Challenges in the Flow Measurement Engineering Study Phases

By Liv Marit Henne and Jean Monnet,
Aker Kværner Stavanger

Summary:

Offshore development of marginal Oil and Gas fields can often be economically profitable if they can be tied in to existing platforms. This usually requires execution of comprehensive feasibility studies, which can often be a long and costly process. Close cooperation in a multi-discipline engineering team is necessary to assure that all possibilities and aspects of the design task have been evaluated.

Integration of a new flow measurement module on an existing installation is often the simplest solution, yielding low total cost as the module can be assembled and fully tested on shore. However on many installations one is required to integrate the new equipment in existing modules.

Flow measurement is a crucial element in the development of marginal fields which has to be evaluated, taking into consideration all critical aspects such as: available space, weight, location accessibility, maintenance and integration to existing metering systems. In particular, special attention should be given to the possible use of new flow measurement technologies and principles.

1. INTRODUCTION

For the past 35 years the North Sea has been populated by a number of types of platforms and rigs, essential for the development of offshore oil and gas fields. This rough environment has largely contributed to technology process developments including fiscal and flow measurement.

During this period Aker Kværner has been at the front End in MMO (Maintenance Modification Offshore) and has acted as an Engineering Contractor involved in most Norwegian fields development.

Aker Kværner is pleased to share their experiences in the accomplishment of those integrations study challenges to keep installation and study cost to a lower level.

2. ENGINEERING CONTRACTOR

What kind of role does Aker Kværner play in this relationship?

Aker Kværner is well acquainted with national and international standards as well as the requirements of most oil and gas related companies operating in the North Sea.
Aker Kværner has a good overview over the metering equipment available on the market.
Aker Kværner is a multi-discipline profession company. The most important disciplines regarding the metering design are process layout, installation, telecommunications, safety and instrumentation. These factors enable Aker Kværner to come up with the most optimal metering solutions.
Aker Kværner does not manufacture any metering equipment, but cooperates closely with suppliers to acquire the optimal solution for the customer.

3. STUDY PHASES

As an engineering contractor Aker Kværner is involved in different phases of the engineering process. The study is classified in 5 phases. Each phase is not necessarily performed by the same company. The study can give a basic cost evaluation with recognised levels of accuracy.

- Idea studies – no specific requirement.

- Feasibility study – cost estimate within ± 40 %.
  The technical work in this phase should focus on new and modified equipment in systems that obviously will be affected by the actual design requirements.

- Concept study – cost estimate within ± 30 %.
  The objective of the concept phase is to select and define the modification concept for realising a business opportunity, implement HSE requirements or reduce operational expense, and demonstrate that execution risk is satisfactory to the company requirements and business plans.

- Pre-engineering – cost estimate within ± 20 %.
  The technical documentation to be further matured defining basis for project execution (detail engineering and construction).

- Detail engineering

To achieve the required level of accuracy the disciplines involved must be well coordinated.
When starting to evaluate conceptual design; there is not always enough information available to develop an accurate budget for a relevant metering system. It is however essential that the requirements can be established at the earliest possible stage, to provide a clear perspective for the project team. Consequently, a study period is required to look at different solutions. The project needs to reach a more mature state. Relevant data for the requirement specification are production profiles, process conditions, field life and required standard of metering.
Many new developments are often small satellite fields. These need to be installed within the boundaries of the existing field infrastructure, utilizing an existing plant. This can create a challenge for existing metering systems that may need to be upgraded in order to bring the metering up to the required standard. To make marginal developments economically viable, metering is often less than full fiscal standards to reduce cost.

4. OFFSHORE SURVEY

Offshore Survey is a very important part of the engineering and is performed for the different study phases as it can give an absolute value to the study. Meeting with offshore personal is normally arranged prior to arrival on board; description and reason for the survey are given to the flow metering technician who will act as co-ordinator for other offshore disciplines.

In the case of integration of new metering equipments many aspects should be reviewed which might involve different engineering disciplines such: Instrument, Electrical, Piping, Structural, Process, Safety, and Maintenance etc. It could be necessary for different specialists to be part of the survey as documentation may not always been updated. Generally it is always beneficial for the project that engineering is familiar with the platform and can establish direct contact with offshore personal.

During survey all technical aspects should be reviewed in order to assess all possible alternatives such:

- Computer hardware & software, upgrading
- Structural , supporting
- Piping , tie-in possibility
- Maintenance, accessibility to equipment
- Location, installation possibilities
- Shut Down requirement
- Prefabrication work including all alternatives
- Utilities requirements
- Hot work necessity
- Temporary equipment, cable etc
- Safety escape route etc ,
- Demolition
- Down time
- Standby spare parts

Offshore survey should be considered as a major requirement to assure successful project performance.

5. ENGINEERING TOOLS

The engineering Contractor main challenge for the project is to assure that all phases will be accomplished in time and within the cost estimation. The flow metering installation will usually depend on shut down activity requiring a constant follow-up for engineering activities, vendor deliveries and test prior to installation.
To accomplish these tasks Aker Kværner use several interconnected tools.
For the detail engineering and vendor follow up the main tools used are:

- PEM (Project Execution Model)
- PDMS / 3D CAD (Plan Design Management System) / (3 Dimensional Computer Assisted Drawing)
- T IME (Technical Information Management Environment)
- MIPS (Material Integrated Production System)
- ELECTRONIC SURVEYING

For the concept study and pre-engineering, a useful tool that is used:

- Meter Run Dimension, Weight and capacity.

5.1 **PEM**

The Modification Task part of the Aker Kværner Project Execution Model for M&M defines the following main phases:

The main intention with PEM is to ensure a consistent development of activities with inter discipline dependencies. These activities are controlled through defined level of completion requirements towards defined milestones.

A set of Execution & Management Key Deliverables are defined and for each Key Deliverable a quality level chain is established with check lists defining the content of the information for each quality level. Each quality level shall be achieved within a certain milestone (ref. Fig. “Execution Key Deliverables” & Management Key Deliverables”).
Typical Execution Key Deliverables with established checklists are:
Study Report
Procurement; Supplier documents & drawings (SDD)
System Engineering; P&IDs
Engineering Register
3D Model /Layout
Installation method

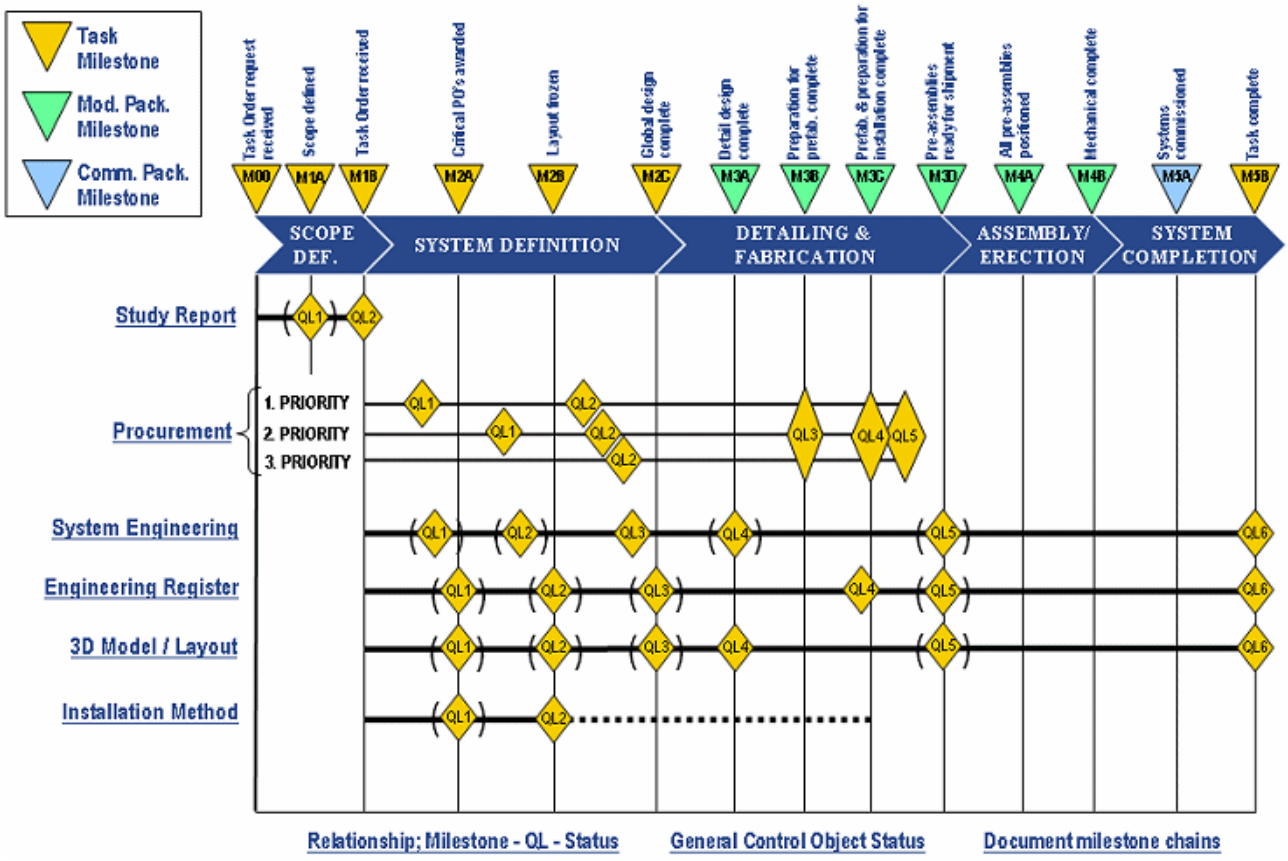

Fig.: 5.1 A “Execution Key Deliverables”

5.2 PDMS (3D CAD)

PDMS is a fully integrated 3D multi-discipline design environment for Piping, Structural, Electrical (cable tray), HVAC, Mechanical, Instrument and Safety. PDMS consists of the following main modules:

- Catalogues and Specifications
- Design (all disciplines)
- Draft (Drawing production from the 3D model, all disciplines)
- Isodraft (Isometric Drawing Production, Piping/Electrical/HVAC)
- Clasher (Clash Detection system, Interactive or Batch)
- Reporter (Various Model and Material reports as object Status, CoG, BOM etc.)

Associated with the 3D model is the walk-through system "Review Reality" which provides an excellent means of design verification and hands-on feeling of how the design will work in practice.
To minimise duplication of data, and to avoid data inconsistency, SQL is used to integrate and link data in the 3D model with data stored in other database systems used by the project (i.e. MIPS & TIME).

5.3 **TIME**

TIME is a multidiscipline engineering application used as standard by all disciplines to track changes to technical information. TIME is use for planning, control and follow-up of the production environment and there are five distinct modules.

TIME Activity for all engineering and procurement related work defined as engineering and procurement activities.

- TIME **Document Plan** is the network activities for the project, deliveries from these activities are defined as input to fabrication-, installation- and commissioning. References to engineering, procurement, fabrication, installation and commissioning activities can be established for all the deliverables.

- TIME Document Control manage all deliverables in the project, Expedites issues for IDC and comments, mark-up and revisions in the fabrication and installation phases, Engineering Numbering System, DFO (documentation for operation) activities etc….

- TIME Document Expediting, manage all supplier documentation, delivery plan, document numbering, distribution for discipline review, and expedite document delivery plan etc…

- TIME Engineering Register for all tags, cables and lines. Line sizing and electrical load list management etc. It provides electronic checklists for 3D modelling and document/drawing production. Linked to CADView 3D review, and to Tektonisk datasheets. TIME is linked to fabrication and commissioning application Sireko MIPS

5.4 MIPS

MIPS is a multidiscipline- and “total construction and material management”- system, designed to follow up all kinds of projects within the Contractor’s organisation.
MIPS covers all phases of the Contractor EPCI execution model from start of system engineering to hand over of a tested and installed product to the client.

All information necessary for the total construction and material administration will be gathered in one common database accessed by the Sireko MIPS, which makes sure that each information element only has one occurrence.

Main output formats are: Material requisitions, Purchase orders, Material tracking reports, progress reports as activity charts / histograms, work orders with details, mechanical completion check sheets and certificates, preservation status and commissioning certificates.

5.4 ELECTRONIC SURVEYING

Over the last ten years Aker Kværner has been using electronic surveying and this has proved to be a success. Significant investments in surveying equipment has been made and Aker Kværner presently employs approximately 20 surveyors.

There are several advantages by using electronic surveying. This is relevant for the integration of metering skid into a module contributing to reduce hot work offshore and reduced installation man hours.

We obtain documentation of what is measured into a 3D-model within an accuracy of 3 mm

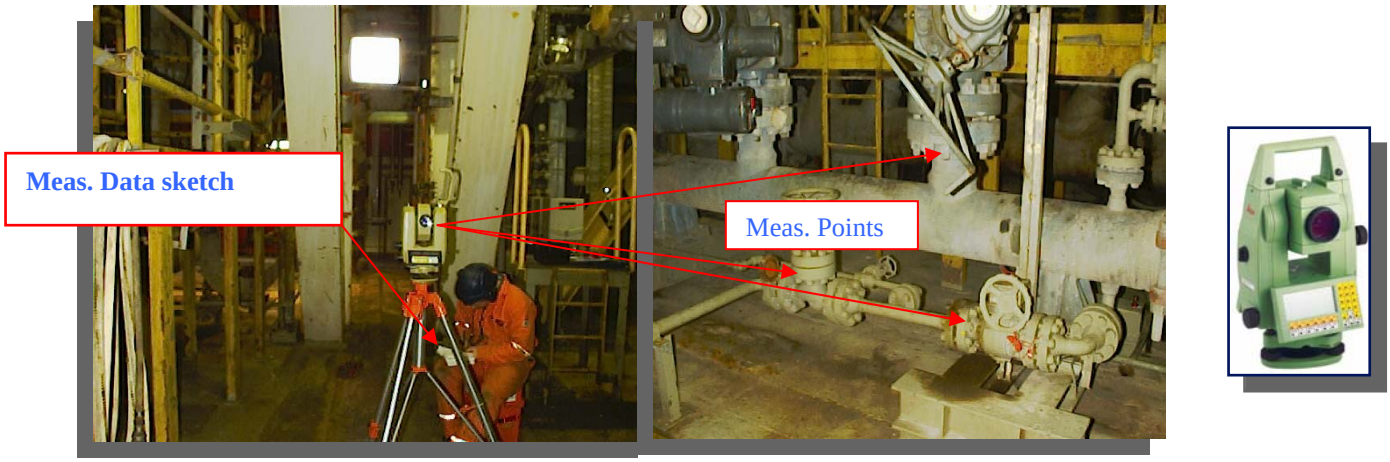

Fig.: 5.4 A / Typical offshore electronic surveying.

5.5 WEIGHT/SPACE ESTIMATION

This is an Excel tool developed by Aker Kværner and is related to USM gas fiscal metering skids as shown on the sketch See fig 5.5A. By inputting pipe & valve data, total skid weight and dimensions are resolved for this typical layout. It gives a prompt answer for the study group during Concept and Pre-engineering study phases.

The accuracy expected is good, weight and dimensions are determined for skid equipped with double expanding gate valves for upstream & downstream manifolds. Results are to be adjusted if other valves are used or if manifolds are different.

Meter Run Dimension, Weight and Capacity

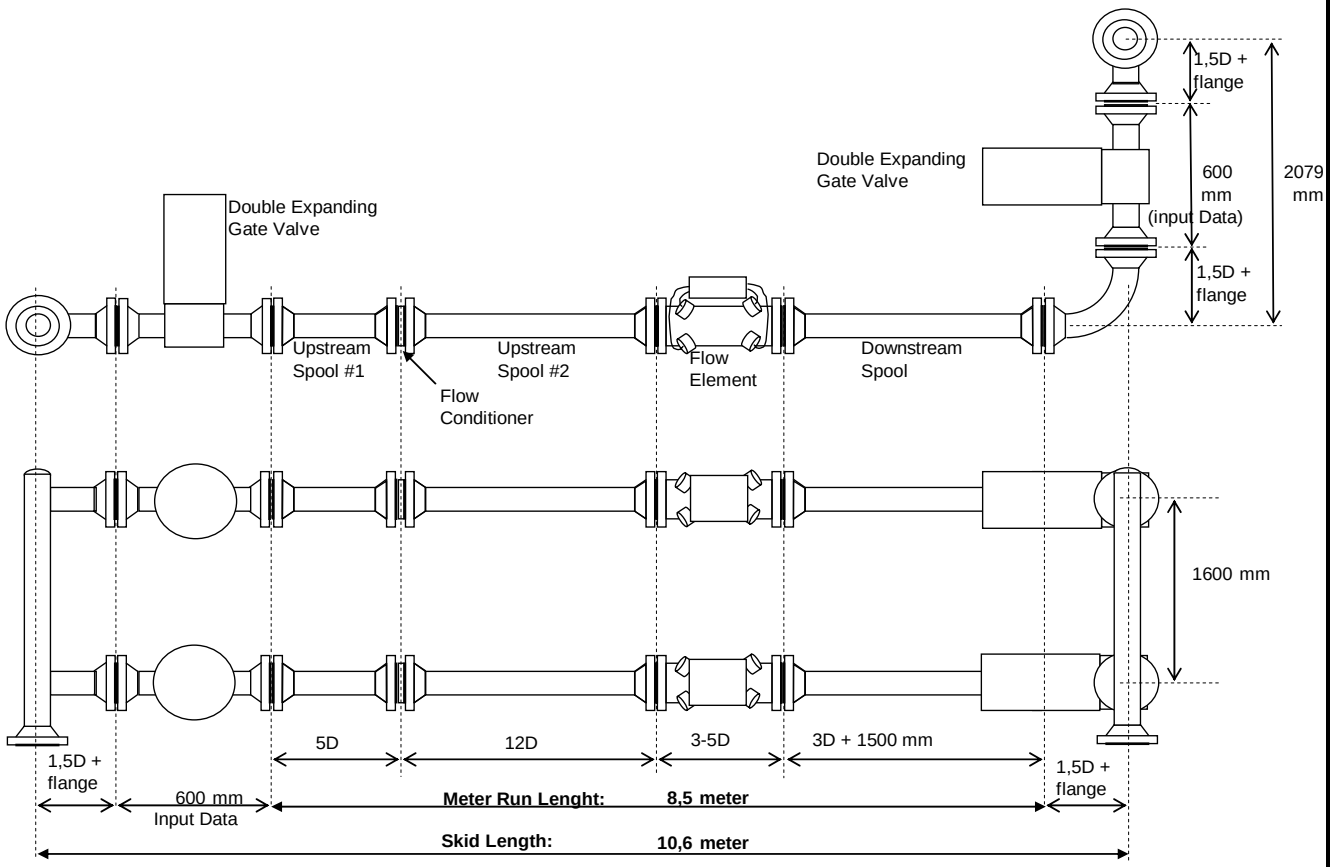

Input Pipe Data	
Pipe OD (mm):	323,85
Wall Thickness (mm):	10,00
Nominal Pipe Size:	12"
Pipe Class:	1500#

Input Valve Data	
Face to Face (mm):	600
Weight incl. act.(Kg):	500,0

Meter Run Weight Details	
Flow Element:	1204,0
Pipe:	464,0
Flanges & Flow Cond:	2191,0
Branches & Field Instr:	400,0
Total Weight Meter Run:	**4259,0**

Other Weight Details	
Valves 4 ea.	2000,0
Bends 2 ea. (4 flanges & 2 bends)	1367,0
Headers 2 ea. 6 flanges & 4 m pipe	2193,5

Dimension Details	
Lenght of bend and flange (mm)	739

Calculated Data		
Meter Run Length:	8,5	m
Meter Run Weight:	4259	Kg
Skid length	10,6	m
Skid height	2,1	m
Skid width	1,6	m
Skid Weight	18302	Kg

Capacity:	min	max
m/s	1	15
actual m3/h	261	3916

Fig. 5.5A / Weight Dimension Tool Lay out

6. NEW TECHNOLOGY

New technology needs to be proven in test loop in order to gain an insight into product performances. It is well recognised that test loops will never reflect actual field conditions even if the product has been tested extensively.

One of the principle major standard requirements for the engineering contractor for equipments to be delivered and installed are:"Only proven instrumentation / equipment should be used". This is mainly to assure that products taken into operation have been fully tested and well proven; in summary:" No prototype can be used which can jeopardise the project".

Despite this restriction; within offshore oil and gas field development, in the North Sea and elsewhere, Oil Companies and Manufacturers have contributed largely to the development and promotion of new products, via pilot project.

Those products based on new technical solutions have very often as main objectives to reduce installation cost, to cover a wide range of process production with high accuracy, to have a low maintenance cost (OPEX), a high availability (Long lifetime reliability), a low cost (CAPEX) and a weight and space savings. Those factors can directly very often contribute to the project feasibility or viability.

New products can be classified into two distinct entities"Main Products" and"Sub Products (auxiliary)". Main products are related to flow measurement, and sub products for auxiliary equipment: such as valves, filters, density transmitter etc

For the flow measurement in the Norwegian sector, Norsok Standard I-104 Chapter # 4-1 states:

General Rule

"The measurement system which fulfils the functional and technical requirements and has the lowest life cycle cost shall be selected".

6.1 Main Products

In the past 15 years products such as: USM, MFM, water in oil meter, oil in water meter, gas chromatograph etc have been subject to extensive development, with many interesting papers issued at different workshops providing new Standards and Guidelines to all parties involved in flow metering. Those products have contributed largely for satellite fields to be developed and most particularly for marginal fields. Recently new products for wet gas measurement have been made which are still subject to intensive field testing and look to be very promising in the near future.
Coriolis Mass Flow Meters used in process control has started to be used as fiscal measurement on the Norwegian sector where it was introduced on the Draugen platform by Shell and taken into operation in the summer of 2000. The Shell Draugen gas export project was challenged with several issues such as: gas and condensate in the same metering station, small volumes of gas and condensate , less maintenance, space, weight and cost. After a study involving several vendors the solution to use coriolis meter looked to be an optimum.

This was encouraged by PSA (Petroleum Safety Authority) following a concept study involving Aker Kværner. A paper was issued two years ago under the 21 st workshop in 2003 "Experiences with a Fiscal Metering System using Coriolis Meter" and concluded that the Coriolis meter was proven to be suitable for fiscal purposes.

It is just amazing to think that a 200 years old discovery made by Gaspard-Gustave De Coriolis born in 1792 today forms the basis for maybe one of the most important measurement principles employed in world of industrial metrology and process control.
Due to the Coriolis meters compact design, which gives space reduction and reduced weight, it compares favourably with traditional flow measurement and is certainly a beneficial meter for integration on existing platform.
The shell Draugen fiscal meters for gas and condensate consisted of five Micromotion Coriolis as shown on the Fig. 6.1-A, composed of, one meter (stream 1) for the liquid, one meter (stream 2) for alternatively gas/liquid, two meters (stream 3 & 4) for gas and one check meter acting as a master meter.
Prior to meter principle qualification for this application one meter (1, 5") was tested extensively at K-Lab (Kårstø) for gas and Con-Tech Services A/S (Stavanger) for liquid.
Due to the Coriolis measuring principle the meter do not require the traditional upstream / downstream straightening lines and can be easily integrated on a skid. The fig. 6.1-B shows the Draugen overall skid dimension (Two parts for installation).

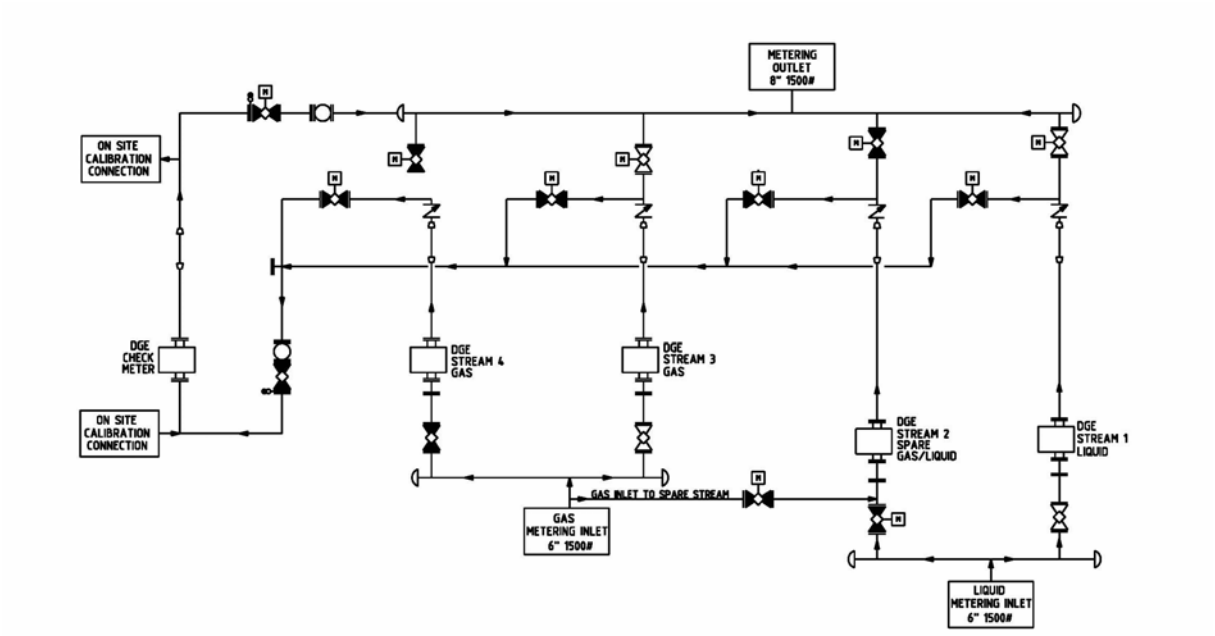

Fig: 6.1.A / Draugen Shell Coriolis fiscal meters Flow Diagram

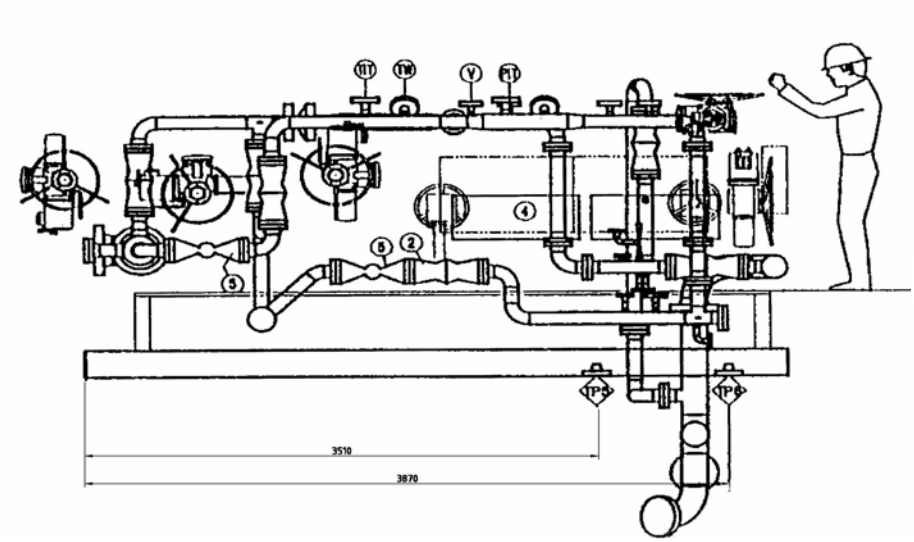

SIDE VIEW A-A

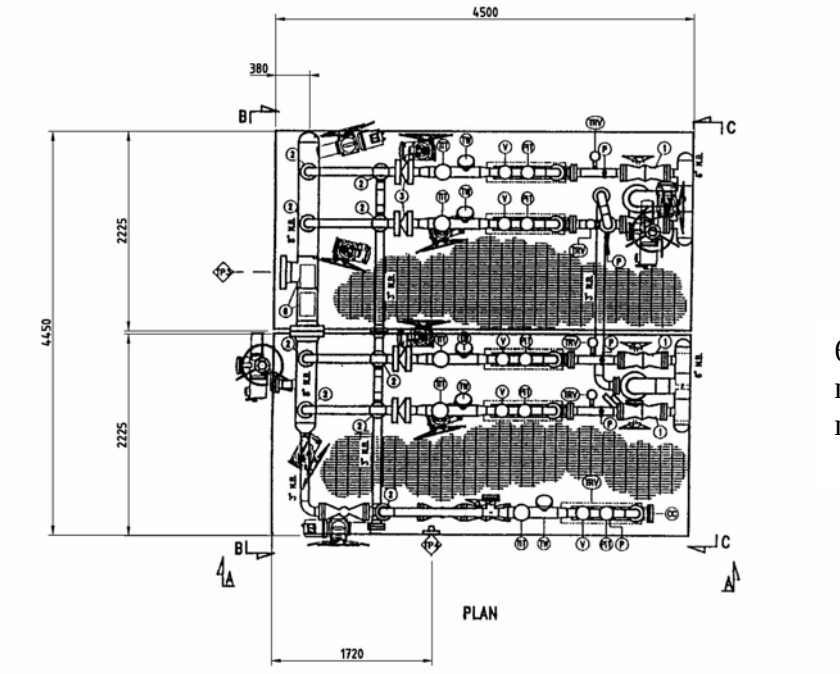

6.1.B / Draugen Shell Coriolis fiscal meters skid for Gas & Condensate mounted in two parts.

6.2 **Sub Products**

Metering sub-equipment classified as new product should not be under estimated. As example we can mention some specific items reviewed by Aker Kværner during Projects for Statoil. This concerns one Double Block & Bleed valve for USM transducer (DB&B), one transducer calibration chamber for the Draupner platform and one wet gas sampling panel for the Sleipner platform.

6.2.1 **Daupner Platform**

The Draupner S and E platforms in the North Sea form a key hub in Norway's network of submarine gas pipelines, with pressure, volume and quality monitoring of gas flows as their most important functions. Draupner S was installed in 1984 as part of the Statpipe system.
It tied the Statpipe lines from Heimdal and Kårstø together for onward transmission of dry gas to Ekofisk. The first gas flowed through the platform in April 1985. Draupner E was installed in 1994 as part of the Europipe I gas trunk line system from the Sleipner fields to Emden in Germany. With seven risers measuring 28 to 42 inches in diameter and associated manifolds, these installations occupy an important place in Norway's gas transport system to continental Europe. The fig. 6.2.1 A shown the Draupner flow diagram with this 12 USM and two GCs.

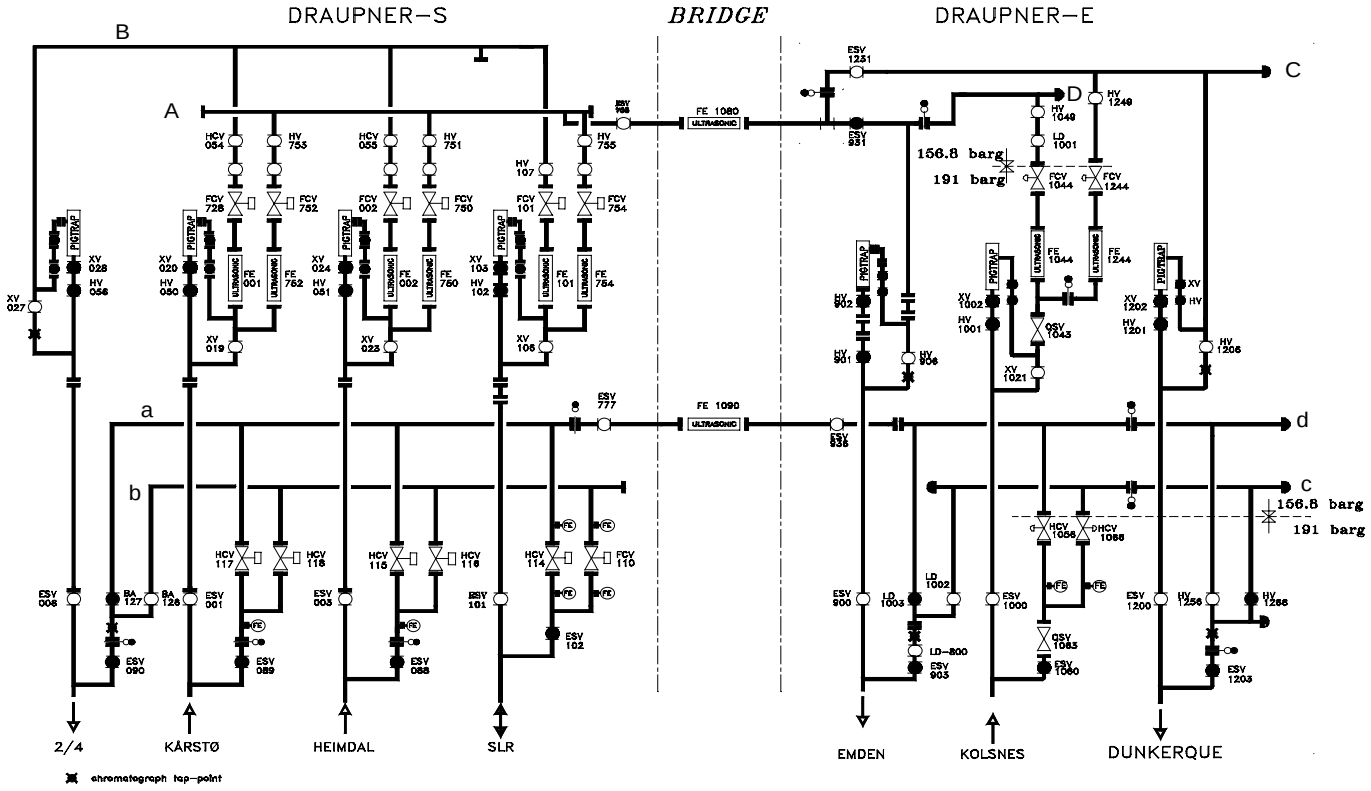

Fig. 6.2.1-A – Draupner flow diagram
Today the Draupner platform is operated by GASSCO, however the philosophy has changed since most USMs are no longer used for fiscals purposes.

DB&B TRANSDUCER

Experience from USMs installed during Statpipe and Europipe I projects has shown transducer problem due to liquid in the pipe; picture 6.2.1D is evidence of today's situation. This required chord transducers pairs to be replaced frequently (usually lowest level) and consequently the meter to be shut down with depressurisation of the line.
To overcome this operation one DB&B valve was specially designed for USM's transducers in 1990's during the Zeepipe project involving AKER KVÆRNER. The fig. 6.2.1B show the valve and transducer assembly and picture 6.2.1C show the assembly on the USM.
Six ultrasonic meters from Daniel ranged from 20", 24"and 30"were installed with this item allowing replacement of transducers pairs with meter under full operation.
It should be noted that during USM calibration one chord failure test was performed at British gas to prove meter accuracy, this is now part of Norsok Standard I-104 Chapter # 5.2.2.4.

This "sub–product" was of great advantage due to lack of space around the meters as we could not install any retractable hydraulic tools. (On the Norwegian sector retractable tools are not so often used).

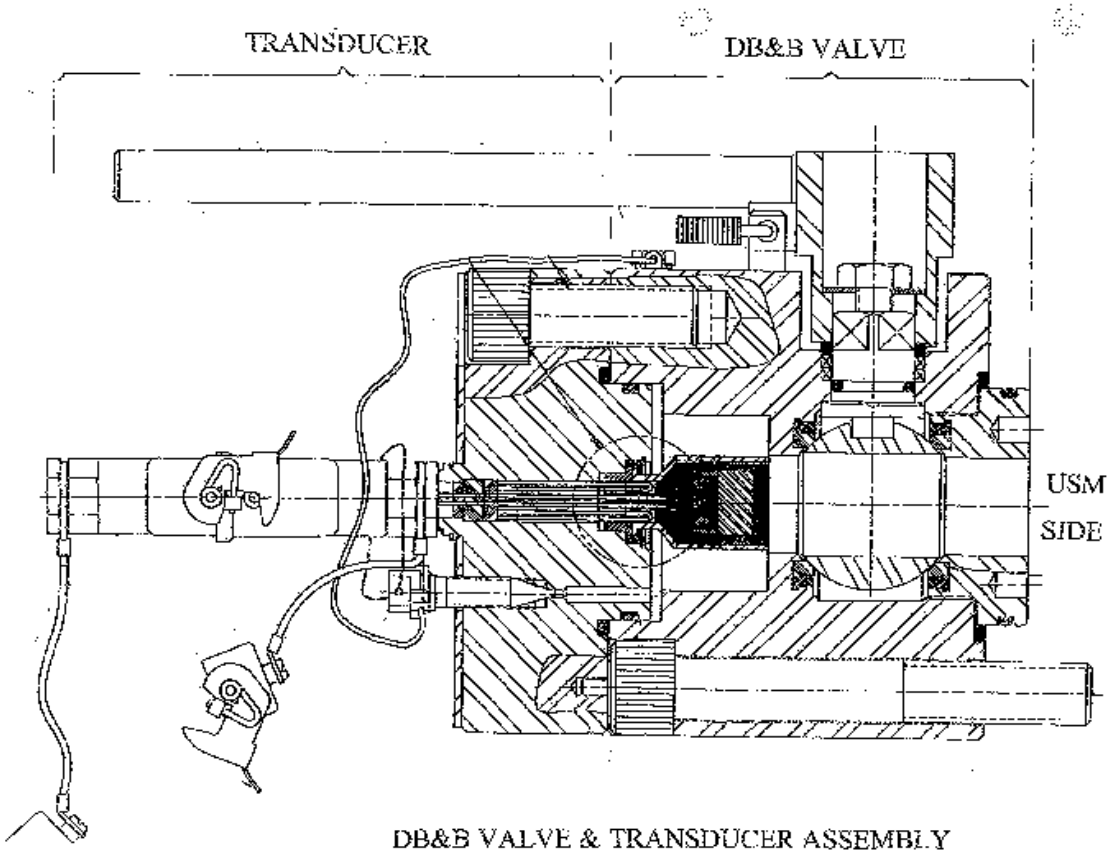

Fig. 6.2.1 B / Double Block and Bleed valve with USM transducer assembly.

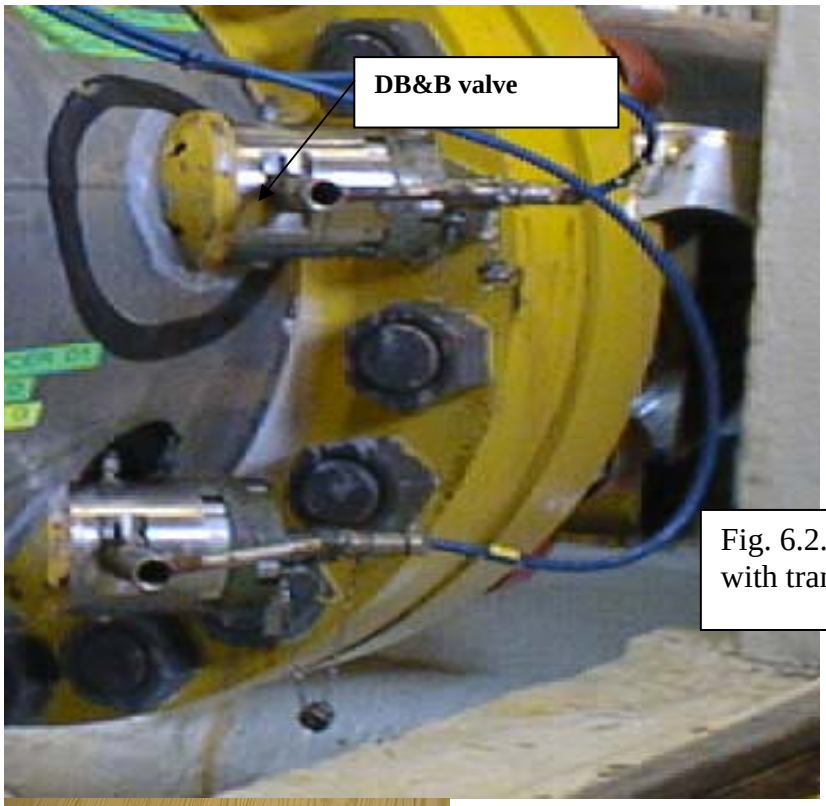

Fig. 6.2.1 – C Pictures showing DB&B valve with transducer assembly on Daniel USM.

Fig. 6.2.1 – D Pictures showing two transducers, one heavily polluted with oil.

CALIBRATION CHAMBER

The Draupner platform has a total of 12 USMs installed during two different periods where only 7 USMs transducers were equipped with DB&B valves. These 7 USMs totalising 60 transducers (28 pairs) convinced Statoil to install on board the platform a transducer calibration rig in order to perform this activity saving time and decreasing this OPEX.
The system is adapted for the two different type of driving unit Mark I and Mark II installed on the platform. New transducer assembly test certificates are issued by the platform in order to update the metering log book, (New Chord average Delay time, Chord Delta Time etc...).
The fig 6.2.1E shown the calibration arrangement

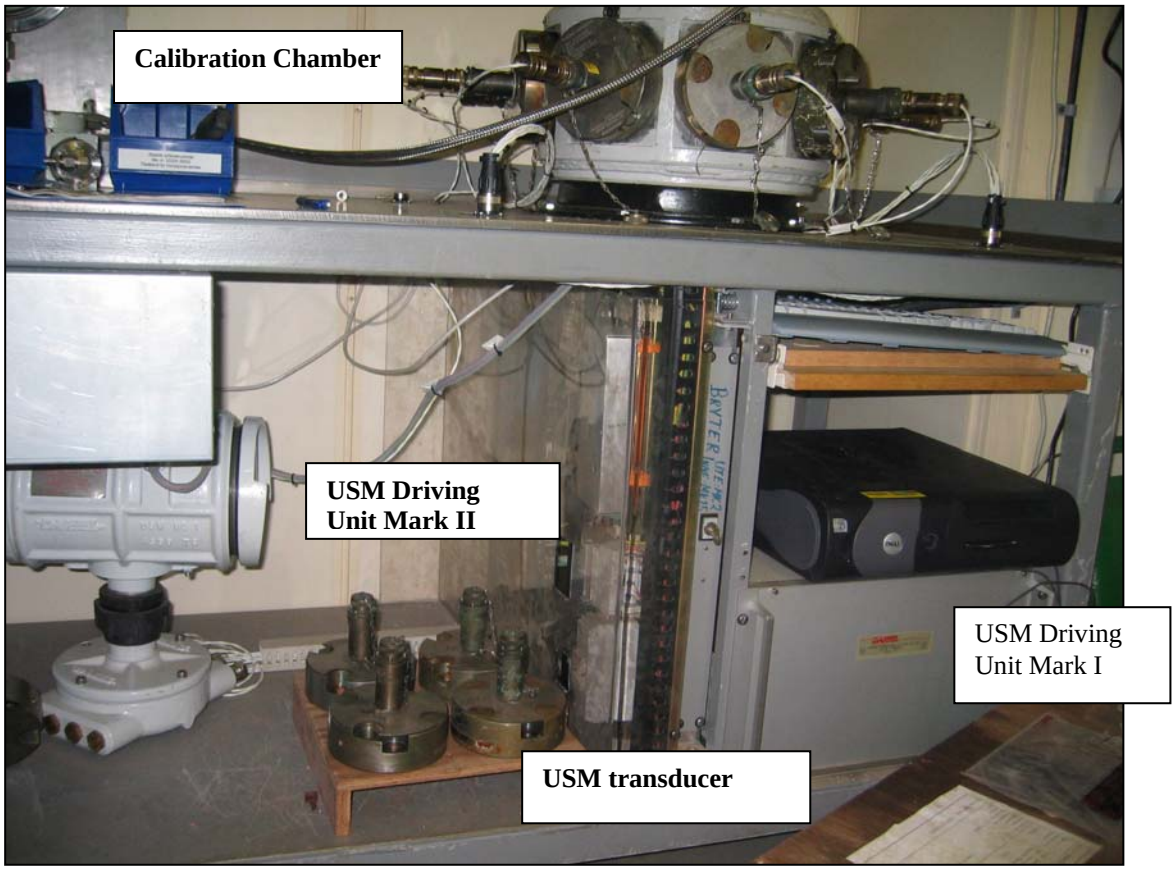

Fig 6.2.1E calibration arrangement

6.2.2 SLEIPNER PLATFORM

A wet gas sampling panel was specifically designed by Aker Kærner to gather water and condensate from Alfa Nord tie in to Sleipner west. This was required by shell in order to have the ability to, analyse C10+ fraction, CO2 determination and calculate MEG (methanol) content.
The sampling is done by routing the process stream through a sample container. A pressure reduction valve is installed upstream the sample container. The pressure drop over the valve and succeeding temperature drop will generate liquid fallout. The liquid will be collected in the sample cylinder. The gas sampling is done by connecting a standard sample cylinder with backpressure to the sample container.
Water and condensate sampling must be done when it is expected that there is liquid in the sample container. The sample line from the process will then be closed and the pressure reduced to atmospheric conditions. Standard sample cylinders will be connected to the bottom of the sample container to take samples of condensate and water.
The fig. 6.2.2 A shown the flow diagram

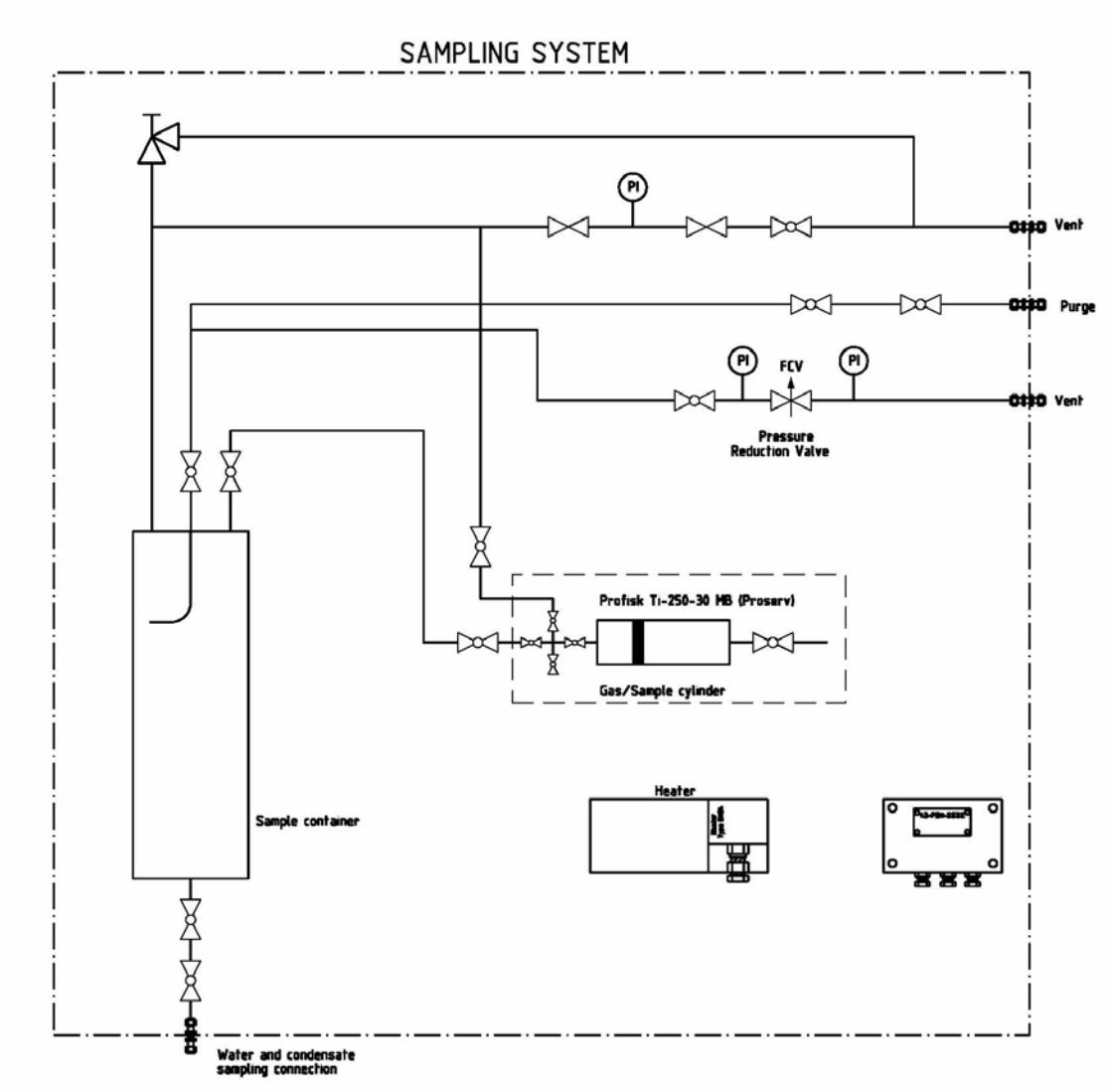

Fig. 6.2.2 A Sampling panel flow diagram

7. SPACE AND WEIGTH

The objectives “Weight and space saving” are certainly one of the most important factors for the installation of flow measurement equipment on an existing platform where lack of space is a major challenge for the engineering contractor and can influence the customer to proceed (due to increase cost).

These two factors can be reduced and can involve both “main” and “sub product” as classified in chapter 6. The following are two typical examples that demonstrate space and weight considerations. They are taken from the Draupner platform and the Gullfaks fields.

7.1 Draupner

One of the challenges very often met in the installation of new fiscal metering is lack of space in the existing flow metering cabinets, that are required to house new computers and to connect field devices.
As already mentioned in the chapter 6.3 in Draupner phase II with new Daniel US meters of type Mark II that were integrated into the existing metering systems. Previously 6 USMs installed on S platform were of type Mark I.
The main difference between Mark I and II is that signal treatment is done in a safe area for the Mark I while signal treatment for Mark II is done locally. Consequently most of the space in the metering room was occupied by the Mark I USM. By upgrading some existing Mark I meters to Mark II, space could have been easily recovered from existing panels, creating new places for new equipment such as new supervisory computer for the all Draupners USM.
If control room space is critical for a new study one should always consider looking for the possibility to gain space by upgrading equipment.
As demonstrated, this approach can be beneficial as the cost of modifying the metering room (if at all possible) is out weighed by the advantages of meter upgrades and space creation.

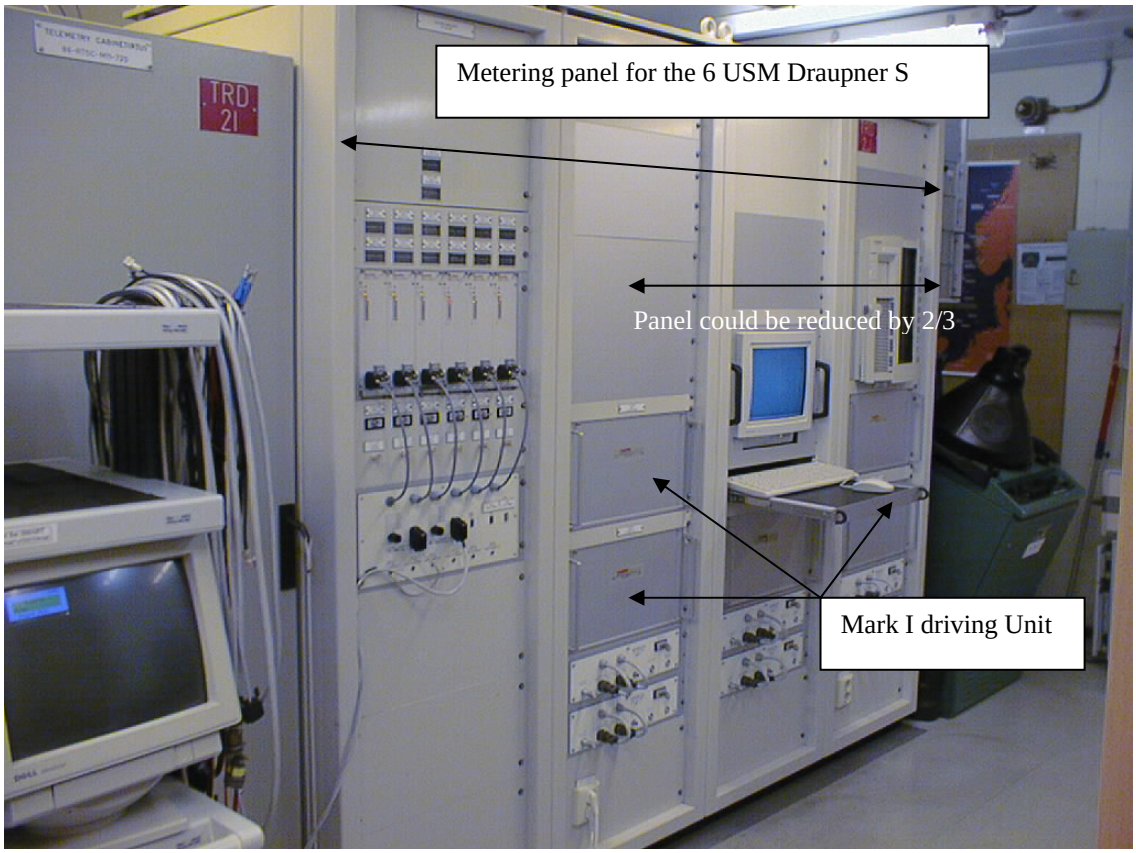

Fig 7.1A / Metering panel for the 6 USM Draupner S

7.2 Gullfaks

One example where space and weight were determining factors is certainly the Gullfaks A & C phase II project for the Gas export metering skid based on two USM runs. Started in 1999 by Statoil, the detail engineering involved different parties. Aker had the responsibility for the Gullfaks C project, UMOE was in charge of the Gullfaks A and KOS supplied the design and skid manufacturing for both platforms.

One of the main objectives and requirements stated by Statoil was to have the possibility to have a common design in order to assure calibration maintenance with one spare meter. This requirement challenged all parties to define a concept to cover all particularities from both platforms such available space, pressure drop, pipe stress level, flow capacity , upstream downstream length (with space for two densitometers), finally temperature and pressure transmitters used for the comparison integrity condition monitoring.

After a long process involving; offshore survey, calculation, several layout options were reviewed by all parties with the following result:

Gullfaks C

a) 2 x 14" USMs and 20ID meter tubes, carbon steel, FC11A spec.
b) 2 x 12" USMs and 20ID meter tubes, carbon steel, FC11A spec.
c) 4 x 10" USMs and 20ID meter tubes, carbon steel, FC11A spec.

Gullfaks A

d) 2 x 14" USMs and meter tubes, duplex, FD22XA spec.
e) 2 x 12" USMs and meter tubes, duplex, FD22XA spec.

Finally the option e) for the Gullfaks A was retained with one of these advantage using Duplex material combine with compact flange instead of ANSI, weight and space was reduced (7 tons could be saved and overall length reduced).

Following, weight table's comparison are given as example. The Fig. 7.2.A /shown a typical Dimension flanges comparison

Flanges Weight Comparison

Flange Type	Dimension	Weight Duplex	Weight Carbon Steel	Saving %
ANSI	12"-1500#	296 kg	303 kg	**2,3 %**
Compact	12"-1500#	89 kg	91 kg	
Saving %		**70 %**		

Fig. 7.2.A / Typical flanges dimension comparison.

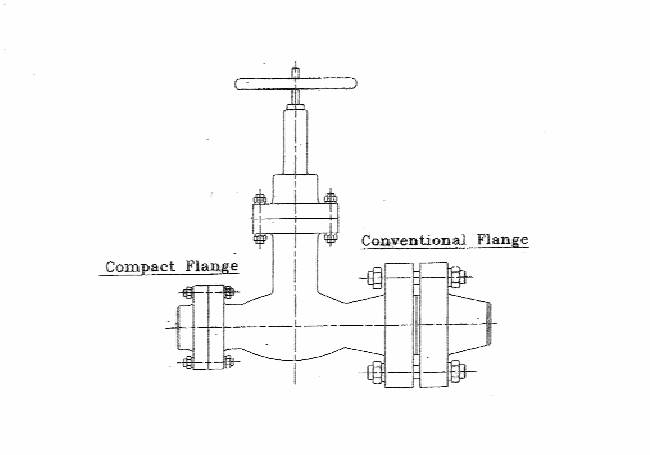

Fig. 7.2.C / Gullfaks C Metering Skid

8. INSTALLATION

Satellites fields with their sub sea wells are usually connected to existing platforms topside facilities according to two concepts depending on platform feasibility, new module or integrated on existing facilities.

8.1 New Module

One concept is to integrate a new module on existing platform, restricting offshore hook-up and commissioning. This offers an ideal situation where metering skid; manufactured and partly commissioned at vendor premises offers the maximum guaranty to the project.
Such an example is on the Bp Blane field in the British sector which will be connected to the Ula Platform located in the Norwegian sector. The figures 8.1.A / shows a concept model done at the preliminary study stage (concept).
This model was produced with readily available material and was made by one person in a short time and corresponded to BP design expectation. Metering skid can be identified "symbolised by plastic straw".
(Sometime it feels good to know that pure craft work talent is still needed and appreciated).

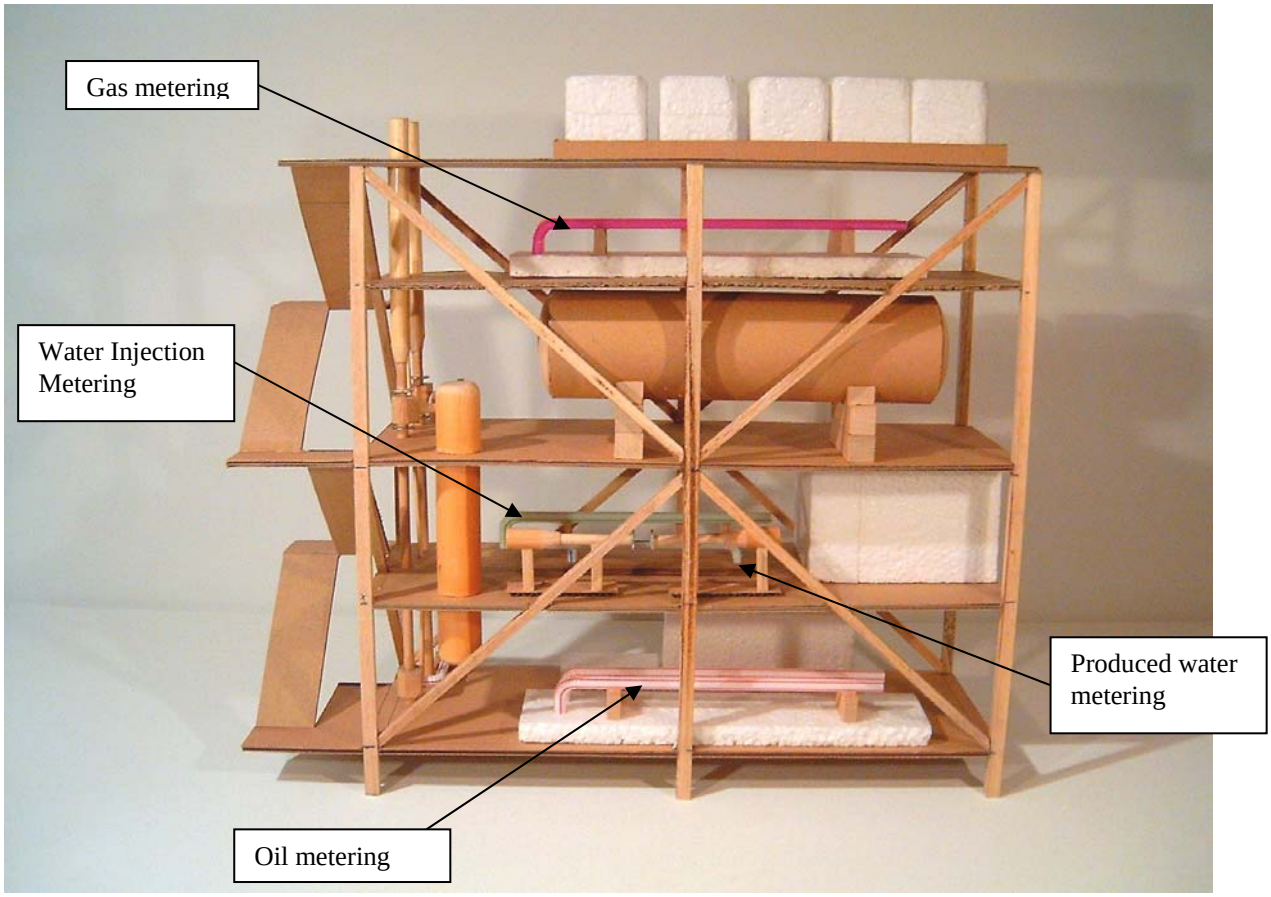

Fig.: 8.1.A / Blane concept model "now on 3D CAD"

8.3 Integrated skid

Sometime new satellite field requires having this fiscal flow metering skid to be integrated into existing modules. In this case flow measurement skid can be often subject of several concept scenarios. Most of the time study is reviewed together with selected vendor during the details engineering phase**.** These installations can require sometime considerable pre-commissioning work offshore in order to allow the new metering skid to be integrated with existing systems and this may involve demolition or temporary equipment locations such cables tray etc.
This work demands close co-ordination between different engineering disciplines, including meter skid vendor and eventually his sub-suppliers with offshore survey to review all feasibility in order to minimise installation work and time offshore. This can be a complex process and need to be evaluated in order to estimate the realistic man-hours necessary to complete all work task to the start up date**.** Gullfaks C phase II is a typical example, the metering skid installed in the module M24 D required the three main parts; inlet manifold, meter runs and outlet manifold to be divided into several sections in order to be re-assembled in place.
Fig.8.3-A shown the metering skid for the two gas meter runs assembled.

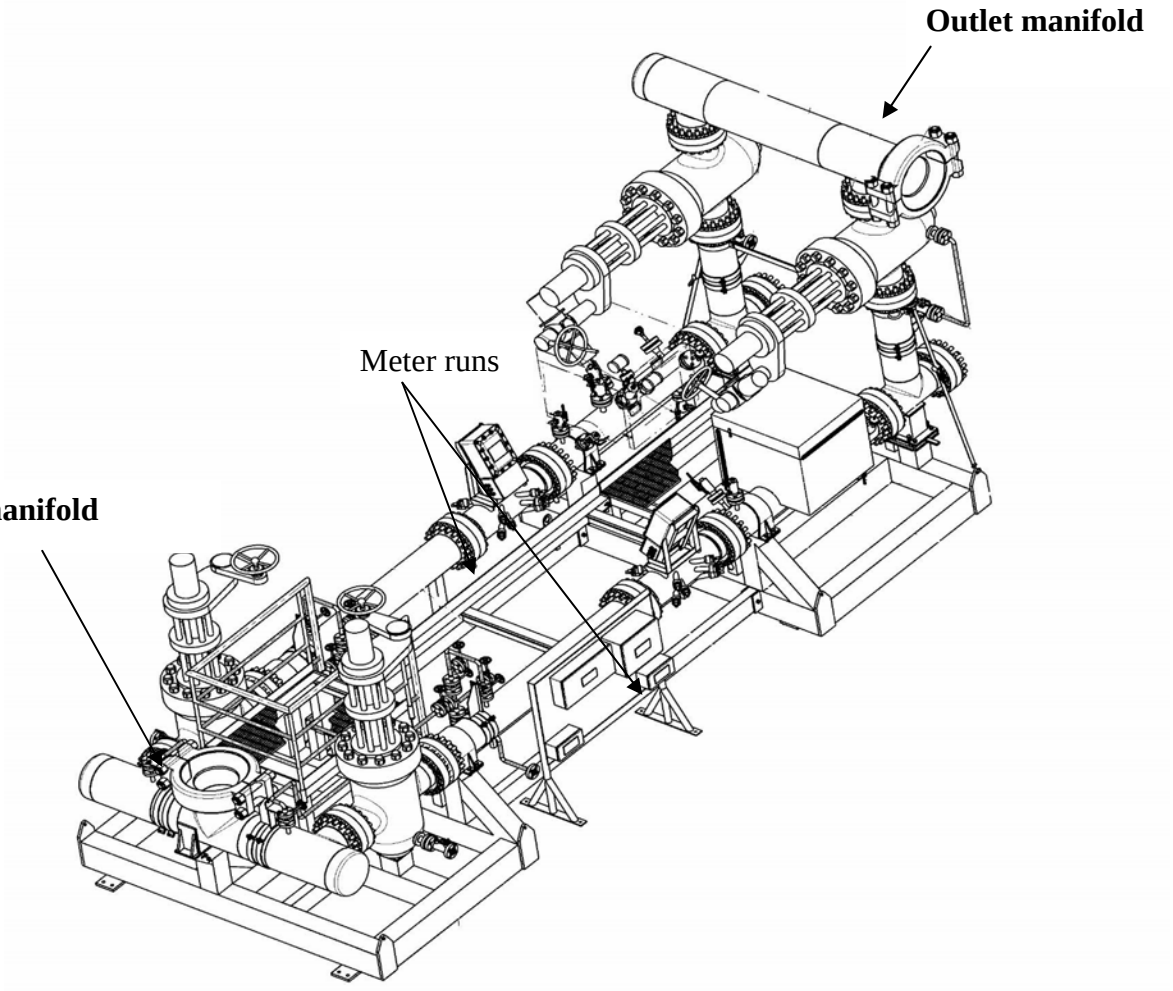

Fig. 8.3.A / Gullfaks C Phase II Gas Fiscal metering skid.

The skid was pre-assembled at FMC sub-supplier yard and tested before it was dismantled as shown on the Fig.: 8.3B and shipped as loose items. FMC issued a very detailed installation procedure with the main purpose to describe the methods and operations required to the Contractor (AKOP) in order to ensure that the dismantled gas metering skid was transported and installed in the correct manner by suitably, qualified personnel under the supervision of FMC representative.
The procedure highlighted several of the following aspects: transport, storage, handling, lifting, and installation (mechanical & Instrumentation) including the N2/HE leak test.

The installation was accomplish during 2 offshore rotations involving 4/5 technicians and one supervisor from FMC.

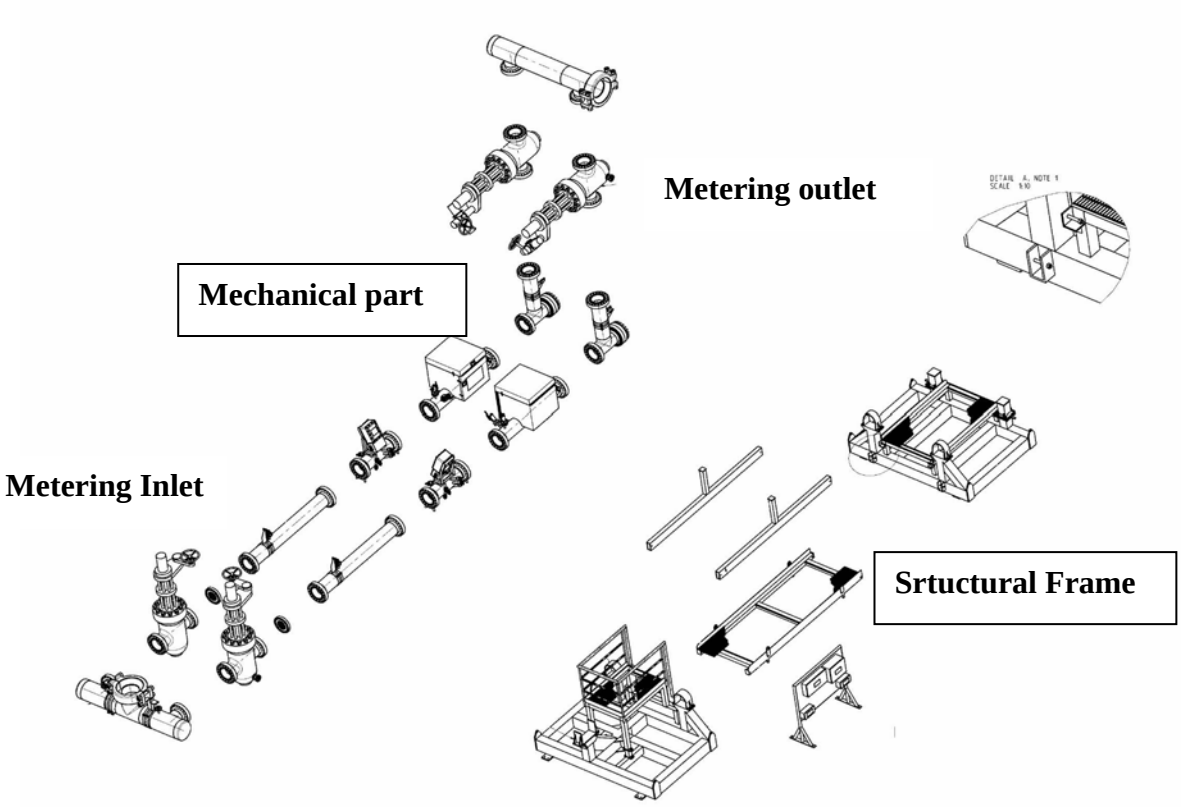

The fig. 8.3.B / shown the skid dismantlement overview.

9. VENDOR & ENGINEERING CONTRACTOR EXPECTATION

From the day of Purchase Order up to the start up, Vendor and Engineering Contractor will have to fully co-operate and establish a good confidence in order to both assume the entire responsibility to their respective tasks and to complete the job at the satisfaction of the end user “Oil Company”. This requires a constant follow-up for the delivery of every milestone, as defined in “PEM/TME”. From experience from main project, Aker Kværner does not usually expect major problem but it is important that if any question should arise from vendor or Engineering contractor they should be highlighted at once to the end user (Oil Company) as they could have consequences on the start up date.

10. CONCLUSION

Aker Kvaerner as an Egineering Contractor has been an actor in MMO from the start of the North Sea oil and gas fields development.

With a multi-discipline knowledge in fiscal flow measurement projects and extended experience in integrated metering skids and new modules, Aker Kvaerner is a key player to successful co-operation between vendors, PSA and clients.

Failure to identify problems at an early stage (construction site problems, late documentation, test procedures, planning changes etc.), may have disastrous consequences to the project and the engineering company. It is therefore a pre-requisite that the engineering company must be able to identify and resolve such problems in a professional manner.

Conducting offshore surveys is a very important part of this process. Aker Kvaerner is continuously improving applied engineering tools, using new technologies in order to reduce study time and installation cost. New technology as a "main product" is a very important part where Aker Kvaerner follows the development and gets acquainted with possibilities and limitations.

REFERENCE

1. Norsok Standards : I-104 " Fiscal Measurement System For Hydrocarbon Gas".

2. Franks Svendsen VTM AS, "Experiences with fiscal metering system using coriolis meter": 21 st International North Sea Flow Measurement Workshop, Norway.

3. GASSCO webside www.gassco.no

ACKNOWLEDGEMENTS

The authors wish to thank: Tove Haaland (Statoil/Draupner), Skule Smørgrav (FMC) , Svein Ole Østdahl (FMC), Colin Lightbody (Daniel), Svein Bakken (Emerson), Anfinn Paulsen (GASSCO), Reidar Sakariassen (MetroPartner as), Nordvald Stokkenes (Statoil/Gullfaks C) and their colleagues : Stine Jørpeland, Janne Gro Sagrov, Marie Aarsland, Nigel Scott, David Colclough, Truls Sønsteby, Øystein Fosså, Søren Knudsen, Egil Salamonsen, Sverre Mo, Tor Olaf Høiaas and Randulf Fjermeros for their advise and help.

North Sea Flow Measurement Workshop
October 2005

Specification of Wet Gas Measurement Equipment for Fiscal Allocation

Dr Max Rowe[1], Britannia Operator Limited[2]
Mr Rod Bisset[3], Britannia Operator Limited
Mr Anthony Alexander, Petrofac Engineering Ltd

1 INTRODUCTION

In the UK North Sea new developments are increasingly utilising existing infrastructure for processing and transportation of hydrocarbons. Utilising existing infrastructure for such developments brings challenges as to how to cost-effectively allocate the produced hydrocarbons (as well as water, fuel usage, and emissions) back to each field – particularly where these fields are under different ownership.

When a new field is to be accepted by a host, it is necessary to define a functional specification for the measurement equipment. This is usually documented as part of the allocation agreement. The question that needs to be addressed is: "What is an acceptable measurement specification?". The ultimate answer will be one which meets standards set by relevant Government authorities and is acceptable to all parties who approve the allocation agreement. One approach, often used, is to apply standard guidelines derived from industry best practice, e.g. 1% uncertainty for a gas fiscal flow measurement. This approach has the advantage of being simple to apply, but may involve some measurements being made with an unnecessary degree of accuracy. Another approach is to undertake modelling of uncertainty in the measurement system to establish the criticality of each measurement (See for example [1]). Scheers and Wolff ([2]) point out the need to consider the whole measurement system through to allocated revenue and propose that the optimum uncertainty of each measurement should be established by evaluating the trade-off between measurement costs and the losses and risks of uncertainty in the measurement. In this paper an extension of these approaches is applied to the Britannia facilities in which uncertainty modelling was applied to the propagation of uncertainty through the whole measurement and allocation system and was used to establish the impact on each company or field's revenue stream.

Figure 1 – Britannia Facilities and Satellites

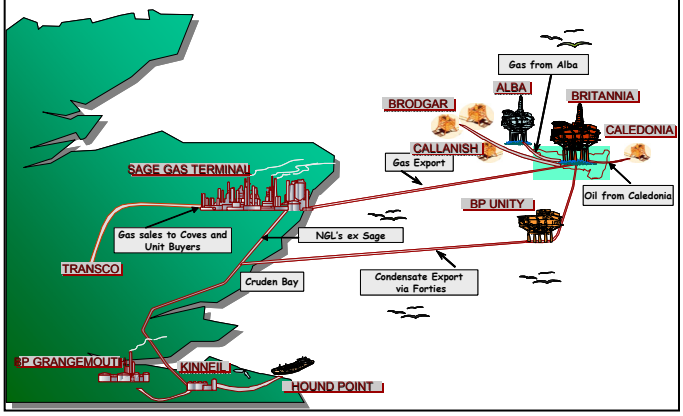

[1] ConocoPhillips (U.K.) Limited, seconded to Britannia Operator Limited
[2] Britannia Operator Limited is a joint venture company of ConocoPhillips (U.K.) Limited and ChevronTexaco U.K. Ltd
[3] Rhomax Engineering Ltd (A division of Tyco Engineering Services), seconded to Britannia Operator Limited.

The Britannia platform was constructed to develop the lower cretaceous Britannia gas-condensate field over a thirty year field life. Following initial processing on the Britannia platform, liquids are exported to the BP Operated Forties Pipeline System (FPS) and processed onshore at Kinneil along with oils from many other North Sea fields. Similarly gas separated offshore is exported via a dedicated pipeline to the Scottish mainland at St Fergus where it is commingled with gas from other fields and processed in the ExxonMobil Operated SAGE terminal. First gas was in 1998. Since then additional facilities have been installed on the Britannia platform to accept gas from the neighbouring Alba oil field and to process hydrocarbons from Caledonia, a black oil field developed as a sub-sea satellite (see Figure 1). In 2004, UK Government approval was obtained for the development over Britannia facilities of two further sub-sea satellites: Brodgar – a gas-condensate field – and Callanish – a black oil field. Additional facilities will be installed to achieve first production by January 2007. With Britannia's long field life and its current transition from a single asset operation to a processing hub, it is ideally placed to secure further satellite business. As part of the preparations for accepting Callanish and Brodgar, the Britannia Coventurers[4] have put in place an allocation agreement to accommodate the new fields and define a fair and equitable method of allocating all products back to each source field. The allocation agreement includes the specification of the measurement systems to be used in the allocation.

The allocation system requires a set of measurements of each field's inputs to the allocation envelope (see Figure 2) and measurements at each output from the envelope. Both gas and liquids from the Britannia platform are commingled with hydrocarbons from other facilities in their respective offtake systems (FPS and SAGE – see Figure 1). The allocation algorithm thus involves two stages, apportionment of products leaving the platform and then allocation of the final sales product streams. The three revenue generating hydrocarbon product streams are: sales gas, natural gas liquids and stabilised crude oil. The total revenue generated on a day will be a function of the measured flow and composition of each of these streams and the prevailing product prices. How this value is allocated back to individual fields and field owners will however depend upon the measured flows and compositions at all of the inputs.

[4] ConocoPhillips, Chevron and BP

Figure 2. Allocation Envelope

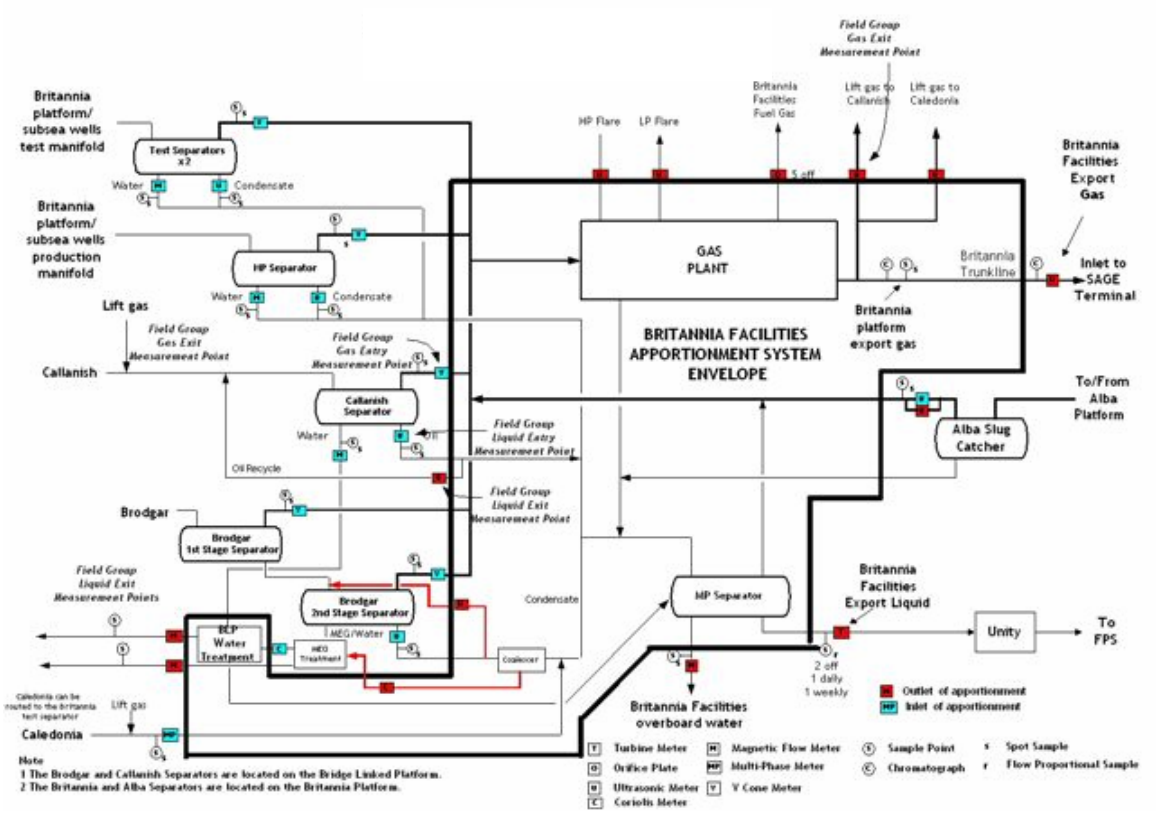

2 METHOD

A spreadsheet implementation of the allocation algorithm was developed and populated with typical anticipated daily flow rates and compositions at each input and output measurement point. It is beyond the scope of this paper to present the allocation algorithm but it is an empirical representation of the physical process equipment based on component liquid recovery factors ascertained through a suite of process simulations. Representative product prices for each of the three main revenue generating output streams were entered into the spreadsheet and from these the total day's revenue allocated between fields and field owners was determined. This information was saved as the base case.

The main inputs to the allocation algorithm are the measured values of flow rate and composition (expressed as percentage by weight of each of a series of hydrocarbon components and CO_2). Excluding recycle streams, there are 45 such inputs (e.g. Callanish C_2 weight percent or Britannia mass flow rate). A sensitivity analysis[5] was performed to establish the sensitivity of each field's and/or owner's allocated value to each of these 45 inputs. One of the inputs was varied by a small percentage, holding all other variables at their base values[6], and the value allocation re-calculated and compared to the base case.

[5] A Monte Carlo analysis could equally have been used to establish correlations between uncertainties in measurements and allocated values.
[6] Note – compositions were always re-normalised so that the total of the component weight percents equalled 100%.

By repeating this process for each of the input measurements one at a time it was then possible to plot the sensitivity of each field and/or field owner's value allocation to the uncertainty in the input measurement.

As some of the measurements on Britannia will be made with existing equipment whose uncertainty is already known, the next step was to establish the maximum measurement uncertainty in each other measurement which could be tolerated without any field / owner seeing an uncertainty in their allocated value greater than that which they would experience from the uncertainties in the measurement systems to be retained. This approach was applied twice: firstly, to consider random errors and secondly to consider systematic bias.

The measurement community place a great deal of emphasis on minimising systematic bias in measurement systems. Some degree of random uncertainty is usually tolerated on the basis that with a symmetrical probability distribution, over and under measurements will cancel out. In order to meet the fundamental criterion for all allocation systems of being fair and equitable, the allocation system mirrors the chemistry and physics of the plant. Since there are non-linearities in the plant behaviour, a symmetrical distribution for the uncertainty of an input measurement may lead to an asymmetric distribution in the resulting allocated revenue. (e.g. a +1% change in an input measurement may lead to a +0.1% change in the revenue allocated to a field, whereas a -1% change in the same input measurement may lead to a -0.15% change in the revenue allocated to the same field). A simplified example is to consider the pressure at which a separator operates. The lower the pressure the higher the proportion of gas to liquid recovered. The pressure in the separator will be a non-linear function of the flow rate through the plant upstream of the separator. If we consider the plant upstream to be a simple pipe, then we can apply Darcy's formula which states that the pressure (P) is related to the flow rate (Q) by the equation:

$$P = K\rho\, Q^2$$

Consider an uncertainty of +/-δ in the measurement of flow rate. When there is an error of +δ then:

$$P_+ = K\rho\,(Q+\delta)^2 = K\rho Q^2 + (2K\rho Q\delta + K\rho\delta^2)$$

Whereas, when there is an error of –δ then:

$$P_- = K\rho\,(Q-\delta)^2 = K\rho Q^2 - (2K\rho Q\delta - K\rho\delta^2)$$

The absolute value of the errors in the result therefore differ by $2K\rho\delta^2$ introducing an asymmetry which, whilst small relative to δ (assuming $\delta<<1$), may be amplified in further calculations.

When considering systematic bias, it was necessary therefore, not only to calculate the propagation of any systematic bias in each measurement, but also any systematic bias in the allocated value arising from the propagation of random errors through asymmetry in

the allocation algorithm. The asymmetry found in the Britannia algorithm was slight, but since systematic bias in the measurement systems is expected to be very small, the bias introduced by random errors was a significant factor.

3 RESULTS

Given the potential commercial sensitivity of presenting actual results, the methodology will be illustrated numerically in this section using a hypothetical set of fields, but the same allocation algorithm. The discussion and conclusions in the following sections will however report the lessons learned when the method was applied to determine the functional specifications for flow and composition measurements at the inputs to the Britannia allocation envelope.

This example will consider three fields (Field A, Field B and Field C) owned by four companies (Company 1, Company 2, Company 3 and Company 4) in the equities shown in Table 1.

Table 1 – Field Ownership (Example)

	Company 1	Company 2	Company 3	Company 4
Field A	50%	20%	10%	20%
Field B	60%	40%	0%	0%
Field C	0%	20%	0%	80%

Under typical conditions the mass flow by component at the arrival separator for each field may be expected to be as shown in Table 2.

Table 2 – Typical Mass Flow by Component (Example)

	Field A		Field B		Field C	
Tonnes/day	Liquids	Gas	Liquids	Gas	Liquids	Gas
N_2	0.07	60.24	0.05	87.69	0.29	9.84
CO_2	1.40	251.37	2.85	131.54	1.11	6.30
C_1	12.55	4442.38	15.29	2718.49	21.95	312.33
C_2	6.78	690.86	29.63	350.77	24.97	88.52
C_3	10.24	411.10	77.60	328.85	56.99	69.66
iC_4	4.33	87.90	32.86	109.62	21.75	11.83
nC_4	11.58	183.67	92.18	131.54	59.27	24.63
iC_5	8.59	68.76	48.00	131.54	35.22	6.53
nC_5	13.34	87.63	73.32	175.39	51.07	7.54
C_6^+	562.07	337.35	1646.55	219.23	3,285.92	11.31
Total	630.95	6621.25	2018.33	4384.67	3558.53	548.50

These fields result in 32% of the inlet mass being exported from the platform as liquids and 68% as gas. The mass allocated to each field was calculated by the allocation algorithm to be as shown in Table 3.

Table 3 – Allocated Mass in base case (Example)

	Field A	Field B	Field C
Allocated mass of export liquids (Te)	1099.49	2939.08	4445.54
Allocated mass of export gas (Te)	10613.72	6509.49	1075.76

For the purpose of this example, the liquids have been assumed to realise £150/Tonne and the gas £100/Tonne. The allocation algorithm may thus be used to allocate the total revenue stream back to each field and company as shown in Table 4.

Table 4 – Allocated Revenue in Base Case (Example)

	Field A	Field B	Field C	**Total**
Company 1	£613,148	£655,087	£0	**£1,268,234**
Company 2	£245,259	£436,725	£154,881	**£836,865**
Company 3	£122,630	£0	£0	**£122,630**
Company 4	£245,259	£0	£619,525	**£864,784**
Total	**£1,226,295**	**£1091811**	**£774,406**	**£3,092,513**

If a 5% increase in the measurement of Field A gas C_1 is now introduced, the Field A component mass flow will be modified to that in Table 5.

Table 5 – Modified Field A Gas Composition Resulting from Measurement Uncertainty (Example)

Component	**Mass (Tonnes)**
N2	57.79
CO2	241.17
C1	4475.27
C2	662.84
C3	394.42
iC4	84.33
nC4	176.22
iC5	65.97
nC5	84.07
C6+	323.66
Total	6565.76

This revised composition was obtained by increasing the C1 mass by 5% from 4442.38 to 4664.49 and then normalising the gas composition to preserve mass. The change in measured composition leads to a revised revenue allocation as shown in Table 6.

Table 6 – Allocated Revenue following Increase in Field A C_1 (Example)

	Field A	Field B	Field C	Total
Company 1	£610,203	£657,237	£0	**£1,267,440**
Company 2	£244,081	£438,158	£155,342	**£837,582**
Company 3	£122,041	£0	£0	**£122,041**
Company 4	£244,081	£0	£621,369	**£865,451**
Total	**£1,220,406**	**£1,095,395**	**£776,712**	**£3,092,513**

It can be seen that Field A's allocated revenue is reduced by £5889 which is 0.5%. Field B and Field C receive an extra £5889 between them. If we apply a 5% change to each input variable in turn the impact on the allocation can be summarised in a graph as in Figure 3.

Figure 3 - Value Difference by Field for a 5% Change in Each Input

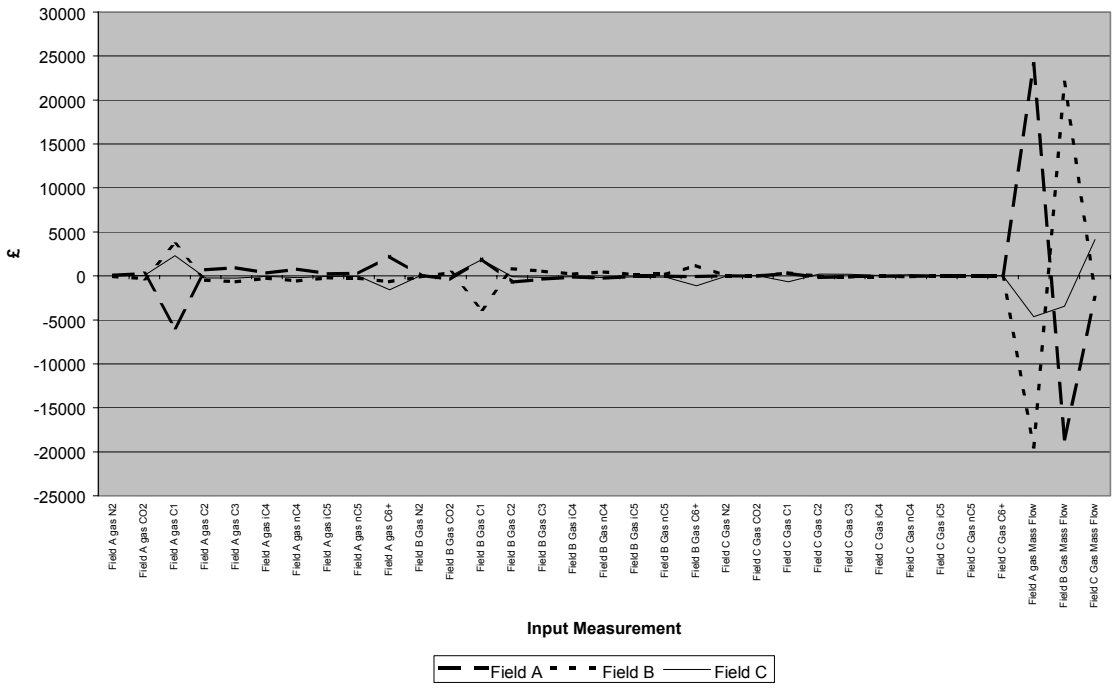

From this it is apparent that the allocation is most sensitive to the mass flow measurements for each field. Whilst the sensitivity to composition is less, the most important compositional measurements are the C_1 weight% for Fields A and B and C_6^+ weight% for Field A.

If the expected uncertainty of the mass flow measurements is +/-1% (symmetrical distribution) then we can calculate the maximum uncertainty which could be tolerated in

measuring composition without increasing the uncertainty in the revenue allocated to a field. These define the functional specification (based on propagation of random errors) for each measurement. The lower (i.e. limiting) values are tabulated in Table 7.

Table 7 – Functional Specification based Limiting Factor Random Errors (Example)

Component	Maximum Uncertainty
Field A gas C1	4%
Field A gas C3	27%
Field A gas nC4	33%
Field A gas C6+	11%
Field B Gas C1	7%
Field B Gas C2	31%
Field B Gas C6+	21%

4 DISCUSSION

For the purposes of this discussion, the difference between the measured value used in the allocation algorithm and the actual prevailing physical conditions (if they could be known) will be referred to as a "measurement error". The measurement error will arise from uncertainty in the measurement equipment and timing differences. It is worth noting that timing differences can be a very significant source of measurement error in this context. For example, the use of onshore laboratory analysis of spot samples for compositional measurement often means that the results are not available when the allocation is run and so values from prior periods have to be utilised.

Any measurement error at the inputs to the allocation envelope will not alter the total quantity of each product stream produced at the outputs. A measurement error in the mass flow will result in a shift in the allocation between fields. A measurement error in a compositional component will result in changes to the other components for that stream (through the normalisation) and is most likely – due to the way the Britannia algorithm works – to result in a change in the ratio of liquids to gas allocated to that field. Depending on the relative product prices, this will typically have a smaller impact on the allocated revenues.

The methodology presented allows the sensitivity of each input measurement on the allocated revenue to be assessed. When applied to the Britannia allocation envelope it showed that the most critical measurements were the mass flows for the higher rate fields as would be expected. The next most critical measurements were the gas compositions of those fields – particularly the C_1 and C_6^+ fractions. It was found that the weight

percentages for these two components need to be within $^{+}$/- 6% (symmetrical uncertainty distribution) in order not to be the dominant factor on the allocation errors for a field[7].

Gas flow is measured at the arrival separators using V-cone meters. All differential pressure meters are known to over-read in the event of liquid carry-over [2]. With the expected conditions on Britannia this over-reading – if not compensated for – would be expected to be of order 0.5%. Using the methodology of Steven and Peters [2] it is expected that this can be compensated for, but it is estimated that there could still be a residual bias of 0.05%. It was found that a random measurement error of +/-6% in determining the C_1 and C_6^+ fractions would generate – through the non-linearity and asymmetry in the allocation algorithm – a systematic bias in the allocated revenues which is of the same order as the bias which may be expected to propagate from any residual bias (+/-.05%) in the flow measurement of gas off the arrival separators.

The figure of $^{+}$/- 6% as a functional specification for measuring gas composition is not just an instrumentation specification. The transfer of the measurement into the allocation system must also be considered. The allocation algorithm will be run every twelve hours to enable allocation to be performed both on a gas-day (06:00-06:00) and on an oil day (18:00 – 18:00). Since gas is delivered into the UK National Transmission System and traded on the day, the allocation of gas has to be established quickly after the end of the day. Thus it is necessary to have a gas composition available for use in the allocation algorithm on each day which is within $^{+}$/- 6% of the actual composition on that day. The functional specification for gas composition therefore implies a combination of measurement uncertainty and timeliness (coupled with what is known about the likely variability of the composition).

5 CONCLUSIONS

The methodology presented provides a means of applying a set of objective criteria to establish appropriate functional specifications for the measurement systems used to obtain the inputs to an allocation system. Attempting to establish functional specifications for the measurement systems in the absence of this kind of analysis runs the risk of introducing a level of uncertainty or bias in the allocated revenue which may prove unacceptable to some fields / owners. Alternatively it may lead to over-specifying parts of the system which have little impact on the final allocated revenues and introduce additional capital expenditure and operating costs.

It is not sufficient to look at the uncertainty of measurement equipment alone. The timely flow of information into the allocation system must also be considered. For example, using a flow-proportional sampling system gives a more representative compositional measurement than spot sampling. However if the flow proportional sample is collected

[7] Given the ownership positions in the fields using the Britannia facilities, the functional specification could have been derived based on company net positions. Since however the field owners may at some stage choose to trade equity in one or more of the fields, the methodology should be applied using field allocations of revenue. Given that much of the equity in satellite fields is owned by some of the Britannia owners, these owners will also want to see their overall company position across all fields.

over a seven day period then the gas allocation system would need to use the previous week's measured composition. Using daily spot sampling it would be possible to use a measurement taken on the day being allocated – albeit with a greater measurement uncertainty. If the expected day to day variability of the property being measured is greater than the measurement uncertainty of spot sampling, then it may be better to use spot sampling.

Since non-linearity in the process chemistry may introduce asymmetry in the allocation algorithm, it may be that random errors which might normally be considered acceptable to a metering / measurement engineer (given that they are symmetrical and cancel one another out) may not be acceptable in the context of the allocation as they may cause a systematic between fields' allocations.

6 ACKNOWLEDGEMENTS

The authors wish to acknowledge the support of the Britannia co-venturers for this work and also the many colleagues who have discussed and reviewed aspects of it and ultimately shaped the methodology.

7 REFERENCES

[1] M. BASIL & AW JAMIESON. Uncertainty of Complex Systems Using the Monte Carlo Techniques, North Sea Flow Measurement Workshop, Gleneagles, Scotland, October 1998.

[2] L. SCHEERS & C. WOLFF. Production Measurement Management, North Sea Flow Measurement Workshop, Gleneagles, Scotland, October 2002.

[3] R. STEVEN & RJW PETERS. Wet Gas Metering with V-Cone Meters, 3rd International SE Asia Hydrocarbon Measurement Workshop 9th -11th March 2004.

Estimation of the Measurement Error of Eccentrically Installed Orifice Plates

Neil Barton, National Engineering Laboratory
Edwin Hodgkinson, Kelton Engineering Ltd
Michael Reader-Harris, National Engineering Laboratory, UK

Introduction

An inspection of the fiscal metering station on a large Middle Eastern gas field revealed that the orifice plates in all three 16-inch metering runs had been incorrectly inserted in their carriers and O-rings sealing the plates had been damaged. As a consequence, all of the orifice plates were eccentric within their carriers. This paper describes the subsequent investigation into this problem and the estimation of the resultant flow-measurement error.

Initial Inspection and Testing Work

Figure 1 shows the three flow meters. The displacement of three plates (FE-001, FE-002 and FE-003) was measured as being 36 mm, 56mm and 39 mm and they were significantly outside eccentricity limits set in ISO 5167 [1]. In all three cases the O-rings were incorrectly sized and had been sheared when the plates had been inserted. The FE-002 plate had a clear 11 mm gap under the plate.

FE-001

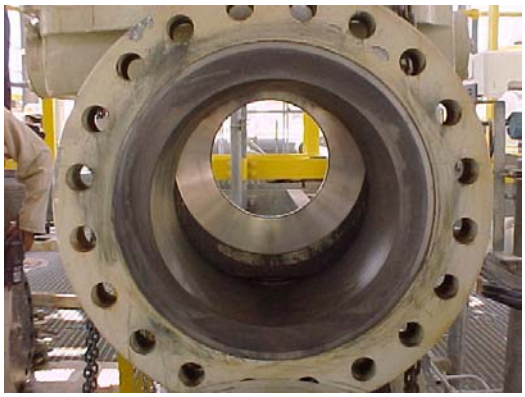

FE-002

FE-003

Figure 1. The orifice plates on initial inspection

After further investigation it was established that the number of turns of the elevator screw required to correctly seat the orifice plate during installation had been incorrectly marked on the outside of the orifice-plate carrier.

To assess leakage rates through the damaged seals, the metering tubes were removed, the upstream flanges blanked off and the orifice plate holes were sealed closed. A pressure was fed into the tapping on the upstream side of the blanked orifice plate with a compressed air supply and the leakage flow rate was measured. For plates FE-001 and FE-003 a leakage flow rate of 10.5 Nm^3/hour was measured for a 1 bar pressure difference across the plate. For plate FE-002 the leakage rate exceeded the range of the flowmeter used in the tests.

Review of Published Information on Eccentric and Leaking Orifice Plates

In general very little information has been published on leaking or eccentric orifice plates. Some work has been performed in the development of fully eccentric orifice plates in which the lower edge of the orifice coincides with the pipe bore. This type of orifice plate is used in slurry flows, as it allows particulates travelling along the pipe bottom to pass through the plate. This type of plate differs from the plates in this problem in that it is more eccentric and the tappings are positioned at the top of the pipe with the orifice at the bottom rather than on the side of the pipe.

Fully eccentric orifice plates are described in ISO/TR 15377 [2]. This document gives the discharge coefficient of an eccentric orifice plate with a diameter ratio of 0.6 to be 0.629. Comparing this with the discharge coefficient values given for concentric plates [1] suggests that a fully eccentric plate would be in error by -4.2% if it was mistakenly assumed to be concentric.

Yadav et al [3] provide detailed measurements of discharge coefficient of a 40mm eccentric orifice plate, in water flow, over a range of flow rates. The data presented agrees well with ISO/TR 15377 and shows that the discharge coefficient is independent of flow rate above a Reynolds number of 70000. In our case this suggests that the metering error caused by eccentricity is likely to be independent of flow rate for the flow rates at which the station operates.

In the mid-eighties Norman et al [4, 5] of British Gas performed experiments to assess the effect of eccentricity on 150mm orifice plates in atmospheric pressure air flows. This data is also presented in ISO TR 12767:1998 [6]. These tests provide very detailed information on the effects of eccentricity with a number of alternative tapping arrangements up to an eccentricity value at slightly lower eccentricities than in our case.

Similar work was performed by Husain and Teyssandier [6] on a 50 mm orifice plate in water flow. The data generated in this work agreed well with the work of Norman et al and it was concluded that eccentricity effects are not a function of line size, Reynolds number (i.e. flow rate) or fluid density.

Miller & Kneisel [7] ran a series of tests on 100 mm orifice plates with different diameter ratios. The results of these tests agree well with those of Norman et el and Husain and Teyssandier, but they are for a larger range of eccentricities.

No detailed information has been found on the effect of leakage past orifice plates. The only document found on this subject was on the Daniel website [8] which suggested that errors exceeding 8% in magnitude were possible in our case.

However, no detailed information is given on the tests performed or the size of meter tested; therefore it is unclear as to how representative these tests are of our problem.

Computational Fluid Dynamics Investigation

A CFD-based study was subsequently initiated to investigate the problem further. A range of simulations were run to determine how plate eccentricity and leakage affected the flow measurement error. Figure 2 shows a typical computational domain and the computational mesh used for a simulation without leakage.

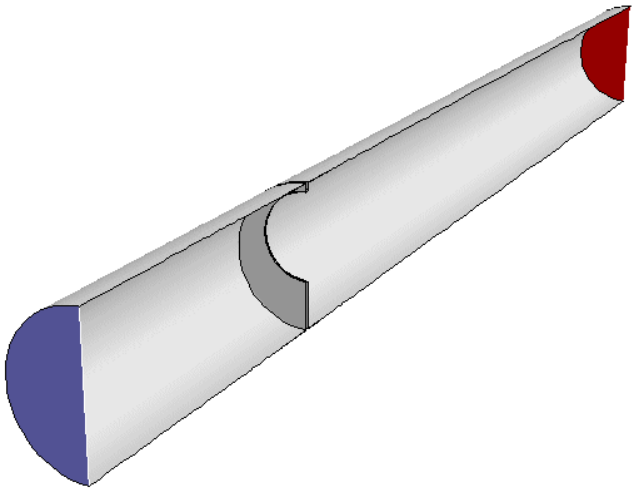

a) Computational domain

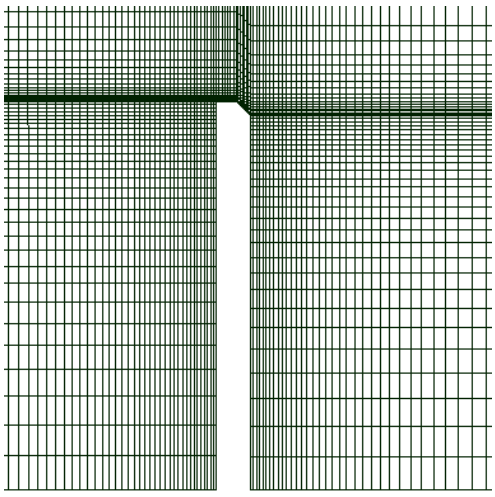

b) Mesh detail

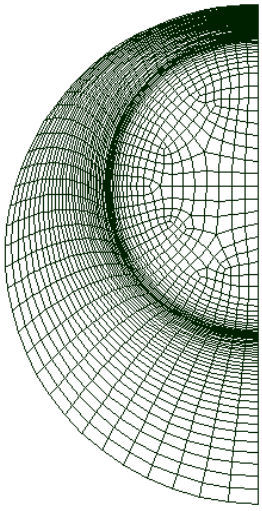

c) Mesh detail

Figure 2. The computational domain and mesh

Figure 3 shows how an eccentric orifice plate causes the jet issuing from the orifice plate to be pushed towards the top of the pipe. This results in a distorted pressure distribution on the pipe walls downstream of the orifice plate (see Figure 4). Figure 4 shows that the effect of eccentricity will vary depending on the radial and axial location of the tappings and the number of tappings used. In particular, Figure 4 suggests that the results of tests performed with small orifice plates with flange tappings may not always be representative of larger, flange-tapped flowmeters.

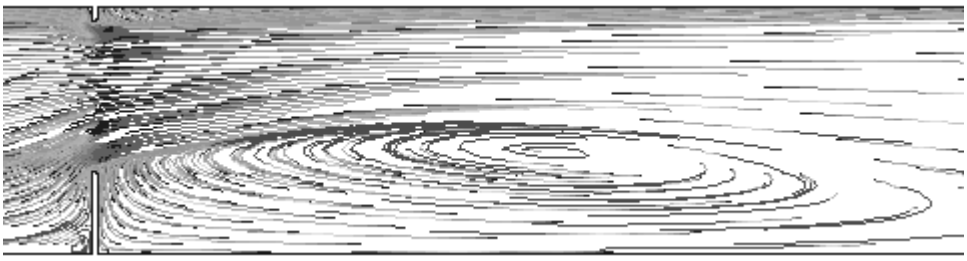

Figure 3. Streamlines showing the predicted flow pattern in eccentric plate

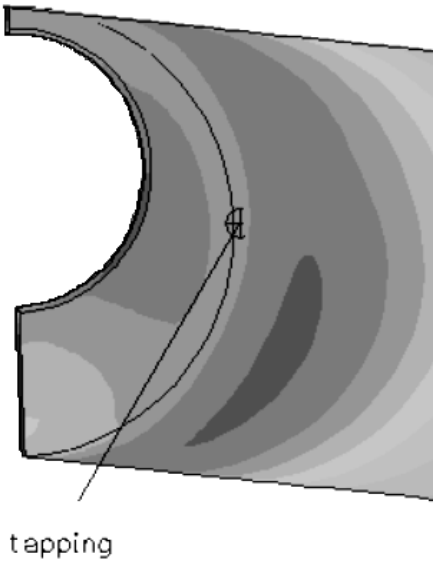

Figure 4. Predicted pressure contours downstream of an eccentric orifice plate
(high pressure = dark grey, low pressure = light grey)

Figure 5 compares the CFD predictions for the gas metering station with data from air flow and water flow tests [5 & 7]. In Figure 5 eccentricity is defined as:

$$Eccentricity = \frac{x}{D}$$

where

x is the displacement of the centre of the orifice hole from the pipe axis (m)
D is the pipe diameter (m)

Eccentricity values for plates FE-001, FE-002 and FE-003 were 0.088, 0.14 and 0.095 respectively. A fully concentric plate has an eccentricity of zero and a fully eccentric plate, with the orifice edge just at the pipe wall, has an eccentricity value of 0.197.

In general, a very good agreement was achieved between the CFD simulations and published test data, although some discrepancies were apparent at higher eccentricities. This is partly caused by the scaling effect previously mentioned and partly by assumptions and simplifications inherent in the CFD simulation method.

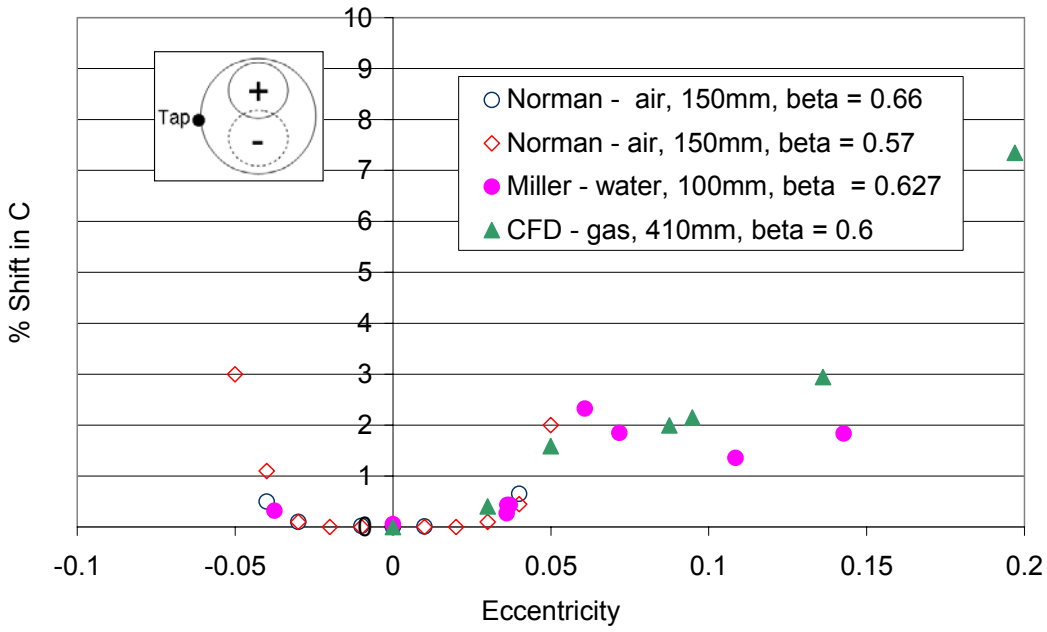

Figure 5. Predicted and measured effect of orifice plate eccentricity

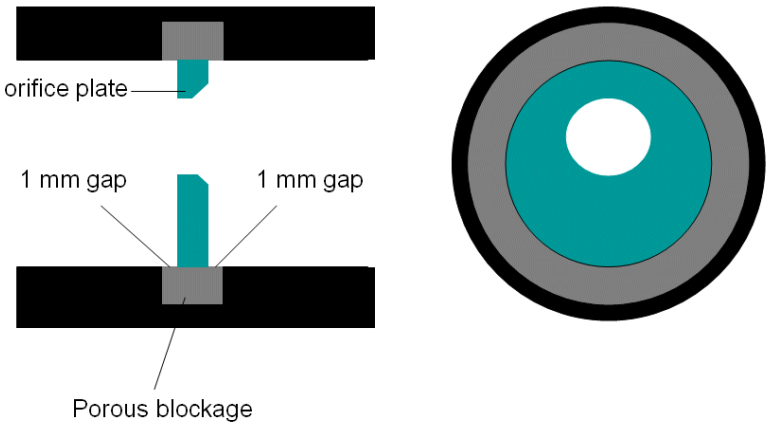

Figure 6. Geometrical arrangement of porous blockage

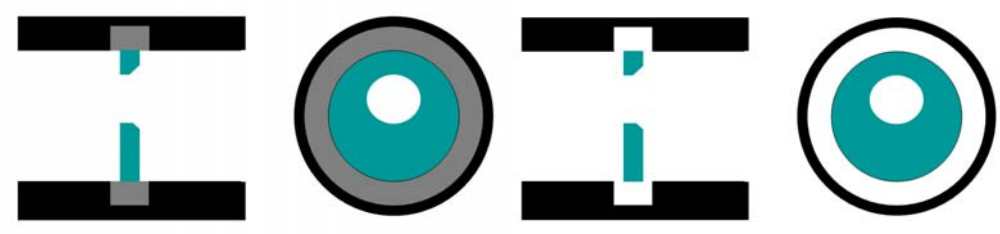

a) Leak 1 (even leakage) b) Leak 2 (high leakage)

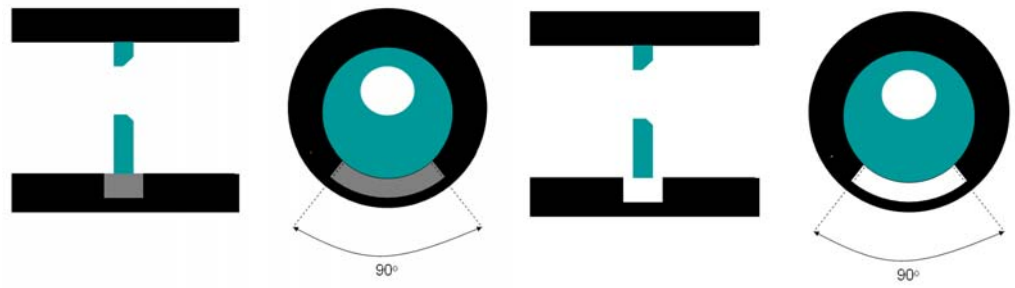

c) Leak 3 (leakage at pipe bottom) d) Leak 4 (high leakage at pipe bottom)

e) Leak 5 (11mm gap under plate)

Figure 7. Different leakage scenarios modelled

A series of simulations were also run to assess the effect of leakage on the eccentric plates. To facilitate this, an annular volume was added to the simulation geometry which was intended to be a simplified representation of the slot in the carrier body (as shown in Figures 6). This slot connected the upstream and downstream sides of the orifice plate and allowed a peripheral leakage flow to pass under the plate. Depending on the leakage scenario being modelled, the slot was filled with porous material whose flow resistance could be adjusted to control the leakage rate through the slot.

Figure 7 shows the five leakage scenarios considered. In the Leak 1 scenario (Figure 7a) the resistance to flow in the slot was set to a constant value around the whole pipe circumference. Simulations were run of the orifice plate in the leakage tests and the porosity of the slot blockage was adjusted until an appropriate value had been found which matched the leakage test data.

In the Leak 2 scenario (Figure 7b) no porous blockage was present. This simulation produced an even leakage around the plate periphery which should be significantly higher than occurred in reality.

In the Leak 3 scenario leakage was only permitted at the bottom of the pipe (Figure 7c). As in the Leak 1 models, the blockage porosity was adjusted to match leakage tests. It is believed that the Leak 3 simulations were most representative of the actual leakage behaviour in plates FE-001 and FE-003.

The Leak 4 scenario was similar to the Leak 3 scenario, but with no porous blockage in the slot (Figure 7d).

In the Leak 5 scenario there was no leakage at the periphery of the orifice plate, but an 11mm gap was included under the plate (Figure 7e).

Figure 8 shows the predicted error caused by the different leakage scenarios. It was found that Leaks 1 and 3 cause negligible additional error, Leak 4 causes an additional error of about -0.6%, Leak 2 causes an additional error of about -0.9% and Leak 5 causes an additional error of -4%. The results also show that the flow measurement error caused by leakage depends only on the total leakage flow rate and is independent of the distribution of leakage around the periphery of the plate.

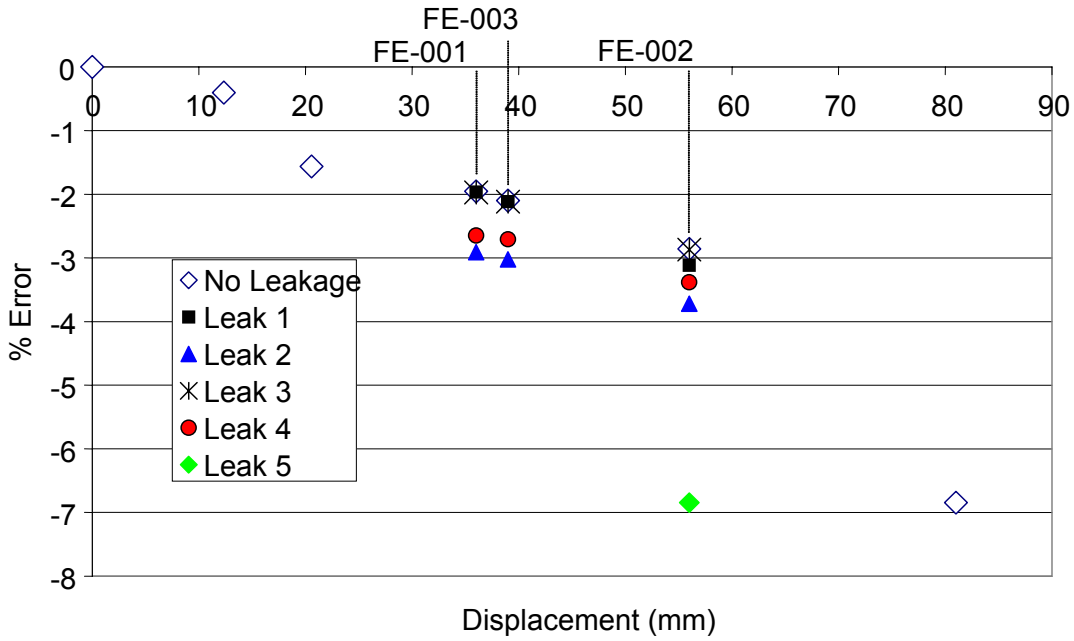

Figure 8. Predicted flow measurement errors

Estimation of Total Flow measurement Error

Over the first two year period of mis-measurement it was believed that the seals in the orifice plates were compromised but that the orifice plates were concentric. Over the second mis-measurement period of one year the plates were eccentric and the seals were definitely leaking.

Based on this information and the results of the CFD study, correction factors were developed representing high and low seal leakage scenarios, as shown in Table 1. These correction factors were used in the following equation to correct historic flow measurements:

$$Corrected\ Flow\ Measurement = CF \times Measured\ Flow\ Rate$$

	Leakage Scenario	Mis-measurement Period 1	Mis-measurement Period 2
FE-001	Low	1	1.019
FE-002	Low	1	1.068
FE-003	Low	1	1.021
FE-001	High	1.009	1.028
FE-002	High	1.009	1.068
FE-003	High	1.009	1.030

Table 1 Correction Factors CF

Figures 9 and 10 show the corrected gas flow data over the May 1999 to May 2002 period for both scenarios. The low leakage scenario predicts that the measured volume of gas passing through the metering system was 12586 mmscf less than the actual volume of gas. The high leakage scenario predicts a discrepancy of 18343 mmscf. A compromise value of 15471 mmscf was agreed between the gas vendor and their customers for compensation purposes. This volume of gas had a monetary value in excess of $10,000,000 US.

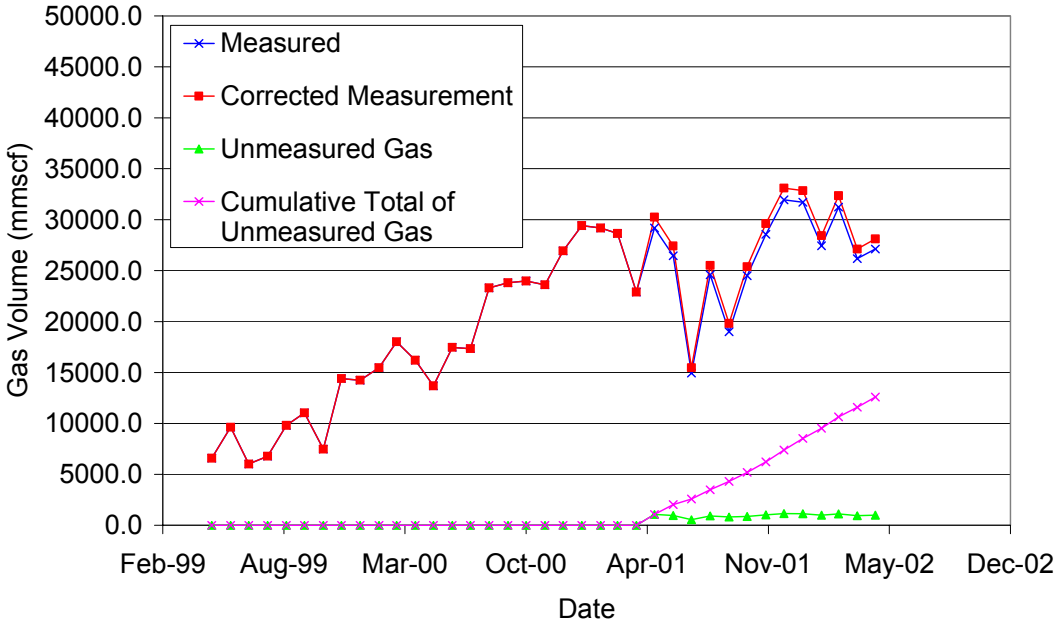

Figure 9. Corrected gas flow measurements (low leakage scenario)

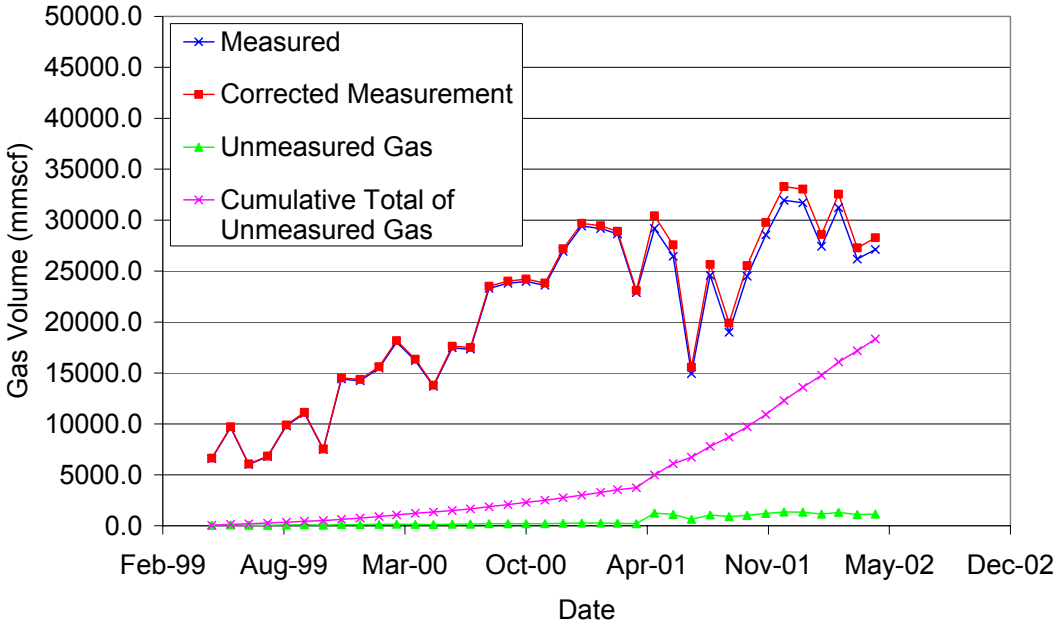

Figure 10. Corrected gas flow measurements (high leakage scenario)

Conclusions

CFD simulation methods and published test measurements have been used to estimate the error of a metering system over a period when its orifice plates were eccentric and when leaking O-rings allowed some gas to bypass the meter.

It was found that plate eccentricity effects would result in errors of between -2% and -3% for individual meters. Validation against test data suggests that these estimates of error should be within 1% of the actual error, but it is unclear whether the simulations over-estimate or under-estimate the error.

Simulations were also run to assess how leakage at the periphery affects the metering error. Various alternative leakage scenarios were modelled and it was found that the leakage rate has an effect on the error, but that the leakage distribution does not.

Correction factors, based on the CFD results, were then used to predict the system's mis-measurement over a three-year period.

8 REFERENCES

1 INTERNATIONAL ORGANIZATION FOR STANDARDIZATION. Measurement of fluid flow by means of orifice plates, nozzles and Venturi tubes inserted in circular cross-section conduits running full. ISO 5167-1:2003. International Organisation for Standardization, Geneva, 2003.

2 INTERNATIONAL ORGANISATION FOR STANDARDIZATION. Measurement of fluid flow by means of pressure-differential devices – Guidelines for specification of nozzles and orifice plates beyond the scope of ISO 5167-1. ISO/TR 15377:1998. International Organisation for Standardization, Geneva.

3 YADAV, H.S., ATHAR, M. & SRIVASTAVA, G.S.. Flow characteristics of eccentric orifice plates. J of the Inst of Eng (India), Vol 72, Pt Civil En, pp 135-141, 1991.

4 NORMAN, R., RAWAT, M.S. & JEPSON, P. . Buckling and eccentricity effects on orifice meter accuracy. International Gas Research Conference, pp 128-138, 1983.

5 NORMAN, R., RAWAT, M.S. & JEPSON, P. An experimental investigation of the effects of plate eccentricity and elastic deformation orifice meter accuracy. International Conference on the Metering of Natural Gas and Liquefied Hydrocarbon Gases, pp 211-231, 1984.

6 INTERNATIONAL ORGANISATION FOR STANDARDIZATION. Measurement of fluid flow by means of pressure-differential devices – Guidelines to the effect of departure from the specifications and operating conditions given in ISO 5167-1. ISO TR 12767:1998. International Organization for Standardization, Geneva.

7 HUSAIN, Z.D. & TEYSSANDIER, R.G.. Orifice eccentricity effects for flange, pipe and radius (D-D/2) Taps. ASME 86-WA/FM-1, ASME Winter Annual Meeting, California 7-12 December 1986.

8 MILLER, R.W. & KNEISEL, 0. Experimental study of the effects of orifice plate eccentricity on flow coefficients. J of Basic Eng. Trans ASME, Vol 91, Pt D, pp121-131, 1969.

9 ROLLINS, R.. Effect of Various Conditions in Primary Element on Orifice Meter Measurement. Emerson Process Website. http://www.emersonprocess.com/daniel/Products/Gas/Orifice/Senior/AppNotes/Effect%20of%20Various%20Conditions%20in%20Primary%20Element%20on%20Orifice%20Meter%20Table%20by%20Rollins%201980%2013KB.pdf

23rd International North Sea Flow Measurement Workshop
Tønsberg, Norway, 18 - 21 October 2005

DENSITY AND CALORIFIC VALUE MEASUREMENT IN NATURAL GAS USING ULTRASONIC FLOW METERS

Kjell-Eivind Frøysa and Per Lunde,

Christian Michelsen Research AS (CMR), Box 6031 Postterminalen, N-5892 Bergen, Norway.

ABSTRACT

Multipath ultrasonic transit time flow meters (USMs) are today extensively used by industry for volumetric flow metering of natural gas, for fiscal measurement, check metering, etc. As natural gas is typically sold on basis of mass or energy, the density and/or calorific value (GCV) of the gas is measured in addition. In current fiscal metering stations this is typically made using additional instrumentation like e.g. densitometers, calorimeter or gas chromatographs.

In addition to the flow velocity and the volumetric flow rate, USMs give measurement of the velocity of sound (VOS) in the gas. The VOS is a quality parameter which contains valuable information about the gas. For example, under certain conditions the density and GCV of the gas can be derived from the VOS. This provides a potential for mass and energy flow rate measurements by the USM itself. Various approaches in this respect have been presented over the recent years, by various research groups.

The present paper describes a new method for calculation of density and GCV of natural gas, from measurements of the pressure, temperature and the VOS only. That is, in the present method, no instrumentation is needed in addition to the USM itself and the pressure and temperature sensors. The method can thus be used on existing USM metering stations with only a software upgrade. Such a feature may be of interest for fiscal metering stations (e.g. for backup and redundancy) as well as simpler metering station (where density and GCV are not measured today, but where such information may be of interest e.g. for monitoring). Results for different real natural gas compositions are presented, and contributions to the measurement uncertainty discussed. The paper is intended to provide insight into the potentials and limitations of methods for calculating gas density and GCV from VOS also on a more general basis.

1. INTRODUCTION

Over the last decade, multipath ultrasonic transit-time meters (USM) have been developed to competitive alternatives to more conventional orifice plate and turbine meters for fiscal metering of natural gas (e.g. sales and allocation metering). Basically, these meter types are all volumetric flow meters. As gas is not sold on basis of volume, but in terms of either mass (e.g. in Norway [1]) or energy (in several European countries), the density or calorific value of the gas is needed in fiscal gas metering stations, in addition to the volumetric flow rate. These gas properties are today measured using either densitometers, gas chromatographs (GC) or calorimeters.

As the use and maintenance of e.g. GCs is work demanding and costly, reducing the number of GCs in metering stations is a highly addressed topic these days. Another aspect of importance is the ability to detect drift in GC instruments, and operation outside of GC specifications. In this respect, USMs may offer a potential to further reduce the cost of mass and energy flow measurement. Such possibilities may be of particular interest for monitoring and regulation purposes in connection with gas commingling for export, for allocation metering, as backup to GC analysis, etc.

In addition to the flow velocity and volumetric flow rate measurement, the USM also gives a measurement of the velocity of sound (VOS) in the gas, cf. Fig.1. Traditionally, the VOS has been used for quality check of the USM, e.g. by intercomparison between the various acoustic paths of the meter, by comparison of the measured VOS with a calculated VOS (from component analysis using a gas chromatograph), etc.

There is today an increasing interest in exploiting the potentials of USMs for direct mass and energy measurement, using the volumetric flow rate measurement in combination with the VOS measurement. Developments in recent years have resulted in methods for calculation of the density and calorific value from the measured VOS in the gas.

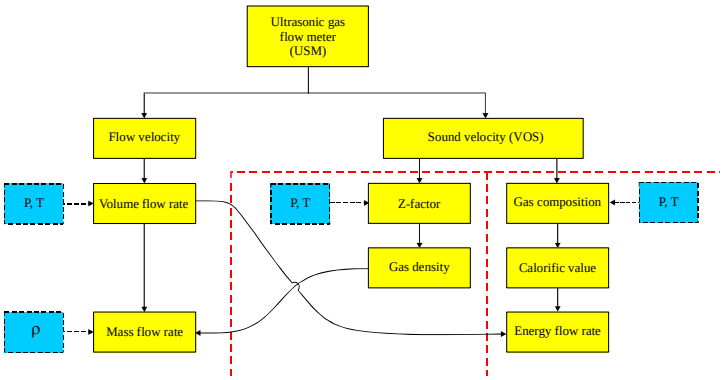

Fig. 1. Applications of USMs in measurement of natural gas (after [9]).

Mass flow rate measurement. With respect to USM mass flow measurement of natural gas, this topic has been addressed by several companies and research groups. For low pressure flare gas metering applications, Panametrics [2,3] and CMR [4] presented methods for density measurement in the 1980s, based on use of the measured VOS in combination with the ideal gas law.

For high-pressure applications, a group at NEL [5] proposed a method based on measurement of VOS, pressure (*P*), temperature (*T*), and daily or weekly compositional knowledge (molar fractions of the various hydrocarbon components, CO_2 and N_2). In this approach then, the gas composition must be known, except for possible compositional variations in the field's production. The algorithm is based on iterative correlation using an equation of state for natural gas at high pressures (e.g. the AGA 8 (94) equation [6], the GERG / ISO method [7], or other).

Beecroft [8] reported briefly an attempt to establish an algorithm for calculating the density from VOS based on USM measurements at the Trent and Tyne fields in the North Sea, comparing with independent reference measurements of density. He concluded that "currently, knowledge of the gas composition is required to allow an accurate calculation of density, and is likely to remain that way for the foreseeable future".

An alternative method was presented and demonstrated in 1999 [9], based on measurement of VOS, *P* and *T*, no knowledge about the actual hydrocarbon components in the gas, and some (weak) knowledge on the molar fractions of CO_2 and N_2 [18, 10-13, 25-26]. Results from flow testing at Statoil K-Lab were presented for pressures in the ranges 32-86 bara, temperatures 31-50 ^oC and flow velocities 5-20 m/s [9]. Relative deviation between the USM density measurements and the reference density (from GC analysis) of less than ±0.1 % was demonstrated. This algorithm has been implemented in FMC Kongsberg Metering's MPU 1200 gas flow meter [14], as a software upgrade (no hardware changes) [9].

Although this "1999-algorithm" actually requires no knowledge on the gas composition (hydrocarbon components), the accuracy of the method depends on the composition. In the

present work, methods have been developed to optimize such algorithms and further increase the robustness with respect to gas composition, pressure and temperature.

Energy flow rate measurement. With respect to energy flow measurement of natural gas, a number of companies and research groups have addressed the use of VOS for calorific value measurement. In the 1980s a Japanese group [16] proposed a method for LNG-based natural gas (with no CO_2 or N_2). The method was based on measurement of VOS, P and T, in combination with the ideal gas law (limiting the method to low pressures). In 1994 Lueptow *et al.* [17] presented a method for natural gas at low pressures (ideal gas law), based on measurement of VOS, P and T. As discussed in the paper, the method did not account for the inert components CO_2 or N_2, which limits the accuracy of the method as such gas components are normally present.

Over the recent years, several methods for high-pressure natural gas have been proposed. In 1996 CMR described a method based on measurement of VOS (at line conditions), P and T, and some (weak) knowledge of CO_2 and N_2 [18-20]. The algorithm was based on iterative correlation using an equation of state for natural gas (e.g. the AGA 8 (94) equation [6], the GERG / ISO method [7], or other), in combination with the ISO 6976 standard for calorific value calculation [21].

At the Southwest Research Institute in the USA [22], an alternative approach was proposed based on measurement of VOS (at standard reference conditions, 1 atm. and 15 ^oC) and some knowledge of CO_2 or N_2. In this approach a separate VOS cell is needed in addition to the USM, for measurement of the sound velocity at standard reference conditions. A group at NEL [23] has announced an alternative method, based on measurement of VOS (at line conditions), P, T, CO_2, and the dielectric constant of the gas (to avoid measurement of N_2). Thus, a separate permittivity cell is needed in addition to the USM.

A joint Gasunie and Ruhrgas research group has presented a method based on (a) measurement of VOS, P and T at line conditions (high pressure), and (b) measurement of VOS, P, T and CO_2 at some reference conditions (low pressure, e.g. 5 bara) [24, 28]. In this approach, thus, a separate VOS cell is needed in addition to the USM, for measurement of the sound velocity at the reference conditions. The measurements at reference conditions are used to avoid e.g. the N_2-measurement.

One advantage of the method proposed by CMR [18-20, 25-26] is that basically, no additional instruments are required in addition to instruments normally used as a part of the gas metering station. The method is based on use of measurements from the USM, the pressure transmitter, and the temperature element / transmitter. With respect to the molar fractions of CO_2 and N_2, it may be sufficient to have a typical (estimate) value of these, so that online measurements of these may not be required. Another possibility may be to use infrared technology (IR) to measure CO_2.

Alternatively, if a density measurement is available in the metering station (which is normally the case), one may use this measurement to avoid either the CO_2 or N_2 estimate. As a further alternative, if density measurements are available both at line conditions and some other pressure condition (e.g. standard reference conditions, which may be the case in some metering stations), one may possibly avoid estimation of both the CO_2 and N_2 molar fractions. Consequently, three alternative approaches are proposed which may be used optionally, dependent on the actual

instrumentation of the gas metering station at hand, without introducing extra instruments in the metering station.

Although this methodology actually requires no knowledge on the gas composition (hydrocarbon components), the accuracy of the method depends on the composition. In the present paper, solutions have been developed to further improve the robustness with respect to gas composition, pressure and temperature.

The present paper discusses various strategies for density and GVC calculations from the VOS measured by a USM (Section 2). In Section 3, some basic problems being faced in this context are raised, and possible solutions of these problems are discussed. In Section 4, examples of output from existing algorithms for density and GCV calculations from VOS are given. Uncertainty considerations are discussed in Section 5. Conclusions are given in Section 6.

2. GENERAL SOLUTION STRATEGIES

Various strategies for calculation of density and GVC from the VOS measured by a USM are discussed in the present section. Important questions in this context include (a) to which extent additional instrumentation is required for the metering station, (b) to which extent knowledge on the gas composition is required, and (c) which accuracy can be achieved, with such methods.

The mass flow rate q_m is given by

$$q_m = \rho q_V \,, \tag{1}$$

where q_V is the actual volumetric flow rate (at line conditions) and ρ is the density at line conditions. The energy flow rate q_e can be given by various equivalent expressions, such as

$$q_e = \left(H_S \frac{\rho}{\rho_0} \right) q_V \,, \qquad q_e = \left(H_S \frac{Z}{Z_0} \right) \frac{P T_0}{P_0 T} q_V \,, \qquad q_e = \left(\frac{H_S}{\rho_0} \right) \rho q_V \,,$$
$$q_e = \left(\frac{H_S Z_0}{m} \right) \frac{\rho R T_0}{P_0} q_V \,, \qquad q_e = \left(H_S \right) \frac{\rho}{\rho_0} q_V \,, \tag{2}$$

where ρ_0 is the density at standard reference conditions, H_S is the superior (gross) calorific value (GCV), Z and Z_0 are the compressibility factors at line and standard reference conditions, respectively, P and T are the line pressure and temperature, respectively, P_0 and T_0 are the pressure and temperature at standard reference conditions, and m the molar weight of the gas. (Apart from the grouping of terms, some of the expressions given in Eq. (2) are identical (nos. 1, 3 and 5). The motivation for this grouping will be more clear in connection with the discussion of GCV measurement methods related to Table 1 below.)

Mass flow rate measurement. Basically, the USM measures the volumetric flow rate at line conditions, q_V . If the density ρ is calculated from the measured VOS, the mass flow rate q_m can be found without extra input parameters (extra measurements), through a straightforward multiplication, cf. Eq. (1). The question is thus how ρ is calculated from the VOS. This is discussed in Sections 3 and 4. In Fig. 2a, a schematic sketch of a method for such density

calculation for low pressure natural gas is indicated. The ideal gas law and hydrocarbon relations are used to estimate the density. *c* is the VOS. In Fig. 2b similar methods for high pressure natural gas are indicated. In this case a high pressure equation of state (like the AGA 8 (94) equation [6], or other) is used. In addition, input of the inert gas components is required.

(a)

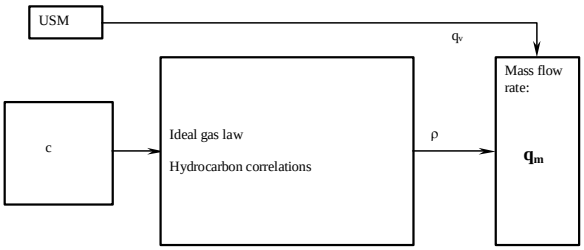

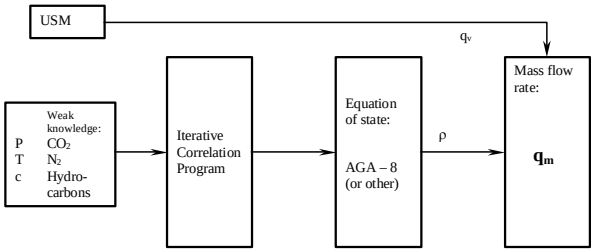

(b)

Fig. 2. Various approaches used for measurement of the mass flow rate using USMs (schematic): (a) Method for low pressure gas [4], (b) Methods for high-pressure gas [5,18,10-13,25-26].

Energy flow rate measurement. In the case of the energy flow rate, q_e, the situation is somewhat different. In order to obtain the energy flow rate from the volumetric flow rate at line conditions, q_V, a calculation down to standard reference conditions (1 atm., 15 °C) is needed before multiplication with the GCV, H_S, cf. Eq. (2). Depending on the instruments available in the USM metering station, there may be several strategies for this.

In Table 1, three different scenarios (or methods) are discussed. These include (1): a metering station with a USM, and pressure and temperature measurements, (2): a metering station like (1) but with a densitometer included in addition, and (3): a metering station like (2) but where also the density at standard reference conditions is measured. In Eq. (2) five equivalent expressions for the energy flow rate are given. The two first expressions are related to method no. 1 of Table 1. In each of the two expressions, the parenthesis contains the unknown expression in a metering station of type (1) above, needed to calculate the energy flow rate. This means that not only the GCV is needed, but also one of the expressions denoted as "alternative “measurands”" in Table 1. Similarly, the third and fourth expressions of Eq. (2) corresponds to a metering station of the type (2) above, and thereby to method 2 in Table 1. The fifth expression of Eq. (2) corresponds to a metering station of type (3) and to method 3 in Table 1.

Table 1. Three different scenarios (or methods) for estimation of the energy flow rate from the USM measurements in USM metering stations.

Method No.	Type of instrumentation	Parameters involved		Alternative “measurands”	
		Measured	Estimated	A	B
1	USM Line cond.: Pressure Temperature	q_v, c P T	CO_2 N_2	$H_S \frac{\rho}{\rho_0}$	$H_S \frac{Z_0}{Z}$
2	USM Line cond.: Pressure Temperature Densitometer	q_v, c P T ρ	CO_2 or N_2	$H_S \frac{1}{\rho_0}$	$H_S \frac{Z_0}{m}$
3	USM Line cond.: Pressure Temperature Densitometer Ref. cond.: Densitometer	q_v, c P T ρ ρ_0		H_S	

This means that in order to upgrade the metering station by a software upgrade only, to provide the energy flow rate, one of these alternative "measurands" are needed. It is possible to develop algorithms for estimation of these measurands from the VOS. In fact, the challenges discussed in Section 3 are quite similar for development of methods for estimation of these measurands, as they are for the estimation of density and GCV (as discussed in Section 3). In the remaining part of this paper, only the estimation of density and GCV will be discussed, and not the estimation of these alternative measurands. This is done partly to simplify the presentation, and partly because the GCV is an interesting parameter in itself, also when the GCV is not sufficient in order to calculate the energy flow rate.

In order to obtain a precise estimate of the GCV from the VOS, additional input is needed. In addition to the pressure and temperature, at least two more input parameters are in general needed. Different strategies have been used by different research groups, cf. Fig. 3. NEL [23] (Fig. 3a) used the dielectric constant, ε, and the CO_2 content, while a Gasunie/Ruhrgas group [24, 28] (Fig. 3b) used the VOS measured at a low pressure, and the CO_2 content. In both these cases, extra measurement instrumentation is needed in addition to pressure, temperature and USM. An upgrade of existing metering stations through a software upgrade only is therefore not possible for these two approaches. Several alternative methods have been presented in refs. [18-20,25-26] (Fig. 3c), such as (a) use of the CO_2 and N_2 contents (Alt. 1), (b) use of the CO_2 (or N_2) content and the density (Alt. 2), and (c) use of the density at line and standard ref. conditions (Alt. 3). The reason for using three alternatives is the flexibility in installing the GCV estimation algorithm in existing metering stations, based on various instrumentation solutions.

(a)

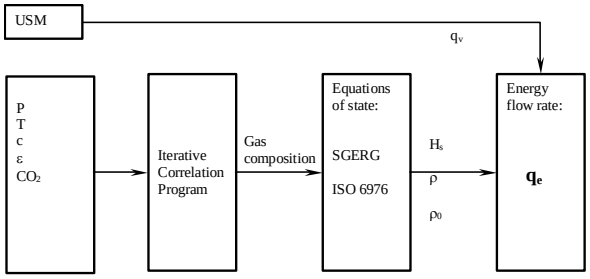

(b)

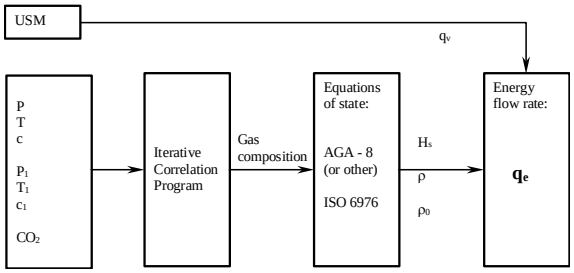

(c)

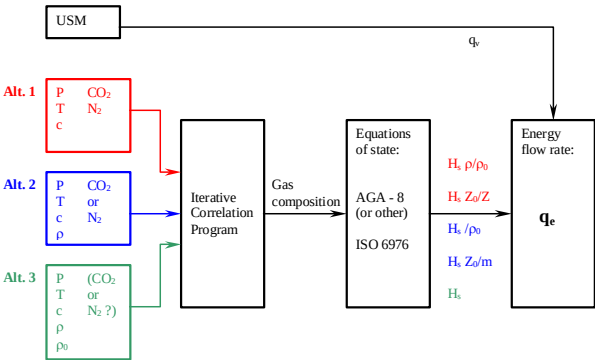

Fig. 3. Various approaches used for measurement of the energy flow rate using USMs (schematic):
(a) NEL method [23],
(b) Gasunie/Ruhrgas method [24, 28],
(c) CMR method [18-20,25-26].

The methods for density and GCV measurement discussed in the present paper can be used in three different modi, depending on the available knowledge about the gas composition:

- "Blind composition approach 1", BCA1 (with no knowledge about the gas composition at all).

- "Blind composition approach", BCA2 (with no knowledge about the hydrocarbon gas composition, but with knowledge about the typical N_2 and CO_2 contents).
- "Typical composition approach", TCA (with knowledge about the typical hydrocarbon gas composition and the typical N_2 and CO_2 contents).

The three approaches may typically be used in the following scenarios:

- BCA1: when no information about gas composition is available.
- BCA2: when the typical contents of the inert gas components (N_2 and CO_2) is available, but not their daily variation.
- TCA: when the typical gas composition is available (hydrocarbons, N_2 and CO_2), but not its daily variation.

As will be discussed in Section 3, the accuracy of the density and the GCV estimate is improved by using the BCA2 option instead of the BCA1, and further improved by using the TCA option.

One advantage of the method presented here in comparison to methods presented by the other research groups, is that basically, no additional instruments are required in addition to the very basic instrumentation of the USM metering station: the ultrasonic flow meter together with pressure and temperature sensors. Thus the method can be implemented in a USM metering station simply by a software upgrade of the USM only, without any hardware changes.

3. PROBLEM DESCRIPTION

In order to apply the VOS measured by ultrasonic flow meters as basis for density and GCV calculations in natural gas, there are several challenges to be solved. These are related to the gas composition of the natural gas, and to establish the relationships between VOS and density and between VOS and GCV, for a particular gas. This is described in the following.

The composition of natural gas varies significantly from gas field to gas field. However, the main component in natural gas is methane (CH_4, often denoted C1). Typically, from 70 to 100 % (molar fraction) of the natural gas is methane. There is also usually a substantial amount of ethane (C_2H_6, often denoted C2). Typically, up to 20 % of the natural gas is ethane. Furthermore, there are smaller amounts of the higher hydrocarbon components propane, butane, pentane, etc. (C_3H_8, C_4H_{10}, C_5H_{12}, etc., often denoted C3, C4, C5, etc.). In addition, there can be up to about 20 % of nitrogen (N_2) and/or carbon dioxide (CO_2), but in many cases much less.

In Table 2, ten natural gas compositions are listed. These gases cover a span in molar weight, inert gas composition and geographical origin. In addition, pure methane has been included, since this is the main component in natural gases. These ten gases are used here as part of the testing of algorithms for calculation of GCV and density from the VOS. However, in the development of the algorithms, a much broader selection of gases have been used.

In order to be able to give precise estimations of the density or GCV of a natural gas based on the VOS, there are several challenges being faced. These include

- The uniqueness problem,

- The effects of higher order hydrocarbon components (C3+),
- The effects of inert gas components.

These challenges are discussed in the following, as a basis for the solution methods discussed here, cf. Section 4.

Table 2. Examples of molar gas composition for gases originating from ten selected natural gas fields. All numbers are given in % (molar fraction).

	Statoil Dry	**Statfjord**	**Åsgard**	**Troll**	**Oseberg**	**K15-FB**	**Nether-land**	**Amarillo**	**Gulf Coast**	**Methane**
Hydrocarbon components:										
Methane, C1	84.0	74.3	86.6	93.2	82.8	71.6	81.3	90.7	96.6	100.0
Ethane, C2	13. 5	12.0	9.6	3.7	8.3	2.4	2.8	4.5	1.8	0.0
Propane, C3	0.9	8.3	0.8	0.4	4.0	0.4	0.4	0.8	0.4	0.0
Butane, C4	0.1	3.0	0.1	0.4	1.5	0.1	0.1	0.2	0.2	0.0
Pentane, C5	0.0	0.6	0.0	0.1	0.5	0.1	0.0	0.1	0.1	0.0
Hexane, C6	0.0	0.2	0.0	0.1	0.0	0.0	0.0	0.0	0.1	0.0
Heptane, C7	0.0	0.0	0.0	0.0	0.0	0.0	0.0	0.0	0.0	0.0
Octane, C8	0.0	0.0	0.0	0.0	0.0	0.0	0.0	0.0	0.0	0.0
Inert gas components:										
Nitrogen, N_2	0.7	0.5	0.7	1.6	0.7	1.5	14.3	3.1	0.3	0.0
Carb.diox., CO_2	0.8	1.0	2.2	0.6	1.7	23.9	1.0	0.5	0.6	0.0

(1) Uniqueness. Firstly, in order to illustrate the challenges of uniquely establishing the relationship between the VOS and the density of a natural gas, and between the VOS and the GCV, an example of some binary mixtures of methane and ethane is studied, as a simplified case. As these two components typically constitute the two main hydrocarbon components of natural gas (cf. e.g. Table 1 above), this is a relevant simplified case.

In Fig. 4, the density is shown as a function of VOS for various methane - ethane mixtures, ranging from 100 % methane at the lower right end, to up to 100 % ethane at the other (upper) end of each curve. The temperature is 0 and 50 °C in these examples. Four different pressures have been used in the calculations: 10, 40, 100 and 160 bara. The calculations have been carried out using the *NATSIM* model [13], according to AGA 8 (94) [6] and ISO 6976 [21], and in agreement with AGA 10 [27]. It is observed that at low pressures, there is uniqueness (a one-to-one relationship) between the VOS and the density. Thus, at such low pressures as 10 and 40 bara, it is - for the temperatures considered here - possible to determine uniquely the density of a binary mixture of C1 and C2 from the VOS, pressure and temperature. The temperature is however also an important parameter in relation to this uniqueness discussion. At low temperatures, non-uniqueness appears at lower pressures than at higher temperatures. A kind of "first turning point P-T curve"[1], describing the transition from uniqueness to non-uniqueness, can be established (not included here), as discussed briefly in Section 5.

Consequently, at higher pressures there appears to be two different possible densities for a given VOS value. This means that in order to be able to convert the VOS to density for a natural gas, additional information about the natural gas is needed. This could - as used in the present work - for example be in the form of user-input with respect to the approximate expected gas

[1] The pressure-temperature (P-T) point at which a minimum in the VOS curve occurs, but so that for lower pressure (and the same temperature) there is no such minimum, is here denoted the "first turning point".

composition (the TCA option, cf. Section 2). From such information, it is possible to determine which of the two candidate values for the density that should be selected. This can be done because an approximate density can be found from the input gas composition. This density can be compared to the two candidates, and thereby picking the correct density (out of the two candidates).

It should be mentioned that even in cases with non-uniqueness, the "blind" approaches BCA1 and BCA2 (cf. Section 2) can be used. However, in this case there is no method to determine the correct one out of the two candidate densities.

It also appears that for pressure-temperature conditions for which the VOS curve has a minimum value (i.e. in cases of non-uniqueness), and when the VOS is close to its minimum value (the "turning point"), the problem is not well-posed. It is therefore not possible to obtain the density to a good accuracy from the VOS value for such combinations of pressure, temperature and VOS. Close to the “turning point” shown in Figs. 4 and 5, the uncertainty of the algorithm is high. In this region, methods for calculation of density from the measured VOS are thus not recommended, cf. Section 5.

Similar limitations apply to the GCV measurement. Fig. 5 is similar to Fig. 4, but in this case the GCV is shown instead of the density. It is seen that qualitatively, the same happens here as in Fig. 4. For low pressures, there is a unique relation between the VOS and the GCV, while at higher pressures, there may be two GVC values for each VOS. Temperature is also a factor in this picture. The discussion is quite analogous to the discussion of the density estimation related to Fig. 4, and will therefore not be repeated here.

(2) Effects of higher order hydrocarbon components (C3+). This challenge is related to the presence of other hydrocarbon components than methane and ethane in the natural gas. Such components need to be taken into account in methods for calculation of density and GCV from the measured VOS.

In Fig. 6, density calculations are plotted as a function of the VOS for gases with methane concentrations in the range 50 to 100 %, concentrations of ethane from 0 to 50 %, and concentration of propane from 0 % to 25 % (integer values only). Only gas compositions with molar weight less than 23 g/mole are used here. The density calculations are shown for a temperature of 50 °C, and for pressures of 10, 40, 100 and 160 bara.

By comparing Figs. 4 and 6 it is observed that the appearance of higher hydrocarbon components transfers the curves of Fig. 4 into a “cloud” of points (not so apparent in Fig. 6, but more apparent e.g. at lower temperatures and higher pressures, not shown here). Therefore, for such gases it is not possible to get 1 (or at maximum 2) possible values for the density from a given VOS value. Instead one gets 1 (or at maximum 2) interval(s) in which the value of the density can be. This means that for precise density estimation, again some additional information is needed. This could for example be in the form of user-input of approximate expected gas composition (the TCA option). This information can be used both for discrimination between the two intervals (in the case of non-uniqueness as described in the description of Fig. 4), and also for picking the “correct” density value within the interval. If such information is not given, the estimated density will have an increased uncertainty (BCA1 or BCA2), but still be of interest.

It can also be shown that the spreading in the "cloud" in Fig. 6 depends on pressure and temperature. The spread is widest for high pressures in combination with low temperatures. This means that in this P-T-region, less accurate results are expected than in other P-T regions, cf. Section 5.

In Fig. 7, similar data are shown for GCV (plotted against VOS). Qualitatively, the same conclusions can be made as in the discussion of density related to Fig. 6.

(3) Effects of inert gas components. In addition to the hydrocarbon components, natural gas may contain significant amounts of the inert gases N_2 and CO_2. This needs to be taken into account in methods for calculation of density and GCV from the measured VOS.

Fig. 8 illustrates how N_2 will affect the relationship between VOS and density illustrated in Figs. 4 and 6. The black curve in Fig. 8 is calculated for mixtures of methane and ethane only (no inert gases, as in Fig. 4). The coloured spots indicate how this relationship is affected by mixing N_2 into such methane - ethane mixtures, in this case for a pressure of 20 bara and a temperature of 0 °C.

The dark blue diamonds show the density as a function of VOS for methane mixed with N_2 (0 - 20 %). In the diamond lying on the black curve (the lower right point), there is no N_2 (only methane). In the neighbouring diamond point, the N_2 molar fraction is 1 %, and then successively increasing to 20 % (at the upper left dark blue diamond point).

The other coloured spots are similar mixes of hydrocarbons and N_2. However, the hydrocarbon part of the gas that was pure methane for the dark blue diamonds, is 95 % methane and 5 % ethane for the pink squares, 90 % methane and 10 % ethane for the red triangles, 85 % methane and 15 % ethane for the blue diamonds and 80 % methane and 20 % ethane for the green triangles.

Similar behaviour is found also for presence of CO_2 in the gas. This means that extra input is needed in order to obtain a precise density estimate when N_2 or CO_2 is present in the gas (as usually is the case). Such extra input could e.g. be to give the concentrations of N_2 or CO_2 as input to an algorithm (the BCA2 or TCA options). These data can either be taken from measurements or from field data. The results using the "blind" approach BCA1, where no gas composition data are provided will have an increased uncertainty in this respect compared to BCA2 and TCA. Alternatively, other input, such as for example the VOS measured at a low pressure could be used instead of one of the N_2 or CO_2 concentration inputs, but that has not been considered here, since that would require another measurement instrument introduced in the metering station. In the present work, the inert gas composition is used as input instead (in the TCA and BCA2 options).

Fig. 9 is similar to Fig. 8 but where GCV is plotted as a function of VOS. The conclusions are similar as above for the density, and two inputs like the N_2 or CO_2 concentrations are needed in order to give an accurate GCV estimate (in the TCA and BCA2 options). The results using the "blind" approach BCA1, where no gas composition data are used, will have an increased uncertainty in this respect compared to BCA2 and TCA. Alternatively, the VOS at a low pressure (cf. alternative 3 of Table 1, and [24, 28]) and the measured density (from a densitometer, cf. alternatives 2 and 3 in Table 1) can be used instead of one or both of the concentration inputs. In the present work, the inert gas composition is used as input (in the TCA and BCA2 options).

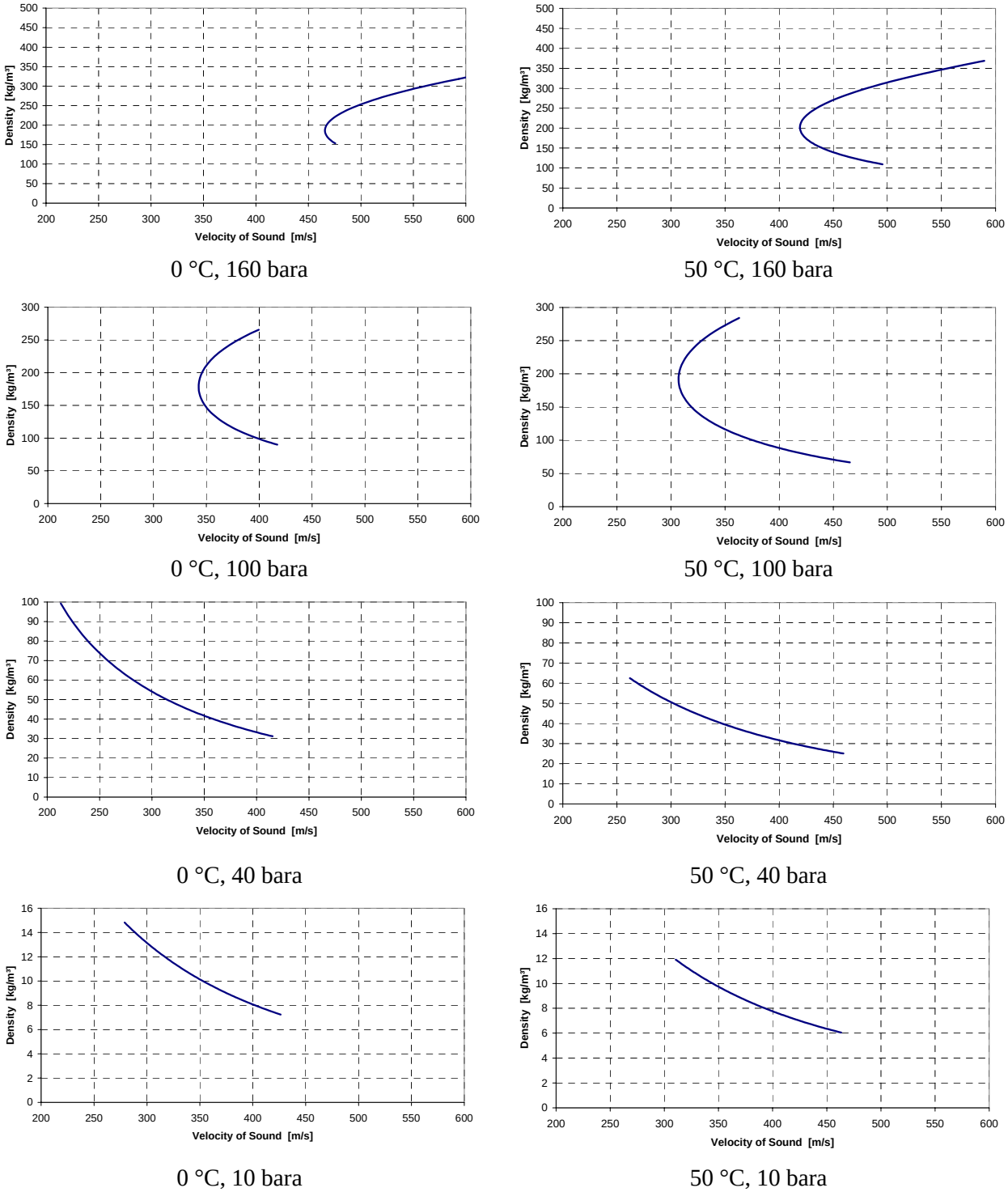

Fig. 4. The density shown as a function of the VOS, for 4 different pressures, and temperatures 0 and 50 °C. In each plot, the natural gas is a binary mixture of methane and ethane, with concentrations ranging from 100 % methane (at the lower right end of the curve) to 100 % ethane. The calculations have been made using the *NATSIM* model [13].

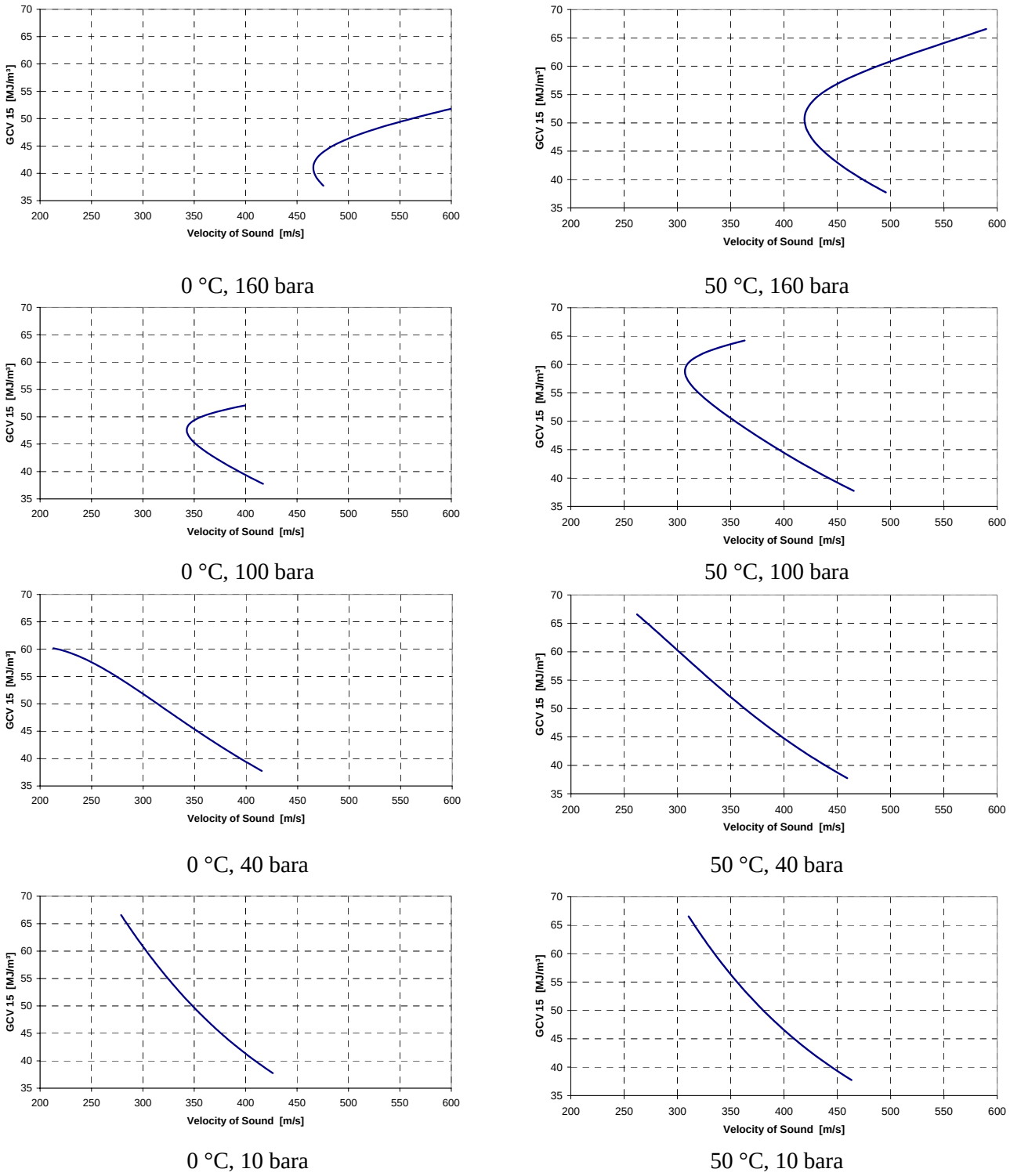

Fig. 5. The GCV shown as a function of the VOS, for 4 different pressures, and temperatures 0 and 50 °C. In each plot, the natural gas is a binary mixture of methane and ethane, with concentrations ranging from 100 % methane (at the lower right end of the curve) to 100 % ethane. The calculations have been made using the *NATSIM* model [13].

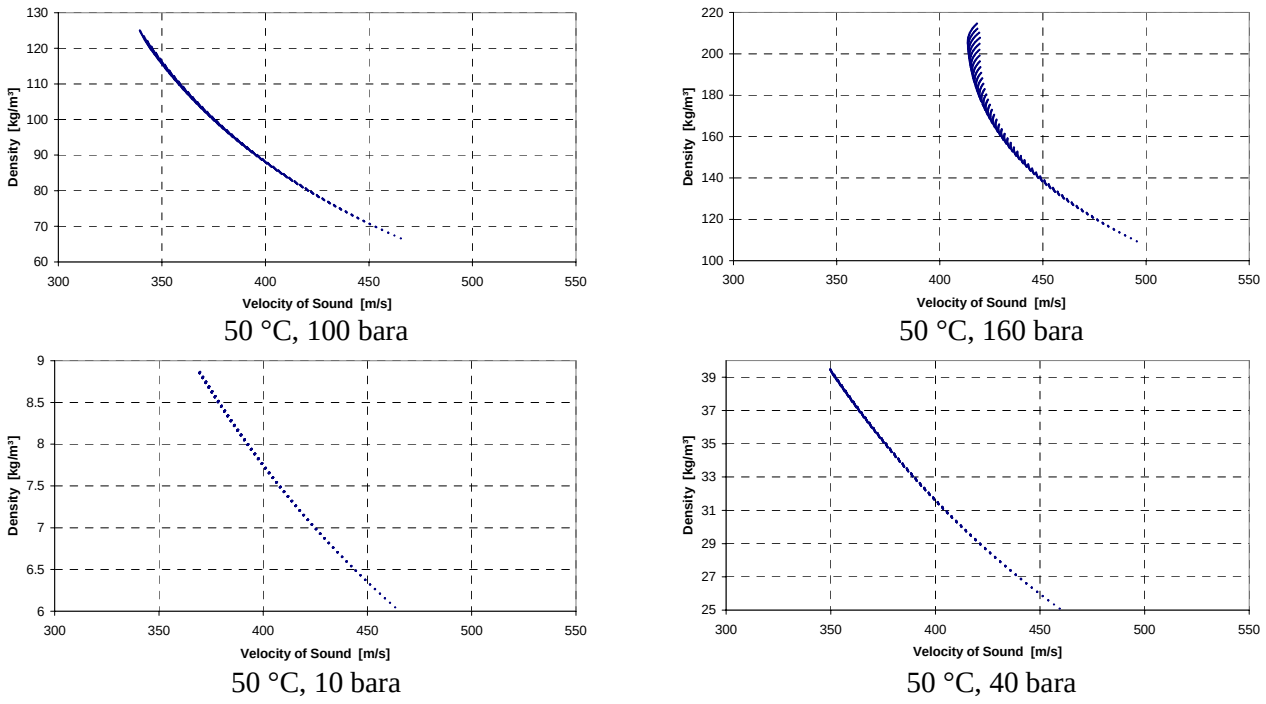

Fig. 6. The density shown as a function of the VOS, for a mixture consisting of methane, ethane and propane. Temperature: 50 °C. Pressure: 10, 40, 100 and 160 bara. The methane concentration is any integer from 50 % to 100 %, concentrations of ethane from 0 % to 50 %, and concentration of propane from 0 % to 25 % (integer values only). Only gas compositions with molar weight less than 23 g/mole are used. The calculations have been made using the *NATSIM* model [13].

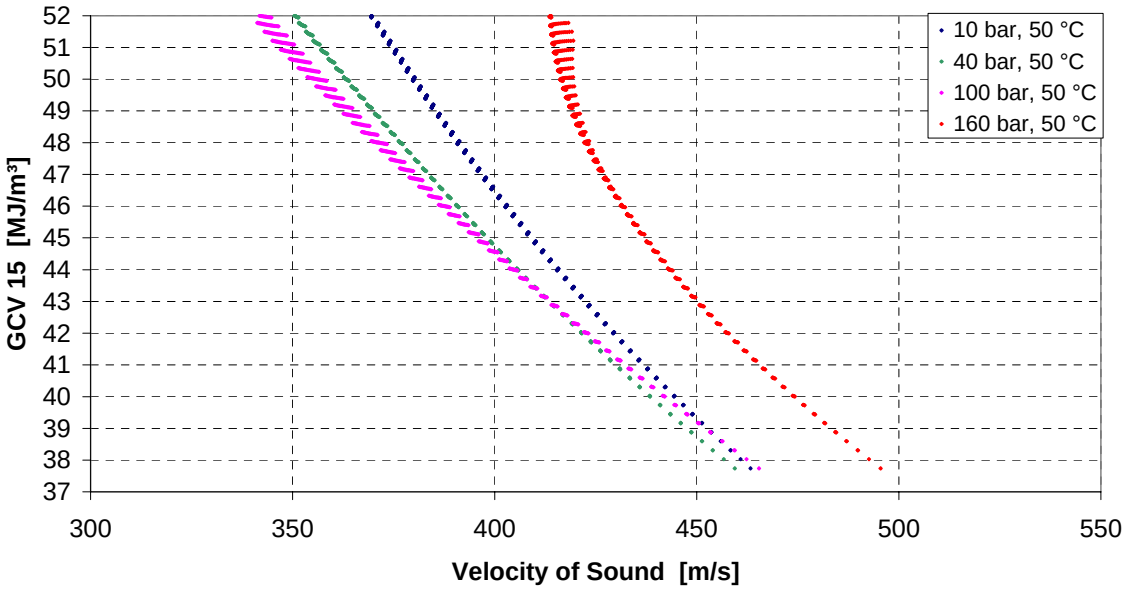

Fig. 7. The GCV shown as a function of the VOS, for a mixture consisting of methane, ethane and propane. Temperature: 50 °C. Pressure: 10, 40, 100 and 160 bara. The methane concentration is any integer from 50 % to 100 %, concentrations of ethane from 0 % to 50 % , and concentration of propane from 0 % to 25 % (integer values only). Only gas compositions with molar weight less than 23 g/mole are used. The calculations have been made using the *NATSIM* model [13].

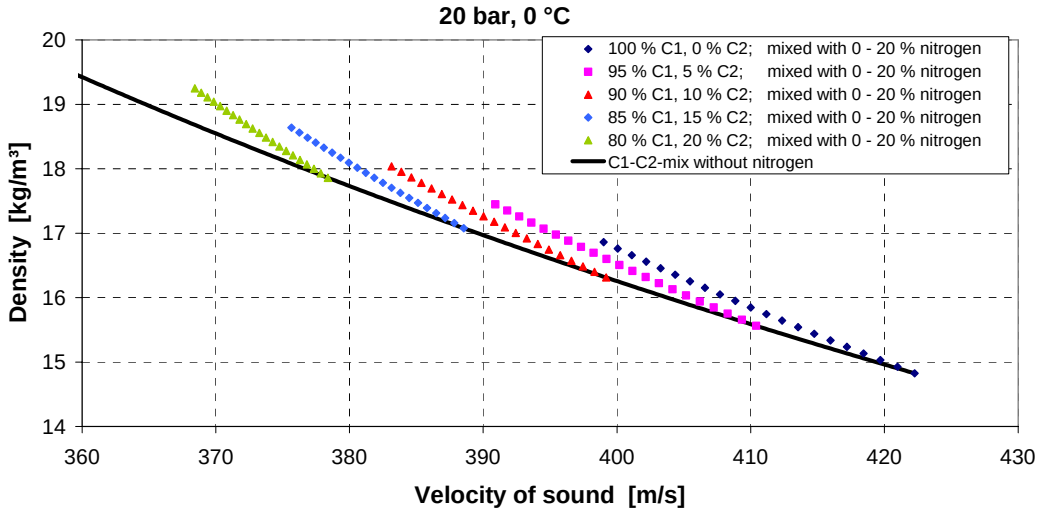

Fig. 8. The density shown as a function of the VOS, for 20 bara and 0 °C. The figure illustrates the effect of mixing N_2 into various hydrocarbon mixtures. More details are given in the text. The calculations have been made using the *NATSIM* model [13].

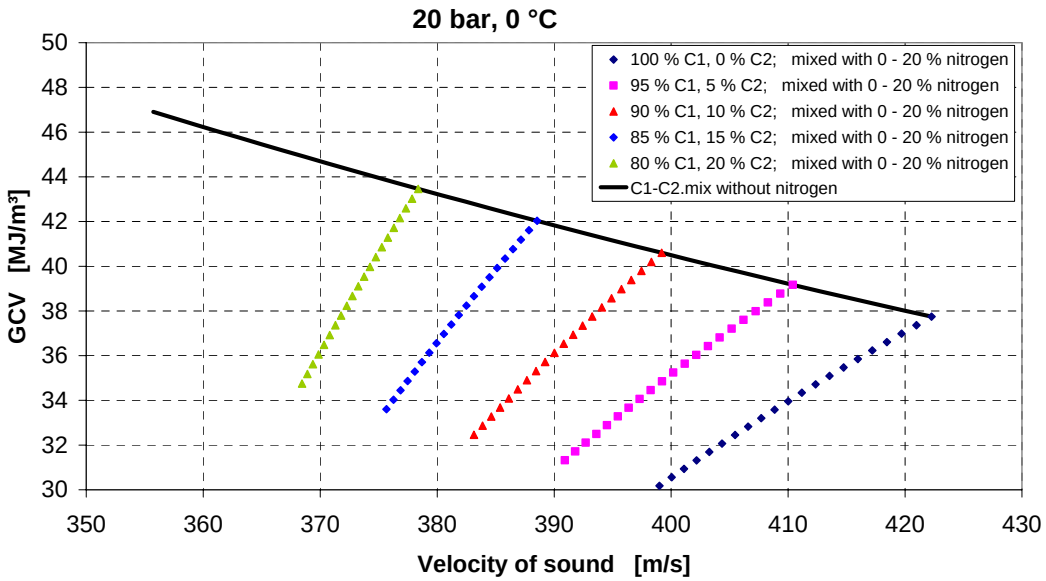

Fig. 9. The GCV shown as a function of the VOS, for 20 bara and 0 °C. The figure illustrates the effect of mixing N_2 into various hydrocarbon mixtures. More details are given in the text. The calculations have been made using the *NATSIM* model [13].

4. EXAMPLE OF REALISATION

In the present section, examples of calculations of density and GCV from the VOS are presented. The examples include a range of gases, also covering a range of pressures and temperatures.

Fig. 10 shows gas density calculated from the VOS for the 10 gases given in Table 2. For each gas example, results are given over the temperature range -10 to 100 °C and four pressures, 20, 60, 100 and 150 bara. The input parameters to the algorithm used in this case (in the TCA option) are

- Pressure,
- Temperature,
- Velocity of sound (VOS),
- Gas composition in the form C1, C2, C3, C4+, N_2 and CO_2.

Note that it is sufficient that typical hydrocarbon gas composition data are used as input, as they are only used to discriminate within the “cloud” that is described in relation to Fig. 6. The use of no hydrocarbon gas composition input (BCA2) would give somewhat less accurate results, cf. Section 5.

The results presented in Fig. 10 are calculated as follows. Firstly, for each temperature - pressure combination, the VOS is calculated from the complete gas composition, using the *NATSIM* program [13], in consistency with AGA 10 [27]. Secondly, the density is estimated from the VOS using the developed algorithm. This estimated density value is then compared to the density value calculated using the complete gas composition (here denoted as the reference density), using the AGA 8 (94) [6] equation of state.

Consider first the data for "Statoil Dry Gas" given in Fig. 10. For temperatures above about 50 °C, the agreement with the reference density is excellent at all pressures shown (deviation less than about 0.04 %). For lower temperatures, the deviation from reference increases at the highest pressure, 150 bara. The reason for this is that as the temperature decreases, the gas is getting closer to the “turning point” shown in Fig. 4 related to the non-uniqueness. Consequently, as the temperature decreases, the problem of calculating the density from the VOS is getting increasingly less “well posed” from a numerical point of view. At 100 bara, the same phenomenon is observed at temperatures below 0 °C. At 20 and 60 bara the agreement with the reference density is excellent at all temperatures considered here.

By considering all the 10 gas types shown in Fig. 10, the same qualitative behaviour as discussed above for "Statoil Dry Gas" is found. That is, at low pressure the results are significantly better than at high pressure, and the results are better at high temperatures than at low temperatures. The main reason for the quantitative difference in the results between the various gas types is that heavy gases are closer to the “turning point” seen in Fig. 4 than light gases are. Therefore, these results are expected to be not as good as for light gases at high pressure and low temperature. It can also be seen that except for the pure methane gas, the "Netherland Gas" is the one that overall provides the best results. This is due to the low content of C4+ in this gas, which makes this gas a simpler task for any density and GCV estimation algorithm.

The practical consequences of the appearance of the “turning points” and how they affect the results in a given application, are briefly addressed in Section 5.

Similarly, Fig. 11 shows the GCV calculated from the VOS for the 10 gases given in Table 2. For each gas example, results are given for the temperatures -2, 30 and 78 °C, at 75 bara pressure. The input parameters to the algorithm used in this case are the same as for the density calculations shown in Fig. 10, see above.

In the left column of Fig. 11, a “blind” approach is used in the sense that only the amount of N_2 and CO_2 is given as input to the algorithm (BCA2), while in the right column, a gas composition specification is used (TCA).

Density from VOS, Statoil Dry Gas

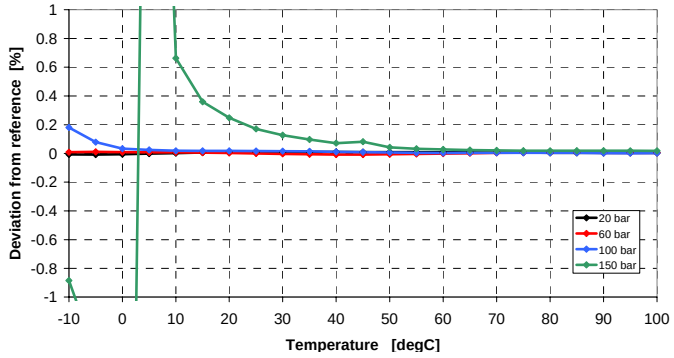

Density from VOS, Statfjord Gas

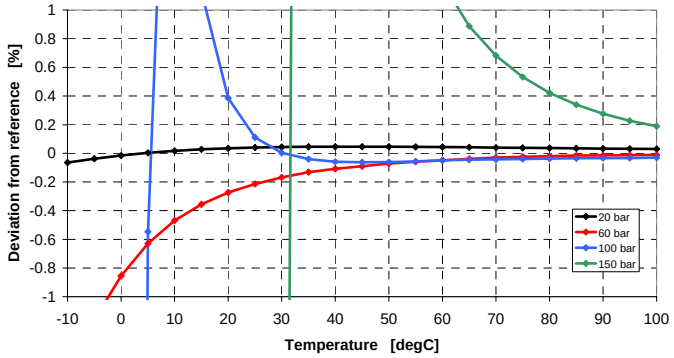

Density from VOS, Åsgard Gas

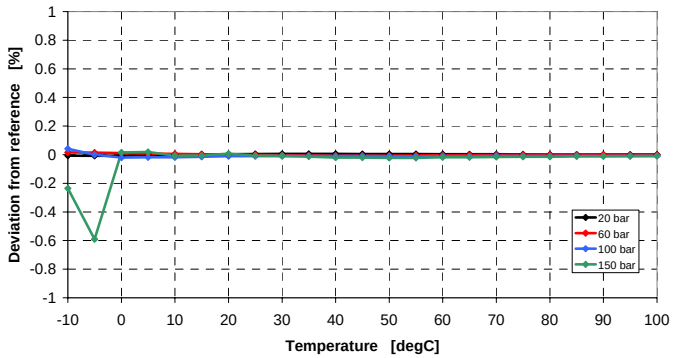

Density from VOS, Troll Gas

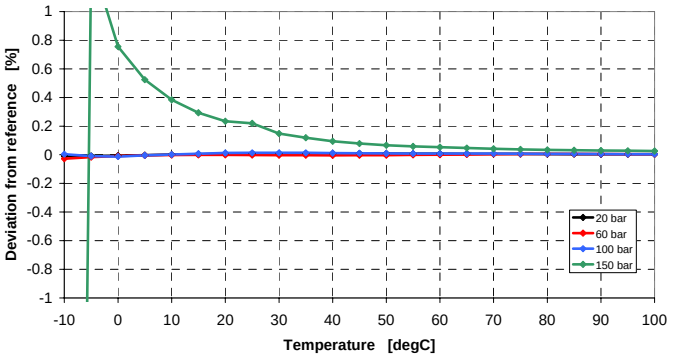

Density from VOS, Oseberg Gas

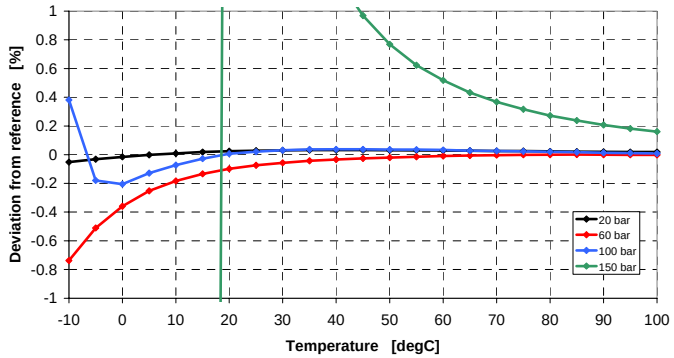

Density from VOS, K15-FB Gas

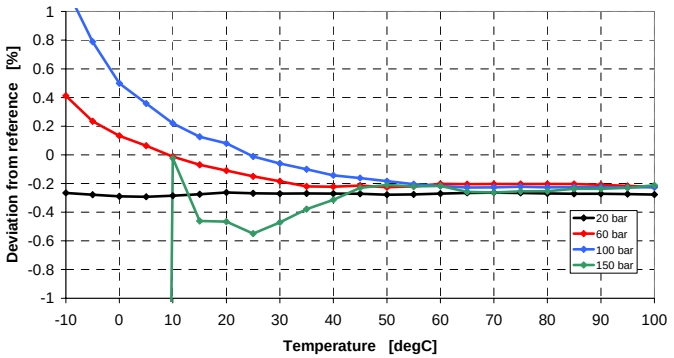

Density from VOS, Netherland Gas

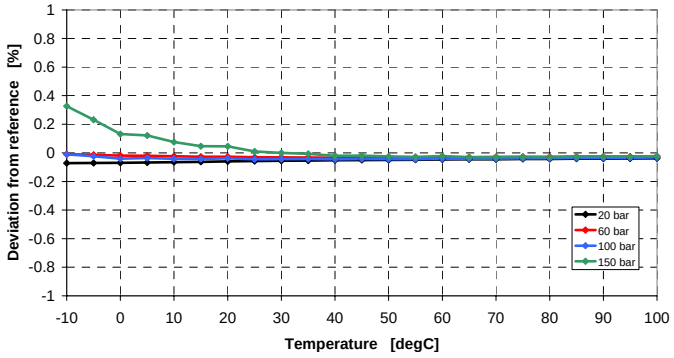

Density from VOS, Amarillo Gas

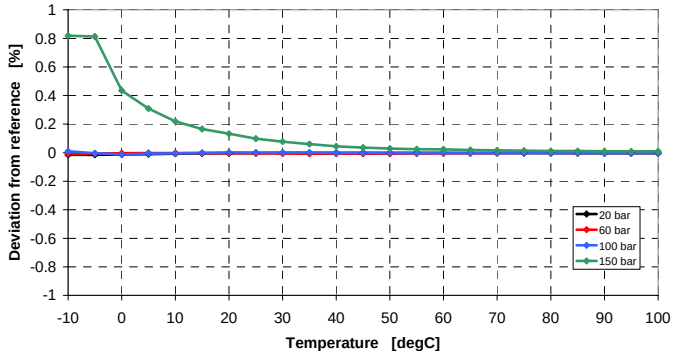

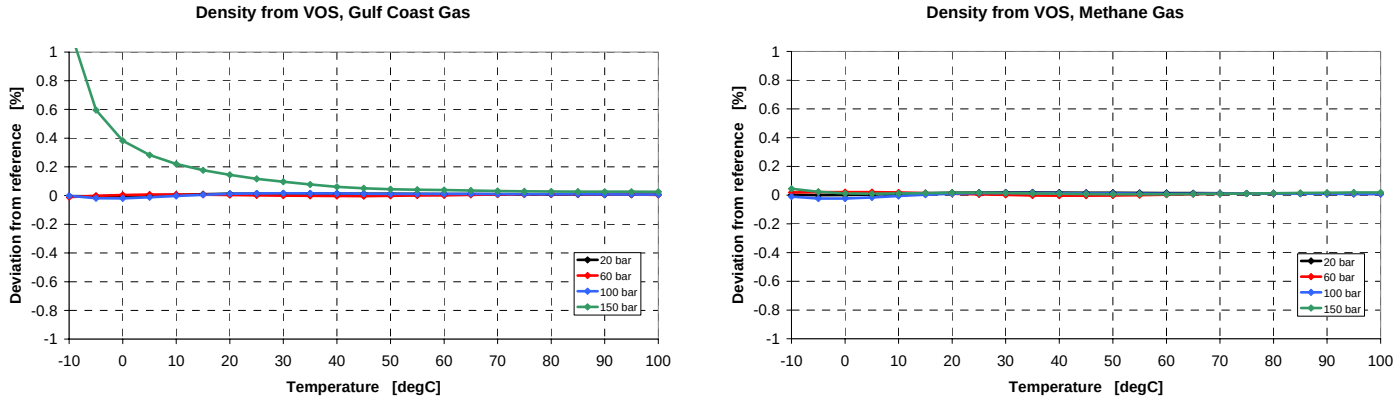

Fig. 10. Deviation from reference, for estimation of gas density from the VOS, for 10 selected example gases (Table 2), over a temperature range from -10 °C to 100 °C, and for pressures 20, 60, 100 and 150 bara.

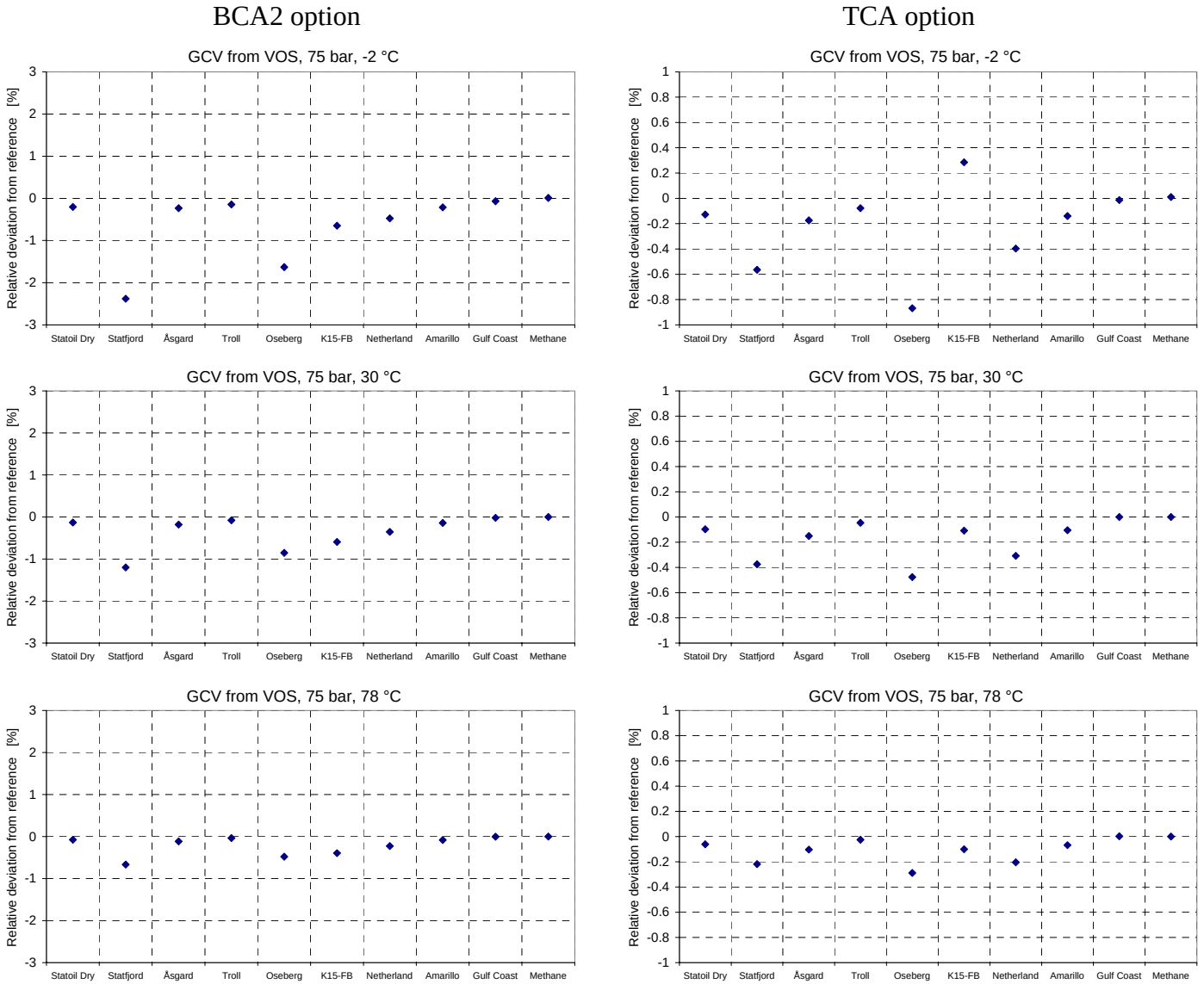

Fig. 11. Deviation from reference, for estimation of GCV from the VOS, for 10 selected example gases (Table 2). Temperature: -2, 30 and 78 °C. Pressure: 75 bara. Two different operational options of the algorithm are shown; a "blind composition approach" (BCA2, left) and the "typical composition approach" (TCA, right).

Fig. 11 is calculated as follows. Firstly, for each temperature- pressure combination, the VOS is calculated from the complete gas composition, using the *NATSIM* program [13], in consistency with AGA 10 [6]. Secondly, the GCV is estimated from the VOS using the developed algorithm. This estimated GCV value is then compared to the GCV calculated using the complete gas composition (here denoted as the reference GCV), using the procedure described in ISO 6976 [21].

For the "blind composition approach" (BCA2) (left column), the deviation from the reference GCV is smaller than about 2.5 %, for the 10 very different gases considered, for this pressure (75 bara), over this temperature range (-2 to 78 °C). In most cases the deviation is within 1 %.

For the "typical composition approach" (TCA) (right column), the deviation from the reference GCV is smaller than 1 %, for the 10 gases at these pressure-temperature conditions. In most cases the deviation is within 0.4 %.

Thus, as expected, the uncertainty of the GCV estimation algorithm is larger in the BCA2 approach than in the TCA approach. It can also be seen that in the same way as for the density estimation from VOS (Fig. 10), the results are better at high temperature than at low temperature. The explanation for this is the same here as for the density estimation case, and will not be repeated here.

For lower pressures than 75 bara, the results are comparable to or better than the results at 75 bara. Like in the density case, the results will not be so good at higher pressures than 75 bara as in Fig. 11, especially for low temperatures (not shown here).

5. UNCERTAINTY CONSIDERATIONS

Contributions to the uncertainty of the methods presented here for gas density and GCV measurement are discussed in the following. Since a complete analysis of this topic will be beyond the scope of the paper, the discussion will be kept at a simplified and preliminary level.

An estimation of the uncertainty of the methods for calculation of gas density and GCV from the VOS, has to account for a number of uncertainty contributions, including

- The uncertainties of the underlying models used in the density and GCV methods (AGA 8 (94) [6], AGA 10 [27], ISO 6976 [21]),
- The uncertainty of the algorithm for calculation of gas density and GCV from the VOS,
- The uncertainties of the input parameters to the algorithm:
    - Pressure
    - Temperature
    - Velocity of sound (VOS)
    - N_2 content
    - CO_2 content
    - Gas composition

For simplicity, the uncertainty contributions due to the underlying models used in the density and GCV methods (AGA 8 (94) [6], AGA 10 [27], ISO 6976 [21]) are not covered in the present preliminary discussion.

The uncertainties of the algorithms for calculation of gas density and GCV from the measured VOS have been addressed in Section 4, and are not further discussed here.

The uncertainty of the input parameters to the algorithms will contribute to the uncertainty of the density and GCV measurement in different ways, depending e.g. on the pressure, temperature and gas composition. A complete analysis of this topic will be beyond the scope of the present paper. However, some examples can be given to briefly point out some typical trends.

The uncertainties of the pressure and temperature measurements will typically not be dominating contributions to the uncertainty of the calculated density and GCV.

The uncertainty of the VOS is an important parameter. It can be shown that typically, a standard uncertainty of 0.3 m/s in the VOS corresponds to a relative standard uncertainty of about 0.2 % for the calculated density, and about 0.1 % for the calculated GCV. This means that in order to use this method in fiscal metering applications (custody transfer and allocation metering, etc.), the VOS should be measured (by the USM) with a standard uncertainty less than e.g. 0.3 m/s (corresponding to 0.075 % = 750 ppm).

Close to the "turning point" shown in Figs. 4 and 5, the uncertainty is much higher. In this region, methods for calculation of density and GCV from a measured VOS, are not recommended.

As a practical approach to this challenge, a diagnostic computer program can be made which for a given gas composition, pressure and temperature can determine whether one is close to the "turning point" or not. The program can also determine whether the spread of the "cloud" described in Section 3 is large or small, and in this way indicate whether low or high uncertainty can be expected related to uniqueness and higher order hydrocarbon components.

In cases where the gas composition is not known (BCA1 or BCA2) no such pre-calculations can be carried out for diagnostics purposes. However, in cases where there uniqueness is not a problem, the uncertainty may not increase dramatically. Cf. e.g. Fig. 11 (left column), in which the deviation from the reference GCV is still within 1 % in most cases, at 75 bara pressure.

The contribution from the uncertainty of the N_2 concentration can be illustrated through the following example. A standard uncertainty of 0.1 % (for example if the concentration is taken to be 3.1 % instead of 3 %) corresponds to a relative standard uncertainty of about 0.02 % for the density, and about 0.15 % or less for the GCV. This means that a variation in the N_2 concentration of a few tenths of a percent may be acceptable, especially for estimation of density.

The contribution from the uncertainty of the CO_2 concentration can be illustrated through the following example. A standard uncertainty of 0.11 % (for example if the concentration is taken to be 3.1 % instead of 3 %) corresponds to a relative standard uncertainty of about 0.03 % for the density, and about 0.2 % or less for the GCV, over a large pressure and temperature range. This

means that a variation in the CO_2 concentration of a few tenths of a percent may be acceptable, especially for estimation of density.

The contribution from the uncertainty of the specified gas composition (or the uncertainty due to using a “blind” approach (BCA1 or BCA2) will typically be larger the lower the temperature is, larger the larger the pressure is, and larger the larger the molar weight of the natural gas is. This effect is illustrated by the difference between the “blind composition approach" (BCA2) and the “typical composition approach" (TCA) in Fig. 11.

It may also be noted that in order to obtain an uncertainty of e.g. 1 % of mass flow rate (95 % confidence level) (as prescribed e.g. by NPD [1]), even an uncertainty of around 0.7 % (95 % confidence level) in density can be tolerated if the volumetric flow rate has an uncertainty of 0.7 % (95 % confidence level). However, that would not be in accordance with e.g. the NPD requirements for the density measurement.

6. CONCLUSIONS

Mass and energy measurement of natural gas is today possible using an ultrasonic flow meter (USM) in combination with pressure and temperature measurements, a typical hydrocarbon gas composition, and estimates of the molar fractions of CO_2 or N_2. That means, without use of either densitometer, gas chromatograph or calorimeter, which are instruments required in traditional fiscal metering stations. Such methods have evolved from the capabilities of USMs to measure the velocity of sound (VOS) in the gas, which may be used to calculate the density and the gross calorific value (GCV) of the gas. Consequently, the USM may be used for measurement of the mass and energy flow rates, in addition to the traditional volumetric flow rate measurement provided by the USM.

In the present paper, various methods and strategies are discussed for calculation of gas density and gross calorific value (GCV) from the measured velocity of sound (VOS). In the development of such algorithms, several challenges are faced, including uniqueness problems, effects of higher order hydrocarbon components (C3+), and effects of the inert gas components (N_2 and CO_2).

Methods are presented here which are based solely on the measured VOS, in addition to pressure and temperature measurements, knowledge of a typical hydrocarbon gas composition, and estimates of the molar fractions of CO_2 or N_2. No instruments are required in addition to the USM and the pressure and temperature sensors.

The methods for density and GCV measurement discussed in the present paper can be used in three different modi, depending on the available knowledge about the gas composition: (1) “blind composition approach 1”, BCA1 (with no knowledge about the gas composition at all), (2) “blind composition approach”, BCA2 (with no knowledge about the hydrocarbon gas composition, but with knowledge about the typical N_2 and CO_2 contents), and (3) “typical composition approach”, TCA (with knowledge about the typical hydrocarbon gas composition and the typical N_2 and CO_2 contents).

The "blind" modi (BCA1 or BCA2) are typically used when gas composition data are not available. The TCA modus may be used e.g. when a typical gas composition is available, but its daily variations are not known, such as e.g. in allocation metering stations, blending, etc. In the

BCA1 and BCA2 modi, the uncertainty of the measured density and GCV is higher than in the TCA modus.

The algorithms developed here for gas density and GCV measurement have been tested over a broad range of gas compositions, and over a range of temperatures and pressures.

For density, results of the order of 0.1 % or better are obtained at 20 bara over a temperature range from -10°C to 100 °C, using the TCA approach. As the pressure increases, the results at the lower temperatures are less accurate. However, at 100 bara the results are still within 1 % in all cases except for the heavy natural gas from Statfjord. For most gases, the results are well below 0.2 % at 100 bara.

For GCV, results at 75 bar have been presented. For the "blind approach" (BCA2), the deviation from the reference GCV is smaller than about 2.5 %, for the 10 very different gases considered, for this pressure (75 bara), over this temperature range (-2 to 78 °C). In most cases the deviation is within 1 %. For the TCA approach (right column), the deviation from the reference GCV is smaller than 1 %, for the 10 gases at these pressure-temperature conditions. In most cases the deviation is within 0.4 %.

Such figures relate to the uncertainty of the algorithms involved for calculation of density and GCV from the VOS, and do not represent the total measurement uncertainty for the density and GCV.

The various uncertainty contributions to the methods presented here for measurement of gas density and GCV have been discussed briefly, at a preliminary level. The accuracy of the density and calorific value measurements depends largely on the accuracy of the VOS measurement, which should be ±0.3 m/s (about ±0.075 %) or better (standard uncertainty). This puts requirements to improved control of transit time measurements in the USM, such as systematic effects due to e.g. (a) transducer time delay correction (“dry calibration” values), (b) diffraction time delay correction, (c) variation of these corrections with P, T, pipe diameter and gas composition, (d) sound refraction (flow profile effects on transit times), (e) finite beam effects, and (f) cavity flow effects.

Since the methods presented here require no additional instrumentation in the metering station, apart from the USM itself and the pressure and temperature sensors, existing USM metering stations can be updated to measure the gas density and the GCV (i.e. the mass and energy flow rates), by a software upgrade only. This may be of interest e.g. for USM based check metering stations and other USM metering stations in which density and/or GCV measurement are not made today.

To which extent fiscal accuracy can be achieved with such methods, will be subject of further study. The results presented here, in addition to flow test results for mass flow measurement using a commercial USM, have definitely been promising in this respect.

ACKNOWLEDGMENTS

The work has been supported by The Research Council of Norway (NFR), Statoil ASA and Gassco AS, under CMR's 4-year strategic institute programme “Ultrasonic technology for

improved exploitation of petroleum resources" (2003-06). In addition, the work has evolved from and been inspired by project cooperation over a number of years, related to USM fiscal metering of gas (custody transfer, sales and allocation metering), involving several partners: The Research Council of Norway (NFR), Fluenta AS (now Roxar Flow Measurement), FMC Kongsberg Metering, Statoil, Norsk Hydro, ConocoPhillips, The Norwegian Society for Oil and Gas Measurement (NFOGM), the Norwegian Petroleum Directorate (NPD), GERG (Groupe Européen de Reserches Gazières), and Gassco AS.

REFERENCES

[1] "Regulations relating to measurement of petroleum for fiscal purposes and for calculation of CO_2 tax", Norwegian Petroleum Directorate (NPD), Stavanger, Norway (November 2001).

[2] **Smalling, J.W., Braswell, L. D. and Lynnworth, L. C.:** "Apparatus and methods for measuring fluid flow parameters." US patent no. 4,596,133, dated June 24, 1986 (filed July 29, 1983).

[3] **Smalling, J.W., Braswell, L. D., Lynnworth, L. C. and Russell Wallace, D.:** "Flare gas ultrasonic flow meter", Proc. of *39th Annual Symposium on Instrumentation for the Process Industries, January 17-20, 1984*, pp. 27-38.

[4] **Lygre, A.:** "A method for estimating density, isentropic exponent and molecular weigth of natural gas at low pressures", CMR Report CMI 871412-1, Christian Michelsen Research, Norway (1988) (Confidential).

[5] **Watson, J.:** "A review of important gas flow measurement parameters." Proc. of *Practical Developments in Gas Flow Metering, One Day seminar - 7 April 1998*, National Engineering Laboratory (NEL), East Kilbride, Scotland (1998).

[6] "Compressibility factors of natural gas and other related hydrocarbon gases", A.G.A. Transmission Measurement Committee Report No. 8; American Gas Association; Second edition, November 1992; 2nd printing (July 1994).

[7] ISO 12213-3, "Natural Gas - Calculation of compression factor - Part 3: Calculation using physical properties", International Organisation for Standardisation, Genéve, Switzerland (1997).

[8] **Beecroft, D.:** "Is a wet gas (multiphase) mass flow meter just a pipe dream?", Proc. of the *16th International North Sea Flow Measurement Workshop, Gleneagles Hotel, Perthshire, Scotland, 26-29 October 1998.*

[9] **Lunde, P., Frøysa, K.-E., Fossdal, J. B. and Heistad, T.:** "Functional enhancements within ultrasonic gas flow measurement", Proc. of the *17th International North Sea Flow Measurement Workshop, Oslo, Norway, 25-28 October 1999.*

[10] **Tjomsland, T. and Frøysa, K.-E.:** "Calculation of natural gas density from sound velocity. Description of theory and algorithms implemented in the Deca code", CMR report no. CMR-97-F10015, Christian Michelsen Research AS, Bergen, Norway (June 1997) (Confidential).

[11] **Frøysa, K.-E., Furset, H. and Baker, A. C.:** "Density and ultrasonic velocity calculations for natural gas. Sensitivity analysis of DeCa", CMR report no. CMR-98-F10002, Christian Michelsen Research AS, Bergen, Norway (December 1998) (Confidential).

[12] **Nesse, Ø. and Frøysa, K.-E.:** "Ultrasonic natural gas density estimation. Sound velocity measurements in nitrogen", CMR report no. CMR-98-F10026, Christian Michelsen Research AS, Bergen, Norway (December 1998) (Confidential).

[13] **Baker, A. C., Frøysa, K.-E. and Midttun, Ø.:** "*NATSIM* user guide. A program for calculating compressibility, sound speed, density, heat capacity and calorific value of gases," CMR Technical Note no. CMR-TN98-F10030 (December 1998) (Confidential.)

[14] "Ultrasonic gas flow meter MPU 1200. Specifications", Bulletin SSKS001, Issue/Rev. 04 (5/02), FMC Measurement Solutions (2005). Web page: http://info.smithmeter.com/literature/docs/ssks001.pdf

[15] **Lunde, P. and Frøysa, K.-E.:** "Handbook of uncertainty calculations - Ultrasonic fiscal gas metering stations", Norwegian Petroleum Directorate, Norwegian Society for Oil and Gas Measurement (NFOGM), Christian Michelsen Research, Norway (December 2001). ISBN 82-566-1009-3.

[16] **Haruta, M., Uekuri, K. and Kiuchi, Y.:** "Continuous measurement of calorific value of natural gas." Proc. of *Symposium on Natural Gas Energy Measurement, Chicago, 1986*, p. 401-427.

[17] **Lueptow, R. M. and Phillips, S.:** "Acoustic sensor for determining combustion properties of natural gas." Meas. Sci. Technol. 5, 1375-1381 (1994).

[18] **Tjomsland, T. and Frøysa, K.-E.:** "Calorific value of natural gas. Possible determination from temperature, pressure and sound velocity", CMR report no. CMR-96-F10022, Christian Michelsen Research AS, Bergen, Norway (December 1996) (Confidential).

[19] **Baker, A. C. and Frøysa, K.-E.:** "A technique for the calculation of the energy content of a natural gas", CMR report no. CMR-97-F10028, Christian Michelsen Research AS, Bergen, Norway (December 1997) (Confidential).

[20] **Baker, A. C. and Frøysa, K.-E.:** "Further work on ENCON", CMR report no. CMR-98-F10029, Christian Michelsen Research AS, Bergen, Norway (December 1998) (Confidential).

[21] ISO 6976, "Natural gas - Calculation of calorific value, density, relative density and Wobbe index", 2nd ed. International Organization for Standardization, Geneva, Switzerland (1995).

[22] **Morrow, T. D. and Behring, K. A .:** "Energy flow measurement technology, and the promise of reduced operating costs", Proc. of the *4th International Symposium on Fluid Flow Measurement, Denver, Colorado, USA, June 27-30, 1999.*

[23] *Flow Tidings - The Flow Programme Newsletter*, Issue 31, Summer 2001, National Engineering Laboratory (NEL), East Kilbride, Scotland.

[24] Collection of papers and presentations, titled "Energy flow measurement system", dated December 13, 2001. Gasunie Research, Groeningen, the Netherlands.

[25] **Lunde, P. and Frøysa, K.-E.:** "Mass and energy measurement of gas using ultrasonic flow meters". In: *Proc. of 25th Scandinavian Symposium on Physical Acoustics, Ustaoset, Norway, 27-30 January 2002.*

[26] **Frøysa, K.-E. and Lunde, P.:** "Mass and energy measurement of natural gas using ultrasonic flow meters. Recent results". In: *Proc. of 27th Scandinavian Symposium on Physical Acoustics, Ustaoset, Norway, 25-28 January 2004.*

[27] "Speed of sound in natural gas and other related hydrocarbon", A.G.A. Transmission Measurement Committee Report No. 10, American Gas Association (2003).

[28] **Panneman, H. J., Koreman, C. W., Toonstra, S. and Huijsmans, F.:** "Energy Flow and Wobbe Metering Based on Velocity of Sound Measurements and Using a Corrective Technique", Proc. of the *20th International North Sea Flow Measurement Workshop, St. Andrews Bay Resort, Scotland, 22-25 October 2002.*

HOW TODAY'S USM DIAGNOSTICS SOLVE METERING PROBLEMS

JOHN LANSING, Manager, Gas Ultrasonics, Daniel Measurement & Control

ABSTRACT

This paper discusses both basic and advanced diagnostic features of gas ultrasonic meters (USM), and how capabilities built into today's electronics can identify problems that often may not have been identified in the past. It primarily discusses fiscal-quality, multi-path USMs and does not cover issues that may be different with non-fiscal meters. Although USMs basically work the same, the diagnostics for each manufacturer does vary. All brands provide basic features as discussed in AGA 9 [Ref 1]. However, some provide advanced features that can be used to help identify issues such as blocked flow conditioners and gas compositional errors. This paper is based upon the Daniel USM design and the information presented here may or may not be applicable to other manufacturers.

INTRODUCTION

During the past several years there have been numerous papers presented which discuss the basic operation of USMs [Ref 2]. These papers discuss the meaning of the five basic diagnostic features. Following is a summary of the five features available from all manufacturers' of USMs.

Individual path velocities

Individual path speed of sound

Gains for each transducer

Signal to noise for each transducer

Accepted pulses, in percentage, for each transducer pair

Although these features are very important, little has been written on how to interpret them. Part of the reason is that the analysis does vary by manufacturer.

In addition some manufacturers provide additional diagnostics such as swirl angle, turbulence, AGA 10 [Ref 3] SOS vs. the meter's reported SOS, and many others.

This paper will go into more detail on all of the above features and more. It is important to understand that the meters being analyzed in this paper are of the chordal design, and therefore some of the analysis would not apply to other designs.

Graphs shown in this paper are from Excel spreadsheets and were automatically generated by Daniel's CUI (Customer Ultrasonic Interface) software that is used to communicate with the meter. Note that these graphs were not individually developed but rather automatically generated while collecting a "Maintenance Log," or by using a feature called "Trending."

Obviously it is important for users to collect periodic maintenance log files. These log files provide a "snap-shot" of the meter's operation at that point in time. Many utilize some of the data for entry into their company database for tracking over time. However, a large number of users don't perform any tracking or trending of data.

Looking at a single inspection, which may be done either monthly or quarterly, can give the user an indication of the meter's health. However, to truly monitor how a meter is doing over the long-term, a method needs to be employed that "trends" key variables. This is important since many diagnostics change slowly over time. Trending helps identify these changes and makes problems much more obvious than merely viewing a single inspection report.

ULTRASONIC BASIC DESIGNS

Before discussing diagnostics it might be helpful to review some of the basic designs that are used today. Figure 1 shows 5 types of velocity integration techniques [Ref 4]. As one can see the methods differ and thus responses to different velocity profiles may also differ. This is particularly true when trying to perform comparisons on velocity and SOS. The various meter configurations in Figure 1 provide different velocity responses to profiles, and are thus analyzed differently. Additionally, looking at differences in SOS between the various paths will require analysis somewhat differently. Analysis in this paper will be of design D in Figure 1.

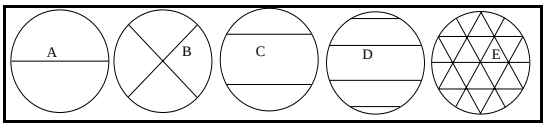

Figure 1 - Ultrasonic Meter Designs

BASIC DIAGNOSTIC INDICATORS

One of the principal attributes of modern ultrasonic meters is the ability to monitor their own health, and to diagnose any problems that may occur. Multipath meters are unique in this regard, as they can compare certain measurements between different paths, as well as checking each path individually.

Measures that can be used in this online "health checking" can be classed as either internal or external diagnostics. Internal diagnostics are those indicators derived only from internal measurements of the meter. External diagnostics are those methods in which measurements from the meter are combined with parameters derived from independent sources to detect and identify fault conditions. An example of this would be using gas composition to compute the gases SOS and comparing it to the meter.

Gain

One of the simplest indicators of a meter's health is the presence of strong signals on all paths. Today's multipath USMs have automatic gain control on all receiver channels. Transducers typically generate the same level of ultrasonic signal time after time. Any increase in gain on any path indicates a weaker signal at the receiving transducer. This can be caused by a variety of problems such as transducer deterioration, fouling of the transducer ports, or liquids in the line. However, other factors that affect signal strength include metering pressure and flow velocity.

Figure 2 shows how gains change with velocity. This example was taken at the time of calibration for a 16-inch meter. A log file was generated for each velocity during the calibration. By using software that "trends" specific features, a summary of gains (left axis) vs. velocity (right axis) can be very easily developed. As can bee seen on the graph this meter was calibrated from 26 to 0.15 m/s.

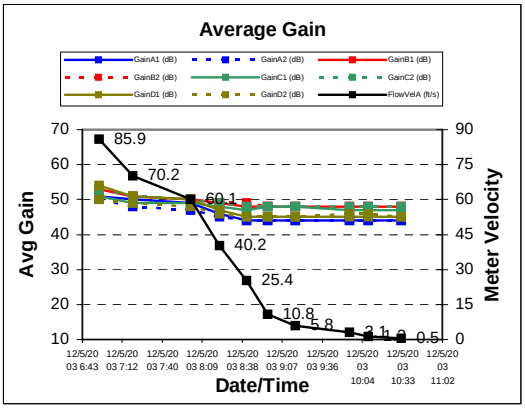

Figure 2 – Gain Changes with Velocity

Figure 2 shows that all chord gains increased about 6 dB, or in other words about doubled at the higher velocities. This is normal since the signal becomes somewhat attenuated by the higher velocity. Thus, in looking at gains alone one should also consider velocity changes when comparing to the gains noted on previous logs.

If this meter was operating at 750 Bar, and then the pressure was reduced to 375 Bar, the gain change would be about the same as this example. Since most pipelines don't typically experience this type of pressure change, generally speaking gain changes will be from velocity or perhaps a transducer contamination.

Figure 3 is an example of a transducer that is failing. This graph was generated from several CUI log files. An Excel file was developed by combining several periodic maintenance logs into several trended graphs. It is clear that chord D has increasing gains far greater than the others. The increase of all transducers about mid-way in time was due to the velocity increasing, and that can be seen on a separate graph in the maintenance log.

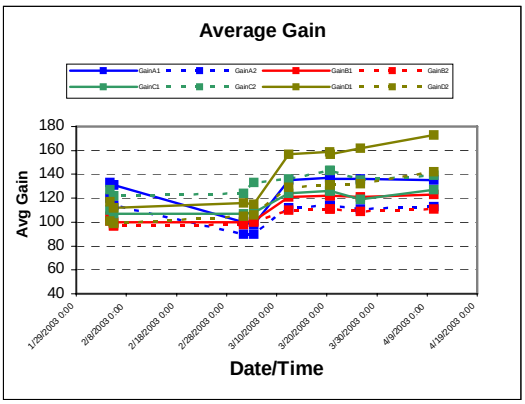

Figure 3 – Gain Increasing on One Chord

This meter had velocities that were typically around 12 m/s and then the operation changed and the meter velocity approached 18 m/s, resulting in the increased gain on all paths. However, Chord D indicated a significantly higher increase in the gain, and then continued to increase while the other chords maintained a relatively stable gain level.

Some may feel the meter's accuracy could be affected with this type of gain increase. In actuality as long as the transit times are being measured correctly then there is virtually no impact on accuracy. By trending gains this customer identified a meter problem before failure, thus avoiding any possible downtime.

Figure 4 shows gains graphed for each transducer during a routine inspection. As can be seen they are relatively consistent. Knowing what is normal for a given meter is more difficult for a technician to keep track because each meter may have somewhat different characteristics due to size and metering pressure. It is important to collect routine maintenance log files, like that shown in Figure 4, so that it's possible to develop the trending graph in Figure 3.

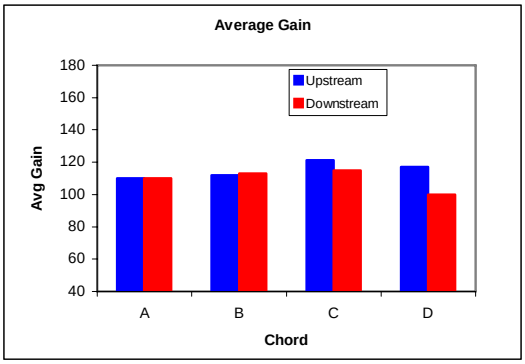

Figure 4 –Transducer Gains - Normal

Figure 5 shows a graph of a meter with a transducer problem. In this case it is quite obvious since the gain levels on chord D are double those of the other chords. The benefit of trending log files to identify gain changes is valuable since it helps identify a potential problem before it becomes significant, allowing the user to be proactive in dealing with the problem rather than reactive.

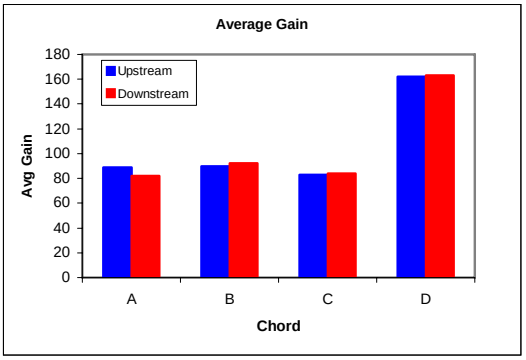

Figure 5 – Transducer Gains - Abnormal

Signal Quality – Transducer Performance

This expression is often referred to as performance (but should not be confused with meter accuracy). All ultrasonic meter designs send multiple pulses across the meter to the opposing transducer in the pair, before updating the output. Ideally all the pulses sent would be received and used. However, in the real world, sometimes the signal is distorted, too weak, or otherwise the received pulse does not meet certain criteria established by the manufacturer. When this happens the electronics rejects the pulse rather than use something that might distort the results.

The level of acceptance (or rejection) for each path is generally considered as a measure of performance, and is often referred to as signal quality. Unless there are other influencing factors, the meter will normally operate at 100% transducer performance until it reaches the upper limit of the velocity rating. Here the transducer signal becomes more distorted and some of the waveforms will ultimately be eliminated since they don't fit the pulse detection criteria within the specified tolerance. At this point the meter's performance will drop from 100% to something less.

Typically this will occur on the outer chords (A&D) for the British Gas design meter. Even though the paths are shorter, the chord position is closer to the wall, and thus there is more distortion in the received waveform.

Figure 6 shows the performance of a meter, taken from data obtained during a calibration, and then trended to show what happens at higher velocity.

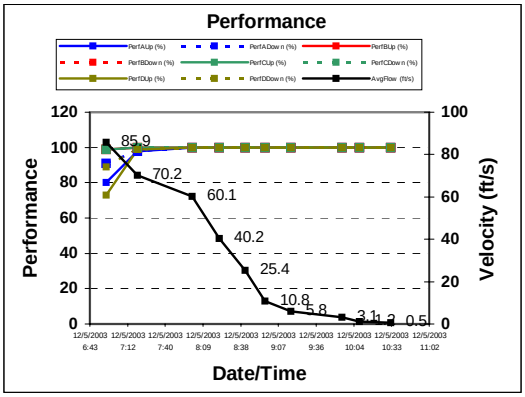

Figure 6 – Performance vs. Velocity

Figure 7 shows the results of a maintenance log file where all transducers are operating at 100% performance. This is what one would expect unless the meter is near maximum velocity.

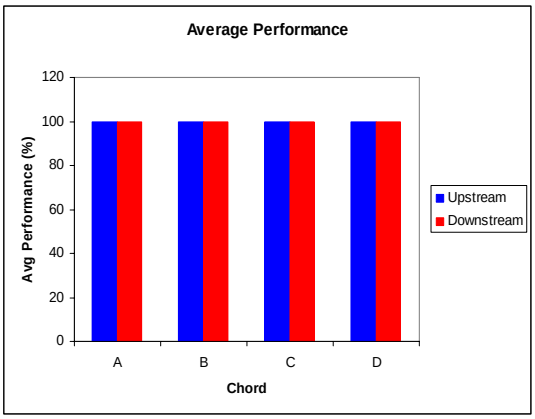

Figure 7 –Transducer Performance Summary

Figure 8 shows the summary from a maintenance log file where Chord D is running less than 100% while all others are at 100%. Although the meter is still most likely operating accurately, this is an indication additional attention is needed to address a problem that may be developing.

As mentioned above, there are several reasons why pulses can be rejected. Additional causes may include extraneous ultrasonic noise in the same region the transducer operates, distorted waveforms caused by excessive gas velocity, and to some degree, contamination on the face of the transducer.

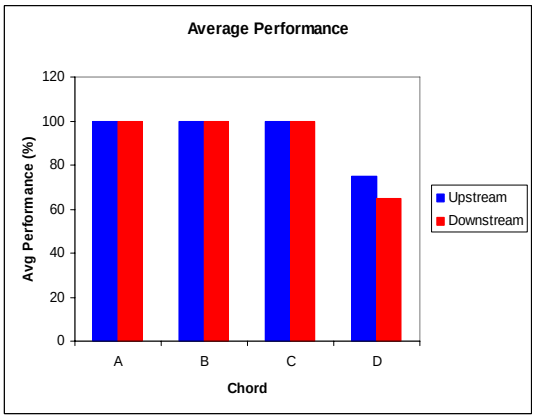

Figure 8 – Transducer Performance Summary

In the example show in Figure 8, the cause can be from a transducer that is either beginning to fail, or it could be from contamination in front of the transducer. This can occur if a large quantity of debris is present, and users have experienced ice partially blocking the transducer port. With performance low on one pair this warrants further investigation.

Signal-to-Noise Ratio

Signal to noise (SNR) provides information that is also valuable in verifying the meter's health, or alert the user of possible impending problems. Each transducer is capable of receiving noise information from extraneous sources (rather than its opposite transducer). In the interval between receiving pulses, meters monitor this noise to provide an indication of the "background" noise. This noise can be in the same ultrasonic frequency spectrum as that transmitted from the transducer itself.

The measure of signal strength to the level of "background" noise is called the Signal to Noise Ratio, or SNR for short. Typically this is not monitored nearly as often as gains and performance. SNR is generally not an issue unless there is a control valve or other noise generating piping component present. When that occurs, the SNR values will drop. The magnitude of the SNR is a function of the manufacturer's methodology of expressing the value.

Figure 9 shows a trended graph of SNR taken from a meter at the time of calibration. As can be seen the SNR is above 3500 at the lower velocities, and steadily drops to something over 1000 when the meter is at maximum velocity. This is normal due to the increase in signal distortion and gain at higher velocities.

Upon initial inspection of a meter, if it is operating near capacity one might be alarmed to see the SNR for all chords around 1000 rather than the expected value of 2500 to 3000. However, it is important to recognize that the SNR drops at higher meter velocities.

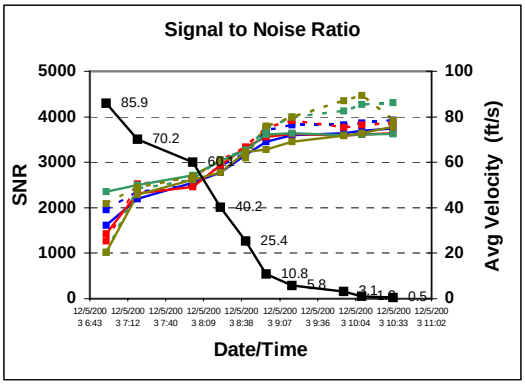

Figure 9 – Trended SNR vs. Meter Velocity

Noise levels can become excessive if a control valve is placed too close and the pressure differential is too high. When this happens the meter may have difficulty in differentiating the signal from the noise. By monitoring the level of noise, when no pulse is anticipated, the meter can provide information to the user, via the SNR, warning that meter performance (signal quality) may become reduced. In extreme cases, noise from control valves can "swamp" the signal to the point that the meter becomes inoperative.

When the ultrasonic noise from a control valve begins to cause the SNR to be too low then action may be warranted. There are several things that can be done to improve SNR. The easiest way to improve SNR is to activate the "Stacking" feature built into the electronics. This feature changes the way transducers are activated.

Normally each transducer is fired once sequentially until all 8 transducers have been fired. This occurs about 31 times per second. When stacking is activated each transducer is fired several times in a row (as opposed to once only). The sum of the waveforms is added up and this effectively filters out the noise that is not synchronous with the transducer waveform. Using this technique can improve the SNR by more than 4 to 1. Figure 10 shows the SNR values of a meter that has stacking turned on. Without stacking this meter would not be operating. With it the meter is running very close to 100% transducer performance.

	Perf (%)	Gain	SNR
Chord A Up	100	44	2292
Chord A Dn	100	43	2533
Chord B Up	100	45	340
Chord B Dn	100	46	329
Chord C Up	100	44	482
Chord C Dn	100	44	498
Chord D Up	100	43	2306
Chord D Dn	100	43	2258
Average Up	100	44	1355
Average Dn	100	44	1404.5

Figure 10 – SNR of Meter with Stacking

The section in yellow shows that the SNR for the middle two chords is below 500, yet this meter was operating with 100% transducer performance. Note that the outer chords have SNR values that exceed 2000. This is partly due to the length being shorter and thus the gain is lower for these. With less gain needed the noise is also amplified less on the outer chords than on the inner accounting for an improved SNR. Also, control valve noise usually causes lower signal to noise levels on the transducers that face the noise source (all would be affected).

Velocity Profile

Monitoring the velocity profile is possibly one of the most overlooked and under-used diagnostic tools of today's ultrasonic meter. It can provide many clues as to the condition of the metering system, as well as the meter. AGA Report No. 9 requires a multipath meter provide individual path velocities.

Once the USM is placed in service, it is important to collect a baseline (log file) of the meter. That is, record the path velocities over some reasonable operating range, if possible. These baseline logs can also be obtained at the time of calibration. However, as the piping in the field will likely be different than that at the calibration facility, there could be some minor changes in profile. Good meter station designs produce a relatively uniform velocity profile within the meter. The baseline log file may be helpful in the event the meter's performance is questioned later.

Figure 11 shows the velocity ratio of each chord relative to the meter's velocity. This ratio is computed by taking each chord velocity average during a period of time and dividing it by the

velocity average as reported by the meter. Since the ratio for each chord remains essentially constant at all meter velocities, changes in the meter's operation are easier to detect than by looking at the actual velocity on each chord.

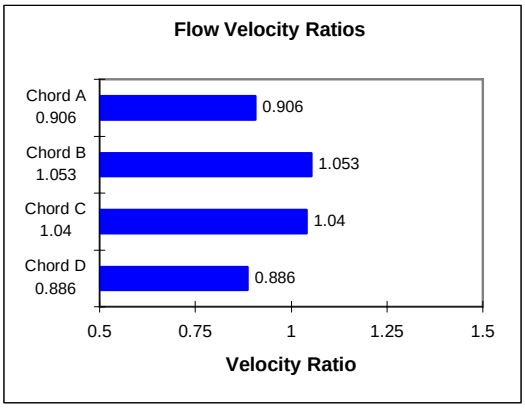

Figure 11 – Chord Ratios at 1 m/s

Typically the ratio for a BG design meter is about 89% (ratio = 0.89) for the A and D chords, and about 104% (ratio = 1.04) for the B and C chords. The difference in ratios is due to the fact that the outer chords are closer to the pipe wall, and thus the velocity of the gas there is less than the gas that is closer to the center of the pipe. When the velocity falls below something like 1 m/s, depending upon meter size and station design, the velocity profile may change. Figure 12 shows the same meter's velocity profile when the velocity is at 0.3 m/s.

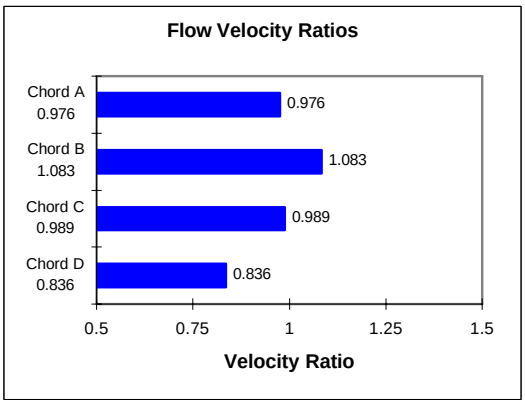

Figure 12 – Chord Ratios at 0.3 m/s

It is clear in Figure 12 and 13 that the velocity profile is very different than that in Figure 11. These were taken from a 16-inch meter at the time of calibration. When one sees this type of "distortion" in the velocity profile, it may be assumed that the meter's accuracy has been affected. Actually this meter's uncorrected reading was within 0.1% at 0.3 m/s when compared to 1 m/s, and within 0.2% at 0.12 m/s compared to the 1 m/s. Thus, just because the velocity profile is distorted, particularly at low velocities, it should not be assumed there is a significant shift in the meter's accuracy.

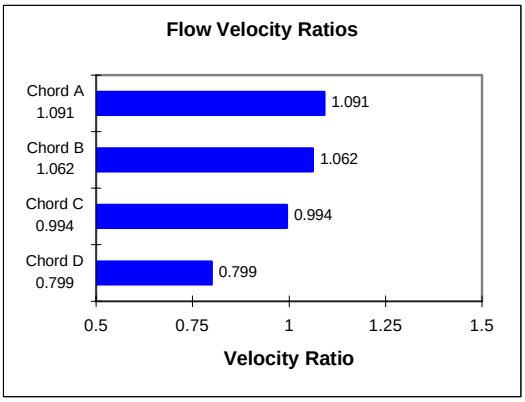

Figure 13 – Chord Ratios at 0.15 m/s

Looking at four chord ratios takes understanding why the velocities are different. Since these can change by small amounts, a simpler method of identifying changes in profile is desired. A single value would be much easier to understand, and also easier to quickly analyze. This value is called Profile Factor.

The Profile Factor is computed by adding the B & C chord values together and dividing by the sum of the A & D chords. The equation looks like this: Profile Factor = (B+C)/(A+D). Assuming the A & D chords are 0.89 and the B & C chords are 1.04 the Profile Factor then computed to about 1.17. This value does vary from meter to meter due to installation design and to some degree the type of flow conditioner and distance of the flow conditioner from the meter. However, the key aspect of the Profile Factor is to monitor when performing a log file and trend it to compare it to the historical norm for that meter

In Figure 11 when the meter was at 1 m/s the Profile Factor was 1.168. As the velocity dropped to 0.3 m/s (Figure 12) the Profile Factor changed to 1.143 and the Profile Factor was 1.087 in Figure 13. By looking at the Profile Factor it is easier to see that the velocity profile is different in the meter than the typical value. Even with this shift in velocity profile, the accuracy of the meter didn't change by more than 0.2% from 1 m/s to 0.15 m/s Again, a change in profile, particularly at low velocities, does not necessarily suggest a significant change in meter accuracy.

The Profile Factor can be a valuable indicator of abnormal flow conditions. The previous discussion showed what happens to the velocity ratios and Profile Factor due to low velocity operation. This profile change is typical when the meter is operated at these lower velocities. Figure 14 shows an ideal profile from a 12-inch meter. This was based on the log file collected at the time of calibration [Ref 5]. Customers have often asked what impact partial blockage of a flow conditioner has on the meter's accuracy. This meter was used to show what happens not only to the profile, but to quantify the change in accuracy.

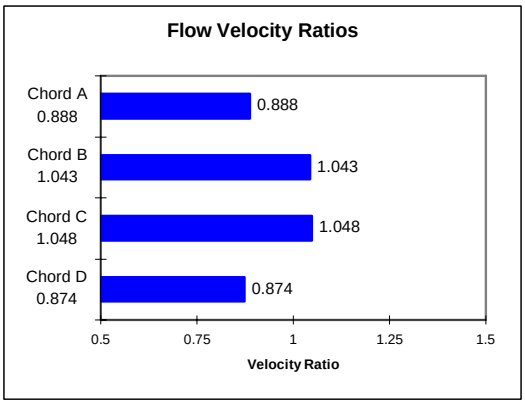

Figure 14 – Normal 12-Inch Meter Profile

The Profile Factor for this meter is 1.187. For the second test, the flow conditioner was modified to have about 40% of the holes blocked with duct tape. Duct tape was used to ensure repeatability. Figure 15 shows the flow conditioner after it was removed.

Figure 15 – Blocked Flow Conditioner

Figure 16 shows the velocity profile during the time the flow conditioner was blocked. This was taken at a velocity of 12 m/s. The profile at two other velocities, 6 and 18 m/s, looked the same.

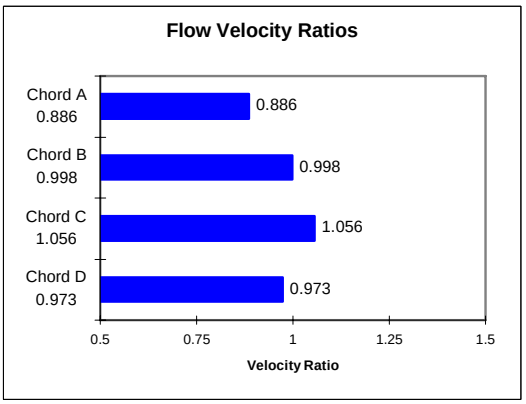

Figure 16 – 12-inch Meter Profile – Blocked

The Profile is obviously distorted with higher-than-normal readings on Chords C & D. The flow conditioner was installed with the blockage at the bottom of the pipe. As the gas flowed through the open holes, there was a low-pressure created just downstream of the blocked area causing the gas to then accelerate downward, thus causing the higher velocity at the bottom of the meter.

The Profile Factor for this 12-inch meter, as determined from Figure 16, is 1.105. This difference doesn't seem like much, but it certainly indicates a significant change in profile. Typically a meter will generate a Profile Factor, after installation in the field, that is repeatable to ±0.02, but that depends upon the piping, and makes the assumption that there are no other changes like flow conditioner blockage.

The next question is what was the impact on accuracy with this distorted velocity profile? Figure 17 shows the result of the three tests velocities and the impact on metering accuracy.

Velocity (m/s)	% Error
18	0.22
12	0.19
6	0.17

Figure 17 – Blocked Flow Conditioner Results

As can be seen the meter was affected by about +0.2% for all flow rates. In this case the meter slightly over-registered with this distorted profile. Later in this paper a more advanced diagnostic feature will also show the meter has blockage, but for now one can see the Profile Factor has indicated a significant change.

Monitoring the profile factor is a very valuable tool to identify a variety of problems. The previous example shows a change that most would say is relatively easy to understand. One of the questions many users have is "How can I determine if my meter is dirty?"

As contamination collects on the pipe wall, and of course on the inside of the meter, the profile will also change. This was discussed in a paper presented in 2004 summarizing the results of several dirty meters that were tested at a calibration facility both dirty and clean [Ref 6 & 7].

The method of determining the meter's condition is relatively simple. The profile tends to change such that the velocities on Chords B & C become higher relative to Chords A & D. This is due to the surface roughness of the upstream piping causing the velocity along the pipe wall to be lower. Thus, for a given amount of volumetric flow, if the velocity along the wall is lower, then the center will have to be higher to make up for it.

In order to determine this change, which typically occurs over time, it would be helpful to "trend" the Profile Factor. The USM software has this feature built-in so that the technician doesn't need to develop these manually. By using several periodic maintenance log files the software will develop a graphical representation of the profile factor, and several other diagnostic graphs as well. Figure 18 shows a 10-inch meter with a normal "trended" Profile Factor.

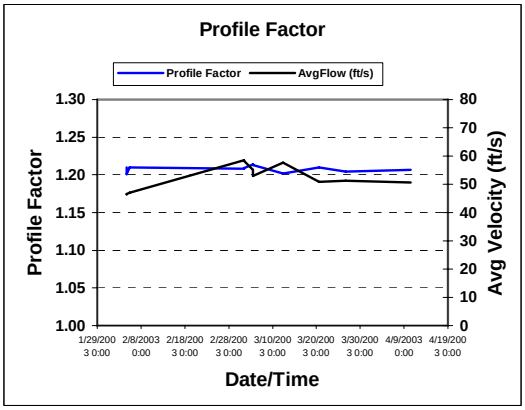

Figure 18 – Trended Profile Factor – Normal

The Profile Factor, which is in blue, to be running about 1.208 for this period of time (approximately 8 months).

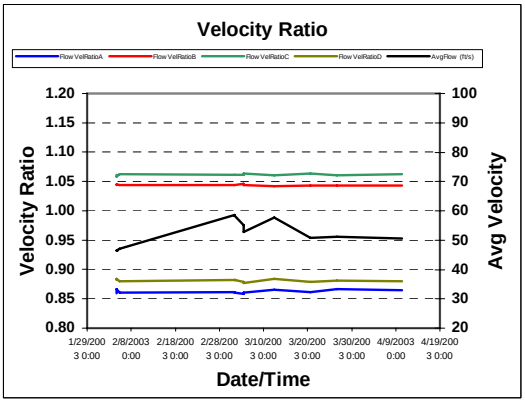

Figure 19 – Chord Ratios of Clean meter

Figure 19 shows the chord velocity ratios for this clean meter over the same period. Notice how the chord ratios remain very stable over these several months.

Figure 20 shows a meter that has some change in the Profile Factor over time. The Profile factor starts out at about 1.198 and gradually increased to about 1.270 after about 9 months. After the first 9 months the Profile Factor basically remains the same, indicating additional contamination is probably not occurring. This meter had been cleaned just prior to the collection of these log files.

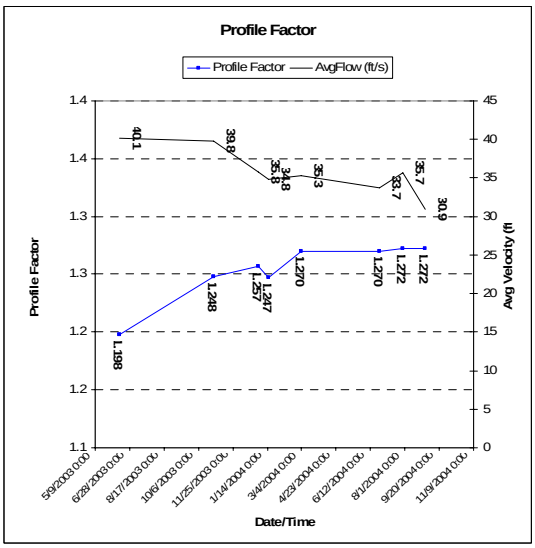

Figure 20 – Trended Profile Factor – Dirty

Figure 21 shows how the chord ratios for this dirty meter were also changing over time. Of course one would expect this since the Profile Factor is developed from all four chords.

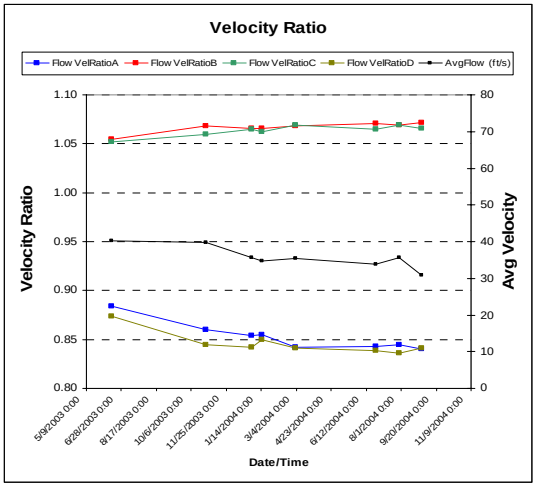

Figure 21 – Chord Ratios of Dirty Meter

As expected the inner chords (B&C) from Figure 21 begin registering faster relative to the meter's average, and the outers (A&D) are now reading lower. Notice how consistent the change is from the beginning to the end of the trend file. Both inners change about the same, and both outers also track each other very closely. This may not always be the case depending upon how uniform the coating inside the meter is.

Figures 22 and 23 show the inside of the dirty meter tube and the meter prior to cleaning. The buildup is relatively thin. As the transducers do not protrude beyond the edge of the meter, the transducer have not contamination on them.

Figure 22 –Dirty Upstream Meter Tube

Although the chord ratio change is subtle, it is apparent when trended and then used to develop the Profile Factor. It is clear change is occurring in this meter. Trending makes it very easy to see that something is happening to this meter. It might not be obvious that change is occurring if the technician were to only look at the monthly maintenance log file. Without periodic collection of maintenance log files, identifying this condition would be more difficult.

Figure 23 –Dirty 10-inch Meter

When a meter becomes dirty one question that is often asked is "how does this affect the meters' accuracy?" Several papers have been published on this issue [Ref 6, 7, 8 & 9]. Figure 22 shows the error results from this 10-inch meter calibrated dirty and clean.

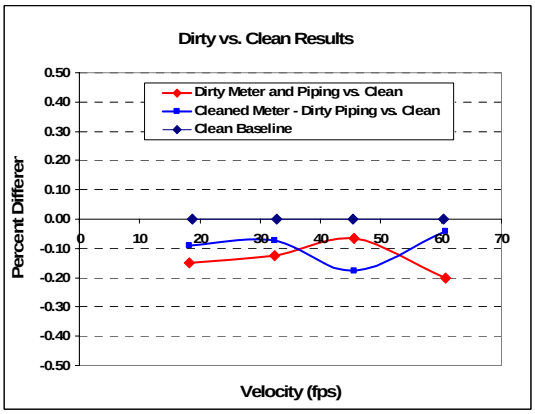

Figure 24 – 10-inch Dirty vs. Clean Results

Figure 24 shows this 10-inch meter registered about -0.14% FWME (slow) when dirty as compared to clean (red line). The blue line represents the meter clean and the piping still dirty. In this case the meter registered approximately -0.093% (slow). This test shows simply cleaning the meter body does not restore the meter's accuracy.

Registering slightly slow has been seen in other sized chordal meters when they become dirty. There is no guarantee that all meters will under-register when dirty, but certainly several results that have been published show this trend.

Figure 26 shows how the Profile Factor shifted back to normal on this meter after being cleaned. Additional flow rate data points were included as the meter was calibrated throughout the range of normal operation.

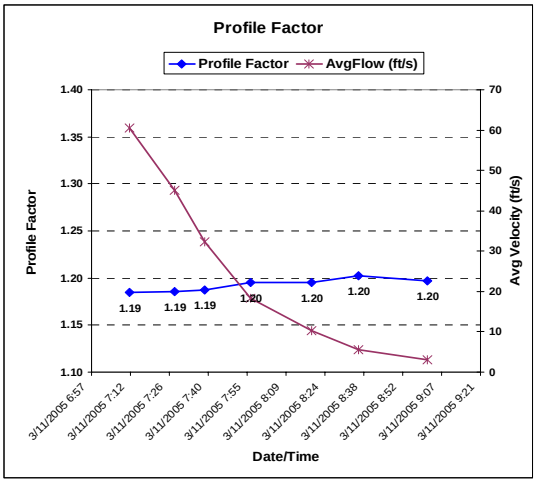

Figure 25 – Profile Factor After Cleaning

This 10-inch meter exhibited an approximately change of approximately 0.074 in the Profile Factor and registered slightly slow when dirty compared to its clean condition. Additional data is required to determine if there is a correlation between Profile Factor change and meter error. If such a correlation exists, then it may be possible to someday predict error based upon Profile Factor change.

Speed of Sound

Probably the most discussed and used diagnostic tool is of an ultrasonic meter is the speed of sound (SOS). The reader may recall that speed of sound on an individual chord is basically the sum of the transit times divided by their product, all then multiplied by the path length. A more detailed discussion on this can be found in a previously presented paper [Ref 10}.

There are at least 2 ways of looking at SOS. The first would be to compare each path's SOS to the meter, or to the other paths. Typically the agreement with today's technology is within ±0.3 m/s during normal operation. At lower and higher velocities there can be some variance from this norm.

Figure 26 shows a trend graph of each chords SOS relative to the meter over a period of several months. This is a very easy way to compare them rather than looking at the absolute value of each chord.

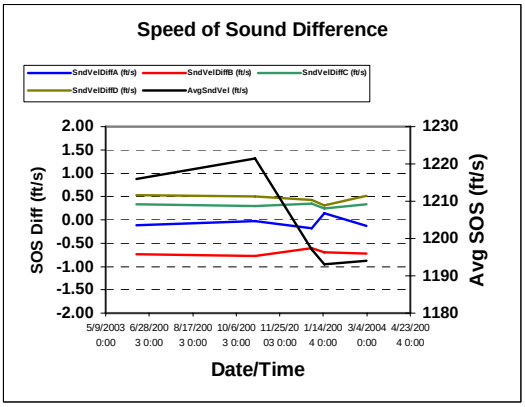

Figure 26 – SOS Difference Over Time

One of the important features about looking at SOS difference is identifying potential buildup on the face of the transducer. If grease or a combination of oils and mill-scale coated the transducer face, one or more of the chords would be changing. Figure 25 shows a meter with a significant difference in SOS between Chord D and the remaining.

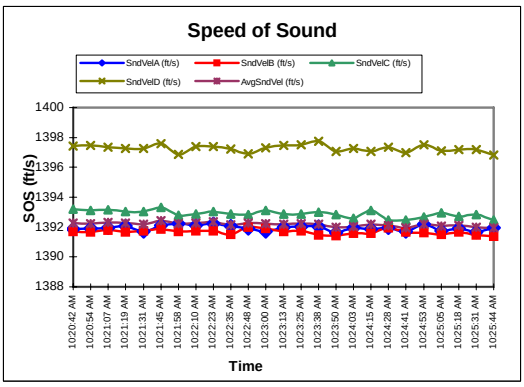

Figure 27 – Chord D Contaminated

Figure 27 was taken from a monthly maintenance inspection log file. This graph shows the actual reading of SOS for each chord, and it clearly shows a SOS difference in Chord D relative to all other chords. Typically all SOS values will be within 1 m/s maximum spread, but here there is about 2 m/s difference in Chord D relative to all others.

Looking at the SOS difference chart, shown in Figure 28, shows how different this chord's reading relative to the others.

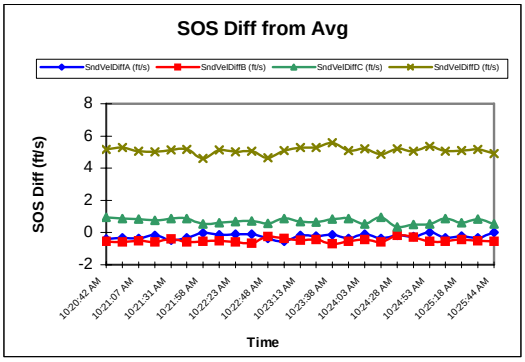

Figure 28 – SOS Difference - Contamination

This SOS difference is graphed at the same time as the graph showing all the meter's reported chord SOS values. Each graph clearly shows a problem, but when the difference between the chords is small, the SOS difference graph makes it easier to see there is a problem.

If the meter is being subjected to significant levels of ultrasonic noise from a control valve, prior to total failure of the meter one might see an occasional pulse detection error. This is also known as a peak switch. This may occur intermittently as shown in Figure 29, or it may be a permanent switch that would continuously show a difference of several fps in SOS.

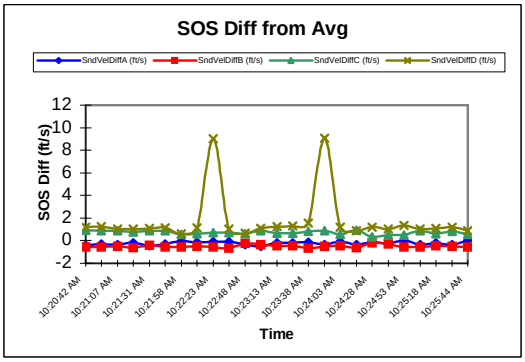

Figure 29 –Intermittent Peak Switch Problem

When this condition occurs the meter will provide an alarm indicating there is a problem. This is a configurable value that is typically set to 0.5% of the meters' SOS reading. This helps identify this condition and it is also logged in the event log, including the date and time it occurred. Once the SOS returns to normal (something less than the 0.5% difference), the alarm will clear.

When a meter is operated at lower velocities, typically less than 1 m/s, and there is a significant difference between the gas and atmospheric temperature, heat transfer can occur. As the heat transfer occurs, internal temperature gradients can develop. When this happens the hotter gas inside the pipe rises to the top. Since the speed of sound in the gas is relatively sensitive to temperature, this will be seen as a SOS difference between the chords. This is often called thermal stratification.

Figure 30 shows an example of a 16-inch meter at the calibration lab. The temperature of the gas is quite a bit higher than the ambient, so at lower velocities there is some stratification inside the pipe. If the gas and ambient temperatures were the same, then no stratification would occur.

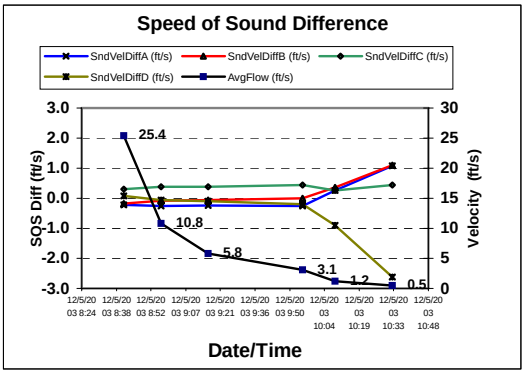

Figure 30 – Thermal Stratification

From this example it appears that somewhere around 1 m/s there is a possibility that thermal stratification can occur. This will cause some increase in measurement uncertainty for at least two reasons. First, the temperature reading by the RTD will most likely not be representative of the average gas temperature. This will lead to errors when converting from uncorrected to corrected volumes. Second, as illustrated in Figures 12 & 13, the velocity profile is also affected. This can cause the uncorrected reading of the meter to be in error if it were different than at the time of flow calibration.

This difference in profile is probably not more than a very few tenths of a percent under most conditions and is supported by the results in Figure 31.

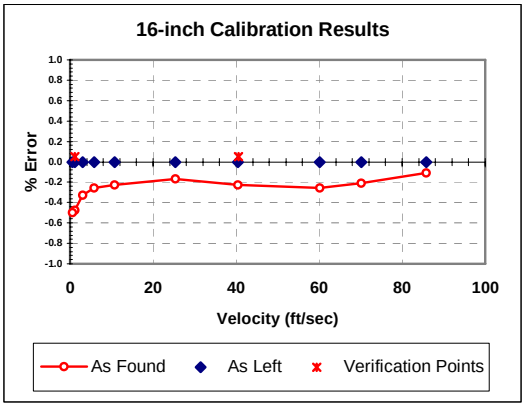

Figure 31 – 16-inch Low-Flow Error

This meter was calibrated to 0.15 and 0.3 m/s. Both error points are virtually the same making it look as though only one data point was taken. The error difference between the 0.15 and 0.3 m/s is less than 0.03%. Thus, even with the chord velocities looking very 'skewed" at the time of flow calibration, as shown in Figures 12 & 13, the metering accuracy is not significantly affected.

ADVANCED DIAGNOSTIC INDICATORS

During the past several years an additional diagnostic feature has been studied by Engineering. This feature, called "Turbulence," is discussed thoroughly in a previous paper [Ref 10]. Essentially Turbulence is a measure of the variability of each chords' velocity readings during the time the meter was sampling, and is provided each time it updates the velocity information. This gives the technician an idea of the steadiness of the flow as seen by the meter.

Typically the level of turbulence on a BG design shows the A & D Chords have 2-4%, and the B & C Chords have 1-2%. This is based upon the history of hundreds of meters. The outer Chords A & D, being closer to the pipe wall, always exhibit higher turbulence by about a factor of 2.

Turbulence can be computed from the maintenance log file for older meters. With the advent of more advanced electronics, it is now computed real-time in the meter and reported on the maintenance log files. This greatly reduces the time for analysis since it is not only stored in the log file, it is graphed out automatically for quick review.

Recently viewing Turbulence has solved several metering problems. Distorted velocity profiles often cause concern about metering accuracy. If the velocity profile, as shown in Figure 14, now appears like that in Figure 16, the cause needs to be determined. Some might feel this is just due to upstream affects and may not believe there is any object blocking the flow conditioner.

Figure 32 shows the turbulence level for this 12-inch meter is normal. It was collected at the time of calibration and the velocity was about 12 m/s.

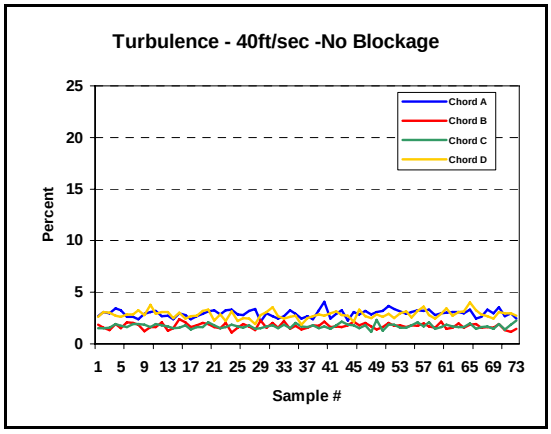

Figure 32 – Normal Turbulence

The 12-inch meter in Figure 32 shows a very consistent level of Turbulence during the period of the test. Figure 33 is the same meter with a blocked flow conditioner as shown in Figure 15.

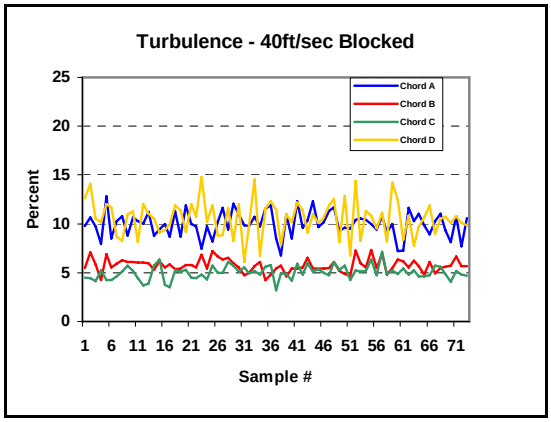

Figure 33 – High Turbulence of 12-inch Meter

It is clear that the turbulence in Figure 31 is about 3 times higher. Certainly the velocity profiles for this meter, shown in Figures 14 and 16, look different. Anyone looking at the blocked profile would immediately recognize there is a problem. It is possible, however, to have a complete blockage of a flow conditioner with something like a porous bag and have a relatively symmetrical profile. In this situation the turbulence would be excessive, indicating

there is a problem with blockage. This has been observed in the field and without Turbulence it would have gone un-detected.

Figure 34 is an example of turbulence is from a 12-inch meter. This meter is installed with a single-bounce meter downstream for checking. This customer uses the single-bounce meter to help insure measurement accuracy. When a deviation is observed, the metering system is investigated. Such a deviation occurred recently and one can also see the elevated turbulence at this time.

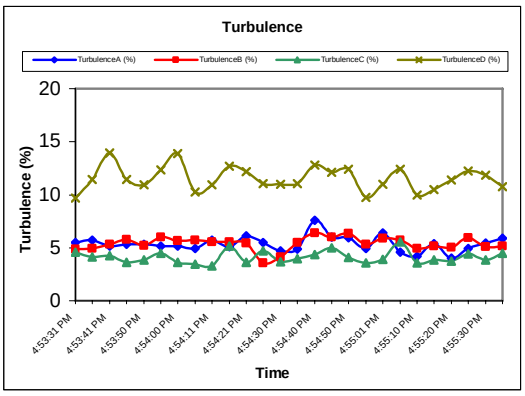

Figure 34 – High Turbulence on 12-inch Meter

This meter is equipped with an older generation of electronics. In order to determine the turbulence it must be manually computed from the log files. Newer generation electronics automatically computes the turbulence and stores it in the hourly archive logs. In this way it is possible to identify to within 1 hour when the blockage occurred.

Figure 35 – 12-Inch Meter Blockage

Figure 35 shows the reason for the shift in meter performance between the 4-path chordal meter and the single-bounce meter. This blockage was just upstream of the flow conditioner.

When looking at the chord ratios with the blockage it is very clear that something has distorted the profile. Figure 36 shows the velocity profile is very non-symmetrical with much higher velocities at the top of the pipe.

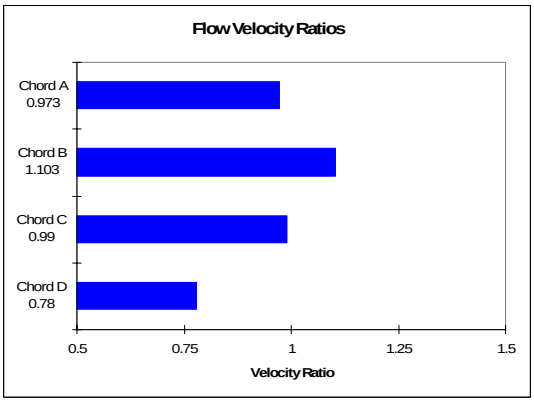

Figure 36 – Chord Ratios of 12-Inch Meter

Figure 37 shows the chord ratios after the blockage is removed. This is the look of a normal profile.

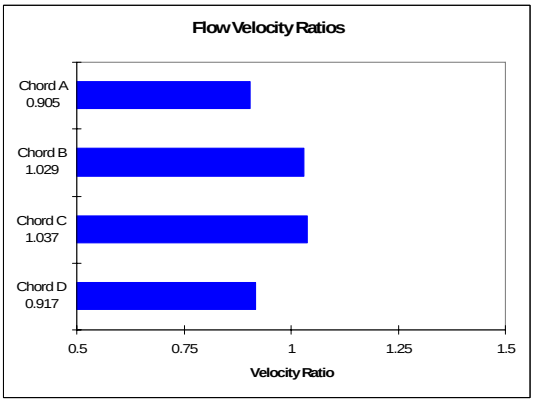

Figure 37 – Chord Ratios of 12-Inch Meter

After the blockage is removed the turbulence levels return back to a more normal value of 2-4% for the A and D chords and 1-2% for the B and C chords, as shown in Figure 38.

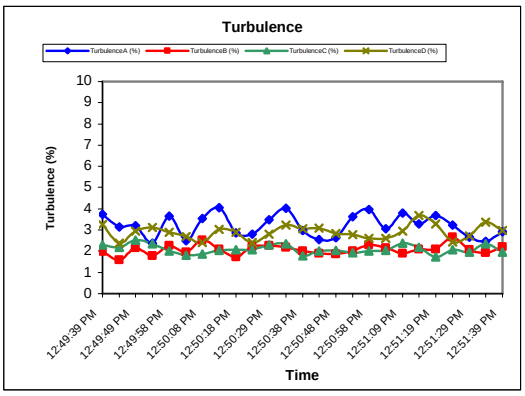

Figure 38 – Chord Ratios of 12-Inch Meter

Another way of looking at distorted velocity profiles is to compare the sum of Chord A & B with the sum of Chords C & D. This is discussed in detail by a paper presented by Klaus Zanker [Ref 10]. He defines this as Symmetry. Figure 39 graphs the Symmetry, and we see that there is a significant shift from the normal.

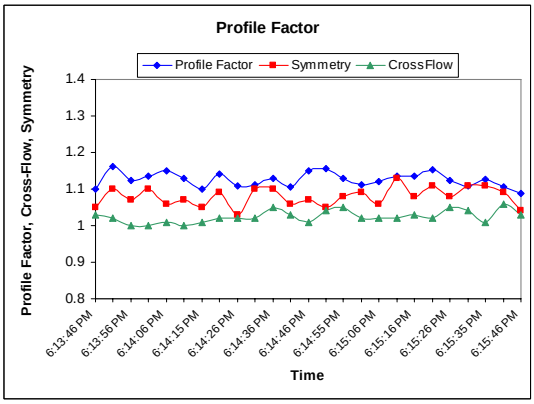

Figure 39 – Symmetry of 12-Inch Meter

Figure 39 is a graph not only of the profile factor (blue line), but the red line represents symmetry and the green is Crossflow. Crossflow is also defined in Klaus' paper as Chords (A+C)/(B+D). Note the Profile Factor is not very steady, indicating a very turbulent, changing flow pattern. Normally both Crossflow and Symmetry will be very close to 1.00, but as we can see the Symmetry is closer to 1.10. Figure 40 show the same graph after the obstruction is removed.

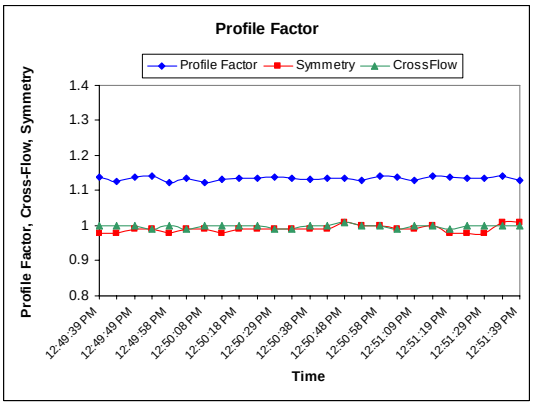

Figure 40 – Symmetry of 12-Inch Meter

With the obstruction removed the Symmetry and Crossflow both return to normal (approximately 1.00), and the Profile Factor is more consistent.

Another diagnostic tool is comparing the computed SOS to that reported by the meter. This has been done for years by using an external program and reporting the difference on the inspection report. This is one good method for identifying if the metering system has a problem. Figure 41 shows such a calculator.

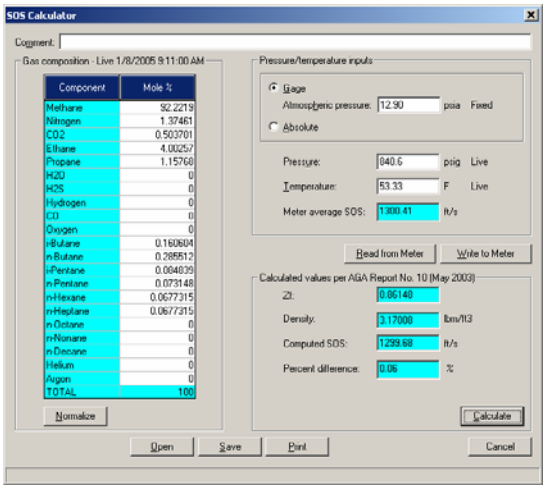

Figure 41 – Actual SOS vs. AGA 10 SOS

The problem with doing this only at the time of inspection is that there can be an intermittent problem that would go undetected. The latest generation of ultrasonic electronics can now perform this on a real-time basis and also store on the hourly log files. This permits a more thorough monitoring of not only the meter, but the gas chromatograph as well.

Figure 42 shows a graph of the meter's reported SOS and that from the meters' computed SOS using the AGA 10 algorithm.

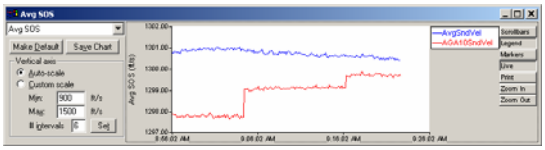

Figure 42 – Actual SOS vs. AGA 10 SOS

This example shows how the SOS, in red, moves closer to the meters' reported SOS (in blue). The cause of this is most likely a delay in the gas sampling process. In this case the GC has a 12-minute update interval (two-stream GC). By seeing how the computed SOS trails the meter's SOS one can see the impact having the sample updated in the GC quicker to insure more timely computation.

Generally if the computed AGA 10 SOS does not agree with the meter's reported SOS, more often than not the problem is with the temperature measurement or the gas chromatograph. The big benefit for computing SOS on a real-time basis is to help insure meter station health.

If the meter and AGA 10 SOS agree it should not be assumed the meter's accuracy has not changed. The AGA 10 SOS comparison shown in the 10-inch dirty meter example did not show any deviation over time. Since there was no contamination on the transducers, the meter's path length was unaffected, and thus the meter's SOS registered correctly.

CONCLUSIONS

During the past several years the industry has learned a lot about USM operational issues. The traditional 5 diagnostic features, gain, signal-to-noise, performance, chord velocities and SOS have helped the industry monitor the USM. These 5 features provide a lot of information about the meter's health. Getting an initial baseline on the meter at the time of installation, and monitoring these features on a routine basis can generally identify metering problems identified in advance of failure.

One major benefit to the USM is that it provides information that can also be used to diagnose the entire metering facility. By looking at the AGA 10 SOS vs. the meter's reported SOS, potential problems with gas analysis or temperature can be spotted. However, as powerful as the basic diagnostic indicators are, new features are being developed.

These more advanced diagnostic indicators, such as Turbulence, Symmetry, Crossflow and real-time SOS computation are paving the way to allow the meter to become virtually maintenance-free. In the future it is likely that a meter will have enough power and intelligence to quickly identify potential measurement problems on a real-time basis.

As the industry learns more about the USM, and the operation of their own measurement system, the true value of the ultrasonic meter will be recognized. The USM industry is still relatively young and technology will continue to provide more tools to help solve today's measurement problems.

REFERENCES

1. AGA Report No. 9, *Measurement of Gas by Multipath Ultrasonic Meters*, June 1998, American Gas Association, 1515 Wilson Boulevard, Arlington, VA 22209
2. John Lansing, Basics of Ultrasonic Flow Meters, American School of Gas Measurement Technology, 2000, Houston, Texas
3. AGA Report No 10, *Speed of Sound in Natural Gas and Other Related Hydrocarbon Gases*, July 2002, American Gas Association, 1515 Wilson Boulevard, Arlington, VA 22209
4. BSI 7965:2000, Guide to the Selection, Installation, Operation & Calibration of Transit Time Ultrasonic Flowmeters for Industrial Gas Applications
5. Larry Garner & Joel Clancy, Ultrasonic Meter Performance – Flow Calibration Results – CEESI Iowa – Inspection Tees vs. Elbows, June 2004, Estes Park, CO
6. John Lansing, *Dirty vs. Clean Ultrasonic Flow Meter Performance*, North Sea Flow Measurement Conference, October 2004, St. Andrews, Scotland
7. John Lansing, *Dirty vs. Clean Ultrasonic Flow Meter Performance*, AGA Operations Conference, 2002, Chicago, IL
8. John Stuart, Rick Wilsack, Re-Calibration of a 3-Year Old, Dirty, Ultrasonic Meter, AGA Operations Conference, 2001, Dallas, Texas
9. James N. Witte, *Ultrasonic Gas Meters from Flow Lab to Field: A Case Study*,

AGA Operations Conference, 2002, Chicago, IL

10. Klaus Zanker, *Diagnostic Ability of the Daniel Four-Path Ultrasonic Flow Meter*, Southeast Asia Flow Measurement Workshop, 2003, Kuala Lumpur, Malaysia
11. Klaus Zanker, The Effects of Reynolds Number, Wall Roughness, and Profile Asymmetry on Single and Multi-Path Ultrasonic

23rd International North Sea Flow Measurement Workshop
Tønsberg, Norway, 18 - 21 October 2005

RECIPROCITY AND ITS UTILIZATION IN ULTRASONIC FLOW METERS

Per Lunde, Christian Michelsen Research AS, Box 6031 Postterminalen, N-5892 Bergen, Norway.
Magne Vestrheim, University of Bergen, Allégaten 55, N-5007 Bergen, Norway.
Reidar Bø, Christian Michelsen Research AS, Box 6031 Postterminalen, N-5892 Bergen, Norway.
Skule Smørgrav, FMC Kongsberg Metering, Kirkegårdsvn. 45, Box 1012, 3601 Kongsberg, Norway.
Atle K. Abrahamsen FMC Kongsberg Metering, Kirkegårdsvn. 45, Box 1012, 3601 Kongsberg, Norway.

ABSTRACT

In ultrasonic transit time flow meters for gas and liquid (USMs), the flow direction, the flow velocity and the sound velocity are estimated from the measured up- and downstream transit times. At no-flow conditions, the up- and downstream transit times of such meters should ideally be the same, or the difference should be negligible. This may not be the case unless special precautions are made. In order to reduce the possibility of the meter to detect a false flow at no-flow conditions, USMs are typically "dry calibrated" before being installed in the field. "Dry calibration" (which may be made in different ways), in general involves measurement of (a) the time delays due to electronics, cables and transducers, (b) the socalled "Δt-correction" (for each acoustic path, also denoted "zero flow offset factor"), and (c) geometrical parameters. Various Δt-correction approaches may be used by different manufacturers, but these are basically similar and have the same purpose: to reduce the false flow detection and improve the accuracy at low and no-flow conditions ("zero flow adjustment"), without significantly affecting the accuracy at the high velocity measurements. The AGA-9 report and the API MPMS Ch. 5.8 standard both prescribe need for "zero flow verification test (zero test)" or "zeroing the meter", for gas and liquid USMs, respectively.

Advances in USM technology based on the electroacoustic reciprocity principle have provided methods for reduction or even neglection of the need for "Δt-correction" of USMs. That means, if the USM measurement system is reciprocal, and operated in a "sufficiently reciprocal" way, the "Δt-correction" may be negligibly small over the operational range of pressure and temperature, and irrespective of whether the transducers are equal or not. Thus, "dry calibration" may be simplified, since reciprocal operation may provide possibilities for "auto-zeroing" of the USM.

However, reciprocal operation is not an "obvious" property of an USM. Even though the USM measurement system consisting of two transducers, electronics, etc. (e.g. an acoustic path), may be reciprocal, it may not necessarily be reciprocally *operated*. Control and careful design is essential to realize reciprocal operation at no-flow conditions in an acoustical measurement system such as a USM.

In the present paper, reciprocal operation of USMs is discussed on basis of general electroacoustical principles, and related to utilization in ultrasonic flow metering of gas and liquid. Criteria for "sufficient reciprocal operation" of a USM are developed. It extends earlier works by (a) taking into account finite-valued electrical impedances of the electronics and the transducers employed in the meter, (b) deriving specific design criteria for "sufficient reciprocal operation" of a USM, in terms of requirements for the electrical impedances of the electronics and transducers, and (c) giving criteria for transducer manufacturing reproducibility, in terms of bounds for variations of the phase of the transducer impedances. In addition, use of the transducer input signal as the reference for the transit time measurements is discussed in this respect, which is shown to provide reduced requirements for achieving "sufficient reciprocal operation". Laboratory measurements and USM "dry calibration" measurements made over a range of pressures, temperatures and signal levels ("firing voltages"), in combination with theoretical calculations, are used to demonstrate reciprocal operation and validity of the theoretical results, also for transducers not being equal in performance (due to production variations). Violation of reciprocity by e.g. "nonlinear driving" of the transducers is demonstrated. Consequences for USMs are addressed, such as e.g. (a) simplified "dry calibration" and cost reduction, (b) improved linearity at low flow velocities, and (c) improved accuracy at low flow velocities (in relation to temperature, pressure, ageing drift, etc.). The paper provides insight into the significance and potentials of utilizing reciprocity in USM technology, as well as the improvements already achieved by realizing "sufficient reciprocal operation" in high precision flow meters for gas and liquid.

1. INTRODUCTION

Ultrasonic transit time flow meters for gas and liquid (USMs) are gaining increased popularity for custody transfer and allocation metering of gas and oil. AGA recommendations on gas USMs were

issued in 1998 [1] (this document is presently under revision), a handbook on uncertainty evaluation of gas USM metering stations was prepared in 2001 [2,3], an API standard on liquid ultrasonic meters was issued in February 2005 [4], an ISO standard on gas USMs is under development [5], etc.

In such meters the flow direction, the flow velocity and the sound velocity of the fluid are estimated from the measured up- and downstream transit times. These transit times are obtained by transmitting and detecting acoustic pulses up- and downstream with respect to the direction of the flow, using ultrasonic transducers and dedicated electronics. One or several acoustic paths may be used, depending on the accuracy required. For further details, cf. e.g. [1-6]. Fig. 1 shows a cross-section of such a meter, schematically.

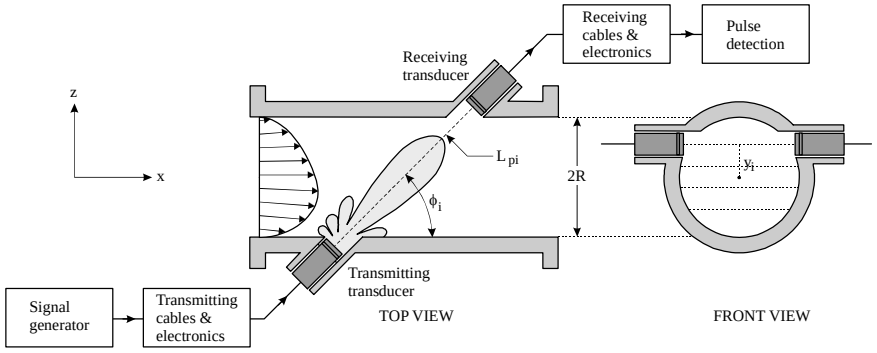

Fig. 1. Schematic illustration of a single path in a multipath ultrasonic transit time flow meter with non-reflecting paths (for downstream sound propagation). (Left: centre path example (y_i = 0); Right: path at lateral chord position y_i.)

In ultrasonic transit time flow meters with reflecting or non-reflecting paths, the volumetric flow rate (at line conditions) is given as [1-6]

$$q_{USM} = \pi R^2 \bar{v}_A, \qquad \bar{v}_A = \sum_{i=1}^{N} w_i \bar{v}_i, \qquad \bar{v}_i = (N_{refl,i} + 1)\frac{2\sqrt{R^2 - y_i^2}\,(t_{1i} - t_{2i})}{t_{1i} t_{2i} \left|\sin 2\phi_i\right|}, \tag{1}$$

where (cf. Fig. 1), R is the inner radius of the USM meter body; $\bar{v}_A$ is the axial volume flow velocity (at line conditions); N *is* the number of acoustic paths; i is the path number; w_i is the integration weight factor for path no. i; $\bar{v}_i$ is the average axial flow velocity along path no. i (i.e. the line integral along the path); y_i is the lateral distance from the pipe center (lateral chord position) for path no. i; L_i is the interrogation length for path no. i; ϕ_i is the inclination angle (relative to the pipe axis) of path no. i; t_{1i} and t_{2i} are the measured transit times for upstream and downstream sound propagation of path no. i; and $N_{refl,i}$ is the number of wall reflections for path no. i ($N_{refl,i}$ = 0, 1 or 2 in current USMs), i = 1, …, N.

For convenience in the discussion, define

$$\Delta t_i \equiv t_{1i} - t_{2i} \tag{2}$$

as the transit time difference for path no. i, i = 1, …, N. At no-flow conditions, the measured up- and downstream transit times of such meters should ideally be the same, i.e. Δt_i should be zero. Alternatively, the difference should be negligible. This may not be the case unless special precautions are made. It is by no means obvious that the upstream and downstream transit times of a single path in a USM are equal in a no-flow situation.

In order to reduce the possibility of the meter to detect a false flow at no-flow conditions, USMs are typically "dry calibrated" before being installed in the field. "Dry calibration" (which may be made in

various ways), in general involves measurement of (a) the time delays due to electronics, cables and transducers, (b) the socalled "Δt-correction"[1] (for each acoustic path), and (c) geometrical parameters. Various Δt-correction approaches may be used by different manufacturers, but these are basically similar and have the same purpose: to reduce the false flow detection and improve the accuracy at low and no-flow conditions ("zero flow adjustment"), without significantly affecting the accuracy at the high velocity measurements [1,4][2]. For typical ultrasound transducers, the Δt-correction may vary with pressure (P) and temperature (T). Whether the Δt-correction is measured at a single P-T point, or at a multitude of P-T points, common practice varies between the USM manufacturers.

For several reasons, it would be highly advantageous to avoid use of any Δt-correction in the USM. Use of Δt-correction may contribute to increase the cost of "dry calibrating" the meter, since this adds another parameter to be measured, possibly over a range of pressures and temperatures. More important, the use of Δt-correction may impose possible uncertainties connected to drift of Δt_i, related to pressure, temperature and ageing characteristics of the transducers. Use of Δt-correction may also complicate the zero-flow validation of the meter in case of transducer exchange, since the "old" Δt-correction value is not necessarily valid after a transducer replacement. Such factors may influence on the USM measurement at low flow velocities, such as false flow detection.

Various authors (e.g. [9-19]) have therefore discussed methods to automatically remove (or reduce) the false flow detection at low- and no-flow conditions in USMs, i.e. to ensure that Δt_i is sufficiently close to zero. These methods have been based on electroacoustical reciprocity, and various approaches to achieve reciprocal operation of the USM.

Reciprocal operation is by no means an "obvious" property of a USM. One has to distinguish between the two concepts "electroacoustical reciprocity" and "reciprocal operation" of an electroacoustic system. Although the electroacoustic system may be *reciprocal*, it does not need to be *reciprocally operated*. By "electroacoustical reciprocity" it is referred to the condition given by Eq. (7) below. Reciprocal operation, on the other hand, means that when the system is (a) driven from one side (I) and a measurement signal is received at the other side (II), and (b) driven in the same way from the other side (II) and a measurement signal is received at side (I), the two measurement signals obtained in the two different driving cases are identical (both with respect to magnitude and phase).

By employing a relationship derived in [7,8] (Eq. (30) of ref. [8], cf. also Eq. (8) below), Hemp [9] indicated a technique by which zero-flow time differences and associated zero drift in an ultrasonic flowmeter can be reduced or even eliminated. Basically it was proposed to drive the transmitter with a voltage pulse and detect the current pulse at the receiver, or *vice versa*. This technique which has been elaborated in more detail in Refs. [10-13], was proposed to achieve reciprocal operation of the electroacoustic system. However, no condition (or design criteria) for "*sufficient* reciprocal operation"

---

[1] By AGA-9 (Section 6.3) [1] the "Δt-correction" is denoted "zero flow offset factor".

[2] By AGA-9 (Section 6.3) [1] and API MPMS Ch. 5.8 (Section 12.7) [4] this procedure is referred to as "zero flow verification test (zero test)" and "zeroing the meter", respectively, and involves checking the meter at "zero flow" conditions, e.g. using blind flanges, at stabilized pressure and temperature conditions.

By AGA-9 (Section 6.3) [1] it is stated that: (1) "To verify the transit time measurement system of each meter, the manufacturer shall perform a Zero Flow Verification Test", and (2) "The manufacturer may also implement a zero flow offset factor, in engineering units of positive or negative feet per second or meters per second. This zero flow offset factor would be applied to the meter's flow-rate output. Use of this factor is intended to improve the accuracy of the low gas velocity measurements, while not significantly affecting the accuracy of the higher velocity measurements. This zero-flow offset factor, if used, shall be documented by the manufacturer".

By API MPMS Ch. 5.8 (Section 12.7) [4] it is stated that: "Zeroing an UFM is a procedure that involves checking the output while the meter is blocked-in. Under these conditions, and if the output of the meter does not indicate zero flow, then the manufacturer's (re-)zeroing procedure shall be followed. Whenever the meter is re-zeroed, it shall be reproved. Normally, a UFM does not require manual zeroing. However changes or replacement of transducers, electronics or transducer cables shall require that the meter zero be checked and if necessary (re-)zeroing procedures shall be followed. In any case, changes or replacement of transducers, electronics or transducer cables shall require the UFM to be reproved".

was discussed, for a set of given transducers and electronics. That is, the effects of finite impedances of the transducers and the transmitting and receiving electronics were not accounted for.

By Sanderson and Torley [14] the technique of reciprocal operation proposed by Hemp [9-11] to reduce zero drifts in USMs was tried out experimentally in an ultrasonic transit time clamp-on flow meter for liquid, using voltage transducer driving and current detection of the received signal.

In connection with ultrasonic gas flow meters for household application, von Jena et al. [15,16] also demonstrated high degree of reciprocal operation (at low firing voltages), as well as violation of reciprocal operation by non-linearity (at high firing voltages). The "zero offset" (i.e. Δt_i) was measured as a function of firing voltage of the transmitting transducer, for different terminating electronics (for reciprocal as well as non-reciprocal set-ups). They concluded that zero-point stability can be achieved if (i) the response of the active components, i.e. the transducers, is linear, and (ii) "if the electrical termination of the input and output is made symmetrical" ("electrical symmetry").

Also by Martin et al. [17] a specific realization of electrical symmetry was proposed to achieve reciprocal operation of a liquid flow meter. Experimental data obtained for a USM given in Ref. [18] further demonstrate the importance of reciprocal operation of USMs.

On a general basis (i.e., from the theoretical principle of electroacoustic reciprocity, cf. e.g. Section 2), it is well known that if reciprocal operation of the measurement system holds, the transducers are allowed to be different in their characteristic parameters (as also pointed out in refs. [9-13] and [15,18], in connection with application to USMs). On the other hand, in a recent simulation study of the effects of non-identical ultrasonic transducers on reciprocity and "dry calibration" in transit time flow meters, van Deventer and Delsing [19] claimed that reciprocal operation holds only when the transmitting and receiving transducers are identical. They concluded that since it is only possible to manufacture identical transducers within a certain tolerance range, "dry calibration" of Δt_i is necessary, to establish a Δt-correction in the USM. These results are not in agreement with the conclusions of the present work.

In the present paper, reciprocal operation of USMs for gas and liquid is discussed on basis of a relatively general theory for linear, reversible and passive electroacoustic systems where the USM is represented in terms of a two-port electroacoustic system[3]. It extends earlier works by (a) taking into account finite-valued electrical impedances of the electronics and the transducers employed in the meter, (b) deriving specific design criteria for "sufficient reciprocal operation" of a USM, in terms of requirements for the electrical impedances of the electronics and transducers, and (c) giving criteria for transducer manufacturing reproducibility, in terms of bounds for variations of the phase of the transducer impedances (Section 2). In addition, use of the transducer input signal as the reference for the transit time measurements is discussed in this respect, which is shown to provide reduced requirements for achieving "sufficient reciprocal operation". Control and careful design is essential to realize reciprocal operation at no-flow conditions in an acoustical measurement system such as an USM. Laboratory measurements and USM "dry calibration" measurements made over a range of pressures, temperatures and signal levels ("firing voltages"), in combination with theoretical calculations, are used to demonstrate reciprocal operation and validity of the theoretical results, also for transducers not being equal in performance (due to production variations) (Section 3). Violation of reciprocity by e.g. "nonlinear driving" of the transducers is demonstrated. Consequences for USMs are addressed, such as e.g. (a) simplified "dry calibration" and cost reduction, (b) improved linearity at low flow velocities, and (c) improved accuracy at low flow velocities (in relation to temperature, pressure, ageing drift, etc.) (Section 4). The paper is intended to provide insight into the significance and potentials of utilizing reciprocity in USM

[3] Alternatively, and with the same results, the present analysis could have been based on the much more general theory of passive, linear electroacoustic systems due to Primakoff and Foldy [7,8]. This is so because Eq. (8) derived and used here is the same as Eq. (30) in [8], which was shown to be more generally valid than the two-port system model used here.

technology, as well as the improvements already achieved by realizing "sufficient reciprocal operation" in high precision flow meters for gas and liquid.

2. THEORY

In the present section the USM measurement system is represented in terms of a two-port electroacoustic system, and the theory of such systems is used to derive specific criteria for "sufficient reciprocal operation" of a USM.

2.1 Conditions for electroacoustic reciprocity in USMs

Consider a single path in a USM as shown in Fig. 1, at a no-flow situation. It is assumed that this electroacoustic system is (a) linear (i.e., that the signal levels are sufficiently low), (b) reversible (i.e., that the transducers can be used as both transmitter and receiver of sound), and (c) passive (i.e., that the power delivered by the transducer to the electrical or acoustical systems to which it is connected is derived from power absorbed by the transducer from these systems).

Denote the transducers at the left and right hand sides of the USM path shown in Fig. 1 by I and II, respectively. The portion of the path between the transmitting and receiving electronics (i.e. the two transducers I and II, and the fluid medium) can be described as shown in Fig. 2a. Here, V_I and I_I are the voltage and current at the electrical terminals of Transducer I, respectively, and V_{II} and I_{II} are the voltage and current at the electrical terminals of Transducer II, respectively. The directions chosen here for positive voltage and current are defined in the figure. All quantities are complex-valued, accounting for magnitude and phase.

(a)

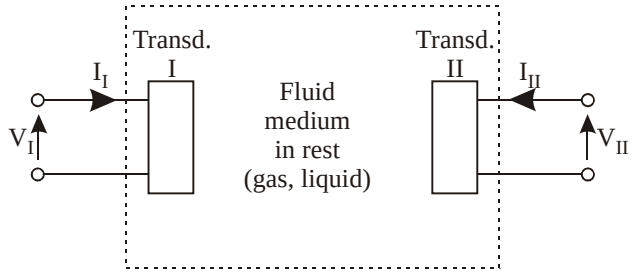

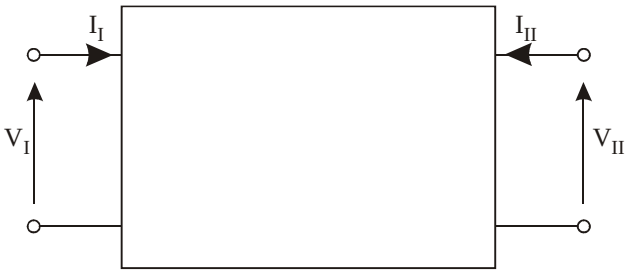

(b)

Fig. 2. (a) Schematic illustration of the "mid" part of the single USM path shown in Fig. 1, including the two transducers and the fluid medium. (b) Two-port ("black box") representation of the electroacoustic system shown in Fig. 2a.

The system shown in Fig. 2a can be represented by the two-port ("black box") electroacoustic system shown in Fig. 2b, where the "black box" includes the two transducers and the fluid medium inbetween. This two-port electroacoustic system is described by the two equations

$$\begin{aligned} V_I &= Z_{11} I_I + Z_{12} I_{II} \\ V_{II} &= Z_{21} I_I + Z_{22} I_{II} \end{aligned} \tag{3}$$

where Z_{11}, Z_{22}, Z_{12} and Z_{21} are the Z-parameters (impedance parameters) of the system. Note that the system is completely described by Z_{11}, Z_{22}, Z_{12} and Z_{21}. That means, if these four parameters are known, the properties of the electroacoustic system (the "black box") is also known. The two impedance parameters Z_{12} and Z_{21} (which are also referred to as transfer impedances) are defined as

$$Z_{12} = \left.\frac{V_I}{I_{II}}\right|_{I_I=0}, \qquad Z_{21} = \left.\frac{V_{II}}{I_I}\right|_{I_{II}=0}, \tag{4}$$

respectively.

Next, consider two-way operation of path no. *i* of the USM shown in Fig. 1, i.e. upstream and downstream electroacoustic signal propagation (still at no-flow conditions). Two-port electroacoustic representation of this situation is shown in Fig. 3, where parts (a) and (b) of the figure apply to up- and downstream propagation in path no. *i*, respectively. In part (a), $V_I^{(1)}$ and $I_I^{(1)}$ are the voltage and current at the input terminals of transducer I, which acts as transmitter of an acoustic signal to transducer *II*, acting as the receiver. At the output terminals of transducer II the voltage is $V_{II}^{(1)}$ and the current is $I_{II}^{(1)}$. In part (b) of the figure, the situation is *vice versa*. That is, transducer II is now the transmitter and transducer I is the receiver. The notation is also the same, except that superscript (1) is replaced by (2), reflecting downstream propagation[4].

(a)

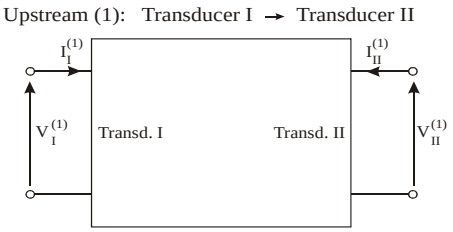

(b)

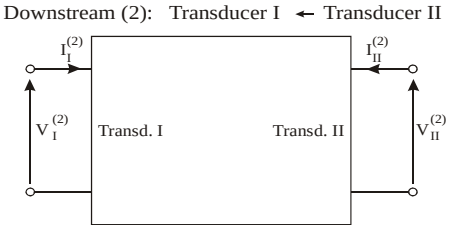

Fig. 3. Two-port ("black box") electroacoustic system representation of (a) upstream and (b) downstream signal propagation in the "mid part" of the single USM path shown in Fig. 1 (i.e. transducers and fluid medium), at no-flow conditions.

From Eqs. (3), the two-port equations for this situation become

$$\begin{aligned} V_I^{(1)} &= Z_{11} I_I^{(1)} + Z_{12} I_{II}^{(1)} \\ V_{II}^{(1)} &= Z_{21} I_I^{(1)} + Z_{22} I_{II}^{(1)} \\ V_I^{(2)} &= Z_{11} I_I^{(2)} + Z_{12} I_{II}^{(2)} \\ V_{II}^{(2)} &= Z_{21} I_I^{(2)} + Z_{22} I_{II}^{(2)} \end{aligned} \tag{5}$$

From Eqs. (5) it follows that

$$\left[V_I^{(1)} I_I^{(2)} - V_I^{(2)} I_I^{(1)}\right] \pm \left[V_{II}^{(1)} I_{II}^{(2)} - V_{II}^{(2)} I_{II}^{(1)}\right] = \left(Z_{12} \mp Z_{21}\right)\left[I_{II}^{(1)} I_I^{(2)} - I_{II}^{(2)} I_I^{(1)}\right]. \tag{6}$$

Eqs. (6) - which in fact are two equations (by applying the upper sign or the lower sign, respectively) - represent two general relations (properties) for a two-port electroacoustic system being operated in two directions. So far nothing has been assumed about reciprocity. If one of the conditions

[4] The notation of Primakoff and Foldy [8] is used here, as also used by Hemp [9-13].

$$Z_{12} = Z_{21} \qquad \text{or} \qquad Z_{12} = -Z_{21} \tag{7}$$

is fulfilled, the electroacoustic system is reciprocal or anti-reciprocal, respectively. In such cases Eqs. (6) reduce to

$$\left[V_I^{(1)} I_I^{(2)} - V_I^{(2)} I_I^{(1)}\right] \pm \left[V_{II}^{(1)} I_{II}^{(2)} - V_{II}^{(2)} I_{II}^{(1)}\right] = 0 \ , \tag{8}$$

where the plus and minus signs apply to reciprocal and anti-reciprocal systems, respectively. That is, in Eqs. (7) and (8) the plus sign is to be taken if the two transducers have electroacoustic coupling of the "same type" (e.g., if one is piezoelectric and the other piezoelectric or electrostatic, etc.), in which case the system displays electroacoustic reciprocity. The minus sign is to be taken if the two transducers have electroacoustic coupling of the "opposite type" (e.g., if one is piezoelectric and the other magnetostrictive or electromagnetic, etc.), in which case the system displays electroacoustic antireciprocity [8][5,6].

The first and second of Eqs. (7) are the conditions of electroacoustic reciprocity and electroacoustic anti-reciprocity, respectively. Eqs. (8) are general relations (properties) of reciprocal or anti-reciprocal two-port electroacoustic systems being operated in two directions. We shall here refer to Eqs. (7) and (8) as the "electroacoustic reciprocity conditions" and the "electroacoustic reciprocity relations", respectively[7].

Eqs. (7) are inherent properties of the electroacoustic system, which is represented by a two-port network. Whether Eqs. (7) are fulfilled or not, - i.e. whether the system is reciprocal or anti-reciprocal or not, for the electroacoustic system at hand, has to be checked by measurements (doing a "reciprocity check").

In the following, reciprocity of the electroacostic system will be assumed, i.e. that the condition $Z_{12} = Z_{21}$ is fulfilled, cf. Eq. (7). The + sign then applies in Eq. (8). Moreover, since the majority of transit time ultrasonic flow meters used today employ piezoelectric transducers, it is in the following assumed that the transducers are piezoelectric.

In general the quantities involved in the electroacoustic system addressed above will vary with time. In the derivation of Eq. (8) a steady state single frequency case was assumed, in which all of the quantities vary harmonically with time, with the same frequency, *f*. In Eq. (8) and in the following, the harmonic

---

5 It is worth noting that in a rigorous analysis, Primakoff and Foldy [7,8] have shown that Eqs. (8) (cf. Eq. (30) of Ref. [8]) are relations of very general validity for electroacoustic systems (far more general than the two-port systems considered here), provided certain sufficient conditions are met. These conditions are:

(a) the transducers are acoustically coupled via stationary bodies (fluid or solid media in contact, at no-flow conditions),
(b) the transducers and the cables, electronics and acoustic media to which they are connected behave perfectly linearly (i.e., the signal levels are assumed to be sufficiently low in amplitude),
(c) the transducers are passive (i.e., that the power delivered by the transducer to the electrical or acoustical systems to which it is connected is derived from power absorbed by the transducer from these systems),
(d) the coefficients in the constitutive relations governing the electroacoustic system satisfy certain "symmetry conditions",
(e) no magnetostrictive media and no static magnetic field are present in the transducers (that is, that the coupling is purely electrostatic or piezoelectric or both), or that no piezoelectric media and no static charge density are present in the transducer (that is, that the coupling is purely electromagnetic or magnetostrictive or both), and
(f) the transducers do not radiate electromagnetic waves from their surfaces.

6 Note that the generality of the relation given by Eq. (8) means that it may be applied e.g. to different types of flowmeters, such as for example ultrasonic flowmeters (various types), electromagnetic flowmeters and Coriolis mass flowmeters [12].

7 A comment on this terminology may be useful. In Refs. [9-13] the relationship given by Eq. (8) (Eq. (30) of ref. [8]) is referred to as the "electroacoustic reciprocity theorem". By other authors (e.g. [7,8]) another relationship (between the source and receiving sensitivities of a transducer) is referred to as the "electroacoustic reciprocity theorem" (Eq. (51) of ref. [7]). These two relationships are not necessarily equivalent. Eq. (8) is a relationship derived by Primakoff and Foldy and used by them in the proof of the source/receiving sensitivity relationship. It thus represents a sufficient condition for that source/receiving sensitivity relationship to be valid, but it has not been shown to be a necessary condition for that source/receiving sensitivity relationship. To avoid confusion, the terminology "electroacoustic reciprocity theorem" is thus not used here.

time variation factor $e^{i\omega t}$ has been omitted, where $\omega = 2\pi f$ is the angular frequency, t is the time, and $i = \sqrt{-1}$. Cases in which the time variation is not harmonic (such as pulsed operation) can be treated with the usual method of Fourier analysis by decomposition into harmonic components, since the equations are all linear and hence the principle of superposition can be used [8]. The results obtained in the following on basis of Eq. (8) will thus apply also for pulsed operation.

2.2 Conditions for reciprocal operation of USMs

Eq. (7) is the condition for *reciprocity* of the electroacoustic system given by Figs. 1-3, but is not sufficient for *reciprocal operation* of this system. Whether a reciprocal system (i.e. fulfilling Eq. (7)) is reciprocally operated or not, will in addition depend on the electrical termination conditions for the system, at the transmitting and receiving sides. In the following the "electroacoustic reciprocity relation" Eq. (8) will be used to derive conditions which are sufficient for reciprocal operation of the system, taking into account the electrical impedances seen by the two transducers I and II towards the transmitting and receiving electronics.

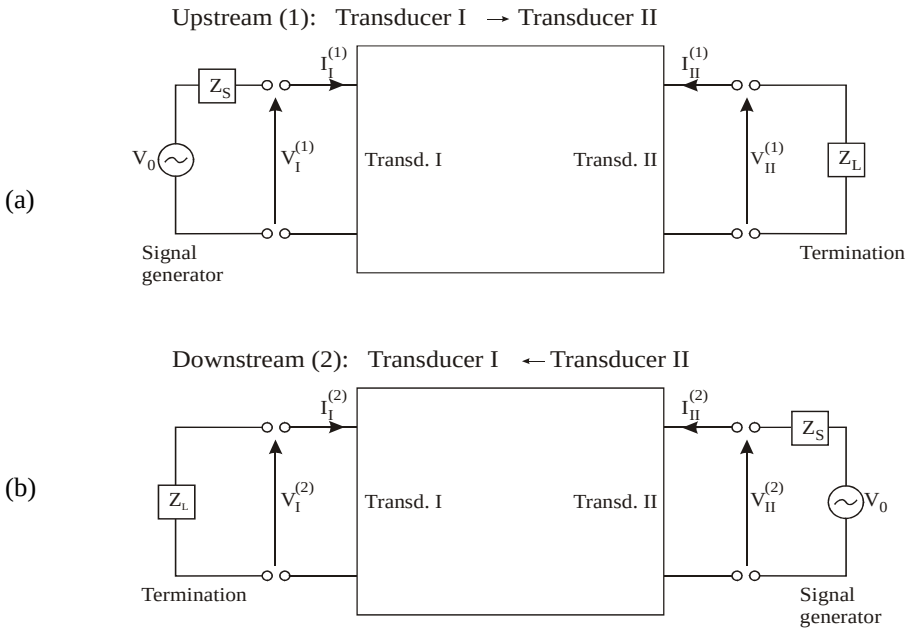

Fig. 4. Two-port ("black box") electroacoustic system representation of (a) upstream and (b) downstream signal propagation in the single USM path shown in Fig. 1, including signal generator and electrical termination, at no-flow conditions.

Consider the situation illustrated in Fig. 4, where parts (a) and (b) of the figure apply to up- and downstream propagation in path no. *i*, respectively. Fig. 4 represents a direct extension of Fig. 3, by including a description of the signal generator / transmitting electronics and the electrical termination at the receiver side. In part (a), a signal generator (including the transmitting electronics and the transducer cable) with voltage V_0 and output electrical impedance Z_S delivers a voltage $V_I^{(1)}$ and a current $I_I^{(1)}$ to the input terminals of transducer I, which acts as transmitter of an acoustic signal to transducer *II*, acting as the receiver. At the output terminals of transducer II the voltage is $V_{II}^{(1)}$ and the current is $I_{II}^{(1)}$. The network is terminated with an electrical impedance Z_L, which represents the input impedance of the transducer cable / receiving electronics. In part (b) of the figure, the situation is *vice versa*. That is,

transducer II is now the transmitter and transducer I is the receiver, and the generator (V_0, Z_S) and electrical load (Z_L) are the same[8]. The input electrical impedances of transducers I and II are defined as

$$Z_I \equiv \frac{V_I^{(1)}}{I_I^{(1)}}, \qquad Z_{II} \equiv \frac{V_{II}^{(2)}}{I_{II}^{(2)}}, \tag{9}$$

respectively.

In the USM, the transit time measurements can be done on the output signals from the receivers[9]. That is, on the voltage $V_{II}^{(1)}$ or the current $I_{II}^{(1)}$ for upstream propagation, and the voltage $V_I^{(2)}$ or the current $I_I^{(2)}$ for downstream propagation. However, a transit time measurement has to be done relative to a "reference signal"[10]. Two different cases are discussed in the following: (a) use of the generator signal (voltage or current) as the reference signal, and (b) use of the transducer input signal (voltage or current) as the reference signal. Both cases are relevant for description of USMs.

2.2.1 Use of the generator signal as the reference signal

In the case where the generator signal is used as the reference signal for the transit time measurement (i.e., the voltage V_0 in the case of voltage generator, or the current V_0/Z_S in the case of current generator), two ratios are of interest: the ratio of the voltage signals $V_{II}^{(1)}$ and $V_I^{(2)}$, and the ratio of the current signals $I_{II}^{(1)}$ and $I_I^{(2)}$. By employing Eq. (9) and the relations (cf. Fig. 4)

$$\frac{V_{II}^{(1)}}{I_{II}^{(1)}} = -Z_L, \qquad \frac{V_I^{(2)}}{I_I^{(2)}} = -Z_L, \tag{10}$$

$$V_0 = \left(Z_S + Z_I\right) I_I^{(1)}, \qquad V_0 = \left(Z_S + Z_{II}\right) I_{II}^{(2)}, \tag{11}$$

it follows from the "electroacoustic reciprocity relation", Eq. (8) (by employing the + sign), that

$$\frac{V_I^{(2)}}{V_{II}^{(1)}} = \frac{I_I^{(2)}}{I_{II}^{(1)}} = \frac{\left(Z_S + Z_I\right)}{\left(Z_S + Z_{II}\right)} \frac{\left(Z_L + Z_{II}\right)}{\left(Z_L + Z_I\right)} \ . \tag{12}$$

In theory, perfect reciprocal operation of the USM is obtained when the generally complex-valued ratio at the right hand side of Eq. (12) is real and equal to 1, so that the magnitude and phase differences between the two measurement signals completely vanish. As outlined in Section 2.1, it follows from the method of Fourier analysis that Δt_i is then equal to zero (also for pulsed signals, irrespective of whether time detection is made in the transient or the stationary part of the signal).

In practice, "sufficient reciprocal operation" of the USM can be obtained when the right hand side of Eq. (12) is "sufficiently close to 1", so that the magnitude and phase differences between the two

---

[8] This assumption, that the generator (V_0, Z_S) and electrical load (Z_L) are the same in Figs. 4a and 4b is a special case, used here since that is relevant for USM applications. Note that Eq. (8) governs also more general cases, where the generator and the electrical load may be different in the two cases of operation, (a) and (b). If so, the present theory can be modified to cover this more general case, and that has to be taken into account if deriving conditions for "sufficient reciprocal operation".

[9] In practice, the transit time measurement is not made on the signal appearing directly at the output terminals of the transducer, but after that signal has propagated through the transducer cable and into the electronics. The latter case can be treated with a slight modification of the present theory. Thus, for simplicity and without loss of generality, the former case is considered here.

[10] For instance, the transit time can be measured as the time difference between corresponding zero crossings in the "measurement signal" and the "reference signal".

measurement signals are sufficiently small, i.e. within the limits determined for the USM (cf. Section 2.3 and Eqs. (24) and (31)).

Four different cases are of particular interest to analyze in this respect, for which the relevant measurement signal ratios are given approximately (from Eq. (12)) as

$$\frac{V_I^{(2)}}{V_{II}^{(1)}} \approx \frac{Z_I}{Z_{II}}\left(1+\left(\frac{Z_{II}}{Z_L}+\frac{Z_S}{Z_I}\right)\left(1-\frac{Z_I}{Z_{II}}\right)\right), \qquad \text{for } \textit{voltage generator and voltage receiver}, \tag{13}$$

$$\frac{V_I^{(2)}}{V_{II}^{(1)}} \approx 1+Z_{II}\left(\frac{1}{Z_L}-\frac{1}{Z_S}\right)\left(1-\frac{Z_I}{Z_{II}}\right), \qquad \text{for } \textit{current generator and voltage receiver}, \tag{14}$$

$$\frac{I_I^{(2)}}{I_{II}^{(1)}} \approx 1+\frac{Z_S-Z_L}{Z_I}\left(1-\frac{Z_I}{Z_{II}}\right), \qquad \text{for } \textit{voltage generator and current receiver}, \tag{15}$$

$$\frac{I_I^{(2)}}{I_{II}^{(1)}} \approx \frac{Z_{II}}{Z_I}\left(1-\left(\frac{Z_{II}}{Z_S}+\frac{Z_L}{Z_I}\right)\left(1-\frac{Z_I}{Z_{II}}\right)\right), \qquad \text{for } \textit{current generator and current receiver}, \tag{16}$$

respectively. The approximate expressions given in each of Eqs. (13)-(16) are based on series expansions, where the four cases are characterized by

- Voltage generator and voltage receiver: $|Z_S| << |Z_I| \; and \; |Z_{II}|, \quad |Z_L| >> |Z_I| \; and \; |Z_{II}|,$
- Current generator and voltage receiver: $|Z_S| >> |Z_I| \; and \; |Z_{II}|, \quad |Z_L| >> |Z_I| \; and \; |Z_{II}|,$
- Voltage generator and current receiver: $|Z_S| << |Z_I| \; and \; |Z_{II}|, \quad |Z_L| << |Z_I| \; and \; |Z_{II}|,$
- Current generator and current receiver: $|Z_S| >> |Z_I| \; and \; |Z_{II}|, \quad |Z_L| << |Z_I| \; and \; |Z_{II}|,$

respectively. The asymptotic approximate expressions for the measurement signal ratios given by Eqs. (13)-(16) are given in Fig. 5, in the limits as $|Z_S/Z_I| \to 0$, $|Z_L/Z_I| \to \infty$, etc. As indicated in the figure, the results fall into two categories. The first category is simply denoted "No"; the other is denoted "OK".

For the category denoted "No" (i.e. by operating the USM either using the combination of voltage generator / voltage receiver, or using the combination of current generator / current receiver), perfect reciprocal operation of the USM is obtained only when the transducers I and II are identical. The ratio of the measurements signals depends heavily on the input electrical impedances of the transducers, Z_I and Z_{II}, and is identically equal to 1 only when these impedances are identical. The phase difference and thus Δt_i vanish only when the transducers I and II are identical. In practice, this will rarely be the case, since transducers - although being of the same design - can hardly be made perfectly identical, and since transducers may have different temperature, pressure and ageing characteristics. Δt_i may thus depend on temperature, pressure, ageing, etc., and a false flow detection may be experienced even at zero flow conditions. In case of non-identical transducers, a "dry calibration" of Δt_i will then be necessary to compensate for the non-negligible Δt_i. Such type of operation of the USM may therefore not be an optimal strategy.

In practice, since there is a specified lower flow velocity limit of the USM, perfect reciprocal operation of the USM is not necessary, and criteria for "sufficient reciprocal operation" of the USM could be determined also for the category "No" (similar to the analysis made in Section 2.3 for category "OK"). However, for the reasons explained above, these criteria would be much more dependent on "equalness" of the two transducers than for category "OK", which is therefore the category of primary interest here.

For the category denoted "OK" (i.e. by operating the USM either using the combination of current generator / voltage receiver, or using the combination of voltage generator / current receiver), reciprocal operation of the USM is obtained automatically in the asymptotic cases indicated in the Fig. 5, irrespective of the properties of the transducers I and II (in fact, irrespective of design of these transducers). By proper design of the electrical impedances of the transmitting and receiving electronics, Z_S and Z_L, in relation to the transducer impedances Z_I and Z_{II} (cf. Section 2.3 for more specific design criteria), the phase difference between the measurement signals (and thus Δt_i) can be made sufficiently small over the whole temperature and pressure range of the USM, and with respect to ageing. Consequently, for such type of operation of the USM no "dry calibration" of Δt_i will be necessary.

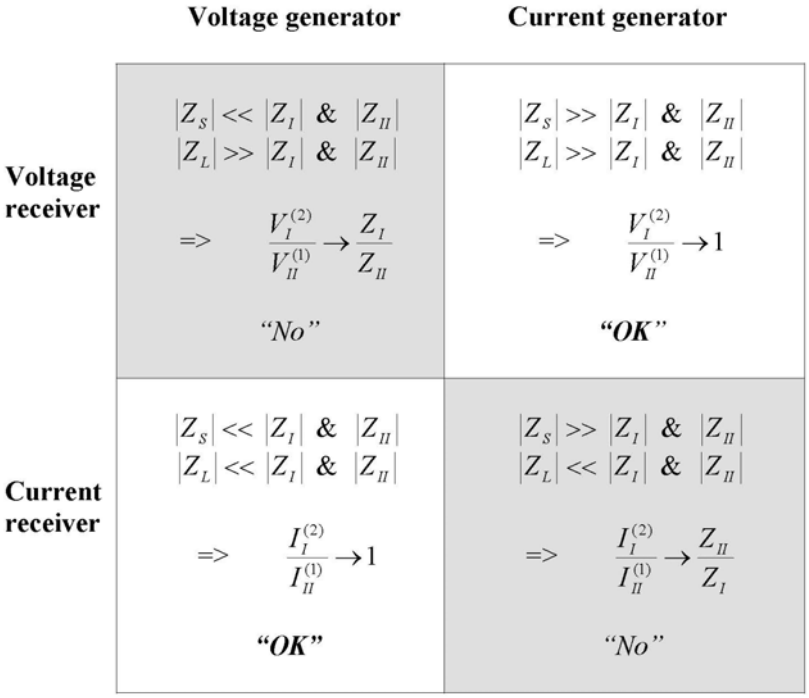

Fig. 5. Four asymptotic special cases of Eqs. (13)-(16), for operation of the USM in which the generator signal is used as the reference signal for the transit time measurement. For interpretation of the categories "No" and "OK", see the text.

Finally, note that in the case of *"electrical symmetry"* (i.e. $Z_S = Z_L$), Eq. (12) reduces exactly to

$$\frac{V_I^{(2)}}{V_{II}^{(1)}} = \frac{I_I^{(2)}}{I_{II}^{(1)}} = 1, \tag{17}$$

which means that this case also falls into category "OK", discussed above[11]. This case was also discussed in ref. [11].

2.2.2 Use of the transducer input signal as the reference signal

In the case where the transducer input signal (voltage or current) is used as the reference signal for the transit time measurement, four different ratios are of interest, dependent on whether the reference signal is voltage or current, and whether the received (measured) signal is voltage or current (cf. Fig. 4).

[11] From ref. [16] it appears that this may be the same type of "electrical symmetry" as referred to by von Jena et al. [15] (cf. Section 1). Also Martin et al. [17] used this type of "electrical symmetry", realized in a slightly different way. Both approaches were based on voltage generation and voltage reception.

For instance, consider one of these cases, e.g. voltage reference and voltage receiver. For upstream propagation, the reference and measurement signals are $V_I^{(1)}$ and $V_{II}^{(1)}$, respectively, so that the phase difference between these is given by the ratio $V_{II}^{(1)}/V_I^{(1)}$. The corresponding ratio for downstream propagation is $V_I^{(2)}/V_{II}^{(2)}$. The other three cases are treated similarly.

Consequently, by employing Eqs. (9) and (10), it follows from the electroacoustic reciprocity relation, Eq. (8) (by employing the + sign), that for the four different cases, the relevant measurement signal ratios are given as

$$\frac{V_{II}^{(1)}/V_I^{(1)}}{V_I^{(2)}/V_{II}^{(2)}} \approx \frac{Z_{II}}{Z_I}\left(1-\frac{Z_{II}}{Z_L}\left(1-\frac{Z_I}{Z_{II}}\right)\right), \qquad \text{for } \textit{voltage reference and voltage receiver,} \tag{18}$$

$$\frac{V_{II}^{(1)}/I_I^{(1)}}{V_I^{(2)}/I_{II}^{(2)}} \approx 1-\frac{Z_{II}}{Z_L}\left(1-\frac{Z_I}{Z_{II}}\right), \qquad \text{for } \textit{current reference and voltage receiver,} \tag{19}$$

$$\frac{I_{II}^{(1)}/V_I^{(1)}}{I_I^{(2)}/V_{II}^{(2)}} \approx 1+\frac{Z_L}{Z_I}\left(1-\frac{Z_I}{Z_{II}}\right), \qquad \text{for } \textit{voltage reference and current receiver,} \tag{20}$$

$$\frac{I_{II}^{(1)}/I_I^{(1)}}{I_I^{(2)}/I_{II}^{(2)}} \approx \frac{Z_I}{Z_{II}}\left(1+\frac{Z_L}{Z_I}\left(1-\frac{Z_I}{Z_{II}}\right)\right), \qquad \text{for } \textit{current reference and current receiver,} \tag{21}$$

respectively. The approximate expressions given in each of Eqs. (18)-(21) are based on series expansions, where the condition $|Z_L| >> |Z_I|$ *and* $|Z_{II}|$ has been used for voltage reception, and $|Z_L| << |Z_I|$ *and* $|Z_{II}|$ has been used for current reception.

Analogous to the situation discussed in Section 2.1, reciprocal operation of the USM is obtained when the generally complex-valued ratio at the right hand side of each of Eqs. (18)-(21) is real and equal to 1, so that the magnitude and phase differences between the two measurement signals completely vanish. In that case Δt_i becomes equal to zero.

The asymptotic approximate expressions for the measurement signal ratios given by Eqs. (18)-(21) are given in Fig. 6, in the limits as $|Z_L/Z_I| \to \infty$, $|Z_L/Z_I| \to 0$, etc. As indicated in the figure, the results fall into two categories "No" and "OK", similarly to the situation discussed in Section 2.1. The meaning of "No" and "OK" and the consequences for the two categories are the same as in Section 2.1.

Hence, for the category denoted "No" (i.e. by operating the USM either using the combination of voltage reference / voltage reception, or using the combination of current reference / current reception), reciprocal operation of the USM is obtained only when the transducers I and II are identical. For further discussion of consequences in category "No" it is referred to Section 2.1.

Since the achievement of "sufficient reciprocal operation" puts significantly higher requirements to "equalness" of the two transducers for category "No" than for category "OK", the four cases classified under category "No" are not considered further here. This concerns Eq. (13) (voltage generator and voltage receiver), Eq. (16) (current generator and current receiver), Eq. (18) (voltage reference and voltage receiver), and Eq. (21) (current reference and current receiver).

On the other hand, for the category denoted "OK" (i.e. by operating the USM either using the combination of current reference / voltage reception, or using the combination of voltage reference / current reception), reciprocal operation of the USM is obtained automatically, irrespective of the

properties or "equalness" of the transducers I and II, by proper design of the output electrical impedance of the receiving electronics, Z_L, in relation to the transducer impedances Z_I and Z_{II} (cf. Section 2.3 for more specific design criteria). For further discussion of consequences in category "OK" it is referred to Section 2.1.

Note also that whereas in Section 2.1 both of the electronics impedances Z_S and Z_L had to be subject to "proper design" in relation to the transducer impedances Z_I and Z_{II}, only the receiving electronics impedance Z_L has to be subject to "proper design" if the USM is operated as in Section 2.2.

The question is thus: what is meant by "proper design" of these impedances. This is the topic addressed in the next section.

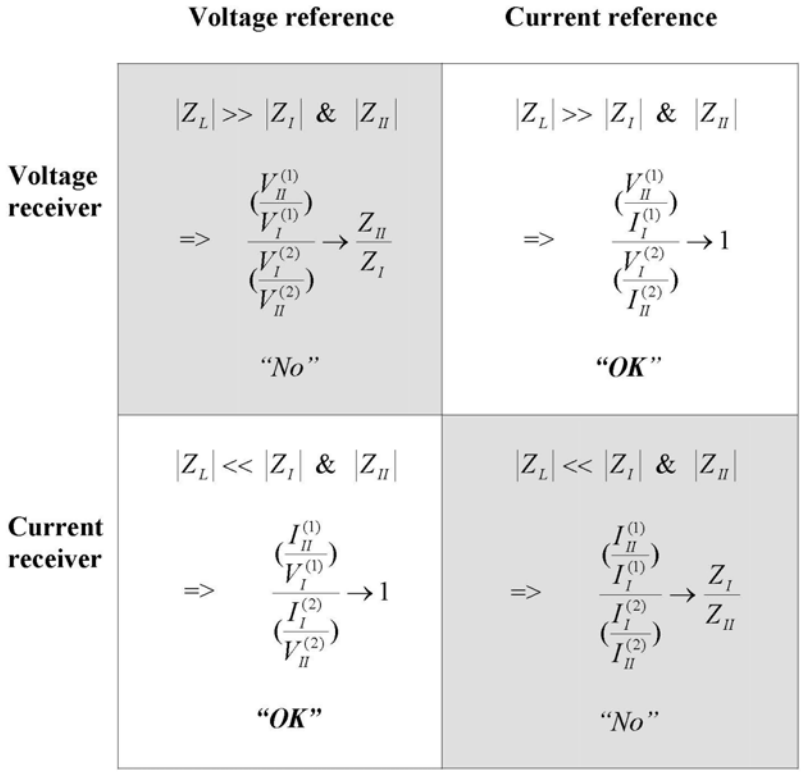

Fig. 6. The four asymptotic special cases of Eqs. (18)-(21), for operation of the USM by employing the transducer input signal as the reference signal for the transit time measurement. For interpretation of the categories "No" and "OK", see the text.

2.3 Design criteria for "sufficient reciprocal operation" and transducer manufacturing

The asymptotic results shown in Figs. 5 and 6 reflect idealized situations, theoretically valid in the limits such as $|Z_S/Z_I| \to 0$, $|Z_S/Z_I| \to \infty$, $|Z_L/Z_I| \to 0$ or $|Z_L/Z_I| \to \infty$, etc. In practice they do not reflect the real situation, that the impedances of the transmitting and receiving electronics have finite values. From Eqs. (14), (15), (19) and (20), it follows that not even for the four cases classified under category "OK", where reciprocal operation of the USM can be achieved irrespective of the values of the transducer impedances Z_I and Z_{II}, the ratio of the measurement signals can be perfectly real and equal to 1. Due to the finite impedances, there will always be a finite phase difference between the measurement signals. It follows that perfect reciprocal operation will never be achieved, and that Δt_i will never be perfectly zero, - not even for category "OK" in a perfectly no-flow situation.

The question is then: how small can we - for category "OK" - make the phase difference, and thus Δt_i, in a no-flow situation? Or formulated in another way, - what are the requirements to Z_S and Z_L, given the transducer impedances Z_I and Z_{II}? That is, what are the requirements to "sufficient reciprocal operation".

To answer that question, we will first need a typical number for the maximum value of Δt_i that can be tolerated in the USM at the specified minimum flow velocity of the USM, say e.g. 0.5 m/s, and still avoid detecting false flow. Such a number can be established using Eqs. (1)-(2). For simplicity, and without much loss of generality[12], consider a path passing through the pipe centerline (y_i = 0), at an inclination angle $\theta_i = 45^o$, and assume that the flow has a uniform (constant) profile. The flow velocity of this path is then given approximately as $v_i \approx c^2 \Delta t_i / 2D$, so that

$$\Delta t_i \approx \frac{2D\overline{v}_i}{c^2}, \tag{22}$$

where $D = 2R$ is the inner diameter of the pipe, c is the sound velocity of the fluid in the pipe, and in the nominator of Eq. (1) the upstream and downstream transit times t_{1i} and t_{2i} have been approximated by $\sqrt{2}D/c$, which is sufficient for the present purpose. In a simplified uncertainty "analysis", neglecting all other uncertainty contributions than the uncertainty of Δt_i, the standard uncertainty of Δt_i is then given approximately From Eq. (22) as

$$u(\Delta t_i) \approx \frac{2D}{c^2} u(\overline{v}_i) = \frac{2D|\overline{v}_i|}{c^2} \left| \frac{u(\overline{v}_i)}{\overline{v}_i} \right| = \frac{2D|\overline{v}_i|}{c^2} E_{\overline{v}_i}, \tag{23}$$

where $u(\overline{v}_i)$ and $E_{\overline{v}_i} \equiv |u(\overline{v}_i)/\overline{v}_i|$ are the standard and relative standard uncertainties of the average flow velocity, $\overline{v}_i$. In order to establish some tentative figures to use in an example to illustrate the method of achieving "sufficient reciprocal operation", consider two USMs, - one operating in natural gas and the other in oil. In the gas example, the sound velocity of the gas is taken as c = 500 m/s (as a tentative upper bound), and the upper limit for the contribution of the standard uncertainty of Δt_i to the standard uncertainty of the USM (as an isolated uncertainty contribution), is taken as $E_{\overline{v}_i}^{\max}$ = 0.4 % at $\overline{v}_i$ = 0.5 m/s[13]. In the oil example, the sound velocity of the oil is taken as c = 1500 m/s (as a tentative upper bound), and the upper limit for the contribution of the standard uncertainty of Δt_i to the standard uncertainty of the

[12] A more rigorous treatment of this topic would require e.g. use of a more complete uncertainty model for USMs than the simplified analysis used here, such as the *GARUSO* model [20, 6]. However, analyses which have been made on this subject using *GARUSO*, where all paths in multipath USMs are considered, and where the simplifying approximations involved here are not used, have shown that the results found using the simplified analysis leading to Eqs. (22)-(23) and Table 1, are sufficiently representative.

[13] From the AGA-9 report [1], the recommended maximum relative deviation (error) of gas USMs from the flow calibration reference measurement is 1.4 % at the low-end of the flow velocity range. By assuming a Type B uncertainty, at a 100 % confidence level and a rectangular probability distribution (with coverage factor $k = \sqrt{3}$) [24], the corresponding relative expanded uncertainty is, according to the "GUM" [24], equal to $2(1.4/\sqrt{3})\% \approx 1.6$ % (at a 95 % confidence level, with coverage factor k = 2). This corresponds to a relative standard uncertainty of 0.8 %. Taking into account that only one source of uncertainty is considered in the text, namely the uncertainty of Δt_i, and that all other uncertainty contributions are neglected, a "safety factor" of 2 is used here relative to the value 0.8 %. That means, the number $E_{\overline{v}_i}^{\max}$ = 0.4 % used in the example of the text corresponds to saying that the standard uncertainty of Δt_i should not contribute more to the standard uncertainty of the USM than 0.4 %, as an isolated uncertainty contribution.

USM (as an isolated uncertainty contribution), is taken as $E_{\bar{v}_i}^{\max} = 0.05$ % at $\bar{v}_i = 0.5$ m/s[14]. (Note that these are tentative example figures only, - another low flow velocity limit for the USM than 0.5 m/s would give other numbers.)

Table 1 gives typical upper limit figures for $u(\Delta t_i)$, i.e. $u(\Delta t_i)_{\max}$, calculated from Eq. (23) and these example figures, for the gas and the liquid USMs, and for some pipe diameters in the range 6" to 20" (15 to 50 cm inner diameter).

Table 1. Tentative and typical upper limit figures for the standard uncertainty of Δt_i in a gas USM and a liquid USM, $u(\Delta t_i)_{\max}$, for some inner diameters of the pipe, D. (Note that these are example figures only, for an assumed specified lower flow velocity limit of the USM taken to be 0.5 m/s.)

	Inner diameter, D		
	6"	12"	20"
Gas USM:	$2.4 \cdot 10^{-9}$ s	$4.8 \cdot 10^{-9}$ s	$8.0 \cdot 10^{-9}$ s
Liquid USM:	$33 \cdot 10^{-12}$ s	$67 \cdot 10^{-12}$ s	$111 \cdot 10^{-12}$ s

To avoid any Δt-correction in the USM, a possible Δt-correction of the USM, Δt^{corr}, should not be larger than $u(\Delta t_i)_{\max}$. Consequently, from these examples,

$$\Delta t^{corr} < \Delta t_{\max}^{corr} = u(\Delta t_i)_{\max} = \begin{cases} 2.4\ ns & (\textit{for gas USMs}) \\ 33\ ps & (\textit{for liquid USMs}) \end{cases} \tag{24}$$

are used as tentative example requirement values for Δt^{corr} in the following, applying only to an assumed specified minimum flow velocity of the USM equal to 0.5 m/s. Consequently, if Eq. (24) is fulfilled for all operating conditions of the USM (with respect to pressure, temperature, ageing, etc.), Δt^{corr} is negligible, and active Δt-correction is not needed in the USM, for flow velocities higher than the min. flow velocity specified for the USM (in the present case 0.5 m/s).

Note that from Eq. (23) and Table 1, the requirements to Δt^{corr} given by Eq. (24) represent "worst case" figures for the diameters considered here (6" and upwards). For USMs larger than 6" diam., the requirements are less severe, and decrease proportionally to the diameter D.

Now, having established Eq. (24), we return to the requirements to be imposed on the impedances Z_S and Z_L to automatically fulfil Eq. (24), leading to conditions for "sufficient reciprocal operation" (defined in Section 2.1.1).

First, to cover all four cases of category "OK" in a single analysis, note that Eqs. (14), (15), (19) and (20) can all be expressed on the form

[14] The API standard on liquid ultrasonic flow meters [4] does not prescribe any linearity requirements for such meters. From the NPD regulations [25], which are used here as an example, the maximum relative expanded uncertainty of liquid USMs is 0.2 % in the working flow velocity range (linearity, at a 95 % conf. level, with coverage factor $k = 2$). The corresponding relative standard uncertainty is 0.1 % [24]. Taking into account that only one source of uncertainty is considered in the text, namely the uncertainty of Δt_i, and that all other uncertainty contributions are neglected, a "safety factor" of 2 is used here relative to the value 0.1 %. That means, the number $E_{\bar{v}_i}^{\max} = 0.05$ % used in the example of the text corresponds to saying that the standard uncertainty of Δt_i should not contribute more to the standard uncertainty of the USM than 0.05 %, as an isolated uncertainty contribution.

$$Ae^{i\Delta\phi} \approx 1 + K(1 - Be^{i\Delta\psi}), \tag{25}$$

where A is the magnitude and $\Delta\phi$ the phase of the measurement signal ratio, i.e.

$$A \equiv \left|\frac{V_I^{(2)}}{V_{II}^{(1)}}\right|, \qquad A \equiv \left|\frac{I_I^{(2)}}{I_{II}^{(1)}}\right|, \qquad A \equiv \left|\frac{V_{II}^{(1)}/I_I^{(1)}}{V_I^{(2)}/I_{II}^{(2)}}\right|, \qquad A \equiv \left|\frac{I_{II}^{(1)}/V_I^{(1)}}{I_I^{(2)}/V_{II}^{(2)}}\right|, \tag{26a}$$

$$\Delta\phi \equiv \angle\left(\frac{V_I^{(2)}}{V_{II}^{(1)}}\right), \ \Delta\phi \equiv \angle\left(\frac{I_I^{(2)}}{I_{II}^{(1)}}\right), \ \Delta\phi \equiv \angle\left(\frac{V_{II}^{(1)}/I_I^{(1)}}{V_I^{(2)}/I_{II}^{(2)}}\right), \qquad \Delta\phi \equiv \angle\left(\frac{I_{II}^{(1)}/V_I^{(1)}}{I_I^{(2)}/V_{II}^{(2)}}\right), \tag{26b}$$

for the four cases described by Eqs. (14), (15), (19) and (20), respectively, K is a quantity dependent on the impedances Z_S , Z_L, Z_I and Z_{II}, i.e.

$$K \equiv Z_{II}\left(\frac{1}{Z_L} - \frac{1}{Z_S}\right), \qquad K \equiv \frac{Z_S - Z_L}{Z_I}, \qquad K \equiv -\frac{Z_{II}}{Z_L}, \qquad K \equiv \frac{Z_L}{Z_I}, \tag{27}$$

for the same four cases, respectively, and B is the magnitude and $\Delta\psi$ the phase of the transducer impedance ratio, defined as

$$B \equiv \left|\frac{Z_I}{Z_{II}}\right|, \qquad \Delta\psi \equiv \angle\left(\frac{Z_I}{Z_{II}}\right), \tag{28}$$

respectively. Note that due to the assumptions made for the impedances Z_S and Z_L for the respective four cases (cf. Section 2.2), one has $A \approx 1$ and $\Delta\phi << \pi/2$ in every case. For transducers which are approximately equal (but not identical[15]) (that is, $Z_I \approx Z_{II}$, i.e. $B \approx 1$ and $\Delta\psi << \pi/2$), Eq. (25) then yields

$$|K| \approx \frac{\Delta\phi}{\Delta\psi} = \frac{\omega\Delta t_i}{\Delta\psi}, \tag{29}$$

since we have $\Delta\phi = \omega\Delta t_i$. "Sufficient reciprocal operation" is thus obtained if the requirement

$$|K| < \frac{2\pi f \cdot \Delta t_{\max}^{corr}}{\Delta\psi} \tag{30}$$

is fulfilled, where $\Delta t_{\max}^{corr}$ is given by Eq. (24). Consequently, "sufficient reciprocal operation" is definitely obtained if the even stronger requirement

$$|K| < \frac{2\pi f \cdot \Delta t_{\max}^{corr}}{\Delta\psi_{\max}} \tag{31}$$

is imposed, where $\Delta\psi_{\max}$ (given in radians) is a representative figure for the maximum phase deviation of the transducers' input electrical impedances, at the frequency f in question, for accepted transducers in a complete transducer production series. $\Delta\psi_{\max}$ may typically be established empirically, from inspection of transducer production over time.

[15] The case of identical transducers is theoretically trivial and also of minor practical interest, and is not addressed further here.

Eq. (31) is here the condition used for "sufficient reciprocal operation" of the USM. If Eq. (31) is fulfilled for all operating conditions of the USM (with respect to pressure, temperature, ageing, etc.), "sufficient reciprocal operation" is automatically achieved. That means, Δt^{corr} is negligible, and active Δt-correction is not needed in the USM, for flow velocities higher than the min. flow velocity specified for the USM (0.5 m/s used in Table 1 and Eq. (24)).

The specific consequences of Eq. (31) for the four cases classified under category "OK" (cf. Eq. (27)) are discussed separately in the following, cf. the cases (a)-(d) below.

(a) **Current generator and voltage receiver**, governed by Eq. (14). From Eq. (27) we have $K \equiv Z_{II}\left(1/Z_L - 1/Z_S\right)$ for this case, so that the requirement given by Eq. (31) leads to the two equivalent requirements

$$\left|\frac{1}{Z_L} - \frac{1}{Z_S}\right| < \frac{2\pi f \cdot \Delta t^{corr}_{\max}}{\Delta\psi_{\max}\left|Z_{II}\right|}, \tag{32a}$$

$$\Delta\psi_{\max} < \frac{2\pi f \cdot \Delta t^{corr}_{\max}}{\left|Z_{II}\right|\left|\frac{1}{Z_L} - \frac{1}{Z_S}\right|}, \tag{32b}$$

for the electronics impedances and the transducer impedances, respectively.

Eq. (31a) represents a "sufficient reciprocal operation" requirement for design and manufacturing of the electrical impedances of the transmitting and receiving electronics, given that typical values for (i) the magnitude and (ii) the variation in phase angle of the transducer impedance are known (for the complete transducer production). Similarly, Eq. (31b) represents a "sufficient reciprocal operation" requirement for reproducibility in manufacturing of the transducers, given that a typical value for (i) the magnitude of the transducer impedance and (ii) the electrical impedances of the transmitting and receiving electronics are known.

(b) **Voltage generator and current receiver**, governed by Eq. (15). From Eq. (27) we have $K \equiv \left(Z_S - Z_L\right)/Z_I$ for this case, so that the requirement given by Eq. (31) leads to the two equivalent "sufficient reciprocal operation" requirements

$$\left|Z_S - Z_L\right| < \frac{2\pi f \cdot \Delta t^{corr}_{\max}}{\Delta\psi_{\max}}\left|Z_I\right|, \tag{33a}$$

$$\Delta\psi_{\max} < 2\pi f \cdot \Delta t^{corr}_{\max}\left|\frac{Z_I}{Z_S - Z_L}\right|, \tag{33b}$$

for the electronics impedances and the transducer impedance reproducibility, respectively (for interpretation, cf. (a)).

(c) **Current reference and voltage receiver**, governed by Eq. (19). From Eq. (27) we have $K \equiv -Z_{II}/Z_L$ for this case, so that the requirement given by Eq. (31) leads to the two equivalent "sufficient reciprocal operation" requirements

$$\frac{1}{\left|Z_L\right|} < \frac{2\pi f \cdot \Delta t^{corr}_{\max}}{\Delta\psi_{\max}\left|Z_{II}\right|}, \tag{34a}$$

$$\Delta\psi_{\max} < 2\pi f \cdot \Delta t_{\max}^{corr} \left| \frac{Z_L}{Z_{II}} \right|, \tag{34b}$$

for the electronics impedances and the transducer impedance reproducibility, respectively (for interpretation, cf. (a)).

(d) **Voltage reference and current receiver**, governed by Eq. (20). From Eq. (27) we have $K \equiv Z_L / Z_I$ for this case, so that the requirement given by Eq. (31) leads to the two equivalent "sufficient reciprocal operation" requirements

$$|Z_L| < \frac{2\pi f \cdot \Delta t_{\max}^{corr}}{\Delta\psi_{\max}} |Z_I|, \tag{35a}$$

$$\Delta\psi_{\max} < 2\pi f \cdot \Delta t_{\max}^{corr} \left| \frac{Z_I}{Z_L} \right|, \tag{35b}$$

for the electronics impedances and the transducer impedance reproducibility, respectively (for interpretation, cf. (a)).

An example can be useful to illustrate typical figures resulting from e.g. Eq. (33a). Consider a gas USM and a liquid USM operating at, say, 150 kHz and 1 MHz, respectively. Assume that in average (for a production series), the magnitude of the transducer impedance $|Z_I|$ is 50 and 500 Ω at the operating frequency, for the gas and the liquid transducers, respectively (for simplicity, as relevant examples). Furthermore, as an example, assume that the maximum phase deviation of the transducer's input electrical impedances, $\Delta\psi_{\max}$, is (say) 10^o (for a production series). From Eqs. (33a) and (24), the "sufficient reciprocal operation" requirement becomes $|Z_S - Z_L|$ < 0.6 Ω for the gas and liquid USMs, in the case when the generator signal V_0 is used as the reference signal for the time detection. Similar calculations can be made for Eq. (33b), as well as for the other three cases governed by Eqs. (32), (34) and (35).

3. MEASUREMENT RESULTS

In the present section, results from experimental laboratory measurements of Δt_i at approximate "zero flow" conditions are used to verify and demonstrate practical realisation of the theory described in Section 2, and illustrate the potentials of utilizing the theory.

Two experimental measurement setups have been used for this purpose. At CMR a 6" test spoolpiece setup was used in measurements at room temperature and low pressure, addressing e.g. the question of nonlinearity in relation to reciprocal operation (cf. Sections 3.2 and 3.3). At FMC Kongsberg Metering a dedicated pressure chamber was used to investigate reciprocal operation over wide pressure and temperature ranges (cf. Section 3.3). The key components of these measurement systems (the standard MPU 1200, 600 and 200 electronics boards and transducers [22]) were equal in the two setups, cf. Section 3.1 (different production units, though).

3.1 Measurement system

A principle sketch of the measurement system is shown in Fig. 7a, designed to achieve "sufficient reciprocal operation" according to the theory outlined in Section 2, cf. Eqs. (24) and (31). The design criterion used for the gas USM is Δt^{corr} < 2.4 ns, in accordance with Eq. (24). Voltage generation and current reception are used to achieve reciprocal operation. Electronic switches are used to realize the

multiplexing between upstream and downstream measurements. The switches are shown for transducer I as transmitter and transducer II as receiver; - they toggle on/off for up- and downstream transmission. The impedances of the electronics components involved are matched so that $|Z_S - Z_L| < 0.55\ \Omega$, which is within the example requirement $|Z_S - Z_L| < 0.6\ \Omega$ for "sufficient reciprocal operation" of gas and liquid USMs discussed in Section 2.3, cf. Eq. (33a). This figure is based on component specifications, so in reality $|Z_S - Z_L|$ is likely to be much smaller than 0.55 Ω.

The transducers and electronics boards (analog and digital) used in these measurements are shown in Figs. 7b and c. These are the transducers and boards used in the FMC Kongsberg Metering MPU 200, 600 and 1200 ultrasonic gas flow meters [22].

(a)

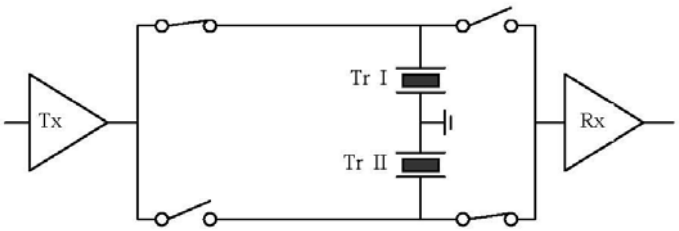

(b)

(c)

Fig. 7. (a) Principle sketch of the measurement system, (b) ultrasonic transducers and (c) electronics board used in the test measurements of Δt_i.

3.2 Effects of nonlinearity (high "firing voltages")

Measurements of Δt_i at approximate "zero flow" conditions have been made at CMR in a 6" test spoolpiece (with a single path), in air at 8.5 barA and about 21 °C. The spoolpiece was put in a water bath for temperature stabilization, to minimize temperature induced convection flow. Since the present measurements aim to measure Δt_i well below 2.4 ns (cf. Eq. (24)), preferably better than 1 ns, even extremely small convection flows can destroy the measurements. An example may illustrate the zero-flow stability requirements: From Eq. (22), Δt_i = 1 ns corresponds to an air flow velocity of about 0.4 mm/s, i.e. 2.4 cm/min. Thus, if the flow is of the order of 2-3 cm/min, it becomes difficult to verify the theory of Section 2. In the measurements presented in Figs. 8 and 9, a sufficient "zero-flow" stability has been achieved[16].

Fig. 8 shows Δt_i measurements for five transducer pairs, for transmitter (Tx) gain setting 1 (the lowest setting available for the "firing voltage" of the transmitting transducer), in air at 21 °C / 9.5 barA. A selection of transducers were used here, consisting of transducers which *had* passed the transducer production QA, as well as transducers which had *not* passed the QA.

[16] This was demonstrated e.g. by interchanging the transducer cables in the pair (at all TX gain settings), and observing that the sign of Δt_i did not change, for the lowest TX gain setting (= 1), cf. Fig. 8. If convection flow was a dominating effect, the sign of Δt_i should change by this cable interchange.

In Fig. 8, Δt_i is shown to be less than about 0.7 ns in 20 out of 23 measurements (the remaining three are about 1.1 and 1.6 ns), and all measurements are well below the "sufficient reciprocal operation" design criterion of 2.4 ns used for the gas USM, cf. Eq. (24). This is so also for the transducer pair no. 4, with relatively high phase difference, 33.5°. The reason for that is probably that $|Z_S - Z_L|$ in practice may be much less than 0.55 Ω. Such results strongly support and strengthen the present realization of "sufficient reciprocal operation", cf. Eq. (24). They also confirm that the transducers do not have to be equal to realize reciprocity.

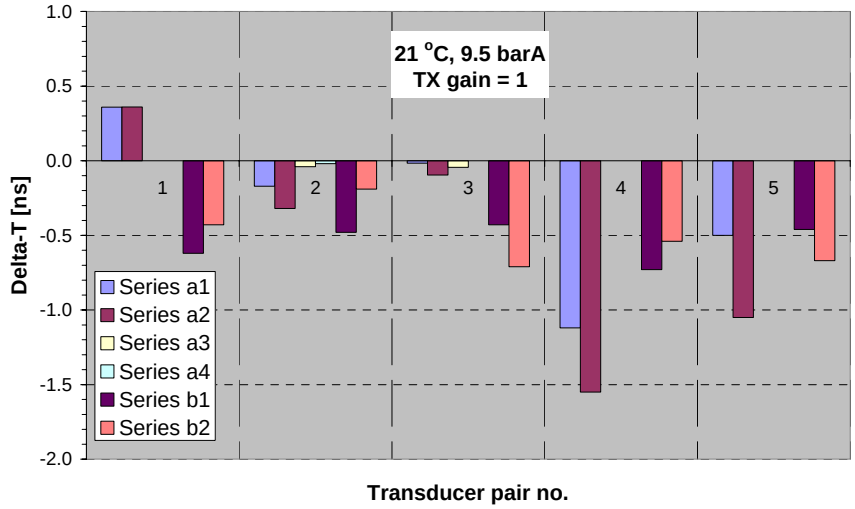

Fig. 8. Δt_i measurements made in the test spoolpiece, at approximate "zero flow conditions", for five different pairs of MPU 1200 ultrasonic transducers, for transmitter (Tx) gain setting 1 (lowest gain available), in air at 21 °C / 9.5 barA.

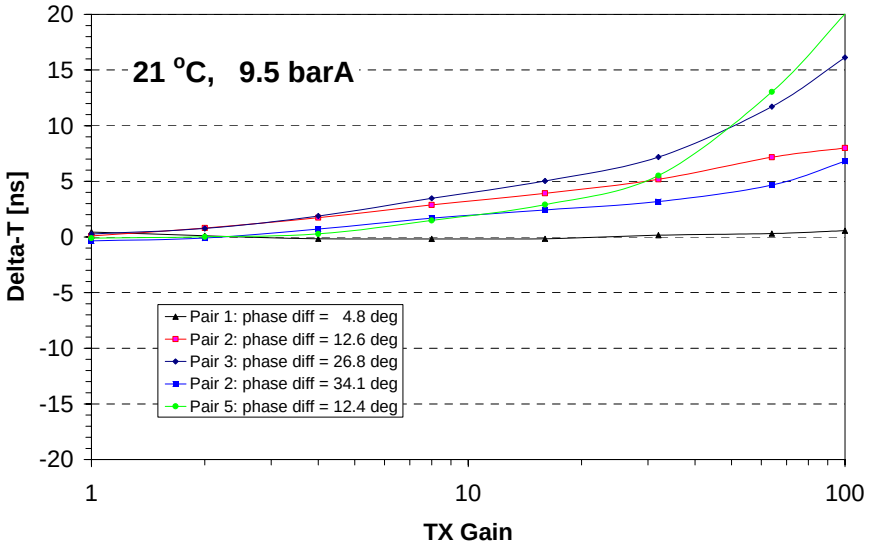

Fig. 9. Δt_i measurements made in the test spoolpiece, at approximate "zero flow conditions", for five different pairs of MPU 1200 ultrasonic transducers, as a function of transmitter (Tx) gain setting (in the range 1-100), in air at 21 °C / 9.5 barA. All pairs are fulfilling "sufficient reciprocal operation" at the lower TX gain settings, cf. Fig. 8.

Fig. 8 demonstrates that "sufficient reciprocal operation" is definitely realized at sufficiently low TX gain settings ("firing voltages"), at low pressure and room temperature, when the system is driven linearly. There is then the question of how higher "firing voltages" will influence on reciprocity.

Fig. 9 shows measurement results for the same five transducer pairs, this time shown as a function of transmitter (Tx) gain setting (i.e. "firing voltage" settings of the transmitting transducer, in the range 1-100, where 1 is the minimum and 100 the maximum setting available for the MPU software and electronics boards used here). Up to TX gain equal to about 70, this setting is proportional to the excitation voltage of the transmitting transducer[17]. Each curve is an average of 4-6 different measurements, taken over a time period of about 6-8 hours. For all pairs, the individual 4-6 measurements have been very repeatable, so that the (averaged) curves in Fig. 9 are highly representative for the individual curves. This reflects stable conditions in the spoolpiece.

A systematic trend of increasing Δt_i with increasing TX gain setting is observed in these results, which is assumed to be caused by increasing nonlinearity in the system (in the transducers or the gas medium), and which probably demonstrates violation of reciprocal operation by non-linear effects (as pointed out and demonstrated also in ref. [15]). Using the tentative example criterion of 2.4 ns given by Eq. (24), "sufficient reciprocal operation" is demonstrated up to about TX gain = 6, for these five transducer pairs.

3.3 Effects of pressure and temperature

In addition to the measurements made at CMR in air at low pressure and room temperature, described in Section 3.2, supplementary measurements of Δt_i at approximate "zero flow" conditions have been made over a range of pressures and temperatures, in a dedicated high-pressure gas transducer measurement chamber belonging to FMC Kongsberg Metering.

Fig. 10 gives an overview of the high-pressure transducer measurement chamber system, and some details, with transducer mounting, etc. In this chamber, 12 transducers of a MPU 1200 ultrasonic gas flow meter [22] can be measured simultaneously, in terms of 6 transducer pairs. The chamber consists of an inner pressure chamber submerged in a temperature controlled water bath. It has entry ports for 12 transducers, and is designed for gas pressures up to 215 barA, using nitrogen. The temperature-controlled water provides even temperature around the pressure chamber, to minimize temperature-induced gas movement (convection flow) in the pressure chamber (approximate "zero flow" conditions). The transducers pairs are all mounted as horizontal centre paths (about 181 mm transducer distance), to further minimize the effect of possible convection flow on the measurements. Measurements are made under the assumption of no flow in the chamber. The transducers are characterized for different operating conditions by changing the gas pressure and temperature by means of a pressure regulator and a water temperature controller. The temperature can be adjusted between 0 and 70 °C. The transducers are mounted in the chamber and connected with transducer cables to a MPU electronics unit. A personal computer (PC) with dedicated software communicates with the MPU electronics through an Ethernet connection. The transducer measurement is done automatically by the computer program after the initial operator set-up.

The chamber is normally used for factory measurement of transducer delay ("dry calibration"), and a quality check of the transducers, before shipment of a meter. "Dry calibration" of Δt_i is normally not made for the gas and liquid USMs considered here [22,23], due to the "sufficient reciprocal operation" design utilized in these meters, according to the theory presented in Section 2 (cf. Fig. 7a), so that no zero flow adjustment or active Δt-correction is used in these meters.

In the present study, however, Δt_i measurements have been made in the chamber in order to test and demonstrate realization of the theory presented in Section 2, over a range of pressures and temperatures. Results of these Δt_i measurements are given in Figs. 11-12. Fig. 11 shows Δt_i measurements for six

[17] Note that for Tx gain equal to about 70 or larger, the input amplifier is driven into saturation. As a consequence, the excitation signal starts to "clip", and at Tx gain = 100, the signal sent through the transmit - receive system is highly distorted.

transducer pairs (representing an arbitrary[18] selection of transducers, and an arbitrary pairing), for transmitter (Tx) gain setting 1 (the lowest setting available), for some combinations of temperature and pressure: 10 °C / 55 barA, 10 °C / 165 barA, 25 °C / 55 barA, 25 °C / 165 barA and 65 °C / 55 barA. In these results, Δt_i is shown to be less than about 1.6 ns in all measurements, except for two values, which are about 1.8 and 2.3 ns. All values are below the "sufficient reciprocal operation" design criterion of 2.4 ns used for the gas USM, cf. Eq. (24). That is, false flow *is* detected, but at a sufficiently low level to be negligible.

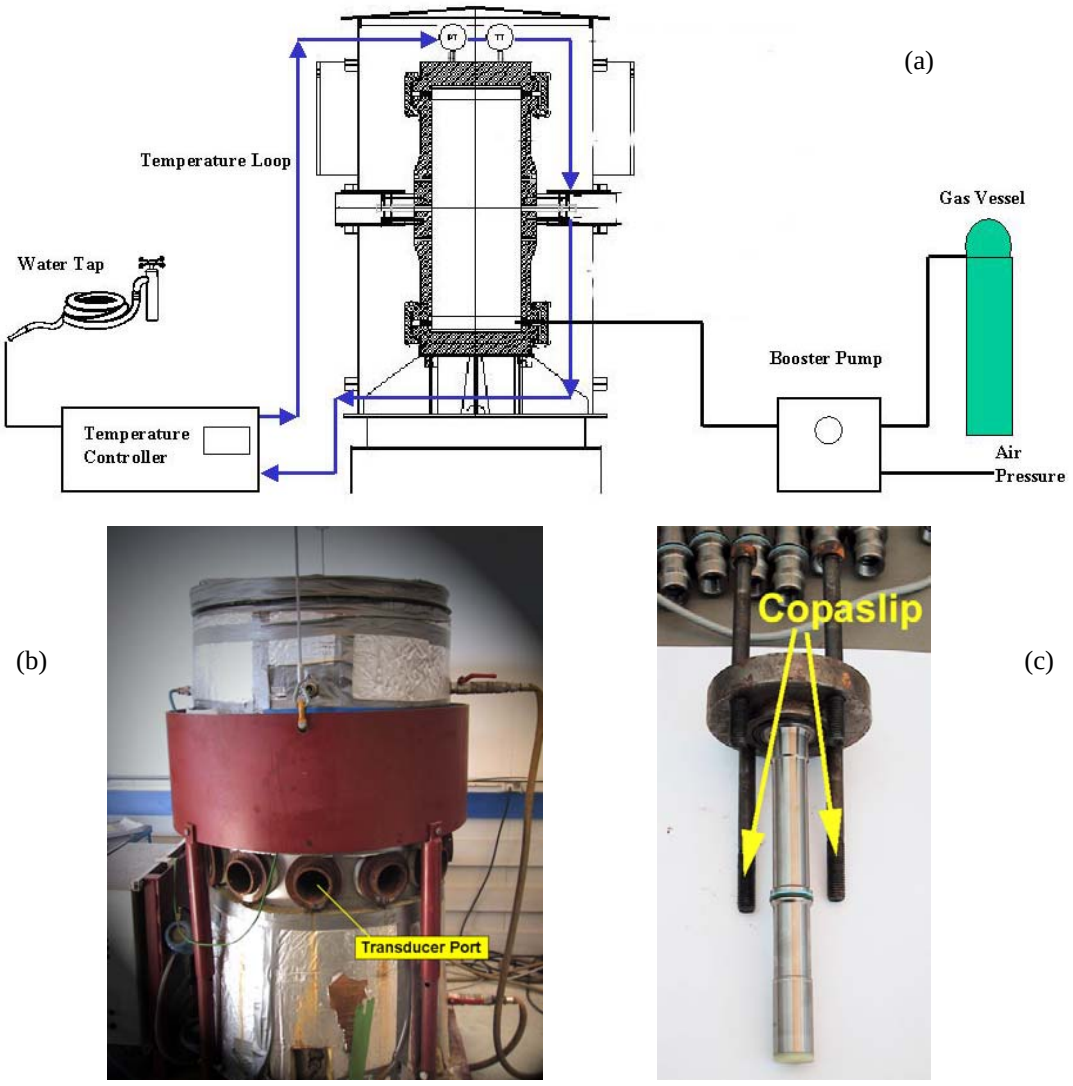

Fig. 10. The high-pressure transducer measurement chamber system used for Δt_i measurements (in nitrogen at "zero flow" conditions, as a function of pressure and temperature), for experimental "verification" of the theory in Section 2. (a) schematic overview, (b) photograph of chamber, and (c) transducer mounting arrangement.

In Fig. 11 (as in Fig. 12 below), each value of Δt_i is an average of 20-30 individual Δt_i measurements (single two-way "shots"), typically. In the data material underlaying Fig. 11, no individual Δt_i measurement was above 6.25 ns in magnitude, and typically the individual Δt_i measurements were below

[18] Only transducers having passed the transducer production QA were used in these pressure chamber measurements.

2.2 ns in magnitude. Such results further supports and strengthens the present realization of "sufficient reciprocal operation", cf. Eq. (24).

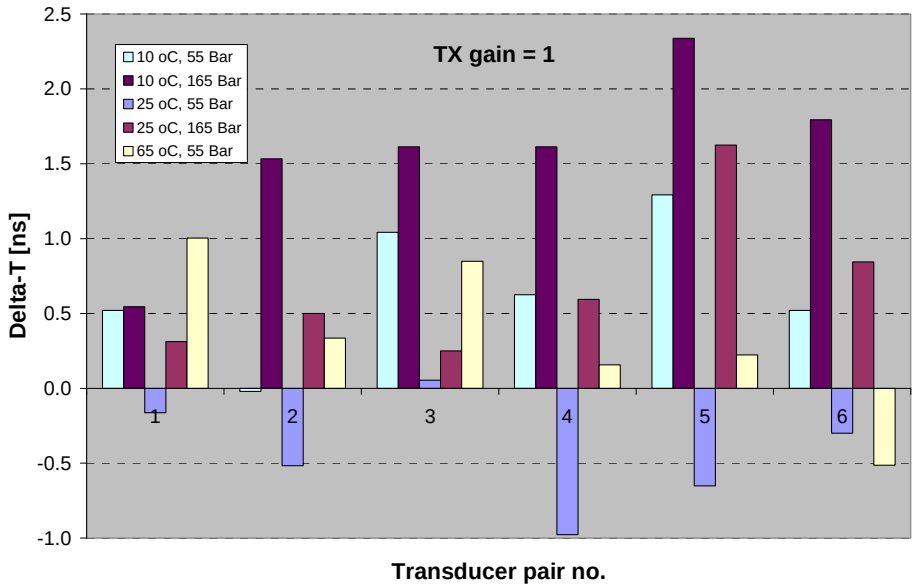

Fig. 11. Δt_i measurements made in the high-pressure chamber, at approximate "zero flow conditions", for six pairs of MPU 1200 ultrasonic transducers (arbitrary paired), for transmitter (Tx) gain setting 1 (lowest gain available), for some combinations of temperature and pressure: 10 ^{o}C / 55 barA, 10 ^{o}C / 165 barA, 25 ^{o}C / 55 barA, 25 ^{o}C / 165 barA and 65 ^{o}C / 55 barA.

Some additional observations can also be made from Fig. 11, at a more detailed level than actually needed here for the discussion of reciprocal operation or not, but which anyway may be of interest for better understanding the USM technology in relation to reciprocity.

From Fig. 11 it is noted that for a given transducer pair, the measured Δt_i may be positive at one *P-T* condition, and negative at another. This could be caused by small convection flows in the chamber, changing by changing *P-T* conditions, regulation system, etc. This could also possibly be explained by Eq. (29), which predicts that a sign change for $\Delta\psi$ leads to a sign change for Δt_i. That is, if the phase difference between the electrical impedances of transducers I and II ($\Delta\psi$, cf. Eq. (28)) changes sign from one *P-T* condition to another, so will also Δt_i.

For the same reason, the measured Δt_i may be positive at one pair, and negative at another (in Fig. 11 this is rarely the case, but Fig. 12 below demonstrates this effect clearly). That is, if the phase difference between the electrical impedances of transducers I and II changes sign from one USM path to another, at no-flow conditions, so will also Δt_i. In a flow meter this comes out as an advantage, since at no-flow conditions, one path may detect *positive* false flow, while another may detect *negative* false flow, depending on which transducer that is fired first in each pair, and the phase difference between the transducers (which may come out as a kind of "quasi-random" effect). So if the false flow detection at each path corresponds to a Δt_i of about (say) 1.6 ns (which according to Eq. (24) is already well below the limit of acceptable false flow detection!), the effective false flow detection of the USM (the integrated effect of all paths) will be even smaller. Such results further supports and strengthens the present realization of "sufficient reciprocal operation".

In Fig. 12, the measured Δt_i is shown as a function of transmitter (Tx) gain setting (in the range 1-100), for the same combinations of temperature and pressure. A tendency of increased Δt_i with increasing Tx gain may be observed in the results. However, the trend is not as clear as the results given in Fig. 9, which may indicate that other effects may possibly also be influent on the results shown in Fig. 12, possibly masking the effect of nonlinearity. It is also noted that the increase in Δt_i with increasing Tx gain is larger for pair no. 6 than for the other pairs, for most of the *P*-*T* conditions investigated here. The reason for that has not yet been clarified.

Thus, using the tentative example criterion of 2.4 ns given by Eq. (24), "sufficient reciprocal operation" has been demonstrated for the gas USM system at the lower TX gain settings, for number of transducer pairs, at all pressure-temperature points investigated here, covering points in the range 10 - 65 ^{o}C, 10 - 165 barA.

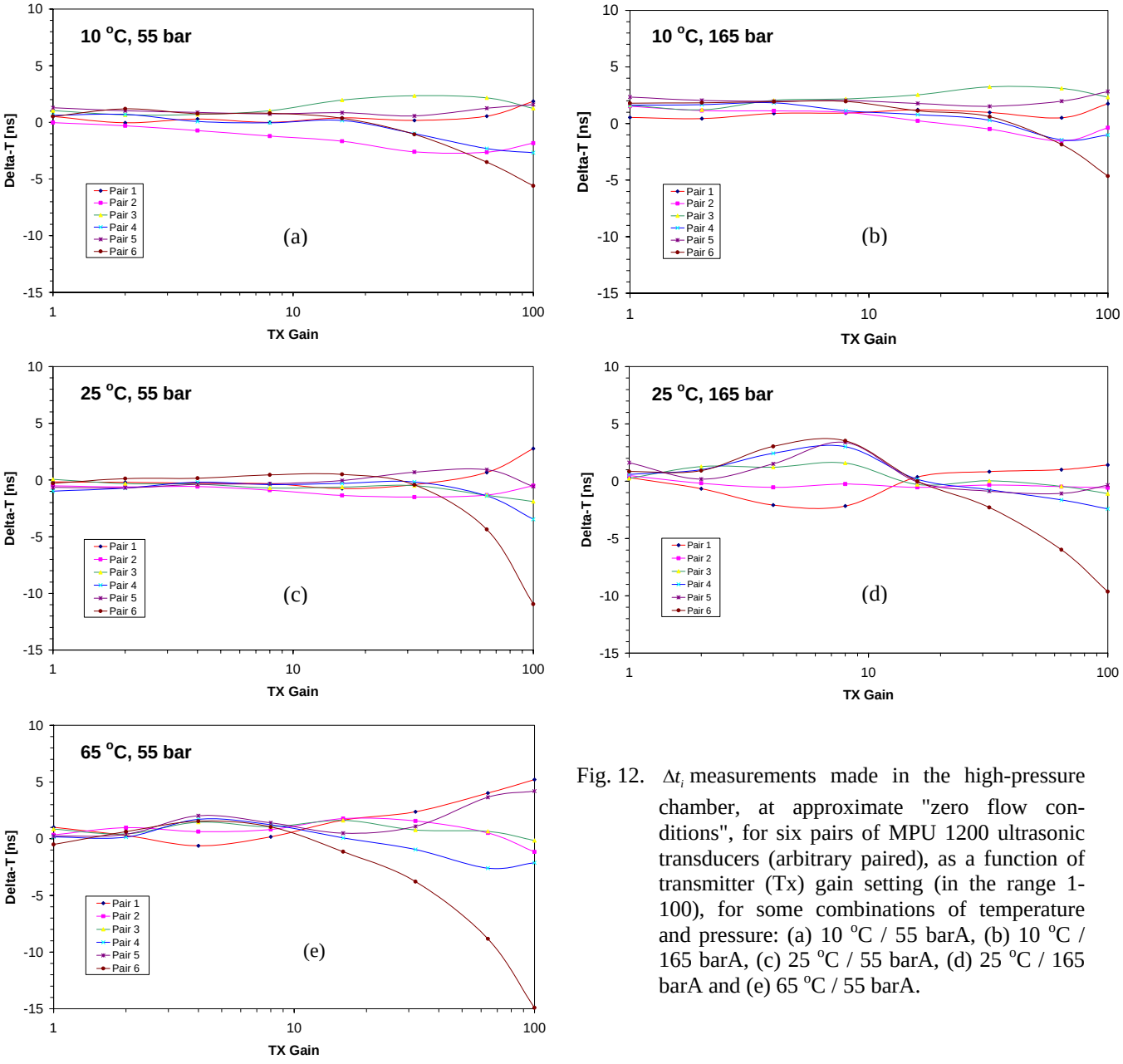

Fig. 12. Δt_i measurements made in the high-pressure chamber, at approximate "zero flow conditions", for six pairs of MPU 1200 ultrasonic transducers (arbitrary paired), as a function of transmitter (Tx) gain setting (in the range 1-100), for some combinations of temperature and pressure: (a) 10 ^{o}C / 55 barA, (b) 10 ^{o}C / 165 barA, (c) 25 ^{o}C / 55 barA, (d) 25 ^{o}C / 165 barA and (e) 65 ^{o}C / 55 barA.

4. CONSEQUENCES FOR ULTRASONIC FLOW METERS

A key question is of course, - "what can *sufficient reciprocal operation* do for the flow meter, if successfully exploited and implemented"? In fact it can do a lot:

- The need for measuring the Δt-correction as part of the “dry calibration” procedure ("zero flow verification") may be eliminated (or reduced), to the advantage of the manufacturer and the customer, such as simplified and reduced "dry calibration" procedures, reduced cost, and improved accuracy.

- By such methods the USM manufacturer can - by design - eliminate (or reduce) the need for active Δt-correction in the USM under field operation, independently of pressure, temperature, transducer ageing, drift, etc. Changes of transducer properties with T (or P) can be made less influent, so that these do not cause significant zero flow timing errors.

  For example, by using sufficiently low "firing voltage", so that the system is driven in a linear manner, it is demonstrated here that the transducers can be very different in characteristics, and "sufficient reciprocal operation" is still achieved. This means that if the transducers for some reason may be subject to significant drift over time (changing characteristics), the reciprocity of the USM system may not be significantly affected by that, as long as the system is driven linearly.

- This contributes to improve accuracy, linearity and reliability of the USM, in flow calibration as well as in field operation of the USM, at low flow velocities, without significantly affecting the accuracy at the high velocity measurements. That means, it can eliminate (or reduce) false flow reading in the range above the minimum flow velocity specified for the USM.

- It provides requirements for reproducibility in transducer production, in terms of the input electrical impedance of the transducer, which may simplify transducer QA, and contribute to cost reduction.

- The transducers are allowed to be different in their characteristic parameters, such as static capacitance, electrical impedance, resonance frequency, source and receiver sensitivities, directivity, etc. This will apply to all conditions of P, T, gas compositions and acoustic path length, as long as the "sufficient reciprocal operation" condition is met. In this connection it is worth noting that Eqs. (13)-(16) and (18)-(21) are derived without *any* assumption of "equalness" of the transducers[19]. Eq. (31) (and thus Eqs. (32)-(35)), on the other hand, i.e. the condition of "sufficient reciprocal operation", has been derived under a relatively weak assumption for the electrical impedances of the transducer production series, namely that the magnitudes are "about equal", and that the phase difference is much less than 90^o, i.e. $\Delta\psi_{\max} << \pi/2$.

  There is another interesting point in relation to "equalness" of the transducers. In ref. [19] it was claimed (on basis of simulation results) that reciprocal operation of the measurement system holds only when the transmitting and receiving transducers are identical (cf. Section 1). From the paper it seems as the authors have used voltage firing of the transmitting transducer and voltage reception at the receiver for simulating the transit time difference, Δt_i. If so, that may explain their findings, since in that case it has been shown above (Section 2) that perfect reciprocal operation of the USM relies on either (1) the transducers I and II being identical ($Z_I = Z_{II}$), or (2) "electrical symmetry" ($Z_S = Z_L$). The authors may possibly have overseen the latter possibility of "electrical symmetry" to achieve reciprocal operation, as well as the possibility of using one of the other cases classified under category "OK" above (e.g. current generator and voltage receiver, voltage generator and current receiver, etc.), for which reciprocal operation can be achieved much more independent of the transducers and their properties, cf. Section 2.

[19] "Sufficient reciprocal operation" can thus be achieved without using Eq. (31). Eq. (31), however, gives a specific *criterion* for that.

Possible *disadvantages* of using reciprocity may include factors such as:

- More careful design of the electronics circuitry is necessary, e.g. according to the conditions of "sufficient reciprocal operation" derived in Section 2, cf. Eq. (31).

- The USM system should be driven linearly, with maximum limits for the signal used for transducer excitation. That is, you cannot drive the transducer as "hard" as you like, which could otherwise be an attractive approach to achieve a high signal-to-noise ratio (SNR), required for accurate time detection [23]. When high excitation pulses are applied to the piezoelectric transducers the linear regime may be transcended, in which case there may be little advantage in reciprocal operation. Linearity of the transducers and the measurement system is an underlying assumption for the theory used in Section 2 to achieve "sufficient reciprocal operation". Investigations have shown that for firing voltages used in some USMs today, linearity may be violated to some extent [21,6]. A high firing voltage may cause a larger Δt-correction (a larger systematic timing error, and a larger false flow detection at low flow velocities, if not corrected for) than a low firing voltage [15].

  On the other hand, reciprocal operation is important only at the lower flow velocities. Noise may be more of a problem at the higher flow velocities (e.g. flow noise), for which reciprocal operation is not important, and higher "firing voltage" can be used to achieve a sufficient SNR.

  Moreover, there is an unsolved question whether a high degree of "equalness" of the transducers can possibly reduce the destroying effect of non-linearity on reciprocity. If so, this could possibly be exploited to use higher signal levels to increase the SNR at low flow velocities under difficult conditions (highly attenuating media) [23]. This interesting question has not been addressed in great detail here, and will require further effort to investigate in full depth.

5. CONCLUSIONS

With fluid flow approching zero, the USM method becomes increasingly dependent upon the reciprocity of the electro-acoustic measurement system. If reciprocity is not fulfilled, the measured transit times of upstream and downstream propagation will not be equal at zero flow, resulting in a zero flow timing offset, which becomes highly important in the low-velocity flow range, and provides false flow detection and degraded accuracy and linearity of the USM in this range. The AGA-9 report [1] and the API MPMS Ch. 5.8 standard [4] both prescribe need for "zero flow verification test (zero test)" or "zeroing the meter", for gas and liquid USMs, respectively.

In the present work, criteria have been established for "sufficient reciprocal operation" of the USM. By such methods the USM manufacturer can - by design - eliminate (or reduce) the need for active Δt-correction, and achieve "auto-zeroing" of the USM. Possible changes of transducer properties with temperature, pressure, and time (ageing, drift) can be made less influent, so that these do not cause significant zero flow timing errors. This contributes to improve the accuracy and reliability of the USM. Moreover, the need for measuring the Δt-correction as part of the “dry calibration” may be eliminated (or reduced), which may reduce costs and in several ways is advantage both for the manufacturer and the user of the flow meter. In addition, criteria have been derived to establish requirements for the reproducibility of the transducer production, which can be used in transducer production QA.

Disadvantages of using reciprocity may include factors such as (a) more careful electrical design is required, and (b) at low flow velocities, the USM system should be driven linearly, with maximum limits for the signal used for transducer excitation. Thus at such low flow velocities it may be more difficult to achieve the signal-to-noise ratio (SNR) which is required for accurate time measurement. For higher flow velocities, however, where high levels of flow noise may force a need for higher signal level to achieve a sufficient SNR, reciprocity is not an important concern.

The techniques to achieve "sufficient reciprocal operation" derived here have been implemented in ultrasonic flow meters for gas [22] and liquid [23]. In the present paper "sufficient reciprocal operation" has been demonstrated for the gas USM [22], with measured Δt_i of the order of 2 ns or less at approximate "zero flow" conditions and low-to-moderate signal excitation levels, over the pressure and temperature ranges 10-65 ^{o}C / 55-165 barA. At presumably more stable measurement conditions, using air at 21 ^{o}C and 9.5 barA, "sufficient reciprocal operation" has been demonstrated to within 0.7 ns, typically.

Similarly, "sufficient reciprocal operation" has been demonstrated for the liquid USM [23] (not shown here), with measured Δt_i of the order of 10-20 ps, using basically the same spoolpiece, electronics units (analog and digital) and software, for the gas and the liquid USMs.

Both results (for the gas and the liquid USMs) are well within the tentative requirements of 2.4 ns and 33 ps used here, respectively, cf. Eq. (24). As a result, auto-zeroing is achieved, and active Δt-correction is not used in these meters.

The methods derived and demonstrated here for "sufficient reciprocal operation" may be of general interest also to other electroacoustic measurement systems than the USM considered here, i.e. to all systems falling into the scheme of Fig. 4, and also to the more general case for which the signal generator (V_0, Z_S) and the electrical load (Z_L) may not be equal in (a) and (b) of Fig. 4.

ACKNOWLEDGEMENTS

Useful discussions with Kjell-Eivind Frøysa, Christian Michelsen Research AS (CMR), are highly appreciated. The work has evolved from and been inspired by project cooperation over a number of years, related to USM fiscal metering of gas and oil (custody transfer, sales and allocation metering), involving several partners: Fluenta AS (now Roxar Flow Measurement), Statoil, FMC Kongsberg Metering, FMC Smith Meter (USA), The Research Council of Norway (NFR), The Norwegian Society for Oil and Gas Measurement (NFOGM), the Norwegian Petroleum Directorate (NPD), GERG (Groupe Européen de Reserches Gazières), Norsk Hydro, ConocoPhillips and Gassco AS. In particular, the work has been supported by The Research Council of Norway (NFR), Statoil ASA and Gassco AS, under CMR's 4-year strategic institute programme “Ultrasonic technology for improved exploitation of petroleum resources” (2003-06).

REFERENCES

[1] **AGA-9**, “Measurement of gas by ultrasonic meters”, A.G.A. Report no. 9, American Gas Association, Transmission Measurement Committee (June 1998).

[2] **Lunde, P. and Frøysa, K.-E.:** “Handbook of uncertainty calculations - Ultrasonic fiscal gas metering stations”, Norwegian Petroleum Directorate, Norwegian Society for Oil and Gas Measurement (NFOGM), Christian Michelsen Research, Norway (December 2001). ISBN 82-566-1009-3 (free download available on web site www.nfogm.no).

[3] **Lunde, P., Frøysa, K.-E., Neumann, S. and Halvorsen, E.:** "Handbook of uncertainty calculations. Ultrasonic fiscal gas metering stations". *Proc. of 20th North Sea Flow Measurement Workshop*, St. Andrews Bay, Scotland, 22-25 October 2002.

[4] **API MPMS Ch. 5.8,** "Manual of petroleum measurement standards, Chapter 5 - Metering, Section 8 - Measurement of liquid hydrocarbons by ultrasonic flow meters using transit time technology". 1st edition, American Petroleum Institute (API), Washington DC, U.S.A (February 2005).

[5] **ISO/CD 18089 Part 1**, "Measurement of flow in closed conduits – ultrasonic meters for gas; meters for custody transfer and allocation measurement", International Organization for Standardization, Geneve, Switzerland (April 2005). (Committee draft standard only.)

[6] **Lunde, P., Frøysa, K.-E. and Vestrheim, M. (eds.):** "GERG project on ultrasonic gas flow meters, Phase II", GERG TM11 2000, Groupe Européen de Recherches Gazières (VDI Verlag, Düsseldorf, 2000).

[7] **Foldy, L.L. and Primakoff, H.**, "A general theory of passive linear electroacoustic transducers and the electroacoustic reciprocity theorem. I", J. Acoust. Soc. Am., **17**(2), 109-120 (October 1945).

[8] **Primakoff, H. and Foldy, L.L.**, "A general theory of passive linear electroacoustic transducers and the electroacoustic reciprocity theorem. II", J. Acoust. Soc. Am., **19**(1), 50-58 (January 1947).

[9] **Hemp, J.**, "Improvements in or relating to ultrasonic flowmeters", UK Patent No. GB 2017914 A (1979).

[10] **Sanderson, M. L. and Hemp, J.**, "Ultrasonic flowmeters – A review of the state of the art", Proc. of Int. Conf. on Advances in Flow Measurement Techniques, 9-11 September 1981, held at University of Warwick, England, organized by B.H.R.A. Fluid Engineering, Cranfield, Bedford, England, pp. 157-178.

[11] **Hemp, J.**, "Theory of transit time ultrasonic flowmeters", J. Sound Vib., **84**(1), 133-147 (1982).

[12] **Hemp, J.**, "Flowmeters and reciprocity", Quart. J. of Mech. And Appl. Maths., **41**(4), 503-520 (1988).

[13] **Hemp, J.**, "A review of the weight factor theory of transit time ultrasonic flowmeters", *Proc. of the 9th Int. Conf. on Flow Measurement (FLOMEKO '98), Lund, Sweden, 15-17 June 1998*, pp. 149-154.

[14] **Sanderson, M. L. and Torley, B.**, "Error assessment for an intelligent clamp-on transit time ultrasonic flowmeter", *Proc. of the Int. Conf. On Flow Measurement in the mid 80s", 9-12 June 1986, National Engineering Laboratory, East Kilbride, Scotland.*

[15] **von Jena, A., Mágori, V. and Ruβwurm, W.:** "Ultrasound gas-flow meter for household applications", Sensors and Actuators A, **37-38**, 135-140 (1993).

[16] **von Jena, A.,** "Triggering and evaluation arrangement for two ultrasonic transducers operable as transmitter and receiver", Patent No. WO9518956 (July 1995).

[17] **Martin, B.J., Temperley, N.C., Wendoloski, J.C., Edwards, G., Drew, P., Vanajek, J.I. and Dencher, P.R.,** "Liquid flow meter", US Patent No. US 6508135 B1 (Jan. 2003).

[18] **Lunde, P., Frøysa, K.-E. and Vestrheim, M.:** "Challenges for improved accuracy and traceability in ultrasonic fiscal flow metering", *Proc. of 18th Intern. North Sea Flow Measurem. Workshop, Gleneagles, Scotland, 24-27 Oct. 2000*.

[19] **van Deventer, J. and Delsing, J.**, "Apparent transducer non-reciprocity in an ultrasonic flow meter", Ultrasonics, **40**, 403-405 (2002).

[20] **Lunde, P., Frøysa, K.-E. and Vestrheim, M.:** "*GARUSO* - Version 1.0. Uncertainty model for multipath ultrasonic transit time gas flow meters". CMR Report No. CMR-97-A10014, Christian Michelsen Research AS, Bergen, Norway (August 1997).

[21] **Lunde, P., Bø, R., Andersen, M.I., Vestrheim, M., and Lied, G.:** "GERG project on ultrasonic flow meters. Phase II - Transducer testing", CMR Report no. CMR-99-F10018, Christian Michelsen Research AS, Bergen (April 1999). (Confidential.)

[22] "Ultrasonic gas flow meter MPU 1200. Specifications", Bulletin SSKS001, Issue/Rev. 04 (5/02), FMC Measurement Solutions (2005). Web page: http://info.smithmeter.com/literature/docs/ssks001.pdf

[23] **Kalivoda, R. and Lunde, P.**, "Liquid Ultrasonic Flow Meters for Crude Oil Measurement", *Proc. of 23rd Intern. North Sea Flow Measurem. Workshop, Tønsberg, Norway, 18-21 October 2005*.

[24] **ISO**, "Guide to the expression of uncertainty in measurement", 1st edition, ISO, Geneva, Switzerland (1995).

[25] **NPD**, "Regulations relating to measurement of petroleum for fiscal purposes and for calculation of CO_2 tax", Norwegian Petroleum Directorate, Stavanger, Norway (November 1, 2001).

North Sea Flow Measurement Workshop 2005

Volker Herrmann, Toralf Dietz, Andreas Ehrlich, SICK MAIHAK

Peter Stoll, Heiko Slawig, Verbundnetz Gas AG

The use of an Ultrasonic „Transfer reference meter“ to investigate differences of two gas meters in series in fiscal natural gas measurement.

Custody transfer meter station design often requires the use of two gas flow meters: The duty meter, and the reference meter. Both meters have to meet custody transfer requirements and therefore have a low measurement uncertainty. These type of installations ensure availability, redundancy and the on-line verification of the measurement.

The standard installation procedure for such meter stations includes a high-pressure calibration for both meters that normally should provide a “zero” difference between the readings. Even at proper station design in a few cases unacceptable deviations can be found directly after field installation of the meter. If there is not a simple reason, often the only appropriate measure is nowadays to check the high pressure calibration of the meters in an official laboratory. Even this extremely expensive and time consuming measure does not always guarantee success since possible installation effects will not be detected this way.

Another possibility is to define a “transfer reference meter package”, using one or two different state-of-the-art gas flow meters. A “transfer reference meter” is considered to be a calibrated meter with the highest achievable insensitivity to installation effects and long term stability.

This paper introduces the use of an Ultrasonic 8 path „Transfer reference meter“ and a reference meter of another technology to investigate differences as high as 0,8% in a German custody transfer station. This method can be used much more effectively since none of the meters under question needs to be taken out of operation or sent back. Additionally, using the more detailed profile information gained from an 8 path meter it is possible to investigate installation effects and detect sources of the deviations.

First results of the investigation of the above mentioned station will be shown and discussed. Possible ways of using transfer reference meters of different technologies and their advantages and drawbacks are also considered.

1 Introduction

VNG – Verbundnetz Gas AG – is the main company for gas transport in the eastern part of Germany. The share of natural gas transferred by VNG is 16% of the gas sales of Germany. The supply region is firmly integrated into the European interlinked system with 4 main delivery points. The natural gas network used for these tasks is composed of high-pressure pipelines having an overall length of about 7,100 kilometres. For supply purposes, VNG AG operates six underground gas reservoirs having a storage capacity of 2.2 billion m³.

As already mentioned, the natural gas is imported from the 4 large stations and delivered to the customers at about 300 transfer points. This explains the outstanding importance, from a metrological point of view, of the measuring technology used in the import stations.

Furthermore, the entire pipeline network is displayed in an online simulation by means of a so-called gas management system. In this context, a basic data supply as reliable as possible (exact quantity values) is also a mandatory requirement for achieving a stable model status. Here, the input measurements are of overriding importance due to their relatively small number.

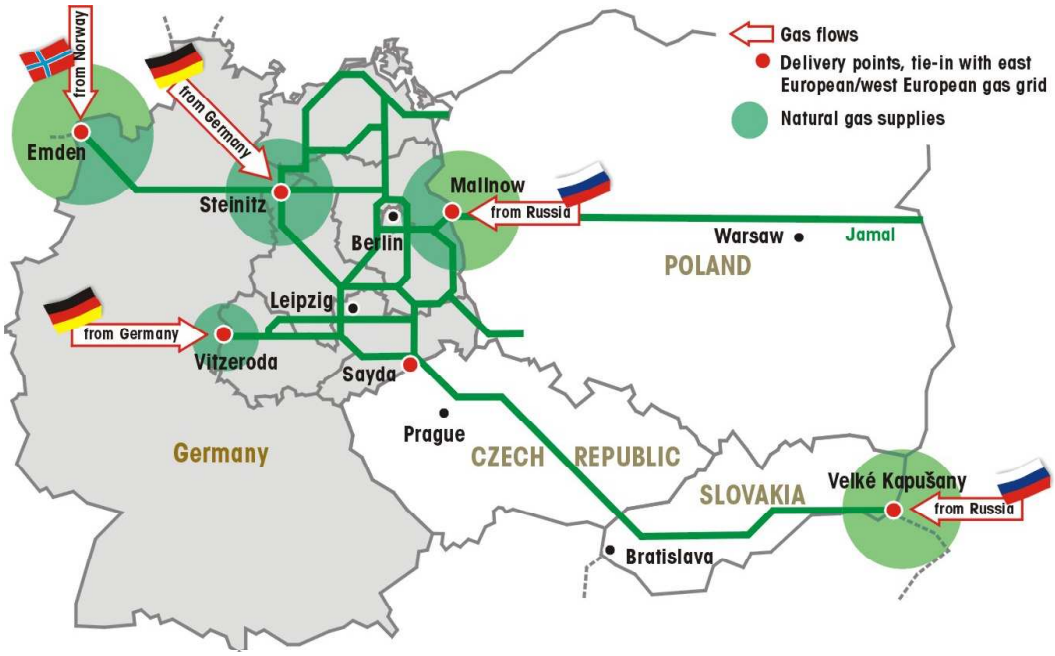

Figure 1 VNG main pipeline network

In Germany, two calibrated measuring devices are usually used in series in custody transfer stations. These devices mostly consist of a turbine gas flowmeter and a vortex flowmeter or increasingly a combination of turbine gas flowmeter and ultrasonic gas flowmeter. In this arrangement, only one meter designated as master meter is always used for invoicing. The second meter serves to detect systematic influences and should normally operate only with a small offset to the master meter. With purchase orders for measuring equipment in the recent past, VNG has been using the approach to define the deviation of the meters between each other not only during high-pressure calibration but also in the system-integrated state, taking a maximum permissible deviation of 0.5% as a basis.

In the present case, this value is not kept over the entire measuring range in a measuring installation. Deviations occur that represent either too large an offset or a non-linear behaviour of the meters. It is assumed that these are the result of system influences which affect the primary measurement, despite compliance with all statutory requirements.

In the previous course of diagnosing such deviations, it has turned out to be very difficult to detect the affected meter in measuring installations and - even more important - to convince the supplier of a possible malfunction, if applicable. Depending on the „know how“ or the willingness of individual firms, troubleshooting and fault detection thus develops into a very lengthy process in most cases.

To date, the next most obvious action in such a case was to retest the meters under high-pressure conditions at a test lab and to calibrate them again. Depending on the magnitude of the system influence, however, satisfactory results can be achieved only very rarely, in addition to the very high cost.

At this stage, the only remaining solution is:

1) to ignore the error, unless it is relevant with regard to invoicing, or

2) to apply other meter technologies at a high cost.

In this context, the logic is to use a kind of portable calibration package for natural gas for fault detection and/or fault assessment, similar to the approach with liquids, e.g. oil.

1.1 Approach to Problem Solution

The possible solution of the above-mentioned problems, presented here, is a **„reference meter section“** that is in this case installed instead of a control section downstream of the primary measurement.

The basic principle was the detection, or elimination, of possible system influences since in such a case no improvement of the measuring characteristics can be expected from the renewed high-pressure tests. With respect to possible system influences, special attention has been given to the flow pattern (asymmetry, swirl) and pulsations. Resulting from this information, a selection of the gas meter technologies to be applied was made.

Alternative variants, such as examinations of flow, pulsation and profile, do not constitute any alternative, neither in terms of time nor in terms of costs, except in simple cases.

As a result of the pro's and con's shown in table 1, the decision was made to use both the ultrasonic-type and the Coriolis gas flowmeter for the set-up of the portable reference meter section. During the first investigation phase, a turbine gas flowmeter was temporarily used as 3rd measuring system for referencing and plausibility analysis, of the results. This will not be required anymore in the final state of the reference meter section.

The reasons for the use of the ultrasonic gas flowmeter are primarily to be found in its well-known stability with undisturbed conditions, as compared to a turbine gas flowmeter, and in its outstanding diagnostic capabilities. Thus, the selected 8-path design allows a very specific statement as to swirl and flow pattern. Furthermore, it is now possible to compare the measured sound velocity of the ultrasonic gas flowmeter with those calculated from the gas composition, provided by a gas chromatograph.

A Coriolis meter was selected for the second measuring method. To date, only very limited experiences has been gained on its use in natural gas; however, this is acceptable within the scope of this investigation. This meter commends itself because of its also very compact fitted length and the expected accuracy.

	Overload withstand capability	Flow pattern, swirl	Pulsation, mech. vibrations	Gas contami-nation	Remarks
Orifice plate	😐	😐	☹	☹	long upstream length required, small measuring range
Vortex flowmeter	☺	☹	☹	😐	long upstream length required
Turbine gas meter	☹	😐	☹	😐	Established measuring system, multiple years of practical experience, extensively researched
Ultrasonic gas meter	☺	😐	☺	☺	4-path design can compen-sate for asymmetry and swirl, but only 8-path design allows quantitative diagnosis
Coriolis gas flow meter	☺	☺	☺	😐	abrasive influences of the gas flow, mechanical changes

Table 1 Technology overview and weighting from a user's point of view

The „reference meter section“ installed at VNG is shown below. All three meters mentioned above were installed at the mounting location in the position of a vortex flowmeter (Figure 2) belonging to a control section. The old control section was completely removed and replaced by the reference meter section (Figure 3).

Figure 2 Meter section with vortex flowmeter prior to modification

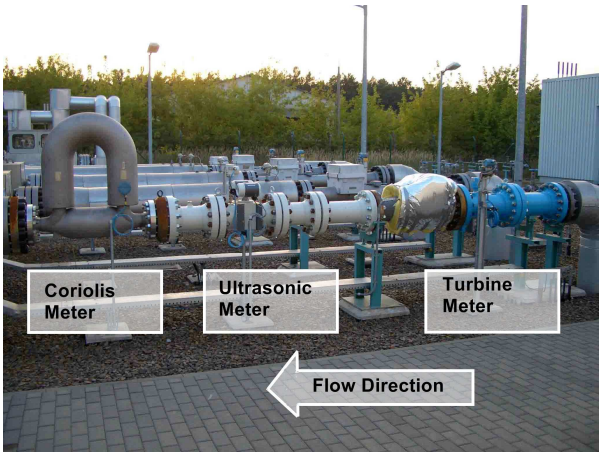

Figure 3 Installed reference meter section with Coriolis, ultrasonic and turbine gas meters (from left to right)

2 Technology and Calibration of the Reference Meters

2.1 8-Path Ultrasonic Flow Measuring System

2.1.1 Description

Standard components of the FLOWSIC 600 gas meter series were used for the 8-path ultrasonic measuring system. The arrangement of 4 additional measuring paths was in particular enabled by the meter body's symmetric construction, which was selected for the stability of the meter body geometry with respect to pressure and temperature (Figure 4). Miniaturised ultrasonic sensors ensure that the flow in the measuring section is influenced to a minimum extent only.

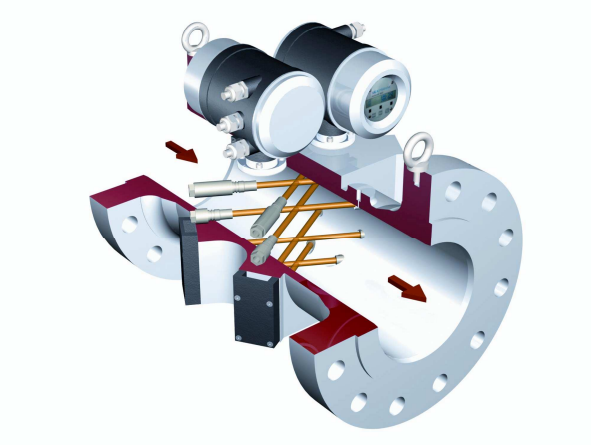

Figure 4 **Arrangement of the 8 ultrasonic measuring paths**

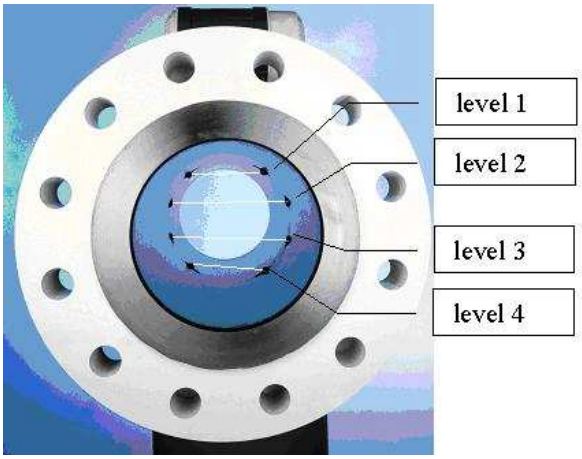

Figure 5 **Distribution of measuring path levels over the cross section**

The geometric position of the measuring path levels (Figure 5) has been maintained, exclusively to the FLOWSIC 600, since this layout provides a very good compensation for the flow pattern [1]. This completely symmetric 8-path arrangement creates 2 paths on exactly the same path level, and thus measurements are taken on the same level in the flow pattern. Due to the fact that the path angles are inverse to each other, tangential components are recorded with opposite sign. This enables a precise and transparent computation of these components. The additional measuring paths make it possible do show precise detailed information on local gas velocity components and to detect the possible causes of deviating measurements. As will be shown hereinafter, the FLOWSIC 600 may thus be calibrated on completely the same standard on air test stands under ambient conditions as well as under high-pressure conditions. The main focus within the scope of this paper, however, has been put on the use for diagnostic purposes.

The measuring result of an ultrasonic path is determined by the local velocity components in axial and tangential direction within the integration range of the ultrasonic signals. Figure 6 is supposed to serve for elucidation. The axial component, in the direction of the pipe axis, is the essential velocity component. Its value is determined by the gas transport. The tangential component is rectangular to the axial one. Tangential components represent swirl-subjected, rotating flows. This rotation is virtually always caused by the customary pipe fitting elements

(double elbows out of plane, U-turns, T-fittings), but may be dampened effectively by suitable measures such as flow straighteners).

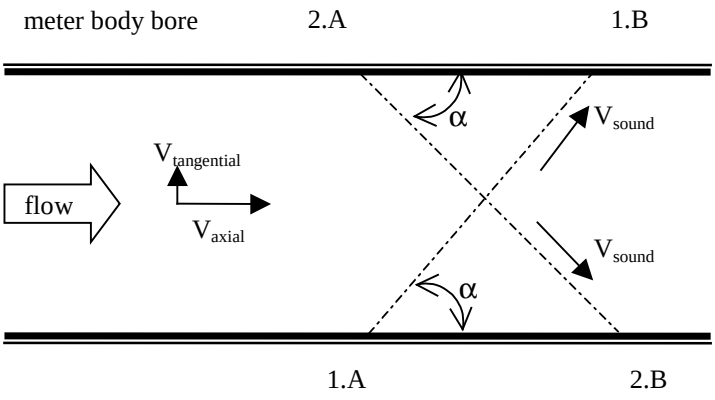

Figure 6 Schematic diagram

Referring to Figure 6, the following is to illustrate the influence of the tangential velocity component. The ultrasonic sensors of the system 1 (sensor 1.A and 1.B) are arranged at an angle α to the pipe axis. The distance between the sensor membranes defines the length of the measuring path (L_1). Accordingly, system 2 is characterised by the sensors 2.A and 2.B, angle α to the pipe axis, and the length of the measuring path L_2. As is well known, the transmitted signals propagate at the sound velocity of the medium. Taking account of the tangential velocity component, as shown in the figure, the signal transit time between the system 1 sensors is then defined by:

$$t_{1ab,1ba} = \frac{L_1}{v_{sound} \pm \cos(\alpha) \cdot (v_{axial} + v_{\text{tangential}} \cdot \tan(\alpha))}$$

For system 2, comparable conditions are the result, only the sign of the tangential velocity component is changed. Consequently, the signal transit time for system 2 is defined by:

$$t_{2ab,\,2ba} = \frac{L_2}{v_{sound} \pm \cos(\alpha) \cdot (v_{axial} - v_{\text{tangential}} \cdot \tan(\alpha))}$$

By calculating the signal transit time difference, it can then be demonstrated for the flow velocity of system 1 that the following is valid:

System 1

$$v_1 \cong v_{axial} + v_{\text{tangential}} \cdot \tan(\alpha)$$

System 2

$$v_2 \cong v_{axial} - v_{\text{tangential}} \cdot \tan(\alpha)$$

Taking the two independently computed gas velocities v_1 and v_2, it is now possible to state the amount of the axial and the tangential component:

Axial velocity component

$$v_{axial} = \frac{v_1 + v_2}{2}$$

Tangential velocity component

$$v_{tangential} = \cot(\alpha) \cdot \frac{v_1 - v_2}{2}$$

When this logic is applied to all four measuring paths it is possible to demonstrate the asymmetry and swirl of the flow pattern and to use them for diagnostic purposes.

2.1.2 Calibration

In order to be able to use the reference meter section as universally as possible, it is particularly interesting to perform the calibration in a wide Reynolds' number range. This can be achieved when the flowmeter is calibrated both on a low-pressure test stand (air, ambient conditions) and a high-pressure test stand. If a relation of the low-pressure and high-pressure characteristic curves can be established, it will be possible to retest the reference meter section more cost-effectively in the future. The retest on a low-pressure test stand would then be sufficient to deduce the high-pressure characteristic curve.

For ensuring that only measurement errors allocated to the flow pattern are identified during flow calibration, the sound velocity has to be verified in advance. Only if the set geometric and time parameter values correspond to reality the measured sound velocity will be in line with the velocity computed theoretically. This would ensure independence from gas type and gas state (in this case air and natural gas). The determined deviations between the measured sound velocities, seen in relation to those computed theoretically from the gas analysis, are depicted in Figure 7 for the tested ultrasonic measuring system. The SonicWare® software was used to compute the theoretical sound velocity. The set of formulae has been standardised and documented in the A.G.A. Report No. 10.

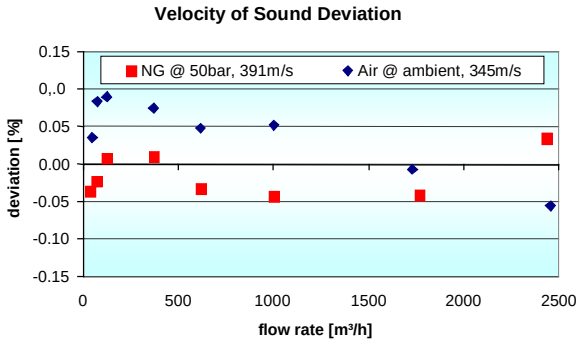

Figure 7 **Illustration of the relative deviation of the measured sound velocity from that computed theoretically**

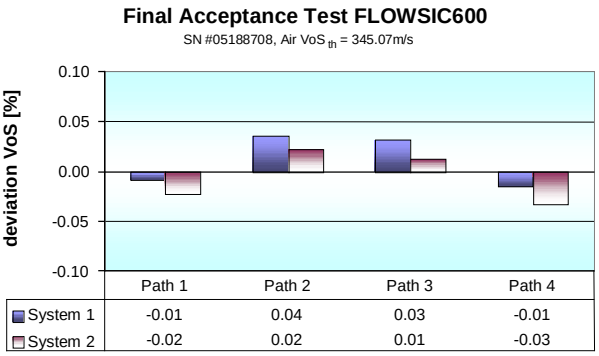

Figure 8 **Illustration of the relative deviation of the sound velocity measurement during final inspection prior to delivery**

All determined deviations between the measured and the theoretically computed sound velocities are in a range of ±0.1%, at average sound velocities of 345m/s (air) and 391m/s (natural gas). Thus, the stability of the geometric and time parameters over a wide working range has been proven.

The flow calibration was performed on the recognised Pigsar® test stand in Dorsten for the high-pressure error curve for natural gas, and on the VNG-owned test stand in Leipzig for the error curve for air.

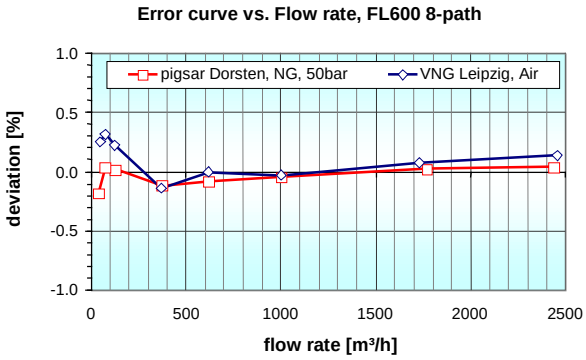

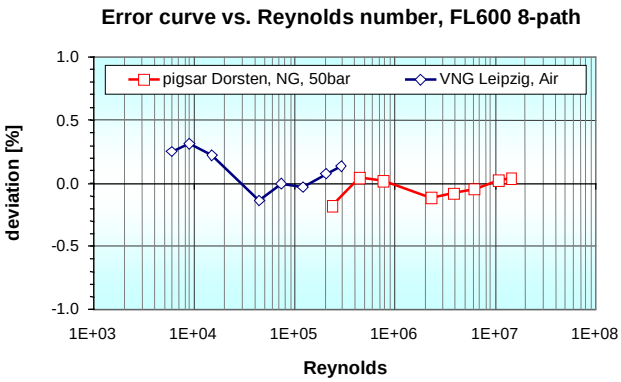

Figures 9, 10 Adjusted characteristic error curves of the 8-path ultrasonic measuring system, shown across flow rate and Reynolds' number range

The average deviation of –0.1% determined from the Pigsar® results was adjusted in both systems of the ultrasonic flowmeter. The adjusted results are shown in Figures 9 and 10, respectively. The conformance of the error curves is clearly below the specified test stand uncertainties of 0.16% for Pigsar® and 0.3% for VNG Leipzig. Figure 11 is supposed to elucidate this. The bi-variate point distribution shown is limited each time by the test stand uncertainties extended by the maximum linearity error of the ultrasonic flowmeter (0.2%). This results in a range of $\pm\sqrt{0.16\%^2 + 0.2\%^2} = \pm 0.26\%$ for Pigsar® and accordingly $\pm 0.36\%$ for Leipzig.

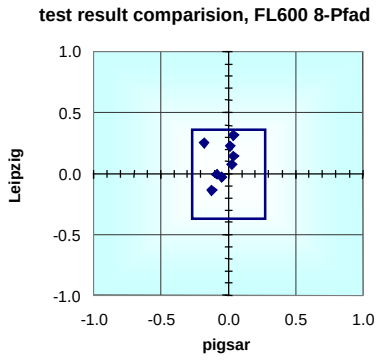

Figure 11 Comparison of high and low-pressure characteristic curves

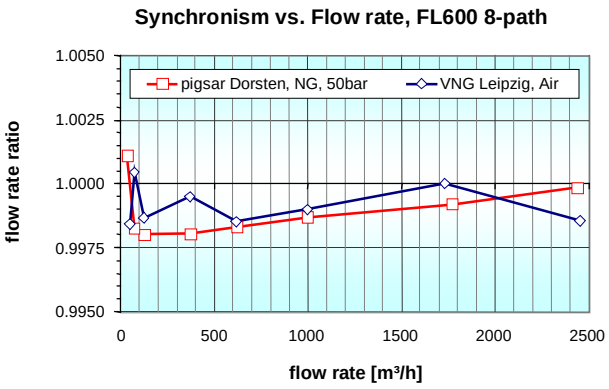

Figure 12 Synchronism of both systems during high and low-pressure test

2.2 Coriolis Gas Meter

Due to the experience already gained by the Emerson company in the field of gas measurement, a CMF400 of the Micro Motion Elite series was selected as the Coriolis gas meter. Its outstanding features are its compact construction, very good repeatability and the specifications that are very suitable for this type of application. The topics of zero drift, temperature and pressure sensitivity were intensively discussed in advance. The result of this discussion was that these influences could be excluded as not being relevant. Further information may be found in [3] and [6].

The meter used was repeatedly calibrated on a water test stand in Veenendall (uncertainty < 0.003%). Both tests performed produced an approximately identical result (<0.1%). The measuring range of 1:50 (Qmin/Qmax) required for the reference meter section has also been adhered to with an adequate uncertainty.

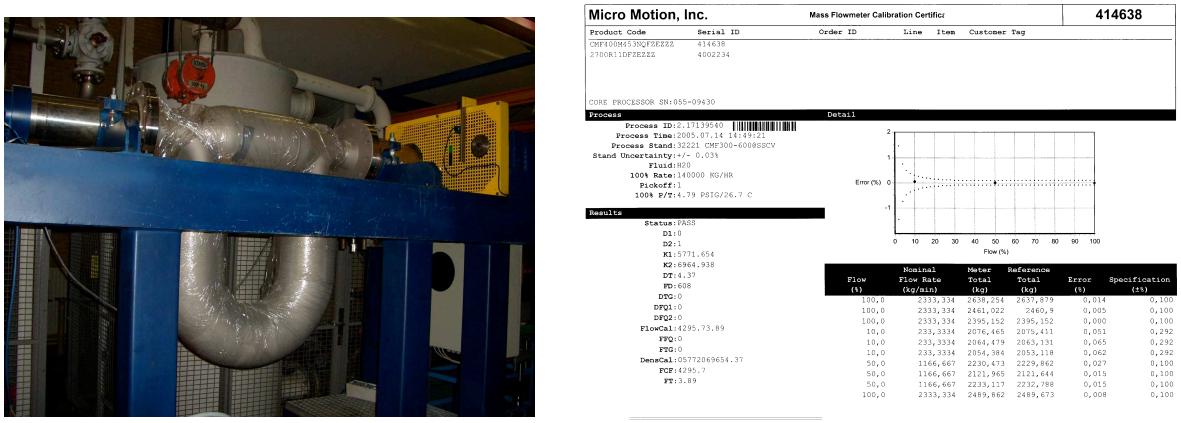

Figure 13 Water calibration, calibration certificate

At the time, no further high-pressure calibration with natural gas was carried out. The results seem to support the possibility of such an approach. In the later course of the series of measurements it is planned to verify the behaviour found in the 1st testing series both on a high-pressure test stand with natural gas and on an air test stand.

2.3 Turbine Gas Flowmeter

Since the turbine gas meter technology is well known, we have refrained from a detailed description within the scope of this paper. Detailed information on the turbine gas meter can be found in [4].

In our case, the description of the calibration results are of more interest. The turbine flowmeter also was tested both in air and under high-pressure condition. Again, the adjusted final result of the calibration is shown. The average deviation of 0.34% determined in the high-pressure test was adjusted by changing the pulse significance.

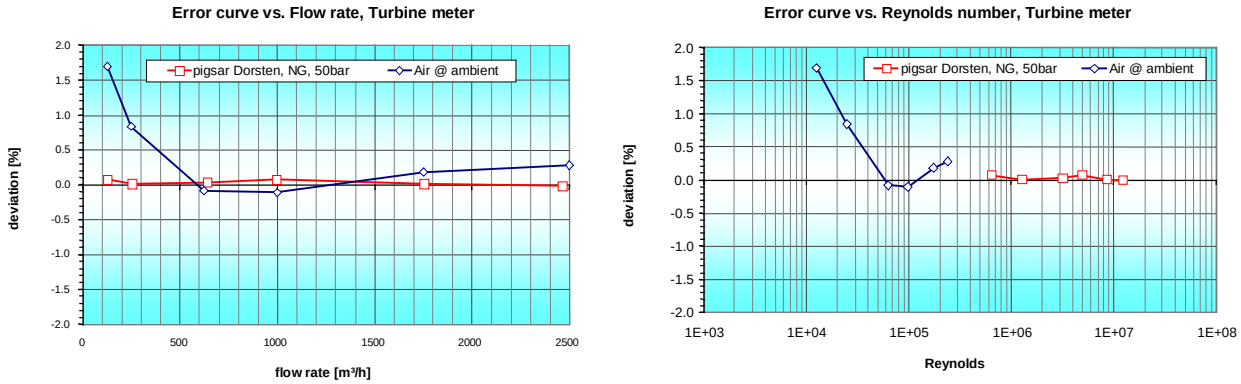

Figures 14, 15 Adjusted characteristic error curve of turbine gas flowmeter, shown across flow rate and Reynolds' number range

3 Signal Conditioning, Data Acquisition

Acquisition and conditioning of signals were done in different ways. First, each meter was equipped with its own flow computer ([5], Figure 16). Through the archiving function of these flow computers, the measured data is available for remote data readout. In order to have a basis of comparison for the meters to each other, all values were related to the converted volume at base conditions. For the ultrasonic meter and the turbine meter, the standard volume conversion is used, based on the gas state readings of a processed gas chromatograph (PGC). The PGC also provided the current value of the standard density required for the conversion of the mass information from the Coriolis gas meter. The station is equipped with 2 PGCs that showed only minimum deviations during the test period.

Figure 16 Quantity weight converter and measured value registration for the remote data inquiry of the reference meter section

In parallel with this, the measuring and diagnostic data was recorded and archived via the serial interfaces of the ultrasonic measuring system.

4 Results

In Germany, larger stations are generally split into a primary and a secondary section where the primary and secondary meters – as described in chapter 1 – must be within the deviation band defined by the operator. If there are deviations in the installation between primary and secondary meters, these can be diagnosed by means of the reference meter package described. The use of two additional independent measuring technologies allows conclusions to be drawn as to which of the installed meters is out of specification and thus a targeted and cost-effective improvement of the situation is made possible.

This approach has been implemented within the scope of this project. Since the data collected and conclusions drawn are not the sole property of VNG and SICK, they are not described here in detail. The installed reference meter section has clearly proven successful in the diagnosis of the deviations. The following will therefore address the technical observations that were obtained in the examination of the reference meter section while disregarding the primary section.

The main part of the measuring results shown herein was recorded in the months of August and September. A period of about 2 weeks was needed until commissioning was satisfactory. During this period, primarily first statements as to the zero point stability and the signal output of the Coriolis gas meter as well as to the synchronism and/or the signal processing of the two ultrasonic meter electronics were made.

At the beginning of the measurement, a clear diurnal variation of the meters between each other could be identified. The temperature, to be more precise, the not representative temperature measurement, very quickly turned out to be one of the greatest influencing factors. Among other things, for instance, the arrangement of the sensors between the turbine gas meter and the ultrasonic measuring system is not ideal. Even so, all these influencing variables allowed the measurements to work within the required ±0.5% range so that the actual measuring programme could be started.

4.1 Plausibility Check of Sound Velocity

After commissioning of the „reference meter section“, the measured velocity of sound was verified against the theoretical velocity of sound . On the first day , a provable difference between the velocities was established. A diurnal variation was also clearly identified in the difference. This variation correlated very well with the direct solar radiation on the reference meter section (Figure 17, 6th Sept. 2005). The protection of the temperature measuring location against direct solar radiation by an insulating mat produced a distinct improvement, although a diurnal variation in the measuring set-up is still visible (Figure 17, from 7th Sept. 2005 onwards). While there were deviations of up to –0.15% caused by diurnal variation, the small deviation of less than ±0.05% observed earlier on the test stands were also reached in the field operation after applying the insulation.

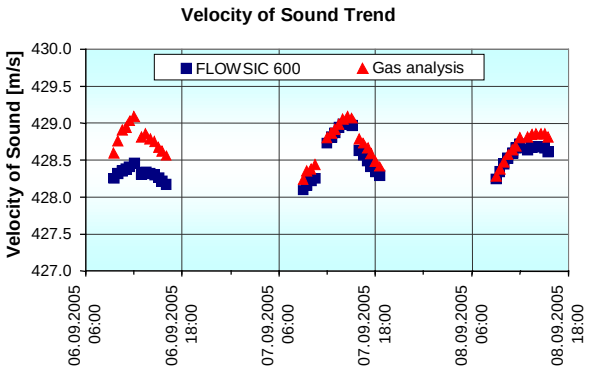

Figure 17 Comparison of measured to theoretical velocity of sound

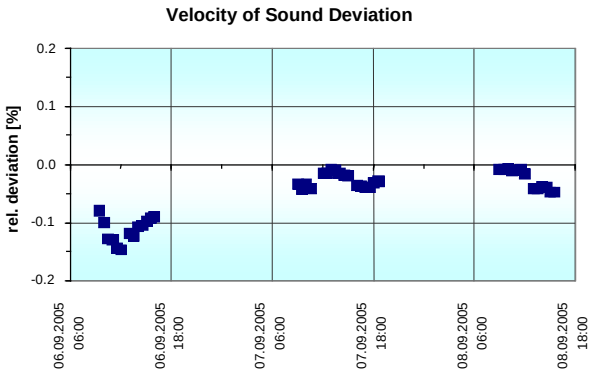

Figure 18 Relative deviation between measured to theoretically computed velocity of sound

4.2 Flow Pattern, Swirl

For an effective and fast assessment it is necessary to convert the offered, path-position-related detailed information on the axial and tangential velocity components into a dimensionless characteristic number. The swirl number K_v described in [2] is suitable for this purpose. Taking the numeric weighting of the path positions into account, the general swirl number definition specified herein can be modified for the ultrasonic meter as follows:

$$K_v = \frac{\sum_{i=1}^{4} w_i \cdot v_{axial_i} \cdot v_{\text{tangential}_i}}{\left(\sum_{i=1}^{4} w_i \cdot v_{axial_i}\right)^2} \qquad w_i = \begin{cases} 0.1382 \text{ for } i = 1 \text{ and } 4 \\ 0.3618 \text{ for } i = 2 \text{ and } 3 \end{cases}$$

Amongst other things, the characteristic numbers specified in the table were determined in [2] by systematic velocity profile measurements using the laser doppler anemometry. These can be used to easily assess and classify the flow situation present.

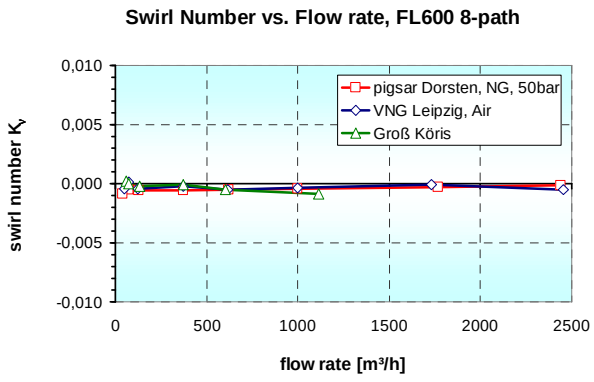

Figure 19 Illustration of determined swirl numbers

	Swirl no. K_v
Double Elbow out of Plane	0.092
OIML mild disturbance	0.115
OIML severe disturbance	0.181
T-fitting succeeded by 90°-elbow	0.134
Fully developed flow profile	0.00

Table 2 Characteristic swirl numbers for typical flow situations

From Figure 19 it can clearly be concluded that, on the test stands as well as in the installation, the swirl components are below those of disturbed flow situations by orders of magnitude. Virtually, a swirl-free flow can be assumed for the ultrasonic measuring system.

4.3 Comparison of Measuring Results

Figure 20 shows the results of the first endurance test phase for the ultrasonic measuring system and the Coriolis mass meter. Illustrated each time is the relative difference in the standard volume of the observed meter to the turbine gas meter, according to:

$$Dev = \left(\frac{V_{\text{meter}}}{V_{\text{turbine meter}}} - 1 \right) \cdot 100\%$$

Each point represented in the illustration corresponds to an acquisition time of one hour. The reduced number of measuring points for the Coriolis gas meter has its reason in the measuring programme. Due to the installation of the Coriolis meter directly upstream of further installation components, no measurements using the Coriolis meter were taken at high velocities. The turbine flowmeter will be removed after completion of this part of the programme, giving the necessary space between the Coriolis gas meter and the other installation components. The ultrasonic meter and the Coriolis meter will then be tested across the flow range that had previously been limited.

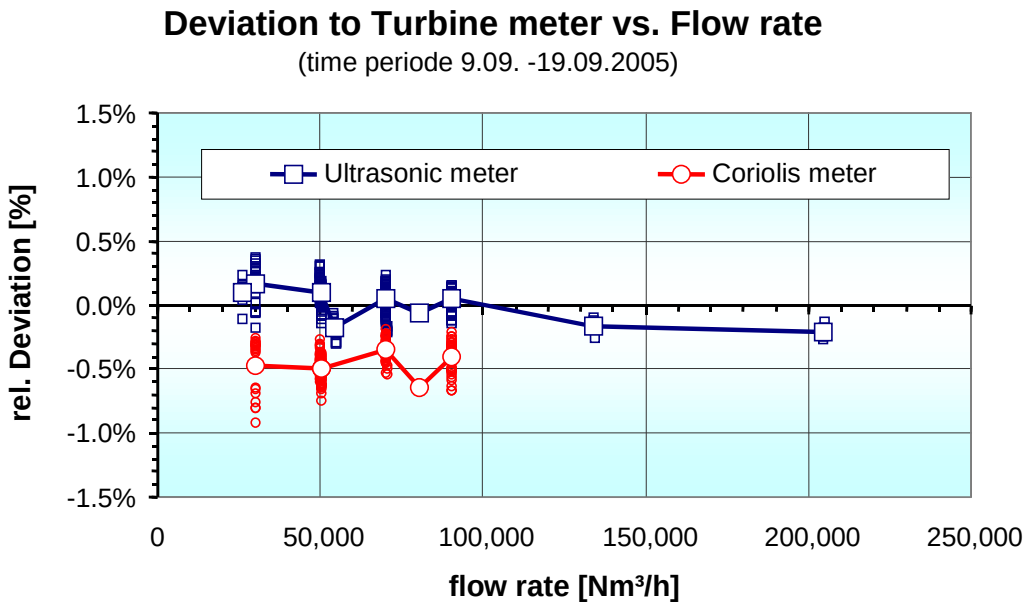

Figure 20 Relative deviations of ultrasonic and Coriolis gas meter to turbine gas meter

Taking account of the uncertainty still present at the current stage with respect to the representative temperature measurement , the following statements can be made:

1. Ultrasonic and turbine gas meter show the characteristic error curve determined during the joint calibration. The average deviations to each other are in the range of ±0.2%.
2. First of all, a stable offset of –0.5% to the turbine and ultrasonic gas meter must be stated for the Coriolis flowmeter. In this context, it should be mentioned again at this point that this meter, as a mass meter, was calibrated with water only. An offset correction was intentionally not made since the question of which meter has to be corrected in which way can not be answered at present. A remedy would be the calibration of the Coriolis meter on a high pressure or low pressure test stand for natural gas. The clarification of the offset will form part of the further programme. A retest on the SICK-MAIHAK air test stand in Dresden is planned at least for the reference meter section of ultrasonic and Coriolis flowmeters. There, the spatial and metrological conditions are available in order to test the entire reference meter section.

In summary it can be said that the target requirements were complied with and „almost better“ than expected performance by the reference meter section under adverse metrological conditions were achieved. All people involved assume that this meter section at this operating site may be used to 100% as a reference for other measurements!

As mentioned before, the crucial influence on the stability of the reference meter section is exercised by the temperature. Even with a temporary solution using makeshift insulation, the influence of temperature is still recognisable. This means that all meters, together with their inlet lines, will have to be insulated when this reference meter section is to be used for outdoor measurement. Moreover, the temperature measurement will have to be arranged close to the relevant meter.

Using the diagnostic data from the ultrasonic gas meter, statements as to the flow and profile behaviour within the reference meter section could be made and verified using appropriate evaluation methods. It has thus become possible to assess or evaluate system influences that cannot be recorded during a high-pressure test, directly in the installation.

Due to the unique situation of being able to examine three meters, which are based physically on most different principles, simultaneously in one meter section, a great deal of data has been recorded, archived, and evaluated. Of course, a final evaluation without further work is not feasible at present, as constantly new considerations also keep on raising new questions. With the time frame available, it was unfortunately not yet possible to answer all identified questions. These would be, for example:

- Cause of the stable offset between ultrasonic/turbine gas meter and Coriolis gas meter
- Optimal arrangement of the temperature measuring points and reducing the influence caused by the difference between gas temperature (about 22 °C) and fluctuating ambient temperature
- Diagnostic opportunities through „acoustic“ temperature computation based on the measured sound velocities (temperature layering of the gas)
- Proof of system influences (none were identified in this case) or detection of normally ignored influences
- Which accuracy or reproducibility is attainable in the future, taking account of the aspects of long-term stability and portability of the reference meter section?
- Development of new re-calibration concepts for high-pressure natural gas facilities

On the part of VNG it can be stated that during the tests series no restrictions whatsoever as to the Coriolis gas meter were recognisable. This means for the future that the permanent series connection of ultrasonic and Coriolis meters will be an absolutely conceivable measuring approach, particularly for bi-directional measurements.

5 Conclusion / Outlook

The use of a reference meter section integrating different measuring technologies for diagnosing installation-conditional deviations under operational conditions has proven to be very successful. The combination of metrological experience of the manufacturers, the application-engineering competence of the operator, and the utilisation of the diagnostic capabilities of state-of-the-art measuring methods, such as the ultrasonic and the Coriolis measuring technique, allows an in depth study of the behaviour of the measuring section. Taking this as a basis, it is possible to optimise station layouts, reduce the cost for additional high-pressure calibrations, and ensure reliable operation.

The plan for the future is to examine the offset between ultrasonic/turbine gas meter and Coriolis gas meter by extended tests. Among other things, the entire package will be tested once again both under high-pressure and low-pressure conditions. At the same time, a statement will be made as to the long-term behaviour of the relative deviations.

As an additional intellectual approach, the idea has arisen to examine whether a sole low-pressure calibration and/or water calibration for meters may be sufficient in the future.

6 Literature

[1] K. J. Zanker “The effects of Reynolds number, wall roughness, and profile asymmetry on single- and multi- path ultrasonic meters” NSFMW Oct 1999

[2] Mickan, B; Wendt, G.; Kramer, R. and Dopheide, D. (1996). Systematic investigation of pipe flows and installation effects using laser doppler anemometry; Part II: „The effect of disturbed flow profiles on turbine gas meters – a describing impirical model“, Flow Meas. Instrum., Vol. 7, (1996), No. 3/4, pp. 151-160

[3] Bas van Ravenswaaij, „AGA Report No. 11 Expands Market For Proven Metering Concept“, 22nd North Sea Flow Measurement Workshop 26 – 29 October 2004

[4] RMG Messtechnik GmbH, manual „Operating Instructions for the TRZ 03 / TRZ 03-K / TRZ 03-L Turbine Meters“

[5] FLOWCOMP Systemtechnik GmbH, data sheet “gas-net F1”

[6] Micro Motion, Inc., Installation and Operation Manual “ELITE® Sensor”, June 2003

Wet Gas Metering with the V-Cone and Neural Nets

Haluk Toral and Shiqian Cai
Petroleum Software Ltd.
Robert Peters
McCrometer

Abstract

The paper presents analysis of extensive measurements taken at NEL, K-Lab and CEESI wet gas test loops. Differential and absolute pressure signals were sampled at high frequency across V-Cone meters. Turbulence characteristics of the flow captured in the sampled signals were characterized by pattern recognition techniques and related to the fractions and flow rates of individual phases. The sensitivity of over-reading to first and higher order features of the high frequency signals were investigated qualitatively. The sensitivities were quantified by means of the saliency test based on back propagating neural nets. A self contained wet gas meter based on neural net characterization of first and higher order features of the pressure, differential pressure and capacitance signals was proposed. Alternatively, a wet gas meter based on a neural net model of just pressure sensor inputs (based on currently available data) and liquid Froude number was shown to offer an accuracy of under 5% if the Froude number could be estimated with 25% accuracy.

Introduction

Wet gas measurements were conducted under a wide range of conditions with a V-cone meter in the test loops at NEL, K-Lab and CEESI. Measurements, comprising high frequency signals from pressure and differential pressure sensors, were analysed by characterisation of the turbulence properties of the flow by means of a pattern recognition / neural net methodology described in previous publications [1,2]

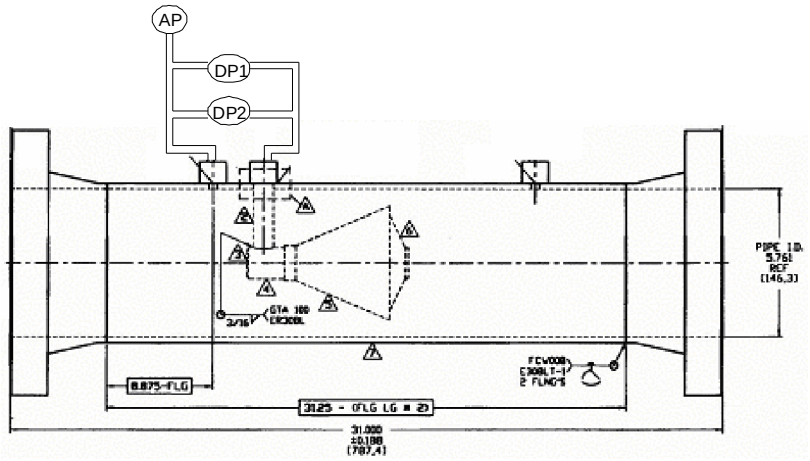

DP1: Standard DP
DP2: ESMER Fast DP
AP: ESMER Fast AP

Figure 1. Schematic Diagram of V-Cone

The V-cone was connected to high frequency absolute and differential pressure gauges and a portable PC as the data acquisition system. The signals were sampled and analysed by extracting characteristic features from fluctuating differential and pressure signals sampled at high frequencies. Examples of such features can be given as standard deviation in the amplitude domain and linear prediction coefficients in the frequency domain. The efficiency of the features for discriminating between different flow conditions is assessed by means of the Saliency test. The features were then related to the superficial velocities of individual phases by means of a back-propagating neural net. A data flow diagram of the concept is shown in figure below.

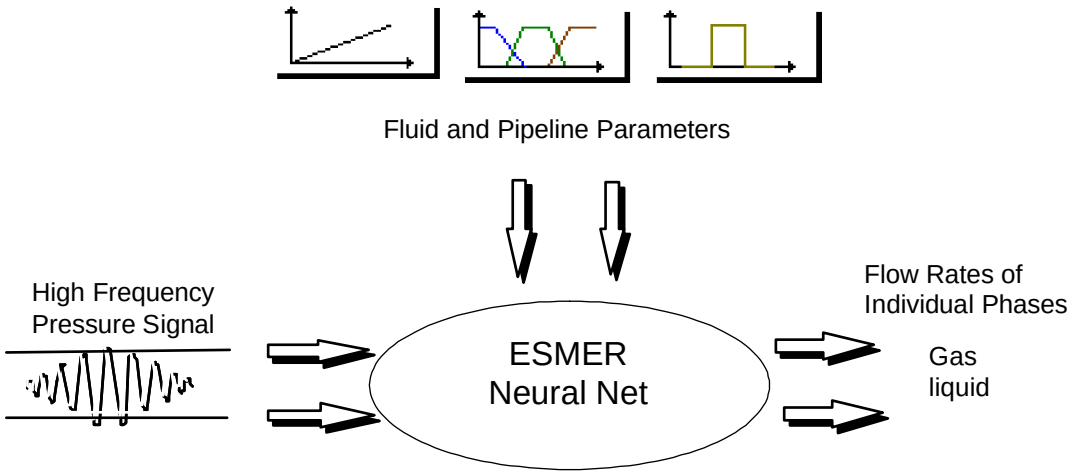

Figure 2. Schematic diagram of the ESMER concept

Test matrices covered a range of flow conditions up to 15% liquid volume fraction, operating pressure up to 90 bar; gas actual volumetric flow of 1000 m3/hr. Kerosene, condensate, field gas and nitrogen was used in different labs in 4" and 6" lines. The chart below gives a graphic summary of the flow conditions.

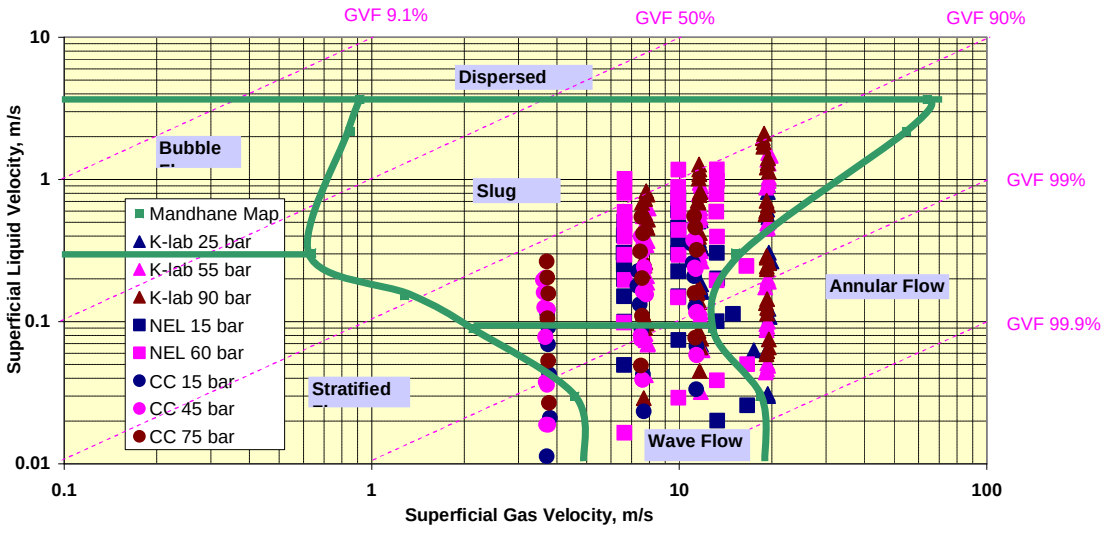

Figure 3. Operating envelope of NEL, K-lab and CEESI test data

Qualitative Analysis

We have started the analysis with the conventional *overreading* graph. Briefly, this graph shows the effect of the liquid fraction on the differential pressure measured across the V-Cone. The liquid fraction is quantified by means of the Lockhart Martinelli number as the ratio of liquid momentum to gas momentum expressed as:

$$X = \frac{m_l}{m_g}\sqrt{\frac{\rho_g}{\rho_l}}$$

and the differential pressure across the V-cone is non-dimensionalised with the theoretical dry gas differential pressure expressed as:

Over-reading = $\sqrt{\Delta p / \Delta p_g}$

where :

Δp_g = theoretical differential pressure across the V-cone calculated from the standard V-cone equation based on (reference) superficial gas velocity [3]

Overreading is partly due to the presence of the liquid phase (greater mixture density than that assumed by the application of the dry gas equation) and partly due to greater frictional losses in the throat of the V-Cone as a result of interfacial interactions between the segregated phases as explained long ago by Lockhart Martinelli [4]

"The pressure drop in the two phase flow is greater than that for the flow of either single phase alone for various reasons, among which are the irreversible work done by the gas on the liquid and the fact that the presence of the second fluid reduces the cross sectional area of flow for the first fluid. Thus during two-phase flow the hydraulic diameters Dl and Dg are always less than the pipe diameter Dp as noted in the Fanning equations…, this reduction of hydraulic diameter will increase the pressure drop greatly."

The overreading graph shows a wide scatter when all data points are included for measurements taken in all laboratories. For example, figure 4a shows the overreading graph for NEL and figure 4b shows the overreading graph for K-Labs.

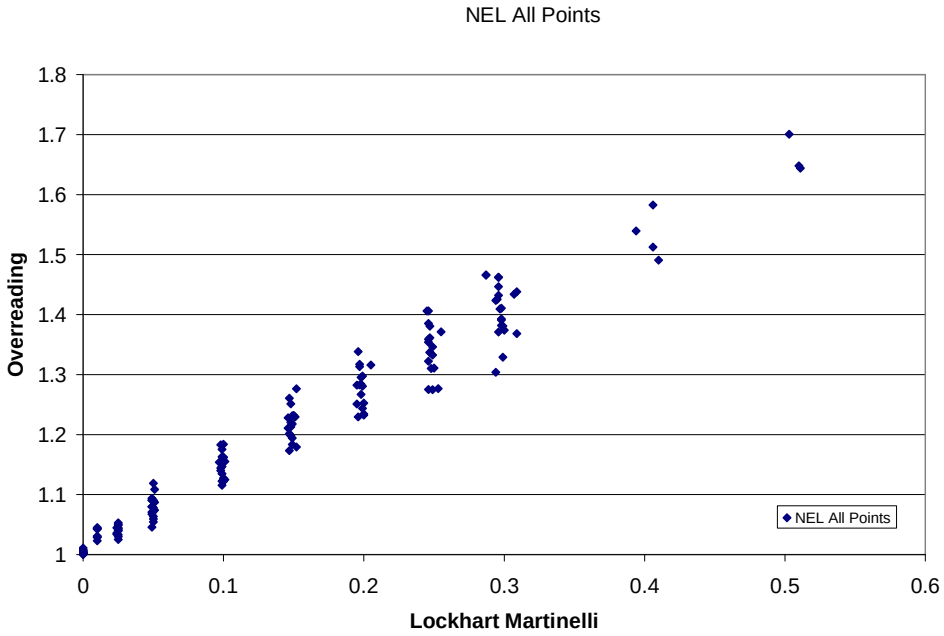

Figure 4 a.Overreading graph for data collected at NEL

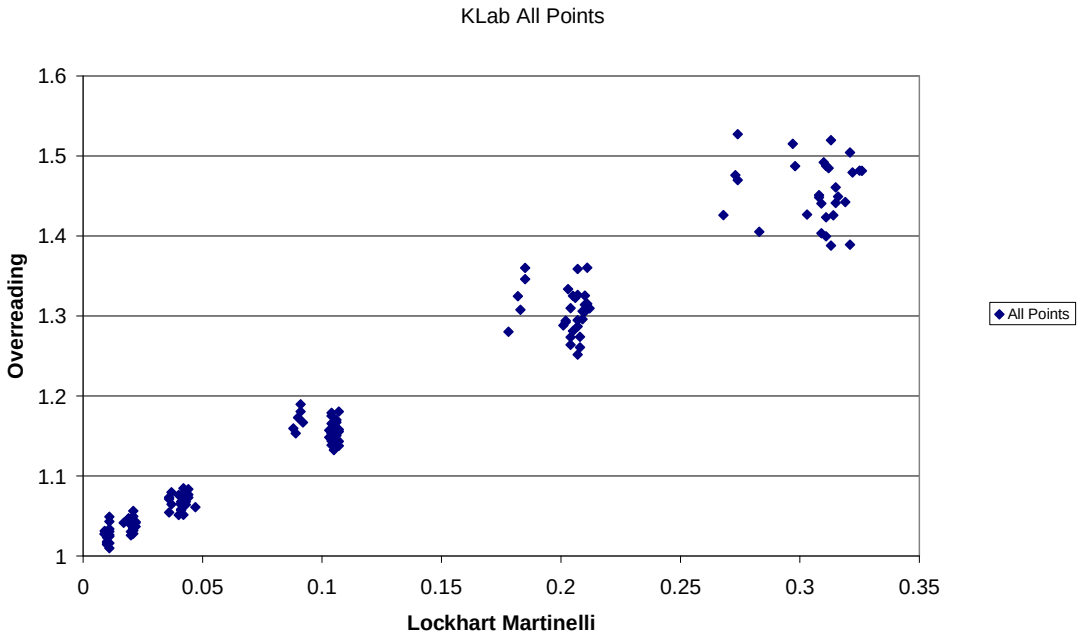

Figure 4 b.Overreading graph for data collected at K-Labs

We have considered a number of possible reasons for the scatter on these graphs including:

- variation in the physical properties
- variation in the density of fluids
- flow regime effects
- experimental error
-

As the physical properties of the fluids are constant at each laboratory, variation in the physical properties can be ruled out as an explanation of the scatter.

Density variations were considered next. As the tests were carried out with the same liquid in each series of tests, we only had to consider the effect of variation in the density of the gas. We have used pressure as a surrogate for examining this effect. Figure 5a for NEL and figure 5b for K-labs shows that density / pressure has a definite effect on the scatter.

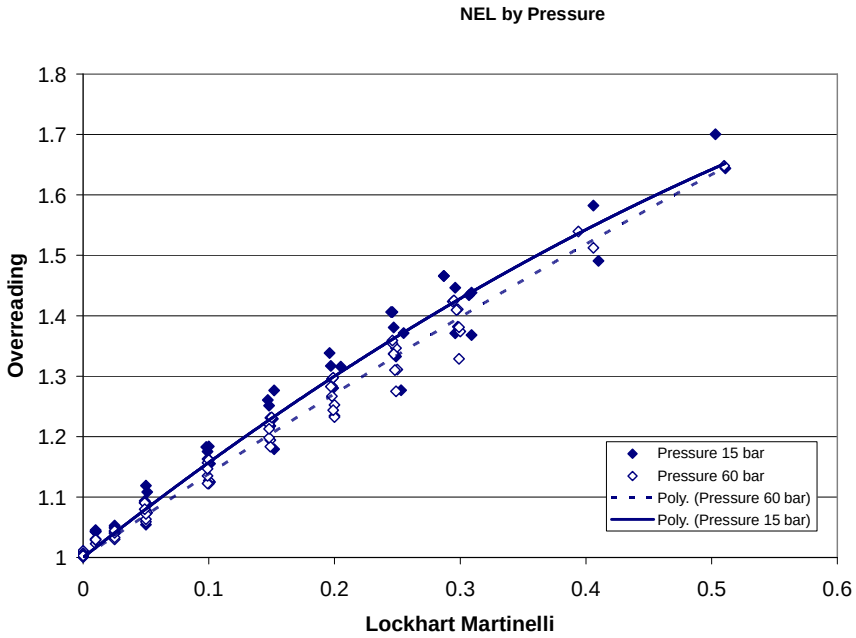

Figure 5 a.Overreading graph for data collected at NEL at different pressures

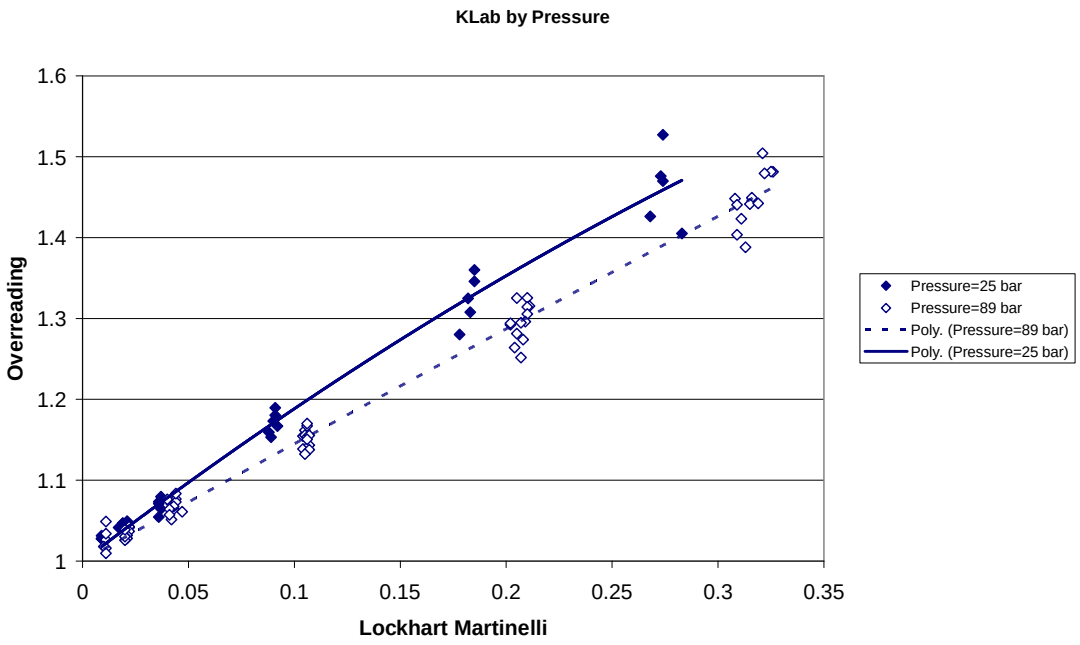

Figure 5 b.Overreading graph for data collected at K-Labs at different pressures

It is seen that overreading increases with decreasing pressure (ie gas density) at the same Lockhart Martinelli number. This can be explained as greater turbulence, and

hence greater interfacial frictional losses arising from the commingled flow of phases of larger density difference.

We have next examined the flow regime effect in further depth. The flow regime effect is of course already taken into account by the Lockhart Martinelli number as a first order effect. The ratio of liquid to gas momentum will exert a decisive effect on the flow regime. The density effect mentioned above can also be considered as a second order flow regime effect.

However, there is another factor at work in establishing the finer characteristics of the flow regime at a given Lockhart Martinelli number and pressure (gas density). This is the ratio of the axial momentum (of the liquid or the gas phase) to gravitational force arising from the difference in density of gas and liquid phases. The Froude number provides the mathematical expression to this ratio. Figures 6a for NEL and figure 6b for K-Labs shows the scatter caused by the variation in Froude number within given Lockhart Martinelli bands. The overreading increases with increasing Froude number because of greater turbulence effects giving rise to larger frictional pressure loss. As expected the Froude number effect was observed to diminish with increasing pressure.

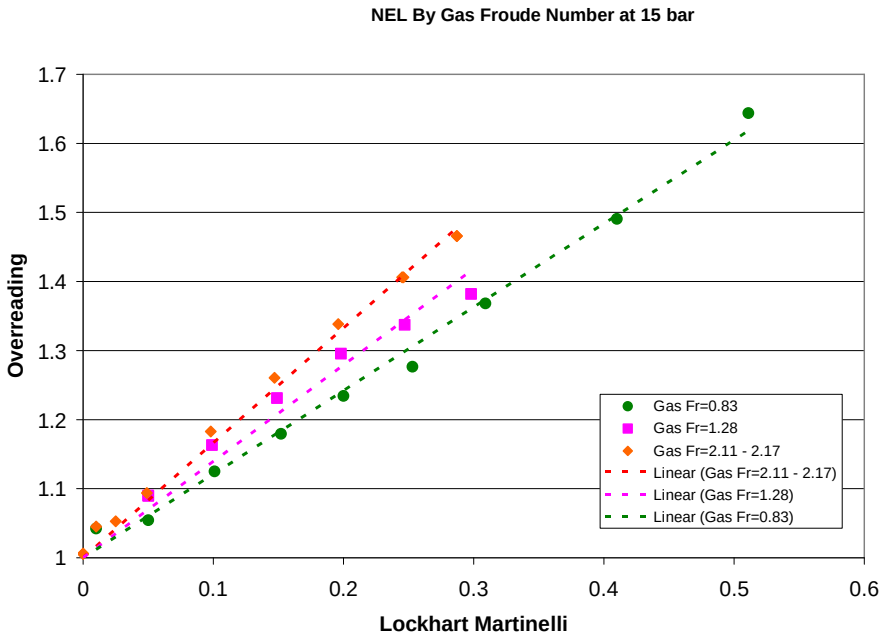

Figure 6 a.Overreading graph for data collected at NEL at different Froude number

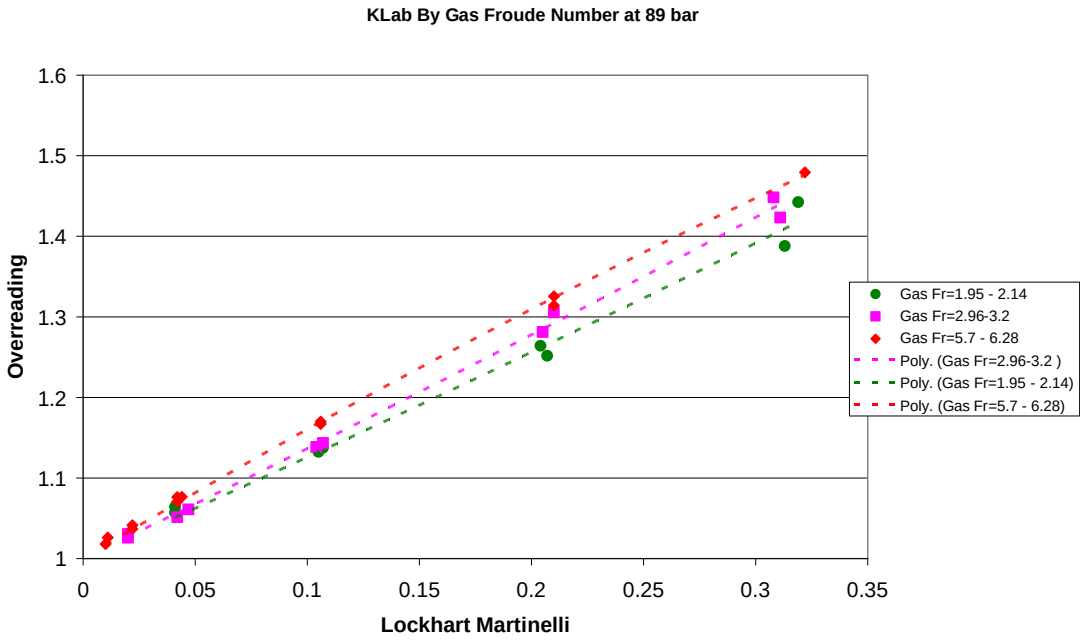

Figure 6 b.Overreading graph for data collected at K-Labs at different Froude number

The importance of the Froude number was highlighted when comparing the results from two labs at the same Froude number. For example, figure 7a, shows two sets of data drawn from NEL at different Froude numbers. As normal, the overreading increases with Froude number. However, the graph of overreading drawn from K-Labs measurements coincide with that from NEL at the same Froude number. This finding confirms the importance of Froude number as a first order effect and also indicates that experimental error is of lesser importance as an explanation of scatter.

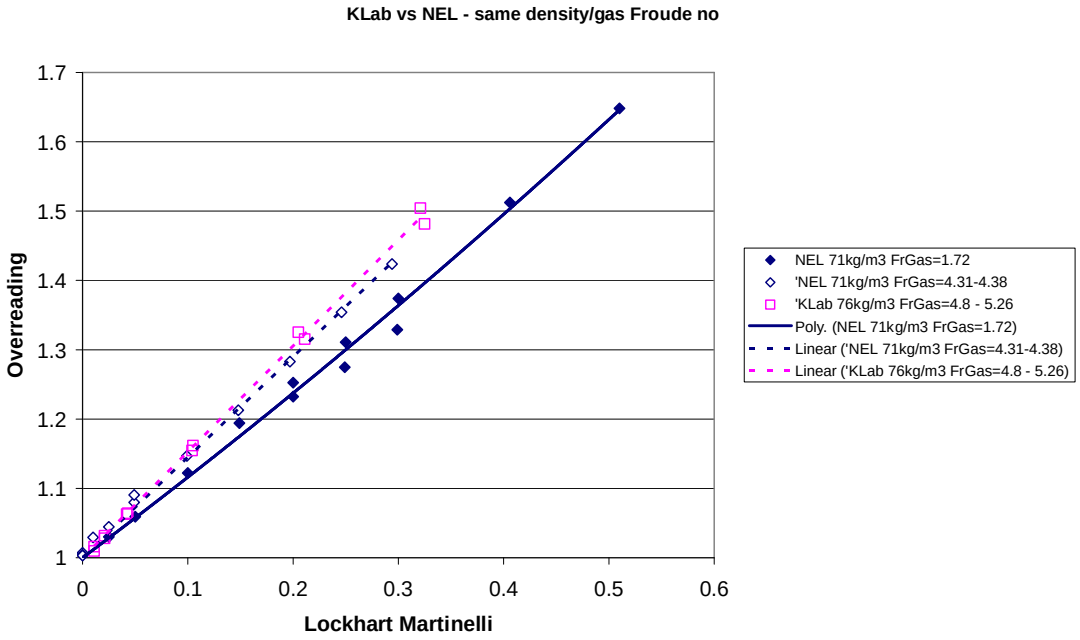

Figure 7 a.Overreading graph for data collected at K-Labs and NEL at same Froude number

The same observation is repeated in figure 7b which shows two sets of data drawn from CEESI at different Froude number against one data set drawn from K-labs at the same Froude number as one of the CEESI data sets. Once again the graphs of overreading at same Froude number coincide irrespective of where the data is coming from.

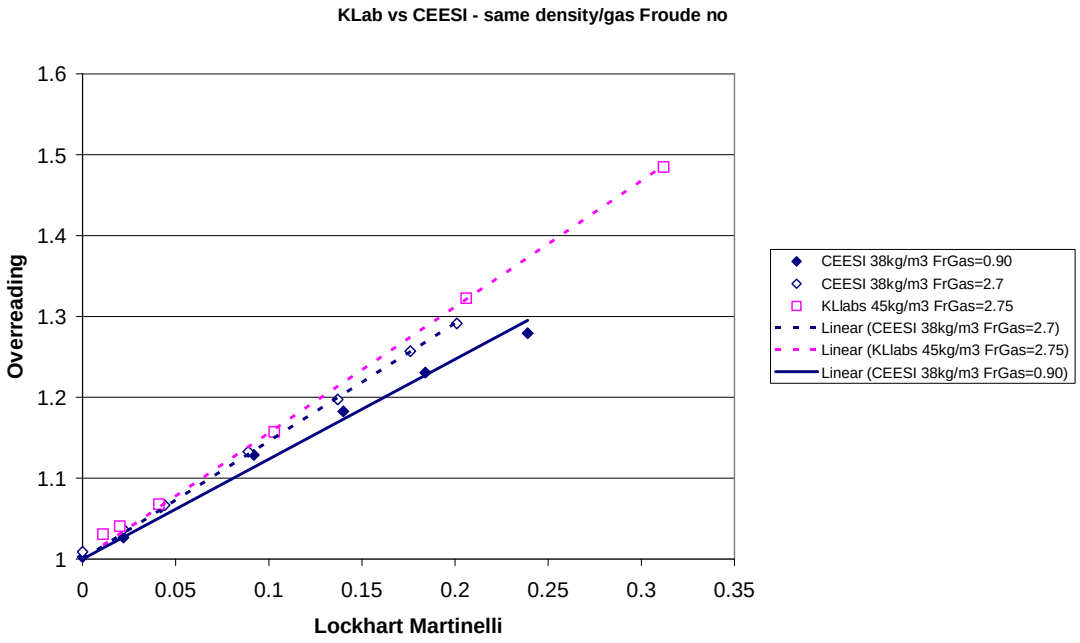

Figure 7 b.Overreading graph for data collected at K-Labs and CEESI at same Froude number

Quantitative Analysis by Neural Nets

The Froude number effect was noted previously; eg see [3], and no claim is made in this paper for originality for noting the effect. However, we believe that the method outlined next for quantifying this effect in relation with others is original to this paper.

After the qualitative analysis described above, we proceeded to carry out a quantitative analysis of the sensitivity of over-reading to various parameters. We have used a back propagating neural net and tried different features, targets and training data. Two configurations of the neural net are reported here. For both configurations, the neural net had eight input nodes and 16 hidden nodes, but different sets of inputs (features) and outputs (targets) were tried as follows

Neural Net 1 Features: The following features were used as input variables (codes are used for reference to figure 9) :

F70:	Liquid Froude Number
X	Lockhart Martinelli parameter
F48:	Gas Froude Number
F53:	$\sqrt{\frac{\Delta p}{\rho_g}}$
F43:	$\sqrt{\frac{\Delta p}{\rho_m}}$
F37:	$\sqrt{\Delta p}$
F69:	$\sqrt{\frac{\Delta p}{\rho_l}}$
Pressure	P

Neural Net 1 Targets: Over-reading was used as the training target.

Neural Net 1 Data: NEL data was used for training and testing. The self test result of the neural net is shown in figure 8. The deviation between actual and prediction was 0.0013 rms

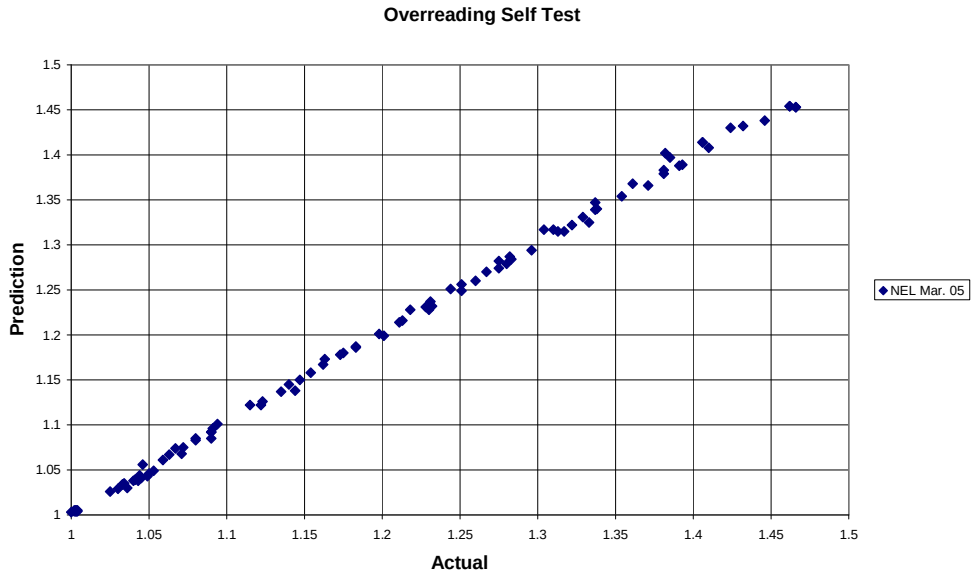

Figure 8 Neural net self test overreading predicted vs overreading actual

We then carried out the saliency test to obtain a quantitative measure of the sensitivity of over-reading to the input parameters [4]. The result of the saliency test is shown on figure 9.

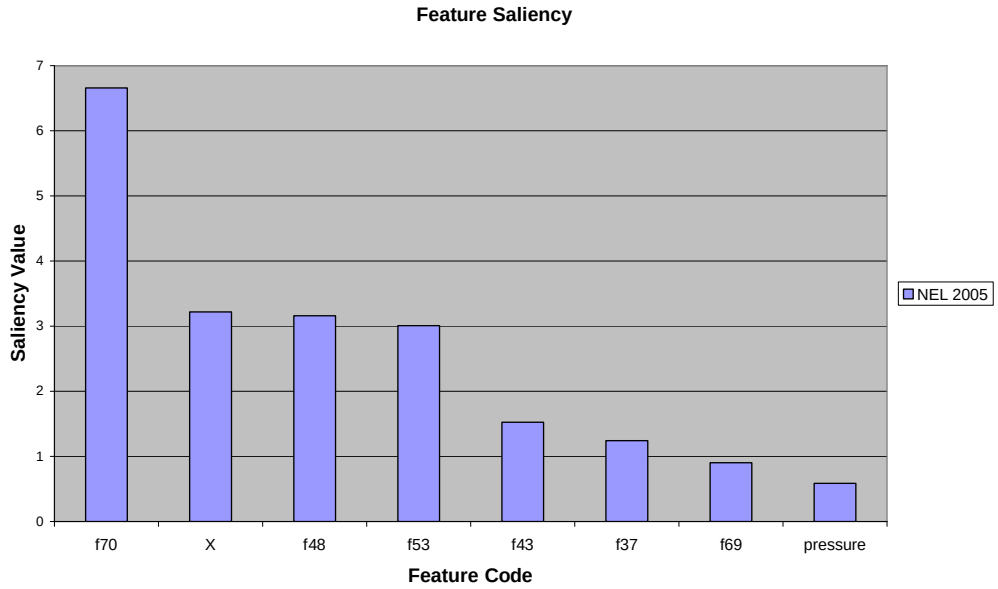

Figure 9 Saliency test neural net 1 – sensitivity of various parameters on overrreading

Neural Net 2 Features:

F65 = $\sqrt{\frac{\Delta p}{P}}$

F53: $\sqrt{\frac{\Delta p}{\rho_g}}$

F37: $\sqrt{\Delta p}$

F70: Liquid Froude Number

F69: $\sqrt{\frac{\Delta p}{\rho_l}}$

Pressure
Density Gas
Density Liquid

Neural Net 2 Targets: Neural net 2 was trained against liquid and gas superficial velocities (two targets).

Neural Net 2 Data: Self test and cross test results for this neural net with two sets of NEL data obtained at different times (May 03 and March 05) is shown below:

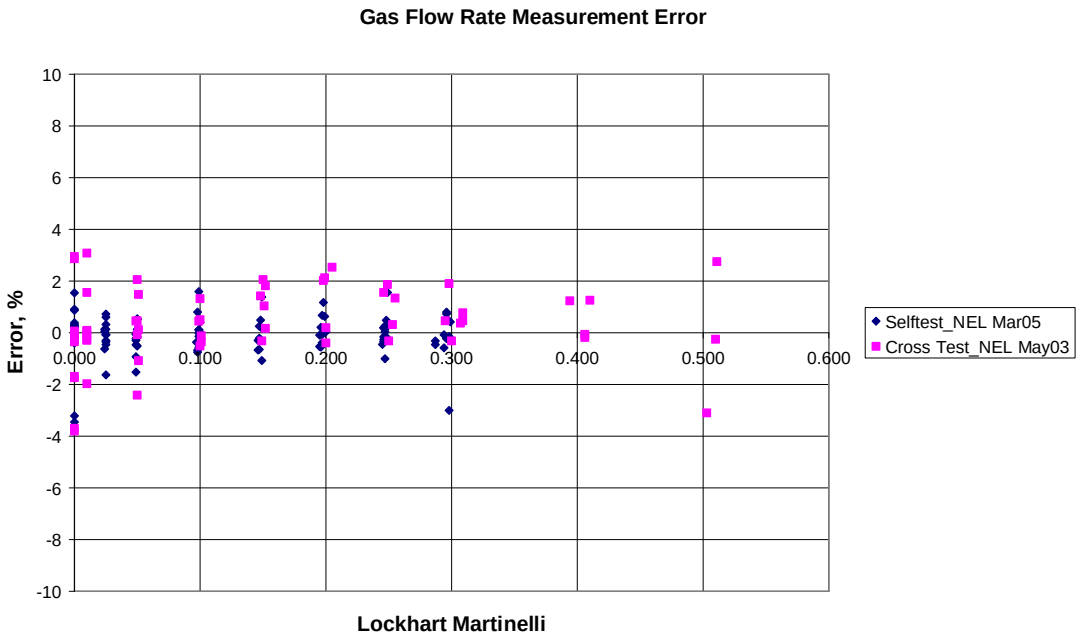

Figure 10 Error in prediction of the gas flow rate with neural net 2 – cross test

The neural net was trained with data gathered in March 05 and back tested against data gathered in May 03. The gas superficial velocity was predicted with an accuracy of rms 1.51 and liquid superficial velocity was predicted with an accuracy of rms 13.74.

The sensitivity of the predictions to input features are shown in figure 11.

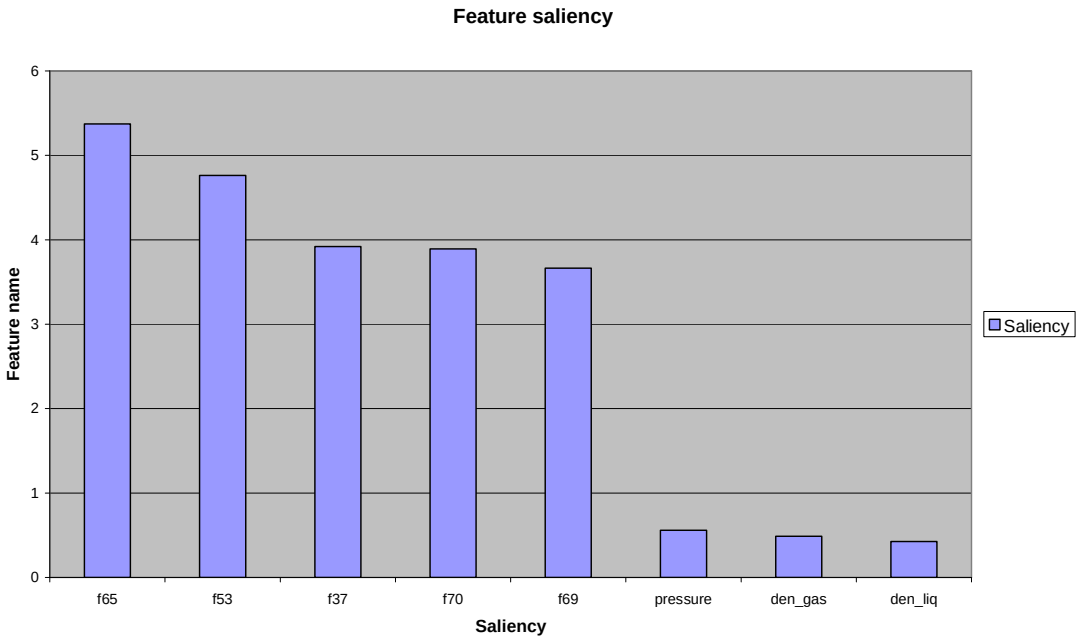

Figure 11 Saliency test neural net 1 – sensitivity of various parameters on liquid and gas superficial velocity prediction

Wet Gas Flow Meter

The brief of an in-line wet gas flow meter is to measure liquid and gas flow rates simultaneously. This requires two measurements (equations) responding in two different ways to the flow rate of liquid and gas flow rate (to solve for two unknowns). One of these measurements (equations) is the mean differential pressure across the V-Cone (Bernoulli equation - momentum balance with appropriate compensation for additional frictional pressure loss arising from interfacial interaction). Another equation can be obtained either from pressure recovery downstream of the V-Cone or from another V-Cone with a different beta ratio. These ideas have been tried before with varying degrees of success.

Another possibility is to extract some features from the differential pressure sampled at a high frequency which respond to the liquid fraction or to the change in liquid and gas flow rates differently. That is, to derive two simultaneous equations from the same measurement. This was tried in the present study. To see how features vary differently to liquid and gas rates we have plotted contour maps of features extracted from the differential pressure signal.

When contours of features are plotted on superficial velocity coordinates one must obtain "intersection" between different feature surfaces (for a solution to the equations) For example, it is not enough to have contours which are laid out diagonally (eg mean DP, standard deviation are typical examples of diagonal contours which do not intersect). Depending on the angle of the diagonal, intersection is still possible (eg variation of mean DP with liquid and gas flow rates is concave but variation of higher order amplitude domain features such as standard deviation, coefficient of kurtosis are convex); but the sharper the angle the better chance for intersection (ie angle =0 -> horizontal contours; angle = 90 vertical contours; angle=45 diagonals).

Figure 12 shows some of the amplitude domain features extracted from the differential pressure signal. These features were extracted from tests conducted at NEL in May 03.

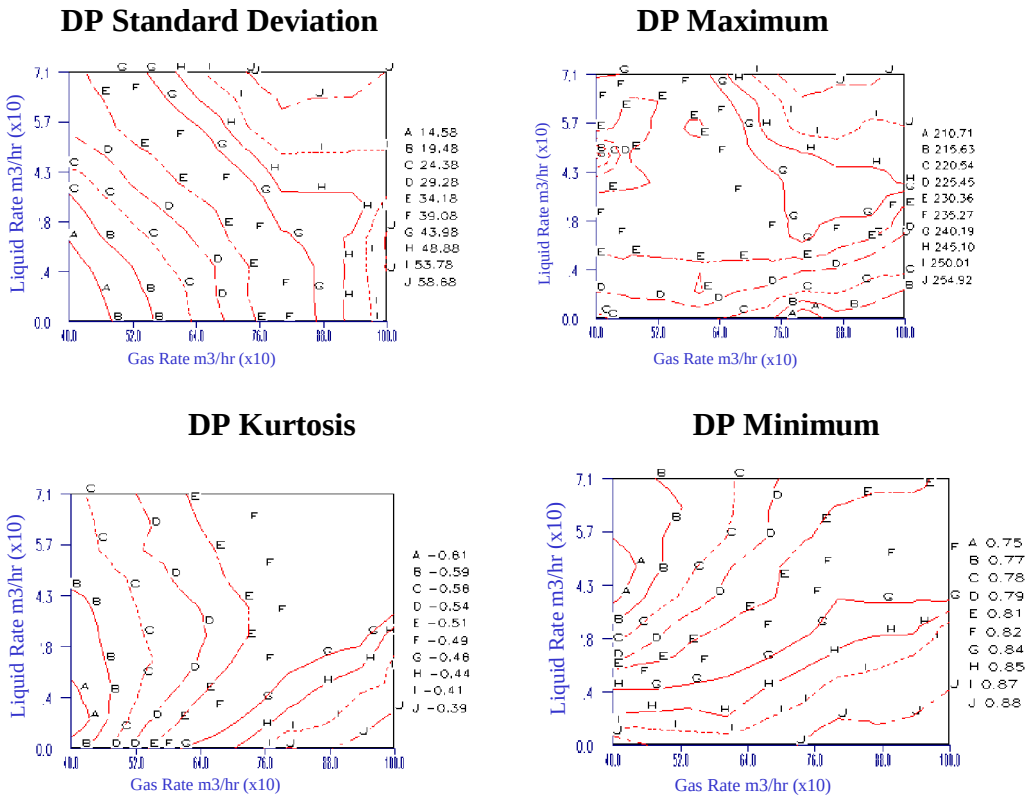

Figure 12 Differential pressure second order features amplitude domain as contour maps on liquid / gas flow rate coordinates.

We have found that while multiple features from the differential pressure provide the intersection points required for identifying liquid and gas rates simultaneously in a given pipeline (or flow loop), for generalization of this method, a stronger (reproducible) imprint of the flow characteristics is necessary. For this it is necessary to add features extracted from another sensor which responds directly to the presence of the liquid phase. For example features extracted from a capacitance sensor in figure 13 show that the capacitance feature surface will intersect with the differential pressure features (eg mean DP rising towards North East, whereas mean capacitance rising towards North West, etc – one can see similar reverse trends in a number of other stochastic features extracted from the respective signals). The measurements shown in figure 13 were made in NEL multiphase flow loop in 1999 – NEL Multiflow JIP [5]

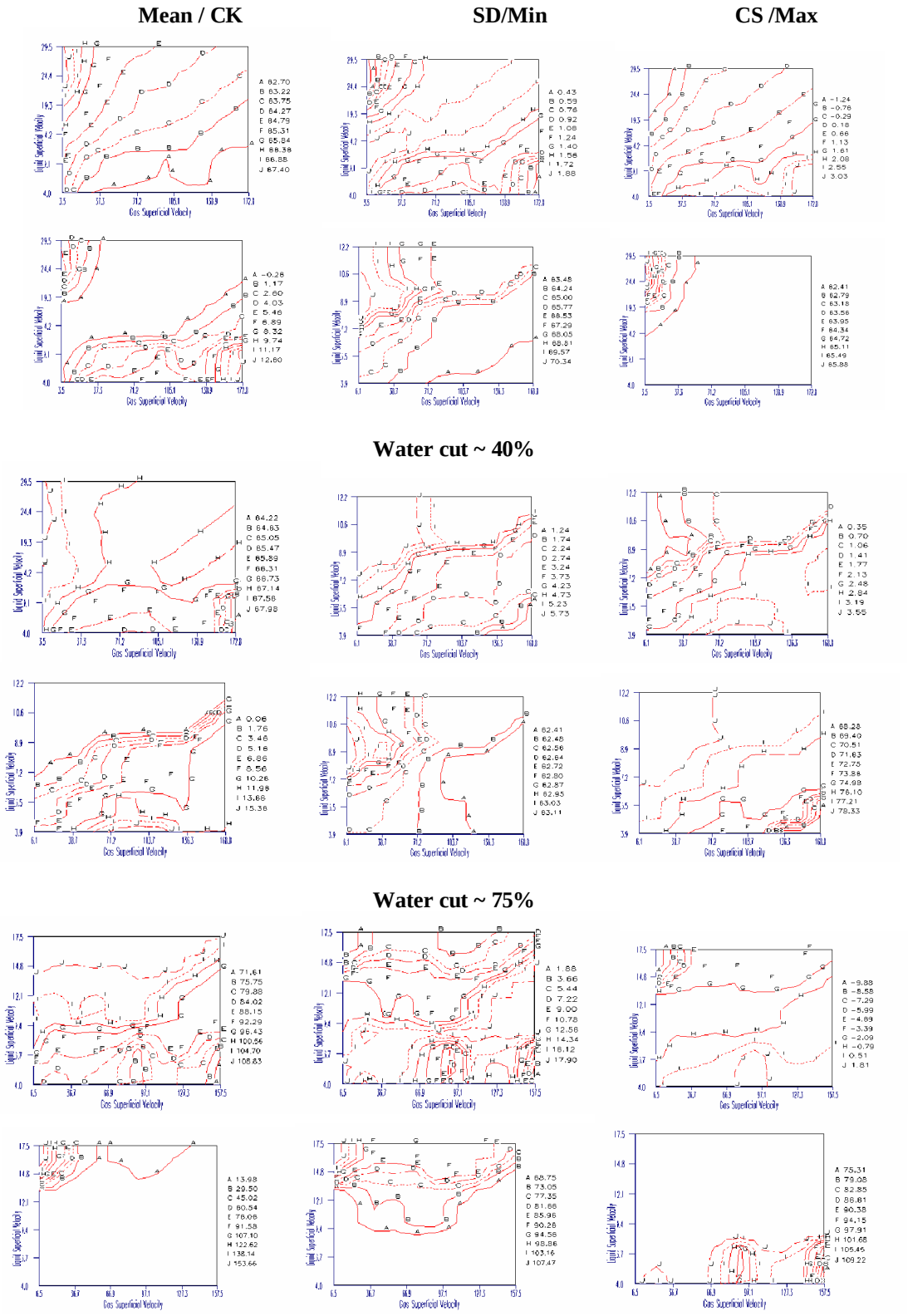

Figure 13 Capacitance sensor second order features amplitude domain as contour maps on liquid / gas flow rate coordinates.

Thus a combination of DP and capacitance sensors will result in a metering system with a greatly enhanced capability for the identification of liquid and gas rates. It can be seen from the trends in contour maps that input-output relations are non-linear and multi-

parameter (eg mean capacitance is not just affected by water composition but also by flow regimes which are in turn affected by superficial velocities and density difference, etc). We believe that only a neural net is capable of finding the relationship between the complex set of causes and effects in multiphase flow.

Finally, we believe that there are still many advantages to the conventional overreading correction approach coupled with a neural net method for correlation of the experimental database. This method of course requires an independent measurement of the Froude number (see Neural Net 2 above). However, an estimate of the liquid Froude number can still result in a relatively good measurement (it is not in the brief of this paper to suggest how this estimate can be made, but a number of options are available including tracers, equation of state, production separator, etc). For example, we have tested the neural net (cross test with erroneous Froude numbers and obtained the result shown in figure 14. It is seen that the rms error in gas prediction is rms 1.51 when the neural net is tested with the correct Froude number. The error goes up to rms 9.13 when Froude number is out by 50% ie when (FrEstimated – FrActual)/FrActual x 100 =50% (figure 14a).

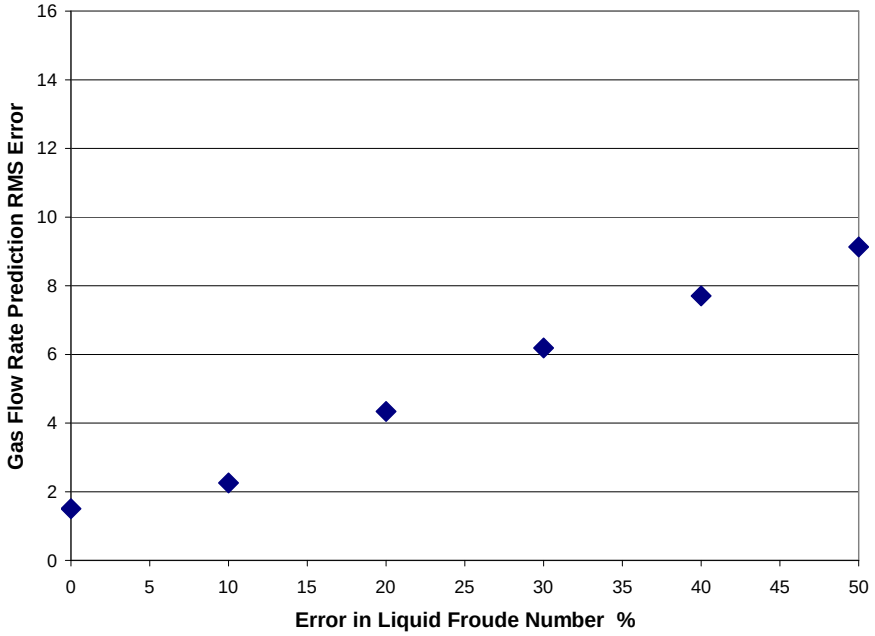

Figure 14a Error in gas rate prediction versus error in liquid Froude number (Neural Net 2)

An interesting byproduct of this investigation was the finding shown in figure 14b that the prediction made by the neural net for the liquid rate is actually better than the input value for Froude number error greater than 20% (Note that this neural net has two targets and the liquid rate is used both as an input feature – via liquid Froude number- and as an output target.)

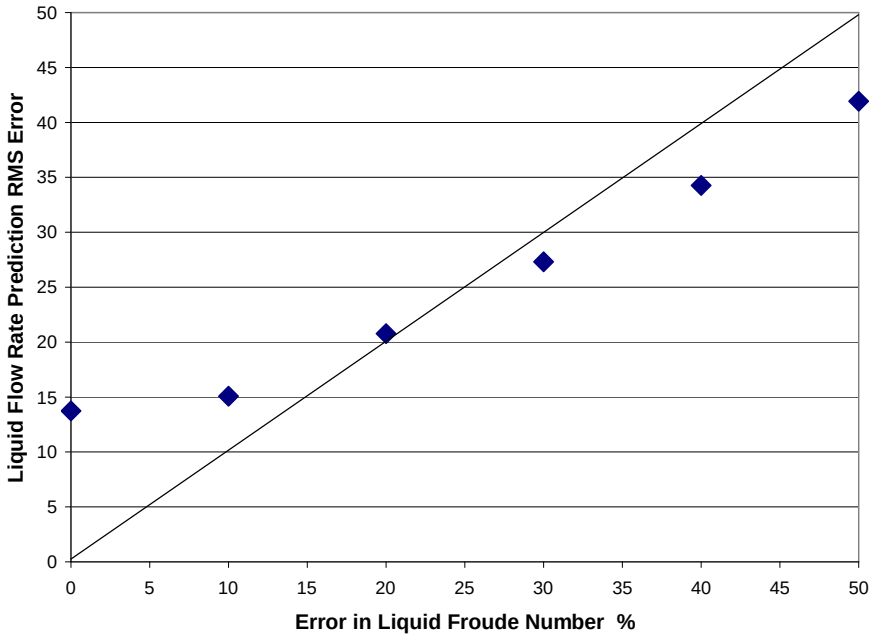

Figure 14b Error in liquid rate prediction versus error in liquid Froude number (Neural Net 2)

Conclusions

1. Back propagating neural nets present a powerful tool for investigating cause and effect relations in wet gas. The effect of Froude number on overreading ratio was quantified by analyzing measurements conducted with V-cones under a wide range of conditions at different laboratories.

2. Back propagating neural nets can also be used as kernel software in a self contained wet gas flow metering system. If the wet gas meter comprises just a V-Cone coupled with a differential pressure sensor and pressure sensor, the liquid Froude number must be input explicitly. In this configuration, the neural net can be self-contained (ie can predict both liquid and gas rates simultaneously) in a given pipeline after suitable training.

3. A general wet gas metering system (ie simultaneous self-contained measurement of liquid and gas rates from a factory calibration) is possible with a combination of differential pressure and capacitance sensors and a neural net for correlating the complex causes and effects between hydrodynamics and phase distributions.

4. A general wet gas metering system is also possible with a neural net trained with features extracted from just the pressure sensors and an external input for liquid Froude number. The error in the gas rate prediction made by the neural net will be under 5% for an error in the Froude number of 25%.

Notation

ρ_l = liquid density

ρ_g = gas density

v_g = superficial gas velocity

Δp_g = theoretical differential pressure across the V-cone calculated from the standard V-cone equation based on (reference) superficial gas velocity

Δp = actual differential pressure across the V-cone (measured)

Frl=Liquid Froude Number = V_l/Sqrt(9.81*Diameter)*Sqrt(ρ_l /(ρ_l - ρ_g)

FrG = Gas Froude Number =Vg/Sqrt(9.81*Diameter)*Sqrt(ρ_g /(ρ_l - ρ_g)

References

[1] Haluk Toral, Shiqian Cai, Richard Steven, Robert Peters, Characterization of the turbulence properties of wet gas flow in a V-Cone meter with neural nets 22nd North Sea Flow Measurement Workshop October 2004 St Andrews

[2] Shiqian Cai, Haluk Toral, Dasline Sinta, Meramat Tajak Experience in field tuning and operation of a multiphase meter based on neural net characterization of flow conditions, (Sarawak Shell Bhd Malaysia) FLOMEKO 2004 Beijing 14-17 Sept. 2004

[3] David Steward, David Hodges, Richard Steven, Robert Peters Wet gas Metering with V-Cone Meters 20th North Sea Flow Measurement Workshop October 2002 St Andrews

[4] Lockhart R.W. , Martinelli R.C."Proposed Correlation of Data for Isothermal Two-Phase Two Component Flow in Pipes" Chemical Engineering Progress Vol 45 No 1

[5] Priddy K. L., Rogers S. K., Ruck D. W., Tarr G. L., and Kabrisky M. (1993) "Bayesian selection of important features for feedforward neural networks," Neurocomputing, vol. 5, no. 2--3, pp. 91--103. http://citeseer.ist.psu.edu/priddy93bayesian.html

[6] A Hall NEL Multiflow JIP Evaluation of ESMER T3 Multiphase Flow Meter 30 March 2000 National Engineering Laboratory Report 069/2000

North Sea Flow Measurement Workshop
18th - 21st October 2005

Three Years of Experience of Wet Gas Allocation on Canyon Express

Aditya Singh, Total E&P USA
James Hall, Letton-Hall Group
Winsor Letton, Letton-Hall Group

1 INTRODUCTION

In September 2002, production was begun from the three fields that together form the Canyon Express System- King's Peak, Aconcagua, and Camden Hills. The 9 wells from these fields are connected to a pair of 12-inch flow lines carrying the commingled wet gas a distance of approximately 92 kilometers back to the Canyon Station platform for processing.

At the 21st NSFMW in October 2003, an initial report was given on the status of Wet Gas Allocation for the Canyon Express project [1]. As discussed in that paper, dual-differential, subsea wet gas meters were chosen for the task of allocating gas and liquids back to individual wells. However, since the gas from all three fields was very dry (Lockhart-Martinelli parameter < 0.01) and because the operating pressures were quite high (250 bar), application of the dual-differential function of the meters yielded errors in both liquid and gas flow rates. Furthermore, as these problems were being uncovered, scale was beginning to collect inside some of the meters. Taken together, these problems produced system imbalances as great as 20%.

To address the problems, one of the individual flow metering elements within each wet gas meter was chosen as the allocation meter, operating as a single-phase gas meter. Using a multi-point flow testing methodology, the response of the individual meters was characterized, with the result that a much improved system flowline balance has been maintained since its application. This methodology was approved by the U.S. Mineral Management Service for the Canyon Express field development.

The experiences of operation of the Canyon Express system for the past three years provide useful guidance for future subsea metering installations. This includes the use of line balance monitoring to identify changes to a meter's response due to deposits, early detection and elimination of hydrate formation, and the use of the meters to indicate the onset of water production from a well. Finally, the survival rate for more than one hundred pressure, temperature, and differential pressure transmitters provide a good indication of what one can expect when deploying meters in very deep water for long periods – over three years at this point in time.

2 WET GAS METER

In the initial design of the Canyon Express project, the decision was made to install the subsea flowmeters for allocation in the jumpers. Because of the lead-times of the

components, fabrication, and calibration schedules involved, it was necessary to select which type of subsea allocation metering device to use by the fall of 2000. At that time, the primary method for wet gas measurement was the use of various differential meters in the manner first suggested by Murdock [2].

Even though production from all Canyon Express fields was expected to be very dry, it was important to identify the onset of water from any well. At the time, Solartron-ISA was in the process of introducing their dual-differential meter, the Dualstream II for wet gas measurement. Since the Dualstream II had shown the potential to provide such an estimate [3], it was chosen for installation on all of the wells.

It was important to calibrate the wet gas meters in a flow loop prior to installation. The initial Canyon Express working pressure of approximately 250 bar was far greater than any application experienced by the Solartron-ISA meters up to that point in time. Only the high-pressure multiphase flow loop at the Southwest Research Institute (SwRI) was able to achieve this pressure; no other wet gas calibration facility operated at even 50% of this figure. Fortunately, SwRI was capable of circulating natural gas, decane, methanol, and water through the meters at varying liquid loads.

The test program for the meter was quite extensive, and covered not only variations in pressure but also liquid loading and, to some degree, liquid composition. Plotted against Gas Volume Fraction, the relative uncertainties for gas flow measurement were generally less than 3% for all gas volume fractions (GVF), and for liquid flow measurement were less than 20% up to 99% GVF. It has been pointed out [4] that the simple Murdock correction is not sufficient to properly model the flow measurement process for very low Lockhart-Martinelli values. Above 99% GVF, the liquid uncertainties expanded out to as much as 80%. Since the introduction of the Dualstream II and its use in the Canyon Express system, Solartron-ISA has modified its design to extend the range to above 99% GVF.

2.1 INITIAL ISSUES

Initially a maximum of 100 - 200 Bbls/D of liquids (production plus injected methanol) was expected through each meter. However, the amount being reported by the meters was far greater, in some cases as much as 2000 Bbls/D. Since each separator on Canyon Station is capable of handling 1750 Bbls/D and was seeing nowhere near this amount of liquid, it seemed clear that something was wrong in the subsea measurement process.

A comparison of the measurements from the redundant differential pressure (DP) transmitters on each wet gas meter showed agreement within 1%. Therefore, having eliminated the sensors as the problem source, only the application of the methodology remained to be considered.

It is well known that differential meters over-read the true gas flow rate when liquids are present. A typical differential over-read curve is shown in Figure 1, with the device over-reading plotted against the well-known Lockhart-Martinelli (L-M) parameter. The exact shape of the curve depends on the geometry of the meter, the

properties of the fluids passing through it, and the pressure in the pipe, but it is linear with respect to L-M, a measure of "wetness".

The Solartron-ISA Dualstream II utilizes the characteristic that different differential devices exhibit different curves similar to the one in Figure 1. The meter incorporates two differential devices in a single wet gas meter. The initial problem with the incorrect liquid estimates by the meters was traced to the following:

The typical Canyon Express operating parameters were:

$$Q_g = 50 MMSCFD$$

$$Q_l = 100 Bbls / DAY \text{ (including methanol)}$$

$$\rho_g = 160 kg / m^3$$

$$\rho_l = 800 kg / m^3$$

$$\text{Lockhart-Martinelli : } X = \frac{Q_l}{Q_g}\sqrt{\frac{\rho_g}{\rho_l}}$$

Lockhart-Martinelli ≈ .005

This extremely small value of L-M was causing the problem in the liquid estimate. Asking that two differential meters each are accurate to within 0.2 - 0.3% is demanding far too much, especially when exposed to production fluids for long periods of time. Since the meter determines the wetness of the gas by calculating the difference in the over-read of the two differential devices, the difference in two values, each with non-negligible uncertainty, can cause significant errors in the resulting computation.

An example in reference [1] showed an estimated liquid rate of about 1 kg/sec, or 680 BBLD, about ten times the true rate. Additionally, because the estimate of liquid production is too high, the gas rate calculated by the meter's algorithm was always 4-6 MMSCFD too low.

2.2 MULTI-POINT SUBSEA CALIBRATIONS

The decision was taken to use either the Dualstream II's wedge or Venturi meters as the allocation device for gas, using it as a single-phase meter. It was decided that the best choice would be the wedge meter, because of the fact that the Venturi's DP transmitters had been observed to saturate on the high producing wells. The high range DP's on the wedge meters were able to function correctly up to approximately 100 MMSCFD.

Since the meters were already installed on the sea floor, it was important to find a way to verify the performance of each device. Given that (1) intervention to replace a meter would be enormously expensive, and (2) gas production was so prolific that any prolonged reduction in rates must be considered only as a last resort, a creative way to verify and, if possible, to calibrate each meter was needed.

It was decided that online calibration of individual subsea allocation meters using the meters on the Canyon Station platform as a reference was a viable approach. This is largely due to the fact that variations in liquid hold-up during the tests were known to be small due to the relative dryness of the gas production. This fact facilitated the test scheme highlighted below. For systems where there is more liquid hold-up and thus more variation in liquid hold-up with varying flow rate, this test scheme may become unmanageable.

The method developed for Canyon Express involved careful calibration of individual meters using a multi-point method. While flow through all other meters on an individual flow line is held constant (or as nearly so as possible), flow through the meter under test and the reference meter on the platform are observed at three or more flow rates ranging from full flow down to shut-in. Changes in the flow of the other meters on the line must be monitored as well, and the differences accounted for in the calculations.

Three or more measurement points are used to determine **k** (meter factor) and **b** (meter bias). The measurements made while the well is flowing (not shut in) define **k**, i.e. the amount of change in reference reading corresponding to a given change in the reading of the meter under test. The meter bias can only be determined when the well is shut-in.

The relationship between flow measured at the reference meter at the gas outlet of the separator and that observed at the meter under test is

$$Q_{ref} = k_i \cdot Q_i + b_i \qquad (1)$$

Changes in the flow from the other wells are accounted for by modifying the above equation as follows:

$$k_i = (\Delta_{ref} - \sum_{j=1}^{j=m} k_{j \neq i} \times \Delta_{j \neq i}) / \Delta_i$$

This equation merely says that in order to account for the change in the flow through the reference meter due to the i^{th} well, the change in the flow of each of the other wells (represented by j, where $j \neq i$) must be subtracted from the total measured change in the reference meter. Since the equation involves **changes** in measured flow, it does not involve meter bias factors.

While this approach will lead to a determination of $\mathbf{k_i}$, the following tasks remain: (a) it requires that the multi-point tests be complete on all wells before we have a solution; i.e., this is an iterative process and the **k**-factors must be known for all the wells on the flowline, and (b) it doesn't address the issue of determining the bias terms $\mathbf{b_i}$ which remain. In order to determine these bias terms, the well under test must be shut in. This is the only point at which the flow condition through the wedge meter is precisely known.

An example of this technique is shown in Figures 2 and 3.

As reported in 2003, this procedure has been utilized periodically to verify and adjust, if necessary, the meter factor and bias for each wedge meter. Once a meter's characteristics have been determined, why would they ever change? Factors that can affect the response of a meter are discussed in the next section.

3 FACTORS AFFECTING METER PERFORMANCE

During these first three years of operation, changes in the calibration parameters of the subsea wet gas meters have been noted. In each case, these changes have been attributed to factors other than a drift in the meters themselves. Changes in the characteristics of the individual wells have certainly been a major influence in the need to constantly monitor and periodically recalibrate the meters.

Experience on the Canyon Express project indicates that it is important to consider the many factors that can cause inaccuracy in subsea flow measurement and consequently in allocation. Our observations are summarized below.

3.1 SCALE BUILDUP

As reported in our 2003 paper [1], one of the first problems to be identified was a drift in the imbalance on both flow lines in the 15-20% range.

When a choke insert was retrieved from one of the wells, it revealed that the inside was covered with a thick scale. A camera looking back inside the jumper toward the meter confirmed the existence of scale on the walls of the jumper and meter. Since the meter had experienced a reduction in diameter due to a buildup of scale, this change of geometry would have increased the differential pressure across the meter and caused a corresponding over-reading in its response. The differences between the Venturi and wedge flow rate measurements were likely an effect of scale in some of the meters, causing the large errors in liquid estimates. The worst result of the scale, though, was the increased error in gas measurement.

In order to attempt to stop the scale production within the meters, scale inhibitor was injected, but the scale that had already formed could not be removed without a multi-million dollar intervention, and even then there were no guarantees that the meter's original geometry could be restored. It was obvious that this was an extremely serious problem, and something had to be done.

The solution was to perform a multi-point calibration on all of the subsea meters, as described in section 2.2. With no changes in the meters' characteristics, all k-values should have been equal to 1.0 and all b-values equal to zero. This was not the case. The k-values ranged from 0.74 to 1.04 and the b-values from 0.73 to –2.58.

Utilizing the calibration parameters, the flow line imbalance was maintained within the range of $\pm$ 3%. However, after a period of two months, the line imbalance abruptly changed. This was traced to a change in the characteristics of the meter

whose k-factor had been measured as 0.74. Redoing the multi-point calibration on that well yielded a new k-factor of 0.89. The supposition is that some of the scale that had built up inside the meter had become dislodged and thus, the internal geometry had been increased.

This experience illustrates the need for constant monitoring of the flowline balance as an indication of changes in a subsea meter's performance.

3.2 DIFFERENTIAL PRESSURE TRANSMITTERS

Since differential flow meters utilize DP transmitters to measure the pressure change across a restriction in the flowline, it is important to insure that the transmitters are functioning properly. Because it is not feasible to retrieve and replace malfunctioning transmitters on the Canyon Express meters, redundant units are utilized. All of the meters contain low range and high range redundant transmitters on both the wedge and the Venturi sections. Some of the meters use triple redundancy and others use double redundancy on both of these ranges.

With redundant transmitters, the question arises as to which unit is correct when there is a difference in readings. Possible criteria for determination are the following:

- If any unit is saturated (maximum output), eliminate it from the calculation.
- If the redundant units are within reasonable agreement, take their average.
- For triple redundancy, if one unit differs from the other two, average the two that are in agreement.

The above criteria can be built into the meter's processing algorithms. However, there are cases where an algorithm cannot decide the correct value to use from redundant transmitters. As an example, consider Figure 4. The figure shows the difference between the DP value used in the wedge flowrate calculation and each of the two high-range DP sensors. Points to note:

- The two sensors began to diverge around January 25.
- Between that date and February 14, the algorithm didn't know which DP was correct, so it used the average of the two.
- On February 14 the calculation stopped using the DP1 values and only used DP2.
- Since there was an extra set of redundant transmitters, an ROV was used to switch the connection from bank 1 to the spare bank.
- After the DP1 sensors were changed on March 5, the agreement between the two sensor banks was excellent.

The lesson learned here was that the system cannot always be depended upon to identify malfunctioning components. Deviations between the sensor value used in the flow calculation and the value from the individual sensors must be monitored to insure that there is consistency in the measurements.

Given that the conditions to which the transmitters were subjected during the past three years, the failure rate has been remarkably low. The table shown in Figure 5 summarizes the current condition of the transmitters. This includes not only the DP's, but also the separate pressure and temperature units. None of the transmitters in bank 2 of the flowmeter on well 305-4 have been functioning, because the connector was damaged during installation.

As mentioned earlier, the DP transmitters on the Venturi meters on some of the high producing wells were always saturated, thus rendering them unusable. This was the primary reason for selecting the wedge portion of the wet gas meter as the gas measurement device. During normal operation, care was taken to assure that the DP's on the wedge meters did not saturate. However, a situation occurred during the calibration process when the flow from some of the wells was reduced. This caused a reduction in the line pressure, allowing an increase in flow from the producing wells. An example is shown in Figure 6. There were only two wells flowing during this calibration (305-1 & 305-2). During the period when the high producer (305-2) was flowing at 75% and 50% rate, the line balance was better than 1%. However, at times when 305-2 was at full flow, the imbalance rose to more than 15%.

3.3 HYDRATE FORMATION

During the initial design of the Canyon Express project, the possibility of blockage due to hydrate formation was recognized. For this reason, the system was equipped for continuous methanol injection. Even without methanol injection at a well during steady state flow, it was felt that the jumper and flow meter did not need methanol flow because the heat from the produced fluid was sufficient to inhibit hydrate formation. While this was true for the jumper, Canyon Express demonstrated that this was not necessarily true for the meter.

As shown in Figure 7, the flow meter assembly consists of the metering pipe containing the two differential elements and the assortment of redundant transmitters. A manifold is connected across each differential device and then the capillaries leading to the DP's are connected to it. Unfortunately, there isn't the ability to flush the meter's capillary lines from the surface with methanol.

Hydrate formation in the capillary lines has caused significant problems in the past year because of the need to shut-in the wells for extended periods due to hurricanes in the Gulf of Mexico. After the wells were restarted, there was an initial flow of some liquids from some of them. Coupled with the fact that the jumper and the meter were at ambient water temperature (2 deg C), several of the meters exhibited erratic behavior. Temperatures measured in the flow meters have decreased from their initial values to a range of 5 °C to 33 °C. At the low end of this range, conditions exist for hydrate formation. In fact, the meter on that well (217-2) has been considered as non-functioning and hydrate blockage is a possible cause. The typical location of the flowmeter and jumper is shown in Figure 8.

Consider the example shown in Figure 9. Notice that at the time shown, the wedge meter on well 305-4 was varying wildly, but the separator showed no significant change. Looking at the output of the Venturi portion of the meter on 305-4, a

consistent value is seen. This is a possible indication of hydrate blockage in the capillary lines leading to the wedge meter's DP transmitters. The redundant DP's on the wedge were in agreement, indicating that they were all measuring the same (incorrect) pressure.

A similar application of the Dualstream II wet gas meters was in Statoil's Mikkel field [5]. In that case, an insulation material was applied not only to the capillary lines, but also around the flowline. It was reported that this helped inhibit hydrate formation, but the problem at startup was not completely eliminated.

3.4 CHANGE IN LIQUID PRODUCTION

At the beginning of the Canyon Express project, the metering problem related to the gas being too dry. As some of the wells have begun to produce water, the challenge is now to quickly identify the well(s) at fault and account for the over-read in the allocation. Often it is easier to notice the onset of water flow by a daily review of the flowline balance as opposed to an increase in liquid flow at the separator. This is particularly true when the wells are located at a great distance from the platform (92 km in the case of canyon Express). When looking at the separator, the liquid hold-up in the flowline may mask the initial onset of a break through. An example of a gradual change in line balance increase is shown in Figure 10.

Once water production has been identified, it must be accounted for in the allocation calculations. In the case of Canyon Express, the use of the wet gas output by the meter was not possible because of the following:

- The meters on two of the wells had saturated DP transmitters on the Venturi portion of the meters. This eliminated the possibility of a wet gas correction on those wells.
- For the other wells, since the calibration of the wedge portion of the meters have changed since installation, it is reasonable to assume that the Venturi portion has also changed, but not necessarily by the same amount. Thus, the Venturis must also be calibrated using the multi-point technique. The algorithms used to calculate the gas and liquid densities utilize the Venturi flowrates. Therefore, the software must be modified to use corrected Venturi flowrates.
- In theory, is would be possible to calculate a wet gas correction using the Murdock parameters.

$$Q_g = \frac{Q_{giv}}{1 + c_v + M_v X} = \frac{Q_{giw}}{1 + c_w + M_w X}$$

$$Q_g = \frac{Q_{giw} - M_w Q_l \sqrt{\rho_g / \rho_l}}{1 + c_w}$$

where M and c are the Murdock primary and secondary constants and were determined for the Canyon Express meters at SwRI. The difficulty is assigning a

precise liquid flowrate through each meter. It is a combination of water, methanol and condensate.

If only one of the wells on a flowline is producing water and the rate is constant, it is possible to calculate the over-read due to that well by measuring the flowline imbalance. In order to eliminate the effect of liquid hold-up in the flowline, it may be necessary to make this measurement over a period of several days.

4 CONCLUSIONS

After three years of operation of the Canyon Express Project, considerable experience has been accumulated. Since at the time it held the record for deepwater hydrocarbon production, application of the technologies discussed here were challenging and required considerable flexibility. It is believed that the Canyon Express experiences will benefit future deepwater flow metering projects. The knowledge acquired thus far is summarized as follows:

In spite of the problems encountered, subsea metering for fiscal allocation was a success. Even though the technology needs enhancements to advance further, this is a definite step forward from well testing by difference. Using the multi-point calibration technique has allowed an excellent line balance to be maintained as long as the GVF was >99%. Since subsea commingled flow is essential to the timely progression of new projects, subsea metering is as well.

Differential flowmeters can operate successfully in deepwater applications. After three years of operation in the deepwater environment, only one of the Solartron-ISA meters is currently not functioning. It is possible that this is due to hydrate blockage, since this is the coldest well.

It is important to select the range of the DP transmitters correctly. As shown earlier, the differential meters will fail to perform correctly if the DP's are saturated. Consideration must be given to the maximum flow expected through the meters. As soon as this is exceeded, the well's flow must be reduced.

With regard to the transmitters, there are two goals for future applications: (1) Retrievable transmitters that can be re-calibrated, rescaled or replaced when necessary; (2) Smart transmitters that can be rescaled remotely from the surface.

Hydrate formation in flowmeters is a serious concern. As wells mature and their liquid production increases, the possibility of hydrate formation in the flowmeter increases. This is particularly true for flowmeters with capillary impulse lines. Putting some insulating material around the meter may help, but eliminating the capillary lines would be the best solution.

Consider alternate flowmeter location. To date, the location of choice for subsea wet gas and multiphase meters has been in the jumper. Because of the expense and difficulty of retrievability, alternate locations should be seriously considered for future projects. Some subsea meters that can be installed on the wellhead tree are now being offered.

Continual monitoring of flowline balance is mandatory. As discussed above, the formation of deposits on the inside surfaces of the flowmeters will affect the meter's calibration and therefore, the flowline balance. This is also true when water break through occurs. In order to maintain equitable allocation, re-calibration may be required.

Multi-point flowmeter calibration is a viable means of maintaining flowline balance. This technique has been utilized successfully on Canyon Express for the past three years. Now that some of the wells have shown water production, a variation of this approach will be required, depending upon the number of wells on a flowline that are producing at the same time. However, for wells producing dry gas, this method is vastly preferable to allocation by difference.

5 REFERENCES

1. Cooley, C., Couput, J.-P., Letton, W., and Hall, J., "Wet Gas Allocation on the Canyon Express Project", 21st North Sea Flow Measurement Workshop, Tonsberg, Norway, October 2003.

2. Murdock, J.W., "Two Phase Flow Measurement with Orifices", Journal of Basic Engineering, December 1962.

3. Tait, A., Lund, J., and Clark, S., "A Wet Gas Meter for Gas/Condensate Flow Measurement", 9th International Conference on Multiphase Technology, Cannes, France, June 1999.

4. Boko, J., Couput, J.-P., Escande, J., Gajan, P., and Strzelecki, A., "Wet Gas Metering with Venturi Meters in the Upstream Area: Further Results for the Correction Factor", North Sea Flow Measurement Workshop, Kristiansand, Norway, October 2001.

5. Jacobsen, E., Denstad, H., Diwning, A., Daniel, P., and Tudge, M., "Validation and Operational Experience of a Dualstream II Wet Gas Meter in a Subsea Application on the Statoil Mikkel Field", North Sea Flow Measurement Workshop, St. Andrews, Scotland, October 2004.

6 ACKNOWLEDGEMENTS

The authors wish to acknowledge the unflinching support of the Canyon Express Partners in the work reported here. As the characteristics of the well production have changed and new challenges have arisen, the Partners have continued to work together to find and support the most equable and technically correct solutions.

We also wish to express our appreciation to personnel from Solartron-ISA, Intec Engineering, Kvaerner Oilfield Products and Calsep, Inc. for their continuing support on this program.

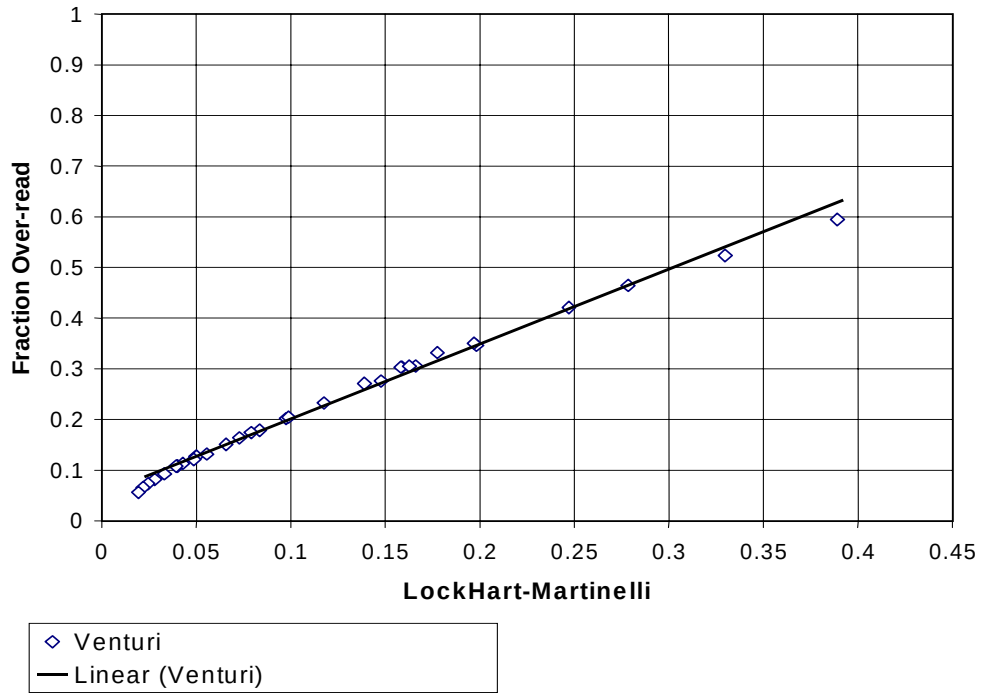

Figure 1. Typical Differential Meter Over-Read as a function of 'wetness'.

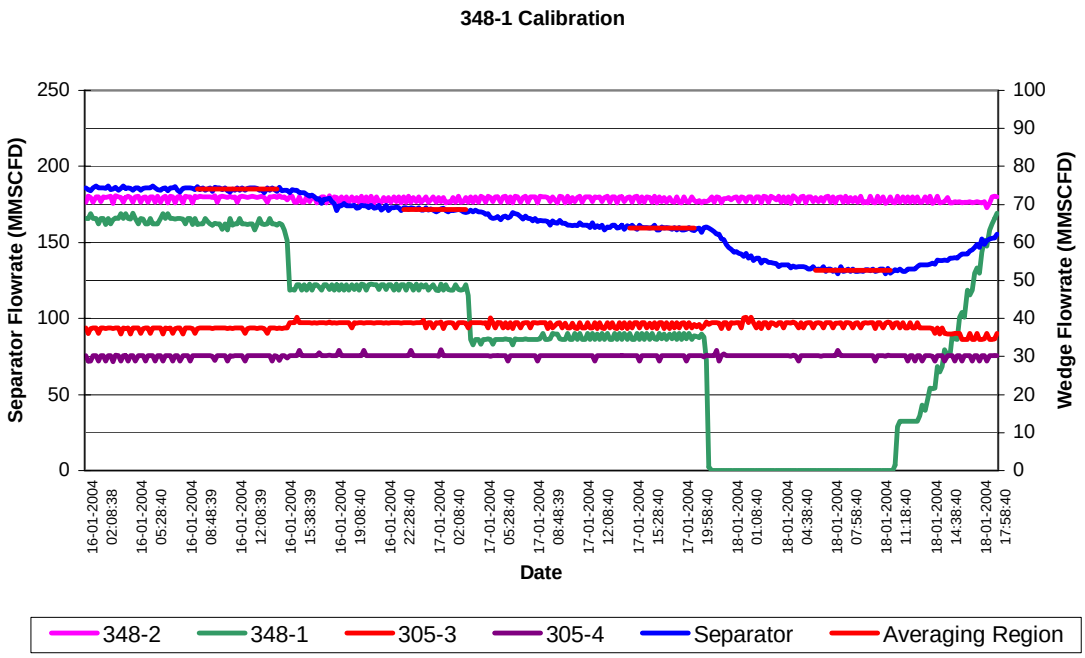

Figure 2. Example of Procedure used for Calibration of Canyon Express Meters

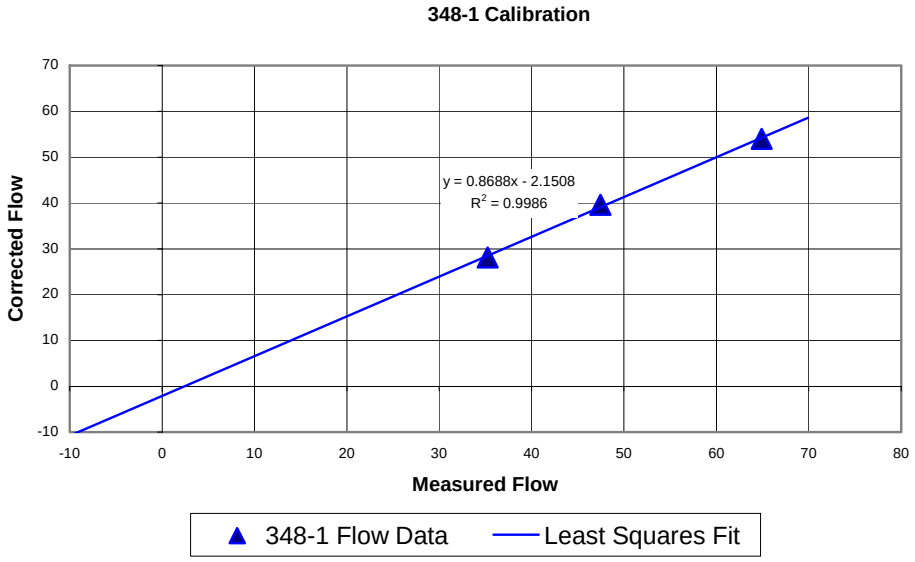

Figure 3. Calibration Curve for Canyon Express Meter

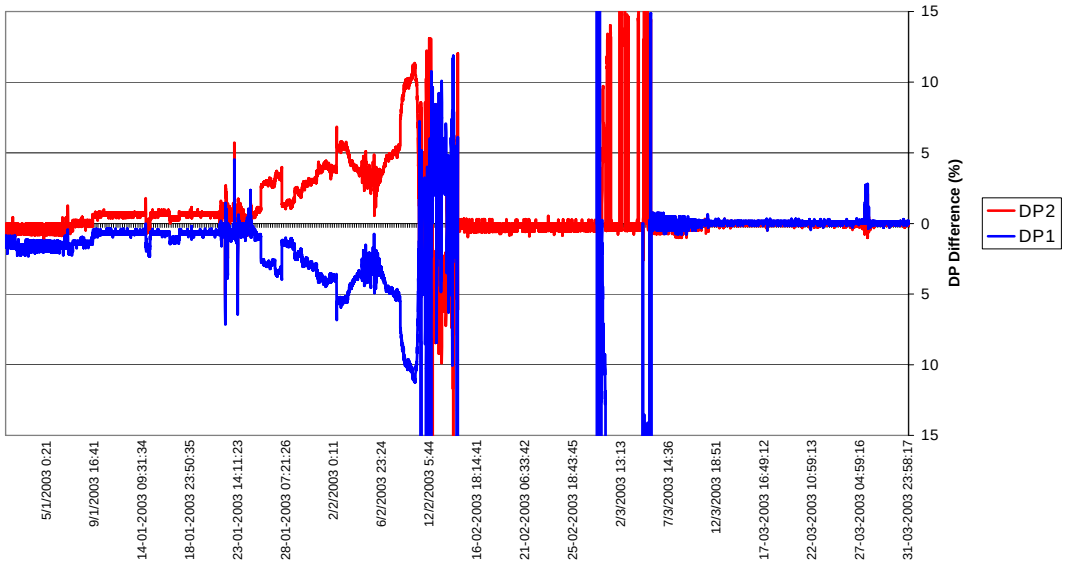

Figure 4. Example of Malfunctioning DP Transmitter

	305-1	305-2	305-3	305-4	348-1	348-2	133-2	217-2	217-3
WH1	OK	OK	OK	OK	OK	**Int**	OK	OK	OK
WH2	OK	OK	OK	**N/A**	OK	OK	OK	**X**	OK
WH3							OK	OK	OK
WL1	OK	OK	OK	OK	OK	OK	OK	OK	OK
WL2	OK	**X**	OK	**N/A**	OK	OK	OK	**X**	OK
WL3							OK	**X**	OK
VH1	OK	OK	**X**	OK	OK	OK	OK	OK	OK
VH2	OK	**X**	**X**	**N/A**	OK	**X**	OK	**X**	OK
VH3							OK	OK	OK
VL1	OK	OK	**X**	OK	OK	OK	OK	**X**	OK
VL2	OK	**X**	**X**	**N/A**	OK	**X**	OK	OK	OK
VL3							OK	**X**	OK
P1	**Int**	OK	OK	OK	OK	OK	OK	OK	OK
P2	OK	**X**	OK	**N/A**	OK	OK	OK	OK	OK
P3							OK	OK	OK
T1	OK	**Int**	**Int**	OK	OK	OK	OK	OK	OK
T2	OK	OK	OK	**N/A**	OK	OK	OK	OK	OK
T3							OK	OK	OK

Int = intermittent

Note: Bank 2 connector is broken

meter is not working

Figure 5. Summary of Current Status of Transmitters on Canyon Express Flowmeters

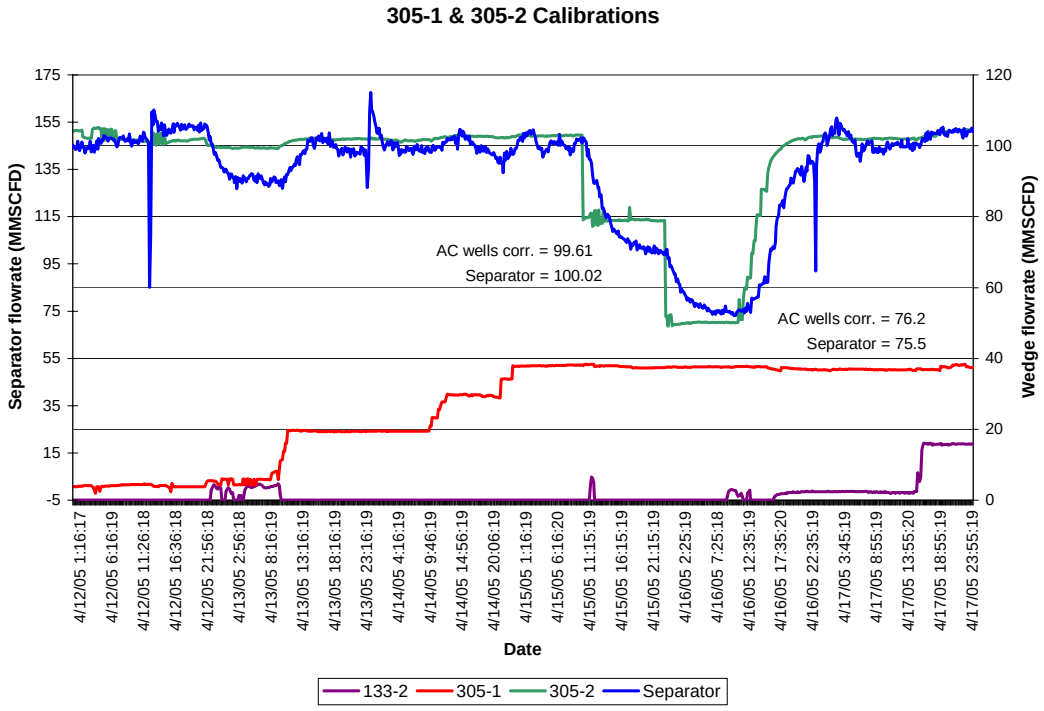

Figure 6. Example of the Effect of Saturated Wedge DP Transmitters

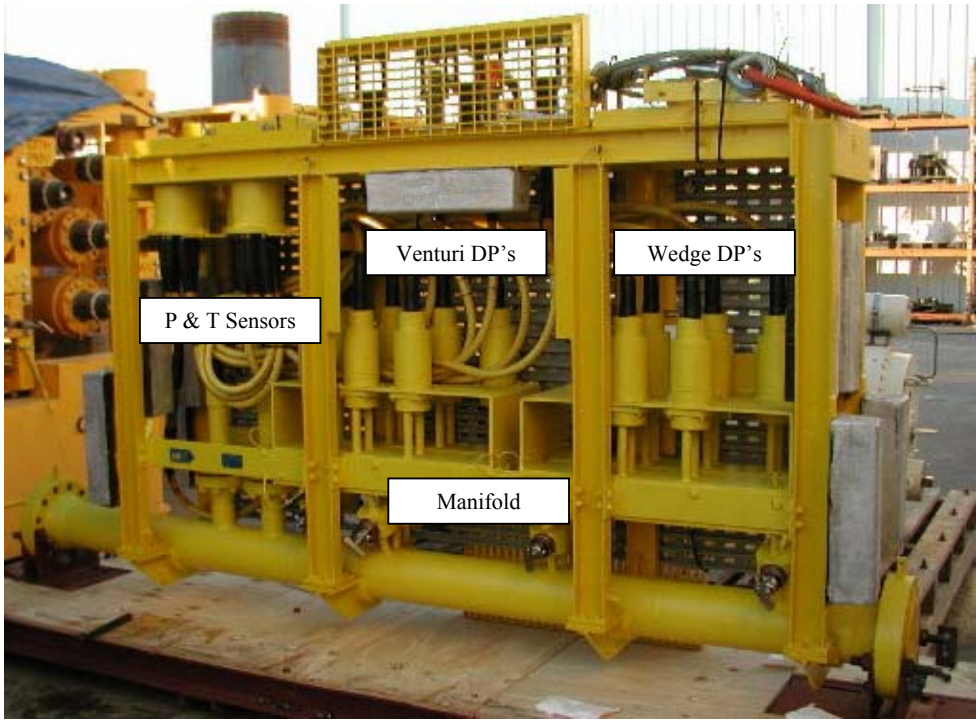

Figure 7. Dualstream II Assembly for the Canyon Express Project

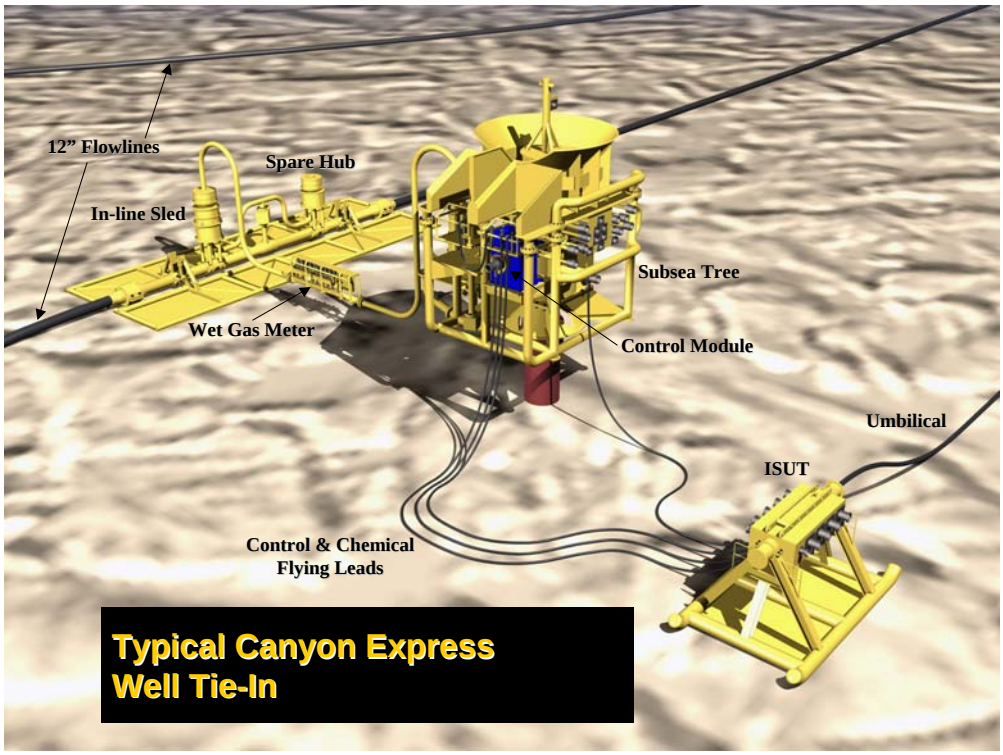

Figure 8. Installation of Metering Skid in Jumper on Canyon Express Well

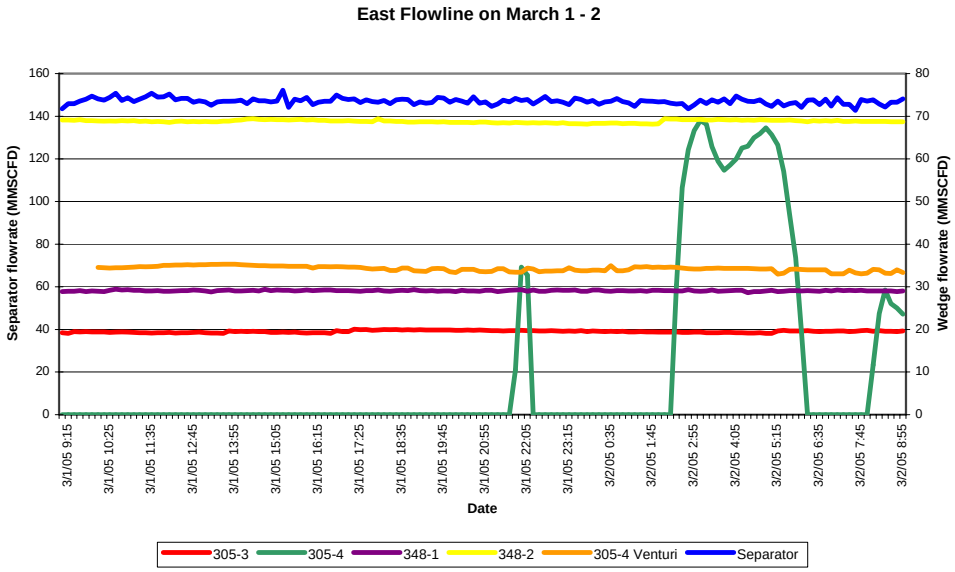

Figure. 9. Example of Hydrate Blockage in the Wedge Capillary Lines

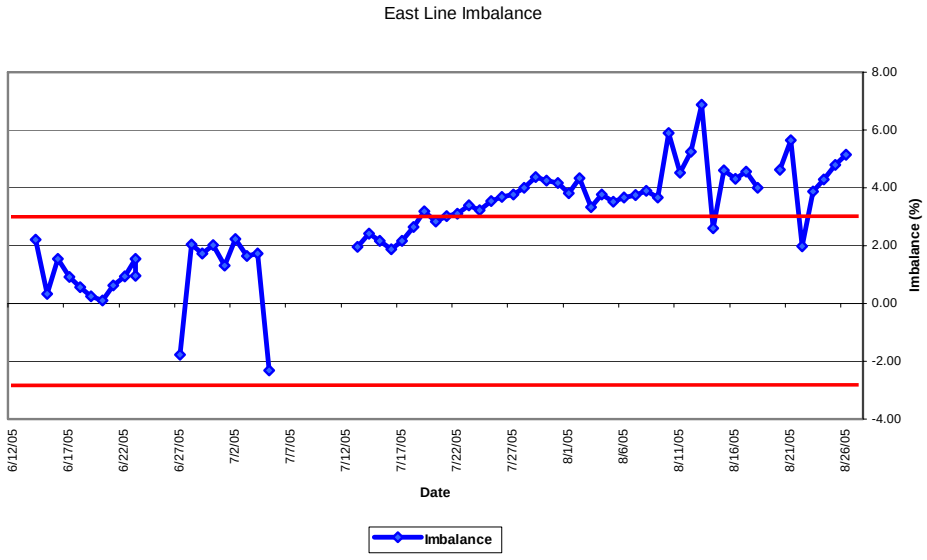

Figure 10. Change in Flowline Imbalance

Wet Gas Measurement in the Southern North Sea

David S. Geach - ConocoPhillips (U.K.) Ltd
Andrew W. Jamieson - 4C Measurement Ltd

Abstract

ConocoPhillips has some 18 wet gas Venturi meters currently in use in the UK sector of the North Sea.

The paper covers:-

The experience gained in operating these meters:

- The importance of gas flow calibration. Flow calibration of these meters clearly shows that the discharge coefficient value given in ISO 5167 is clearly not applicable and the discharge coefficient can vary by > ±2%.
- The effect damage has had on the discharge coefficient of one meter arising from a broken choke impinging on the meter convergent section.
- Calibration repeatability over time
- The methods used to correct the over-reading (namely Murdock, Chisholm and de-Leeuw).
- Flow verification tests carried out on two meters installed in the Southern North Sea.
    - First, a sub sea meter located some 34km from the host platform. This not only demonstrated applicability of using a correct wet gas correlation but also gave valuable information on how gas, condensate and water flow along a pipeline
    - Second, a topside meter installed on an unmanned satellite, where verification was conducted over about a year. This showed very good agreement between the Venturi meter readings and high quality separator gas and condensate meters it was tested against.

A way forward: From the experience gained we propose a practical and cost-effective method of monitoring the liquid content of wells/satellite fields in a wet gas allocation system.

1. Introduction

ConocoPhillips uses Wet Gas Venturi meters extensively in its Southern North Sea operations. New gas fields are too small to justify full-scale separation and are tied back to host facilities using existing pipeline infrastructure and separation facilities.

The following are examples of the advantages of Wet Gas Venturi meters.

- They are robust instruments and are not damaged by high flow rates.
- They do not 'dam' the flow (unlike orifice plate meters).
- They use proven technology that has been widely accepted within the oil and gas industry, such as differential pressure, static pressure and temperature transmitters.
- They can operate at higher differential pressure than orifice plate meters without incurring permanent meter damage (differential pressure up to 4 bar can be used).
- When combined with smart differential pressure transmitters they have a relatively large turn down approaching 10:1.
- Provided sufficient care is taken in the manufacture and the selection of the secondary instrumentation they are very suitable for subsea use.
- Extensive work has been carried out to develop practical correlations for the over-reading of Venturi meters due to liquid entrained in the gas flow.

The design requirements for Venturi-type flow meters are contained within ISO 5167:2003, Parts 1 and 4. Note that this standard does not apply to wet gas. For example, piezometric rings are not suitable for wet gas applications as the rings will fill with liquid. Furthermore the Venturi section of ISO5167 was originally developed for single phase liquid applications. The 2003 edition acknowledges that Venturi meters are increasingly used for gas applications, and that they should be calibrated over the expected operating flow range. We present calibration data in this paper which highlights these issues.

In this paper we discuss three aspects of wet gas Venturi metering.

- Meter calibration issues including the effects of damage on a Venturi
- The most appropriate wet gas correction correlation
- Verification of operational Venturi meters.

Combining the findings from these aspects we suggest a practical and cost effective method for verification of wet gas Venturi meters that requires limited shutdown of associated facilities.

2. Venturi Meter Calibration Issues

2.1. Gas Discharge Coefficient

We present calibration data for the meters currently in use.

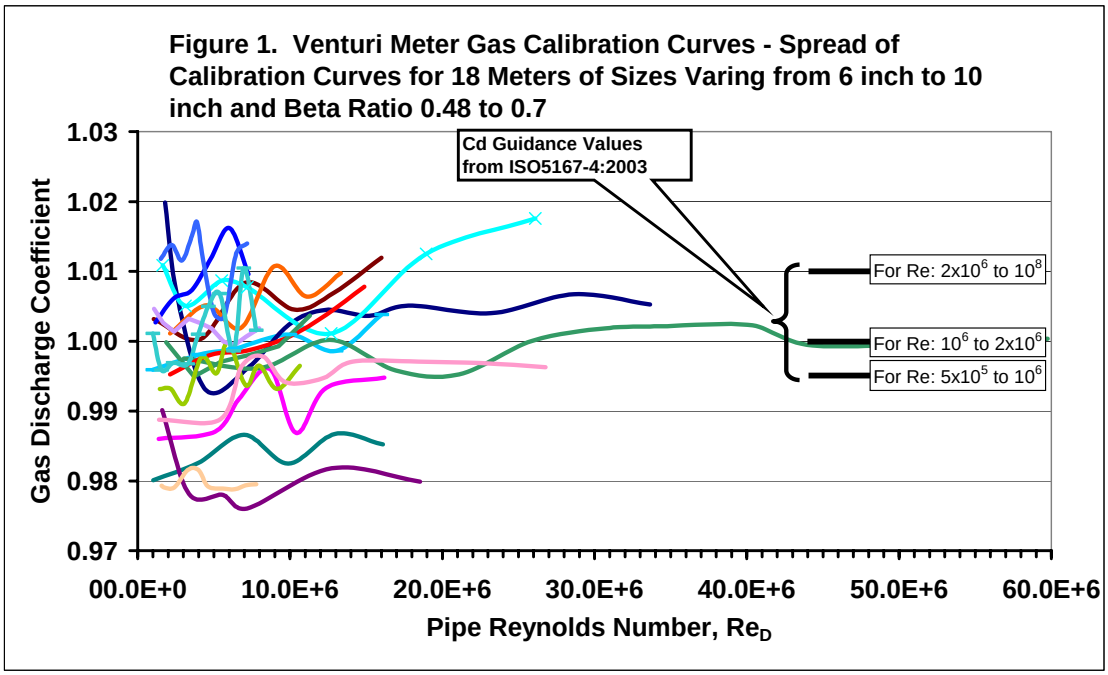

Figure 1 above shows similar gas calibration curves for 18 Venturi meters with diameters ranging from 6 to 10 inches and beta ratios ranging from 0.48 to 0.7. The meters were calibrated at the Advantica Flow Centre at Bishop Auckland on sales-quality natural gas. For the meters calibrated, the variation in discharge coefficients is about 4%. The curves themselves are evidently not linear, and many show sharp kinks. This confirms findings by Jamieson et al (Ref [1]).

These data confirm the statement in Note 1 of ISO5167-4:2003 that in many cases the discharge coefficients lie outside the range predicted by part 4 by 2% or more. However, the data are in conflict with Annex B, Table B.2, of the above standard, which is given for guidance when classical Venturis are used outside the scope of ISO5167-4. In particular this table gives a discharge coefficient of 1.01 for throat Reynolds Numbers between $2x10^6$ and 10^8. This would lead to an average bias of about -1.5% for the ConocoPhillips meters. On the right hand side of Figure 1 we have indicated the recommended values from Table B.2.

The important issue is that unless you can accept a meter calibration uncertainty of about 3%, potentially with a large bias, then you should follow the advice of ISO5167-4 and determine the value of the discharge coefficient from an actual calibration on gas. We consider that considerably more work must be done to clarify the guidance given by the standard on this issue.

We now split out these meters by manufacturer. Figure 2 and 3 below show the Discharge Coefficient calibration curves for meter Manufacturer A and Manufacturer

B. It is evident that the variations in calibration curves are similar and therefore cannot be attributed to the manufacturer.

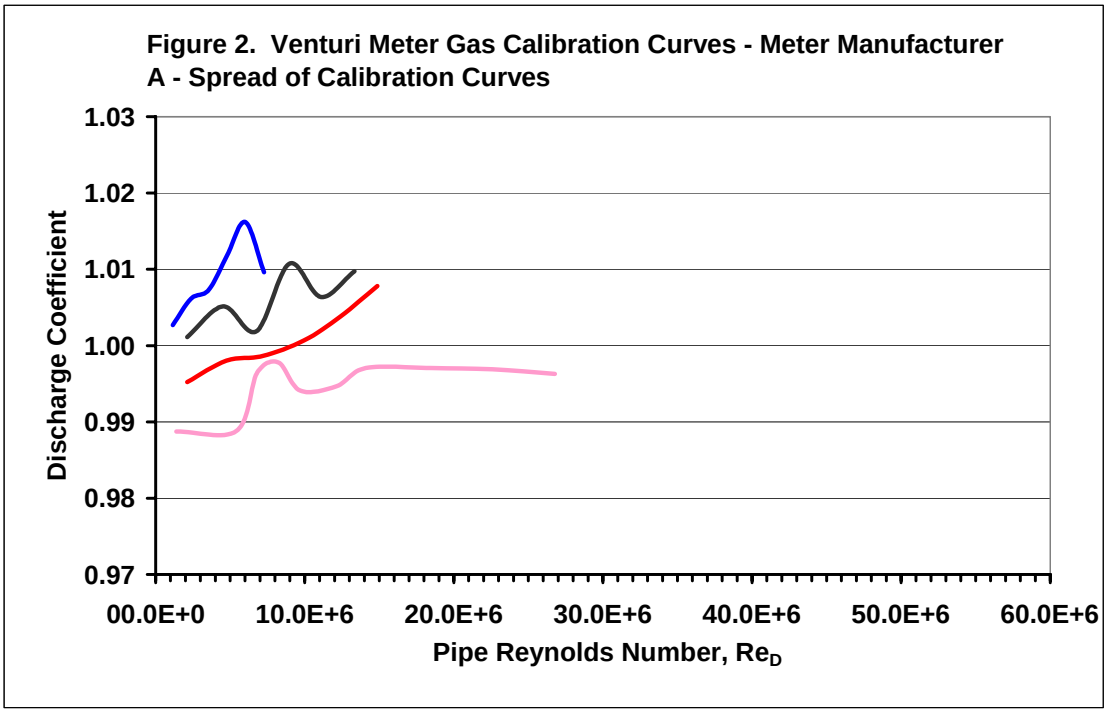

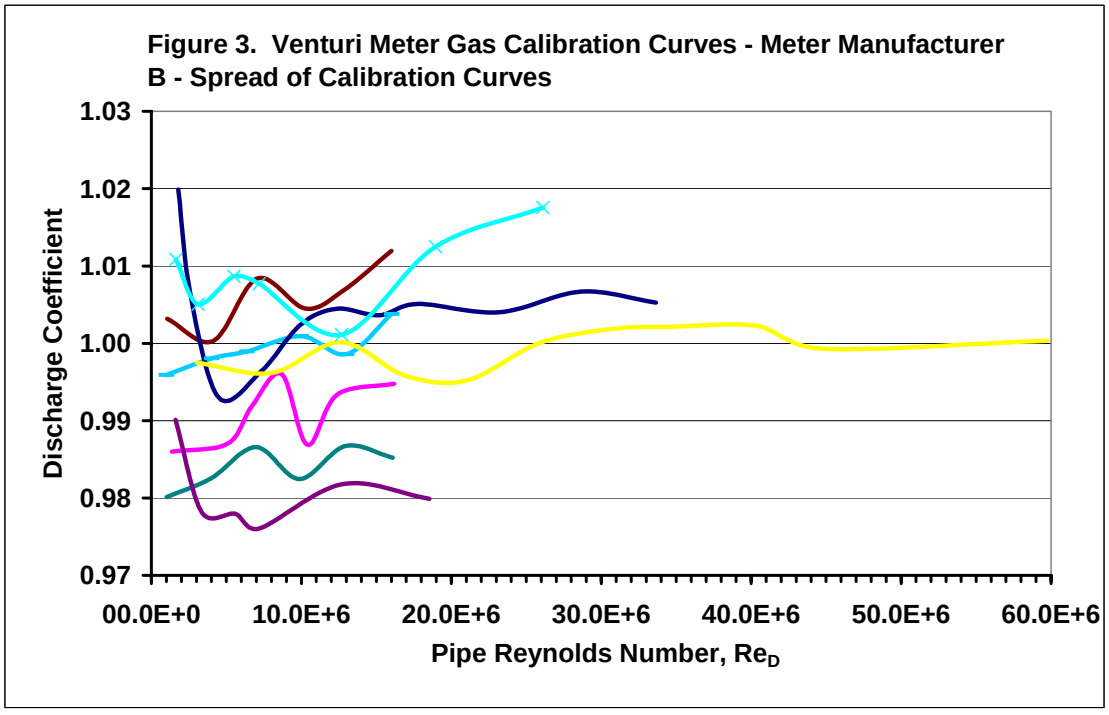

Three of the meters supplied by Manufacturer B are nominally identical. Figure 4 below, shows the gas discharge coefficient curves for three 6 inch meters. These meters are identical within machining tolerances, being manufactured using the same computer numerical controlled (CNC) boring machine. The tapping holes were drilled using a vertical borer and deburred to remove any burrs. These calibration curves differ by as much as 2%, and the shape of the curves is markedly different.

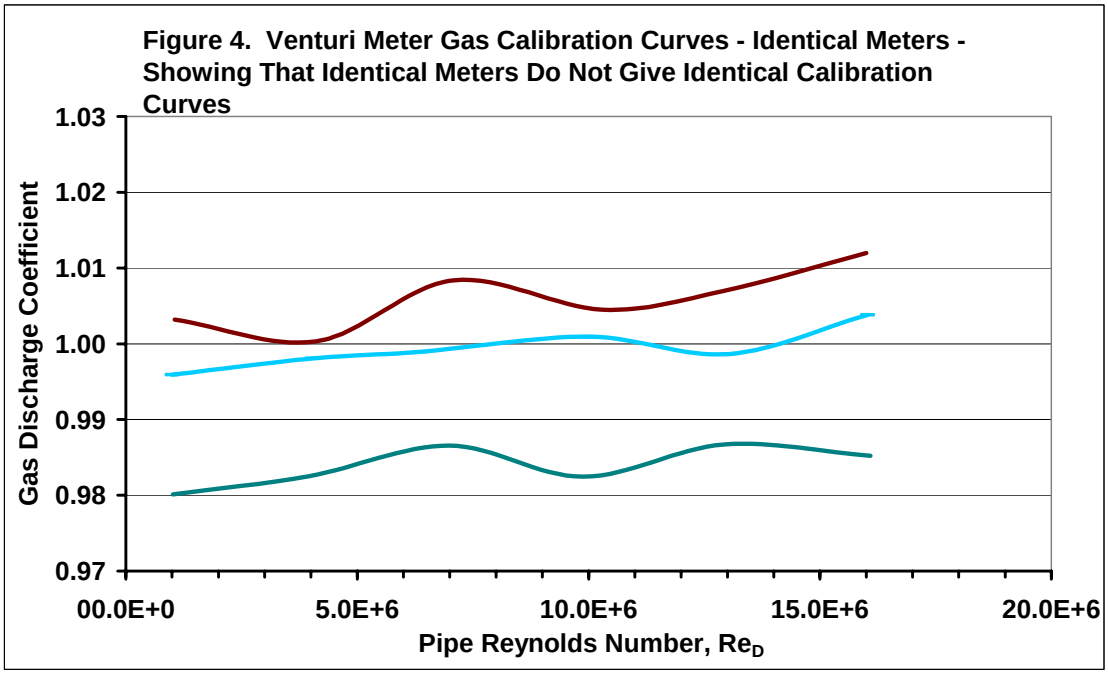

2.2. Liquid Discharge Coefficient

The correlations used to correct for liquid entrainment in wet gas require both the gas and liquid discharge coefficients which are usually not the same. Liquid discharge coefficients were determined on the water calibration facility at the E.ON Hams Hall Calibration Laboratory.

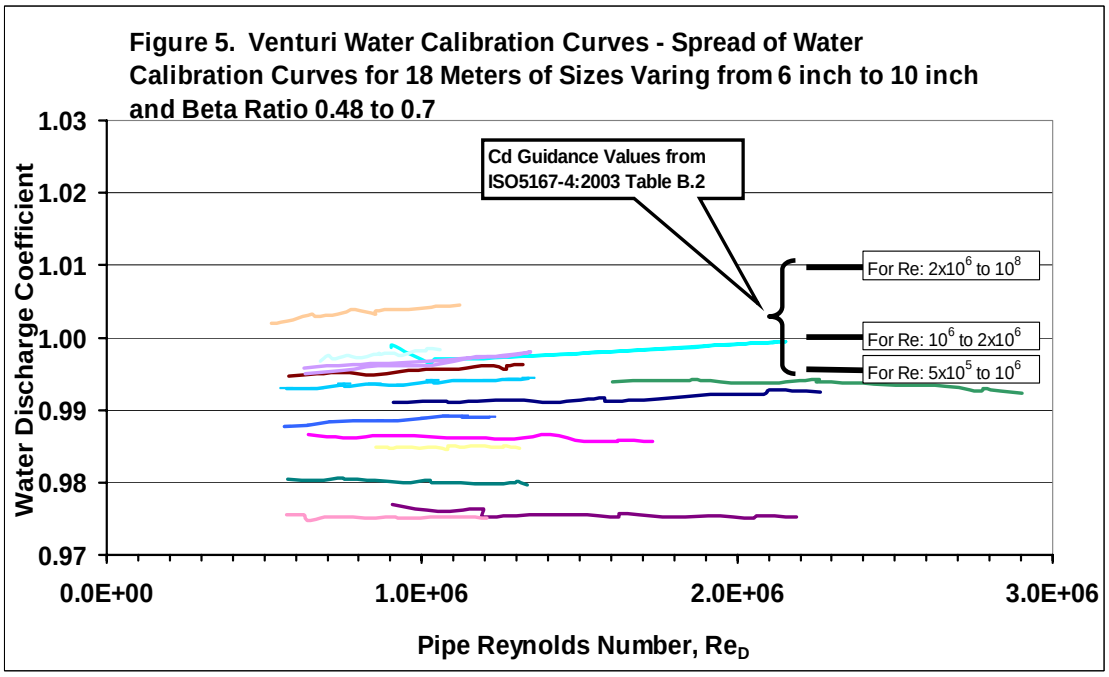

Figure 5 above shows the water discharge coefficients for the same meters given in Figure 1. The water discharge coefficient curves are significantly more linear than the gas curves. The spread in water discharge coefficient, about 3%, however, is similar that that for the gas curves. ISO5167-4:2003 gives a value of 0.995 ±1% for throat Reynolds Number up to 10^6. Our calibrations are clearly in conflict. Note, however, that the liquid discharge coefficient has a second order effect in the wet gas calculations. We have not investigated this effect in detail at this stage.

We give below the calibration curves for both liquid and gas for the last six meters calibrated. These show that the water discharge coefficient curve lies below the gas curve. It may be practical, therefore, simply to take the lowest value of the gas discharge coefficient as the liquid discharge coefficient and dispense with the water calibration.

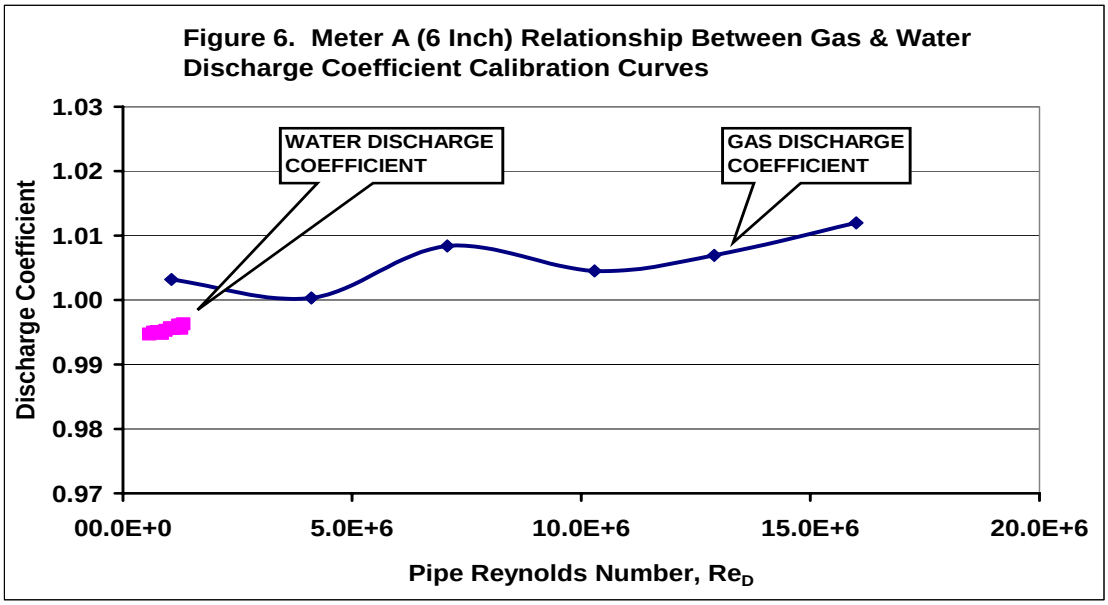

Figure 6. Meter A (6 Inch) Relationship Between Gas & Water Discharge Coefficient Calibration Curves

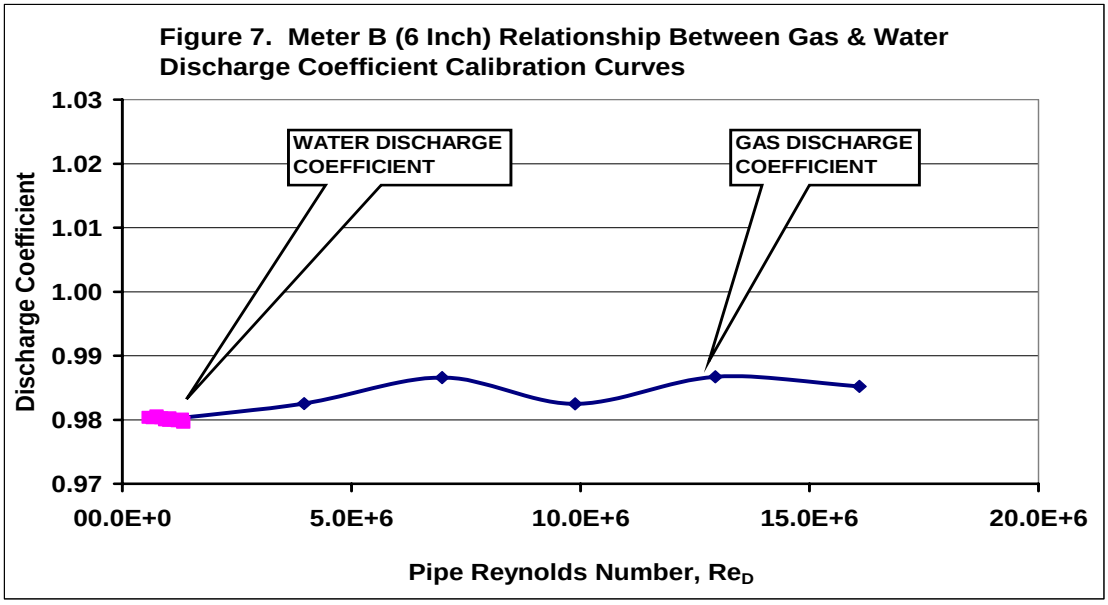

Figure 7. Meter B (6 Inch) Relationship Between Gas & Water Discharge Coefficient Calibration Curves

Figure 8. Meter C (6 Inch) Relationship Between Gas & Water Discharge Coefficient Calibration Curves

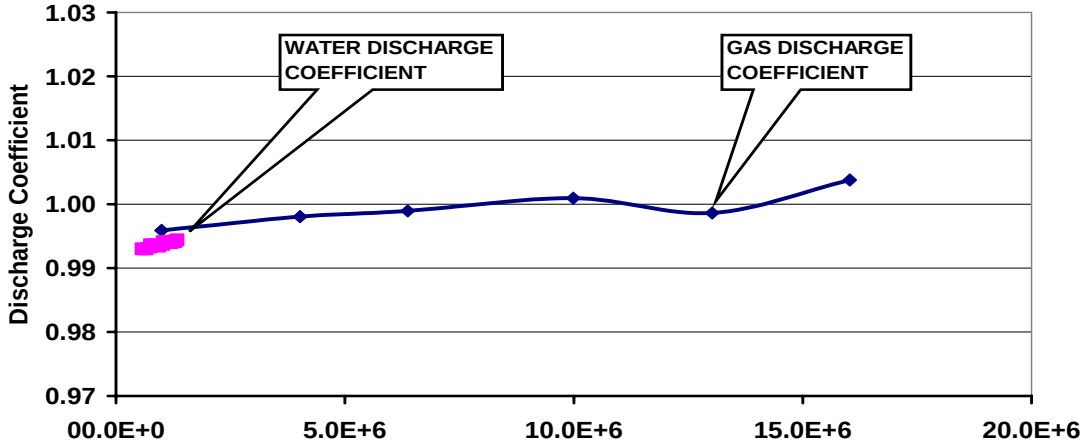

Figure 9. Meter D (8 Inch) Relationship Between Gas & Water Discharge Coefficient Calibration Curves

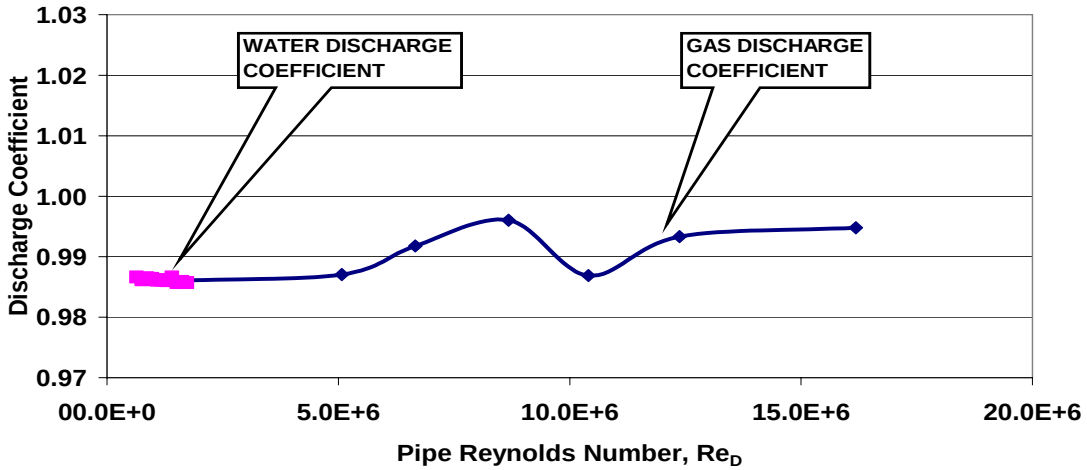

Figure 10. Meter E (8 Inch) Relationship Between Gas & Water Discharge Coefficient Calibration Curves

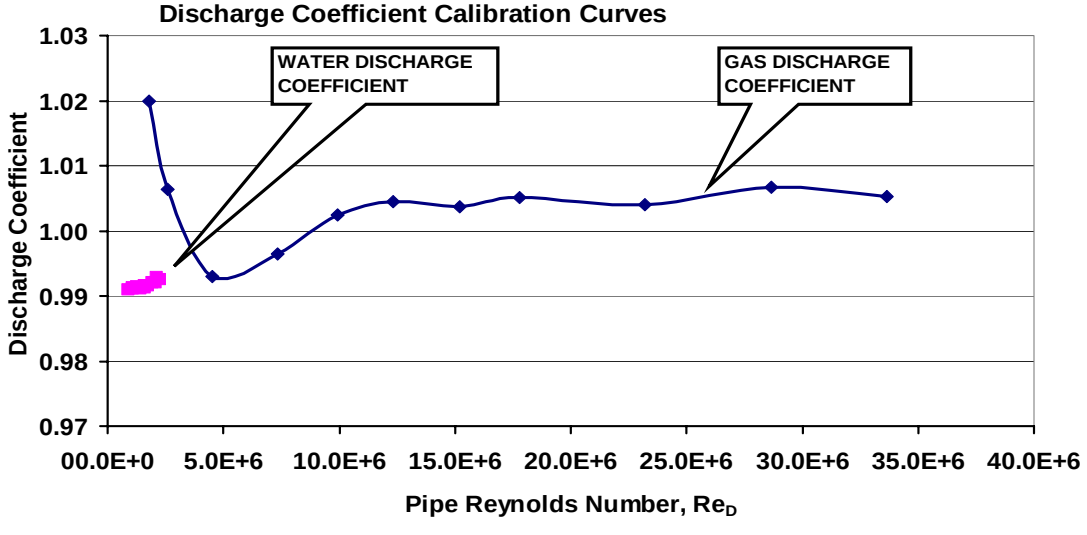

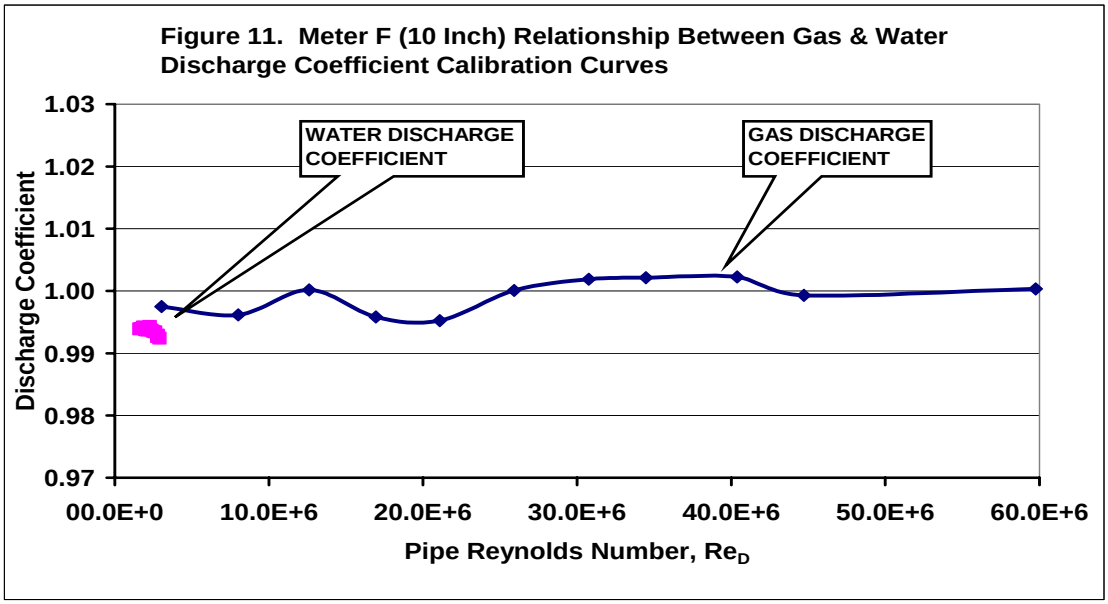

2.3. Effect of Damage to Meter on Discharge Coefficient

This section discusses the effect of damage from a broken choke on a Venturi meter.

The meter was installed immediately down-stream of a well head choke valve. The choke failed and part of the tungsten carbide flow control element was swept into the throat of the Venturi meter. The well was shut-in and the meter spool was removed from the line.

Figure 12 below shows the two recovered parts of the choke flow control element reassembled.

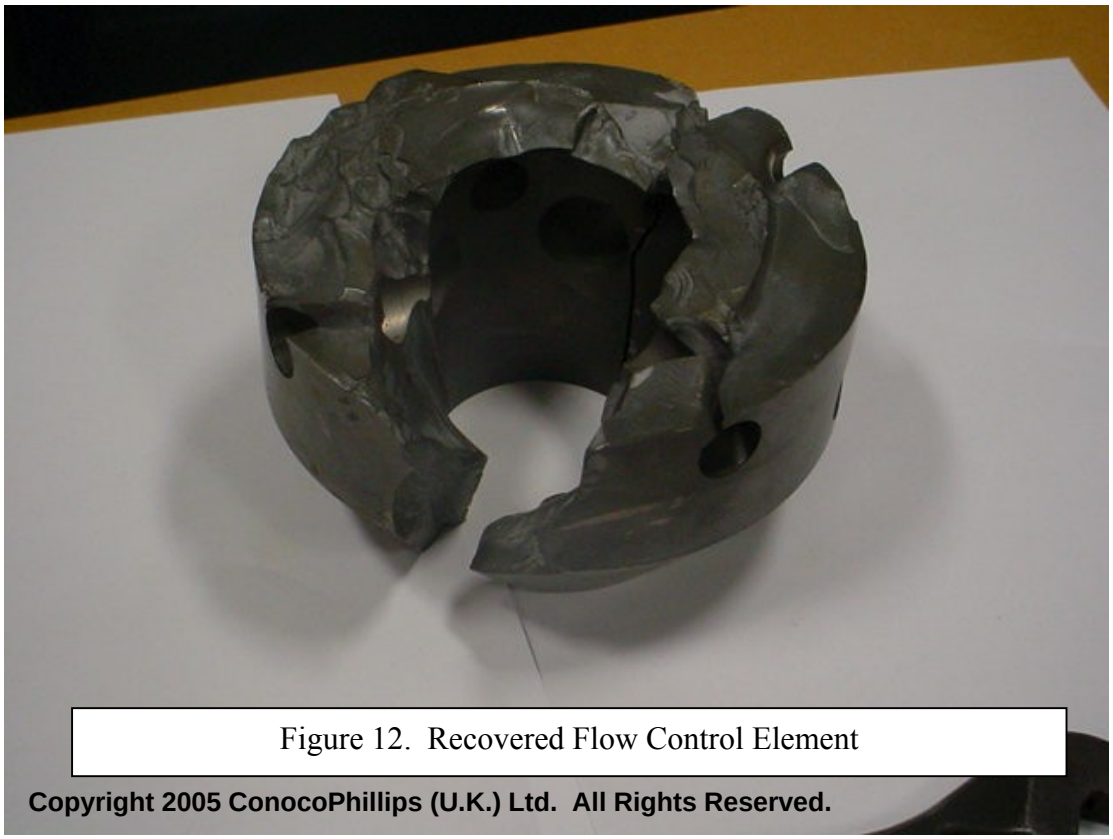

Figure 12. Recovered Flow Control Element

Figure 13 below shows the significant damage sustained by the upstream conical section. Note the deep scores. No damage was noted in the throat section or around the pressure tappings.

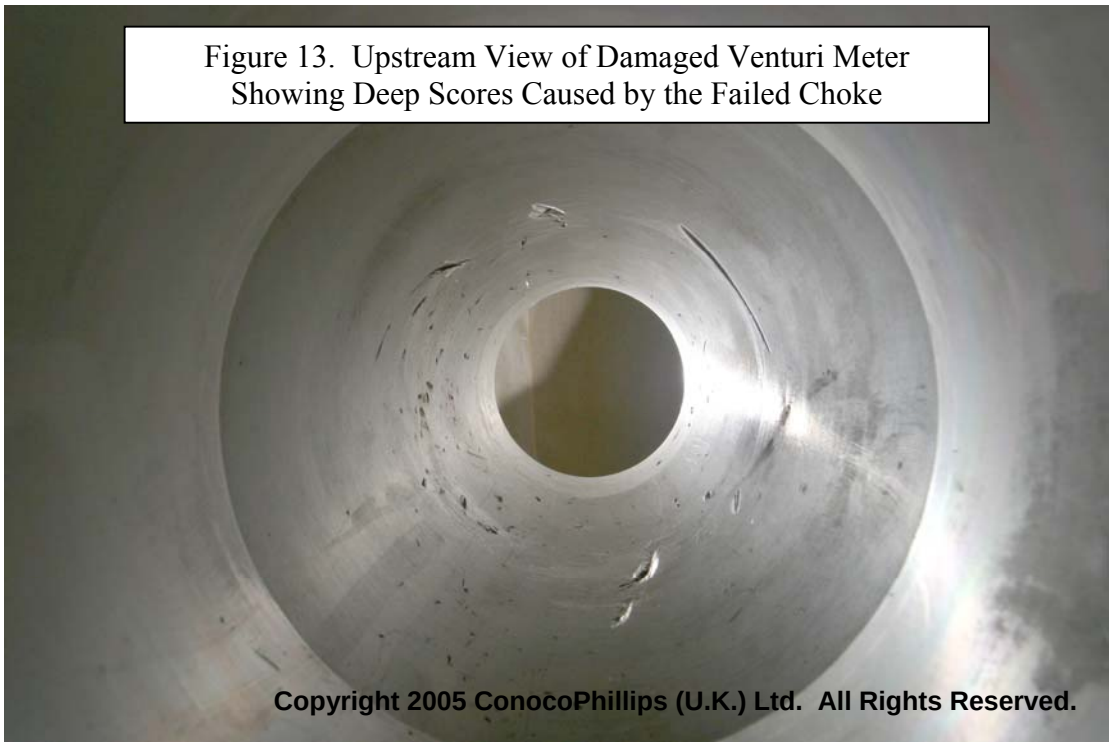

Figure 13. Upstream View of Damaged Venturi Meter Showing Deep Scores Caused by the Failed Choke

Figure 14 below shows the downstream conical section. Apart from slight pitting this section of the meter was not damaged.

Figure 14. Downstream View of Damaged Venturi Meter

Our original plan was to re-machine the damaged section of the meter, recalibrate it and return it to service. However, we decided to determine the effect that the damage

would have had on the flow calibration. Accordingly the meter was recalibrated at Bishop Auckland where its original calibration had taken place.

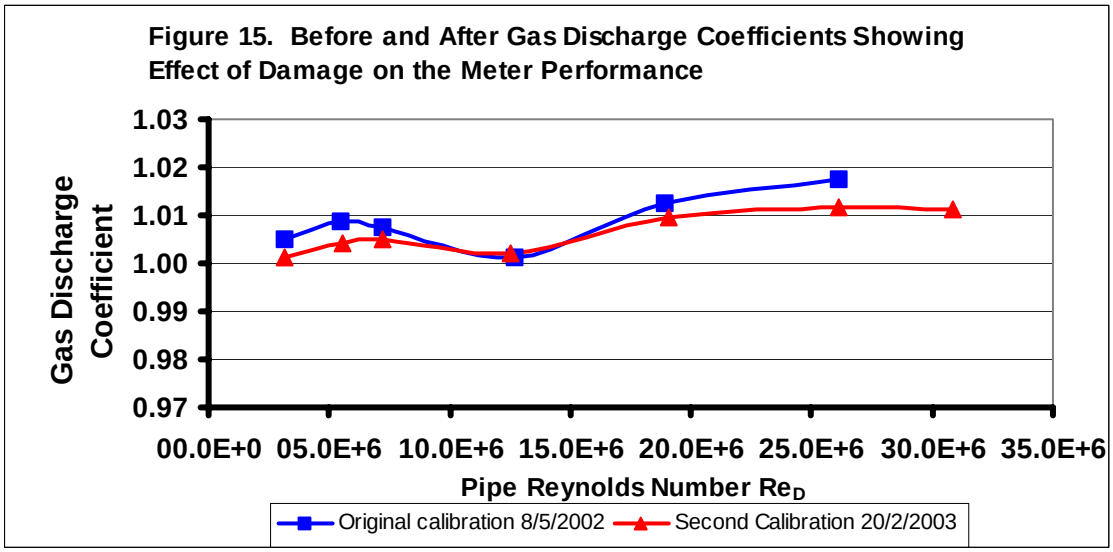

Figure 15 above shows the original calibration performed before the meter was installed prior to first production, and the calibration curve following the damage caused by the choke valve failure. It is evident that the damage had little effect on the meter discharge coefficient. We considered that the difference was as likely to be due to the uncertainty of the calibration as to a shift in calibration. Accordingly the meter was reinstalled without re-machining. We can offer no guidance as to the degree of damage that would result in a significant shift in discharge coefficient.

3. Wet Gas Correction

The equation for measuring dry gas flow using a Venturi meter is:

$$Q_g = \frac{Cd_g}{\sqrt{1-\beta^4}} * \varepsilon * \frac{\pi}{4} * \left(d'\right)^2 * \sqrt{2 * h * \rho_g}$$

Where:

Q_g	Mass flow rate
Cd_g	Discharge coefficient
d'	Venturi throat diameter at operating conditions (m)
ρ_g	Gas density at upstream tapping (kg/m^3)
β	Venturi Throat/Pipe Diameter ratio
h	Differential pressure (mbar)
ε	Expansibility factor

Liquids flowing through the meter in the gas flow will cause an increase in differential pressure over and above that would occur if there were no liquids present. This causes the meter to over-read in terms of dry gas, as follows.

$$Q_{g(ind)} = \frac{Cd_g}{\sqrt{1-\beta^4}} * \varepsilon * \frac{\pi}{4} * \left(d'\right)^2 * \sqrt{2 * h_{(ind)} * \rho_g}$$

Where:

$Q_{g(ind)}$ Indicated mass flow rate
$h_{(ind)}$ Indicated differential pressure

It is therefore necessary to apply a correction to obtain a correct dry gas reading. This is applied in the form:

$$Q_{drygas} = \frac{Q_{g(ind)}}{Wet\ Gas\ Correction}$$

Where:

Q_{drygas} Venturi dry gas mass flow rate

The correlations currently used in wet gas metering were largely introduced by Shell Research. From field experiments at Coevorden in the Netherlands, Washington (Ref [2]) related the performance of Venturi meters to the earlier work carried out at NEL on orifice plate meters by Murdock and Chisholm. At low liquid fractions (less than 1%) and high pressures (around 100 bar) there is little to chose between the modified Murdock or Chisholm corrections.

Shell Research followed this work up by extensive testing at SINTEF in Norway covering a wide range of pressure and liquid content. The correlation from this work and the extent of the data, though not the detailed data set, has been published and is available in the public domain. Ref [3] is the most relevant. In this work de Leeuw showed that Murdock and Chisholm corrections are not suitable for general application particular at lower pressures and higher liquid fractions. Murdock takes no account of pressure; Chisholm does not take into account gas velocity. The de Leeuw correlation is much more appropriate for general application and the Murdock and Chisholm correlations should be retired.

Work carried out at NEL has revealed yet another dependence, this time on the β value of the Venturi meter, Ref [4]. The work at NEL can best be regarded as extending de Leeuw's work, and impacts at higher liquid content. De Leeuw's correlation is currently gradually being accepted as meter specialists realise the shortcomings of Murdock and Chisholm at higher liquid content and at lower pressure; the NEL work has not yet had the chance to be assimilated.

The following Figures 16 and 17 are taken from de Leeuw's paper cited above.

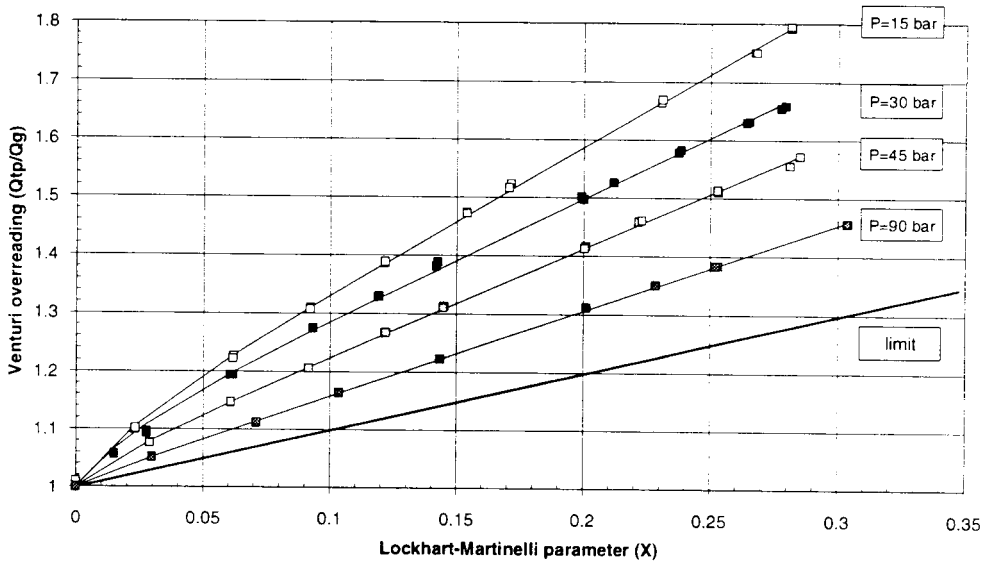

Figure 16. Trondheim Test Results Showing Venturi Overreading Against Liquid Fraction, Expressed as the Lockhart-Martinelli Parameter. Frg=3.2

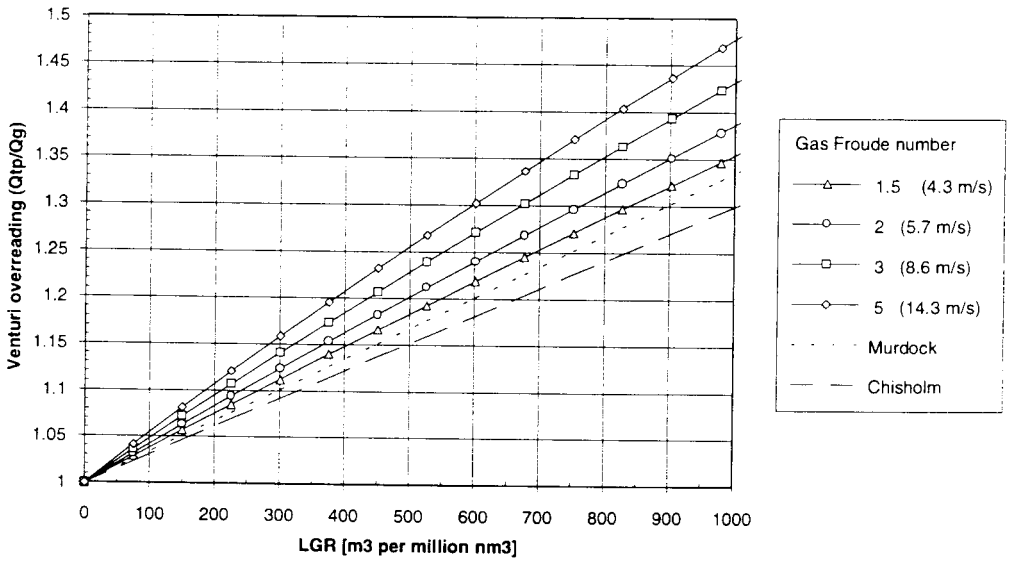

Figure 17. Illustrative Comparison Between the new Venturi Correlation and the Murdock and Chisholm Orifices relationships, for the Case ρ_l=700kg/m^3 and ρ_g=80kg/m^3

Figure 16 shows the test points measures at SINTEF, and gives the over-reading measured for the Venturi (4@ nominal diameter, β = 0.4) at pressures ranging from 15 to 90 bar, against the Lockhart-Martinelli parameter, a convenient parameter for

expressing liquid fraction in multiphase flow studies. The SINTEF test loop uses diesel and nitrogen as working fluids. The lowest pressure was 15 bar, corresponding to a nitrogen density of 17 kg/m^3. Evidently this is the reason for de Leeuw restricting his correlation to gas densities above 17 kg/m^3. The NEL work was also based on nitrogen, and again the lowest test pressure was 15 bar.

Figure 17 illustrates the difference between de Leeuw correlation and the Chisholm and Murdock relationships. It shows the predicted Venturi over-reading for liquid and gas densities of 700 and 80 kg/m3 respectively plotted against the LGR (liquid to gas ration – m^3 liquid per million Sm3 gas) for different Froude Numbers. The gas Froude Number is often used as a convenient parameter relating to gas velocity in multiphase studies, as is the superficial gas velocity (v_{sg}), the velocity calculated assuming the gas is the only phase present. Figure 17 shows clearly the strong dependence of over-reading on gas velocity, and also that Chisholm and Murdock predict much lower over-readings.

4. SubSea Venturi Meter Verification

An opportunity was given in 2003 to verify a subsea Venturi meter measuring the wet gas production from a single well field in the Southern North Sea. The gas and liquids production was commingled in a subsea pipeline with the fluids from other fields and was transported a to central processing facility, where the combined gas and liquid production from the pipeline was metered at the outlets of a production separator.

4.1. Gas Measurement

The gas was metered by an orifice plate metering station designed and operated in accordance with ISO5167.

The meter verification was carried out by shutting-in the other fields producing into the 34km long pipeline and flowing only to the test field. Following a 24 hour stabilising time the test field meter readings were then compared with the gas, condensate and water readings from the production separator on the central processing facility.

It had been intended to carry out the meter verification at the same flow rate as when the test field produced normally into the pipeline. However, shortly before the verification started, the well annulus pressure was too high, and it was necessary to increase the well tubing pressure to ensure safe operation. This meant that the gas flow rate had to be reduced to about 90% of the then current normal production. This was considered acceptable. Production from the test field was steadily declining, and a verification at the reduced flow rate was considered to be more representative of average production conditions until the next planned verification.

However, there were further difficulties, with the consequence that the gas flow rate was reduced to 50% of the current normal production from the test field. Half way through the verification period, the difficulties were sufficiently resolved to allow the well flow rate to be increased back to 90% of the current normal flow.

During the stabilisation period, a preliminary comparison of the test field and central processing facility metering figures showed that the test field was indicating some 17% higher than the central processing facility.

It was clear that the verification was not proceeding in the straightforward way that had been intended. It was considered that it was essential to continue the test, not merely because it would take a long time to set up another one, but because it was evident that much more information would come from the test. It was agreed to continue for the full verification period and gather as much information as possible to allow ConocoPhillips to evaluate possible options thoroughly. The enforced need for two flow rates during the verification period meant that it was possible to look for a flow dependence in the difference between the test field and central processing facility metering figures.

Figure 18 below shows the gas data from the test field meter and central processing facility gas meters. The time scale is 4.5 days. The stabilisation and test periods are indicated. The average over-reading by the test field meter over the verification period was 16.7% (referred to the central processing facility metering readings) or 14.3% (referred to the test field meter reading).

Figure 18. Subsea Venturi Meter Verification - Gas Measurement

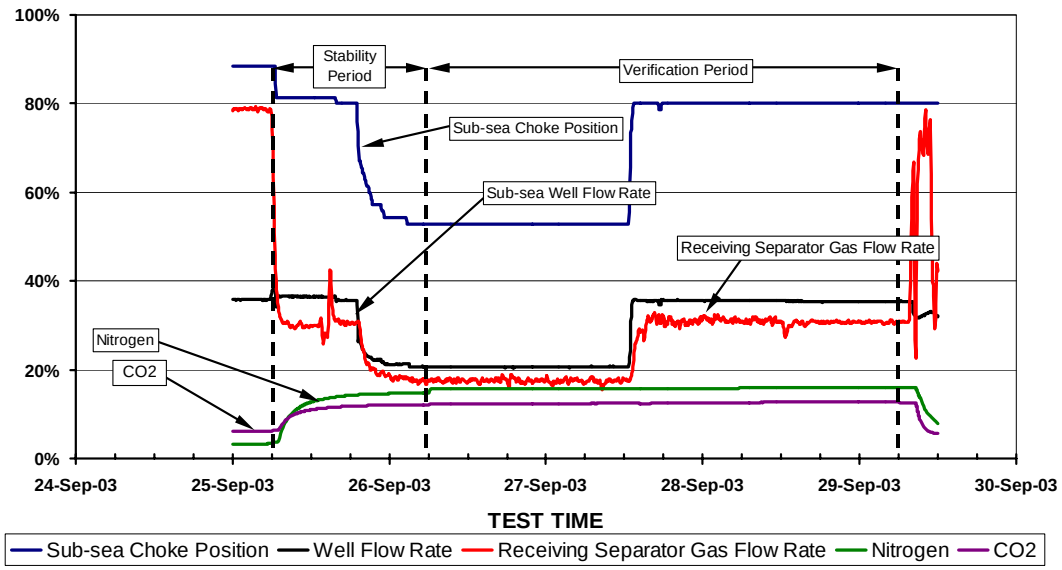

Figure 18 also shows the choke settings for the test field well. The field production follows these settings quite precisely, and the field flow rate was very stable.

Finally Figure 18 also shows the molar concentrations of nitrogen and carbon dioxide measured by the gas chromatograph on the central processing facilities. The concentration of these inert components are significantly different from the average composition of all of the fields producing into the pipeline, and so they provide an excellent indication of when test field gas filled the pipeline. The blips at 06:00 each morning are when the automatic calibration of the GC was performed. It is evident that by the end of the stabilisation period, the test field gas filled the pipeline.

In summary:

- During the verification period, the test field meter read higher than the central processing facility metering by 16.7%
- The difference between the test field and central processing facility metering figures appears to be flow related.
- Test field gas filled the pipeline in the stabilisation period.

4.2. Water Production

The produced water was measured by a 4" magflow process meter with no pressure or temperature corrections.

Figure 19. Subsea Venturi Meter Verification - Water Measurement

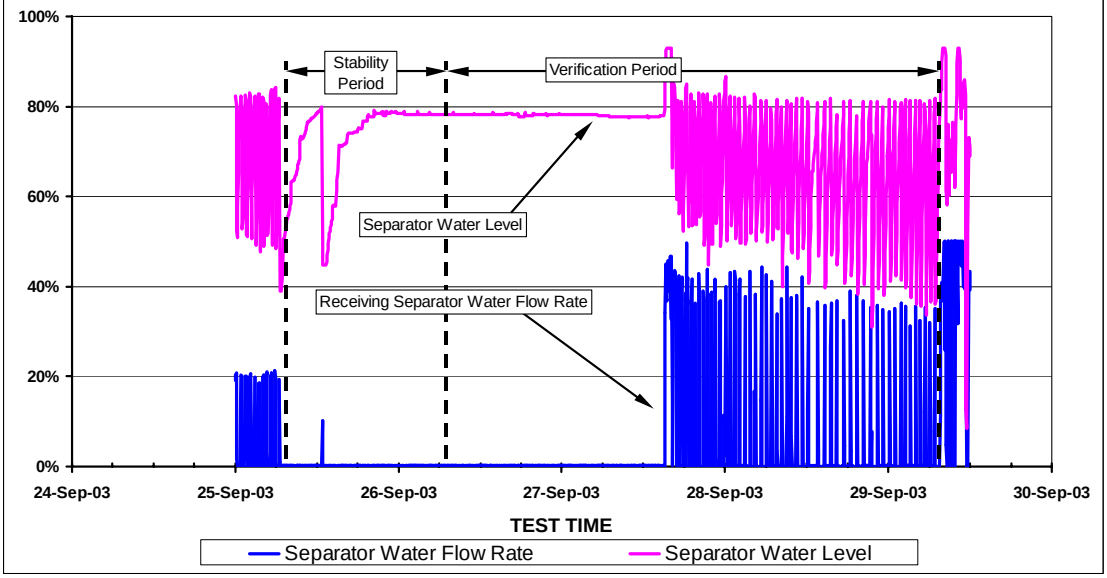

Figure 19 above shows the plot of the water production during the verification. The bottom trace shows the water flow rate; the upper the variations in separator interface level. The spike at about mid-day on 25 September corresponds to the water being drained prior to the test. The separator was operated in batch flow mode.

When only the test field was flowing into the pipeline the gas velocity would be reduced and liquid would accumulate in the low spots until a new equilibrium level was reached. Water would then be produced out of the pipeline onto the central processing facility and into the separator at about the same rate as it was being produced from the test field. Accordingly, to estimate the water production during the verification period it is appropriate to take the average water flow rate for the period when water was produced into the separator, applying that flow rate to the whole verification period, and calculate the corresponding volume of water.

4.3. Condensate Measurement

The condensate was measured downstream of the production separator by turbine meters maintained to fiscal standards. However, the uncertainties in determining condensate production from the well proved to be much greater than the uncertainties

in these meters. The separator was operated in batch flow mode. Condensate was drained before the test was started and shortly after the end of the test.

Figure 20 below shows the plot of the condensate production during the verification period. Total condensate measured was 30.2m^3. Unlike the water, condensate appears to have been produced continuously into the separator throughout the verification. In the pipeline, condensate would have lain on top of the water and would have been swept through in preference to water. Accordingly, the assumption was made that the total condensate measured over the verification period was a high estimate of the condensate produced from the test field and there was a large uncertainty, say 50%, in its value. The measured condensate was 30.2m^3. Thus the estimate of the condensate produced during the test lay between 15 and 30m^3. There was no point in applying temperature and pressure corrections to these values.

Figure 20. Subsea Venturi Meter Verification - Condensate Measurement

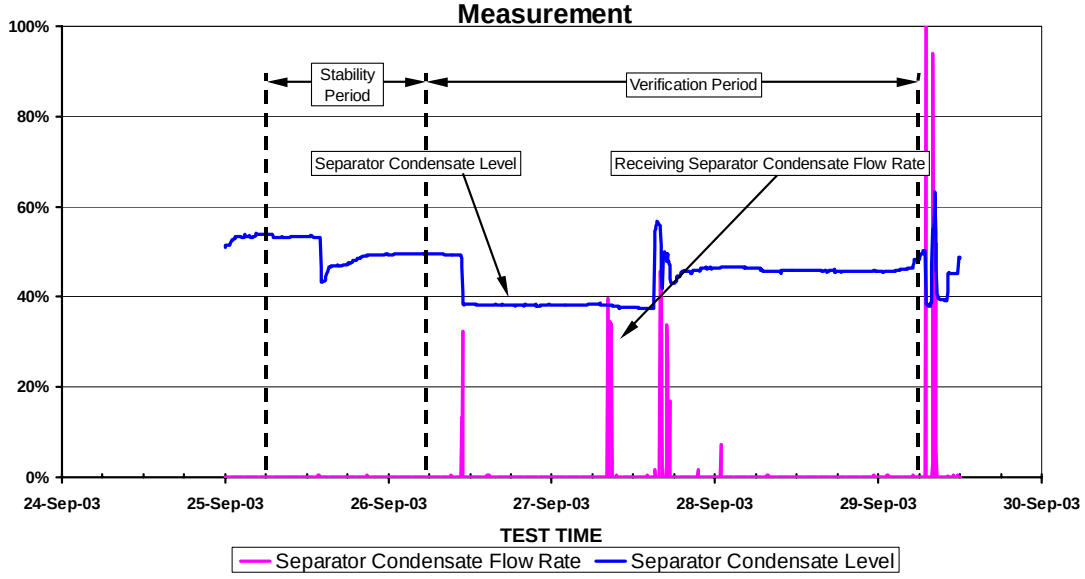

4.4. Discussion of Findings

The 16.7% difference between the test field meter readings and the central processing facility meters was considerably larger than anticipated. The following issues were discussed as possible reasons for the over-reading of the test field meter.

Associated instruments of the test field meter

The possibility that the associated instrumentation, namely differential pressure transmitter, temperature sensor and pressure transmitter could have drifted or changed suddenly in calibration was reviewed.

The instruments had shown little drift from start of production and a previous verification of the test field meter where the agreement was 2.8%. The drift on the differential pressure and pressure transmitters would need to be about 28% to account for the over-reading. This was not considered possible with the equipment installed. The drift on the temperature sensor would need to be about 80°C to account for the over-reading. This was evidently not the case, as temperatures measured at the test field meter during the verification were about 44° and 51°C, both sensible values. It

is even more unlikely that two or all of these sensors could have gone faulty at the same time to give the over-reading. Further more, in a recent shutdown the differential pressure transmitter (ranged 0 – 3000 mbar) gave a reading of -12 mbar and the other sensors responded as expected.

Errors in the test field subsea control system
The test field metering calculations are made in the subsea control system. By carrying out an offline calculation it was evident that the control system was working correctly.

Deposition on the inside of the Venturi meter
The velocities in the meter are high; often in excess of 25 m/s, and much higher in the throat of the venturi. It is most unlikely that deposits or scale could stick. If there was sand production, this would lead to erosion of the throat giving lower readings. Further if erosion was occurring in the venturi meter, it would be observed in other items of equipment where the consequences could be even more serious.

Blockage of impulse lines
There were no signs that there was a "locked-in" differential pressure due to blocked impulse lines to the differential pressure transmitter. When the test field well was shut in shortly before the test the differential pressure went down to -12 mbar, and during the test the differential pressure trend followed the choke settings closely.

Errors in central processing facility gas meters
If an orifice plate had been inserted the wrong way round in its carrier, the orifice meter would have under-read by about 20%, nearly explaining the over-reading. During the calibrations immediately before the test, the orientation of the orifice plates had been carefully checked to ensure they were correctly installed.

Choice of Venturi meter for service on test field
Venturi meters are chosen for subsea wet gas metering as they are robust, use proven components in the associated instrumentation, and there is little to go wrong.

Debris from well/broken choke
The possibility for debris lodged in the throat of the Venturi meter was seriously considered.

In September 2000, the choke trim had failed and had broken up into several pieces. When the choke was replaced it was not possible to recover all the parts. As the meter is downstream of a long sweeping elbow it was not possible to check if parts of the choke had stuck in the throat of the Venturi meter. Initially we considered this the most probable reason for the Venturi over-reading. However, during detailed discussions with the choke manufacturer it became evident that choke fragments could only lodge in the Venturi meter under very exceptional circumstances. As the exit diameter of the choke was smaller than the Venturi throat diameter, only a long, thin shard could have passed through the choke exit, turned sideways on, and then lodged in the throat. It would then have had to remain lodged in that position for two years.

Furthermore, there was no evidence in the production records of a sudden increase in differential pressure reading at the time that the choke failed. From the previous example given in this paper (section 2.3) of a choke failure, the fragment lodged in the Venturi meter only because it was bigger than the Venturi throat. It was therefore concluded that the over-reading by the test field meter was not due to well debris or a broken choke.

Appropriate wet gas correction

The predicted over-readings for the test field using the de Leeuw correlation were 1.227 at the high flow rate and pressure, and 1.203 at the low flow rate and pressure. This was based on a liquid to gas ratio of 258m^3 liquid per 10^6Sm^3 gas, corresponding to the liquid and gas measured during the verification period. The corresponding over-readings predicted using the Chisholm correlation were 1.065 and 1.058 and the over-readings using the Murdock correlation were 1.052 and 1.043. The observed over-reading was 1.167 on average, 1.155 at the high flow rate and pressure and 1.175 at the low flow rate and pressure.

Evidently both Chisholm and Murdock predict an over-reading that is too small. The de Leeuw and NEL work shows that the Chisholm and Murdock correlations should not be used for the conditions existing at the test field.

The over-readings predicted by the de Leeuw correlation appear to be somewhat higher than the observed over-reading, about 21% compared to about 16.5%. Furthermore the de Leeuw correlation predicts a higher over-reading at high pressure than at low pressure. The observed over-readings are the other way round. We calculated the liquid to gas ratios (LGRs) so that the de Leeuw over-readings match the observed over-readings. This resulted in a 20% lower LGR for the high pressure high flow rate gas (171m^3 per 106Sm^3) than for the lower pressure low flow rate gas (219m^3 per 106Sm^3). This probably corresponds to the situation where formation water is flowing at a more or less constant rate into the well bore, but the gas flow rate varies. However, the gas velocities are sufficiently high for all of the liquid to be removed.

Note that the pressures and densities of the gas at the test field meter (21bar, 14.4kg/m^3, and 15bar 10kg/m^3) are comparable with the SINTEF data set regarding pressure but not density. De Leeuw gives a minimum density of 17kg/m^3 based on the density of nitrogen at 15bar. There is no reason to believe that the de Leeuw correlation is invalid at our densities, but further work may be required to confirm this.

Water, the most of the liquid produced, was only produced at the host facility during the second half of the verification period, presumably because the pipeline was stabilising to a new liquid level. It was therefore very difficult to estimate the likely error in both water and condensate produced. It is probably more correct, and more useful, to turn things round and use the observed Venturi meter over-reading and the de Leeuw correlation to estimate the liquid throughput. These observations involve changes in accurate differential pressure readings, and a well founded correlation, in contrast to relatively poor water and condensate measurements at a separator at the end of a long pipeline.

5. Production Field Comparison

There is a similar installation to the test field described above, except that the Venturi meter is installed on a top-sides satellite and the de Leeuw correlation is implemented in the flow computer. The Venturi meter was calibrated on both gas and water before installation and is one of the meters shown in Figures 1 and 5. We consider that this installation follows best current practice. For this paper we shall call this field the "production field". Gas from the production field is routed through a subsea pipeline to a similar host facility as the test field. The major difference is that the production field has been producing on its own to the separation facilities for about a year. Therefore there has been a continuous verification of the production field Venturi for this period.

Figure 21 below shows the total hydrocarbon percentage difference between the host facility meters and the production field Venturi meter. The average difference for the 12 month period is 0.38%. We consider this very satisfactory. The scatter in the points is more a function of operating the pipeline and line packing and not the performance of either the host facility meters or the production field Venturi meter.

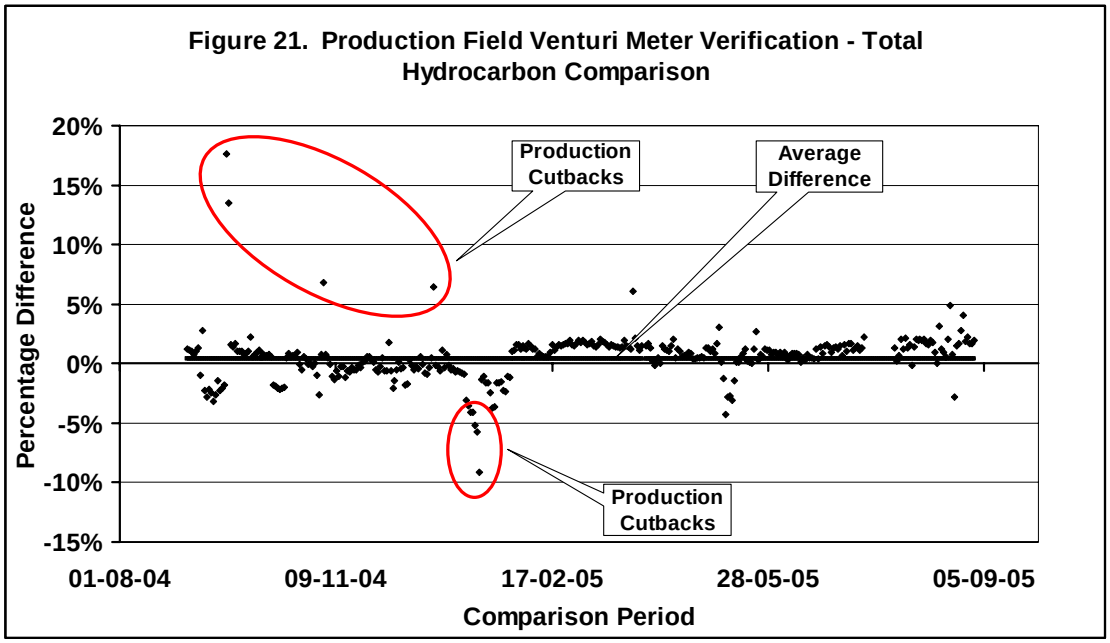

Figure 22 shows the difference for gas. Here the average difference was 0.67%.

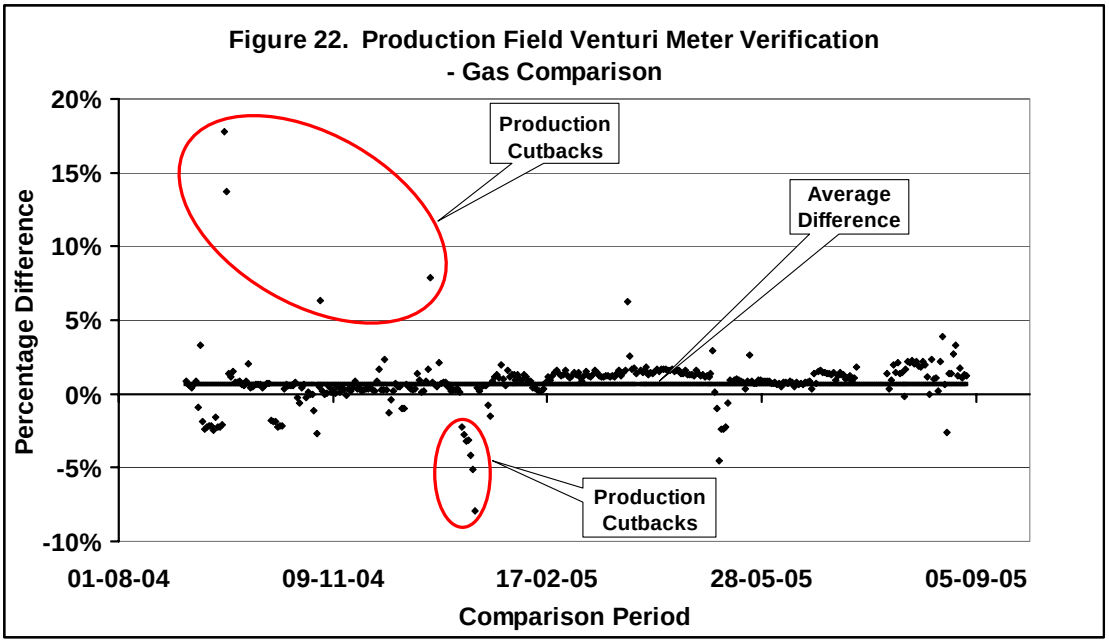

6. Conclusions and Way Forward

- Venturi meters show such a wide spread in their discharge coefficients that for serious gas metering they must be calibrated before use.

- For wet gas applications they are commonly calibrated using both gas and water. It may be practical to use the lowest value of the gas discharge coefficient as the value for the liquid discharge coefficient, eliminating the need for a water calibration.

- In an example where significant damage was sustained in the convergent section of a Venturi meter there was a minimal shift in discharge coefficient saving costs of re-machining and further recalibration. It should be noted that no damage was seen in the throat section or around the pressure tappings.

- Verification of a subsea Venturi meter showed that the de Leeuw correlation was much more appropriate. The Chisholm and Murdock correlations were inaccurate and we consider they should no longer be used for Venturi wet gas metering.

- The gas was found to flow through the pipeline very quickly (hours rather than days) compared to the liquids. The arrival of the gas and stabilisation of the pipeline could be monitored easily by observing the change in gas composition.

- Water and condensate behaved differently. Water accumulated in the pipeline until a new equilibrium level was reached, whereas condensate flowed through

more continuously. The errors in estimating both water and condensate quantities were large.

- Continuous verification of a topsides Venturi meter incorporating the de Leeuw correlation over a period of one year showed a difference of less than 1% for both hydrocarbon and gas comparisons.

Current practice is to try to estimate the liquid throughput and derive a wet gas correction factor using one of the available correlations. However in our case there was the large volume of the pipeline between the test field meter and the central processing facility meters. This meant that errors in estimating the liquid hold-up in the pipeline and hence the possible errors in estimating the liquid actually flowing through the test field meter were too large for this approach to be useful.

The above conclusions suggest strongly that it is probably more correct, and more useful, to turn things round and use the observed Venturi meter over-reading and the de Leeuw correlation to estimate the liquid flowing through the test field meter. These observations use accurate differential pressure readings, and a well-founded correlation, in contrast to relatively poor water and condensate measurements at a separator at the end of a long pipeline. The adjustment to make the test field gas figure agree with that of the central processing facility is made by the correction factor in the wet gas equation used to represent the over-reading due to liquid. By making observations at different flow rates it is possible to determine whether liquid is entering the well at a constant or varying rate and adjust the correction factor accordingly.

From our findings stabilisation took 12 hours, verification would take a less than a day. We had allowed four days' shutdown for our verification exercise. For a verification exercise of all fields in a multi field wet gas pipeline system the shutdown period could be minimised by good organisation.

References

[1] Jamieson, A.W. et al. Unpredicted behaviour of Venturi flow meter in gas at high Reynolds Numbers. NSFMW 1996

[2] Washington, G. "Measuring the flow of wet gas", NSFMW 1991

[3] de Leeuw, H. "Liquid correction of Venturi meter readings in wet gas flow", NSFMW 1997

[4] Stewart, D.G. et al. "Venturi meters in wet gas flow", NSFMW 2003

Lessons from wet gas flow metering systems using differential measurements devices: Testing and flow modelling results

J. Cazin[†], J.P. Couput[†], C. Dudézert[†], J. Escande[‡], P. Gajan[*], A. Lupeau[*], A. Strzelecki[*]

† Total, Corporate Technical Center 64018 Pau cedex, France

‡ Gaz de France, Direction de la recherche, 1ch de villeneuve, 94140 Alfortville, France

* Office National d'Etudes et de Recherches Aérospatiales (ONERA),
2 av Edouard Belin BP 4025 31055 Toulouse Cedex, France

Abstract:

A significant number of wet gas meters used for high GVF & very high GVF are based on differential pressure measurements. Recent high pressure tests performed on a variety of different DP devices on different flow loops are presented. Application of existing correlations is discussed for several DP devices including Venturi meters. For Venturi meters, deviations vary from 9% when using the Murdock correlation to less than 3 % with physical based models. The use of ΔP system in a large domain of conditions (Water Liquid Ratio) especially for liquid estimation will require information on the WLR

This obviously raises the question of the gas and liquid flow metering accuracy in wet gas meters and highlight needs to understand ΔP systems behaviour in wet gas flows (annular / mist / annular mist).

As an example, experimental results obtained on the influence of liquid film characteristics on a Venturi meter are presented. Visualizations of the film upstream and inside the Venturi meter are shown. They are completed by film characterization. The ΔP measurements indicate that for a same Lockhart Martinelli parameter, the characteristics of the two phase flow have a major influence on the correlation coefficient. A 1D model is defined and the results are compared with the experiments. These results indicate that the flow regime influences the ΔP measurements and that a better modelling of the flow phenomena is needed even for allocation purposes.

Based on that, lessons and way forward in wet gas metering systems improvement for allocation & well metering are discussed and proposed

1 INTRODUCTION

In addition to "conventional" multiphase applications, the oil & gas industry has to cope with an increasing number of applications for metering systems usable in wet gas range which corresponds to the upper end of multiphase GVF range i.e. 95% < GVF < 100% for :

- Reservoir monitoring on individual wells or in place of test separators
- Allocation on individual wells or flow lines
- Production optimisation

Expected capability of such wet gas meters are ranging from high accurate gas measurements to true 3 phase wet gas meters able to give gas, water & condensate in wet gas conditions

If manufacturers are now proposing several options to measure liquid and gas, gas and water or three phases, proposed technology and related performances (operating envelope, accuracy) still have some limitations in the wet gas range .

As an example, most of the wet gas meters used for very high GVF are based on differential pressure measurements using Venturi and other differential pressure geometries.
In order to better assess performance and identify ways of improvement , TOTAL and GDF have entered into a number of testing and R&D programs addressing differential pressure systems behaviour (Venturi & V cone based) both in low & high pressure conditions.
On one side this paper describes results obtained with Venturi based wet gas meters in HP & LP conditions and discusses application of published models & correlations.
On the other side, it describes some results obtained on Venturi behaviour modelling in wet gas flows (annular / mist / annular mist).
Results obtained on various flow loops and basic research are pointing out the question of the gas and liquid flow metering accuracy, highlighting difficulty to implement wet gas meters and to apply flow loop results to real cases by maintaining accuracy.
For confidentiality reasons, system and flow loop references are not published.

2 THE FLOW LOOPS

In the last years, TOTAL and GDF were involved in some flow loop tests. During these experiments, various thermodynamic and flow conditions were tested, with varying fluids, meter installation - horizontal or vertical, presence of a mixer or not - from one loop to another.

Some tests were performed under low pressure conditions (less than 7 bars), notably at the ONERA loop in France, and others under high pressure conditions (until 250 bars).

Testing loops use combination of fluids which range from air and water to real hydrocarbons. Tests were performed in two phase or 3 phase flow conditions.

Baker's vertical and horizontal maps have been used to represent the expected flow regimes types. *Figure 1* and *Figure 2* illustrate the variety of regimes that one can encounter and it show that the regimes during these tests might have been mainly annular and dispersed annular.

In most of the tests, as flow patterns visualisation devices were not installed, flow regime prediction studies were also conducted in some cases using flow simulators like OLGA for instance. Prediction models are built using experimental data and as a consequence their accuracy is greatly dependent on the conditions of the experiments runs (pipe diameter, orientation, fluids, thermodynamics…).

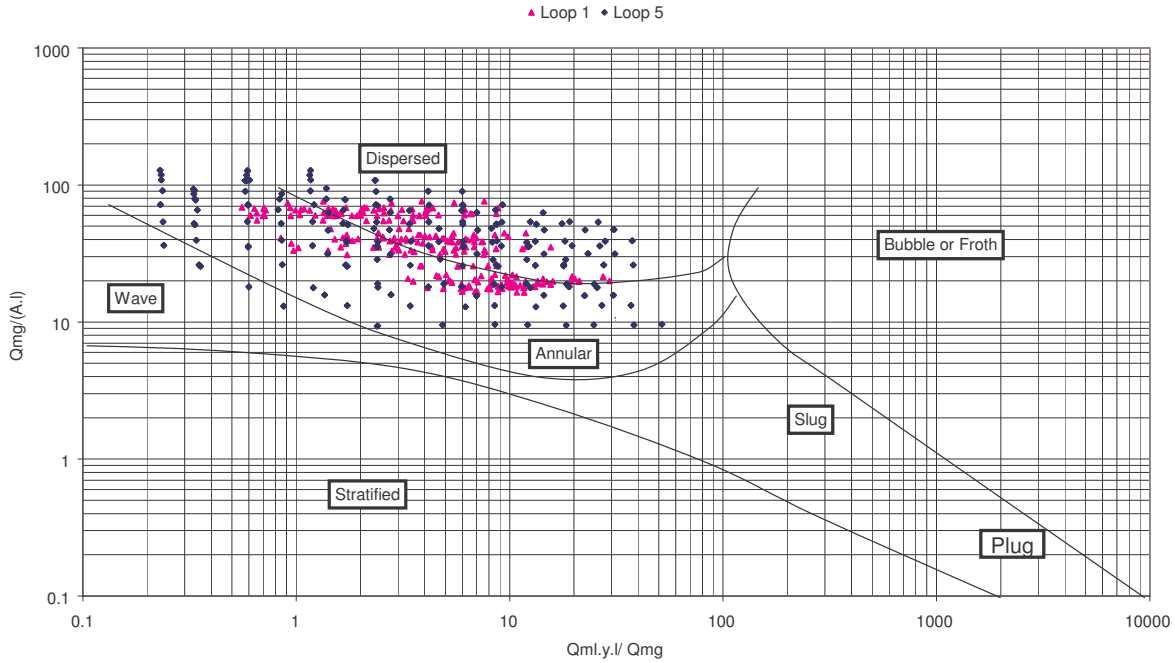

Figure 1 : Loop tests points displayed in the Baker Map – horizontal

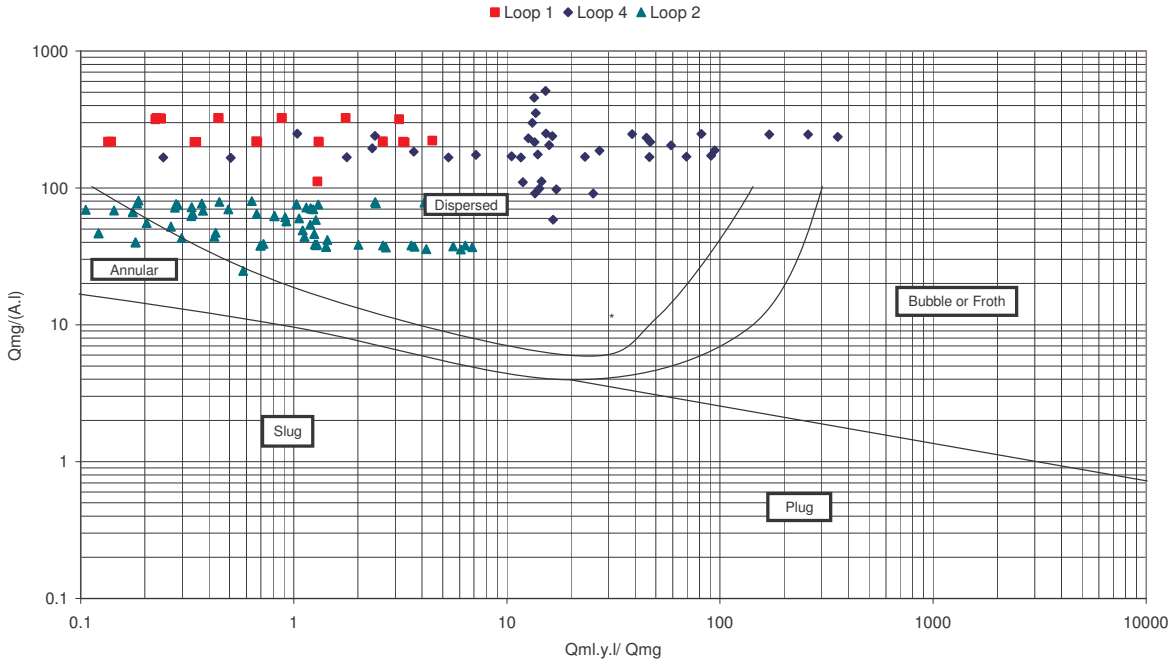

Figure 2 : Loop tests points displayed in the Baker Map - vertical

3 VENTURI BASED WET GAS METER SYSTEMS

3.1 Industrial status

Most of the wet gas meters of the market are using Venturi geometries, alone or in combination with other devices.

If total flow rates are generally derived from a differential pressure measurement across a Venturi meter or a V cone, liquid fraction and water fraction are either measured from a second Δp measurement and / or from specific fraction measurements (gamma attenuation, microwave absorption…)

3.2 Venturi modelling

In principle, mass flow calculations using pressure drop measurements in a Venturi are straightforward as based on the Bernoulli's equation.

Such principles have been very successful in homogeneous flows but need to be corrected when liquid phase is present.

Three types of models and approaches can be applied: physical models, statistical models, and intermediate models between these two approaches.

The corrected equation for wet gas mass flow is then:

$$Qm_g = \frac{Y\sqrt{2\rho_g \Delta p}}{\Phi_g}$$

Where Qm_g, ρ_g, Δp and Y are respectively the gas mass flow rate, the gas density, the pressure drop along the device and a corrective coefficient depending on the device geometry, and accounting for the pressure loss and the compressibility of gas. Φ_g is the over-reading factor accounting for the presence of liquid and is the main topic of this section.

3.2.1 Statistical models

They are built on statistical processing of tests data. The obtained corrections are very sensitive to the conditions under which the equations were established. We can quote Murdock's and Steven's correlations [1]. The latest takes into account the gas Froude number and the Lockhart Martinelli parameter while Murdock only uses the Lockhart Martinelli parameter.

Murdock: $\phi_g = 1 + 1.26 X_{LM}$

Steven: $\phi_g = \frac{1 + AX_{LM} + BFr_g}{1 + CX_{LM} + DFr_g}$

A, B, C, D are parameters depending on the ratio between gas and liquid densities. Fr_g and X_{LM} are the gas Froude and Lockhart Martinelli numbers.

The Lockhart Martinelli number equation is (the indexes g and l refer to gas and liquid):

$$X_{LM} = \frac{Qm_l}{Qm_g}\sqrt{\frac{\rho_g}{\rho_l}}$$

3.3 Simple physical model: the Equivalent Density Correction

Such a model is based on the calculation of an equivalent density of the a fluid flowing at the superficial velocity of the gas and given the same momentum flux in a pipe section than the two phase flow. It uses a slip factor K between the gas and the liquid phase $K = \frac{\overline{U_g}}{\overline{U_l}}$. It permits to deduce a Φ_g factor from the following expression is:

$$\Phi_g^2 = 1 + CX_{LM} + X_{LM}^2$$

$$C = \frac{1}{K}\sqrt{\frac{\rho_l}{\rho_g}} + K\sqrt{\frac{\rho_g}{\rho_l}}$$

If the liquid flows as very small droplets, K equals 1 and one obtains an simplified expression called in this paper "droplets model-physical correction".

3.4 An intermediary approach between physics and statistics

3.4.1 It is the most commonly used approach, with the De Leeuw correction [2]/[3] *:*

$$\Phi_g^2 = 1 + CX_{LM} + X_{LM}^2$$

$$C = \left(\frac{\rho_l}{\rho_g}\right)^n + \left(\frac{\rho_g}{\rho_l}\right)^n$$

$$n = 0.606\left(1 - e^{-0.746 Fr_g)}\right) \; for \; Fr_g \geq 1.5$$

$$n = 0.41 \; for \; 0.5 \leq Fr_g \leq 1.5$$

4 VENTURI METER PERFORMANCE

4.1 Venturi performances for gas metering

The three types of correction were tested on the data from the different test loop programs and a summary of their accuracies in terms of mass flow rates prediction is given

4.1.1 Murdock's **correction** for Venturi

The Murdock's correction, being a very simplified correction, does not lead to very good accuracies as can be seen in the *Table 1*. The errors on gas mass flow rates are of about +/-8% and even reach 103% at 6 bars.

Loops β ID	1 0,5 5"	2 0,6 2"	3 0,65 2"	4 0,6 5"	5 0,6 6"
6 b			103%		
15 b					9%
30 b					7%
45 b					6,5%
50 b		9%			
60 b					6.3%
100 b				+/-6%	
80=>240	1.3=>8.7%				

Table 1: Performances of the Murdock's correction on the test loops data

4.1.2 De Leeuw's **correlation**

The correlation fits well with the data with which it was created (Sintef) with an error of +/-2% on gas mass flow rate. However, it can be seen in the *Table 2* that in other conditions, its accuracy varies with the tests pressures, with the beta parameter and the inner diameter. Notably, it shall not be used when pressure is low as the error on gas mass flow rates reaches +/-28% in the loop 3, at 6 bars. Apart from low pressure conditions, accuracy ranges from 3% to 6,4%.

Loops β ID	Sintef 0,4 4"	1 0,5 5"	2 0,6 2"	3 0,65 2"	4 0,5 5"	5 0,6 6"
6 b				+/-28%		
15 b	+/-2%					+/-5,5%
30 b	+/-2%					+/-4%
45 b						+/-4,5%
50 b			+/-3%			
60 b	+/-2%					+/-3,5%
90 b	+/-2%					
100 b					+/-6,4%	
80=>240		+/-5%				

Table 2: Performances of De Leeuw's correction on the test loops data

4.1.3 Droplets model - physical correction

The results displayed in the *Table 3* clearly show that the accuracy of the droplets model correction increases when pressure grows. This may be accounted for by a better atomization of the liquid film from the pipe wall when the pressure increases. This model can reach very good accuracy with +/-2.9% errors at the loop 1 from 80 to 240 bars.

Loops β ID	1 0,5 5"	2 0,6 2"	3 0.65 2''	4 0,6 5"	5 0,6 6"
6 b			+/-45%		
15 b					+/-16%
30 b					+/-11%
45 b					+/-9.5
50 b		+/-8,7%			
60 b					+/-5.4
100 b				+/-3,4%	
80=>240	+/-2.9%				

Table 3: Performances of the droplet model correction on the test loops data

4.1.4 Example of gas flow rates measurements curves

The curves below display some data points from the loops tests. The errors on gas mass flow rates are plotted against the Lockhart Martinelli parameter for the Murdock and De Leeuw correlations and for the droplet model correction. In *Figure 3* the data from the loop 5 corresponding to a gas Froude number of 1.39 are extracted at 60 bars, in *Figure 4* all the points from the loop 1 corresponding to a pressure of 80 bars are plotted.

In these conditions, the flow maps predict a misty regime and it can be seen that the droplets model is the best correction with an accuracy of +/-3%. The Murdock's and De Leeuw's correlations are less accurate with errors between 2% and 8%.

This indicates that when the flow regime is known, here the droplet regime, a physical approach is best suited to gas flow rates calculations than statistical correlations and leads to a good accuracy.

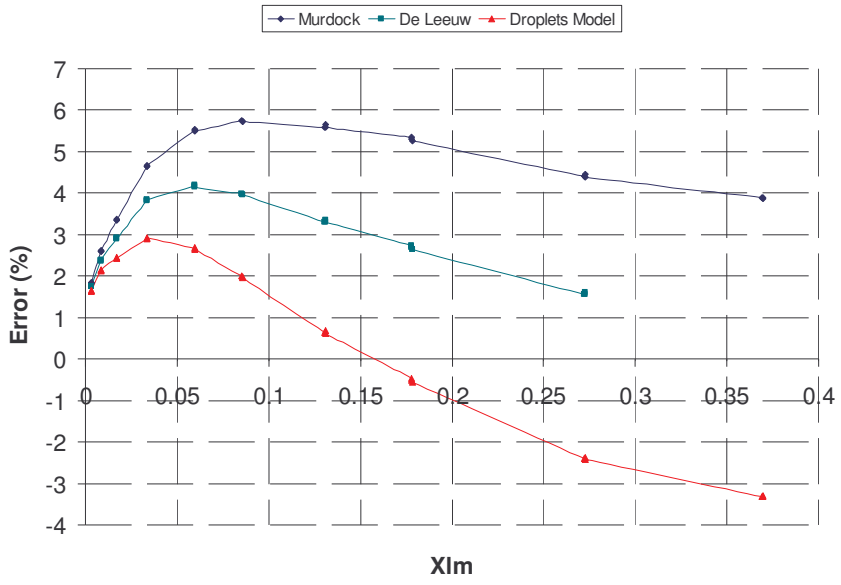

Figure 3 : Performances of the corrections at the loop 5, 60 bars, Fr_g=1.39

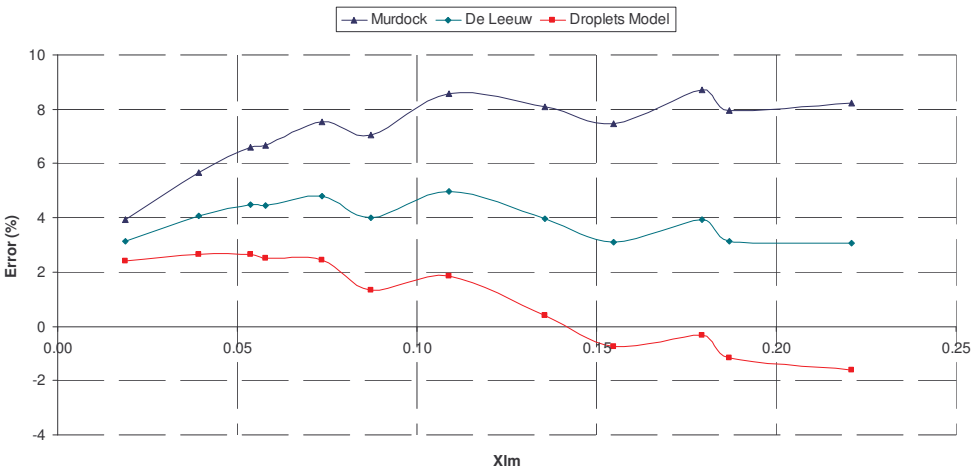

Figure 4 : Performances of the corrections at the loop 1, 80 bars

4.2 Liquid measurement using double Δp devices: 3 phase wet gas metering application

Operators needs concerning wet gas are the measurement of gas flows as well as of liquid flows. Besides, the correction of gas flow rates requires the knowledge of the liquid content of the flow. Therefore, it is of paramount importance to use an additional measurement device to enable the calculation of the liquid flow.

A strategy in use is to install a second pressure drop device to get more information. The new measured pressure drop could be of several types, between different locations: inlet and outlet of the Venturi, pressure drop measurement from different device …

Different responses of the pressure drop devices will be required when liquid loading is varying so that information can be extracted to calculate liquid flow rates.

Moreover, the behaviour of each device must be well known to predict accurately the gas and liquid flow rates.

In this paper, we have tested such devices in three phases systems. Tests run under three phases conditions – gas and liquid hydrocarbons and water – showed that the water cut is playing an important role in the behaviour of the devices and consequently that behaviour in 3 phases could be significantly different from behaviour in 2 phases. In the *Figure 5*, displaying the difference between the two pressure drops measurements of a Δp system, a discontinuity can be seen when the water in liquid ratio meets the value of 60%. This value corresponds with the transition point between water continuous and oil continuous domains.

Consequently, to calculate the flow rates of gas and liquids in a large range of WLR, one must also know and measure the water cut.

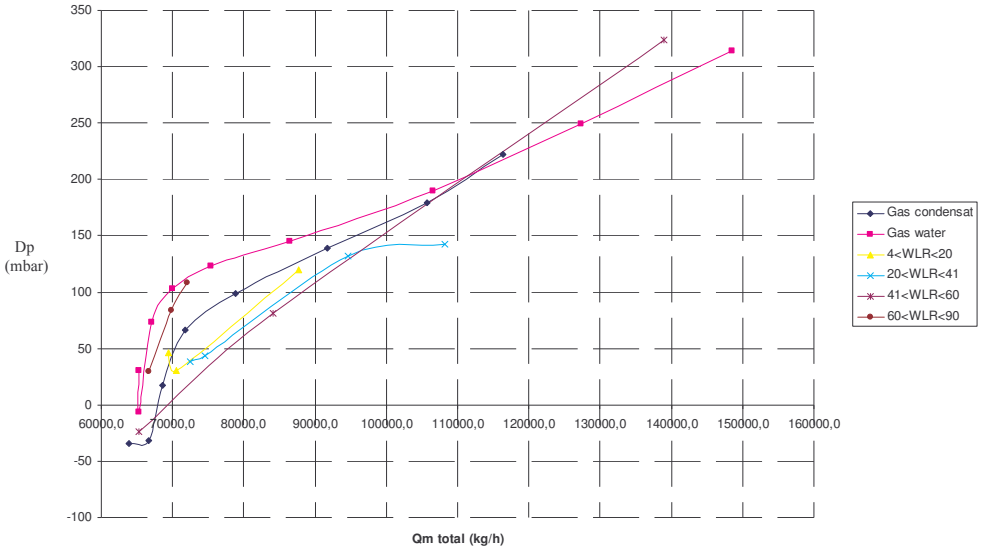

Figure 5 : Difference between the two measures of a Δp system

4.3 Conclusions and lessons

Most of correlations and models which are generally used to correct the Venturi meter gas mass flow rates according to the liquid loadings are mainly statistical and do not use accurate physical approaches. They present a great dispersion in the results and their performances vary as geometries and flow conditions vary. As a consequence, claimed accuracy of published correlations cannot be generalised / extrapolated and will not strictly apply without specific meter calibration.

On the other side, physical models based on flow morphology are very accurate when applicable; this is the case of droplets models applied to Venturi meter correction in mist flow. Such assumptions need to be extended to more complex flow regimes like annular & annular mist flows through a better understanding of fluids behaviour in Venturi. An example of this approach is presented in the following part of this paper.

Behaviour of Venturi and other ΔP systems in 3 phase wet gas conditions is obviously a new area which has to be considered in detail when establishing correction for liquid when 3 phases are present.

Points to be also considered when testing, interpreting and generalising flow loop tests concern both the flow regimes knowledge and prediction - annular, dispersed annular, stratified… - and the extrapolation of two phase results to three phases conditions - gas, liquid hydrocarbons, water.

5 DETAILED ANALYSIS OF THE FLOW PHENOMENA IN THE VENTURI METER AND THEIR REPERCUSSION ON ΔP MEASUREMENTS

As indicated previously, to improve the metering methods of wet gas, it is necessary to improve our knowledge of the basic phenomena which take place in the pipe, to model them and to deduce correction laws which take into account the characteristics of the two phase flow upstream of the flow meter. However, the knowledge of the characteristics of the two phase flows under real flow conditions, is difficult to reach (150 bars, 200°C) and the approach developed at ONERA consists of making a detailed study on the influence of various parameters under low pressure conditions, with air and water, in order to define those necessary to be measured in situ in order to ensure a significant improvement of the metering accuracy. Results presented in previous papers [4][5] showed that a law of correction must take into account the quantity of liquid in gas but also the distribution of this liquid flowing at the wall as a film and in the core region as droplets. This law must also take into account the size of these droplets. In this paper we will focus on the behaviour of the liquid film on the wall and its influence on the law of correction. From the experimental analysis a 1D model was developed. It will be compared to low pressure results in annular flow regime.

5.1 Experimental study

5.1.1 Experimental procedure

5.1.1.1 ONERA wet gas test facility

The wet gas tests were carried out at low pressure on the ONERA experimental flow loop (*Figure 6*). The gas flow (air) is generated by means of high pressure tanks. The gas flow rate up to 0.21 kg/s, is controlled by a sonic nozzle located upstream of the test section. The mass flow rate of liquid (water) can be varied from 0 to 0.1 kg/s. The liquid line is equipped with electromagnetic flow meters. This loop can be used from atmospheric pressure to 5 bars. A separator is used to recover the liquid.
The test section is placed in a vertical downwards orientation. It is composed of:

- a flow conditioner,
- a liquid film injector,
- a Venturi meter.

The pipe diameter (D = 2.R) is 100 mm. Two identical Venturi flow meters with a β of 0.6 were machined in steel for ΔP measurements and in Perpex for flow visualisations. The half angles of the upstream convergence and the downstream diffuser were respectively 10.5° and 7.5°.

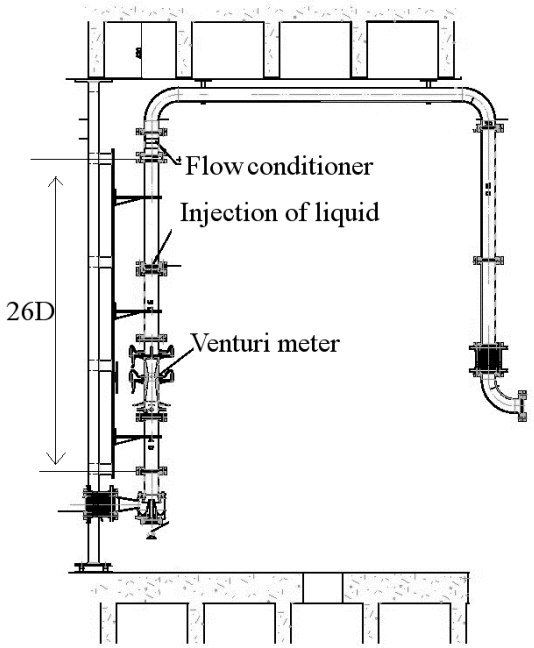

Figure 6 : Experimental test set-up

5.1.1.2 Experimental techniques used for analysing the film behaviour.

Two different techniques are used to analyse the film behaviour. In order to determine the entrainment phenomena through the Venturi meter, flow visualisations are performed. In this case, an argon laser sheet parallel to the pipe axis is used to illuminate the film and the images are recorded by a CCD camera placed perpendicular to the laser sheet. Different zones are analysed from the inlet of the convergent section to the outlet of the diffuser.

The film thickness is determined from a film conductance method described by Hewitt [6]. It consists of measuring the electric impedance between two flush-mounted electrodes.

5.1.2 Results

5.1.2.1 Visualisation of the liquid film behaviour through the Venturi meter

Examples of visualizations of the liquid film through the Venturi meter are shown in *Figure 7*. The results indicate that the film behaviour depends mainly on the location and on the liquid volume flow rate Qv_l. As a matter of fact, even if an amplification of the disturbance is observed when the gas volume flow rate Qv_g is increased, the influence of the gas velocity does not seem to be the main parameter. On the contrary, the film characteristics change greatly when the liquid flow rate is increased. In the convergent part of the meter, the gas acceleration induces a diminution of the wave amplitude and a thickening of the film. Nevertheless, the movies reveal instantaneous breaking of waves linked to entrainment. For the higher liquid flow rates tested, an intermittent appearance of large waves is observed. At the end of the convergent section, the waves seem to be disorganised. In the throat section, the film becomes thicker and the wavelength greatly diminishes.

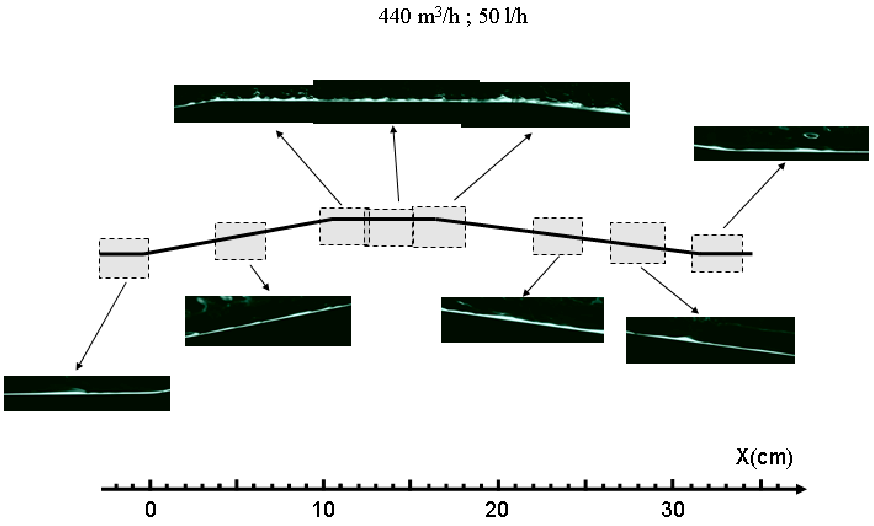

Figure 7 : Visualization of the liquid film behaviour through the Venturi meter (Qv_g = 440 m^3/h ; Qv_l = 50 l/h ; Re = 10.7 10^4; Re_{liquid}=44)

5.1.2.2 Film behaviour upstream of the convergent section

The analysis of film thickness signals shows that the ONERA's test conditions correspond to 3 flow regimes [7][8]. At low liquid flow rate, the liquid surface is dominated by ripples. For higher liquid flow rate, the disturbance wave regime described by Asali and Hanratty [9] is reached. Among this last regime, two film behaviours are distinguished: the "regular wave" and the "dual wave" regimes. Hanratty [10], observes that when the air velocity is sufficiently high (10 m/s), liquid atomization may occur on the wave crests. Such a result is also observed on visualisations for the highest liquid flow rate.

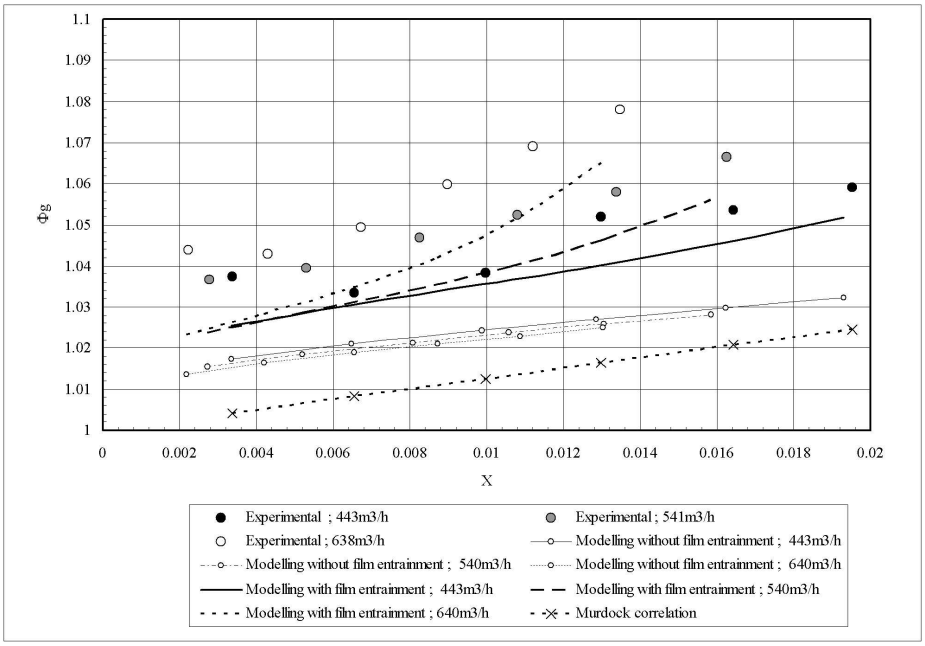

Figure 8 : Correction factor plotted with respect to a Lockhart Martinelli parameter measured in annular flow regime

5.1.2.3 ΔP measurements

The influence of the annular flow regime on the Venturi metering is shown in *Figure 8*. For low values of the Lockhart Martinelli parameter, the correction factor decreases and then increases. This behaviour may be linked to the film regimes presented previously. The film surface is covered by ripples which do not encourage liquid

atomisation. For sufficiently high liquid flow rates, high amplitude waves appear and liquid atomisation occurs on the wave crests, as observed in the visualisations.

5.2 FLOW MODELLING

The flow modelling method used for this work follows the approach described by van Werven *et al* [11]. Nevertheless some differences appear in particular on the film description. In our model (Lupeau [7], Lupeau *et al* [8]), the flow is divided in two regions: the convergent section and the throat. In each zone, integrated balance equations (mass and momentum conservation) are applied on the gas flow, the liquid film and the dispersed flow. In each pipe section, each flow is defined by its local velocity v and its flowing area S. In these equations, source terms are used to describe the momentum and mass exchanges. This concerns the momentum gas/liquid film interaction at the interface, the momentum exchange between the gas and droplets and the mass exchange between the film and the droplets due to the entrainment. The model supposes that no mass exchange between the liquid and the gas occurs in the meter (evaporation and condensation). In the convergent section and in the throat, we consider that no mass flux exits between the film and the droplets. We only suppose, as Werven *et al* did, that an atomisation occurs at the inlet of the Venturi throat section. The flow rate and the size of the droplets atomised at this point depends on the film thickness at the convergent section outlet and on the fluid properties. They are deduced from correlations (Lupeau [7], Lupeau et al [8])

Examples of the film thickness and differential pressure distributions calculated by the model are presented in *Figure 9* and *Figure 10*, respectively. The flattening of the film in the convergent observed in the visualisations is reproduced by the model. Furthermore the influence of the liquid entrainment from the film on the pressure is shown in Figure 10. In Figure 5, comparisons with the experimental results indicate that the model is able to predict this parameter within 1.5 %. If we analyse the correction factor calculated with and without taking into account the film atomisation at the throat inlet, we clearly demonstrated the importance of the droplet acceleration on the ΔP measurements. By this way, we observe that it is very important to have a good description of the film behaviour in the convergent because the thickness of this film will have a great influence on the rate of atomisation and at fine on the ΔP increased in the Venturi throat.

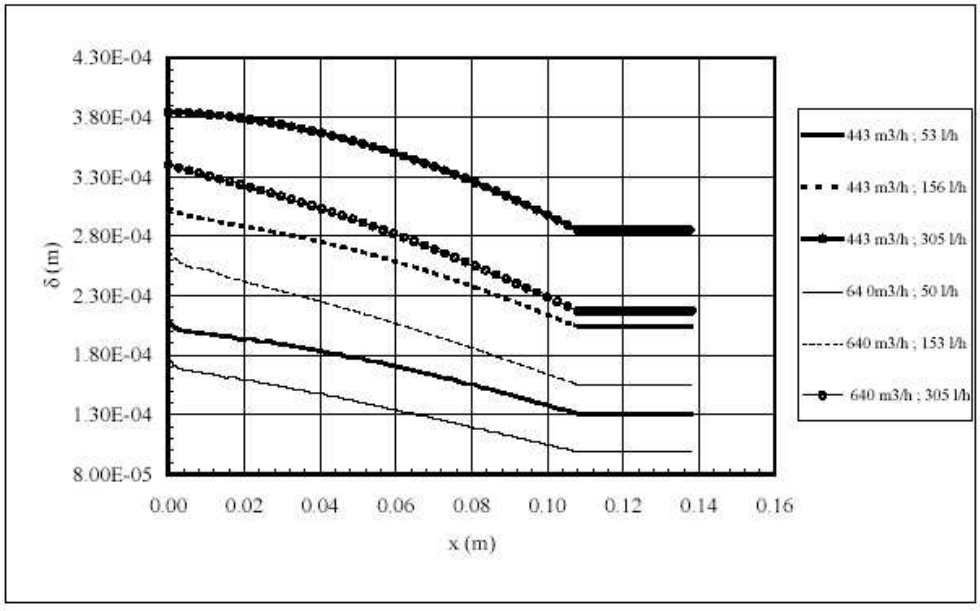

Figure 9 : Film thickness distribution in the Venturi meter calculated by the model

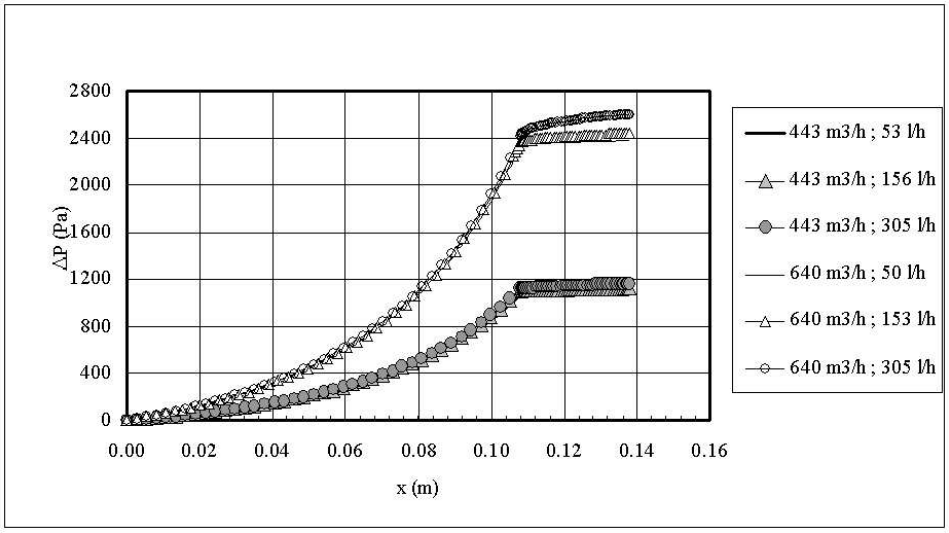

Figure 10 : Differential pressure distribution calculated by the model

5.3 APPLICATION OF MODEL TO HIGH PRESSURE CONDITIONS

The objective of this modelling work is to extrapolate the low pressure results to high pressure configuration. The main difficulty here is to determine the upstream boundary conditions in terms of liquid distribution in the pipe between droplets and liquid film (*f* factor) and droplet size. One possibility is to determine these quantities from published correlations using the superficial velocities and properties of both fluids. In figure 11, we present an attempt of this approach applied to results obtained on the loop 4. The error bars correspond to 2%. We can observe that, most of the correction factor calculated from the model, reproduced the tests within 2%. Nevertheless, for some points, the deviation is more important. A more precise analysis of the results shows that many factors can explain these results. The first concerns the accuracy of the correlations used to determine the inlet conditions. The second deals with the correlations used in the code. An effort is now needed to improved these correlations.

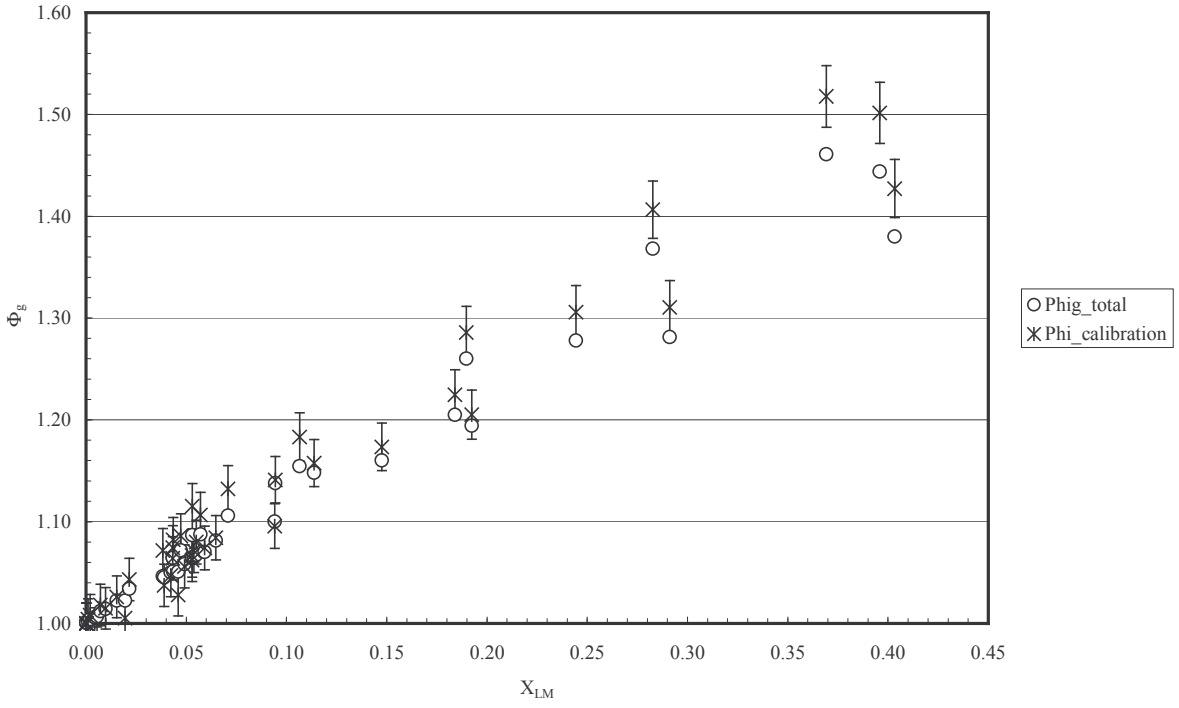

Figure 11 : Validation of the model on high pressure results (Loop 4, 100 bars)

6 CONCLUSIONS

High pressure tests analysis shows that the application of available correlations is not straightforward and published correlations do not necessarily offer the required accuracy when Venturi systems are used in various high pressure conditions. We notice that the accuracy can be improved by selecting Venturi models (mist, film) suited to flow conditions, which indicates that wet gas metering improvement using Venturi meter will require liquid content knowledge but also flow typology information. So the implementation of ΔP based Venturi meter could require more information than expected as such systems will be sensitive to the flow typology upstream the meter and inside the meters also. Information gained so far show also the limitations of ΔP measurements to derive liquid content specifically in 3 phases conditions.

This seems to indicate that wet gas metering will require:

- Three phase meters as the knowledge of the watercut is needed to accurately measure the liquid flows.
- Knowledge of flow morphology upstream meter
- Venturi behaviour information when using Venturi based systems

This is in fact opening a new area for accurate wet gas metering with the following questions:

- Shall we consider wet gas flows as significantly different from multiphase flows ?
- Shall we measure liquid repartition / structure like film thickness …?
- Shall we still use Venturi meters which are generating flow pattern modification ?

An experimental and modelling work performed on a two phase flow varying from annular to dispersed flow regime, proved that the influence of the flow typology can be taken into account in a one dimensional model to predict accurately the correction factor. This approach verified on low pressure tests, was applied to higher pressure configurations. Even if encouraging results were obtained, it seems now necessary to continue this modelling effort in order to ameliorate the prediction of the flow regime upstream of the Venturi meter.

7 BIBLIOGRAPHICAL REFERENCES

[1] Steven R., Wet gas metering", PhD Thesis, Univerity of Strathclyde, Glasgow, (2001)

[2] DeLeeuw H.: Wet gas flow measurement by means of a venturi and a tracer technique, North sea Flow measurement Workshop, (1994)

[3] DeLeeuw H.: Venturi meter performances in wet gas flow, *B.H.R. Group 1997 multiphase*, 567-582, (1997)

[4] Bissières D, Couput J.P , Estivalezes J.L., Gajan P. , Lavergne G. , Strzelecki A., Wet gas flow simulation for venturi meters, 1st North America Conference on Multiphase Technology, Banff, (1998)

[5] Lupeau A., Escande J., Couput J.P., Gajan P., Strzelecki A., Influence of the characteristics of an annular dispersed flow on the behaviour of a Venturi meter, 4th North America Conference on Multiphase Technology, Banff, (2004)

[6] Hewitt G.F., Measurement of two phase flow parameters, Academic Press, (1978)

[7] Lupeau A., Etude de la modélisation du comportement d'un écoulement annulaire disperse. Application à la mesure de debit de gaz humide à l'aide d'un débitmètre à venture, PhD Thesis, Supaero, 2005

[8] Lupeau A., Platet, Gajan P., Strzelecki A., Escande J., Couput J.P., Influence of the presence of an upstream annular liquid film on the wet gas flow measured by a Venturi in a downward vertical configuration, accepted for publication in Flow Measurement and Instrumentation, 2005.

[9] Asali J.C., Hanratty T.J., Ripples generated on a liquid film at high gas velocities, Int. J. of Multiphase flows, 19(2), (1993) 229-243

[10] Hanratty T.J., Interfacial instabilities caused by air flow over a thin liquid layer, In "Waves on fluid interfaces" (edited by Meyer, R.E.), , Academic press, New York, (1983) 221-259

[11] van Werven M., van Maanen H. R. E., Ooms G. and Azzopardi B. J.., Modeling wet-gas annular/dispersed flow through a Venturi, AIChE Journal, 49(6), (2003), 1383-1391

ISO 3171 Production Hydrocarbons Allocation Sampling for challenging "Tie-ins" with pressures close to RVP breakout.

By Mark Jiskoot, Managing Director, Jiskoot Ltd.

Summary

Introduction

There are an increasing number of applications where sampling is required for crude oils and condensates at close to vapour breakout in production environments.
These are typified where the quality measurement must be extracted/made in the "oil" leg of a separator. The exertion of back pressure (pressure loss) on the liquid leg to expand the operating envelope is generally not acceptable due to the effect that this will have on the separator efficiency and this frequently precludes the use of normal metering technologies.

These conditions represent some of the hardest for quality determination.

In conventional separators, velocities are low to promote separation of the gas and liquids and the therefore the gas pressure within the liquid phase is close to breakout. Frequently there is an envelope of less than 0.5 bar below the operating pressure at which the fluid will start to cavitate. Concurrent with the low velocity is the expectation of some free water that would require mixing to ensure representivity.

There are frequently also severe restrictions on space and the piping arrangement in which to achieve a representative off-take. The "rules" that are applied to representative sampling are equally applicable to the use of water monitors (watercut, OWD) and to densitometers.

An integrated quality measurement system that prevents any impact on the process and also provides the required mixing to allow extraction of a representative offtake that can be used for physical samplers as well as process instrumentation such as densitometers, viscometers and water cut monitors can be achieved by careful design. Jiskoot has adapted its CoJetix technology to meet these goals.

Sampling Requirements

Conventional sampling requires that four steps be met :

- Adequate dispersion and distribution of the pipeline content cross section
- Representative sampling of the batch
- Sampling handling and mixing
- Laboratory analysis

Our industry should never overlook any of the above steps, whether the objective be extracting a physical sample or to provide a representative flow to a process analyzer; but we are frequently surprised by how often the overall requirements are overlooked.

Dispersion and Distribution
A cursory reading of the current standards provides a table informing the user of the potential problems with poor mixing at low velocities. Unfortunately many miss the small print and assume that if they meet the requirements in the "table", they have adequate mixing. Those that do this fail to take the opportunity to assess their process against a much more detailed and accurate methodology which also accounts for viscosity and density. For close on 20 years models representing the dispersion and distribution of oil/water mixes have been published both in the ISO (3171 – Annex A), API (8.2 – Appendix B) and the IP (6.2 – Appendix B)standards and its all the more surprising that they are not used as these calculations are easily accessible on the internet. The models allow the calculation of dispersion quality in many configurations including downstream of a variety of devices including meters, valves as well as the more common elbows, reducers, pumps etc.

There are many specialised situations where a deeper understanding is required, for example :

It is not commonly understood that although a vertical pipe reduces the gravitational segregation of oil/water mixes, over a short length it also promotes slug formation and can spin the water towards the circumference of the pipe, i.e. make distribution worse.

Or, for example, that the use of a metering system as a mixing device may not always be successful due to the possibility that the inlet manifold can act as a slug creator (if there is a free water phase at inlet). Under such circumstances the mixing of water into oil in each stream may be acceptable, but the commingling of the streams in the outlet header can yield a poor cross sectional distribution. Given that these methods are available, why do some process engineers still overlook the actual process and make subjective judgments that should fail an easily applied audit of the process? Both engineers and auditors are at fault here.

Representative Sampling of the Batch
This is all about getting a sample to be physically extracted from the pipeline and deposited into a sample receiver that fully represents the batch in question. It remains a constant surprise that many engineers still fail to read the standards in regard to the actual requirements for sample frequency and many appeared blinkered by the de-facto marine discharge requirement of 10,000 samples per batch. Collecting 10,000x1ml samples of a high RVP product and either transporting it under pressure, or mixing and decanting it into a smaller pressurised receiver for transportation to a laboratory is frequently at a detriment to the overall measurement uncertainty. Poor handling and mixing can often result. It should be under this heading that we discuss the sampling mechanism and "Isokinetic" as applied to both in-line and fast loop sampling systems. **Isokinetic -** Implicitly an "in-line" sample probe with a large opening through the head may have a velocity closely matching that of the process through the sample chamber. (Though this may not be true when the opening size is relatively small in comparison to the bluff body of the stem that supports it!)

However over time two clarifications of the desirability of Isokinetic sampling must be qualified:

1. As the size of the opening to the sampling device increases relative to the expected droplet size, then Isokinetic sampling becomes irrelevant. This was first highlighted in qualification notes from testing within the IP Section 6 part 2
2. If a "Fast Loop" is driven isokinetically i.e. matching the velocity at the inlet to the velocity in the main pipeline, then there is a significant problem at low flow velocities that water and sediment can fall out in the sample loop this is in contradiction to the objective of the "Fast Loop" which is to deliver a representative and well mixed stream to the sampler or analyser.

Sound engineering design should recognise the use of large sampler or sample loop openings and abandon the use or application of the work Isokinetic to oil sampling.

Sample Handling and Mixing
Consideration of the volume of sample that is actually required for analysis and retention and the required sampling frequency is valuable. A 4 litre, high pressure, sample will normally be more than adequate to represent a batch in a production environment.

We also often find demand for high pressure sample receivers to be used on stabilised crude i.e. with an RVP below a bar, this is simply a waste of money.

Even with higher RVP products the sample used for water determination will need to be depressurised for analysis.

Density and On-line water content measurement
We realize that there is growth in demand for using on-line water monitors particularly for allocation (sometimes called Watercut or OWD's – but NOT correctly described as BS&W monitors), indeed there is a paper later this morning dedicated to this subject. But without adequate pre-conditioning of the process stream (pipeline mixing) and suitable and regular re-calibration these devices render little more than trending information.

Sampling technology continues to move from the old style and less accurate "in-line" samplers to fast loop systems. By fast loop, we tend to classify them as a loop with a piping size of 1" or larger nominal diameter and typically a loop flowrate of 4-10 m3/hr. These rates and velocities concur nicely with the demands of OWD's and densitometers.

There are many reasons for this slow migration, the general comprehension by engineers that fast loop systems offer easier installation in a congested process environment and simplified maintenance. Also since a loop is required for density measurement which, according to the standards "should meet the same requirements as for sampling" and more recently the body of evidence that fast loop technology is simply more representative.

It is possible to classify sampling systems into various categories and further to consider the mixing. Since the 1980's there have been significant water injection tests of all types of systems. From the "DIY" samplers constructed by sites, to in-line systems with "Static Mixers" or Power and Jet Mixers.

There have also been a considerable number of tests of fast loop systems with the same types of preconditioning and more recently with the direct integration of fast loops with JetMix systems so-called CoJetix.

One statement of fact :
NO sampling system, unless installed in a biased pipeline profile will measure the absolute water content, ALL sampling systems tend to under measure water content, the only question is by how much. Call this uncertainty or call this systematic bias, gathering real data from over 200 water injection of various systems yields the following summary.

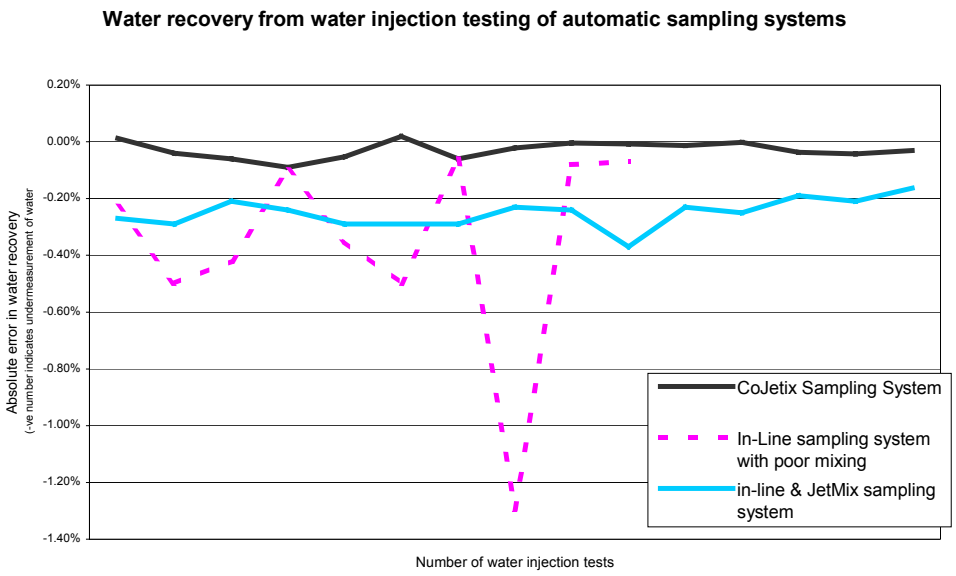

The reason for these results are somewhat obvious:

The under measurement will depend in greatest part in the dispersion and distribution of the water in the pipeline cross section. To minimise these influences a balance between the mixture quality and the size of the opening and flow profile through sampling device seeking to collect a sample are paramount. A fast loop is implicitly more competent than an inline probe by virtue of its larger opening extracting water droplets from a pipeline of equivalent dispersion quality.

Whatever you do for mixing, you MUST pay the price in energy terms, be it through pumping power (pressure loss) in your pipeline or by adding energy such as with a JetMix.

Back to back comparisons of an in-line ("Isokinetic"!) probe behind a static mixer and a CoJetix system indicate a significant average offset (0.15%)

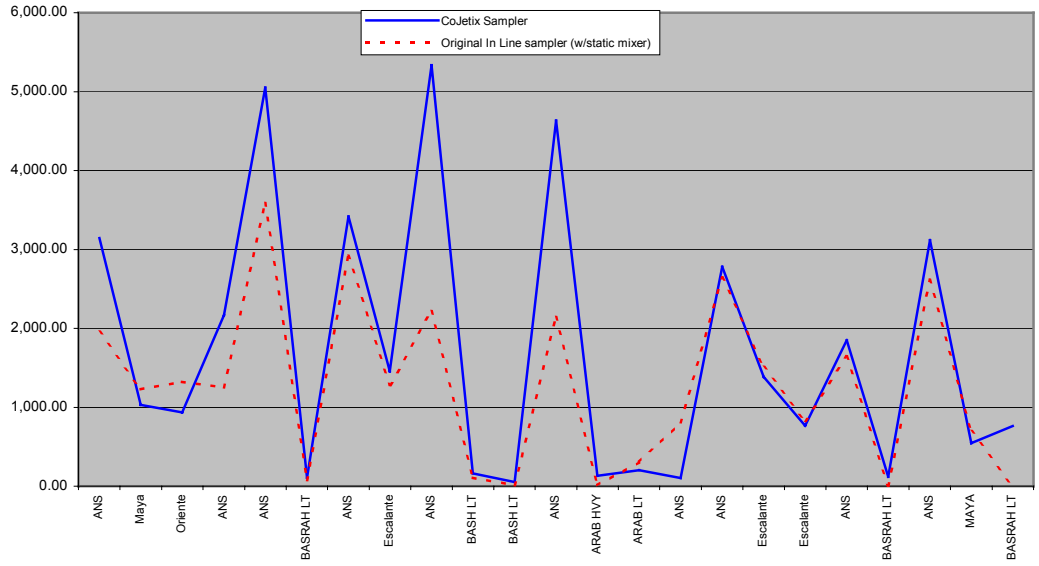

We have also been comparing the results of a variety of water cut monitors back to back against a marine unloading environment, our conclusions are that provided the users rigorously follow the calibration procedures and understands the limitation of the technology, that they are capable of providing excellent trending information.

The summary below indicates the scatter between two different manufacturers units and a proven (physical) sampling system. The two units are in the same loop with a sampler, both density compensated – running batches of the same "blended" crude, sulphur is plotted as a possible cause for the scatter.

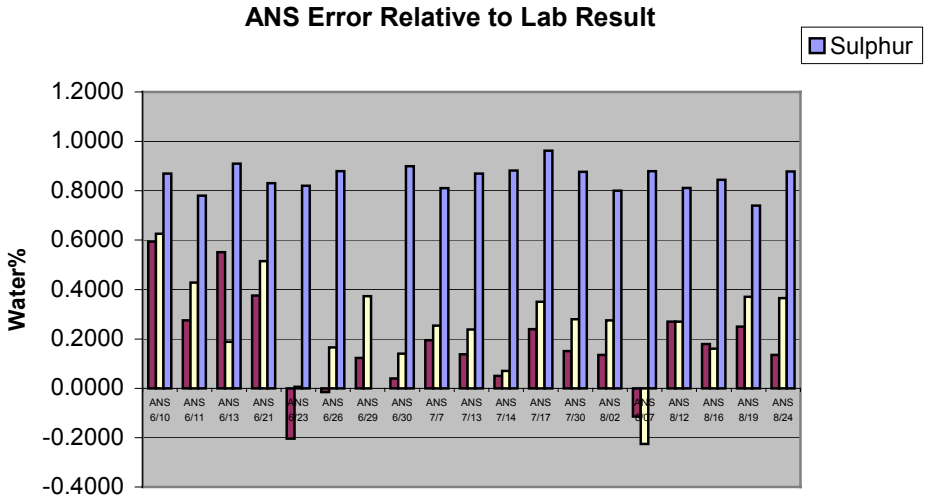

Design Study
Process Values

Liquid Process Data			
Line Size	8”	8”	8”
Pipeline Fluid	Condensate	Condensate	Oil
Flowrate Range	2696 to 12750 bbls/d	6785 to 84800 kg/h (10.6 to 122.1 m^3/h)	8818 to 422700 kg/h (11.4 to 540.5 m^3/h)
Density	645 to 654 kg/m^3	643.1 to 694.1 kg/ m^3	746.8 to 782 kg/ m^3
Viscosity	0.5112 cP	1.2 to 1.6 cP	2.0 to 3.75 cP
Line Temperature	55 to 75 °C	30 to 50 °C	42 to 67 °C
Operating Pressure	28 to 63 Barg	11 to 15 Barg	7 to 63 Barg
Water Content	Unavailable	0 to 2%	0 to 2%

Pipeline Mixing
Given that the RVP is within 6psi (0.5 bar) of the process pressure any reduction in process pressure will cause gas breakout.
Since the flow velocities are low, some form of mixing will be required as the separator is expected to allow up to 2 % carryover of water in the oil leg.
The use of a static mixer in this environment would not have worked, (in one case a 50:1 turndown – we would typically suggest, even if pressure losses are acceptable that 5:1 is the attainable limit). The maximum allowable backpressure was 0.5 bar at maximum flowrate and this should have been the static mixer back pressure AT MINIMUM FLOWRATE (and therefore significantly higher at higher flowrates.)

Some form of power (Jet) mixing was therefore desirable. In seeking to employ a pump to extract flow from the pipeline, considerations of available pressure losses within the suction pipeline and the NPSHa vs NPSHr (and specific engineering constraints applied by the buyers) require due care in selection of and positioning of the pumps. If suction head can be increased through elevation, this should be implemented.

A careful design requires consideration of a variety of issues, these include:
- Droplet dispersion and distribution vs. sample system inlet sizing.
- Configuration of the inlet and outlet connections, all the intermediate piping.
- Elevation.
- The obstruction potentially caused by the insertion of an offtake quill and a re-injection jet.

Nominal calculation of the initial distribution yielded the following result.

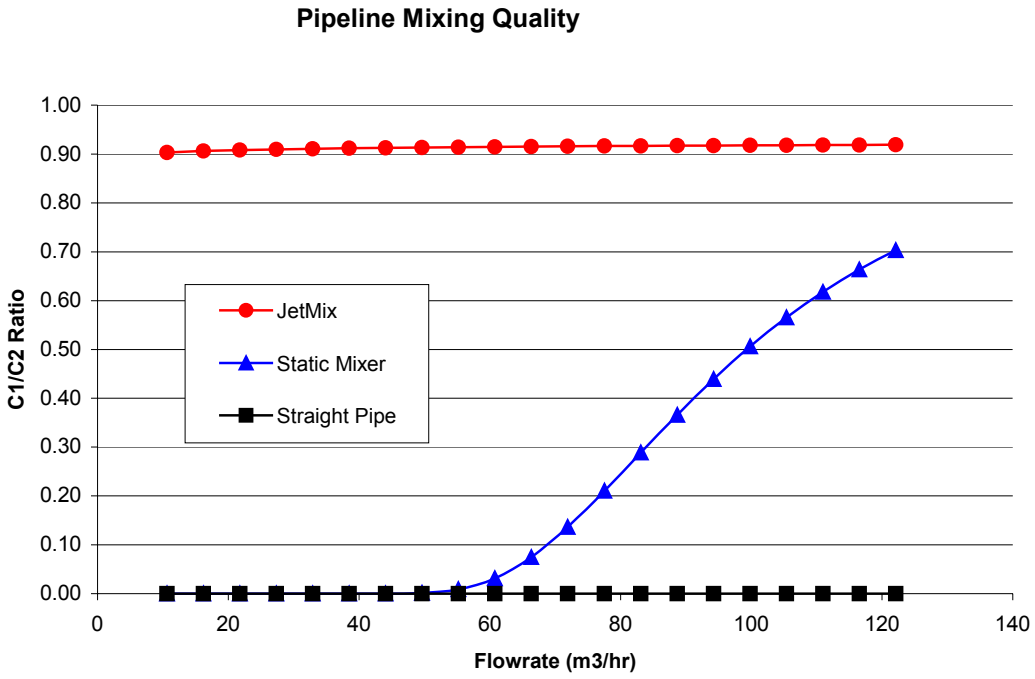

The energy dissipation required for mixing to allow extraction of a sample with a conventional in-line sample probe or fast loop provided an energy addition requirement and pump sizing that was untenable, therefore the energy addition was curtailed in favor of increasing the suction inlet profiling capability of the offtake quill and changing the system into a CoJetix, this allows the mixing energy requirement and therefore demand pumping rates to be reduced.

JetMix nozzle

A further constraint on the design is the compromise between volume and jet velocity (pump outlet head requirements). Jet velocity in conjunction with the jet diameter provides the means for both dispersion and distribution. Small diameter jets at high velocity provide good local energy addition but limited distribution capability due to their faster diffusion. Larger jets provide longer term bulk movement of the flow.

The pipeline section in to which the offtake quill and jet were inserted was increased to ensure that the installation would not impact the overall system pressure losses through obstruction.

The use of a CoJetix also allowed the implementation of the densitometer loop and the use of a water cut monitor, samples are collected into a constant pressure receiver.

Co-Jetix fiscal condensate sampling and analysis system

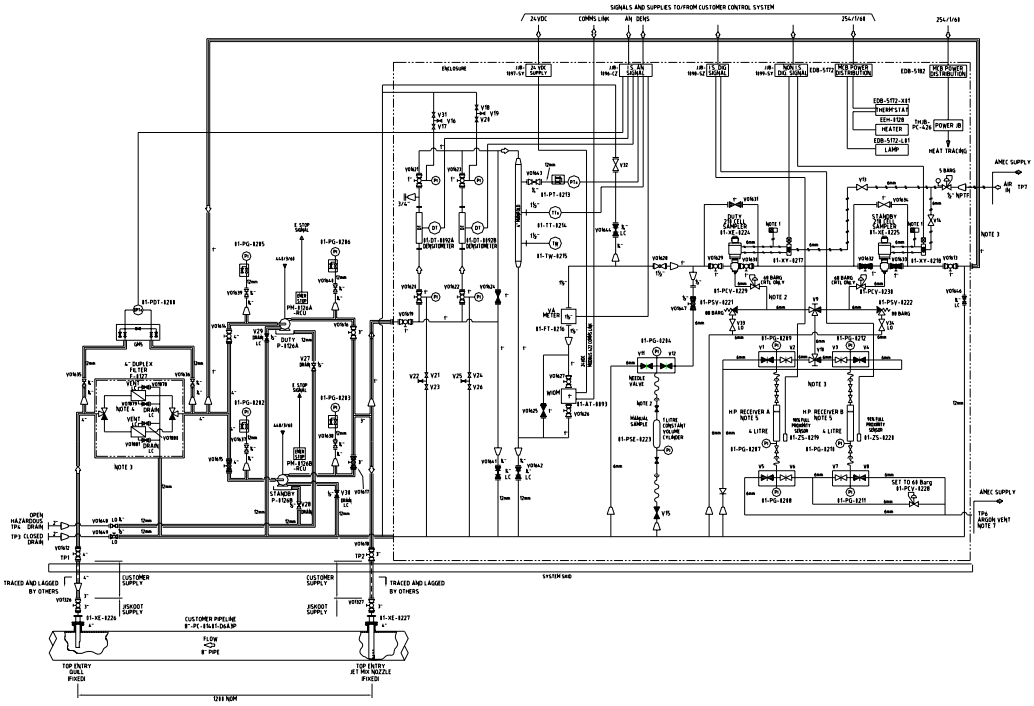

Due to the high RVP of the product the system was designed to be able to use plain and compact (constant pressure) sample collection receivers which can be mixed in a laboratory. These can be mixed with a ShearMix (pressurised shearing vessel) into which the sample is decanted for homogenization. The ShearMix can be used with almost any vendors constant pressure cylinders and allows samples to be extracted from the top and bottom of the vessel to ensure convergence in the analysis results.

CPC sample receiver

ShearMix - CPC mixer

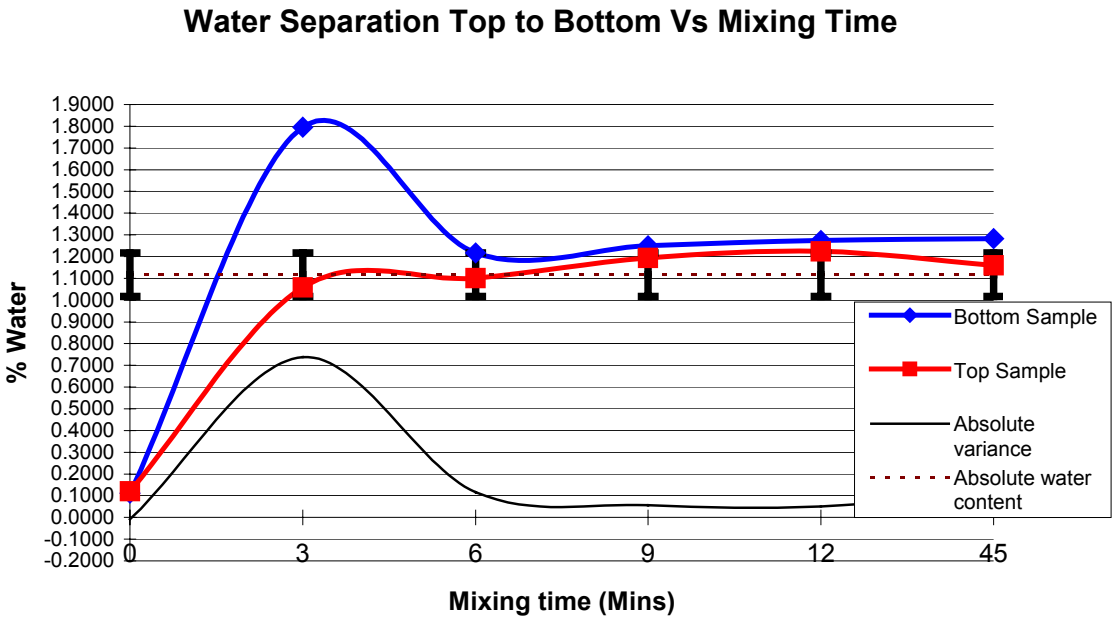

A more recent application of this CoJetix style design is to a system where no sampling is implemented but the problem of providing representivity to a watercut monitor remains, under these circumstances the same approach is taken.

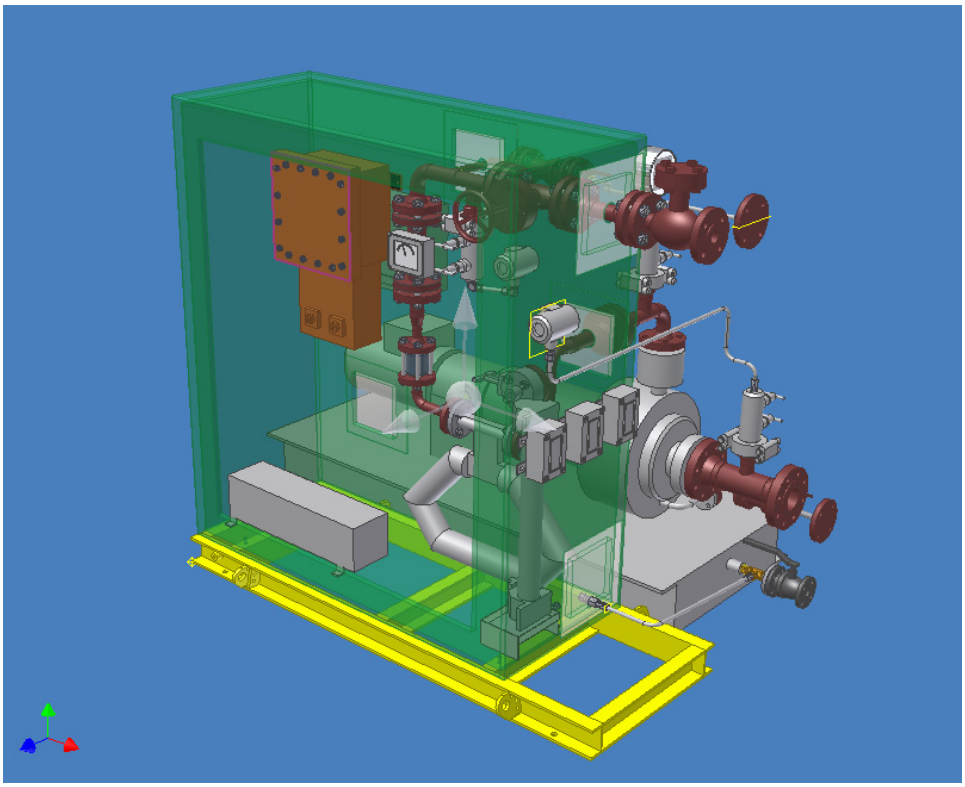

Sampling system 3D design model

This style of design, whether it be for a physical extraction of sample, density measurement OR water cut measurement singularly or concurrently can be used in almost any application where measurement uncertainty is important to the overall process audit.

Your income stream in either joint venture environments or where production is taxed on the basis of your measurement depends upon the best measurement achievable.

The Effects of Water in Oil on the Performance of aFour Path Chordal Ultrasonic Flow Meter in a Horizontal Flow Line

By

T. Cousins, D. Augenstein, and S. Eagle

Caldon Inc.

ABSTRACT

A series of flow tests were performed at the Ohio University multiphase test facility to evaluate the performance of a four path ultrasonic flow meter (UFM) in the presence of water in oil. The tests used a clear Perspex flow meter and piping, so that the flow behaviour could be observed and correlated with UFM performance.

Tests were initially carried out at a wide range of water-cut (water volume fraction), in order to verify meter operation. These tests showed that at higher velocities the water was fully dispersed and UFM operation appeared normal, although the true flow rate performance of the meter could not evaluated due the the lack of a suitable reference measurement. At lower velocities, water separated and formed a “river” along the pipe bottom. Under some circumstances the bottom acoustic paths could fail to operate due to refraction and dispersion effects when the ultrasound encounters the oil/water interface region.

Further tests were then carried out to attempt to quantify the UFM performance with water-cut in the range of 1% and 7%. For these tests, more of an attempt was made to quantify the uncertainty in flow rate measurement. At higher velocities, the combined oil and water volumetric flowrate measured by the UFM was within the experimental uncertainty of the test method. At lower flow rates, the performance of the flowmeter was degraded by water drop out affecting the lower path velocity measurement.

This paper describes the hydraulic behavior and gives advice on operational limits for good flow measurement in oil/water flows. The test data shows that the conditions in which good measurement can be obtained correspond well with the API[4] guidelines for good mixing in sampling applications.

1 INTRODUCTION

There has always been concern as to the effects of water in oil mixtures on the performance of Ultrasonic flowmeters (UFMs). Opinions have often been formed from circumstantial evidence, and seem to have been influenced by other factors such a gas in the fluid or the presence of particulate matter, rather than just the effects of water. To try and understand these effects and quantify the performance of a 4-path ultrasonic meter, Caldon designed a set of tests to be performed at the Ohio University Corrosion Research Center. Amongst other studies, Ohio University carries out testing on the effects of gas, water and oil mixtures on the corrosion of pipes and therefore seemed to be a good laboratory location for Caldon’s oil/water testing.

The tests were carried out in two stages, The second stage of testing built upon the better understanding gained from the previous first stage and the test method was substantially revised.

The series of tests were performed with two different viscosities (4 cP and 20 cP) and with "coarse" control of water content. These tests are more applicable to larger volumes of water content. In the second series of tests, a more direct flow comparison was performed and the water-cut was limited to between 1% to 7%.

The results give sufficient information to provide some basic precautions in how to use UFMs to measure fluids that consist of water in oil mixtures. To obtain a reasonable uncertainty of measurement of the combined volume the water and oil should be well mixed. When the flow becomes stratified, at lower velocities, then there is greater potential for meter performance to be degraded.

2 INITIAL TESTS INCLUDING HIGH WATER-CUT

The first series of tests were carried out using the following method:

The liquids were pumped from a single tank. Within the tank, the water and oil were separated by gravity, e.g., with oil on the top and water on the bottom. The oil was pumped out from the higher section of the tank and water from a lower section. The flow return was near the top of the tank. A picture of the facility is shown in Figure 1 below.

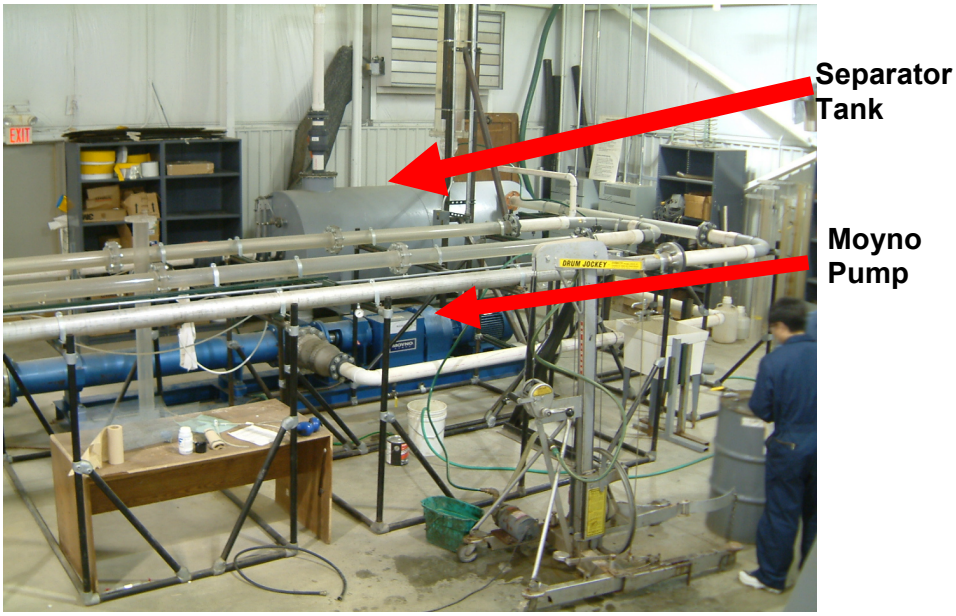

Figure 1: Flow/Separator Tank

The pumps used were semi-positive displacement type (Moyno), allowing the flow rate to be estimated by the RPM of the drive motor. It was intended that the water-cut would be controlled by varying the ratio of pump motor speeds. However, it was discovered early in the tests that the tank volume was too small to allow sufficient separation of the water and the oil before the liquid was drawn back in through the pumps. Therefore, the pump speed ratio was used to

roughly set the water-cut. To measure the water-cut a diverter valve was used to by-pass the full flow stream into a settling tank. The water and oil volumes in the setlling tank were then measured off-line to determine water cut.

The test liquids used were water, LVT200 (~ 2.5 cS viscosity and 0.82-0.83 specific gravity) and Duopac 90 (viscosity 18.6cS, 0.851 specific gravity).

The ultrasonic flow meter was a 4-inch Caldon 4-path meter, the operation of which has been described before (e.g. see References 1 and 2). The meter used 1.6 MHz transducers and the body was made of Perspex. It was installed in a 4" Perspex flow line approximately 150 pipe diameters long. This test set up allowed for proper development and observation of the oil/water flow distribution. Photographs of the meter body and test line are shown below.

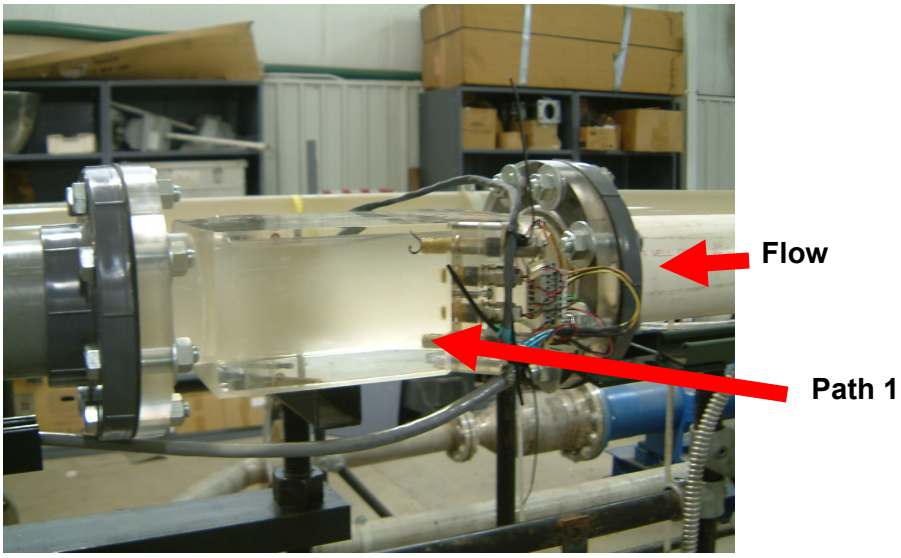

Figure 2 Test Meter

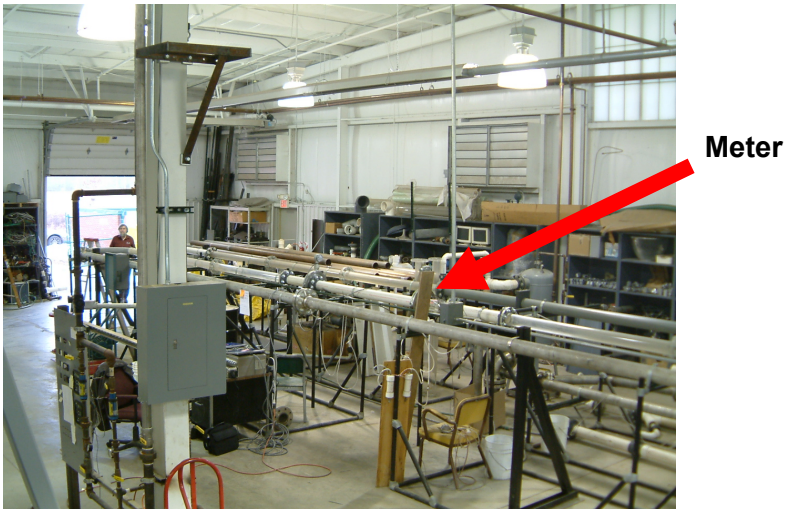

Figure 3 Meter Installation

2.1 Initial Test Results

During the tests diagnostic data was recorded to monitor features that define the UFM's quality of operation (e.g., gains, signal to noise ratio, standard deviation of the samples and velocity of sound).

In the case where no water was purposefylly added to the oil the diagnostic results indicated excellent performance. For example, the signal-to-noise ratio (SNR) was around 90 for all paths and flows. The flow velocity profile was also acceptably symetrical. In reality a pure oil test was not possible as there was always a background contamination level of water in oil. However, this did create the opportunity to carry out some tests with small quantities of water to see the effects.

A series of low velocity tests were performed where the presence of water was observed to vary in the bottom of the pipe from a small rivulet to almost a quarter fill. Under these conditions, with water still running separately from the oil, the transducers submerged below the water gave a good signal and those above the water line gave a good signal, but any on the oil/water interface gave a very poor signal.

The results of the intial series of tests can be summarised as follows:

- At velocities greater than 2.6 to 3.1 m/s, the meter worked at all water cut levels tested (0%-25% for 2cS, 0-75% for 18.6cS). At these velocities, the water droplets appear to be completely dispersed. There was some degradation of SNR and increase in gain, but not consequential with regard to meter operation.

- For 2 cSt oil, at velocities less than 3.1 m/s, the water droplets began to drop out and a layer of water developed on the bottom of the pipe. By 1 m/s, the droplets had essentially dropped out and the water was running along the bottom of the pipe. At these velocities, there is a transition region at the water/oil interface. This transition region has surface "waves" (for lower velocities) or a combination of waves with large to small droplets breaking off waves (for higher velocities). The height/thickness of the transition region is a function of the velocity, relative densities, viscosity and water cut.
  - For acoustic paths below the water/oil transition region (depending on the water-cut and velocity), the acoustic paths work well – as if in pure water.
  - For acoustic paths above the water/oil transition region (again depending on the water-cut and velocity), the acoustic paths work well – as if in pure oil.
  - For acoustic paths within the water/oil transition region, the acoustic paths are degraded in performance or may have failed.

- For 18.6 cSt oil, water droplets began to drop out at velocities less than 2.6 m/s. Under these conditions, the observations discussed above are still valid. The intersection of the water/oil transition region with a transducer path adversely affects its performance. However, the transition layer was thinner and more defined than that of the 2 cSt oil. This localizes the effect of the transition layer to one path and the effect upon that path is not as great as with the 2 cSt oil. For example, during these tests, no path failed at any time.

- With 2 cSt oil, for water-cuts below 10%, the UFM operated without any apparent performance degradation (irrespective of the velocity). With 18.6 cSt oil, at a flow rate of 0.6 m/s and low water cuts, the transition region can interfere with the bottom path. Under this

condition, increased gain, low SNR and rejects eventually cause the software to reject the path due to poor acoustic quality. The remaining three paths are unaffected. Obtaining low water-cut at low flow rates was very difficult with the configuration at Ohio University. This was due to the lowest pump speed for the water pump being too high for our purposes.

- At velocities ~ 1.5 m/s, the oil/water distribution is most noticeably in a transition region between stratified and well mixed flow, and this is the area where things are most difficult for the meter. With 2 cSt oil, and if the water-cut was high enough, the meter had 2 or even 3 acoustic paths in and out of failure. With 18.6cS oil, although multiple transducer paths were adversely affected, at no time did any path fail.

The next figures show a typical set of observations, taken at high velocity. The water-cut during the time of these observations was approximately 20%.

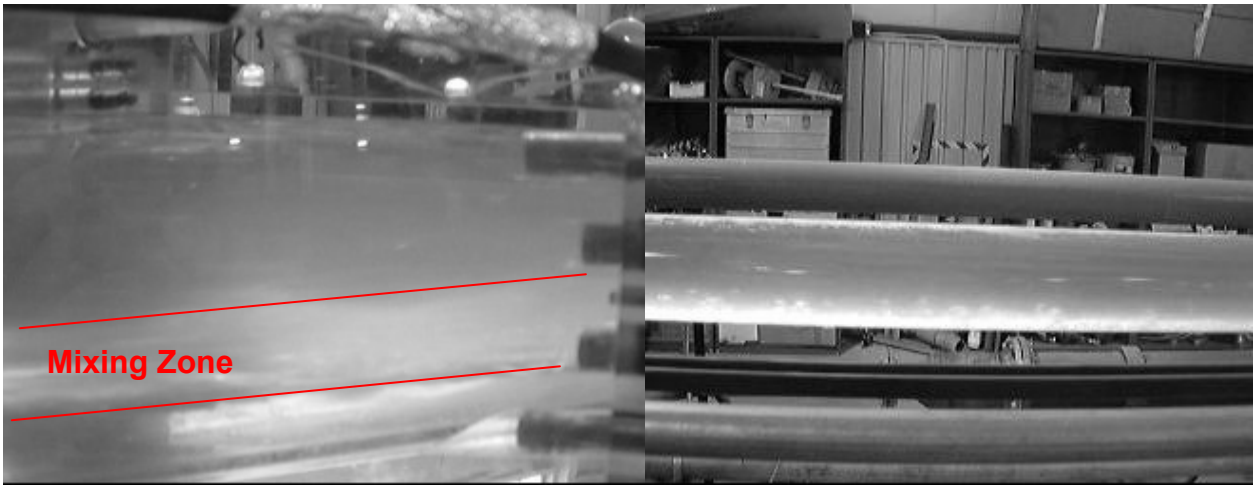

Meter Body **Upstream Pipe**

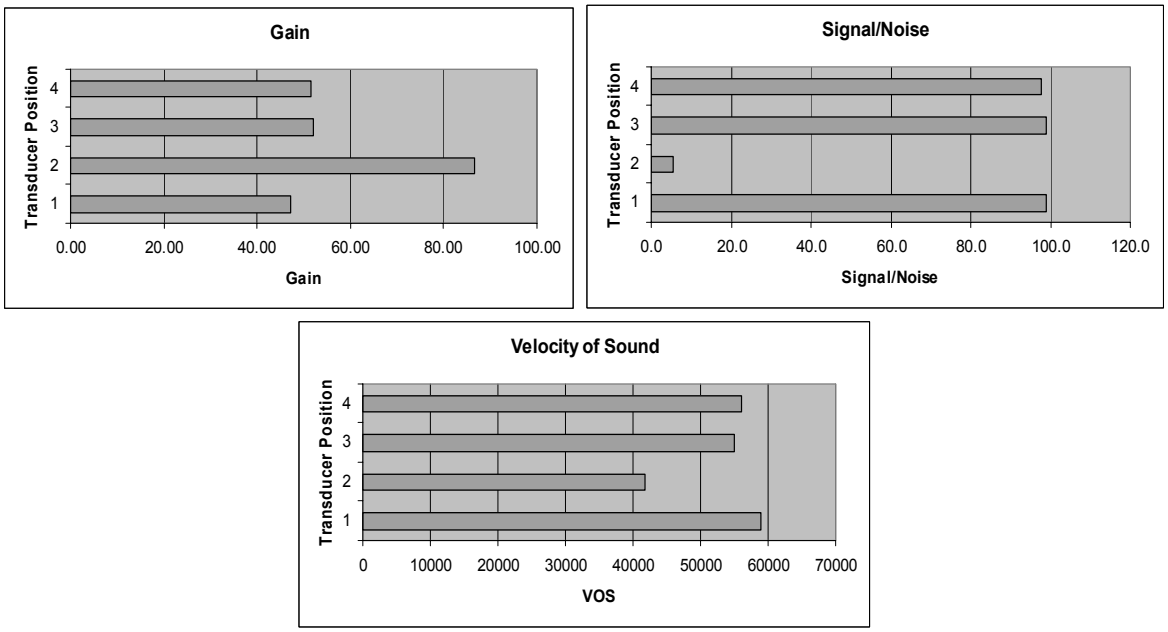

Figure 4 High Flow 20% Water Data

The mixing zone is a very turbulent shear layer of varying percentages of water and oil, with varying degrees of signal attenuation. The velocity of sound (VOS) for paths 3 and 4 (top paths) was a value of around 55,000 in/s (1,400 m/s) which is normal for the oil and around 59,000 in/s (1,500 m/s) for path 1 indicating water on the bottom. In between the value is invalid because of the poor signal quality, as shown by the plots of SNR and gain.

Figure 5 below shows the flow with a small volume of water at a velocity of below 1m/s. The graphs illustrate the effect of the stream on the gain and signal to Noise ratio, indicating that the interface between the water and the oil is impacting the bottom path.

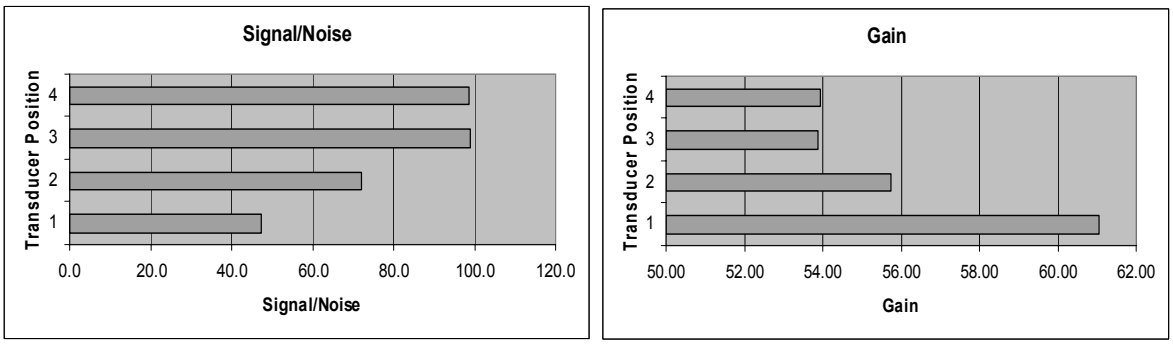

Figure 5 Data For Low Flow <1% Water

3 WATER IN OIL TESTS AT 1% - 7% WATER-CUT

Following the first series of tests a decision was made to perform more controlled tests over the 1 to 7% water-cut range. This test was felt to be more applicable to the majority of custody transfer applications. The test method was changed to give a more consistent volume of water to oil. Instead of using the pumps separately to mix the liquids, the tank was filled with the required volumes of oil and water, and the mixture was then pumped until it was fully mixed/dispersed. The reference measurement method was to use the pump RPM measurement as the method of calibration. The method utilized the output from the Moyno semi-positive displacement pump. A resolver was mounted on the pump shaft which produced a pulse train, which was used to gate the meter pulses.

This method was not able to give a good absolute measurement, but was very repeatable, to within 0.2%. Thus, the experiment used the calibration with 0% water in oil, at velocities above 1.5 m/s, as the baseline for all of the tests. The data is all referred to this datum. The criteria of higher velocity was used because of the fact that it was not possible to remove all traces of water from the system, and therefore the higher velocity data was considered to be more representative of the performance without water present.

The meter used for the tests was again the 4” Perspex LEFM 240C meter described earlier. The meter was installed with Path 1 on the bottom and Path 4 on the top. Water cuts tested were nominally 0% (Baseline), 1%, 3%, 5% and 7%. A check was made on the water-cut by taking a draw sample of the mixture into a long calibrated vertical tube, and allowing it to settle out. The proportion of water to oil could then be determined by comparison of the depths. The viscosity of the oil in these tests was 13 cSt and the specific gravity was 0.89.

3.1 Results

Before data was logged at any given water-cut, the test rig was run at a high flow rate for at least 30 minutes to ensure good mixing. The picture below shows a typical mixed flow at high flow rates, the “milky” appearance being caused by the water being well mixed through the oil in the form of many small droplets.

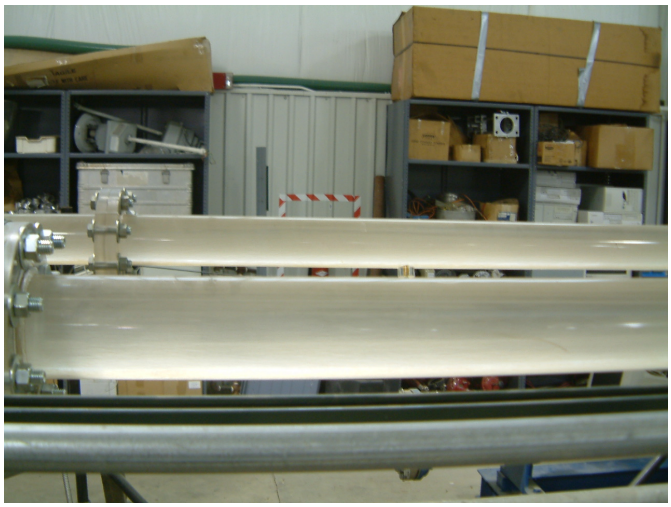

Figure 6 Mixed Flow Prior to Testing

The initial calibration of the meter is shown in Figure 7. It should be noted that the calibration at the low end is non-linear. This is explained later, when it was realized that there was still water in the line, and that it was gradually settling in the lower port, and therefore the calibration at the low end had some degradation.

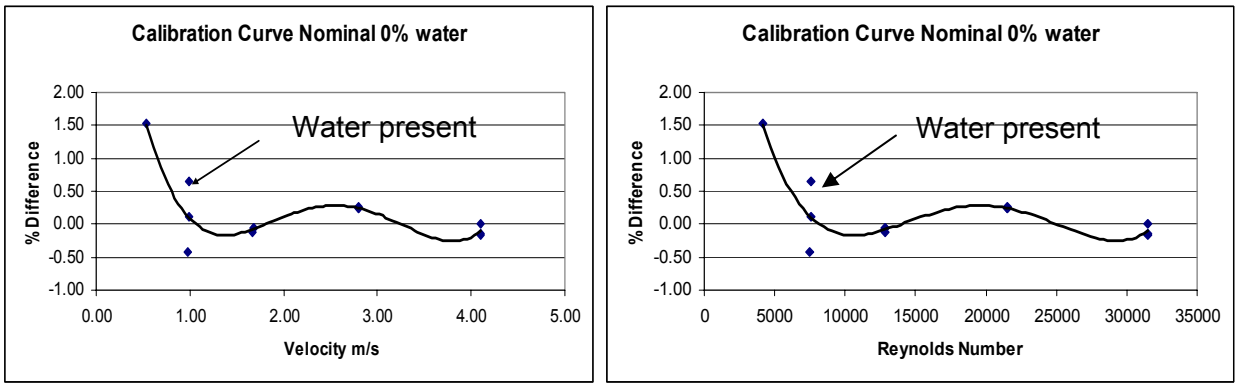

Figure 7 Initial Calibration

Tests were then carried out at water-cuts of 1, 3, 5 and 7%. The results, plotted as a percentage difference relative to the 0% water-cut baseline, are shown in Figure 8 below. During these tests, the meter was configured such that the results were computed using all four paths, even those whose path velocities would normally be rejected owing to poor signal diagnostics. Therefore the poor performance at low velocities is exaggerated owing to the inclusion of spurious velocity data from path 1.

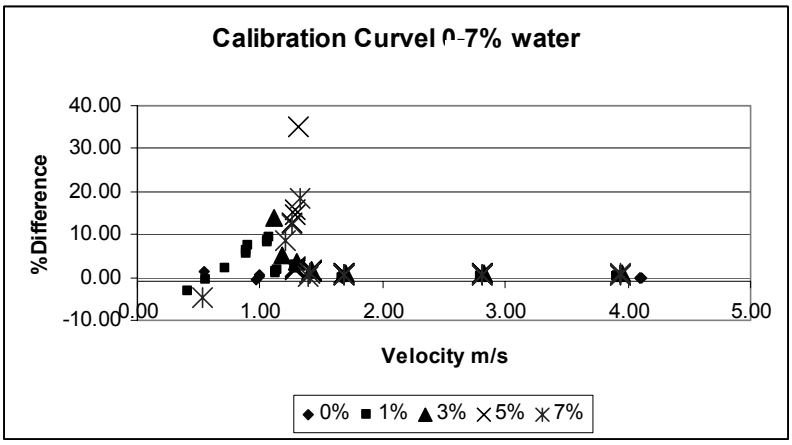

Figure 8 Calibration of the Meter with 1-7% Water content

A summary of recorded diagnostic data for individual paths is shown in Figures 9 - 12. In Figure 9 the data is a conglomeration of water-cuts and therefore variations with water-cut can not be distinguished.

Figure 9 shows that the signal to noise ratio for paths 1 and 2 (in the lower part of the pipe) are reduced by the presence of water at velocities of less than approximately 1.3 m/s.

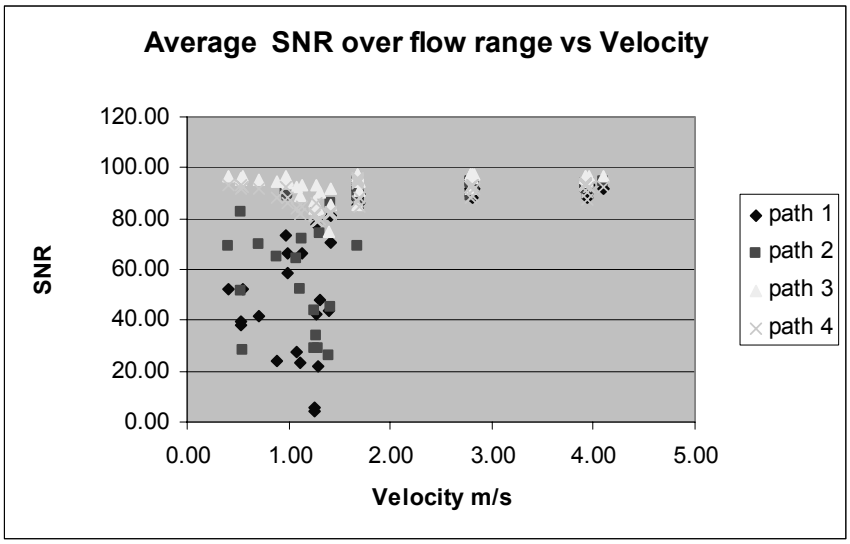

Figure 9 Signal to Noise Ratio Data for all Water-Cuts

Figure 10 shows an increase in average gain over all paths as the water-cut increases. Again the effects are most pronounced at velocities below 1.3 m/s velocity,

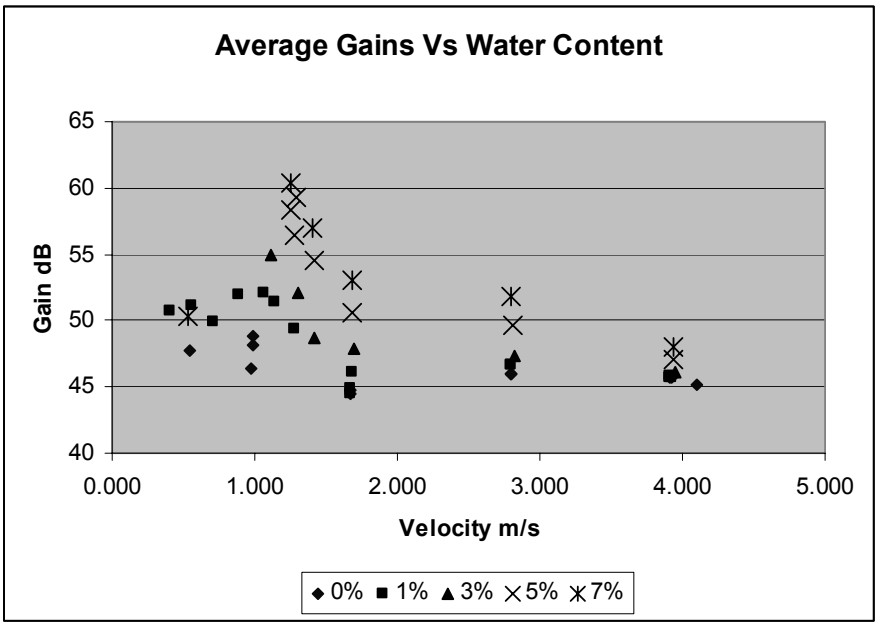

Figure 10 Average Gain Data for all Water-Cuts

Figure 11 shows the flatness ratio (i.e. the ratio of the velocities measured on the outside paths divided by the velocities measured on the inside paths) vs velocity and water-cut. It can be seen that this ratio is constant at velocities above 1.3 m/s.

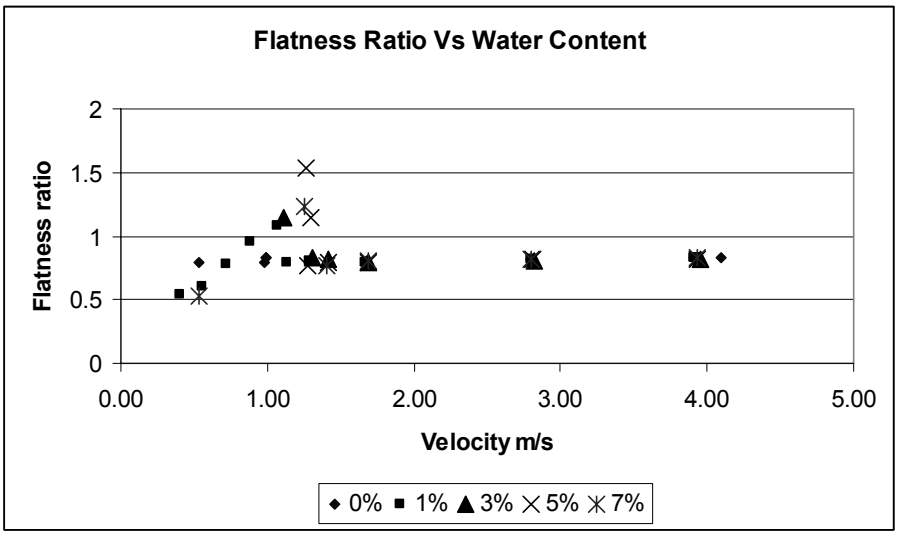

Figure 11 Flatness Ratio vs Water-Cut

Figure 12 shows the variance of the velocity measurements (i.e. the scatter) vs velocity and water-cut. It can be seen that the varience is low at velocities above 1.3 m/s and sometimes very high at lower velocities with water present.

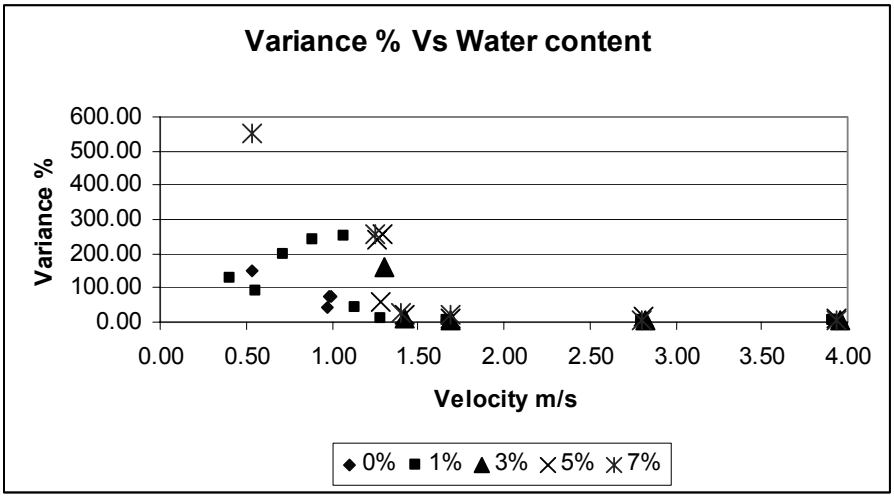

Figure 12 Variance vs Water-Cut

3.2 Discussion of Results for 1-7% Water

3.2.1 Performance at Velocities Greater than 1.3 m/s

Above a velocity of approximately 1.3 m/s (corresponding to a Reynolds number of around 10,000) the meter performed within the uncertainty of the calibration system at all water-cuts tested (i.e. up to 7%). Under these conditions there was no observable change in the meter's performance. As shown in Figures 9 – 12, the flatness ratio, gains, variance and SNR all remain relatively constant in this regime. These observations are also supported by examining the velocity profile measured by the meter. At velocities greater than 1.3 m/s, there is no change in measured velocity profile with water-cut, as shown in Figure 13.

These observations can be related to the distributon of the water in oil. Above a velocity of 1.3 m/s visually the water appears to be well distributed throughout the oil, as shown in Figure 14.

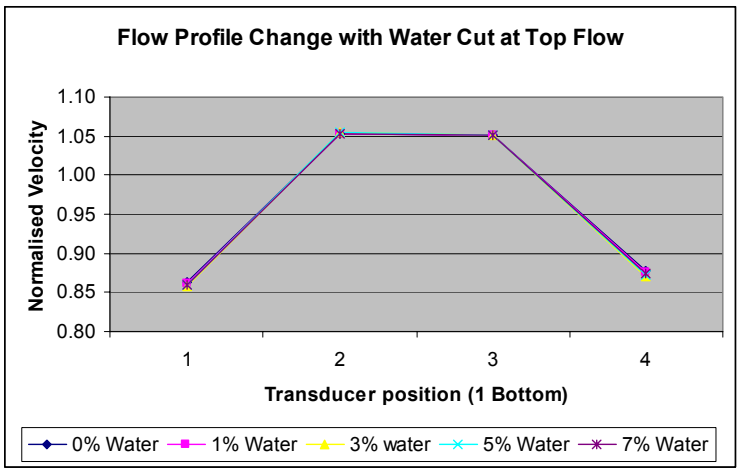

Figure 13 Change in Measured Profile with Water-Cut (velocity > 1.3 m/s)

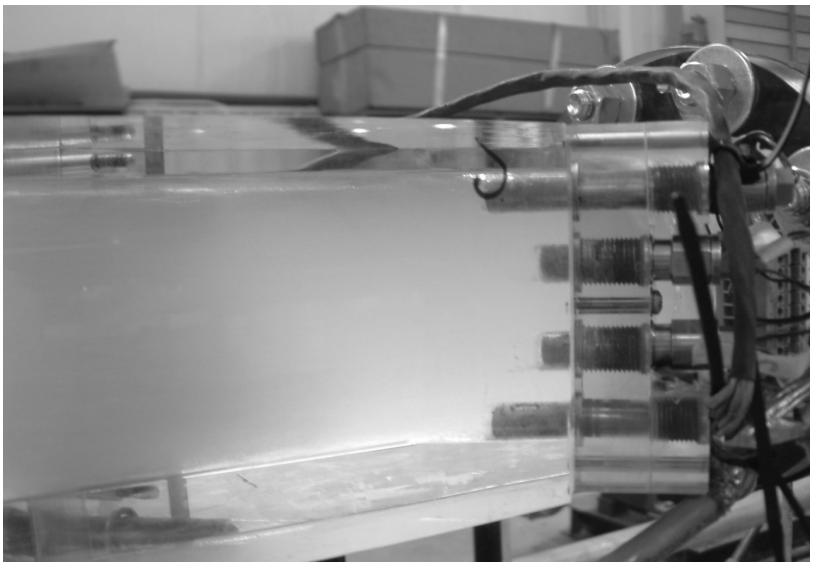

Figure 14 A Photograph Taken at 5% Water-Cut at Highest flow

3.2.2 Performance at Velocities Less than 1.2 m/s

Below 1.3 m/s (Reynolds number of 10,000) the presence of water begins to dramatically change the meter performance. The calibration now begins to open out and become non-repeatable. At this point the velocity measurement on the bottom path becomes inaccurate as shown in Figure 15.

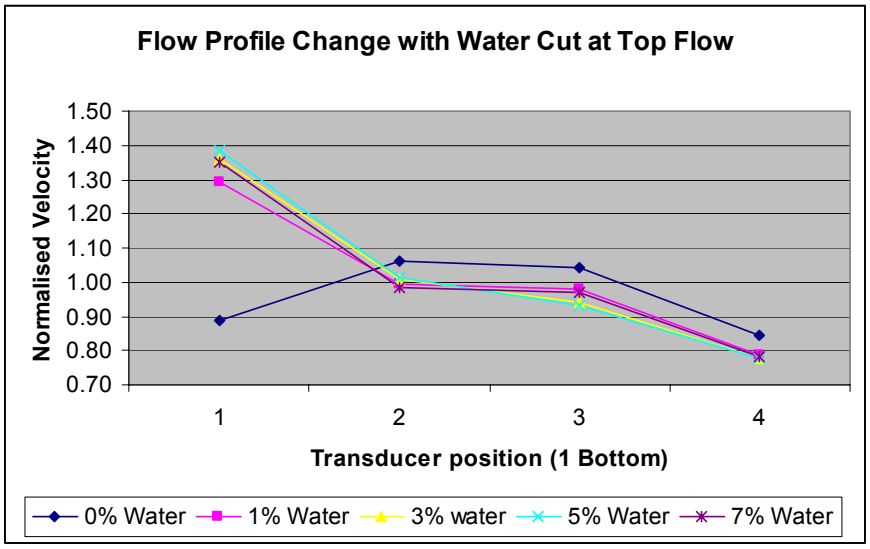

Figure 15 Measured Flow Profile Variation with Water Cut at ~ 1 m/s Velocity

When the data was examined what was disconcerting was the fact that the magnitude of the effect at this velocity did not seem to be dependent on the water-cut. The velocity on path 1 was also very unstable in these conditions and changed with time in the presence of water, as shown in Figure 16. The only notable difference between the behaviour at 1% and 7% water-cut was the time after change of flow it took for the effect to reach a maximum.

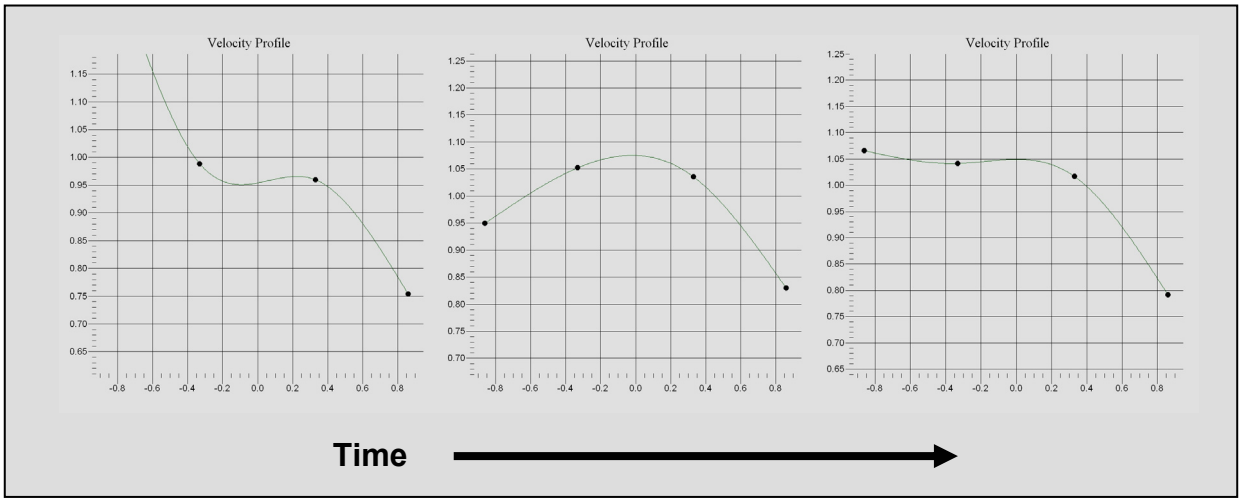

Figure 16 Changes in Measured Velocities with Time at 1% Water-Cut

At a velocity of about 1 m/s there was not an obvious rivulet of water at the bottom of the pipe, particularly at the lower water cuts. This could be observed at lower flows, with globules of water tracking along the bottom of the pipe rather than a continous stream at the lower water-cuts. On examination, the real cause of the problem at these conditions appears to be the formation of a 'glob' of water in the bottom transducer ports. This was observed clearly during the tests as shown in the Photograph in Figure 17.

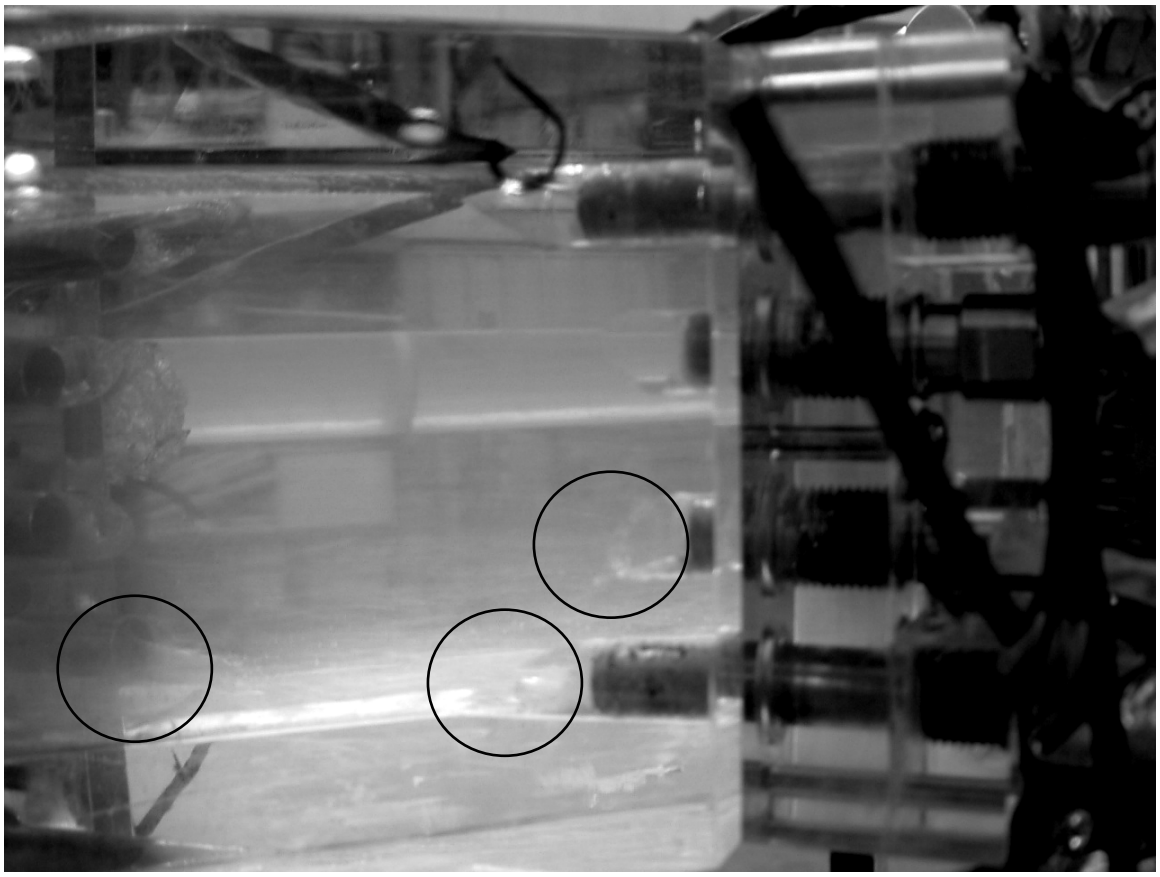

Figure 17 Formation of Water 'Globs' in the Lower Transducer Ports

It can be observed from the figure above that there are small formations of water in the second from bottom path. However, this did not appear to affect the velocity measurement on that path, even though a lower signal to noise ratio was observed.

The 'glob' of water that formed in the lower transducer ports could be observed to change in size with time. At the lower flows there was not sufficient velocity, or turbulence, to provide a vortex action to completely remove the glob of water. However, its size is added to and reduced by the action of the flow. The glob is essentially stationary except at the boundary, where it wobbles like a piece of jelly, occasionally shedding pieces of itself. The disconcerting feature of this effect is the fact that it does not appear to matter how much water is present, it will ultimately build up to a similar level in the lowest transducer ports.

At lower velocities of around 0.5 m/s there was indication that the effect of the 'glob' was mitigated and the velocity profile returned to a more parabolic shape, indicating a sensible velocity measurement on the bottom path.

As can be seen from the SNR, gain and variance plots, the ultrasonic signals on the bottom path are dramatically affected at these low flows. The shape of the 'glob' of water refracts the ultrasound, causing deflecton of the 'beam' and distorting the waveform of the received signal. With the shape of the glob shifting with time then the way that the signal is affected changes with time also, resulting poor repeatability as well as inaccuracy.

What is unclear is if the onset of this effect of is a function of velocity or Reynolds number, or perhaps some other parameters. The changes in performance and the appreance of the 'globs' all occur close to the transition from laminar to turbulent flow. This leaves the following questions unanswered;

- If the flow was turbulent would it remove the 'glob'?
- Will viscosity, density and surface tension differences significantly alter these effects?

These questions can only be answered by further tests.

4 CONCLUSIONS

The use of clear piping has provided additional insight into UFM operation when operating under conditions of water mixed with oil. Three flow regimes of water and oil mixtures have been observed. These are fully mixed flow, stratified (separated) flow and transitional flow. Based on observations and measurements in these regimes, the following conclusions can be made:

Fully Mixed Flow

At velocities greater than 3 m/s, independent of the oil viscosity and water-cut, the water is well dispersed through the oil. Under these conditions, the UFM may see some acoustic degradation (dependent on the water-cut), but the degradation is not consequential with regard to the UFM flow measurement operation. When calibrated, the meter performance does not change by more than the uncertainty of the test method.

Transitional Flow

At velocities less than 3 m/s and greater than 1.3 m/s, the water begins to drop out and a layer of water develops on the bottom of the pipe. At these velocities, there is a transition region at the water/oil interface. This transition region has surface "waves" (for lower velocities) or a combination of waves with large to small droplets breaking off waves (for higher velocities). The height/thickness of the transition region is a function of the velocity, relative densities, viscosity and water cut.

- For acoustic paths below the water/oil transition region (depending on the water-cut and velocity), the acoustic paths work well – as if in pure water.
- For acoustic paths above the water/oil transition region (again depending on the water-cut and velocity), the acoustic paths work well – as if in pure oil.
- For acoustic paths within the water/oil transition region, the acoustic paths are degraded in performance or may have failed.

The velocity at which good mixing is observed to occur corresponds closely to API's mixing requirements for product sampling.

Stratified (Separated) Flow

Below 1.3 m/s, the droplets have essentially dropped out and the water runs along the bottom of the pipe. For lower watercuts, below 5%, the water travels along the pipe bottom, but does not interfere with the bottom path (at least for the design of the meter tested). However, by some mechanism (such as the coalescence of droplets that traveling along the pipe wall) water can accumulate in the bottom transducer ports. to forming a 'glob'. This glob changes shape and size with time, but will not clear itself at low velocities. This glob degrades the acoustic signal (due to refraction), such that eventually the flow meter rejects that path's data from the flow calculation.

At higher water-cuts, the water stream can cover the bottom path. The bottom path may still be rejected from the flow calculation depending upon the character of the 'waves' of water. However, eventually the water will cover the bottom path such that its acoustics are acceptable. However, the next path from the bottom may then start to go through conditions similar to those that affected the bottom path.

Water-Cut Measurement

Although not presented here, the test data also shows that the measured sound velocity can reasonably be used to estimate water-cut, where the water cut is determined by a linear combination of the oil sound velocity and water velocity.

5 REFERENCES

1. T. Cousins & D Augenstein (2002) "Proving of Multi-path Liquid Ultrasonic Flow Meters" *North Sea Flow Measurement Workshop*, St Andrews, Scotland, October 2002

2. T. Cousins & J. Thorogood (2004) "Small Volume Proving of Ultrasonic Flow Meters" *S E Asia Hydrocarbon Flow Measurement Workshop, Singapore*, March 2004

3. T. Cousins, H. Estrada & D. Augenstein (2004) "Installation Effects and Diagnostic Interpretation Using the Caldon Ultrasonic Meter" *North Sea Flow Measurement Workshop*, St Andrews, Scotland, October 2004

4. API Chapter 8 "Sampling"

The 21st International North Sea Flow Measurement Workshop
Thursday, 1000, 20 October 2005
Uncertainties in Pipeline Water Percentage Measurement
Bentley N. Scott

Abstract

Measurement of the quantity, density, average temperature and water percentage in petroleum pipelines has been an issue of prime importance. The methods of measurement have been investigated and have seen continued improvement over the years. Questions are being asked as to the reliability of the measurement of water in the oil through sampling systems originally designed and tested for a narrow range of densities. Today most facilities sampling systems handle vastly increased ranges of density and types of crude oils. Issues of pipeline integrity, product loss and production balances are placing further demands on the issues of accurate measurement. Water percentage is one area that has not received the attention necessary to understand the many factors involved in making a reliable measurement.

A previous paper[1] discussed the issues of uncertainty of the measurement from a statistical perspective. This paper will outline many of the issues of where the errors lie in the manual and automatic methods in use today. A routine to use the data collected by the analyzers in the on line system for validation of the measurements will be described.

Introduction

Composite samplers have been used as the standard by which water content is determined in pipelines. Losses and gains between tankage and pipeline, marine unloading and shore may reflect an acceptable mean value but is the system within acceptable control limits? Results for composite samplers are only available at the end of a batch and there is no recourse if something goes wrong with the sampling system during the batch. At the end of the batch only a single number is available to argue about the water delivered. The exposure of personnel to hazardous liquids and the errors associated with processing the samples are additional issues. On line real time analysis of the water content can be obtained with analyzers on the market today. Real time data makes it possible to know when the water arrived providing several beneficial operational advantages. Knowledge of when the water arrives and the magnitude provides an opportunity to do something with the water before it hits the pipeline or tankage. The real time data can show if the water was several short periods of time or if it was across the entire load. In addition, real time analyzers can be used as a comparison of the validity of the composite samplers, something not done until recently.

Originally pipelines only shipped products with a narrow range of densities and due to this fact composite samplers only required testing against one density of oil. Today pipelines ship products with extremely large variation in density and molecular chemistry but the older methods of validation are still in place using one or two densities. Samplers are typically proved on one type of product with the assumption that it is valid for all densities and types. Original API methods suggested testing on the lightest density oil. If the oil becomes heavy, cold and very viscous does the sampler provide the same acceptable deviation from acceptance tests? There are many more issues and questions which must be asked to determine the overall system performance.

The better a process can be understood and the errors controlled the easier it is to assure a good measurement. Each process will be analyzed for the potential errors and their sources. Finally, a new analysis routine will be investigated to compare the on line measurements.

1 – Uncertainty

The petroleum industry generates and uses volumes of data used to buy, sell and balance production. Unfortunately, the documentation with this data typically does not contain statements of uncertainty. Decisions about expectations and corrective actions cannot be made without a statement of uncertainty typically expressed as a standard deviation from a mean value. The standard deviation can only be obtained through taking enough data that can then be used to generate the statistical comparisons against some other method. If there is no other standard to compare against then the uncertainty cannot be obtained. There have been statements about loading losses by crude types and losses for load and receipt terminals but are these statements qualified for all of the contributing factors?

If one composite sample is obtained and laboratory methods performed with two different analysis techniques, what does the uncertainty analysis represent? The composite sample container, Sample 1, is mixed then a sample pulled that is Sample 2. Now the laboratory takes this Sample 2 and pulls two more samples one for titration, Sample 3, and another for distillation Sample 4. This results in a statistical analysis determining the uncertainty between the two laboratory methods and the ability to pull the Samples 3 & 4 from Sample 2. Therefore, if the sample itself is processed using two independent laboratory methods this routine will only check the uncertainties of the two laboratory methods and the operator's ability to pull a sample from the larger composite sample. Nothing can be said about the uncertainty of the actual in line measurement because the sample into the composite sampler has nothing for comparison.

If API Chapter 8.2 is followed to prove the composite system, the allowable deviation for 1% level of water in a batch is 0.11% and for under 0.5% water the allowable is 0.09%. These numbers are relational to the testing of the composite system by water injection. If the system has been tested on several crude types it is likely that they do not represent the entire spectrum of crude types being shipped through the system after the testing was completed. Therefore, the results may or may not fall in the allowable deviation seen during the injection water testing. Therefore the remaining question is how can the measurement be validated not only across crude types but also for every batch shipped?

Can anything be said about accuracy of the measurement? Accuracy must be compared against a known standard. There does not exist a standard by which to measure the water in the crude oil that is flowing with a specific chemical structure, density, temperature, pressure, viscosity and water content equal to what is in the line. The best that can be done is to qualify a system against an independent measurement for the validity of measurement uncertainty, not accuracy. Independent means that it is not dependent upon the same sample or method of measurement.

If an on line analyzer is installed in a separate fast loop or in line then this is independent of the sampling mechanics of the composite system. This analyzer can be used to aid in arriving at the uncertainty of the measurement when using the composite system. The analyzer should be located in a position that is viewing the main liquid stream in the same homogeneous state as the mechanical sampler. If both methods are reproducible then the resulting uncertainty analysis will be meaningful and one can be used to aid in validation of the other.

2 – Discussion of Data for a Pipeline

The following data in Table 1 was collected by the operators and entered manually into a worksheet and is representative of many types of data collection in the field. The unusual aspect of this table was that it contains several laboratory methods (Karl Fisher and centrifuge) instead of the usual one lab method and the density was quite consistent through the entire month of data.

The data is from a composite sampler on a pipeline across a month where all of the data was

Table 1. Hand Entered Batch Data

Date	Batch #	Analyzer %Water	KF %Water	Grind Out %Water	Avg.Batch Density	API at 60	Obs.Grav.	Obs.Temp	(BBLs)
4/1/2003	52	0.17	0.40	0.20	0.8575	32.2	33.3	75	197931
4/4/2003	55	1.27	1.14	0.60	0.8567	32.1	32.0	58	115454
4/6/2003	56	0.45	0.39	0.15	0.8559	32.2	32.1	58	78690
4/9/2003	57	0.17	0.37	0.10	0.8548	32.4	33.3	72	196547
4/10/2003	58	0.10	0.24	0.10	0.8571	32.1	33.0	72	78624
4/12/2003	59	0.12	0.23	0.10	0.8564	32.1	33.1	74	182087
4/14/2003	60	0.24	0.22	0.10	0.8552	32.0	33.0	74	78626
4/16/2003	61	0.23	0.21	0.10	0.8538	32.2	33.2	73	197371
4/17/2003	62	0.26	0.30	0.10	0.8565	31.7	33.0	78	78733
4/20/2003	63	0.40	0.40	0.10	0.8500	33.0	33.2	63	183877
4/23/2003	65	1.03	0.85	0.50	0.8507	32.8	32.9	62	78546
4/25/2003	66	0.67	0.67	0.70	0.8548	31.7	33.4	83	65583
4/27/2003	67	0.69	0.60	0.30	0.8541	32.1	33.6	80	130832
4/29/2003	68	0.40	0.50	0.25	0.8548	31.9	33.4	80	120000
									1782901

obtained with one operator using a laboratory that followed API standards closely. The real time water analyzer was installed after the static mixer and sampling system. The results are shown in Figure 1. The dotted lines represent the best-fit line through the data. In this case the on line analyzer compared favorably with the composite by titration but composite by centrifuge shows the water much lower. More data may change the analyzer trend line to fall more correctly without a skewed slope against the titration. Another question this trend may ask is if the titration is biased at higher water percentages. One centrifuge point (batch 66) which appeared to be a bad data point was correct with respect to titration. Possibly this was an error in the entry of the centrifuge result or some operator influence, as it would be expected to follow

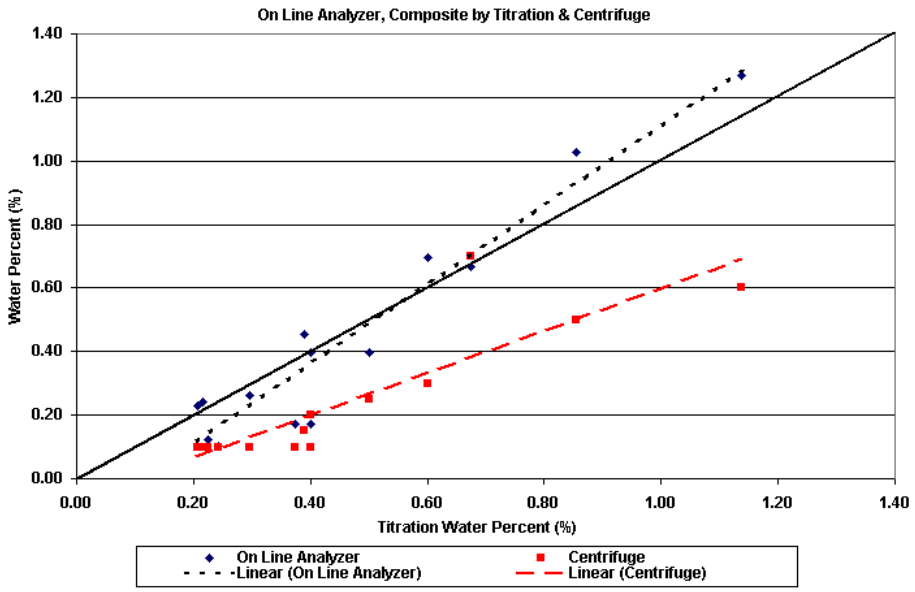

Figure 1. Water Percentage Analyzer & Centrifuge vs Titration

the same trend as the other centrifuge points.

Another aspect of this data is seen when the trend lines are compared with the least error line that is a 45 degree line between the two graph end points. The centrifuge versus the titration is showing the centrifuge consistently low while the comparison with the on line analyzer shows titration slightly less in water than expected. Normally centrifuge is expected to produce a lower water percentage than titration. Since all of the data consisted of moderate crude density and viscosity the centrifuge results would have been expected to be closer to the same water result as the titration.

3 – Ship Unloading Data

The following examples were from an on line analyzer and a composite sampler using titration as the laboratory method. All of the data collection was by computer with checks for the composite sampler built into the data collection.

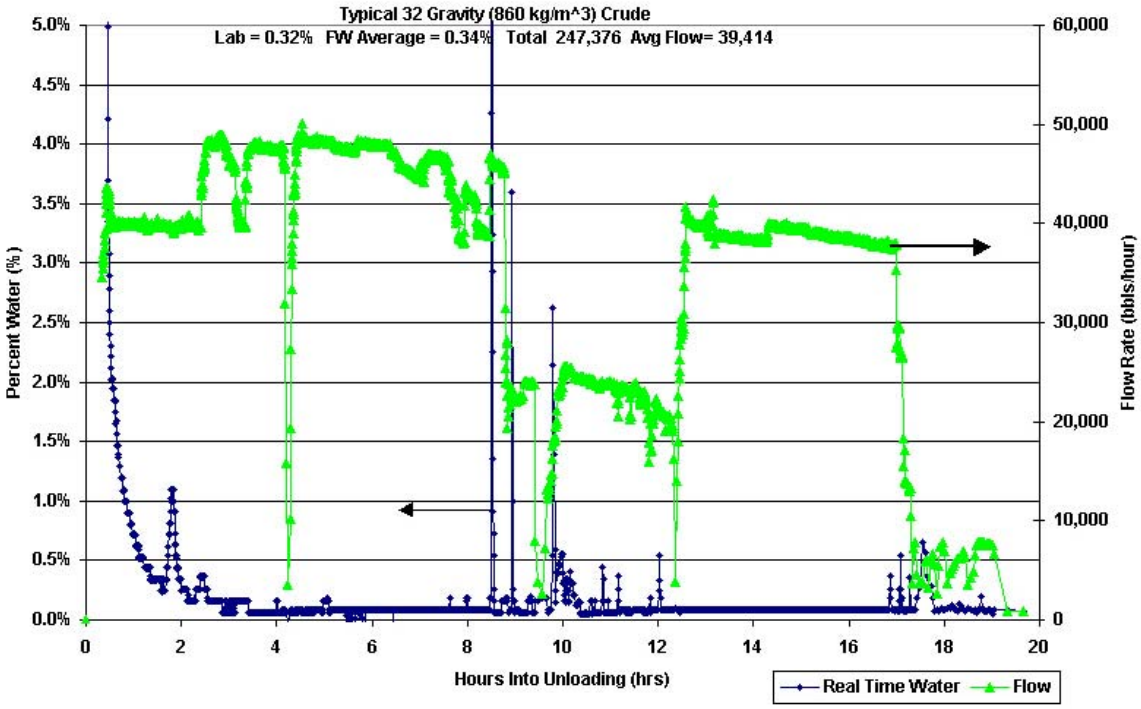

Figure 2. Medium Crude Density Ship Unloading Profile

In the ship unloading profile of Figure 2 the flow started and stopped, ran at one half the rate for several hours and had some very large water spikes. The results from the composite sampler were 0.32% water using titration and the flow weighted average from the on line water analyzer gave 0.34%. Very good results with the lab compared to the on line analyzer with the standard density crude oil. What happens when the same facility receives a higher density and viscous oil?

Figure 3 is a graph for a ship unloading profile for a 21 degree API density crude oil. Now the laboratory results from the composite sampler are much higher than the on line analyzer. Which one is correct? This question would not be asked without the on line analyzer for comparison. The composite sampler was not tested against this heavy crude.

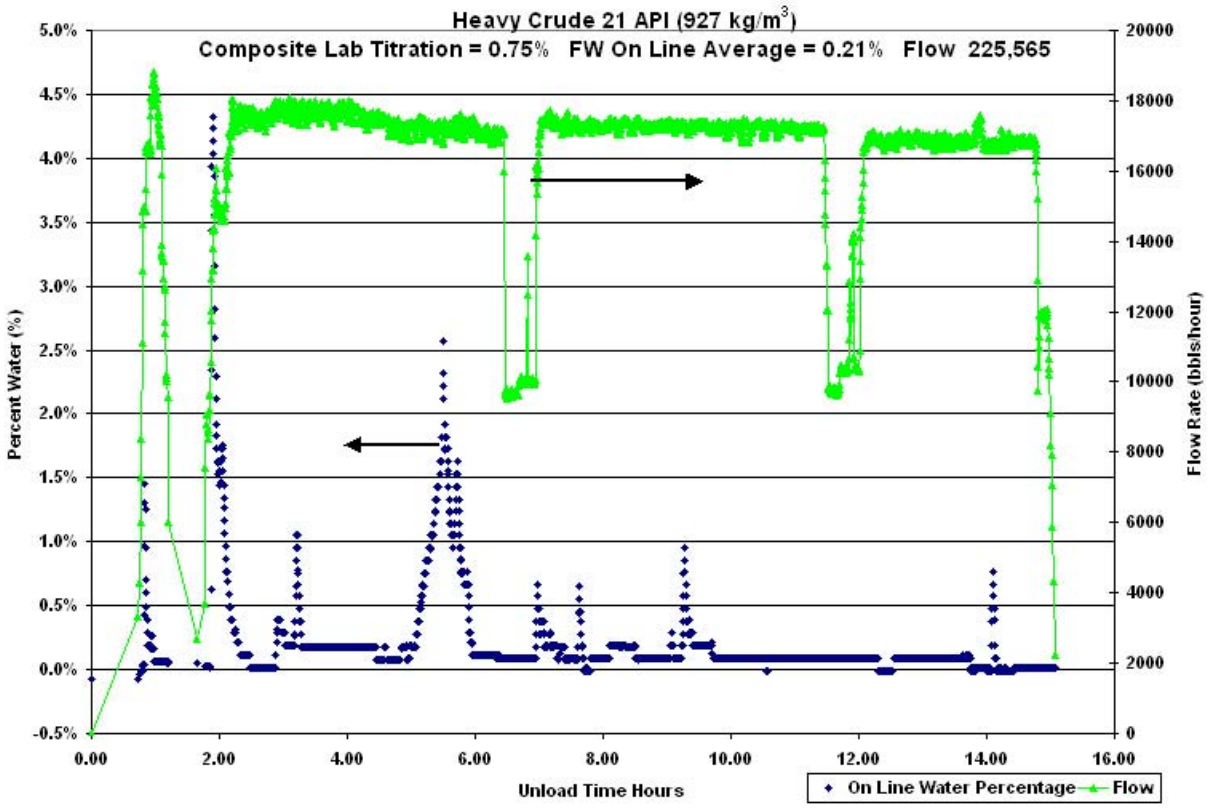

Figure 3. Heavy Crude Oil Ship Unloading Profile

The measurement of density affects the offset calculated for the on line water analyzer baseline and defines where zero water percentage is with respect to density. Was it simply an offset calculation problem or a density measurement issue? Did the sampler have trouble with the higher viscosity of this crude oil? Was there bias in handling the heavy, cold crude oil in the laboratory? Was there a chemical interference with the titration from some component in the crude oil? Although the chemical interference was suspected and partially proven, no answers to these questions were acceptable with enough certainty to be accepted as true. The composite sampler was correct because it was the standard.

4 – Uncertainty Components

In the petroleum industry the measurement of water cut using centrifuge could have the following uncertainty components (not all inclusive): sample probe location in the main pipeline (center 1/3, wall, top, bottom), sample probe size, valve type and size, upstream conditioning (mixer, elbow, two elbows), flow rate in main line, flow rate in sample probe, difference in pressure between line and atmosphere, temperature differences between ambient and liquid, sample container material, size and type of seal for lid, volume of sample, time before processing sample, mixing of sample before extraction to centrifuge tube, solvent type used, de-emulsifier type, temperature of centrifuge, oil type and viscosity, type of centrifuge tube, operator reading the meniscus, solids content, and clarity of the water.

Table 2 is a partial description of what may define systematic and random uncertainties. These components of the total uncertainty need to be separated and discussed as to the contributions in each portion of the measurement. The British Standard Methods for Sampling Petroleum Products, Part 2 (BS3195: Part 2:1989, IS)3171:1988) defines the formula for uncertainty calculations where the Relative Systematic Uncertainties are additive while the Relative Random Uncertainties are relational to one fourth of the sum of the squares of the relative random uncertainties. Relative uncertainty is the uncertainty of a factor divided by the value of the factor.

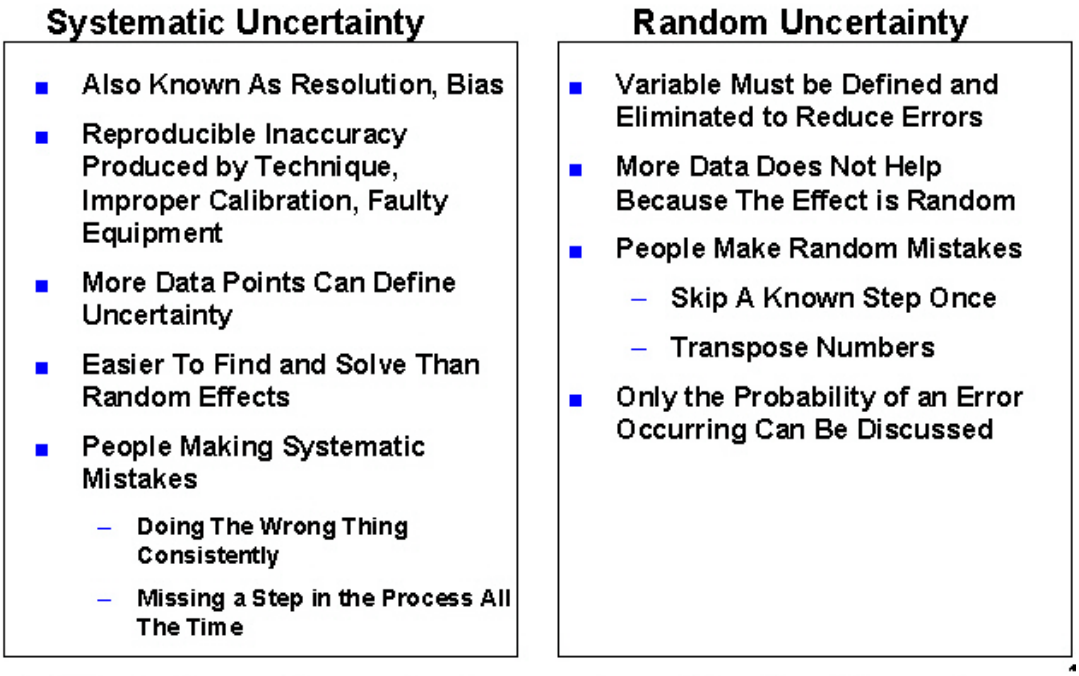

Table 2. How to Recognize Systematic and Random Uncertainty

As defined by the British Standard, there are two numbers for each line below, one for the systematic and one for the random uncertainty:

1. non-homogeneity of the water content
2. changes in the water content caused by sampling
3. uncertainty of the grab volume
4. uncertainty in the flow rate causing non-proportionality of sampling
5. changes in the water content during sampling
6. changes in the water content caused by sample handling and mixing
7. changes in the water content caused by transfer to laboratory apparatus

The systematic uncertainties add therefore, they are the most important source of errors.

5 – Sources of Uncertainty for a Composite Sampler

Table 3 suggests some of the uncertainty components for the composite sampler. Notice that many of these are related to people handling and inspecting the process. Although many can be automated for verification that the process is progressing during a batch sample, all cannot be controlled simply by monitoring. In the British Standard, description of the variables number one through four describe the expected issues with the sampler.

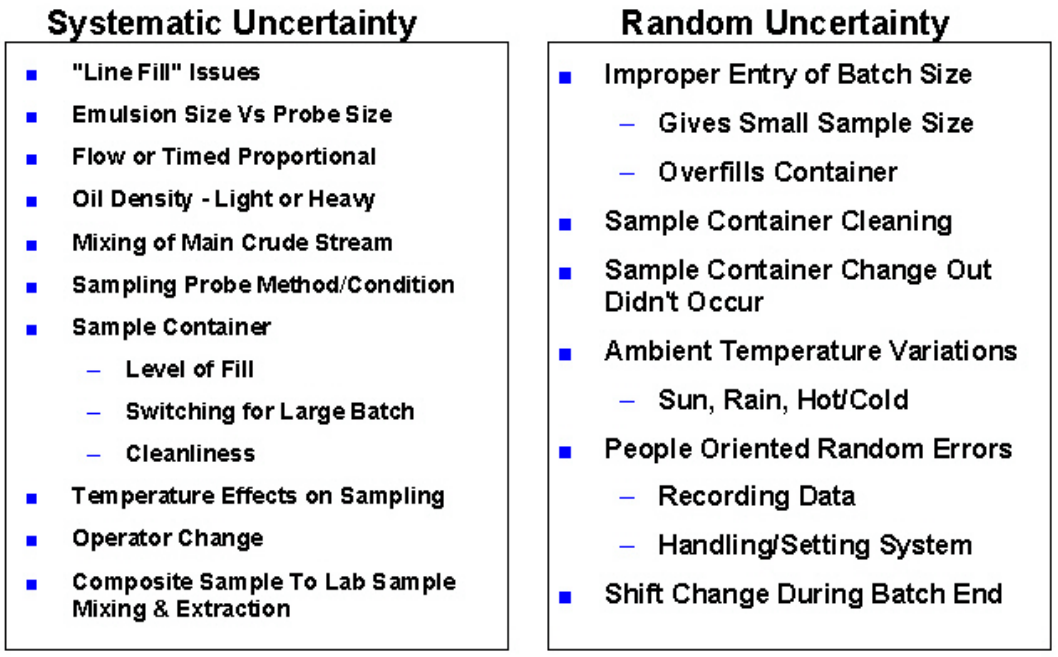

Table 3. Systematic and Random Components for Sampler System

6 – Sources of Uncertainty for a Laboratory Analysis

Table 4 suggests some of the uncertainties that may be found in the laboratory. In these steps the personnel become one of the most important influences to uncertainty. In the British Standard, description of the variables number five through seven describe the expected issues with the laboratory.

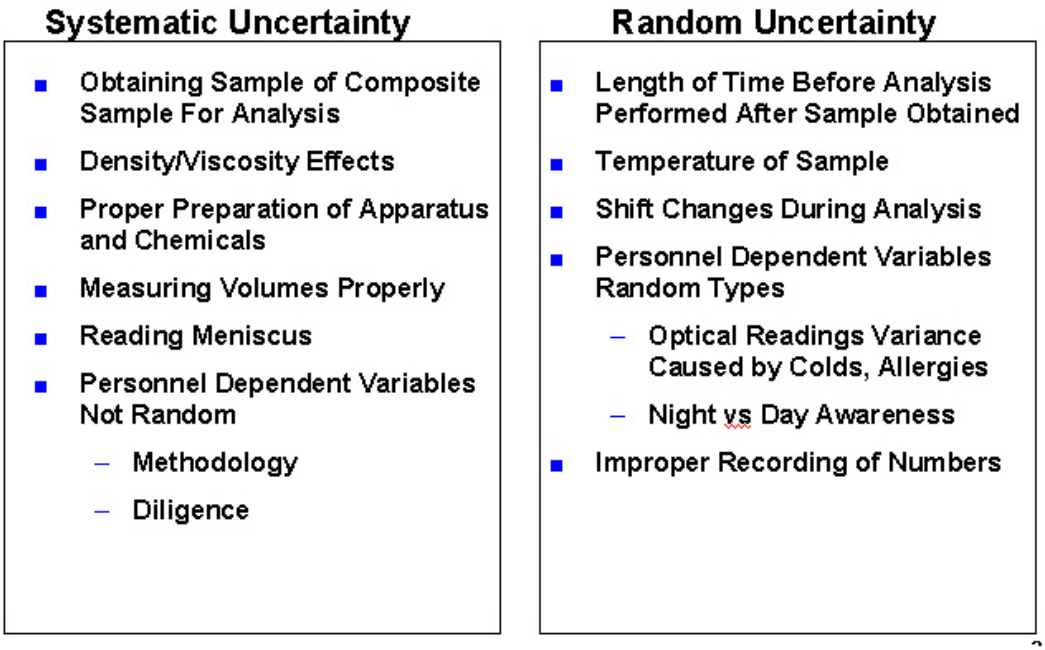

Table 4. Table for Laboratory Uncertainty

7 – Density Measurement Uncertainties

The typical online measurement of density has the potential for being affected by many influences. One of these is the ambient temperature variation in addition to liquid temperatures that are typically compensated. If the sun shines on the analyzer during the day and then turns cold and rains, it is possible that the density measurement is affected. Some vendors recommend insulation to prevent this and possibly a sun shield. The accuracy of the density measurement is stated by one vendor not to be "accurate" unless it is calibrated on that specific crude type. This is due to viscosity and other physical liquid variables. Temperature compensation using the actual liquid temperature measurement instead of making the measurement on the outside surface of the pipe can also affect the answer.

8 – On Line Water Analyzer Measurement Uncertainties

On line water analyzers must see a representative sample of the actual flowing stream just like the composite sampler probe. This has always been a requirement for any analysis for water content, density or sampling system. The analyzer will be only as good as the representative sample that is presented to the measurement section.

Systematic Uncertainty	Random Uncertainty
■ Density Input Wrong – Liquid Temperature Correction ■ Mixing Not Sufficient – Low Flow Rate – Improper Location ■ High Water Exceeding Range ■ Installation Issues – At Elbow, On Top or Bottom ■ Crude Oil Properties – Viscosity/Density/Emulsion ■ Calibration Improper	■ Ambient Temperature Issues? ■ Data Collection/Software Issues – Not Flow Proportional – Batch Signal Wrong – Reset Wrong

Table 5. On line Water Analyzer Uncertainty Table

There has been a lot of information improperly presented in the past as to how "wet oil density" versus "dry oil density" affects analyzers. As the water increases so does the density. The density correction for the baseline zero water content for typical permittivity based analyzers is approximately 0.03% change in water for a 1 kg/m^3 change in density. Therefore, for a 10 kg/m^3 change in density the change is 0.3% water. A summary of the impact is shown in Table 6. These results are with the oil density set at 860 kg/m^3 (approximately 32 API degree) and the water is a 3% salt content which give a water density of 1020 kg/m^3.

Density Oil	860			
Density Water	1020	3% Salt Water		
Absolute Water Percent	"Wet" density	Microwave Analyzer Offset Due To Density Oil+Water	Net Reading (%)	Wet/Dry Density Error (%)
0	860.00	0.000	0.00	0.00
1	861.50	-0.046	0.95	0.05
2	863.00	-0.092	1.91	0.09
3	864.50	-0.137	2.86	0.14
4	866.00	-0.183	3.82	0.18
5	867.50	-0.228	4.77	0.23
8	872.00	-0.363	7.64	0.36
10	875.00	-0.452	9.55	0.45
12	878.00	-0.540	11.46	0.54
15	882.50	-0.671	14.33	0.67
20	890.00	-0.887	19.11	0.89
30	905.00	-1.309	28.69	1.31
40	920.00	-1.717	38.28	1.72
50	935.00	-2.111	47.89	2.11

Table 6. Wet Density Effect on Water Analyzer

The solution is to hold the earlier density within the analyzer memory for excursions above say 5% water. Then the impact of the density is limited to a very small number as shown in Table 7.

Density Oil	860			
Density Water	1020			
Absolute Water Percent	"Wet" density	Microwave Analyzer Offset Due To Density Oil+Water	Net Reading (%)	Wet/Dry Density Error (%)
0	860.00	0.00	0.00	0.00
1	861.50	-0.05	0.95	0.05
2	863.00	-0.09	1.91	0.09
3	864.50	-0.14	2.86	0.14
4	866.00	-0.18	3.82	0.18
5	867.50	-0.23	4.77	0.23
8	872.00	-0.23	7.77	0.23
10	875.00	-0.23	9.77	0.23
12	878.00	-0.23	11.77	0.23
15	882.50	-0.23	14.77	0.23
20	890.00	-0.23	19.77	0.23
30	905.00	-0.23	29.77	0.23
40	920.00	-0.23	39.77	0.23
50	935.00	-0.23	49.77	0.23

Table 7. Hold Density Constant Over 5% Water Measured

9 – Method Comparison for Water Measurement

If no adjustment is made for the "dry oil density" then the data in Table 6 is close to being the error in water percentage for the on line analyzer for those given densities. Now a comparison between the sensitivities using a microwave water measurement which is based on the polar moment of the molecule (the permittivity or at lower frequencies and water percentages, the dielectric constant) and the calculation of water percent using density is made in Table 8. The microwave method is more sensitive to the water molecule because the parameter of measurement is the large difference between the small polar moment of crude oils (2.5) and the high polar moment of water (80). With this additional sensitivity the microwave method's ability to resolve water is approximately 33 times greater than that when density is used for measurement.

MW Water Analyzer	Densitometer & Water %
■ 2,000,000 Hertz Change in Frequency for a 1% Change in Water – Analyzer Primarily Sees **Water 1% / 2,000,000 Hz** ■ Approximately 0.03% Change in Water for a 1kg/m^3 change in Density – **0.03% / 1 kg/m^3** – Generally 33 Times Less Sensitive to Density Changes Than Using Density for Water Measurement	■ If Water has 3% Salt Then Density of Water is 1,030 kg/m^3 and Oil Density is 860 kg/m^3 then: – 0 - 100% Water is a change of 170 kg/m^3 – 1% change in Water is 1.7 kg/m^3 ■ If Water has 3% Salt and Oil Density is 960 kg/m^3 then: – 0 - 100% Water is a change of 70 kg/m^3 – 1% change in Water is 0.7 kg/m^3 ■ Density Highly Dependent upon Water – **Median 1% / 1 kg/m^3**

Table 8. Water Percentage Measurement by MW Analyzer & Density

10 – The Opportunity to Improve Oversight

The opportunity to use more than one independent measurement provides the ability to make a more educated choice as to what method may be less uncertain. Such an opportunity exists using a composite sampler and an on line water analyzer although the sampler results will be considered the correct answer by default. If an additional method was available then there exists an opportunity to better decide which may be the correct answer. The differences between the microwave and density determination of water were given in the previous section. Although these are not totally independent measurements they are sufficient to study as a course of action to better a measurement.

The first issue when using density for water percentage measurement is to determine the dry oil and the produced water density at flowing conditions. If this information can be determined, then the densitometer used for pipeline measurements becomes another check on the final answer to the question "what was the water in the pipeline." The answer lies in the fact that the water analyzer is capable of accuracy at higher water percentages with reduced sensitivity to density. The higher the water percentage the smaller a change in density from the on line

density when the low water density is used as in Table 7. The key to this method is to store all of the data for a batch process such as that for ship unloading, well testing or the like and then process the data at the end of the unloading or testing period. In addition, the ability to store the data and then sort it versus some variable such as density, water percentage or flow rate is of interest in the ease of processing the data.

11 – Sorting and Analyzing the Data

Figure 4 is the data from the first tanker shown in Figure 2 with the no flow rate cases removed and then the remaining data sorted by density.

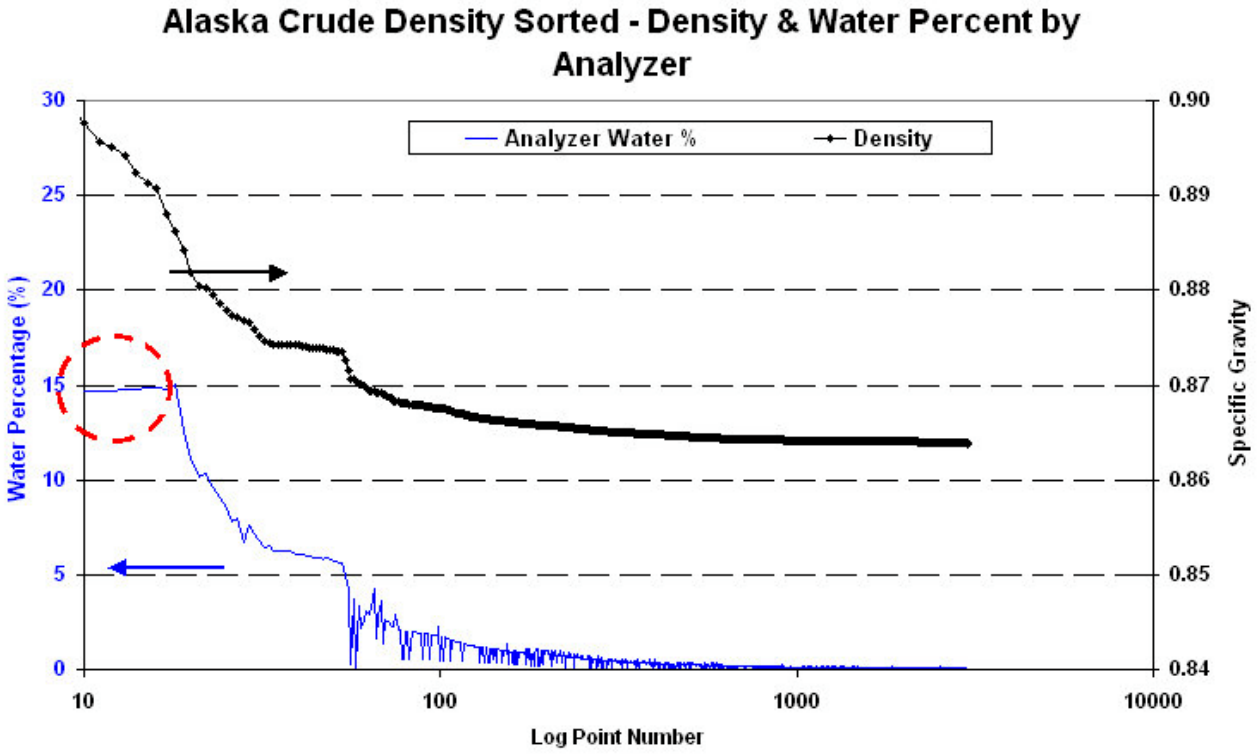

Figure 4. Data Sorted by Density From Figure 2

The circled region is where the water percentage exceeded the range of the analyzer and therefore it demonstrates how high the water can be at times. The region starting at 15% water cut and declining is selected to begin the analysis and the minimum specific gravity is used which corresponds to the minimum water percentage. In a simple iterative process a water percentage by density can be calculated to match with to the microwave analyzer's initial high water data points. The result of this analysis provides the following graph of Figure 5.The resulting density of the oil was 0.864 versus the laboratory of 0.867 and the water density was 1.025. There was no lab density of the water available but, this is close to the expected density from that region. The resulting conclusion is the three methods gave similar results.

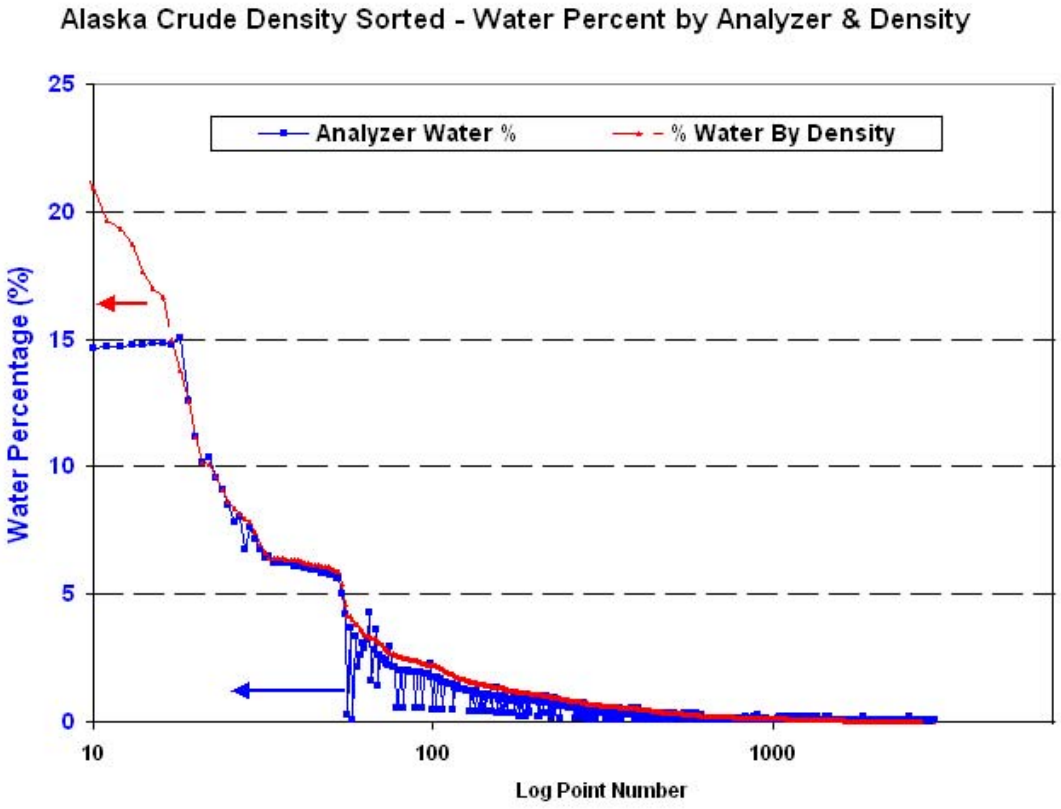

Figure 5. Alaska Water by Analyzer & Density

12 – Another Example

An example with a heavy crude taken from Figure 3 and sorted for density is shown in Figure 6. In this example the laboratory was at 0.75% water while the online analyzer average was 0.21%. Notice that the data is based on the log of the data point number so that the beginning fit to the water calculated by density is obvious. It appears visually that the analyzer would have a resulting average well below the laboratory.

This figure appears to demonstrate data for the density that contains much more noise than the data from the Alaskan crude oil data above. A look at the temperature during the discharge was a next step of analysis since the density is temperature corrected.

Figure 7 shows the temperature and water percentage with time on unsorted data. At several major points where the water was higher the temperature is lower which suggests that the water did not come along with the crude. Theoretically the temperature should be the same or a higher temperature due to the thermal capacity of water being so much higher than the crude oil.

From the observation with temperature the water analyzer was reset to use the line density without any temperature correction. This was not suggesting this is the right answer but instead to compare the results and curve shapes. Figure 8 shows the resulting water by analyzer that levels off to a reasonably consistent number. A question as to the validity of the temperature correction for density at the densitometer would be of interest at this point.

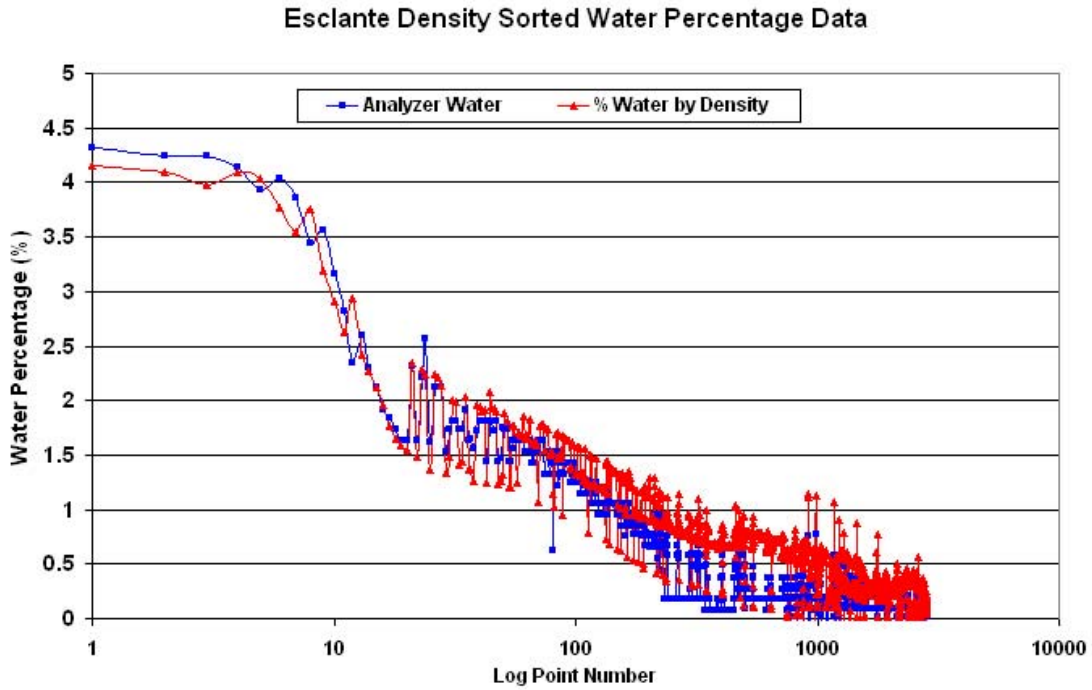

Figure 6. Figure 3 Sorted by Density Heavy Crude

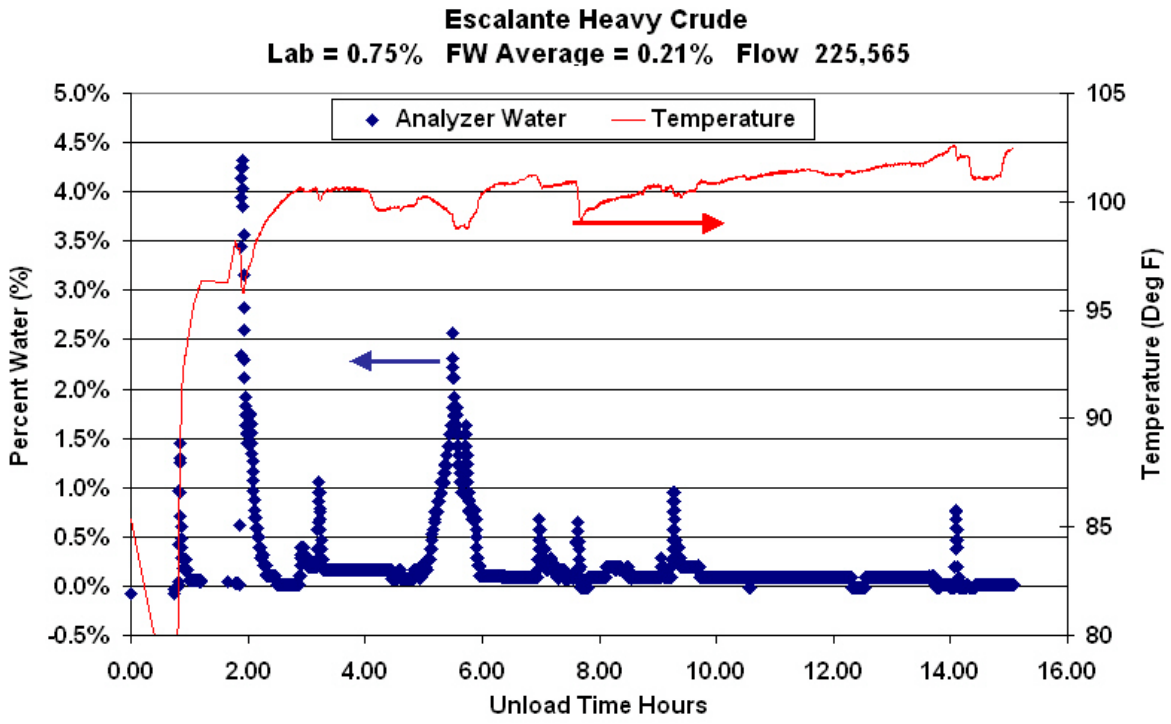

Figure 7. Unsorted Temperature & Water With Time

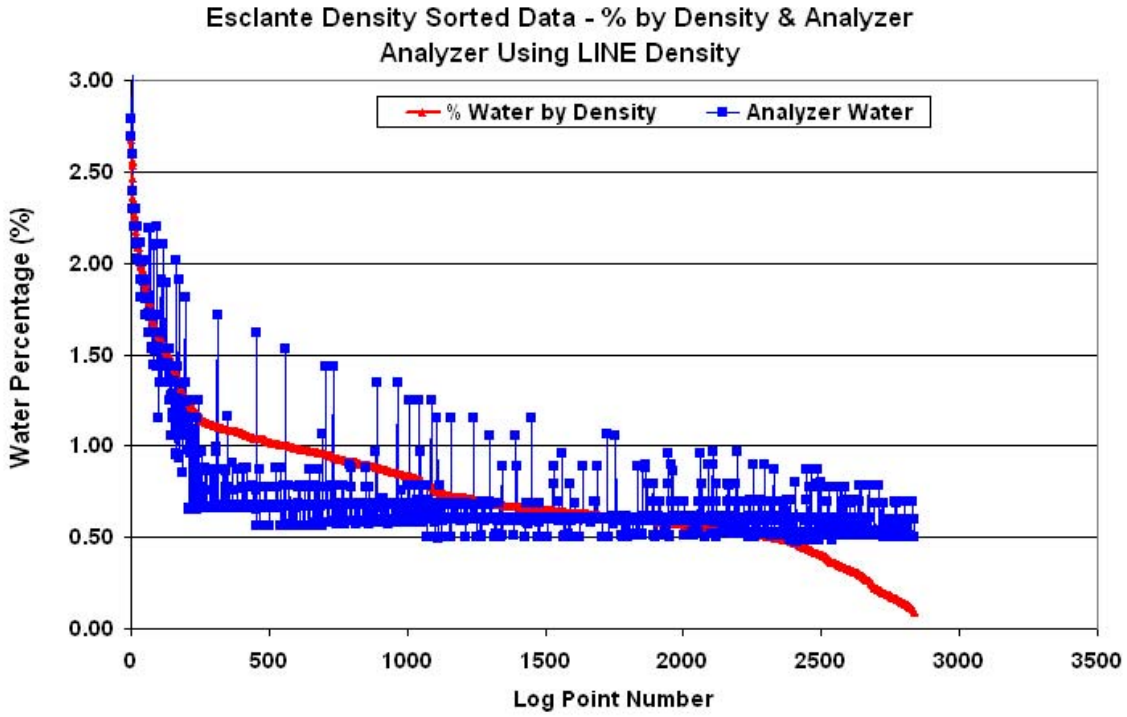

Figure 8. Water Analyzer Using LINE Density

13 – Conclusion

Although the composite sampler will be around for many more years, the on line real time companion may aid in improving the measurement. In addition, data techniques may allow an independent set of measurements by which validation of the results can be compared. When differences occur, they can be identified and resolved if the data obtained during routine operation can determine that a question should be asked. The data obtained from composite samplers is not real time and can only provide answers that are obtained by human involvement after the batch has left the station. Analytical measurement coupled with the computing power that is now available will change the way pipeline data on water cut is collected and analyzed. Methods to prove the viability of this approach are just now being tested. Among the remaining things to be understood and defined are how to automatically process the data and alert an operator that some further inspection of the data or comparisons are required.

With the current price of petroleum products exceeding US$50 per barrel, methods to measure and validate the transfer of crude oil must be improved. Real time on line analyzers should become a valuable tool in this pursuit of a better measurement. If the real example in Figure 3 was used where the difference of 0.54% in water delivered between the composite sampler (0.75% water) and the on line analyzer (0.21%) across 225,565 barrels would be a difference of US$60,903.

The greatest difficulty in moving the technology ahead is the lack of top level management stating that these issues need to be investigated and resolved. Taking data and looking for answers to questions that have not been asked before is time consuming and costly. Independent

vendors will require additional help in the future to truly solve the issues for fiscal measurement and to bring these into this century.

14 – Acknowledgements

This paper would not have been possible without many diligent companies looking for answers to problems in their operations. The time to collect and properly analyze samples is time consuming and requires dedicated personnel. The data shown in this paper represents many man years of work. Many thanks are given to each and every person that have assisted in the collection, processing and transfer of the information which led to this paper. The companies who have allowed data to be collected and questions to be asked include but are not limited to the following: Shell Pipeline, Marathon, BP, ARCO Pipeline, Husky Oil, EXXON, Phillips Petroleum.

15 – References

1. Scott, Bentley N., Uncertainties in Pipeline Measurement. *Proceedings of IPC 2004 International Pipeline Conference*, Calgary, Alberta, Canada. IPC04-0046, October 4 - 8, 2004.

Flow Disturbances and Flow Conditioners: The Effect on Multi-beam Ultrasonic Flowmeters

Jankees Hogendoorn, KROHNE Altometer
André Boer, KROHNE Altometer
Dick Laan, KROHNE Altometer

---

1. INTRODUCTION

Over the past years a lot of experience with the five beam ultrasonic flowmeters on fiscal applications has been obtained [1], [2], [3]. Ultrasonic flowmeters have gained full acceptance and customers are using the five beam ultrasonic flowmeters in a growing number of fiscal transfer metering applications worldwide. More recently, three path ultrasonic flowmeters have been introduced for custody transfer applications [4]. The success of ultrasonic flowmeters can be attributed to their inherent benefits: no moving parts, no wear, low pressure drop, wide rangeability and minimal maintenance.

Many National Weights and Measures Authorities worldwide have approved the use of ultrasonic flowmeters for fiscal metering. An important step forward in the acceptance of ultrasonic flowmeters is the release of a standard by the American Petroleum Institute (API) "Measurement of Liquid Hydrocarbons by Ultrasonic Flow Meters" in February 2005 [5],[6].

Now that custody transfer flow measurement with multi path ultrasonic flow meters are increasingly accepted in the market, further development has been focussed on increasing robustness of installation and on simplifying calibration, commissioning and operating procedures. We have found that proper flow conditioning is an essential part of this development.

This paper describes the experience with different types of flow straighteners focussing on:

- Constructional aspects
- Effects on linearity
- Effects on disturbances
- Effects on turbulence intensity

2. FLOW CONDITIONERS: CONSTRUCTIONAL ASPECTS

2.1 ISO tube bundle flow straightener

The ISO tube bundle flow straightener (according to ISO/DIS 5167-2) consists of 19 tubes arranged in three concentric circles. The length of the bundle 'shall be between 2D and 3D, preferably as close to 2D as possible' [7]. Attention must be paid to a number of geometrical issues as mentioned in the ISO-standard.

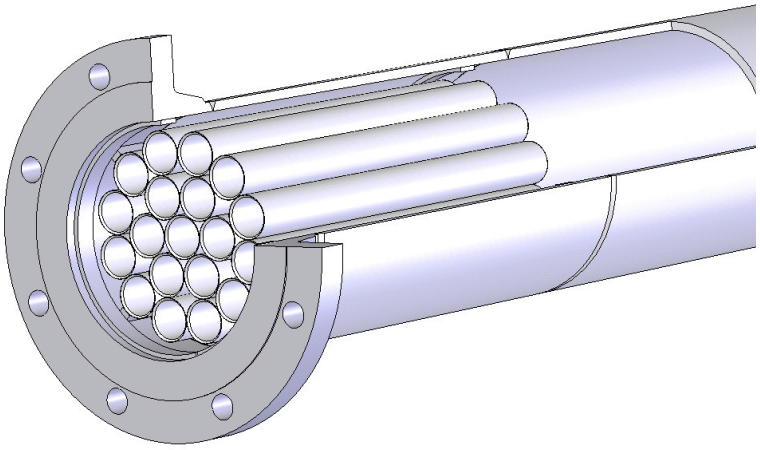

Figure 1 Example of a tube bundle flow straightener according to ISO/DIS 5167-2.

One of the important remarks in the standard is that 'it is important to ensure that the tubes are parallel to each other and to the pipe axis'. If this is not the case the resulting flow profile will be non-symmetric. Even a swirling flow can be introduced.

An extensive flow investigation has been done to gain understanding of the effects of production tolerances on flow profiles.
A glass model of the ultrasonic flowmeter has been build which was mounted in a flow loop. This test rig was filled with a liquid with a refraction index equal to that of the glass. This enables us to carry out precise LDA measurements at any arbitrary spot in the flowmeter (see Figure 2).

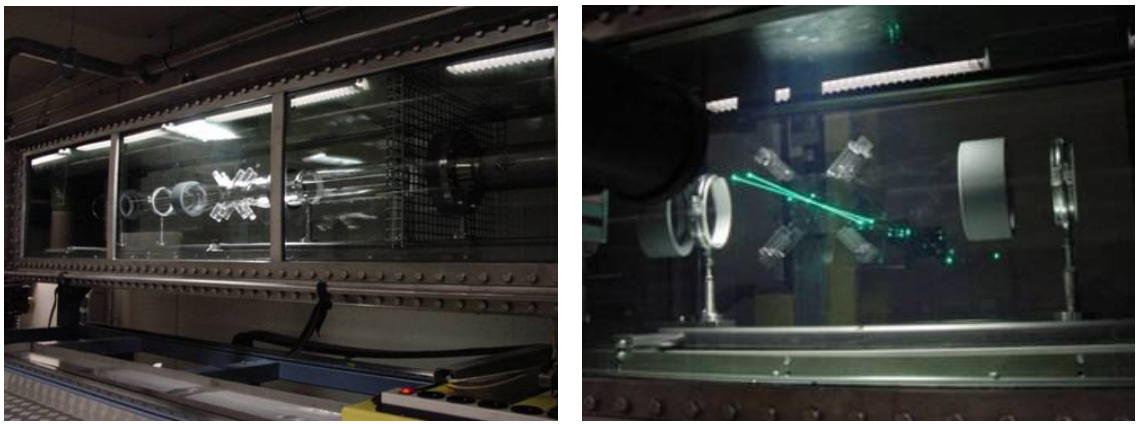

Figure 2 Experimental test rig in which the refraction index of the glass model flowmeter and the liquid are equal.

Figure 3 illustrates the sensitivity of the flow profile to the design and construction of an ISO tube bundle. During this test it turned out that the measured velocity profile was fairly non-symmetric for Reynolds number 3900 and higher (filled markers).
The results indicated by the filled markers were obtained with a tube bundle that was constructed in accordance with the ISO standard. This was confirmed by inspection afterwards.

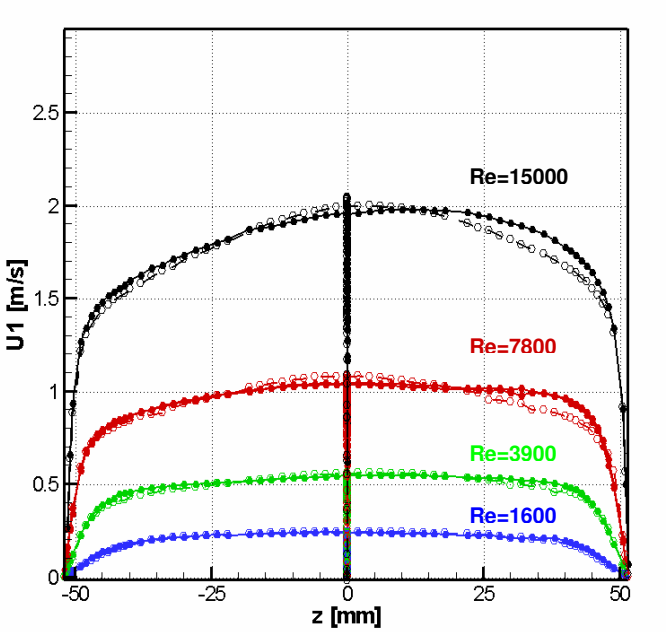

Figure 3 Velocity profile in vertical direction measured with LDA. Filled markers indicate the velocity profile about 7D behind an ISO tube bundle which is not properly constructed. The open markers indicate the velocity profile measured with a properly produced tube bundle.

We conclude that the tube bundle must be build very carefully. A regular check during the different phases in the manufacturing process is very important. Inspection afterwards is not sufficient, since important dimensions can not be measured after completion anymore. We implemented our additional procedures on top of the ISO specifications.
If these procedures are applied, the quality of the velocity profile is guaranteed (open markers). Furthermore, the experience is that a bundle length of 4D is required.

2.2 Etoile flow conditioner

Because the proper construction of an ISO tube bundle is complicated, we have looked at much simpler alternatives such as the Etoile flow conditioner.
The construction of an Etoile conditioner is based on three plates in a star-like configuration (see left-hand figure of Figure 4).

Also for the design of the Etoile flow conditioner it holds that a number of requirements must be fulfilled. The construction must be simple from the manufacturing point of view. So, the number of parts must not be too large, and it must not be too difficult to meet the production tolerances. Otherwise, the conditioner becomes too expensive.
Another requirement is that the construction must be stable during operation. Vibrations and resonance modes must be prevented in order to avoid undesired whistling sounds and rupture due to fatigue.
Since the construction of an Etoile Flow Conditioner is based on plates a thorough resonance analysis has been carried out.

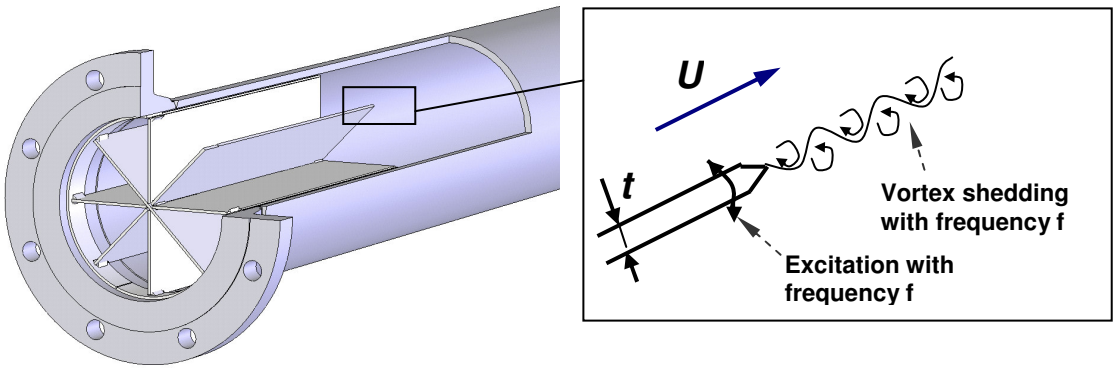

Figure 4 The construction of an Etoile flow conditioner is based on three plates that are put together. At the very end of the conditioning plates (trailing edge) vortex streets are created. As a result of this vortex shedding, an alternating pressure is acting on the conditioning plates.

From literature it's well-known that vortices are generated behind a bluff body and behind a flat plate. As a result of these vortices, an alternating force is acting on the conditioner plate (see right-hand figure of Figure 4). In the case that the vortex frequency matches the resonance frequency of the plate, the oscillation of the plate is amplified.
The vortex frequency is given by the simple relation:

$$\mathrm{Sr} = \frac{f \cdot t}{U} \qquad \text{Eq. 1}$$

Where: U=flow velocity [m/s], f=vortex frequency [Hz], t= thickness of the plate [m] and Sr is the Strouhal number [-].

In this relation the Strouhal number can be considered as constant over the normal flow range with a value of about 0.2. As a consequence the excitation frequency is directly proportional to the flow velocity.
This implies that with increasing flow velocity the excitation frequency increases (blue line in Figure 5).

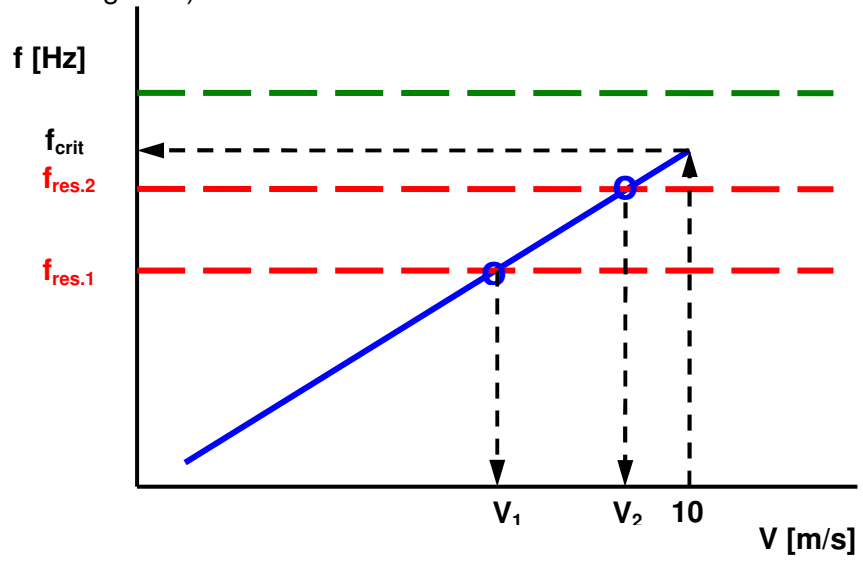

Figure 5 Blue line: relation between vortex frequency and flow velocity (Eq.1), Red lines: resonance frequencies of the conditioner that are in the normal operating range,

amplification occurs at v_1 and v_2,, Green line: resonance frequency of the conditioner above the maximum vortex frequency, $f_{crit.}$.

Because of this mechanism the construction is excited by a frequency band. If a certain frequency matches the resonance frequency of the construction, amplification occurs (crossing of blue solid line with red dashed lines in Figure 5). The solution is to increase the stiffness of the construction in such a way that the resulting resonance frequency becomes higher than the highest excitation frequency f_{crit}. (green line in Figure 5).
This mechanism has been confirmed both by numerical analysis and experiments. An example is shown in Figure 6. The numerical analysis of an Etoile straightener (3 inch pipe) shows the first resonance frequency at 394 Hz.

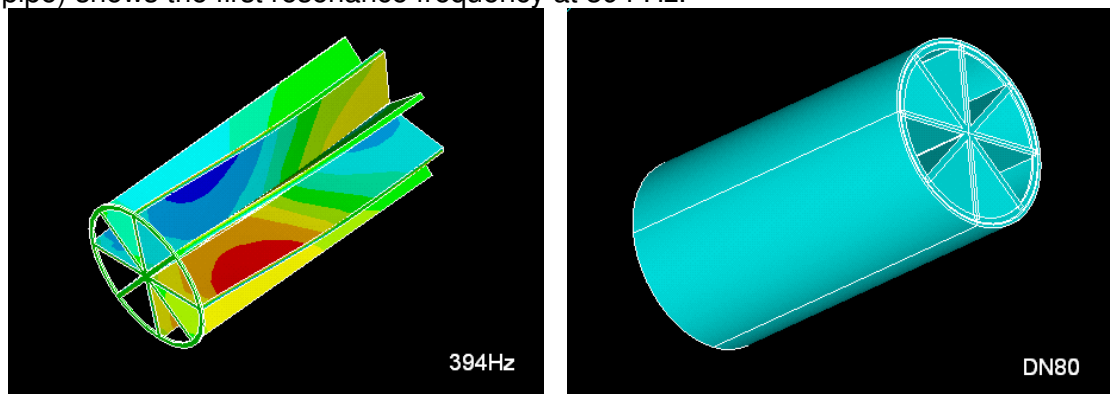

Figure 6 Resonance frequency analyses (3 inch) of an Etoile flow conditioner. The conditioner is fixed to the pipe just in the front by means of a ring. The colors indicate the strain.

According to eq. 1 the flow velocity at this vortex frequency corresponds to 5.9 m/s (with t=3 mm). Experiments in a test rig with equally constructed Etoile flow conditioner generated a whistling tune at 6 m/s. The whistle frequency that has been measured was 378 Hz. This example illustrates that the dynamic behaviour of the Etoile flow conditioner can be predicted fairly accurate.

Depending on the stiffness of the construction more or less resonance frequencies are observed. In a worst case scenario, an Etoile flow conditioner can have several resonance frequencies in the operational flow range. The first mode (with lowest frequency) can be suppressed by welding the conditioning plates to the pipe at several spots in the axial direction. Even than, different resonance modes are still possible, as shown in Figure 7.

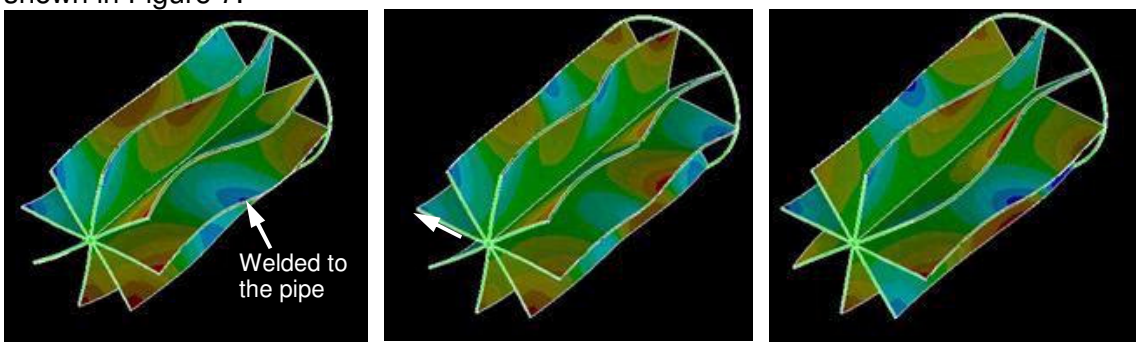

Figure 7 Example of different resonance modes of an Etoile flow conditioner in a three inch pipe. In this configuration the plates have been welded to the pipe on one spot half way the length of the plate.

Important is the requirement that the design must made in such a way that it still can be manufactured.

Design guidelines have been developed for the diameter range starting at 2 inch up to 10 inch. If these design guidelines are followed, resonance will not occur in the normal flow range up to 10 m/s.
The design of sizes of 10 inch and larger is more complex. The plates are getting less stiff and welding to the pipe along the entire length seems unavoidable. However, this is not practical during manufacturing. Increasing the stiffness by increasing the plate thickness won't help: the mass that is added destroys the stiffness that is gained.

3. EFFECT OF FLOW PROFILE DISTURBANCES

3.1 Linearity without flow conditioner

As a first step the linearity has been established in a piping configuration without flow conditioner and without active flow profile disturbances. Three uncorrected linearity curves of a three path ultrasonic flowmeter (3") are shown in Figure 8. A non-linearity of about ±0.2% is observed.

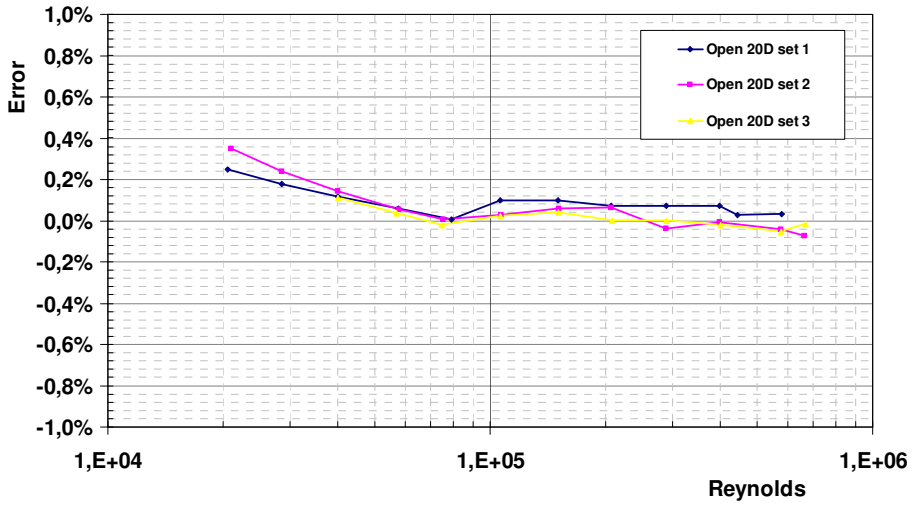

Figure 8 Three uncorrected linearity curves of a three path UFM. No flow conditioning measures have been taken.

3.2 Effect on linearity with an Etoile flow conditioner

Figure 9 shows the linearity of a three path UFM in combination with an Etoile flow conditioner.

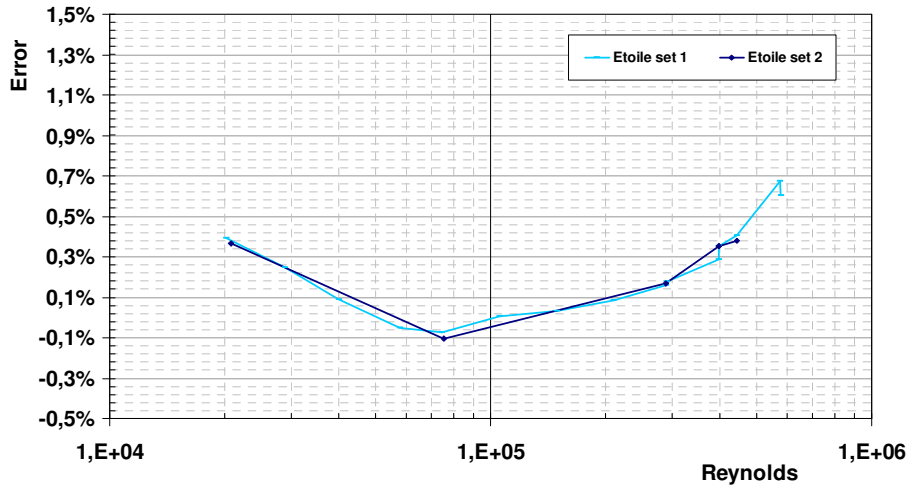

Figure 9 Linearity of a three path UFM with Etoile flow conditioner mounted in a 10D inlet pipe run.

If we compare Figure 9 with Figure 8 it can be observed that an Etoile flow conditioner introduces a non-linearity even in the absence of any disturbance. Whereas the linearity without flow conditioner is about ±0.2%, the linearity now has increased to about ±0.3%. This result is disappointing because the linearity becomes worse. Furthermore, the linearity curve doesn't become horizontal at higher Reynolds numbers.

3.3 Effect on linearity with an ISO tube bundle flow straightener

The effect of an ISO tube bundle straightener is shown in Figure 10. There is no significant change in linearity as a result of the tube bundle. The overall linearity is clearly within ±0.2%.

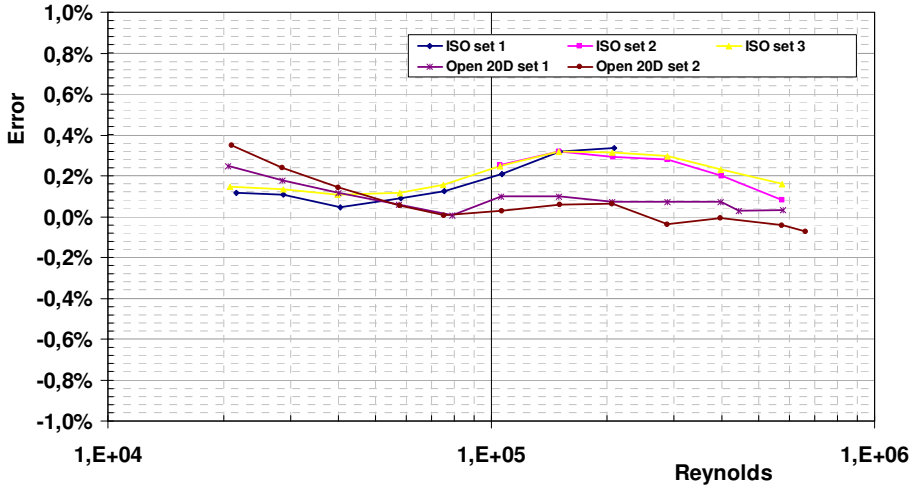

Figure 10 Linearity curves of a three path UFM with ISO tube bundle at 10D compared to the linearity curves without flow conditioner.

3.4 Effects on linearity of different types of disturbances

Different types of disturbances have been used. An overview of the disturbing plates is given in Figure 11. In addition two space bend configurations have been used. One in a normal position, the other 90º rotated along the axial axis.

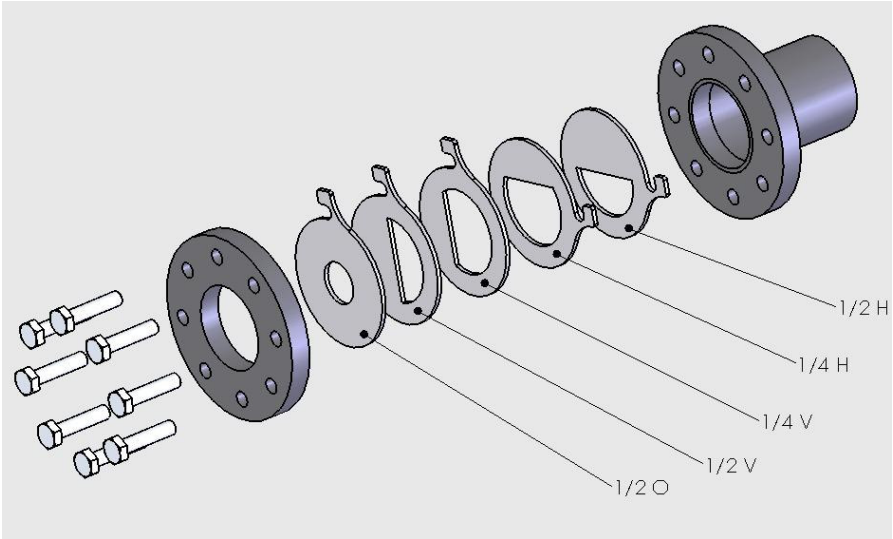

Figure 11 Five standardized flow profile disturbing plates; orifice plate with an inner diameter of ½ D (indicated by ½ O), plate of which half the diameter is blocked in

vertical (½ V) and horizontal (½ H) direction and a plate of which a quarter of the diameter is blocked in vertical (¼ V) and horizontal (¼ H) direction.

These disturbances have been offered to a three path UFM (ALTOSONIC III) in a configuration without flow conditioning. The disturbances have been introduced 20D upstream of the flowmeter. An overview of the result is shown in Figure 12.

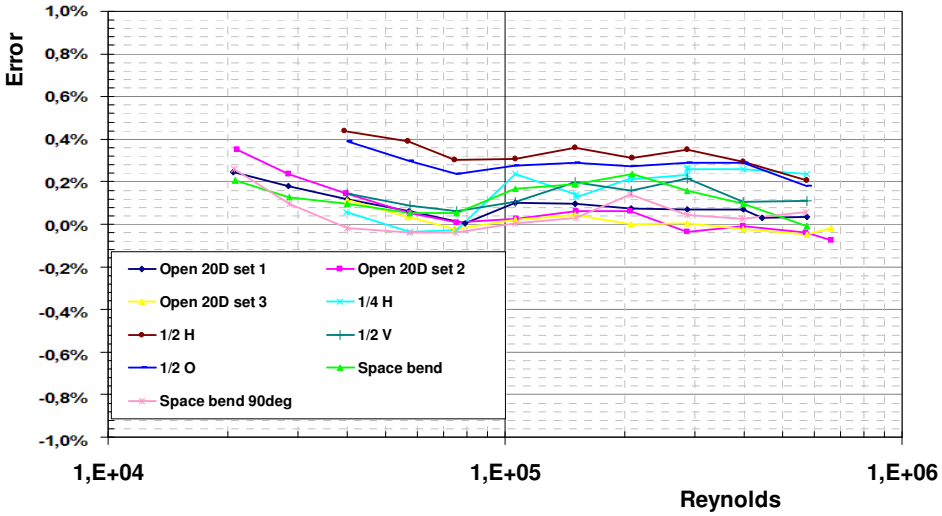

Figure 12 Effect of disturbances on a three path UFM without flow conditioner.

From this figure it can be observed that all curves fall within a bend of 0.4%. It is interesting to see that if there is a shift as a result of a disturbance, the shift is always positive.
Furthermore, it can be seen that the linearity is hardly affected. There is one exception. This is the ¼ V disturbance. The effect of this disturbance turns out to be twice as large as the effect of the ½ H which is 2nd worst.

3.5 Effect of flow disturbances with an Etoile flow conditioner

The attenuating effect of an Etoile flow conditioner is disappointing. Figure 13 shows, the effect of two types flow profiles disturbances (¼V and ¼H). The effect of the ¼V disturbance is even amplified.

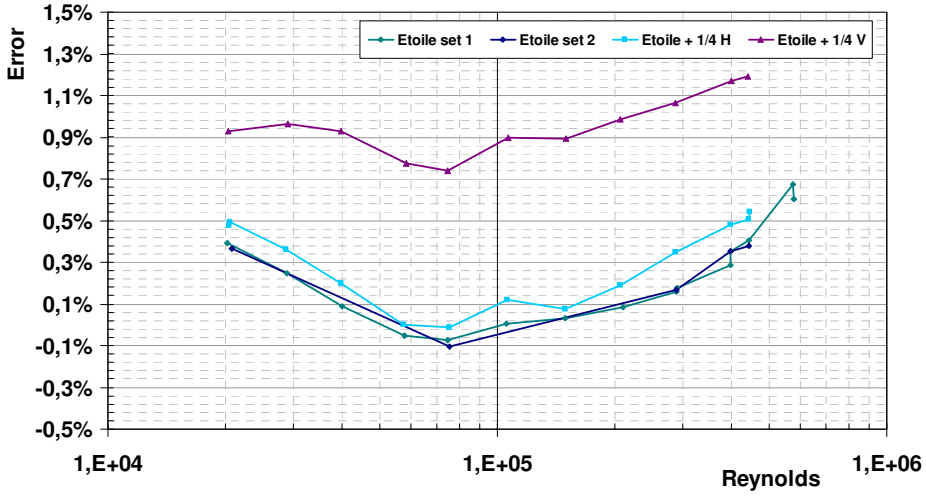

Figure 13 Effect of two different flow profile disturbances with an Etoile flow conditioner.

The linearity is not affected that much. As it was the case in the configuration without straightener, the meter shows an over reading in case of a disturbance here as well.

3.6 Effect of flow profile disturbances with an ISO tube bundle straightener

Extensive tests have been carried out on the sensitivity to flow profile disturbances of a three path UFM in combination with an ISO tube bundle flow straightener. An overview of the results is shown in Figure 14. An initial linearization (for the basis non-linearity observed in Figure 10) has been applied. It is important to note that the scale resolution of the vertical axis is twice as big as in the other figures.
From Figure 14 can be concluded that the linearity is hardly affected in this Reynolds range.

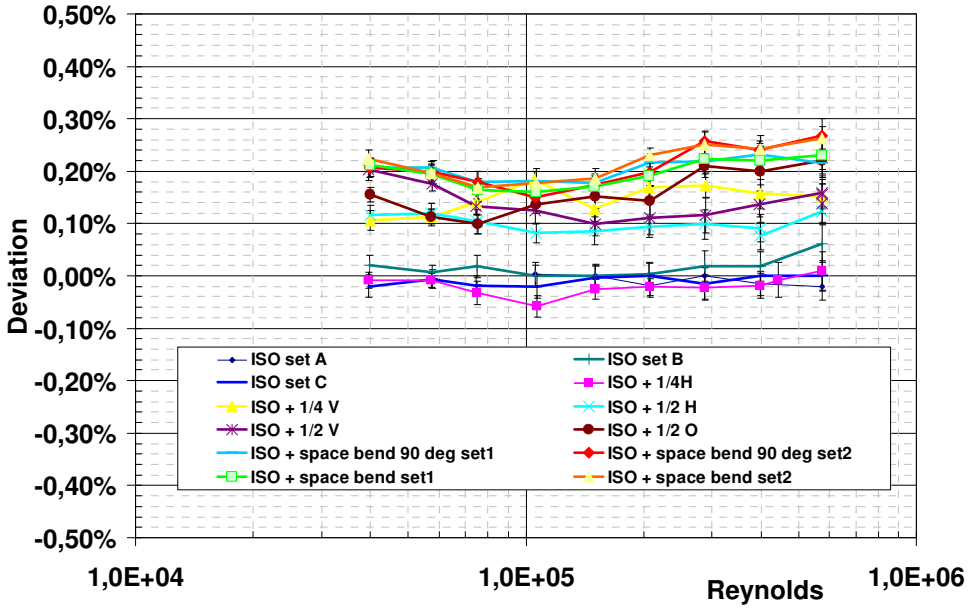

Figure 14 The effect of flow profile disturbances on a three path UFM using an ISO tube bundle flow straightener. The disturbances have been offered 10D upstream of the ISO tube bundle.

The effect on linearity is only about ±0.05%. Furthermore, the shift is always positive. Another very important conclusion is that the value of the shift is relatively low. About 0.1% to 0.2%.
This result shows that if proper measures are taken, the three path ultrasonic flowmeter reading stays within ±0.15% for all disturbances that have been tested.

4. EFFECT ON TURBULENCE INTENSITY

4.1 Turbulence intensity measurements

Turbulence intensity does have an effect on short term repeatability of an UFM. Since an UFM measures the velocity without interfering with the flow, turbulence is being measured as well. There are no inertial forces in the measuring principle that averages out the effect of turbulence. The consequence is that turbulent noise is measured on the actual flow. This can lead to a somewhat longer calibration run in order to get the right repeatability [1], [8], [9]. The higher the turbulence intensity, the stronger the effect is.
Flow straighteners do affect the turbulence intensity significantly. A very direct measure of the effect of turbulence intensity on an ultrasonic flowmeter is the standard deviation that is being measured by the flowmeter. The result of different configurations is shown in Figure 15. The relative standard deviation on the vertical axis is the standard deviation at that specific Reynolds number related to the average velocity at that Reynolds number.

The velocity which is used, is the velocity composed of velocities that are measured along the acoustical paths at three fixed positions in the pipe.

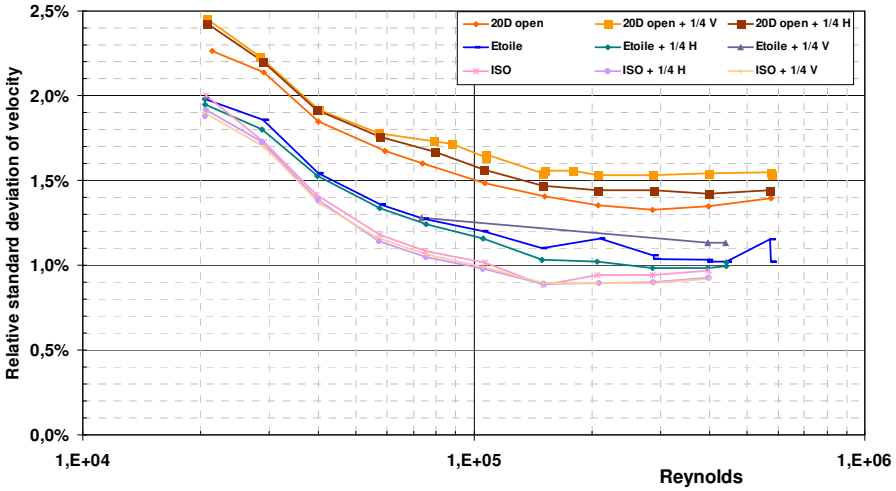

Figure 15 Relative standard deviation of the velocity as function of Reynolds for three different flow straighteners in combination with two flow profile disturbances.

Three different piping configurations have been used: a configuration without flow conditioning measures, a configuration with the Etoile flow conditioner and one with the ISO tube bundle straightener. It can clearly be seen that the configuration without flow conditioning results in the highest turbulence intensity. The configuration with the lowest intensity is the set-up with the ISO tube bundle. From the physical point of view this is expected. The smaller the straightener holes, the smaller the turbulent eddies are and the lower the measured turbulence intensity is.
It can also be observed that the effect of flow profile disturbances is the smallest when using the ISO tube bundle. No significant difference can be noticed between the undisturbed configuration and the situation where the horizontal and vertical disturbance is applied. This is not the case in the configuration with the Etoile conditioner and without conditioner. Especially in the configuration without flow conditioner the relative standard deviation increase to values above 2.0% in case of a disturbance where half the area is blocked (½H and ½V) for Reynolds numbers above 10^5.
Figure 16 shows the effect of a number of flow profile disturbances on the relative standard deviation. It interesting to observe that there is no significant difference.

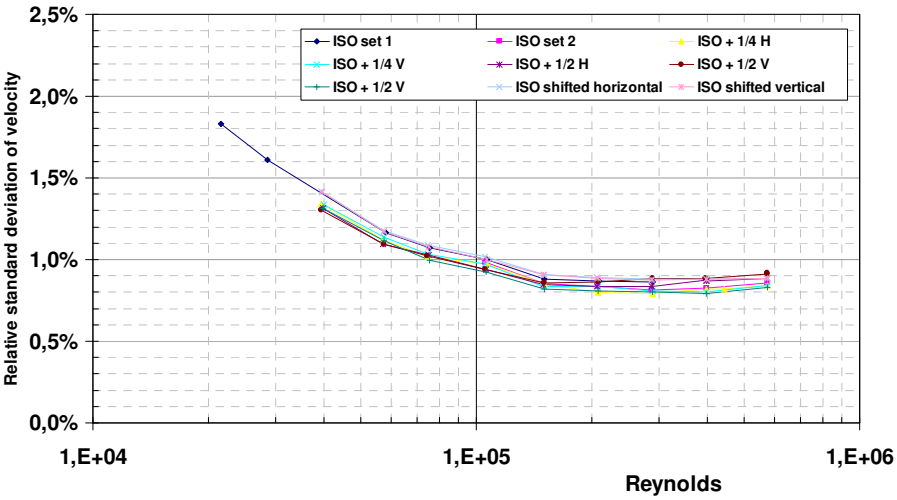

Figure 16 Relative standard deviation of the velocity as function of Reynolds for a configuration with an ISO tube bundle straightener in combination with a number of flow profile disturbances.

It is very important to note that these relative standard deviation measurements are a result of integration along a line (acoustical path). Furthermore, the path configuration is fixed. The velocity profile changes with Reynolds number and the turbulence intensity distribution changes as well. If LDA measurements are carried out in the centre of the pipe on one spot to determine the turbulence intensity as a function of Reynolds, the figure would look totally different. In that case the turbulence intensity would increase with increasing Reynolds number.

5. CONCLUSIONS

Knowing the effect of flow conditioning and upstream disturbances on ultrasonic flowmeters allows design of metering systems less influenced by the environment it is installed in thus simplifying commissioning and operation procedures. In addition this knowledge enables the application of new (offsite) calibration concepts and procedures.

5.1 Constructional aspects

Analysis has shown that both the Etoile and ISO tube bundle flow conditioner must be constructed carefully.
The Etoile conditioner easily suffers from resonance frequencies leading to whistling tunes and even damage due to fatigue. For sizes of 10" and larger it is getting very difficult to develop straight forward design rules in order to get a stable flow conditioner which can be manufactured easily.
The ISO tube bundle must be constructed carefully as well. If the tube bundle is manufactured inaccurate the resulting flow profile shall be non-symmetric and even can have a swirl.

5.2 Linearity

In general the linearity is not improved by using flow straighteners. The effect of an ISO tube bundle is not strong in the Reynolds range that has been studied. The Etoile flow conditioner clearly leads to an additional non-linearity.

5.3 Repeatability

The ISO tube bundle straightener improves the repeatability with a factor of two. This is independent whether there is a flow profile disturbance or not. When using an Etoile conditioner there is still some influence of flow profile disturbances on the short term repeatability. This is not the case with an ISO tube bundle. Consequently, it is advised to always install an ISO tube bundle to generate optimal proving conditions.

5.4 Effect of flow profile disturbances

The ISO tube bundle straightener is much more effective than the Etoile conditioner. Based on experiments with many types of disturbances, it can be concluded that, if there is a shift, the shift is always positive. The maximum shift that has been observed is 0.2%.
The shape of the linearity curve remains similar when using an ISO tube bundle. Furthermore, it has been observed that an ISO straightener reduces the effect of a disturbance approximately with a factor of two.
The Etoile conditioner is less effective. In fact, no improvement with respect to flow profile effect reduction has been observed. This does not imply that the Etoile conditioner is worthless. CFD analysis has shown that in specific cases of unstable flow profiles, the Etoile flow conditioner can be helpful [10].

Summarizing, it can be concluded that a three-beam ultrasonic flowmeter (ALTOSONIC III) stays within ±0.15% (for the disturbance types that have been tested)

when using an ISO tube bundle. This conclusion can be made on the condition that the ISO tube bundle is constructed carefully.

6. REFERENCES

[1] Trond Folkestad, Proving a fiscal 5 path Ultrasonic Liquid Meter with a Small Volume Prover Norsk Hydro ASA Can it be done?, NSFMW 1999.

[2] Maron J. Dahlström, Two years of fiscal performance by the liquid 5path Krohne ALTOSONIC-V Saga Petroleum ASA ultrasonic meter at the Vigdis/Snorre Crossover measurement station, NSFMW 1999.

[3] Jankees Hogendoorn, Experience with Ultrasonic Flowmeters in Fiscal Applications for Oil (-products), NSFMW 1999.

[4] Jankees Hogendoorn, ALTOSONIC III – A Dedicated Three-beam Ultrasonic Flowmeter for Custody Transfer of Liquid Hydrocarbons, NSFMW 2004.

[5] André Boer, Draft API standard “Measurement of Liquid Hydrocarbons by Ultrasonic Flowmeters Using Transit Time Technology”, NSFMW 2003.

[6] Manual of Petroleum Measurement Standards, API MPMS 5.8, first edition February 2005.

[7] ISO/DIS 5167-2, 1999.

[8] Maron J. Dahlström, KROHNE ALTOSONIC V, with master meter approach – Rough road to success with oil ultrasonic fiscal meter at the Snorre B export station, paper 18, NSFMW 2003.

[9] Trond Folkestad, Testing a 12” KROHNE 5-path ALTOSONIC V ultrasonic liquid flowmeter on Oseberg crude oil and on heavy crude oil, NSFMW 2001.

[10] A. Hallanger, CFD Analyses of the Influence of Flow Conditioners on Liquid Ultrasonic Flowmetering. Oseberg Sor – A Case Study, NSFMW 2002.

7. ACKNOWLEDGEMENT

The authors like to thank their colleagues from the KROHNE R&D team for the valuable input for this paper.

23rd International North Sea Flow Measurement Workshop
Tønsberg, Norway, 18 - 21 October 2005

LIQUID ULTRASONIC FLOW METERS FOR CRUDE OIL MEASUREMENT

Raymond J. Kalivoda, FMC Measurement Solutions, 1602 Wagner Avenue, Box 10428 Erie, Pennsylvania, U.S.A.
Per Lunde, Christian Michelsen Research AS (CMR), Box 6031 Postterminalen, N-5892 Bergen, Norway.

ABSTRACT

Liquid ultrasonic flow meters (LUFMs) are gaining popularity for the accurate measurement of petroleum products. In North America the first edition of the API standard "Measurement of liquid hydrocarbons by ultrasonic flow meters using transit time technology" was issued in February 2005. It addresses both refined petroleum products and crude oil applications. Its field of application is mainly custody transfer applications but it does provide general guidelines for the installation and operation of LUFM's other applications such as allocation, check meters and leak detection.

As with all new technologies performance claims are at times exaggerated or misunderstood and application knowledge is limited. Since ultrasonic meters have no moving parts they appear to have fewer limitations than other liquid flow meters. Liquids ultrasonic flow meters, like turbine meters, are sensitive to fluid properties. It is increasingly more difficult to apply on high viscosity products then on lighter hydrocarbon products. Therefore application data or experience on the measurement of refined or light crude oil may not necessarily be transferred to measuring medium to heavy crude oils. Before better and more quantitative knowledge is available on how LUFMs react on different fluids, the arguments advocating reduced need for in-situ proving and increased dependency on laboratory flow calibration (e.g. using water instead of hydrocarbons) may be questionable.

The present paper explores the accurate measurement of crude oil with liquid ultrasonic meters. It defines the unique characteristics of the different API grades of crude oils and how they can affect the accuracy of the liquid ultrasonic measurement. Flow testing results using a new LUFM design are discussed. The paper is intended to provide increased insight into the potentials and limitations of crude oil measurement using ultrasonic flow meters.

1. INTRODUCTION

Because of their non-intrusive design features, there is much excitement today about extending the application of liquid ultrasonic meters (LUFMs) to a wider range of crude oil measurement. They have been used in the petroleum industry for many years in non-custody transfer applications such as leak detection, allocation measurement and check meter measurement. With advancements in multiprocessors, transducers and electronic technology, multipath ultrasonic flow meters are now available with higher levels of accuracy. They are recognized in many European countries for custody transfer service and recently in North America with publication of the API Standard *Measurement of Liquid Hydrocarbons by Ultrasonic Flowmeters Using Transit Time Technology* [1]. Most of the applications, though, have been on refined products or light to medium crude oils.

Crude oil measurement defines a wide range of applications from light condensates with a viscosity of less than 0.5 cP to heavy crude oils with less that 10 API gravity, over 2000 cP. Ultrasonic meters infer the volumetric through-put by measuring the velocity over the flow area. As all velocity meters they are Reynolds Number depended, that is, they are more or less

affected by the relationship between velocity and viscosity. They may also be affected by entrained solids, gases, waxes and chemicals contained in the crude oil, which further complicates their application on crude oils

The present paper explores ultrasonic meter technology and its application on crude oils. In Sections 2 and 3 the LUFM principles and some crude oil characteristics are reviewed briefly, as a reference for the paper. Various influences of fluid properties on the LUFM metering principle are discussed in Section 4, as a background to understand how the LUFM may react on different fluids. Proving issues of the LUFM are then addressed in Section 5. Test results for a novel type of LUFM are presented in Section 6, with conclusions given at the end (Section 7).

2. LUFM PRINCIPLES

In ultrasonic transit time flow meters (UFM) the flow direction, the flow velocity and the sound velocity of the fluid are estimated from the measured up- and downstream transit times. These transit times are obtained by transmitting and detecting acoustic pulses up- and downstream with respect to the direction of the flow, using ultrasonic transducers and dedicated electronics. One or several acoustic paths may be used, depending on the accuracy required. For further details, cf. e.g. [1-6]. Fig. 1 shows a cross-section of such a meter, schematically.

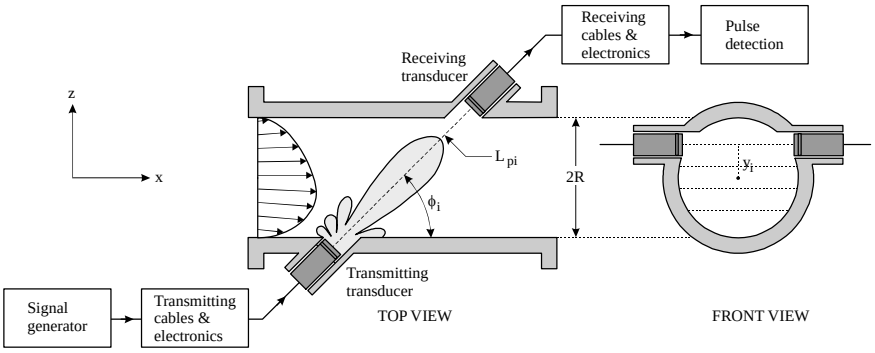

Fig. 1. Schematic illustration of a single path in a multipath ultrasonic transit time flow meter with non-reflecting paths (for downstream sound propagation). (Left: centre path example (y_i = 0); Right: path at lateral chord position y_i.)

In UFMs with reflecting or non-reflecting paths, the volumetric flow rate (at line conditions) is given as [1-6]

$$q_{UFM} = \pi R^2 \bar{v}_A, \qquad \bar{v}_A = \sum_{i=1}^{N} w_i \bar{v}_i, \qquad \bar{v}_i = (N_{refl,i} + 1) \frac{2\sqrt{R^2 - y_i^2}\,(t_{1i} - t_{2i})}{t_{1i} t_{2i} |\sin 2\phi_i|},$$

(1)

where (cf. Fig. 1) R is the inner radius of the UFM meter body; $\bar{v}_A$ is the axial volume flow velocity (at line conditions); N is the number of acoustic paths; i is the path number; w_i is the integration weight factor for path no. i; $\bar{v}_i$ is the average axial flow velocity along path no. i (i.e. the line integral along the path); y_i is the lateral distance from the pipe center (lateral chord position) for path no. i; L_i is the interrogation length for path no. i; ϕ_i is the inclination angle (relative to the pipe axis) of path no. i; t_{1i} and t_{2i} are the measured transit times for upstream and

downstream sound propagation of path no. i; and $N_{refl,i}$ is the number of wall reflections for path no. i ($N_{refl,i}$ = 0, 1 or 2 in current UFMs), i = 1, …, N.

3. CRUDE OIL CHARACTERISTICS IMPORTANT TO LUFM PERFORMANCE

Crude oil characteristics are important to the measurement of crude oil. Viscosity is of primary importance in determining the feasibility and accuracy of measurement with an ultrasonic meter. But also important are entrained gas, water, solids, wax, and corrosive chemicals. These characteristics are defined in Crude Oil Assays[1] and include:

- **API gravity**. Crude oils are normally defined by their API gravity. The definition of API gravity is the density of crude oil at a specific temperature compared to the density of water at a standard temperature, 60 F. The relationship between specific gravity (SG) and API gravity is:

$$\text{SG (60F/60F)} = 141.5 / (131.5 + \text{API}) \quad (2)$$

  API gravity is also loosely related to viscosity. In general as the API number decreases the viscosity increases. Crude oils vary widely from the different production fields, but can be divided by API gravity into four ranges as shown in Table 1.

Table 1. API gravity of condensates and crude oils.

Petroleum Liquids	API Gravity Range	Viscosity [cSt]
Condensate	< 50	0.5 – 0.8
Light crude	35 – 50	< 1 – 20
Medium crude	25 – 34	20 – 500
Heavy crude	< 10 to 24	100 - >2000

  For light crude oils there is a fairly close relation between viscosity and API gravity. But for medium crude oils and heavy crude oils it is important to obtain the viscosity from the assay or from specific tests.

- **Viscosity** can be expressed in many different units. For the petroleum industry the most commonly used viscosity units are:

  - Kinematic Viscosity (symbolically, v), has units of Stokes (St). It is, for our purposes the most suitable viscosity to use. In the metric system the kinematic viscosity unit is cm^2/s (centimeter^2/second). As the value of Kinematic Viscosity is normally small, the unit is often converted by multiplying by 100 and calling the unit centistokes (cSt).
  - Saybolt Universal Viscosity (SSU). SSU can be converted to cSt using a conversation table.
  - Dynamic Viscosity (symbolically, μ), has units of Poise (P). Poise can be converted to Stokes by dividing by the specific gravity, i.e. St = P / SG. In the metric system,

[1] The Hydrocarbon Measurement Committee (HMC) has assays of a wide range of crude oils. This information can be found online at: http://www.melvcon.co.uk/Crude_Oil_Data/crude_oil_data.html. This website is operated on behalf of the UK Energy Institute HMC-4 Oil Transportation Measurement Committees to provide rapid access to crude oil measurement and property data. The data is submitted by major oil companies listed on the site.

the dynamic viscosity unit is Pa·s (Pascal·second). Like Kinematic Viscosity, the Poise is often multiplied by 100 and named centipoise (cP).

The viscosity of all liquids varies with temperature. Table 2 illustrates the effect of temperature on the viscosity of selected products. In absolute terms the more viscous the product the greater temperature affects the viscosity. It is important when evaluating any meter application that the viscosity of each product must be specified over the operating temperature range.

Table 2. Effect of temperature on the viscosity of selected products.

API gravity	**Viscosity in cP @ deg F (deg C)**		
for selective crude oils	**60 (15)**	**100 (38)**	**150 (66)**
48 API	2.7	1.7	1.1
32.6 API	21	9	5
25.3 API	1442	243	93
17.8 API	-	340	-
16.2 API	-	574	-
10 API	-	1294	-

- **Cloud-Point** in a petroleum product is the temperature at which wax crystals begin to form as it is cooled. If a meter is operated below the cloud point, wax can form on the measurement element, which can notably affect the meter's accuracy. Some meters are considerably more tolerant of waxing than other meters. For example, after an initial build-up of wax on the walls of a Smith PD, the rotating blades wipe the surfaces, and the meter factor remains stable. In the case of velocity meters (eg: ultrasonic, turbine) there is a continuous meter factor shift as the wax builds-up.

- **Sediment and Water (S&W).** This is a collective term for non-hydrocarbons found in crude oil. In API MPMS Chapter 1, S&W is defined as "A material, coexisting with yet foreign to a petroleum liquid,… may include free water and sediment (FW&S) and emulsified or suspended water and sediment (SW&S)." Since all pipelines regulate the amount of S&W they will accept, normally less than 1%, a crude oil within these requirements is termed "pipeline quality oil". In general "pipeline quality oil" may not be a problem for measurement with an ultrasonic meter. Crude oil at the production lever and in gathering lines may be a problem, so the characteristics of these crude oils must be carefully considered before making a decision on the type of meter to use.

- **Gases.** Slugs or entrained gas will not damage an ultrasonic meter but it can adversely affect the measurement accuracy. Even a small number of gas bubbles can cause attenuation of the ultrasonic signal. The degree of attenuation depends on a number of factors such as e.g. pressure, bubble size, amount of free gas, signal frequency, etc. (cf. Section 4.1).

- **Chemical Contaminants.** As with S&W, pipelines have strict limits on the type and amounts of chemicals in the crude oils they will transport. Normally "pipeline quality oil" is not a problem. Crude oils at the production level can have a variety of chemicals and it is important to check the compatibility of the meters materials of construction with the crude oil assay.

4. SENSITIVITY OF LUFMs TO FLUID PROPERTIES

Inherent benefits of liquid ultrasonic flow meters include no moving parts, "no" wear (as compared to e.g. turbines and PD meters), low pressure drop, wide rangeability, and potentials of low maintenance. This does not mean that such meters cannot fail, however, or be subject to gradually or abrupt degraded performance. Such factors have been discussed e.g. in [10]. Diagnostic tools are available in present-day LUFMs which in many cases are able to alarm the user in case of degraded performance.

Another important factor, which becomes relevant e.g. when transforming measurement results from one type of fluid to another and different fluid (such as e.g. by flow calibration the meter in a water laboratory facility, for long-time field operation on oil products [10,11]), is the influence of fluid properties on the meter. On a qualitative (overall) level, many of the influences of fluid properties are known, and have been addressed by various authors. However, on a *quantitative* level, the knowledge on such influences is definitely insufficient today, and any contribution to close this knowledge gap should be welcome. The following discussion may represent a contribution to the process of filling in on some parts of this knowledge gap.

The influence of fluid properties on the UFM performance may be classified in two main groups, according to *how* they influence on the UFM:

(a) Signal quality; i.e. the signal attenuation and signal-to-noise ratio (SNR) in the acoustic paths,
(b) Flow profiles and integration mehod; i.e. how the numerical integration method used to combine the individual acoustic path measurements into a full volumetric flow rate measurement, handles different flow velocity profiles met in practice.

These topics are discussed in the following.

4.1. Signal quality: Sound attenuation and SNR

The signal strength, or more precisely, the signal-to-noise ratio (SNR), is crucial for the accuracy of the transit time measurements made in the UFM. Reduced SNR means higher uncertainty of the transit time measurement, and thereby higher uncertainty of the volumetric flow rate measurement.

Noise is classified as coherent noise (signal interference) and incoherent noise ("signals" with random phase relative to the measurement signal). Coherent noise contributions may be e.g. (a) transducer "ringing" effects, (b) spoolpiece borne signals (acoustic cross talk), (c) liquid borne reflections (transducer ports reflections, pipe wall reflections/reverberation), etc. Incoherent noise contributions may be e.g. (a) electromagnetic noise (RFI), (b) flow noise, (c) valve noise, (d) structural (pipe) vibrations, etc.

The "strength" (amplitude) of the measurement signal has to "compete" with such noise contributions, to give a sufficient SNR. To illustrate this situation, SNR requirements[2] for an example of a "standard" zero crossing time detection method is given in Table 3, for incoherent

[2] The example requirements of Table 1 apply to the processed signals on which the time detection is made.

and coherent noise contributions, respectively, and for different pipe dimensions (6" - 20" LUFMs).

Table 3. Signal-to-noise (SNR) requirements for an example of a "standard" zero crossing time detection method, in an ultrasonic liquid flow meter (LUFM) for precision custody transfer measurement.

	Pipe diameter		
	6”	**12”**	**20”**
Incoherent noise	> 45 dB	> 40 dB	> 35 dB
Coherent noise (“worst case”)	> 65 dB	> 60 dB	> 55 dB

It is noted that for single-phase water (with its relatively low viscosity), the 6" and 20" requirements of Table 3 are about "equivalent", since the geometrical attenuation increases about 10 dB from 6" to 20" LUFMs. In viscous oil, however, and in cases with water and/or gas contents, etc., the 20" requirements may be the strongest.

A number of fluid-dependent factors may contribute to attenuate the measurement signal, thereby decreasing the SNR. The sound attenuation coefficient, α, consists of a number of contributions, such as e.g.

$$\alpha = \alpha_{abs} + \alpha_{wio} + \alpha_{gas} + \alpha_{solids} + \alpha_{wax}\,, \tag{3}$$

where α_{abs} is the sound absorption coefficient (due to shear viscosity, bulk viscosity, thermal conductivity and possible relaxation effects), and α_{wio}, α_{gas}, α_{solids} and α_{wax} account for excess attenuation due to water contents, gas contents, solid particles (e.g. wax), and contamination (wax) at transducers, respectively.

The properties of the fluid under measurement may influence significantly on the signal attenuation, and thus on the SNR and the time detection accuracy. Broadly speaking, sound attenuation below about 0.1 dB/cm may not influence much on the meter performance, except for large meters. For 6" and 20" meters, this figure would correspond to about 2 dB and 7 dB increased attenuation, respectively, for centre paths. Various effects contributing to the sound attenuation are discussed in some more detail in the following.

(1) Sound absorption. Sound absorption is the attenuation due to shear viscosity (μ), bulk viscosity (μ_B) thermal conductivity (κ) and possible relaxation effects in the fluid [12]. The influence of absorption on the SNR is accounted for through the sound absorption coefficient α_{abs}, cf. Eq. (3). As an investigation of sound absorption in various oils of different viscosity, being used in flow testing of LUFMs, experimental measurements and calculations have been made for selected samples of such oil types, cf. Table 4. For reference of the measurement method, other oil types (castor oil and rapeseed oil) have also been included in the study, since published data for both viscosity and sound absorption are available for these oil types (which is seldom the case!). On castor oil the agreement with experimental and theoretical literature results [13-15] is better than 0.1 dB/cm over the complete frequency range investigated here (0.5 - 1.2 MHz). The measurements were made using a combined sound velocity / sound attenuation measurement cell developed in ref. [16], applying a modified measurement method. The measurements have been compared with calculations using the classical absorption coefficient (with no description of relaxation effects), given as

$$\alpha_c = \frac{\omega^2}{2\rho c^3}\left(\frac{4}{3}\mu + \mu_B + \frac{(\gamma-1)\kappa}{c_p}\right), \tag{4}$$

where $\omega = 2\pi f$ is the angular frequency, ρ is the fluid density, c is the sound velocity, γ is the ratio of specific heats, and c_p is the specific heat capacity. On lack of bulk viscosity data for the oil types investigated here, we have here used $\mu_B = (4/3)\mu$ as for lubrication oil [28]. The measurement and calculation results are shown over a broad frequency range in Fig. 2. Among these, the oil types of interest for LUFM operation are the five types given in Table 4 from "light oil" to "extra heavy oil". A fair agreement between the measurement results and the classical sound absorption coefficient is observed, for the oil types investigated here. This includes the level of absorption, as well as its frequency dependence. However, the measurements should only be taken as tentative results.

Table 4. Liquid samples used for measurement and calculation of the sound absorption coefficient. The density, sound velocity and viscosity data given in the table are also measured values. All data apply to 20 °C and 1 atm. (Note that the five types from "light oil" to "extra heavy oil" are among those used in flow testing of the new LUFM design described in Section 6.)

	Density	Sound velocity	Viscosity	Absorption coefficient @ 1 MHz [dB/cm]	
Sample	[kg/m^3]	[m/s]	[cP]	Measured	Calculated (α_c)
Water (destilled)	998	1480.0	-		
"Light oil"	809	1347.3	3	0.02	0.007
"Medium oil"	848	1401.5	11.5	0.07	0.02
"Brad Penn"	867	1422.1	16.5	0.04	0.03
"Heavy oil"	865	1441.3	48	0.09	0.09
"Extra heavy oil"	881	1480.0	297	0.45	0.48
Rapeseed oil	915	1470.4	63.5	0.07	0.10
Castor oil	962	1520.8	775	0.78	1.05

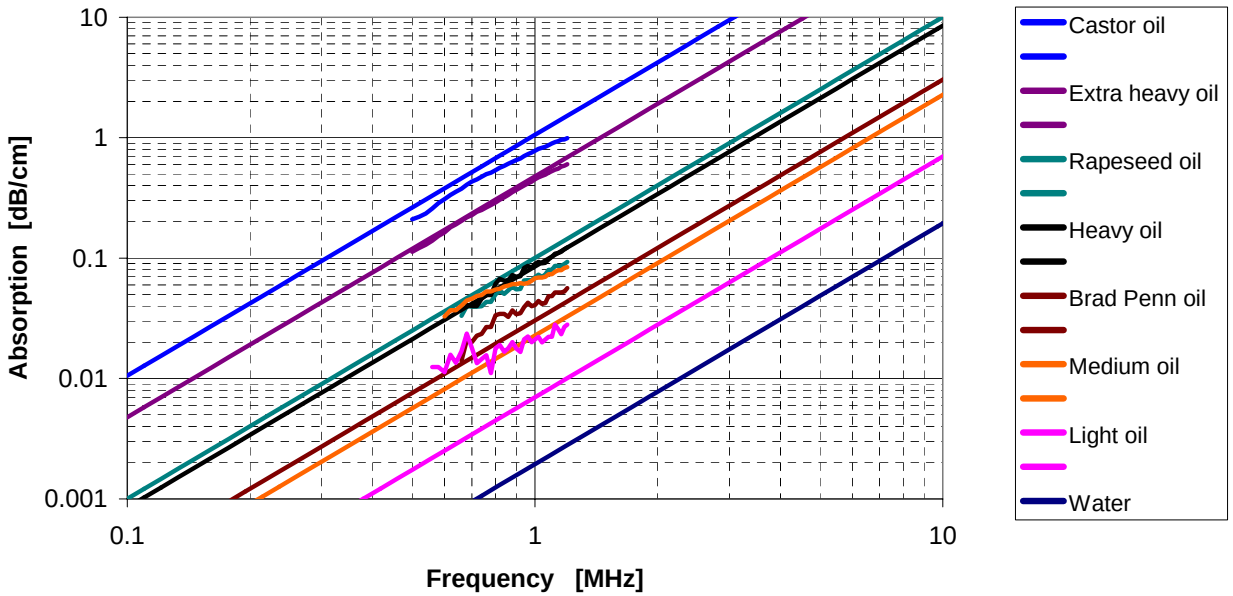

Fig. 2. Measured and calculated sound absorption coefficient α_{abs} for the liquid samples given in Table 4 (various oils and water), at 20 °C, shown as a function of frequency. The "non-straight" lines are measurement results, and the straight lines are calculated (classical absorption) results.

If we take 1 MHz as a typical operational frequency of current-day LUFMs, it is observed that four out of the five oil types (of interest for LUFM operation) investigated in Fig. 2 display sound absorption less than 0.1 dB/cm at 1 MHz. These fluids, with viscosity less than about 50 cP, should normally not represent problems for LUFMs less than e.g. 20" size, in this temperature range.

For "extra heavy oil", with viscosity 297 cP, however, the attenuation is higher, about 0.45 dB at 1 MHz, which means significant higher attenuation for large meters, relative to a low viscosity oil application. For 6" and 20" meters, that would correspond to about 10 dB and 32 dB increased attenuation, respectively, for centre paths. Especially for the 20" meter, this may be a significant attenuation and reduction of the SNR.

Excess absorption may be caused by relaxation effects, due to e.g. internal molecular vibrations, rotations, etc. The influence of relaxation on the SNR is accounted for in the attenuation coefficient α_{abs}, cf. Eq. (3). Such effects may cause significant excess absorption in the frequency band of the relaxation mechanism [12]. That means, at frequencies close to the relaxation time, τ (i.e. $\omega\tau \sim 1$), the energy loss per signal period is maximized. Relaxation effects will also express itself as dispersion (that the sound velocity varies with frequency). For LUFMs relaxation may cause significant extra attenuation if the relaxation frequencies of the oil in question is in the operational frequency band of the LUFM. Whether this is the case or not has to be investigated for the oil type at hand. For the oil types investigated here (Fig. 2) the measurements have not revealed any significant relaxation effects in the frequency band around 1 MHz.

(2) Water-in-oil (emulsion) effects. Water droplets in the oil cause excess sound attenuation due to scattering of the sound waves by the droplets. The excess effect on the SNR is accounted for through the attenuation coefficient α_{wio}, cf. Eq. (3). The major question is of course "how much water can be tolerated in the oil before the LUFM performance is significantly influenced?" Before such a question can be answered, one needs improved insight into which mechanisms that dominate the sound attenuation when water is present in the oil. Parameters of relevance in that context include the water droplet size distribution, the amount of water present in the oil, the pressure and temperature, the oil type (constituting the continuous phase), the LUFM signal frequency, etc. As an example, Fig. 3 shows simulations of the combined attenuation terms $\alpha_{abs}+\alpha_{wio}$ as a function of droplet diameter (over the range 0.1 μm to 10000 μm = 1 cm), for 5 % water-in-oil emulsions, at 1 atm. pressure and a frequency of 1 MHz, using the Waterman-Truell multiple scattering model [17-19][3].

[3] The present results are calculated using the Waterman-Truell multiple scattering model with Allegra-Hawley scattering coefficients [17-19]. This model takes into account the thermal and viscous boundary layer effects close to the droplet surface (inside and outside of the droplet), the generation of sound waves inside and outside of the droplets, and higher order oscillation modes (monopole, dipole, quadropole, etc.). The model is potentially applicable at all frequencies of relevance, from very long to very short acoustic wavelengths relative to the droplet diameter. This includes droplet resonances appearing when the acoustic wavelength is of the order of the droplet diameter.

The Waterman-Truell multiple scattering model for two-phase fluids has expressed good agreement with experimental measurements for a wide range of Exxsol D80-in-water and water-in-Exxsol D80 emulsions [16], and for aerosols (e.g. water droplets in air) [20]. Several other types of models for description of sound propagation in two-phase media have also been implemented and used extensively, for comparison and reference (not shown here).

Fig. 3a shows $\alpha_{abs}+\alpha_{wio}$ calculated for water droplets in the oil types given in Table 4, at 20 ^{o}C. Several important features are noted. Firstly, two dominant "peaks" are observed in $\alpha_{abs}+\alpha_{wio}$, the first one at droplet sizes of about 0.35 μm, the other one at sizes of about 5 mm and above. The first one is due to thermoviscous effects in a boundary layer around each droplet interface. The second one is due to scattering of sound by the droplet itself, i.e. an effect caused by the contrast in the acoustic impedance between the continuous oil phase and the water droplet. At these "peaks" the attenuation $\alpha_{abs}+\alpha_{wio}$ is relatively high, in the range of about 0.5 dB/cm and above. Inbetween the two "peaks" $\alpha_{abs}+\alpha_{wio}$ displays a "valley" with lower attenuation, since in this droplet size range there is no dominating attenuation mechanisms. By comparison with Fig. 2, it turns out that in the "valley", the attenuation is essentially dominated by α_{abs} (given by Fig. 2), and that the excess attenuation due to water-in-oil scattering, α_{wio}, is relatively small. Consequently, for the oil types investigated here and for the 5 % water concentration considered, the simulations indicate that high attenuation may be expected for water droplet sizes in a band below 1-2 μm and in a band above e.g. 2-3 mm (depending on oil type). However, for water droplets in the range of, say, 2 μm to 2 mm, the simulations indicate that the excess attenuation α_{wio} due to water-in-oil is negligible. For very small droplets, less than 0.1 μm, the simulations indicate that the excess attenuation α_{wio} due to water-in-oil becomes small.

It should be emphasized that the present example results are all based on simulations for a 5 % water-in-oil emulsion. For other water fractions the results are different, such as for "pipeline quality oil" (less than 1 % water, cf. Section 3), for which the attenuation will be smaller. However, a discussion of this matter is too large and complex to be covered in the present paper.

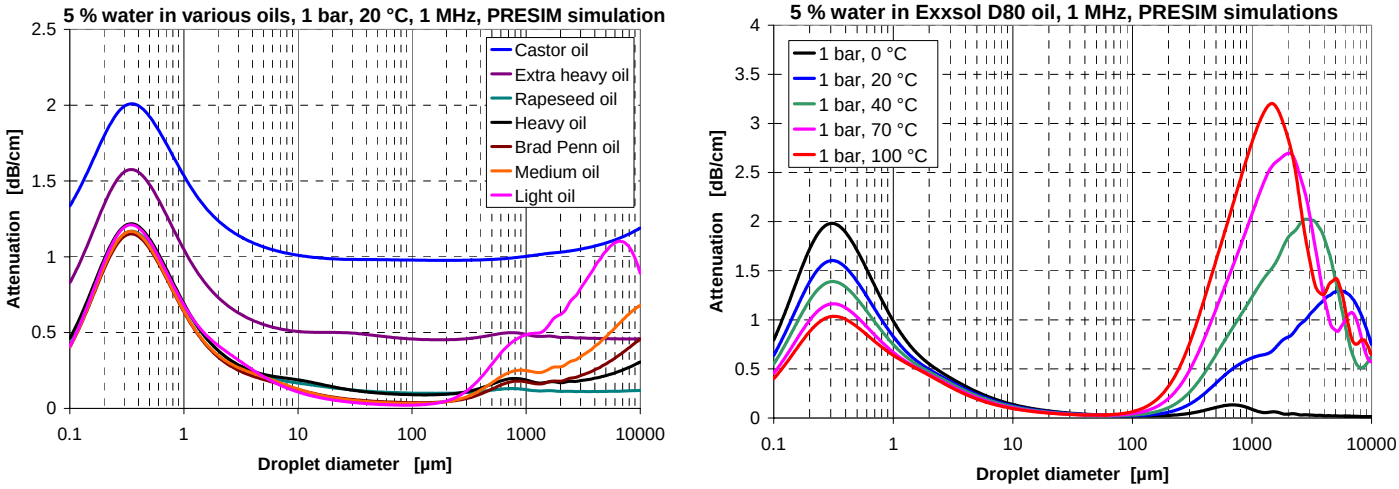

Fig. 3. Numerical calculations (using the Watermann-Truell multiple scattering model) of sound attenuation $\alpha_{abs}+\alpha_{wio}$ in 5 % water-in-oil emulsions, shown as a function of water droplet diameter, at 1 MHz. (a) Selected oils at 1 atm / 20 ^{o}C / 1 MHz (cf. Table 4), (b) Exxsol D80 model oil at 1 atm. and different temperatures in the range 0 to 100 ^{o}C

Additional simulation results (not shown here) indicate that the main characteristics of the results shown in Fig. 3a do not change much by lowering the frequency some hundred kHz, except that the overall level of the attenuation $\alpha_{abs}+\alpha_{wio}$ of course becomes smaller at these lower frequencies.

Additional simulation results (not shown here) also indicate that the influence of pressure on these results should not be large, as expected. The reason for that is of course the low compressibility of the fluids.

There is then the question of temperature influence. Unfortunately, relevant properties of the oil types given in Table 4 have not been sufficiently available to enable any simulation of temperature effects on $\alpha_{abs}+\alpha_{wio}$. On lack of better data, temperature effects were then simulated using the model oil Exxsol D80 as the continuous phase. Simulations of $\alpha_{abs}+\alpha_{wio}$ for 5 % water-in-Exxsol D80 at different temperatures in the range 0 to 100 ^{o}C are shown in Fig. 3b, at otherwise the same conditions as for Fig. 3a. It appears that temperature has a significant influence on the two attenuation "peaks" discussed above, but not so much inbetween the "peaks". The attenuation level of the "left peak" increases significantly at the lowest temperatures in this range, while for the "right peak" the attenuation level increases significantly at the highest temperatures, accompanied by a move of the "peak" towards lower droplet sizes. At these "peaks", the simulated attenuation levels are so high that, if they are correct, droplet sizes in these ranges would definitely have consequences for operation of LUFMs.

It is strongly emphasized here, that before being taken into use as any part of a basis for operation of LUFMs, attenuation results for water-in-oil such as those indicated by Fig. 3 through theoretical modelling, need to be experimentally verified, by measurements. Work has been started also on this experimental part (not shown here)[4].

(3) Gas-in-oil effects. Free gas (e.g. in the form of gas bubbles) in the oil causes excess sound attenuation due to scattering of the sound waves by the bubbles, bubble resoncances, etc. The excess effect on the SNR is accounted for through the attenuation coefficient α_{gas}, cf. Eq. (3). Again, the major question is "how much free gas can be tolerated in the oil before the LUFM performance is significantly influenced?" Parameters of relevance in that context include the bubble size distribution, the amount of free gas present in the oil, the pressure and temperature, the oil type (constituting the continuous phase), the LUFM signal frequency, etc. As an example, Fig. 4 shows simulations of the combined attenuation terms $\alpha_{abs}+\alpha_{gas}$ as a function of droplet diameter (over the range 0.1 μm to 10000 μm = 1 cm), in Exxsol D80 model oil with air bubbles, for different bubble concentrations (10 ppm to 1 %), at 20 ^{o}C and 1 MHz, using the Waterman-Truell multiple scattering model [17-19]. The attenuation $\alpha_{abs}+\alpha_{gas}$ is calculated for two pressures, 1 atm. and 100 bara, shown in Figs. 4a and 4b, respectively.

The 1 atm. results given in Fig. 4a are discussed first. This case is not of much practical interest, since operation at 1 atm. is normally not relevant for the LUFMs in question here, but may be of interest to illustrate the physical mechanisms involved. Several important main features are noted. At bubble sizes of about 5-6 μm the attenuation displays a distinct "peak" due a bubble resonance. At the bubble resonance the attenuation level is dramatically high. Below the bubble resonance, the attenuation level is reduced until it reaches a constant but high level (in the range of Rayleigh scattering). Above the bubble resonance the attenuation level is also gradually reduced, approaching the attenuation of the continuous oil phase, α_{abs}. This happens at very

[4] As mentioned in another footnote, fair agreement with measurements has been obtained using the Waterman-Truell model for oil-in-water and water-in-oil emulsions, but for a low-viscosity oil (Exxsol D80) [16], and for aerosols [20]. To which degree such agreement can be obtained also for water-in-oil emulsions based on high-viscosity oils, remains to see.

large bubble sizes, from 1 mm and upwards. The overall level of the attenuation increases of course by increasing amount of gas in the oil.

At 100 bara the situation is different, both qualitatively and quantitatively, cf. Fig. 4b. The higher pressure contributes to stiffen the bubbles so that the resonance and scattering effects are reduced, and the bubble size at which the bubble resonance occurs is increased, to about 70-80 μm. In addition, higher harmonics of the bubble resonance are observed, as sharp resonance peaks at larger bubble sizes. In addition, a broad resonance occurs at about 1 μm. The simulation results indicate, if they are correct, that sound transmission at such pressures should not be a problem at low bubble concentrations, less than e.g. 100 ppm, except for a band in the vicinity of the bubble resonance. Transmission problems arise however at higher bubble concentrations. For a concentration of e.g. 1000 ppm = 0.1 %, the attenuation may be critically high except for bubble sizes larger than about 0.1-1 mm (depends on pipe diameter). For 10000 ppm = 1 %, the attenuation may be critically high except for bubble sizes larger than about 1-10 mm (depends on pipe diameter).

Note that the calculations shown in Fig. 4 have been made for monosize bubbles, evenly distributed in the oil. They thus represent "worst case" scenarios. Similar calculations made for bubble size distributions (not included here) show that the resonances are then "smeared out", accompanied by a reduction of the attenuation level.

The results shown in Fig. 4 apply to a frequency of 1 MHz. Additional simulations (not shown here) indicate that the attenuation due to gas bubbles decreases if the frequency is lowered, and that the bubble resonance moves slightly towards the region of larger bubbles.

The results shown in Fig. 4 apply to air bubbles in Exxsol D80 model oil. Bubbles of natural gas instead of air may give slightly higher attenuation, due to the lower density of natural gas (at otherwise equal pressure and temperature conditions). On the other hand, higher viscosity oil may decrease the attenuation, especially at the bubble resonances.

Additional simulations (at 70 ^{o}C, not shown here) also indicate that the influence of temperature on the results shown here may not be a dominating effect.

(a)

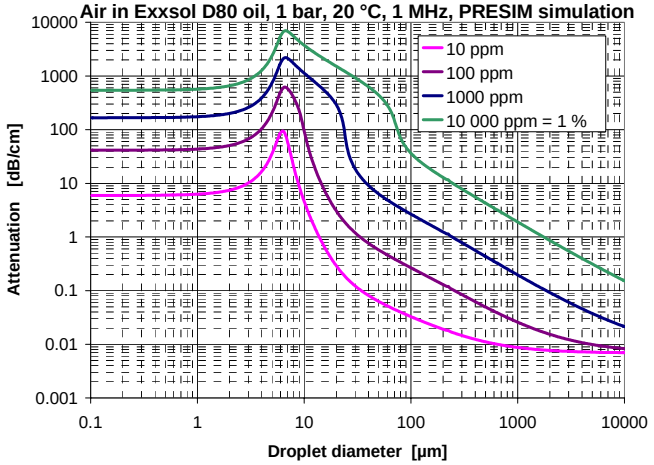

(b)

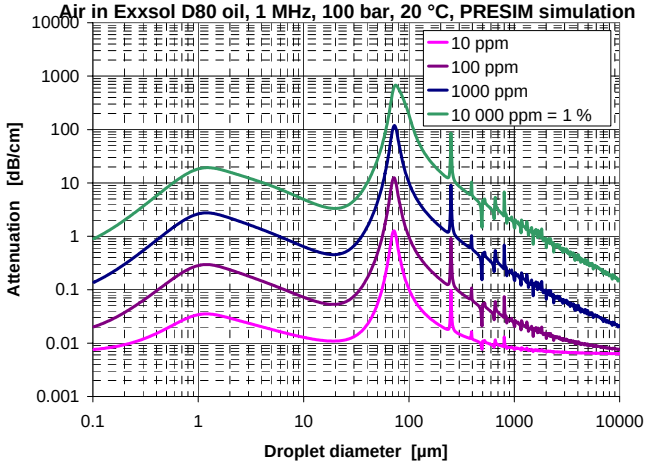

Fig. 4. Numerical calculations (using the Watermann-Truell multiple scattering model) of sound attenuation $\alpha_{abs}+\alpha_{gas}$ in Exxsol D80 model oil with air bubbles, shown as a function of bubble diameter, for different bubble concentrations (10 ppm to 1 %), at 20 ^{o}C and 1 MHz. (a) 1 atm. pressure, (b) 100 bara pressure.

(6) Solid-particles-in-oil (suspension) effects. Wax particles may be present in the oil it if the temperature is below the cloud point (cf. Section 3). Solid particles in the oil causes excess sound attenuation due to scattering of the sound waves by the particles. The excess effect on the SNR is accounted for through the attenuation coefficient α_{solids}, cf. Eq. (3). Again, the major question is "how much solid particles can be tolerated in the oil before the LUFM performance is significantly influenced?" Parameters of relevance in that context include the particle size distribution, the amount of particles present in the oil, the pressure and temperature, the oil type (constituting the continuous phase), the LUFM signal frequency, etc. Before a qualified answer to this question can be given, experimental measurements and numerical simulations using a scattering model accounting for solid particles[5] are needed to improve current-day knowledge on such effects, both qualitatively and quantitatively.

(4) Wax effects (contamination). Wax may also cause other effects. If the temperature is below the cloud point, wax contamination may build up at different surfaces of the LUFM. Possible influences which may be important for the LUFM performance include:

(a) Wax layer build-up at the transducer fronts. Such build-up may shift the transit times and cause a continuous meter factor shift as the wax builds up. For example, a 0.1 mm wax layer on all transducer fronts would result in a systematic meter factor shift of about 0.08 and 0.03 % for a 6" and a 20" flow meter, respectively. Regular in-situ proving of the flow meter will however correct for such misreading.

Wax build-up may also cause excess attenuation and contribute to reduce the SNR. However, due to the relatively small difference in the acoustic impedance between oil and wax, a thin wax layer may not be expected to affect the SNR significantly, unless the layer becomes thick, and if inhomogeneities are present. The excess effect on the SNR is accounted for through the attenuation coefficient α_{wax}, cf. Eq. (3).

(b) Wax build-up in the transducer cavities, at the sides of the transducer. Such build-up may cause reduced acoustic isolation of the transducer from the spoolpiece, with increased level of acoustic "cross-talk" through the spoolpiece as a result. Since such cross-talk acts as coherent noise, this results in reduced SNR, and thus reduced accuracy of the transit time measurements.

(c) Wax build-up on the inner wall surface of the spoolpiece (in the pipe bore itself). Such wax build-up results in a deviation between the actual cross-sectional area seen by the liquid flow and the "supposed" area (i.e. the area in case of no wax present). The consequence is incorrect volumetric flow rate reading, and a systematic shift of the meter factor. The question is of course again; "how much wax build-up can be tolerated at the spoolpiece wall before the meter factor of the LUFM is significantly shifted?" A simple analysis reveals that for a thin wax layer distributed uniformly along the spoolpiece wall with effective thickness L, the relative change in cross-sectional area is given approximately as $\Delta A/A \approx 2L/R$, where R is the pipe radius and $A = \pi R^2$ is the cross-sectional area with no wax present. For a 6" flow meter, thus, a wax layer of 0.1 mm thickness will result in a misreading of 0.27 %, which is a large error, if not discovered and corrected for. For a 20" meter, the misreading is proportionally smaller, about 0.08 %. Such

[5] That means, accounting for both compressional and shear waves in the particle, not only compressional waves, such as the Waterman-Truell model [17-19] used for fluids here.

wax build-up at the spoolpiece wall may be difficult to discover in-situ, although methods for in-situ wax build-up detection may be available. Regular in-situ proving of the flow meter will however correct for misreading due to such wax build-up.

4.2 Flow profiles, numerical integration and VPC

A combination of multipath configuration and numerical integration is necessary in UFMs to achieve sufficient measurement accuracy in cases of disturbed flow velocity profiles. The lateral chord positions y_i and integration weights w_i , $i = 1,..., N,$ (cf. Eq. (1)) are chosen to account for e.g.

- Robustness and accuracy with respect to disturbed (asymmetric) axial flow velocity profiles.
- Compensation for transverse (non-axial) flow components (swirl, cross-flow, etc.).
- Effects of orientation of the meter relative to the flow profiles.
- Reynolds number dependency.
- Pipe roughness effects (influencing on flow profiles).

Although the integration method in actual UFMs may display a high degree of robustness to installation conditions (bends, flow conditioners, etc.) using constant integration weights w_i, there is one effect which needs special treatment: the "velocity profile effect". This effect and its treatment is addressed in the following.

The essence of the "velocity profile effect" experienced in UFMs is that numerical integration using constant integration weights w_i does not in general appear to be sufficient over the complete range of flow velocity profiles experienced at various Reynolds numbers, not even for the ideal situation of a straight pipe run with a very long upstream length. If constant integration weights were used, a distinct "nonlinearity" would appear in the flow calibration curve of the UFM. This effect means that there in some cases could be problems in meeting the linearity requirements of the UFM using such weights, and that special treatment is needed to avoid or reduce this effect.

The effect can be explained as follows. For convenience and without loss of generality[6], consider an example of a UFM with an even number of paths, e.g. $N = 4$. For symmetric flow profiles (e.g. such as expected in straight pipes with long upstream lengths) one then has, from Eq. (1),

$$\bar{v}_A = \sum_{i=1}^{4} w_i \bar{v}_i = 2\sum_{i=1}^{2} w_i \bar{v}_i \,, \tag{5}$$

where

$$\bar{v}_i = \int_{Path\ i} v_{A,i} d\ell \,, \qquad v_{A,i} = v_A(x, y = y_i, z, t) \,. \tag{6}$$

$v_A(x, y, z, t)$ is the axial flow velocity component in the position (x, y, z) at time t. $v_{A,i}$ is thus the value of v_A at the lateral chord position no. i. From Eq. (5) it follows that if the condition

[6] For USMs with odd number of paths, one path will normally be a centre path, and the arguments given in the text (for even number of paths) are not altered.

$$2\frac{w_1\bar{v}_1 + w_2\bar{v}_2}{\bar{v}_A} = 1 \qquad \Leftrightarrow \qquad w_1\left(\frac{\bar{v}_1}{\bar{v}_A}\right) + w_2\left(\frac{\bar{v}_2}{\bar{v}_A}\right) = \frac{1}{2}, \tag{7}$$

was fulfilled for all flow velocity profiles, the UFM would display perfect linearity (in case of symmetric flow profiles considered as an illustration here). In practice, this will not be the case if constant integration weights w_i are used. The weights w_i can be designed so that Eq. (7) is fulfilled for a certain flow velocity profile, but as the flow profile changes (e.g. with changing Reynolds number), it appears that Eq. (7) can not be fulfilled for all profiles, without changing the weights. Alternatively, one can use constant integration weigths and correct these afterwards, depending on the measured flow velocity profile. The latter technique is employed here and denoted "velocity profile correction" (VPC) [21].

The following example can illustrate this situation. Fig. 5a shows a number of symmetrical and experimental flow velocity profiles, measured as a function of relative lateral chord position y_i/R in straight pipe runs, most of them with long upstream lengths. The profiles have been normalized to the average axial flow velocity, $\bar{v}_A$, to give $v_{A,i}/\bar{v}_A$. Most of these flow velocity profile data (in the Reynolds number range 7000 - 10^7) are taken from published literature [22-26], supplemented with some own measurements at lower Reynolds numbers (Re = 1000 - 32000). In addition, the parabolic profile representing laminar flow has been included in the figure. Note that the lateral resolution in the latter data sets (the own measurements) is significantly courser than for the published literature data.

(a)

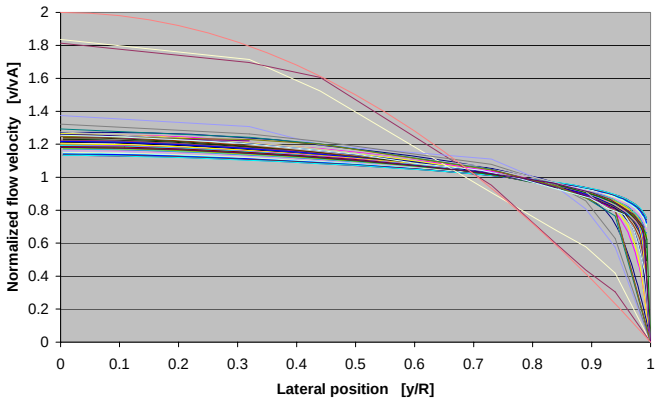

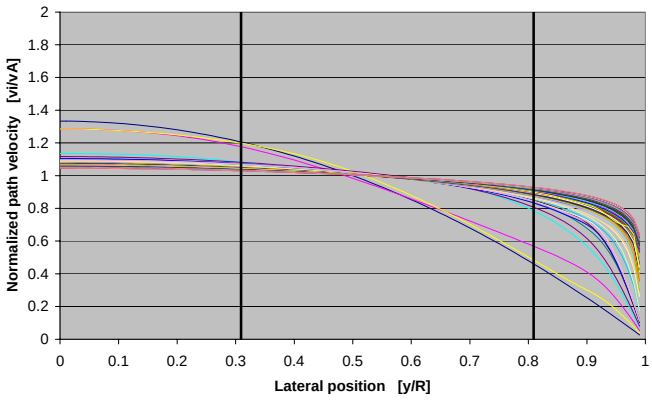

(b)

Fig. 5. (a) Normalized experimental flow velocity profiles, $v_{A,i}/\bar{v}_A$, measured in straight pipe runs, most of them with long upstream length. (b) Integrated (using Eq. (6)) and normalized experimental "flow velocity profiles", $\bar{v}_i/\bar{v}_A$.

In Fig. 5b the experimental flow velocity profiles given in Fig. 5a have been integrated over the relevant UFM paths, using the line integral, Eq. (6), and then normalized to $\bar{v}_A$. Consequently, the figure shows the ratio $\bar{v}_i/\bar{v}_A$ for the various profiles given in Fig. 5a, as a function of relative lateral chord position in the pipe, y_i/R. In Fig. 5b two vertical lines are also indicated. These are the relative lateral chord positions of the paths in a UFM configured with 4 paths in an

"asymmetric criss-cross" pattern ($\phi_i = \pm 45^o$), using the Gauss-Jacobi integration method (y_i/R = 0.3090 and 0.8090)[7].

At the position of these two vertical lines, the two ratios $\bar{v}_1/\bar{v}_A$ and $\bar{v}_2/\bar{v}_A$ are thus determined. These are the two ratios needed in Eq. (7). As can be seen from Fig. 5b, these two ratios overestimate and underestimate the flow, respectively. From Fig. 5b it is also seen that for the lateral chord positions used as an example here (cf. above), the first ratio, $\bar{v}_1/\bar{v}_A$, varies considerably less over the range of profiles than the second ratio, $\bar{v}_2/\bar{v}_A$, does. Consequently, when these ratios are multiplied with their respective integration weights, w_1 and w_2, and then added, according to Eq. (7), and if the integration weights are constant, it is evident that this sum is not a constant (and equal to ½) over the range of flow velocity profiles, as would be required by Eq. (7) for a completely linear UFM calibration curve. That means, the sum may be equal to ½ for some profiles, and different from ½ for others.

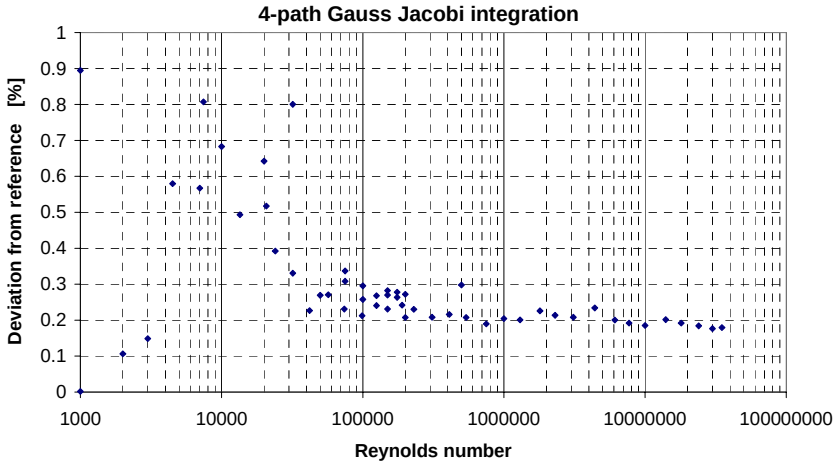

Fig. 6. "Linearity curve" for the illustration example of a 4-path UFM employing Gauss-Jacobi integration, for the "straight-pipe" experimental flow velocity profiles shown in Fig. 5, before applying any VPC.

Fig. 6 shows how this effect turns out for the 4-path Gauss-Jacobi integration method used as an example here, i.e. for the UFM measurement. At high Reynolds numbers, with fully developed turbulent flow, and relatively flat flow velocity profiles which do not change much (cf. Fig. 5), the UFM displays a fair degree of linearity (i.e. the deviation from reference is relatively constant). For Reynolds numbers of 10^5 and below, where the flow profiles are different, the deviation "curve" increases significantly (i.e. the measurement error increases), for the reasons explained above. At Reynolds numbers below about 7000 the deviation "curve" decreases. In essence, thus, for this integration method, there appears to be a distinct "bump" in the linearity curve.

Since the effect is basically due to the flow velocity profiles, this "velocity profile effect" is universal, and will be present in any UFM integration method employing constant weights. However, as can be seen from Fig. 5b and the above explanation, the actual form of the "bump" in the linearity curve will be different for different UFM integration methods (depending on the relative lateral chord positions y_i/R and the weights w_i used). The LUFM described and used in the present work (cf. Section 6) is based on a different integration method than this 4-path

[7] The Gauss-Jacobi integration method is used as a convenient example here, since it is a well-known and well documented integration method, which has also been used as integration method in gas and liquid UFMs.

Gauss-Jacobi integration (which has been used only as an example above, to explain the effect qualitatively).

In the LUFM used in Section 6, the "velocity profile effect" is compensated by employing a "velocity profile correction" technique, VPC [21], involving non-constant integration weights. Improvements achieved using VPC are illustrated in Section 6, cf. Fig. 8 showing LUFM measurement results after use of VPC.

In connection with crude oil operation, an important question is how the "velocity profile effect" and the associated "bumb" will be influenced by the fluid quality. It turns out that since the flow velocity profile depends on Reynolds number, viscosity is the fluid quality parameter of importance in this respect. Increasing viscosity means decreasing Reynolds number and reduced flatness of the flow velocity profiles. Flow velocity profiles relevant for different viscosities, as well as asymmetries in the flow profiles, are taken into account in the VPC method [21].

5. API STANDARD AND PROVING ISSUES

Proving liquid ultrasonic meters is similar to other meters, but because of the sampling methods employed they produce a greater degree of data scatter. API, in developing the ultrasonic meter standard [1] understood these differences, and recommend methods to successfully prove these meters. This section outlines the accuracy requirements, the unique problems with proving ultrasonic meters, the recommendations for proving, and need for in-situ proving.

5.1. Meter accuracy requirements and criteria

Accuracy requirements for the wholesale and retail trade are normally defined by the weights and measures regulations in the country or jurisdiction in which the sale is conducted. Sales within the petroleum industry that are not normally defined by weights & measures, but by a contract between the trading parties, are known as Custody Transfer transactions. A typical contract may define a specific measurement standard such as one of the American Petroleum Industry (API) Standards. Currently API recognizes four types of dynamic measuring devices: (a) Positive Displacement (PD) Meters, (b) Turbine Meters, (c) Coriolis Mass Flow Meters (CMFMs) and (d) recently approved Liquid Ultrasonic Flow Meters (LUFMs). The API Standards are based on best practice and define the proper application of a specific flow meter. Contracts are also based on other recognized standards but all these standards have one thing in common - they all strive to minimize measurement error for a specific application.

The API Standard for LUFMs [1] is specifically written for custody transfer measurement but also addresses other applications such as allocation measurement, check meter measurement, and leak detection measurement.

It states that the meter factor shall be determined by proving the meter at stable operating conditions, (i.e., essentially constant: flow rate, density, viscosity, temperature, and pressure). Since the essential purpose of proving is to confirm the meter's performance at normal operating conditions, in-situ proving is preferred because it eliminates installation and operating effects which can affect a meter's accuracy and repeatability.

5.2. Proving liquid ultrasonic flow meters

Field proving of liquid ultrasonic flow meters is difficult for two reasons:

1. The UFM output pulses are not related in "real time" to the meter through-put. There is a time delay between what is being measured and the pulse output. Reducing the meter's response time and / or increasing the prover volume are recommended.

2. The inertia free measuring principle makes the UFMs far more "sensitive" to operating conditions than conventional meters (turbine and PDs), in the sense that UFMs can follow rapid changes (fluctuations) in the flow. This is normally an advantage, but in *proving* the UFM it may be a disadvantage. The measurement accuracy is improved by taking more samples and / or using a larger prover.

The API Ultrasonic Flow Meter Measurement standard [1] provides suggested prover volumes and the number of runs to achieve custody transfer accuracy.

Typically custody transfer accuracy requires a repeatability of 0.05 % in 5 consecutive prover runs. Since repeatability, by definition, is at constant conditions, the uncertainty of the measurement is due to random errors. Statistically, a repeatability of 0.05 % in 5 runs is equivalent to ± 0.027 % uncertainty at 95 % confidence level. This same level of uncertainty can be met by using more or less repeatability runs. Table 5 gives an abbreviated overview of the number of runs and repeatability required to achieve the stated level of uncertainty. The table is taken from [1] and was derived from [27].

Table 5. Proving an ultrasonic liquid flow meter (from [1], Table B-1).

No. of repeatability proving runs	Repeatability*	Uncertainty (95 % conf. lev.)
3	0.02 %	0.027 %
5	0.05 %	0.027 %
10	0.12 %	0.027 %
15	0.17 %	0.027 %
20	0.22 %	0.027 %

* Per API MPMS, Ch. 4.8, Table A-1 to achieve 0.027 % uncertainty of meter factor

Table 6. Prover volume vs. meter size, for turbine meters (TM) vs. ultrasonic meters (LUFM), to achieve ± 0.027 % uncertainty of meter factor (95% conf. level).

Prover Volume vs. Meter Size				
	5 runs 0.05 %		8 runs 0.09 %	10 runs 0.12 %
	Prover Size (barrels)			
Meter Size	Turbine Meters	Ultrasonic Meters*		
4”	5	33	15	10
6”	12	73	34	22
8”	20	130	60	40
10”	24	203	94	62
12”	48	293	135	89
16”	100	521	241	158

* Per API MPMS, Ch. 5.8 [1] (Table B-2)

For ultrasonic meters the prover volume should also be increased to insure acceptable results. Table 6 provides a comparison between typical prover volumes for turbine meters at 5 repeatability runs, and the same size ultrasonic meter at 5,8 and 10 repeatability runs, to achieve ± 0.027 % uncertainty at 95% confidence level. The ultrasonic meter numbers are taken from ref. [1].

To better handle the random uncertainty, and improve the repeatability of an ultrasonic meter "groups" proving can be used. This method is outline in API MPMS 4.8 "Operation of proving Systems". It states that "The scatter in erratic meter proving data can be normalized by averaging the results of several meter proving runs and comparing the average of these small sets for agreement with the deviation limits." This method was employed in the lab testing of ultrasonic meters by running 14 consecutive runs, eliminating the first 3 to insure stable conditions, and grouping the remaining 11 runs into 5 groups of 7 runs each. The method makes use of all the data and provides significantly better results.

5.3. The need for proving

Validation, proving, a meter is always import for measurement certainty. For ultrasonic meters there are two methods that can be used: (1) In-situ testing in the field under operating conditions, or (2) lab testing under simulated conditions. The method employed depends on the amount of uncertainty that is acceptable. Meters used in the wholesale and retail sales almost universally require in-situ proving. The custody transfer of petroleum products by contract also almost always stipulate onsite proving.

Other applications may use meter factors established in a laboratory, but the measurement uncertainty increases. The installation effects are very difficult to asses quantitatively because of the many different configurations of piping, combined with the effect of in-line accessories like valves and strainers.

Influences of fluid properties on UFM performance have been pointed out and discussed to some extent in Section 4. For example, the presence of water droplets, gas bubbles or wax particles in the oil may cause significantly increased sound attenuation, cf. Figs. 3 and 4. For high-viscosity oils the sound absorption of the oil itself may also be significant. If so, the result may be a degraded signal-to-noise ratio (SNR).

Degradation of the SNR will lead to degradation of the accuracy of the LUFM. In many cases the SNR will not be the same in the in-situ field operation as it was in a factory flow calibration situation. Possible errors should therefore be measured and accounted for in both places, such as by in-situ proving of the LUFM.

Regular in-situ proving of the LUFM will also correct for possible misreading (shift in the meter factor) due to possible build-up of wax at (a) the transducer fronts, and (b) the spool piece wall.

Before better and more quantitative knowledge is available on how UFMs react to different fluids, the arguments advocating reduced need for in-situ proving and increased dependency on laboratory flow calibration (e.g. using water instead of hydrocarbons) [10,11], are highly questionable.

6. DEVELOPMENT RESULTS

The present project has lead to the development of a 6 path liquid ultrasonic flow meter which will be commercialized as Smith Meter™ Ultra[6].

The meter has been developed for the high accuracy measurement of refined petroleum products and crude oils. The main design criteria for the Ultra[6] were to develop a meter that could provide both high reliability and measusment stability in a wide range of petroleum applications. Since most petroleum applications are in harsh outside environments the packaging of the electronics is especially important. Measusment stability, as seen from this paper, depends on the proper application of the meter as well as the operation of the meter. The Ultra[6] has been built with experience in these applications and provides another measurement instrument for the industry. Application is so highly tied to performance that it always key to accurate measusment.

Significant synergies have been achieved, in several respects, between FMC Kongsberg Metering's MPU 1200, 600 and 200 gas ultrasonic flow meters [29], and FMC Smith Meter's Ultra[6] liquid ultrasonic flow meter. This relates to development synergies (cf. e.g. [30]) as well as production synergies.

The product line for the Ultra[6] will be released worldwide in phases for application on 6” - 20” lines and flow rates to 7500 m^3/h.

Fig. 7. 8” Smith Meter™ Ultra[6] Liquid Flowmeter with Signal Process Unit (SPU).

The meter has been tested over a wide range of operation conditions, with and without the patented VPC method [21] (software only). Typical results for an 8" meter on 2 cSt and 30 cSt products are shown in Fig. 8. The linearity is within ± 0.115 % and ± 0.161 %, respectively, over a 10.5:1 turndown ratio, for the two examples shown here.

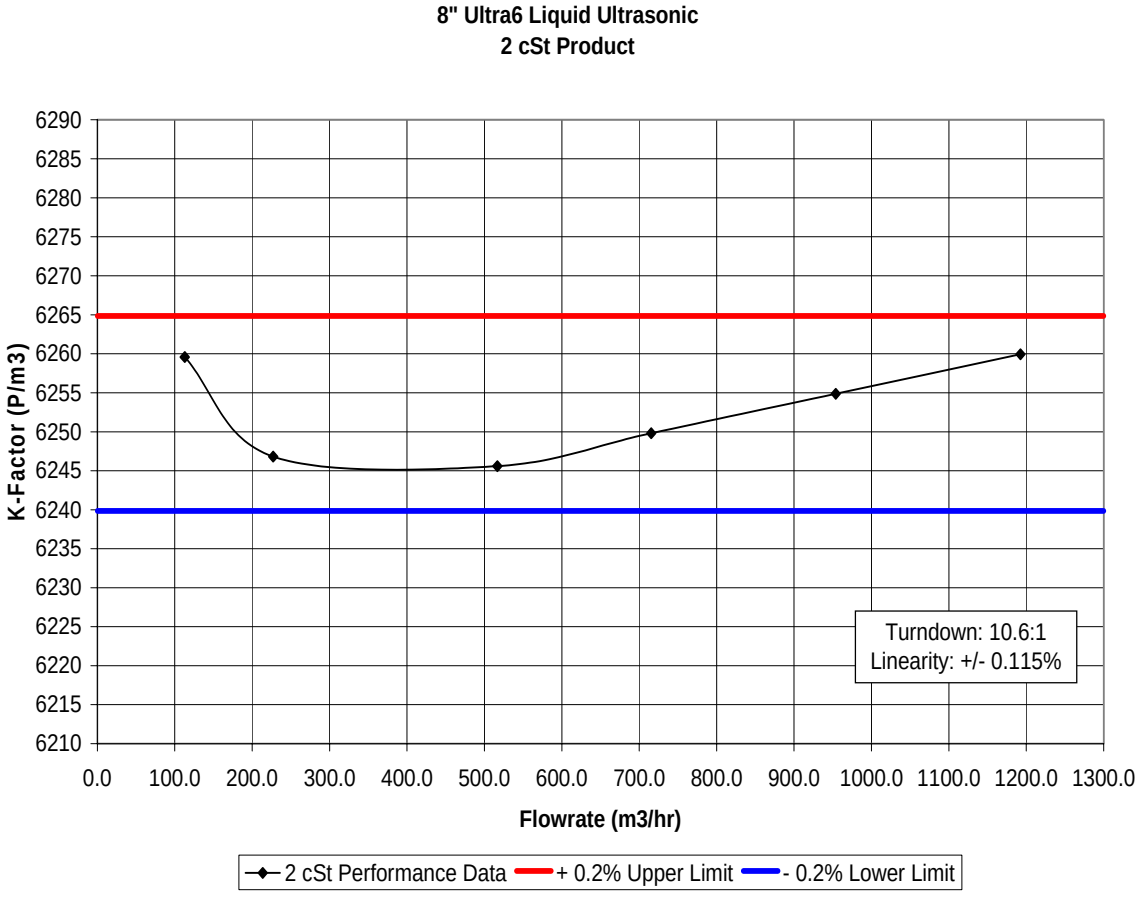

(a)

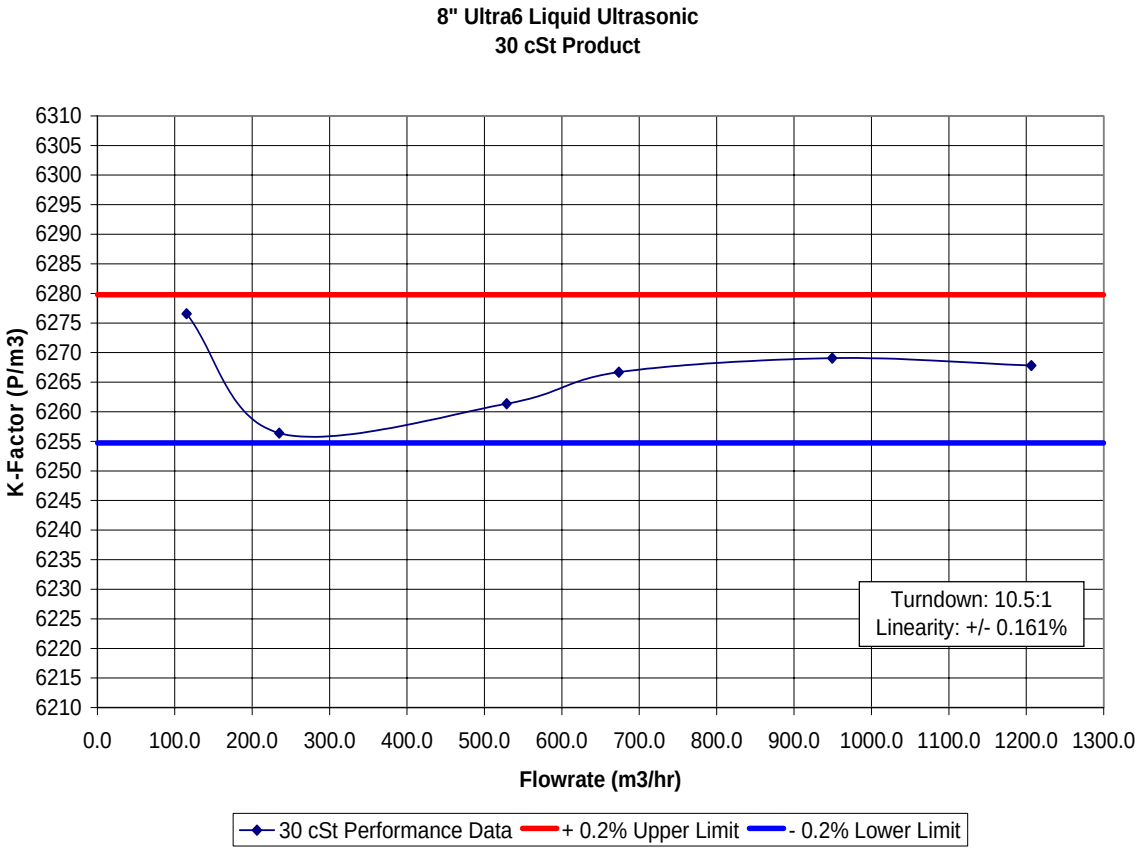

(b)

Fig. 8. Typical test results for an 8" Smith Meter™ Ultra[6] Liquid Flowmeter, on (a) 2 cSt and (b) 30 cSt products.

7. CONCLUSIONS

The advantages of ultrasonic meters make them well suited choice for high volume applications such as pipelines and ship loading / unloading facilities. Like turbine meters they are best operated at the higher flow ranges for optimum accuracy, but with techniques such as VPC, accurate measurement also at the lower flow ranges can be achieved. No pressure loss reduces operating cost. No moving parts increases service life and may reduce the frequency of proving, because usage wear is a key reason why meters are recalibrated.

The measurement technique is susceptible to installation effects and fluid properties. As with all meters, LUFMs need to be proven. In-situ proving, even though difficult, is indisputably the best method to reduce the total measurement uncertainty. Proving the meters in a laboratory offers an alternative, but at substantially higher risk of measurement error. Even though a specific ultrasonic meter may compensate for installation effects such as swirl or cross flow, there isn't any means of verifying this without field proving. The measurement accuracy is further compromised by the fluid property effects that were discussed in this paper. This is especially true for crude oils, because their properties are difficult to simulate even in a laboratory that tests with hydrocarbon fluids. Before better and more quantitative knowledge is available on how LUFMs react on different fluids, the arguments advocating reduced need for in-situ proving and

increased dependency on laboratory flow calibration (e.g. using water instead of hydrocarbons), are highly questionable.

Ultrasonic meters can provide accurate measurement over a wide range of crude oil applications if they are properly applied, proven and operated.

ACKNOWLEDGEMENTS

Significant technical contributions to the present work has been provided by the ULTRA[6] development team, consisting of (in addition to the authors) Kjell-Eivind Frøysa, Reidar Bø, Remi Kippersund and Stig Heggstad, Christian Michelsen Research AS, Norway; Skule Smørgrav, Atle K. Abrahamsen and Tom Heistad, FMC Kongsberg Meterering, Norway; Dave Resch, Jim Breter, Bob Smith and Joshua Rose, FMC Measurement Solutions, U.S.A.; and Magne Vestrheim, University of Bergen, Norway. The work has been supported by The Research Council of Norway (NFR).

REFERENCES

[1] **API MPMS Ch. 5.8,** "Manual of petroleum measurement standards, Chapter 5 - Metering, Section 8 - Measurement of liquid hydrocarbons by ultrasonic flow meters using transit time technology", 1st edition, American Petroleum Institute (API), Washington DC, U.S.A (February 2005).

[2] **AGA-9**, "Measurement of gas by ultrasonic meters", A.G.A. Report no. 9, American Gas Association, Transmission Measurement Committee (June 1998). (Revision in preparation.)

[3] **ISO/CD 18089 Part 1**, "Measurement of flow in closed conduits – ultrasonic meters for gas; meters for custody transfer and allocation measurement", International Organization for Standardization, Geneve, Switzerland (April 2005). (Committee draft standard only.)

[4] **Lunde, P., Frøysa, K.-E. and Vestrheim, M. (eds.),** "GERG project on ultrasonic gas flow meters, Phase II", GERG TM11 2000, Groupe Européen de Recherches Gazières (VDI Verlag, Düsseldorf, 2000).

[5] **Lunde, P. and Frøysa, K.-E.,** "Handbook of uncertainty calculations - Ultrasonic fiscal gas metering stations", Norwegian Petroleum Directorate, Norwegian Society for Oil and Gas Measurement (NFOGM), Christian Michelsen Research, Norway (December 2001). ISBN 82-566-1009-3 (free download available on web site www.nfogm.no).

[6] **Lunde, P., Frøysa, K.-E., Neumann, S. and Halvorsen, E.,** "Handbook of uncertainty calculations. Ultrasonic fiscal gas metering stations". *Proc. of 20th North Sea Flow Measurement Workshop,* St. Andrews Bay, Scotland, 22-25 October 2002.

[7] **Poynter, W. G.,** "Fundamentals of Liquid Measurement – Part 1", *Proc. of 76th ISHM (2001)*, p. 186.

[8] **Spitzer, D.,** "Industrial Flow Measurement", ISA (1990).

[9] **Miller, R. W.,** *Flow Measurement Engineering*, 3rd edition (McGraw-Hill, 1996).

[10] **Estrada, H., Cousins, T. and Augenstein, D.,** "Installation effects and diagnostic interpretation using the Caldon ultrasonic meter", *Proc. of 22nd North Sea Flow Measurement Workshop,* St. Andrews Bay, Scotland, 26-29 October 2004.

[11] **Hogendoorn, J., Laan, D., Hofstede, H. and Danen, H.,** "Altosonic III – A dedicated three-beam ultrasonic flowmeter for custody transfer of liquid hydrocarbons", *Proc. of 22nd North Sea Flow Measurement Workshop,* St. Andrews Bay, Scotland, 26-29 October 2004.

[12] **Kinsler, L. E., Frey, A. R., Coppens, A. B. and Sanders, J. V.,** *Fundamentals of Acoustics*, 4th edition (J. Wiley & Sons, New York, 2000).

[13] **D. Shore, M.O. Woods and C.A. Miles,** "Attenuation of ultrasound in post rigor bovine skeletal muscle", Ultrasonics, 81-87 (March 1986).

[14] **M. Freese and D. Makow,** "High-Frequency Ultrasonic Properties of Freshwater Fish Tissue", J. Acoust. Soc. Amer., **44**(5), 1282-1289 (1968).

[15] **Ping He,** "Acoustic parameter estimation based on attenuation and dispersion measurements", *Proc. of 20th Annual International Conference IEEE/EMBS, Oct. 29 - Nov. 1, 1998, Hong Kong.*

[16] **Ø. Nesse,** "Sound propagation in emulsions", Dr. Scient (Ph.D.) thesis, University of Bergen, Dept. of Physics, Bergen, Norway (January 1998).
[17] **Waterman, P. C. and Truell, R.,** "Multiple scattering of waves", J. Math. Phys. **2**, 512-537 (1961).
[18] **Frøysa, K.-E.:** "Separator instrumentation. A User Documentation of PRESIM 1.0", CMR Report CMR-93-F10011 (August 1993). (Confidential.)
[19] **Allegra, J. R. and Hawley, S. A.:** "Attenuation of Sound in Suspensions and Emulsions: Theory and Experiments", J. Acoust. Soc. Am. **51**, 1545-1564 (1972).
[20] **Lunde, P., Frøysa, K.-E., Fossdal, J. B. and Heistad, T.:** "Functional enhancements within ultrasonic gas flow measurement", Proc. of the *17th International North Sea Flow Measurement Workshop*, Oslo, Norway, 25-28 October 1999.
[21] **Frøysa, K.-E., Lunde, P. and Kalivoda, R.,** "Ultrasonic flow meter with velocity profile correction", US Provisional Patent Application No. 12878, Filed December 8, 2004.
[22] **Laufer, J.,** "The structure of turbulence in fully developed pipe flow", NBS Report No. 1174, National Bureau of Standards, USA (1952).
[23] **Dürst, F., Jovanovic, J. and Sender, J.,** "LDA measurements in the near-wall region of a turbulent pipe flow", J. Fluid Mech., **295**, 305-335 (1995).
[24] **Zagarola, M. and Smits, A.,** "Experiments in high Reynolds number turbulent pipe flow ", Phys. Rev. Lett., **78**(2), 239-242 (1997).
[25] **Perry, A. E., Henbest, S. M. and Chong, M. S.,** "A theoretical and experimental study of wall turbulence", *J. Fluid. Mech.* **165**, 163-199 (1986).
[26] **den Toonder, J. M. J.,** "Drag reduction by polymer additives in a turbulent pipe flow: laboratory and numerical results", PhD thesis, Delft University of Technology, The Netherlands (1995).
[27] **API MPMS,** Section 4.8 "Operation of Proving Systems" and **API,** Ch. 13.1 "Statistical Concepts and Procedures in Measurement", American Petroleum Institute (API), Washington DC, U.S.A.
[28] **Tasköprülü, N. S., Barlow, A. J. and Lamb, J.,** "Ultrasonic and visco-elastic relaxation in lubricating oil", J. Acoust. Soc. Am., **33**, 278-285 (1961).
[29] "Ultrasonic gas flow meter MPU 1200. Specifications", Bulletin SSKS001, Issue/Rev. 04 (5/02), FMC Measurement Solutions (2005). Web page: http://info.smithmeter.com/literature/docs/ssks001.pdf
[30] **Lunde, P., Vestrheim, M., Bø, M., Smørgrav, S. and Abrahamsen, A**, "Reciprocity and its utilization in ultrasonic flow meters", *Proc. of 23rd Intern. North Sea Flow Measurem. Workshop, Tønsberg, Norway, 18-21 October 2005*.

North Sea Flow Measurement Workshop
18-21 October 2005

MULTIPHASE FLOW METERING: 4 YEARS ON

G.Falcone, TOTAL E&P UK PLC and Imperial College London, UK,
G.F.Hewitt, Imperial College London, UK,
C.Alimonti, University "La Sapienza" of Rome, Italy,
B.Harrison, TriPhase Consulting Ltd, UK

---

1 Abstract

Since the authors' last review in 2001 [1], the use of Multiphase Flow Metering (MFM) within the oil and gas industry continues to grow apace, being more popular in some parts of the world than others. Since the early 1990's, when the first commercial meters started to appear, there have been more than 1,600 field applications of MFM for field allocation, production optimisation and mobile well testing. As the authors predicted, wet gas metering technology has improved to such an extent that its use has rapidly increased worldwide. A "who's who" of the MFM sector is provided, which highlights the mergers in the sector and gives an insight into the meters and measurement principles available today. Cost estimates, potential benefits and reliability in the field of the current MFM technologies are revisited and brought up to date. Several measurements technologies have resurfaced, such as passive acoustic energy patterns, infrared wavelengths, Nuclear Magnetic Resonance (NMR) and Electrical Capacitance Tomography (ECT), and they are becoming commercial. The concept of "virtual metering", integrated with "classical MFM", is now widely accepted. However, sometimes the principles of the MFM measurements themselves are forgotten, submerged in the sales and marketing hype.

2 Introduction

Over the past four years, MFM has come a long way from being generally recognised as an area of research, development and technology application, to representing a discipline *per se'* within the oil and gas industry. The benefits associated with MFM, as outlined in the authors' previous review [1], have been confirmed by the way MFM technology has succeeded in fitting with other technologies toward global field-wide solutions.

However, MFM has not yet achieved its full potential nor is everybody in the oil and gas industry aware of what MFM can and cannot do.

Nowadays, it is not surprising to hear of a multi-million dollar contract being signed by an Operator for a Manufacturer to supply fifty MFM's for a field development, but it is debatable whether there has been any revolutionary advancement in MFM solutions since 2001. What has undeniably improved is the confidence in the subsea versions of the MFM technology and in the hardware reliability, the stability of the sensors and the mean time to failure. Also improved is the collaboration between Operator and Manufacturer, forged by working together in the field over the past years.

However, have all the technical routes to MFM innovation been fully exploited? Are there still physical and economic constraints that prevent this technology from moving forward?

3 MFM Trends

Since 2001 there have been several published reviews on the number of MFM installations worldwide [2][3]. However, it remains difficult to establish the official figures, as it is necessary to distinguish between:

- MFM's installed and currently working;
- MFM's installed, but now discontinued;
- MFM's ordered, but not yet delivered;
- MFM's delivered, but not yet installed;
- MFM's used as portable well testing solutions.

This type of information is commercially sensitive due to the high competition in the market of commercial MFM's.

Following a market research by the authors in 2005, it appears that a total figure for MFM installations to date, as defined in the bulleted list above, is in excess of 1,600. Of these, 10% is represented by mobile well testing applications and a further 20% corresponds to wet gas metering. Western Europe, Asia-Pacific and the U.S. together represent 75% of the total number of MFM installations. Asia-Pacific has seen a sharp increase in MFM applications since 2001 and has now overtaken the North Sea, where most of the initial installations of MFM's began. However, the 1,600 figure does not account for all of the installations since the early 1990's as some Manufacturers have disappeared and some of the solutions have been discontinued. The past four years has seen mergers amongst manufacturers, but the entry of newcomers has kept the total number of commercial manufacturers at around twenty. In some ways, these mergers have helped in the disclosure of information to the public domain, but knowledge has also been lost. Some of the smaller manufacturers, who were around four years ago, have experienced mixed fortunes, becoming established "names" and setting trends with the larger providers, while others have not really "cracked" the market.

Table 1 presents a list of the current commercial MFM's, divided into "traditional" MFM's (Gas Volume Fraction, GVF<95-98%), high gas volume fraction MFM's (GVF>95-98%) and Downhole MFM's (DMFM's).

Table 2, **Table 3**, **Table 4** and **Table 5** present possible ways to classify the current commercial MFM's based on their features. Those meters that are still under development have not been included (e.g. IFP, University of Manchester, Imperial College, Robert Gordon University/QuantX). Also omitted are those MFM solutions that need to be integrated with other techniques in order to provide the three flow rates (e.g. pressure pulse, virtual metering).

Although the authors have developed their own views on the MFM solutions available, the tables of MFM's only provide an immediate overview of the MFM market today and indicate what applications the contractors claim they may be used for.

MFM's	High GVF MFM's	DMFM's
Roxar-MPFM	Roxar-WGM	QuantX
Schlumberger/Framo-Vx	Schlumberger/Framo-Vx	Weatherford/CIDRA
Flowsys/FMC-TopFlow	Petrotech-Smartvent	Schlumberger
Jiskoot-MIXMETER		
TEA Sistemi-Lyra	TEA Sistemi-VEGA	
Agar-MPFM	Agar-MPFM 400 loop	
Red Eye-REMMS	Red Eye-REMMS (?)	
Abbon-Flow Master	Abbon-Flow Master	
Haimo-MPFM	Haimo-MPFM	
ESMER	ESMER (e.g. + V-cone)	
Kvaerner-DUET	Kvaerner-CCM	
Kvaerner-CCM		
Accuflow	Accuflow	
Daniel/Emerson-MEGRA	Solartron/Emerson-Dualstream II	
Hydralift-Wellcomp		

Table 1: current commercial MFM's, WGM's and DMFM's

Flow conditioning /Homogenisation	Leave-as-it-is	In-line separation	Isokinetic sampling
Roxar-WGM	Roxar-MPFM	Agar	TEA Sistemi-VEGA
Jiskoot-MIXMETER	Schlumberger/Framo-Vx	Wellcomp	
TEA Sistemi-Lyra	Flowsys/FMC-TopFlow	Accuflow	
Daniel/Emerson-Dualstream II	Daniel/Emerson-MEGRA (for GVF<25%)	Daniel/Emerson-MEGRA (for GVF>25%)	
	Abbon-Flow Master	Red Eye-REMMS	
ESMER (+ V-cone)	ESMER	Haimo-MPFM	
	Petrotech-Smartvent		
	Kvaerner-DUET	Kvaerner-CCM	

Table 2: current commercial MFM's with/without flow conditioning

Gamma source	No Gamma source
Roxar-MPFM	Roxar-WGM
Jiskoot-MIXMETER	Red Eye-REMMS
Daniel/Emerson-MEGRA	Daniel/Emerson-Dualstream II
Kvaerner-DUET	Kvaerner-CCM
Haimo-MPFM	Agar
Schlumberger/Framo-Vx	Wellcomp
TEA Sistemi-Lyra	TEA Sistemi-LYRA (for WC>30%)
	TEA Sistemi-VEGA
	Flowsys/FMC-TopFlow
	Petrotech-Smartvent
	Abbon-Flow Master
	ESMER
	Accuflow

Table 3: current commercial MFM's with/without gamma ray source

Intrusive	Non-intrusive(*)
Roxar-WGM	Roxar-MPFM
Jiskoot-MIXMETER	Schlumberger/Framo-Vx
TEA Sistemi-VEGA	TEA Sistemi-LYRA
Kvaerner-CCM	Kvaerner-DUET
Daniel/Emerson-Dualstream II	Daniel/Emerson-MEGRA
Haimo-MPFM (flow conditioning vessel)	Petrotech-Smartvent
Accuflow	Flowsys/FMC-TopFlow
Red Eye-REMMS	Abbon-Flow Master
Agar	ESMER
Wellcomp	

Table 4: current commercial MFM's intrusive/non-intrusive
(*) Venturi's are not regarded as intrusive devices

X-correlation	No X-correlation
Roxar-MPFM	Roxar-WGM
Kvaerner-DUET	Kvaerner-CCM
Haimo-MPFM (flow conditioning vessel)	TEA Sistemi-LYRA
Flowsys/FMC-TopFlow	Schlumberger/Framo-Vx
	Daniel/Emerson-MEGRA
	Petrotech-Smartvent
	Daniel/Emerson-Dualstream II
	Abbon-Flow Master
	ESMER
	Accuflow
	Red Eye-REMMS
	Agar
	Wellcomp
	TEA Sistemi-VEGA
	Jiskoot-MIXMETER

Table 5: with/without cross-correlation

The cost of MFM's today remains in the range of US$100,000-US$500,000 (varying with onshore/offshore, topsides/subsea, the dimension of the tool and the number of units ordered), even though there has been an estimated increase of 25-50% in production facilities CAPEX since 1999 [4]. This CAPEX rise has been "cancelled out" by the fact that MFM's have become up to 50% cheaper, mainly due to the increased competition in the market and the rise in units sold.
When comparing a traditional production layout (with test separator and test lines) with an installation with MFM, it still appears that the second option involves much lower CAPEX. The installed cost of a separator varies enormously with rates, pressures, temperatures, chemistry of the fluids to be treated, onshore/offshore, but is typically in the range US$1m-5m. It may also require several instruments, depending on its complexity.
The test lines may be omitted in some MFM installations. Carbon steel flow lines of 4-6" in diameter cost approximately US$1.3m-3.6m per Km installed.

OPEX costs associated with test separators can be around US$350,000 per year for offshore installations. In 1999, it was estimated [4] that the OPEX for a MFM was likely to be 25% of the cost of the meter itself for the first year, then US$10-40,000 per year (for both onshore and topsides applications). Today, with the increased reliability of the MFM hardware and more structured training of personnel, OPEX is spread more evenly over the operating life of a MFM.

4 The MFM Community

The oil and gas industry is a global business, yet the MFM expertise is not equally distributed worldwide. Not all Operators have in-house MFM specialists and, within the Service Companies, only a select handful of people can be defined as experts in MFM. As with all in-house specialists in any particular discipline, there is reluctance to share too much of their hard-won knowledge, which can lead to them being isolated from the rest of the company.

With MFM now being accepted as a standard solution for existing and new developments, competition among MFM suppliers has intensified. Despite the existence of a global MFM community, it remains very difficult to release and share confidential data. A small/medium Operator without direct MFM experience will find it almost impossible to obtain a fair and independent view of the advantages and disadvantages of each commercial MFM from discussions with the Manufacturers or other Operators. The old trick of going to see Manufacturer A to ask about the downfalls of the product sold by Manufacturer B (and *vice versa*) only works up to a certain point.

There has been a constant rise in the availability of MFM handbooks, guidelines, recommendations and technical publications, but so far, none of them has described in detail the pros and the cons of each commercially available MFM solution. Such guidelines are usually limited to lists of MFM solutions (full separation, partial separation, in-line, etc.), MFM definitions (what GVF is, how calibration is done, etc.), standards by the International Organization for Standardization (not always directly applicable to the specific case of MFM) and ways to report the performance of a meter. This only captures the performance of a MFM as a "black box", but does not teach how to keep track of all the possible uncertainties and inaccuracies that are inherent in each individual MFM technique. Also, there is the risk of continual reference to original equations or relationships, while their actual implementation in commercial solutions is often adapted to suit a specific approach. There are very few worked examples in the public domain that do not have a "commercial agenda" and are sufficiently accurate to enable a critical and informed selection of meters.

As a result, there is an emerging class of consultants who perform studies on behalf of Operators and Government bodies and mediate between them and the Manufacturers.

5 Example of "forgotten basics"

As previously stated, the hardware and sensors have improved tremendously, but it is important not to forget the principles of the measurements themselves. Let us consider the basic concept of the gamma ray measurement of two-phase flow.

Figures 1, **2** and **3** illustrate the absolute error in phase fraction measurement in a two-phase flow system of air-water, air-oil and water oil, respectively. The calculations

are based on a 4" diameter pipe section made of Perspex material, with single-energy gamma-ray beams passing through pipe walls of 12.7mm of thickness. The sources and energy levels used in this example are those commonly adopted in commercial MFM's, namely, Americium 241 (17.8 and 59.5 KeV), Barium 133 (31, 81 and 356 KeV) and Caesium 137 (33 and 661 KeV). Assuming that all sources can provide the same initial intensity, I_0 = 5,000 counts/s, it is possible to calculate the intensity (I) of a single-energy gamma-ray beam, transmitted through the Perspex conduit in which there are two static or flowing phases, as:

$$I = I_0 \exp\left(-\gamma_{wall} x_{wall} - \gamma_1 x_1 - \gamma_2 x_2\right) \qquad \textbf{Eq. 1}$$

where:

γ_1 and γ_2 are the linear attenuation coefficients of phase 1 and phase 2, respectively;
x_1 and x_2 are the thicknesses of phase 1 and phase 2, respectively;
γ_{wall} is the linear attenuation coefficient of the conduit;
x_{wall} is the thickness of the conduit.

The absolute error in phase fractions is given by [5]:

$$\delta\varepsilon_{1,2} = \pm \frac{1}{(\gamma_1 - \gamma_2) D \sqrt{Ct}} \qquad \textbf{Eq. 2}$$

where:

D is the internal diameter of the pipe;
C is the transmitted count rate;
t is the counting time.

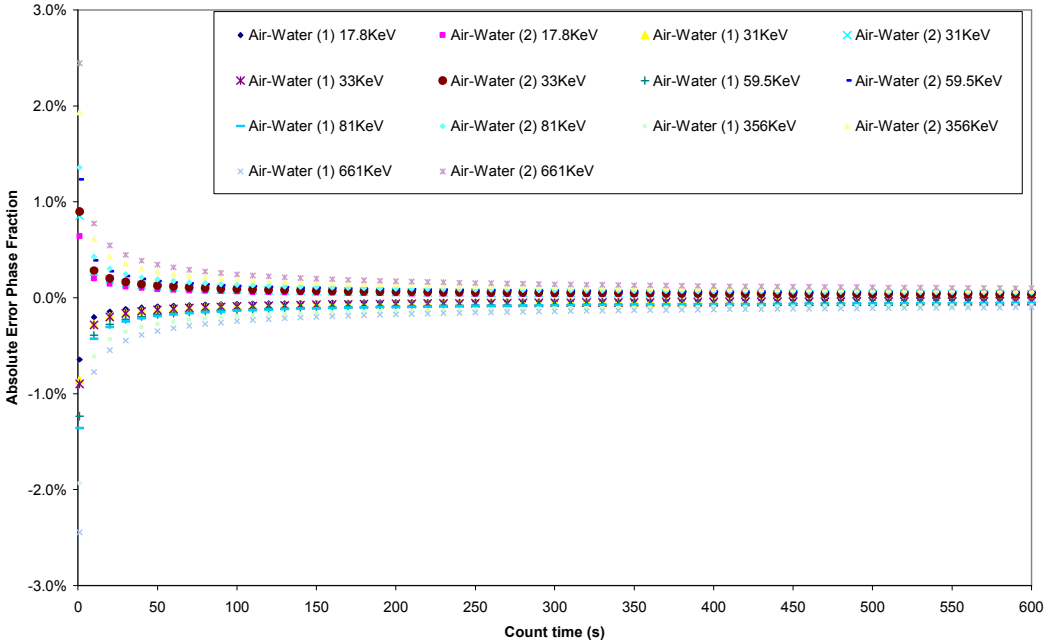

Figure1: Absolute error in phase fraction for an air-water system.

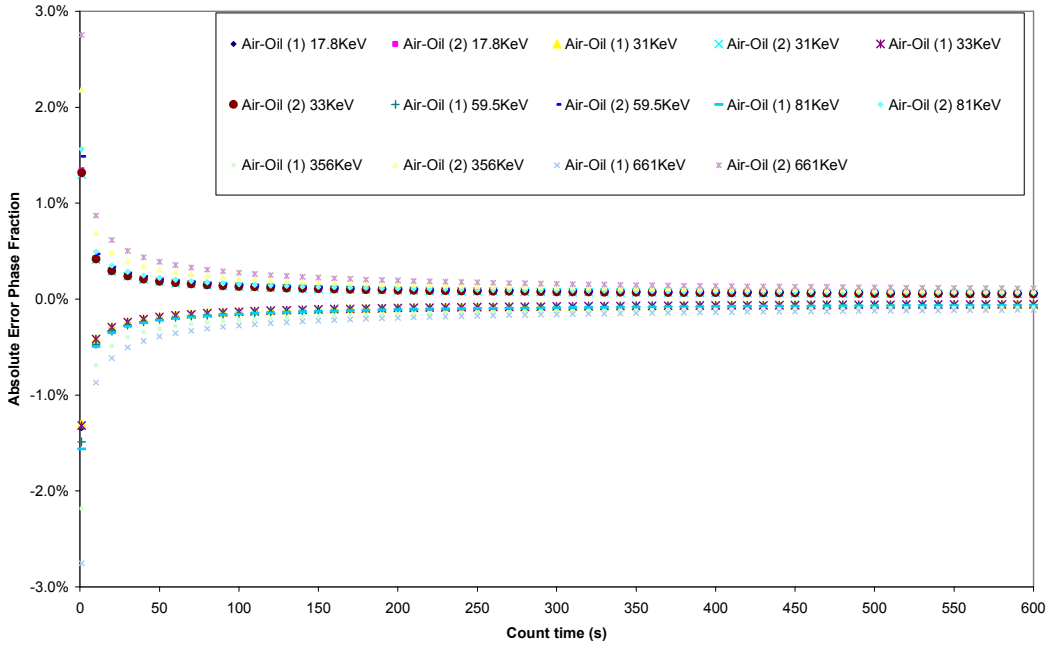

Figure 2: Absolute error in phase fraction for an air-oil system.

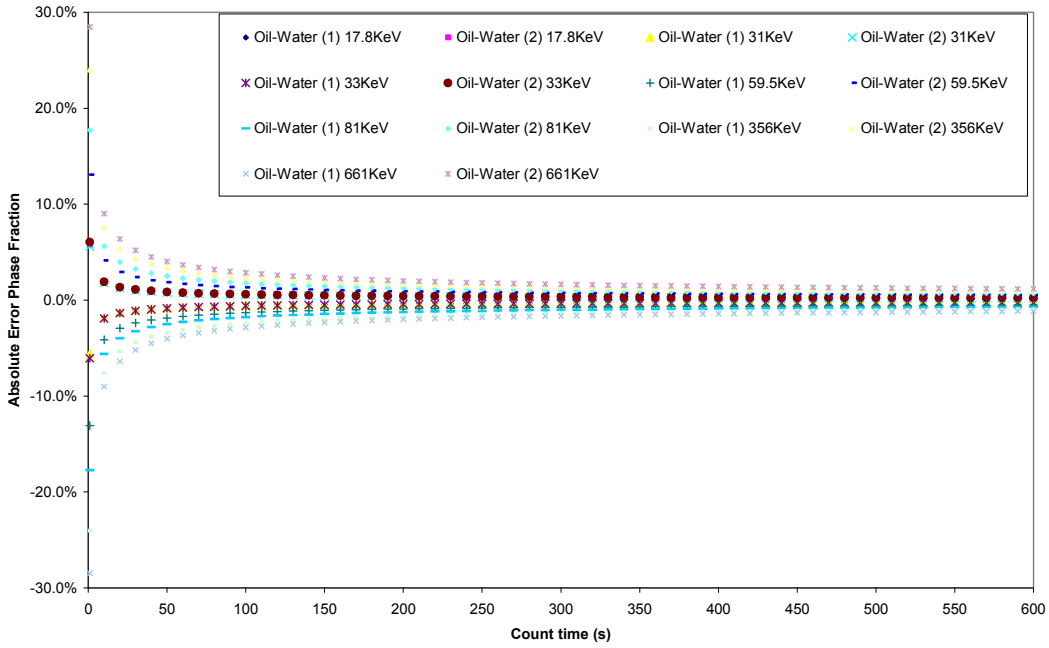

Figure 3: Absolute error in phase fraction for an oil-water system.

The plots above illustrate that the accuracy of the measurement is a function of the counting time. They also show that the measurement errors for air-oil and air-water systems are quantitatively similar, while that for oil-water systems is several times larger due to the small difference between the water and oil density.

Gamma ray measurements are usually associated with a Venturi in order to measure the total (or mixture) momentum from which the phase flow rates are calculated. The

classical equation used to calculate the total flow rate, assuming homogeneous flow, is given by:

$$Q_t = C_q A \sqrt{2 \cdot \left(\frac{\Delta p}{\rho} - g \cdot \cos\theta \cdot L \right)} \qquad \textbf{Eq. 3}$$

where:

C_q is the flow coefficient;
ρ is the bulk or mixture density;
A is the cross sectional area of the Venturi throat;
L is the distance between pressure taps;
ΔP is the measured pressure difference;
θ is the deviation angle from the vertical.

The above parameters can be divided into those that can be measured in the field and those that can be established in the factory. The design of the meter establishes the cross sectional area of the Venturi throat, the distance between the pressure tappings and the full scale of pressure transducer, while the flow coefficient can be determined in the factory by calibration. The remaining parameters are measured in the field. Of course, uncertainties in parameter determination can play an important role.
Figure 4 shows the relative error in mixture density from error propagation. The assumed uncertainty in gas density is 5% while that in liquid density is 1%. The gas fraction and the water cut are affected by an uncertainty of 3%. A strong influence of gas fraction is highlighted.

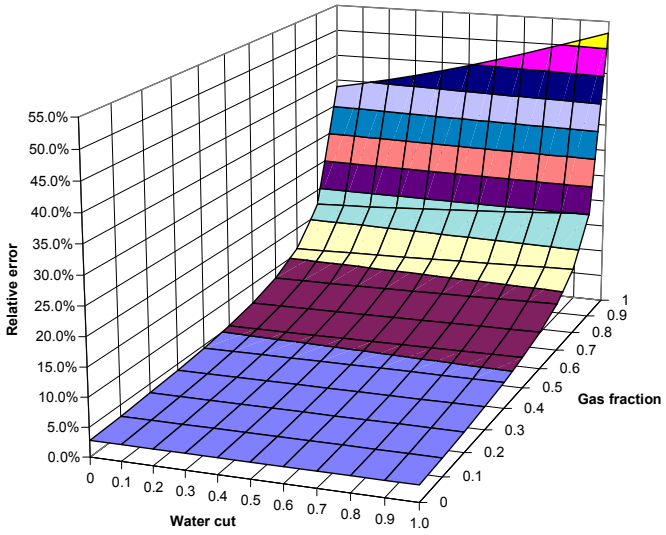

Figure 4: Relative error in mixture density for a gas-oil-water system.

The uncertainties for remaining parameters needed in the design of a 3" DN Venturi, with a cross sectional ratio of 0.5, are reported in **Table 6**.

Parameter	Uncertainty
Distance between pressure tappings	10^{-4} m
Cross sectional area	$1.2\ 10^{-5}$ m^2
Pressure difference	0.1 % of reading

Table 6: Design uncertainties of Venturi's

It is possible to estimate the error propagation from **Eq.3** and so highlight the influence of the measured parameters, pressure difference and mixture density. **Figure 5** shows the error in mixture flow rate vs. the mixture density and the pressure difference. The two parameters exert a considerable influence on the error, especially when they are relatively small in value. Errors can vary between 3.5% and 75%.

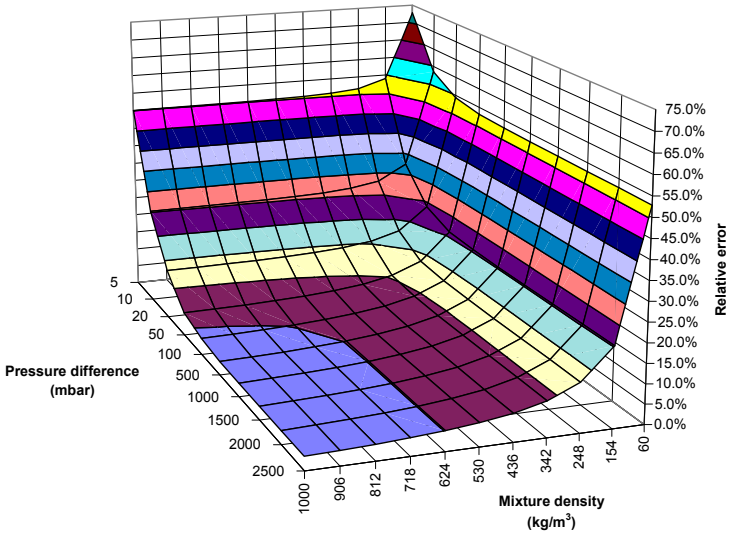

Figure 5: Relative error in mixture momentum for a gas-oil-water system.

The direct consequence of the above is the definition of an envelope of operation (rangeability), where the error is less than a fixed value, as shown in **Figure 6**.

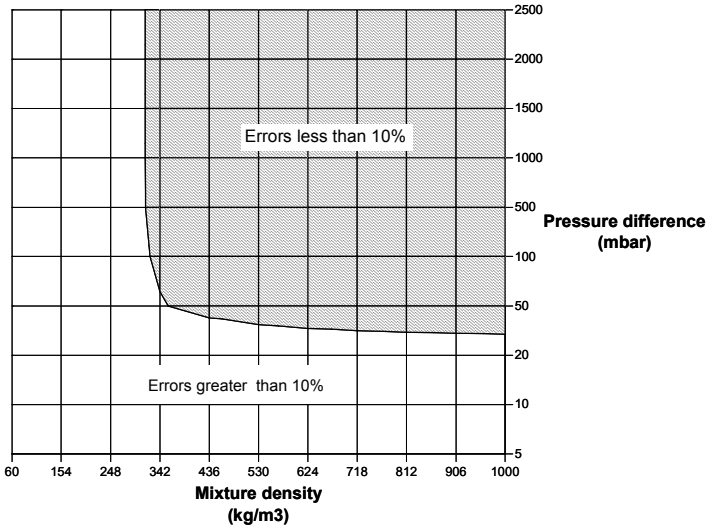

Figure 6: Envelope of operation for a mixture momentum for a gas-oil-water system.

Last but not least, the discharge coefficient is a model calibration parameter that is mainly dependent on the fluid properties. Oil viscosity can be much higher than that of water, whereas the density difference between the two phases is relatively small, so the Reynolds number of the flowing mixture will decrease as the oil fraction increases. For Reynolds numbers lower than 100,000, the discharge coefficient assumes a variable value, but this becomes constant at higher Reynolds numbers. Thus, the higher the oil viscosity, the more important it is to provide an accurate description of

the discharge coefficient pattern vs. Reynolds number. Experimental data, which exhibit this dependency, are shown in **Figure 7** [15]. The oil viscosity, in this case, was only10 mPa·s.

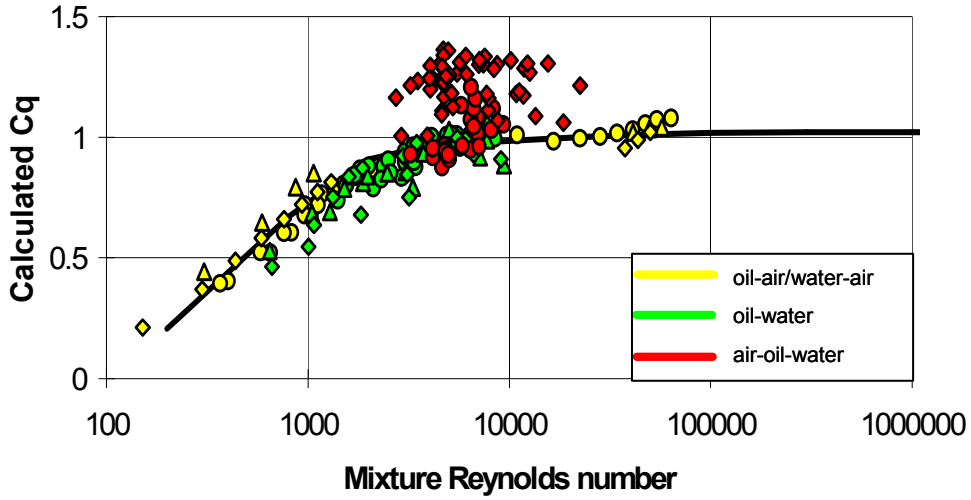

Figure 7: Discharge coefficient vs. Reynolds number.

6 Novel technologies, R&D trends

As mentioned previously, there have been no truly novel MFM technologies breaking through over the past four years. However, some of the novel technologies identified in 2001 have been the subject of rather intensive research that has now led to some significant results.

X-ray and gamma ray tomography [6], ECT [7][8] and microwave techniques [9] have already undergone noticeable improvements since the authors' previous review [1]. If combined with independent velocity measurements (e.g. cross-correlation, Venturi), they could provide the flow rates of each phase.

Water cut meters based on infrared spectroscopy are now commercially available. They aim at measuring the volumetric proportion of oil in a mixture of petroleum and water by passing through the stream a beam of infrared light that is absorbed by oil, but not water. Several infrared wavelengths can be measured to allow extending the range of applicability of this optical technology to low water cuts and to reduce the effects of the presence of gas.

Research has continued into NMR [10]. Surprisingly, Pulsed Neutron Activation (PNA) has not been the focus of any substantial studies, despite the fact that it could be the only way of directly measuring individual component velocities and fractions.

Cheaper "stand-alone" technologies such as pressure pulse [11][12] and acoustic noise interpretation [13] are now commercially available. Although there may cases

where these technologies are not suitable, they should be able to compete with other solutions on price.

The integrated monitoring and metering approach is nowadays referred to as "virtual metering" [14]. Commercial solutions are now available, although virtual metering should be treated as a supplement or back-up to MFM's rather than a replacement.

There is a developing trend in the industry to "mix and match" different MFM solutions from different provider to better exploit their inherent strengths. This has probably been triggered by the need to extend the operating envelope of previously existing MFM's and has led to some positive results.

Direct R&D efforts continue within academia, research organisations and Service Companies. While some oil companies still retain some level of in-house research, the majority of them have opted for contracted research projects, in which they share supervision.

7 Conclusions

The trends in MFM sales and installations, the establishment of wet gas metering as a special niche and the evolution of some novel technologies have been as predicted in 2001 [1]. Also, the interaction between Operators and Manufacturers has improved, but there remains a paucity of quality field data in the public domain. This is why more effort is needed to define much more specific MFM Regulations, with a special focus on the strengths and the downfalls of each MFM metering principle.
Though MFM technology has now been widely applied in hydrocarbon recovery systems, there are still unresolved questions regarding the accuracy and range of applicability of commercial meters. There is a tendency to forget some of the basic limitations, as exemplified here by the cases of gamma densitometry and Venturi meters. Even in the case of straight pipe flows, the structure and local behaviour of multiphase flows is still, in all but the simplest cases, poorly understood and certainly not predictable. Small wonder then that the developing flows through the complex geometries which occur in many metering systems are not captured by the simplified models use to interpret meter outputs. Perhaps the real surprise is that, even after discounting the sales hyperbole common in this field, the meters work even as well as they do! There is a long way to go in this field and the user should realise that MFM's are one piece of the optimised production system jigsaw.

8 References

[1] Falcone, G., Hewitt, G.F., Alimonti, C., Harrison, B.: "Multiphase Flow Metering: Current Trends and Future Developments", paper SPE 71474 presented at the 2001 SPE Annual Technical Conference and Exhibition held in New Orleans, Louisiana, 30 September–3 October 2001

[2] API Publication 2566, First Edition: "State of the Art Multiphase Flow Metering", May 2004

[3] Atkinson, A., Theuveny, B., Berard, M., Conort, G., Lowe, T., McDiarmid, A., Mehdizadeh, P., Pinguet, B., Smith, G., Williamson, K.J.: "A New Horizon in Multiphase Flow Measurement", Schlumberger Oilfield Review, Winter 2004-2005, 52-63

[4] Sheers, A.M., Noordhuis, B.R.: "Multi-phase and Wet Gas Flow Measurement", presented at IBC's 5th Annual Multi-Phase Metering Conference held in Aberdeen, Scotland, 22-23 February 1999

[5] Pan, L.: "High pressure three phase (Gas/liquid/liquid) flow", PhD Thesis, Imperial College London, 1996

[6] Johansen, G.A.: "Nuclear tomography methods in industry", Nuclear Physics A 752 (2005) 696c–705c

[7] Ismail, I., Chondronasios, A., Yang, W.Q.: "Wet gas flow metering by electrical capacitance tomography", paper presented at the 4th South East Asia Hydrocarbon Flow Measurement Workshop, Kuala Lumpur, Malaysia, 7-11 March 2005

[8] Gamio, C., Ismail, I., Zhang, Z.T., Yang, W.Q.: "Review of electrical capacitance tomography for oil industry", Proc. of 4th Int. Symp. on Measurement Techniques for Multiphase Flows, Hangzhou, China, 10-12 Sept. 2004, 116-121

[9] Bentolila, Y., Constant, M.: "Physical approach of volumetric phase estimation based on mixture laws for multiphase flows", presented at the 5th North American Conference on Multiphase Technology, Banff, Canada, 1-6 June 2005

[10] Ong, J.T., Oyeneyin, M.B., Coutts, E.J., MacLean, I.M.: "In Well Nuclear Magnetic Resonance (NMR) Multiphase Flowmeter in the Oil and Gas Industry", paper SPE 89978 presented at the SPE Annual Technical Conference and Exhibition held in Houston, Texas, 26-29 September 2004

[11] Gudmundsson, J.S., Celius, H.K.: "Gas-Liquid Metering Using Pressure-Pulse Technology", paper SPE 56584 presented at the SPE Annual Technical Conference and Exhibition, Houston, Texas, 3-6 October 1999

[12] Gudmundsson, J.S., Durgut, I., Ronnevig, J., Korsan, K., Celius, H.K.: "Pressure Pulse Analysis of Gas Lift Wells", presented at the Fall 2001 ASME/API Gas Lift Workshop, Aberdeen, 12-13 November 2001

[13] Piantanida, M., Mazzoni, A., Tanzi, A., Hope, B.R.: "Multiphase Metering: Experimental Results from the Analysis of Acoustic Noise Through a Choke", paper SPE 50681 presented at the 1998 SPE European Petroleum Conference held in The Hague, The Netherlands, 20-22 October 1998

[14] Rasmussen, A.: "Field applications of model-based multiphase flow computing", presented at the 22nd North Sea Flow Measurement Workshop, St. Andrews, Fife, 26-29 October 2004

[15] Alimonti, C., Annunziato, M., Cerri, M.: "Using a Venturi Meter in Multiphase Metering Systems", 5th International Conference on Multiphase flow in Industrial Plants, Amalfi, Italy, 26-27 September 1996

Is it a MUST to add Upstream Devices for High GVF Multiphase?

Jianwen Dou
Jason Guo
Gokulnath R
Haimo Technologies Inc

Objective

High accuracies in measurement of the gross liquid and net oil flow rates at high GVF levels in the multiphase flow is identified as one of the most demanding needs of the industry, especially in high watercut environments. The underlying factor that decides the accuracy of the net oil flow rate measurement is the accuracy at which the gross liquid & watercut are measured and the prevailing watercut in the flow. It is an established fact that accuracies falter with increasing GVF in the multiphase flow.

The purpose of this paper is to present the performance results of a newly developed Compact High GVF Haimo multiphase meter that addresses the above needs,

- without having to use an Upstream Separation Device for high GVF application
- while retaining the accuracies within ±2% absolute for watercut and 10% relative for liquid and gas flow rates at 90% confidence level.
- while also optimising the footprint, the cost, the weight of the solution

Further developmental work and trials are in progress to achieve the targeted accuracy levels under very high GVF conditions as well.

Contents of the Paper

1.0 Definitions

1.1 GVF – Gas Volume fraction

The gas volume flow rate, relative to the multiphase volume flow rate, at the pressure and temperature prevailing in that section. The GVF is normally expressed as a fraction or percentage.

1.2 WC – Watercut

The water volume flow rate, relative to the total liquid volume flow rate (oil and water), both converted to volumes at standard pressure and temperature. The WC is normally expressed as a percentage.

1.3 Moderate GVF (25-85%)

The Moderate GVF can be considered as the 'sweet spot' of multiphase meters, i.e. the range where they have their optimum performance, and where at the same time traditional single-phase meters are not a viable option.

1.4 High GVF (85-95%)

Entering this High GVF range the uncertainty of multiphase meters will start to increase, with a rapid increase towards the upper end of the range. This increase in uncertainty is not only linked to more complex flow patterns at high gas fraction, but also because the measurement uncertainty will increase as the relative proportion of the fraction of the component of highest value (in this case the oil) decreases. In some cases partial separation is used to move the GVF back into the Moderate GVF range.

1.5 Very high GVF (95-100%)

This upper end of the multiphase range could also be termed the 'wet gas' range. In the lower end of the very high GVF range the measurement performance of in-line multiphase meters may still be sufficient for well testing, production optimisation and flow assurance. For allocation metering, in particular at the high end of this range, often gas is the main 'value' component, and a wet gas meter would be the preferred option.

This corresponds to a Lockhart-Martinelli (LM) value in the range from 0 to approximately 0.3.

1.5 Measuring envelope

The area's in the two-phase flow map and the composition map in which the MPFM performs according to its specifications (elaborated in 1.6)

1.6 Accuracy Specifications

The term "accuracy specifications" in this paper shall refer to carrying out measurements within $\pm$2% abs. for watercut and 10% relative for liquid and gas at 90% confidence level. All data points within any of the Measuring envelopes presented in this Paper are consistently measured within the Accuracy Specifications.

Reader's special remembrance to the above definition is requested while the above term is read in this Paper in different contexts.

2.0 MFM 2000 + Upstream Separation Device (*Accuracy Specifications* applicable upto 99.8% GVF)

MFM 2000 - the basic configuration of the Haimo multiphase meter is a combination of a gas / liquid two phase (inline) and a full range three phase water cut meter. The watercut measurements are carried out independent of the gas / liquid flow rate measurement.

The gas / liquid two phase meter consists of a venturi and one single gamma (59.5 keV) sensor. The three phase water cut meter comprises a dual energy (22 and 59.5 keV) gamma sensor and a flow conditioner located upstream. Measurement of the gas and liquid streams is carried out upstream of the flow conditioner in the two-phase flow meter.

The Dual gamma meter measures the water cut under a stable flow regime, which is critical for the water cut measurement accuracy. Net oil flow rate is finally calculated based on the gross liquid and water cut measurements.

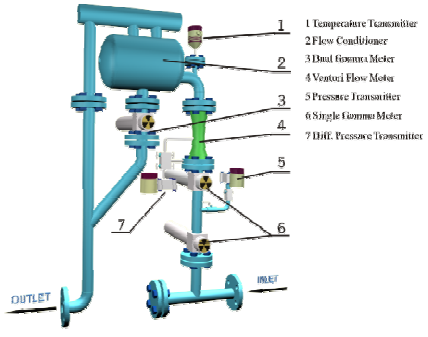

Schematic of Enhanced MFM2000 Series Multiphase Flow Meter

***"Accuracy specifications"* applicable upto 90% GVF**

The combination of the flow conditioner and the dual energy gamma absorption watercut meter helps Haimo achieve the +/-2% abs. error on watercut over 0-90% GVF range with a 90% confidence level

It is a well established fact that the accuracies in measurement of watercut and liquid / gas flow rates fall with increasing GVF. An upstream gas conditioning device is integrated upstream of the MFM 2000 series meters to extend the GVF to 99%)

With an Upstream Separation Device

***"Accuracy specifications"* applicable upto 99.8% GVF**

The gas conditioning unit is used to absorb shock in flow rate of the incoming multiphase flow such as severe slugging, and to separate the multiphase flow initially. The gas conditioning units separates the liquid drops from the flow to ensure no liquid is diverted into the gas leg. The gas leg is fitted with a control valve and vortex meter.

Based on the GVF measurements from the MFM initially when the control valve is fully closed, the control valve mounted on the gas leg regulates its opening to control the gas flow rate through the same leg thus controlling the GVF level in the multiphase leg; the vortex flow meter measures the wet gas flow rate through the gas leg. Sections hereunder detail the measurement philosophy and principles behind the Haimo technology

2.1 The technology within …

Haimo targets a narrow band of accuracies specified in Section 1.6 of this Paper as the Design Basis. Increasing levels of GVF in the incoming multiphase flow affect the measurement of the phase flow rates and phase fractions.

The objective of the design is to maintain these accuracies consistent over all the points falling within the *Measurement envelope* of the meter. It is to be remembered that the accuracy with which the watercut is measured impacts the accuracy of the net oil flow rate, and it is pronounced at high watercut conditions.

The fundamental philosophies and principles behind the same are listed hereunder:

2.1.1 Measurement Philosophy

Separation of Phase flow rate and Phase fraction measurements

Water cut measurement errors are pronounced when the GVF levels are high and/or severe slugging conditions prevail in the flow. Incoming multiphase flow may exhibit one or more combinations of "high GVF" or "slugs" or "high watercut".

Measurement of the total flow rate and Gas Void Fractions are well established using the principles of Venturi and Gamma absorption, and follow a predictable and acceptable accuracy under very high GVF conditions. The effect of increasing GVF or slugging in the multiphase flow is more severe in affecting the WLR measurement accuracy.

The solution to measure WLR accurately is to introduce an independent section made up of "a flow conditioner and a low Dual energy gamma absorption watercut meter" with suitable conditioning done to the multiphase flow during the watercut measurement

Conditioning upstream of the 3 phase watercut measurement

The net oil flow rate from a well is a "calculated" figure from "two measurements" taken by the multiphase meters namely "Water Liquid Ratio" and "Gross Liquid Flow Rate". With higher water cuts coupled with higher uncertainties of water cut measurement, the net oil flow rate inaccuracy worsens.

Haimo's watercut meter is installed downstream of the built-in flow conditioner that conditions the flow, mitigates slugs and reduces the GVF level to the watercut meter. This helps the watercut measurement errors within +/- 2% abs. for the full range of stated GVF in the meter's *Measurement envelope.*

The accuracy of watercut measurement in various comparison tests establishes that the WLR in the multiphase flow outlet to the flow conditioner is same as that of the incoming multiphase flow, but at depleted gas conditions.

2.1.2 Measurement Principle

Low energy gamma absorption technology

Haimo meters utilise the photo electric effect that is associated with the low energy gamma sources, in this case, Americium 241 (Am 241). Am 241 emits alpha and gamma rays. Gamma rays are emitted at 59.5 KeV energy level. A silver foil is used to generate X rays at an additional energy level of 22 KeV.

The photo electric effect mass attenuation coefficient is

- directly proportional to the 4^{th} to 4.8^{th} power of Z – the atomic number of the interacting matter
- and inversely proportional to the 3^{rd} power of the energy level of the gamma source used

Phase fractions are determined by exposing the multiphase flow to two different energy levels of gamma rays 59.5 and 22 KeV. By solving the 2 independent equations generated from exposure to the two different energy levels and the continuity equation, the phase fractions are calculated.

Under this measurement principle, the phase discrimination occurs by measuring the relative presence of the Carbon to Oxygen atoms in the Oil and water respectively. This gives the Haimo technology the unique advantage of measuring oil and water fractions, even if separated by a narrow margin of density.

3.0 Haimo's experience with Upstream Separation Devices

3.1 Installation references

Haimo been offering skid configurations with Upstream Separation Devices from the year 1999. Over 100 of these units that have been supplied are high to very high GVF configurations fitted with Upstream Separation Devices. These units function up to a GVF of 90% without having to use the upstream units and for GVF's above the cut-off value of 90%, the upstream unit comes into play along with its combination of cyclone, control valve and the vortex meter. Skids rated up to 900#, made out of Incolloy and Hastelloy internals for cyclones and for vortex meters and control valves are in operation worldwide.

The presence of the flow conditioner in the skids also helps to allow for a higher GVF handing capacity before the partial separation unit comes into play.

The use of the upstream gas conditioning unit has also proven to be resulting in weight, volume and costs and delivery as commercial disadvantage issues to Haimo and the customers.

The performance of such configurations are well established with various third party live crude FAT reports and field studies.

MFM 2000 series meters with and without Upstream Separation Device

SPE 84505 Multiphase flow meters: Experience and Assessment in PDO co-authored by Busiadi, Khamis, and Bhaskaran, Haridas, Petroleum Development Oman (PDO),Oman, presented at the SPE Annual Conference and Technical Exhibition, Denver, Colorado, 5-8th October 2003 shares more details of the third party testing carried out on such a configuration.

The typical challenges to be addressed while using the upstream devices can be listed as follows:

- Material selection issues
- Footprint, weight and volume.
- Cost and economics

3.2 Material selection and costs associated with Upstream Separation Devices

Exotics

High chlorides and sulphides in the flow may require the use of exotic materials such as Duplex stainless steel, Incolloy, Hastelloy etc. Designing of the process vessel with such materials prove to be expensive, not only from the cost of the raw materials, but also the special fabrication standards and procedures to be followed. Procurement of exotic material – for vessel internals, control valves and vortex meters can also be very expensive impacting on the cost effectiveness of the solution provided

Fabrication

High pressure High GVF skids to be fitted with upstream devices would warrant special standards and skills to be followed for fabrication.

Foot prints, weight and volume

When appropriately designed to handle the required liquid turndown, GVF and slugs, the multiphase meter with an Upstream Separation Device assembly when installed in field should raise a few interesting questions.

For fixed onshore applications, it is possible that footprints and the height are not a major constraint. However, when such a units are to be transported from one well head to another for mobile well testing services, the portability and compactness advantages may be lost.

For offshore applications, it shall be virtually impossible to even move such a unit onto the platform where space is premium. Additional weight caused by the upstream units also poses challenges for easy mobility between platforms, while also impacting the efficiency of the platform in terms of structural design and utilisation.

Costs and delivery

The above can result in considerable costs for the completed units with half of it accounted from the Upstream Separation Device with associated control valve, vortex meter and piping. Longer delivery periods owing to the use of exotic materials and special fabrication needs may not be acceptable to customers looking for quick solutions.

4.0 Motivation to develop the Compact meter solution

Given the above backgrounds and with an effort to develop a balanced solution between "accuracies" and "cost-effectiveness", Haimo embarked on a special project to develop a new meter to extend the *Measuring envelope* of the Haimo MFM 2000 series multiphase meter to *High GVF* conditions without having to use Upstream Separation Devices.

It shall be noted and reinforced here that efforts taken by Haimo are to be within the *"Accuracy specifications"*. The new term "Compact High GVF meter" is used henceforth in this paper.

Partial list of challenges addressed in this new development:

- Wide liquid turndown requirements with associated gas flow rates
- Suitable slip models for Phase flow rate measurement
- Liquid and gas handling capability of the flow conditioner for a wide turndown of liquid and gas
- Sample assurance to the watercut meter downstream of the flow conditioners under gas depleted flow condition for all points falling within the *Measuring envelope* of the meter

The paper shall present the results achieved from the modifications carried out in the skid, rather than focussing on the details of the modification.

In Section 6.0, the results of testing in a third party facility are shared. The testing was carried out on the first prototype design of the Compact high GVF meter in March 2004.

The test was witnessed by a Global Service company offering Field surveillance services and mobile well testing services. The test was carried out in the DOD facility described in Section 6.0

5.0 Description of the Compact solution

5.1 Description of meter tested

The meter tested in the third party facility is a 2 in 1 meter configuration, built with a 3" and 2" venturis, which are valved in such a way to be in series or have only one on-line.

The two sizes of venturis bring a wide Measurement envelope to measure liquid from as low as 20 m3/d (125 bpd) to 2,400 m3/d (8,792 bpd), with corresponding high GVF conditions, better interpreted from the *Measurement envelope* presented hereunder.

A wide turn down meter is chosen to address requirements of customers with large turndown requirements, and limited pressure drop allowance, while also to test the turndown capability of the flow conditioner upstream of the watercut meter.

5.2 *Measuring envelope* of the meter in a 2 phase flow map

(GVF limit set from test points that met with the *Accuracy Specifications*, post testing)

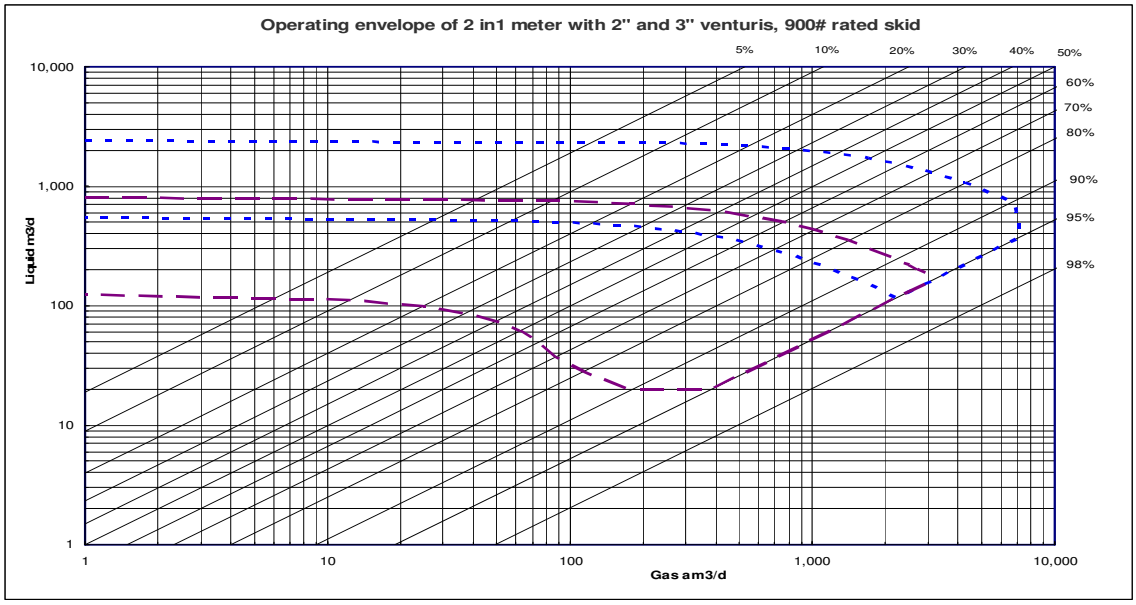

5.3 P&ID of the meter tested

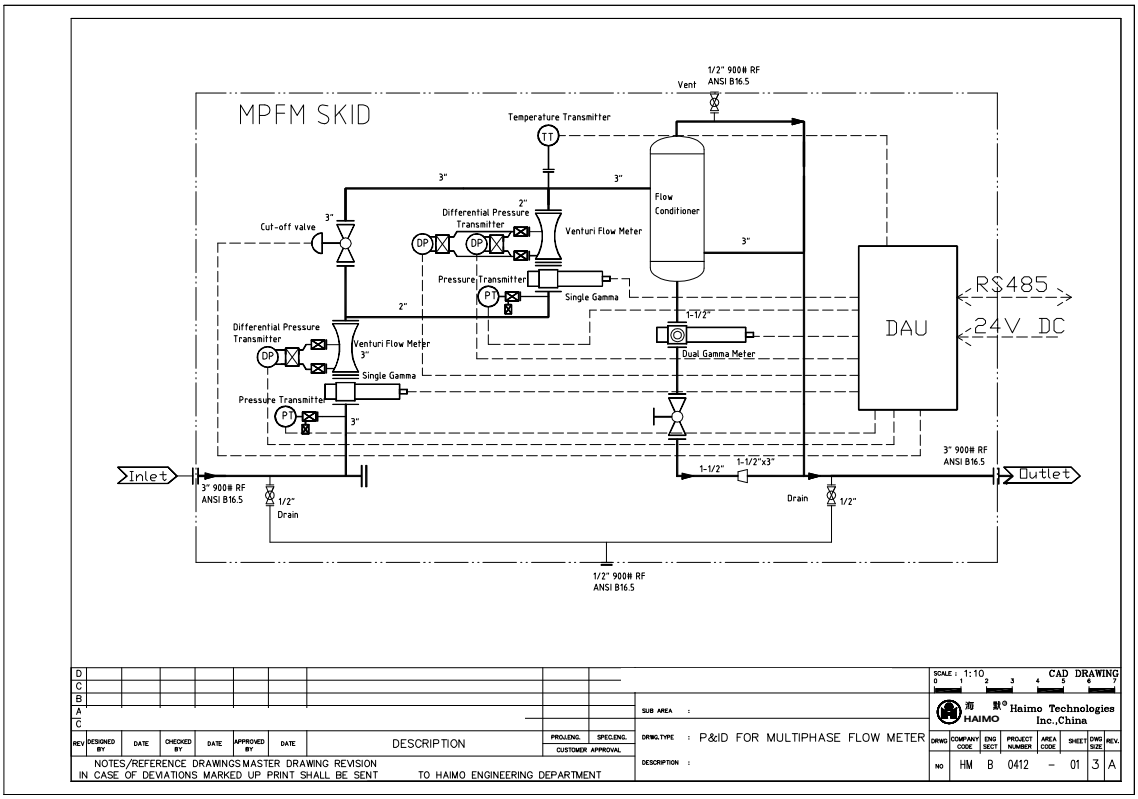

5.4 Picture of the skid during the Third party testing

5.5 Operating Principle

The meter consists of two venturis with in-built single gamma meters installed respectively on two multiphase legs, a flow conditioner and a Dual gamma meter. The phase fractions and flow rates are calculated based on the following measurements:

- Total flow rate of the multiphase fluids (TFR) is measured by the two Venturi tubes. (Lower flow rate is measured by 2" Venturi and higher flow rate is measured by 3" Venturi). The single gamma meter gives an additional input of density for the venturi calculations.

- The cut off valve directs the flow through both the venturis in case of low flow rates, while measurements are just captured from the smaller venturi for flow computations; for higher flow rates, the fluids are routed through the larger venturi alone in this unique valving arrangement

- Single gamma meter also measures the ratio of gas flow to the total flow rate at line conditions (Gas Void Fraction)

- The water Liquid Ratio (WLR) is measured by a Dual gamma meter; the WLR measurement is carried out downstream of the improved flow conditioner. This new vertical flow conditioner has five functions:

    - to buffer the slugs
    - to deplete gas in the outlet to the Dual gamma meter
    - to replenish the Dual gamma meter with fresh samples
    - to provide a homogenised multiphase fluid to the Dual Gamma meter
    - to extract liquid in the gas depleted multiphase that is representative of the WLR of the incoming multiphase flow to the meter inlet.

    In short, the new flow conditioner is a combined device consisting of separation, mixing, conditioning and sampling elements.

- The actual Gas flow rate is calculated as a product of TFR x GVF (calculated from Gas Void fraction)

- The Gross liquid flowrate (GFR) is calculated as a product of TFR x (1-GVF)

- The Water flowrate is calculated as a product of GFR x WLR and the Oil flowrate is a product of GFR x (1-WLR)

- Pressure and Temperature transmitters are mounted in appropriate locations in the skid for correction of measured values to standard conditions and for applying to EOS and/or PVT corrections

5.6 Claimed accuracies of the meter

The Compact meter is set to achieve the *Accuracy specifications* over the *measuring range* of the meter. The typical accuracies expected out of the meter skid are as follows, to be confirmed during the testing in the Third party facility:

***Accuracy Specifications* / Uncertainties :**

Gross liq.flow rate:	+/- 5% relative (GVF<50%)
	+/-10% relative (GVF>50%)
Watercut:	+/- 2 % absolute
Gas flow rate:	+/- 10% relative

Uncertainties are based on 90% confidence level

Repeatability

Gross liq. flow rate:	+/- 2.5% relative (for GVF<50%)
	+/- 5% relative (for GVF>50%)
Watercut:	+/- 1 % absolute
Gas flow rate:	+/- 5% relative

6.0 Performance testing of the meter in the third party facility

6.1 Description of DOD Facility and test procedure

The DOD Multiphase Flow Facility is located in Daqing Oilfield, Daqing City, China. The facility was conceptually designed by National Engineering laboratory (NEL), Glasgow, UK. The test facility is located in the middle of the Daqing oil field, and provides live crude oil, produced water and natural gas for the testing. The tests carried out in the DOD shall be considered as a SAT (Site Acceptance test) as the meter is calibrated with the fluid samples in the field.

It is approved by China National Measurement Institute and China National Petroleum Corporation (CNPC) and by PDO – Oman, and frequently used by Shell, Conoco Phillips among other international operators.

The specifications of the DOD facility are presented in Annexure 1:

6.2 Selection of Test points

The objective of the test was to establish the extent to which the GVF limit of the *Measuring envelope* could be stretched while also meeting with the *Accuracy Specifications*.

The tests were carried out independently for the 2" and the 3" measurement legs for different flow rate ranges. A total of 100 test points were selected to cover testing upto high GVF conditions to evaluate the meter performance from minimum to maximum liquid flow rates, while also varying the watercuts from 0-100%.

While the objective is to establish the meter performance in the high GVF environment, emphasis was placed on maximising the test points at above 80% GVF

For the 2" leg,out of 50 test points:

27 test points were above 80% GVF
17 test points were above 90% GVF
6 test points were above 95% GVF, upto 96.1%

For the 3" leg, out of 50 test points:

31 test points were above 80% GVF
20 test points were above 90% GVF
5 test points were above 95% GVF upto 95.4%

In summary, out of 100 test points, 37 were above the 90% GVF range.

Repeatability tests were carried out on 5 test points each for the 2" and 3" measurement legs

6.3 Test results

The test results are presented for the different measurement sections, separately and combined based on the following graphical charts presented elsewhere in the paper:

△ Liquid flow rate Vs Gross liquid
△ Watercut Vs Gross liquid
△ Gas Vs Gross liquid
△ Liquid Vs GVF
△ Watercut Vs GVF
Detailed test results are presented in Annexure 2

6.4 Analysis of test results

Watercut ABSOLUTE errors:

- The targeted criteria was found to be bettered in the absolute error on watercut plotted against GVF; At 90% confidence level, the watercut was measured within 1.8% for the 2" leg and 1.3% for the 3" leg; both legs combined, the watercut absolute error at 90% confidence level was established to be within 1.8% - better than the targeted criteria of 2% absolute at 90% confidence level

- Abs. errors on the watercut was found falling within 1.8% and 1.5% at 90% confidence level respectively for the 2" and 3" legs; the combined test results when plotted against the Gross liquid showed an absolute error of 1.8% at 90% confidence level

- No charts have been drawn or highlighted for watercut errors against the watercut itself, as the watercut measurement based on dual energy gamma absorption principle is well established to be independent of water continuous and oil continuous flow regimes.

Liquid flow rate RELATIVE errors:

- At GVF below 50%, as expected, the 2" and 3" legs produced liquid flow rates relative errors that were within 5.7% and 1.9% respectively at 90% confidence level; the combined results were within 3.2%.

- Over the 50-95% GVF range, the 2" and 3" legs produced liquid flow rate relative errors that were within 7.3% and 5.6% respectively at 90% confidence level; the combined results were within 6.8%.

Gas flow rate RELATIVE errors:

Relative errors on gas flow rates were plotted against various liquid flow rates.

- At 90% confidence level, the gas flow rate errors were within 11% and 9.8% for the 2" and 3" legs respectively;
- The combined gas errors were within 10.4% relative at 90% confidence level

Repeatability test results were well within the claimed Repeatability figures

7.0 Conclusions and Benefits

- The objective of working out a new solution for high GVF without having to use a Upstream Separation Device seem to have been achieved with excellent test results;

- The new configuration of Compact High GVF meter successfully met and exceeded its Acceptance criteria. The main objective was to asses its performance, confirm the quality of the measurements and check its compliance with the *Accuracy specifications.*

- The consistency of the absolute error on watercut MUCH LOWER THAN 2% for the full range of the GVF and liquid flow rates re-establishes the independence of the watercut measurement technology over the GVF and liquid flow rates, now for high GVF

- The accuracy results obtained for gas flow, gross liquid flow and water liquid ratio measurements demonstrate the following:

    - efficiency of the flow conditioner technology and its great advantage of measuring the water liquid ratio (WLR) independently of the Gas volume fraction (GVF)

    - capability of the flow conditioner to handle the wide turndown of the liquid from the 2 in 1 meter

    - capability of the flow conditioner to handle high GVF without compromising on the efficiency to mitigate slugs, deplete gas and provide a representative sample of multiphase fluid with WLR same as that of the incoming multiphase flow

References

1. N Sea Flow measurement handbook Rev 2
2. SPE 84505 Multiphase flow meters: Experience and Assessment in PDO co-authored by Busiadi, Khamis, Petroleum Development Oman (PDO), Oman and Bhaskaran, Haridas, Petroleum Development Oman (PDO),Oman, presented at the SPE Annual Conference and Technical Exhibition, Denver, Colorado, 5-8th October 2003
3. Multiphase flowmeters – Experience and Assessment, co-authored by Haridas P. Bhaskaran, Khamis Al Busaidi, and presented at the Multiphase Pumping and technologies Seminar in Abu Dhabi, 22-25th Feb 2004
4. Sustaining the multiphase metering technology in the field, co-authored by Gokulnath R, Daniel Sequeira, Jianwen Dou, Haimo International FZE and presented at the Multiphase Pumping and technologies Seminar in Abu Dhabi, 22-25th Feb 2004
5. SPE 88745 Combination of Dual Energy Gamma ray / Venturi multiphase meter and Phase Splitter in Very high gas volume fraction environment co-authored by E.Delvaux, B Germond and N K Jha, Schlumberger and presented at the 11th ADIPEC, in Abu Dhabi, 10-13th October 2004
6. Extending the multi-phase flow meter operating envelope by adding a partial separation device co-authored by Lex Scheers, Shell Global Solutions International, The Netherlands, Martin Halvorsen and Tor Wideroe, FlowSys, Norway, Paolo Nardi, Pietro Fiorentini, Italia and presented at the 4th International South East Asia Hydrocarbon Flow Measurement Workshop, 9 – 11th March 2005

ANNEXURE 1 - DESCRIPTION OF THE DOD FACILITY

The multiphase pipeline size is DN50,80, 100
The operating pressure is 200 – 500 KPa.
The Max. fluid temperature is 80 C.

The test fluids used in DOD are as follows:

Oil phase - Crude oil (water in oil less than 0.5%) from Daging Oilfield
Gas phase - Natural gas (liquid in gas less than 0.5%) from Daging Oilfield
Water phase - Produced water (oil in water less than 0.5%) from Daging Oilfield

The capacity of the DOD facility is given below:-

Max. Oil flow rates:	1,200 m3/d
Max. Water flow rates:	1,200 m3/d
Max. Liquid flow rates:	1,200 m3/d
Max. Gas flow rates:	28,080 Sm3/d

The accuracy of the DOD facility is given below:-

Oil phase:	+/- 1.0 % relative (PD meter)
Gas phase:	+/- 1.5 % relative (Turbine meter)
Water phase:	+/- 1.0 % relative (Turbine meter)

The repeatability of the DOD facility is given below:-

Oil phase:	+/- 1.0 % relative
Gas phase:	+/- 5.0 % relative
Water phase:	+/- 1.0 % relative

The range-ability of the DOD facility is given below:-

GVF:	0 - 100 %
Water cut:	0 - 100 %

The MFM skid is be mounted on the multiphase flow testing pipe section of DOD's facility. The multiphase piping is downstream of the mixing point of the reference single-phase flow meters for oil, gas, and water individual phases. The oil, gas, and water single phase flows shall be first metered by the reference single-phase flow meters respectively.

DOD's own reference temperature and pressure transmitters are located close to the MFM skid. The DOD's reference values of gas flow rate are calculated according to the temperature and pressure reported by the DOD transmitters. This way the inlet single-phase flow rates measured by the reference flow meters could be compared with the flow rates of multiphase flow measured by the MFM skid.

ANNEXURE 2 - TEST RESULTS
PERFORMANCE RESULTS FROM THE 2" LEG

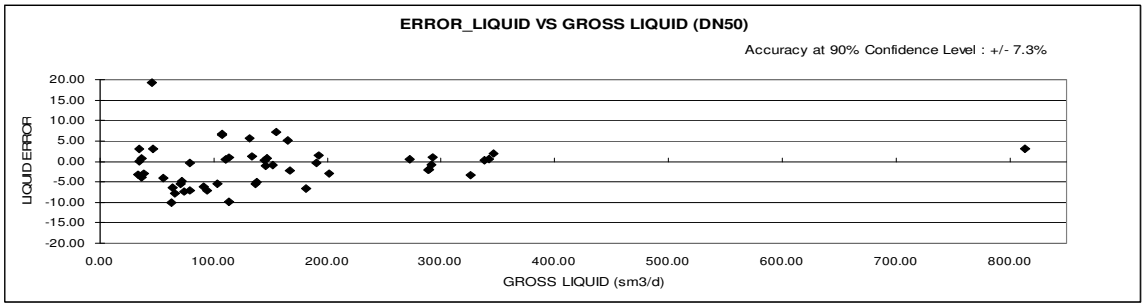

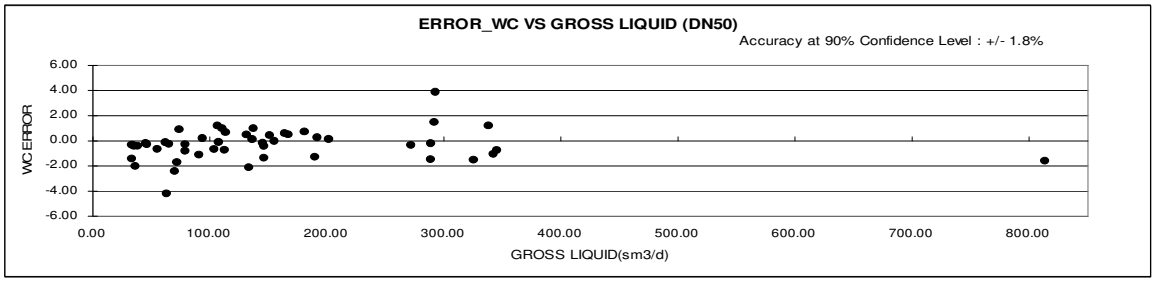

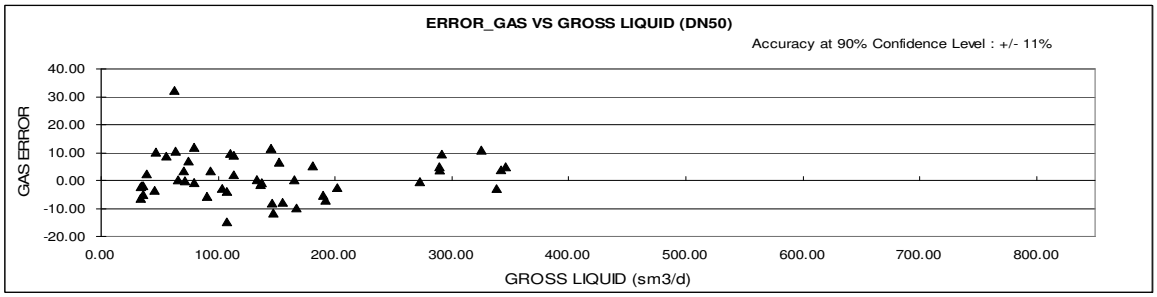

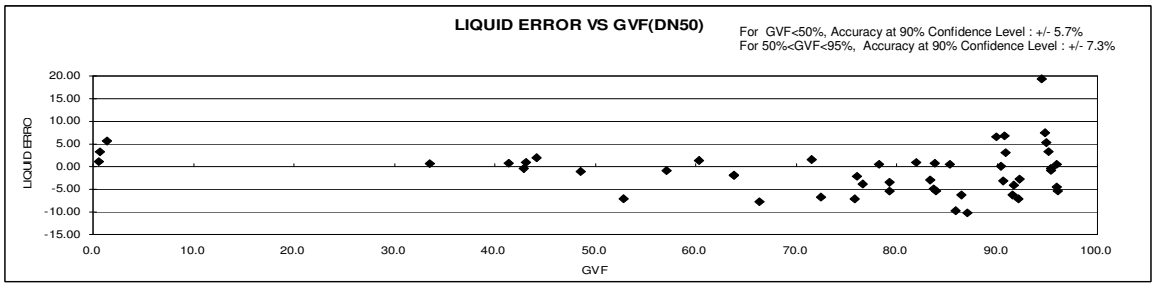

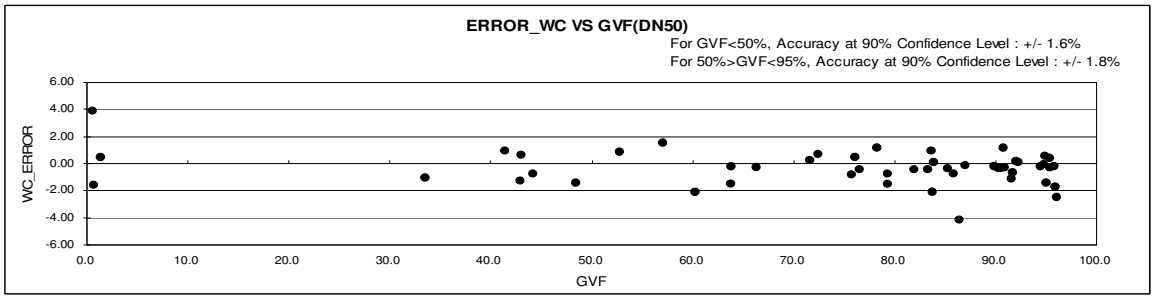

PERFORMANCE RESULTS FROM THE 3" LEG

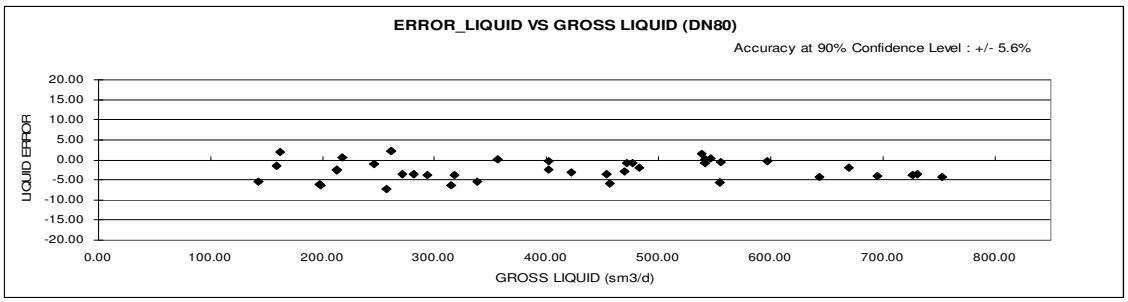

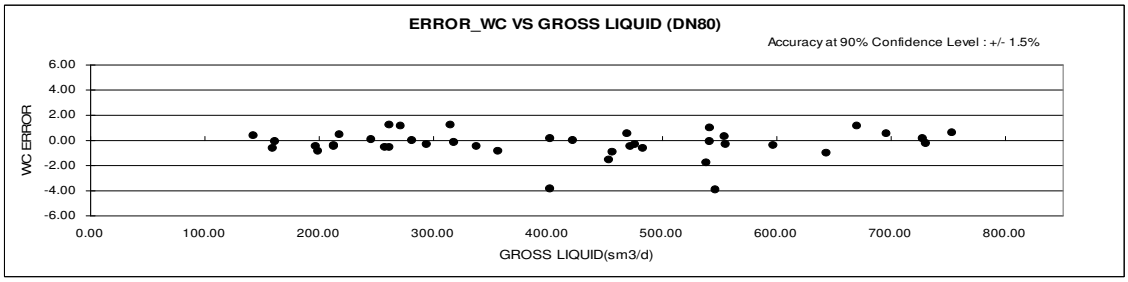

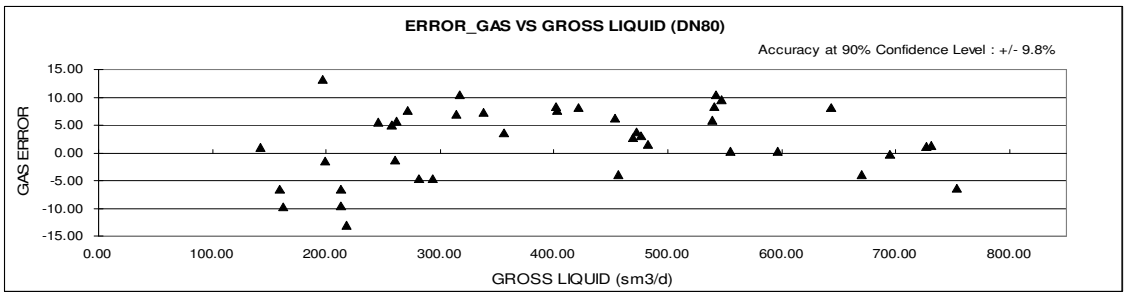

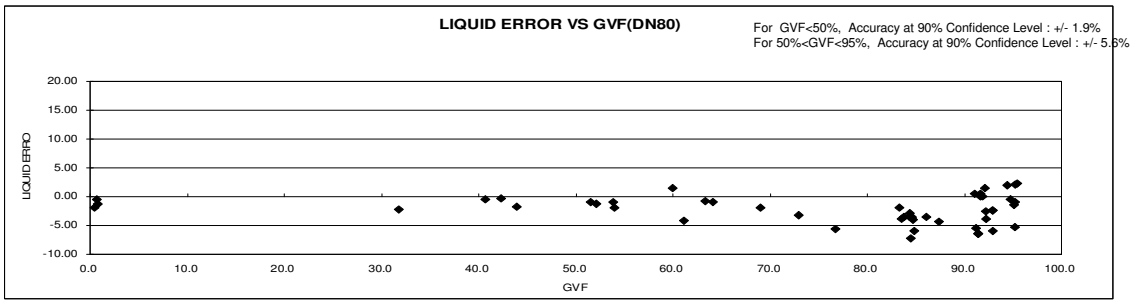

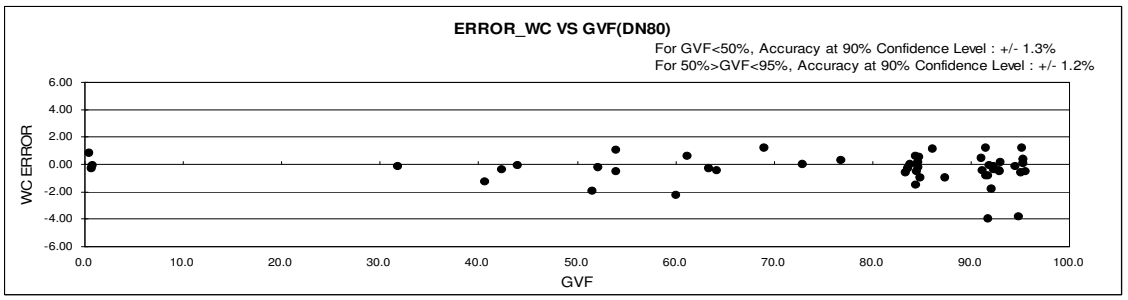

COMBINED RESULTS FROM THE PERFORMANCE OF THE 2" AND 3"LEGS

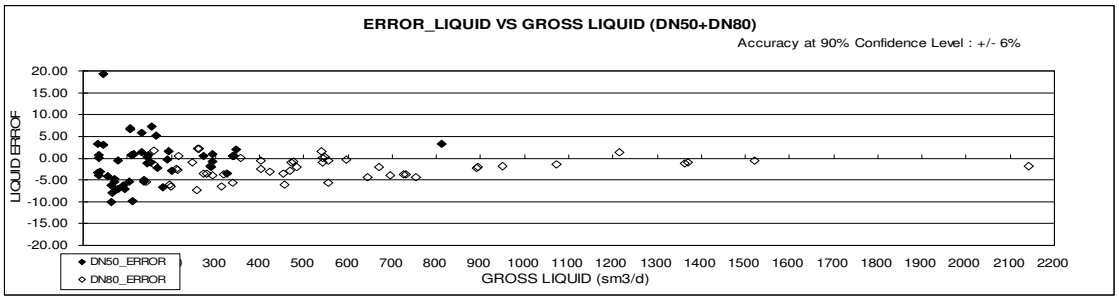

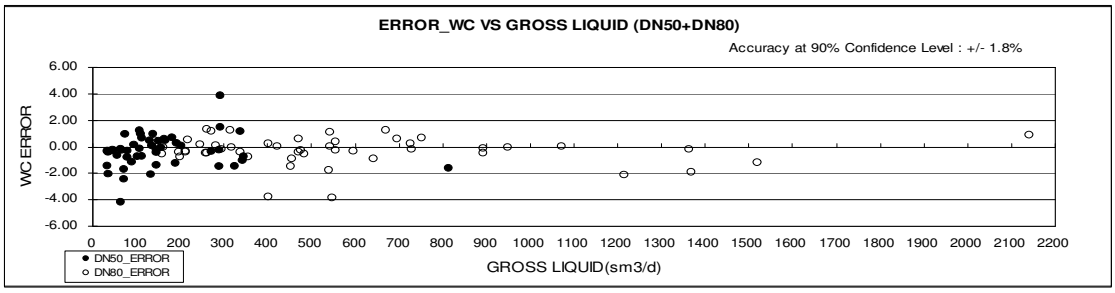

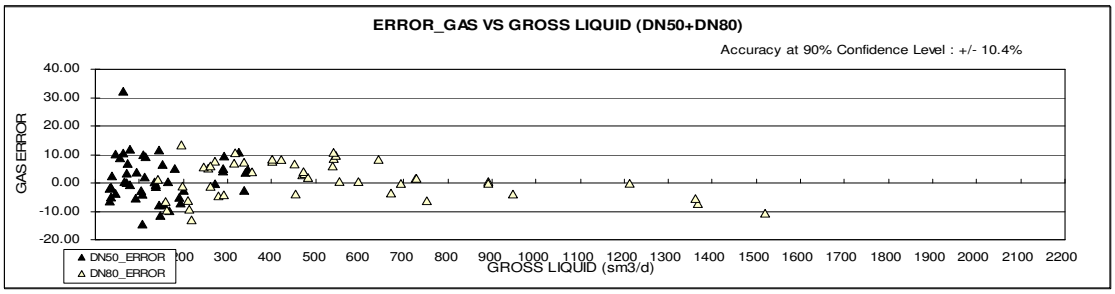

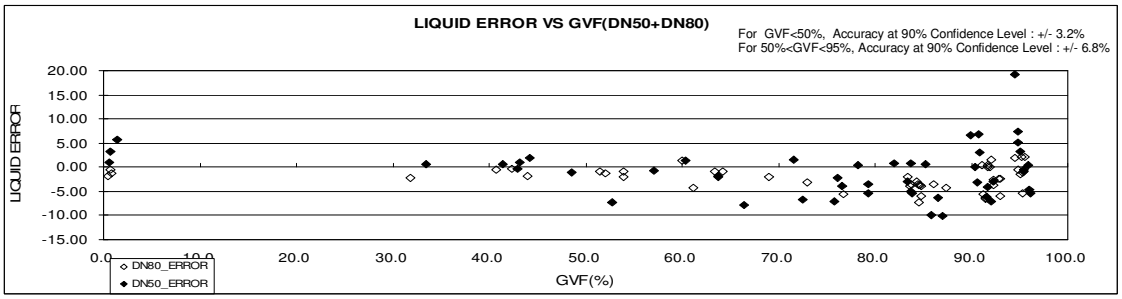

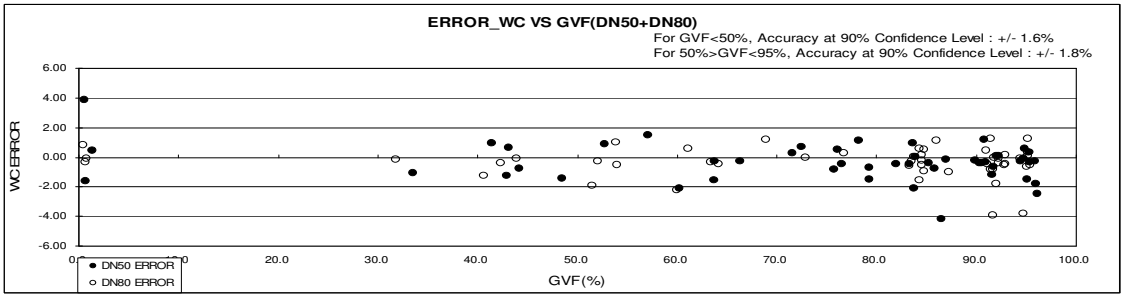

The 21st International
North Sea Flow Measurement Workshop
28 – 31 October 2003, Tønsberg, Norway

Well testing using Multiphase Meters

Karl Herman Frantzen
Roxar AS

Introduction

- Well Testing Background
- Technology Selection
- Principles of Operation
- Learnings From Commissioning & Operation
- Achievements

This paper describes one of the first major roll-outs of multiphase meters in the Middle East area. The project started in 1998 and after trial installations and technology evaluation it was decided to install a series of multiphase meters on unmanned wellhead platforms. A total of 9 meters have been installed and has presently been in service for up to 2 years. Another 7 meters will be put in service on new-built platforms.

The background for considering multiphase meters as an alternative to well testing by traditional methods is

The selected technology and measurement principles is described.

The main experiences for the project is presented and discussed. Of particular interest is the collaboration model applied for the commissioning phase and the continuous follow-up of well test results by use of a field wide model of the production system.

The most important achievements in the project has been that the frequency of well testing has been dramatically increased and the amount of oil lost due to well testing is greatly reduced.

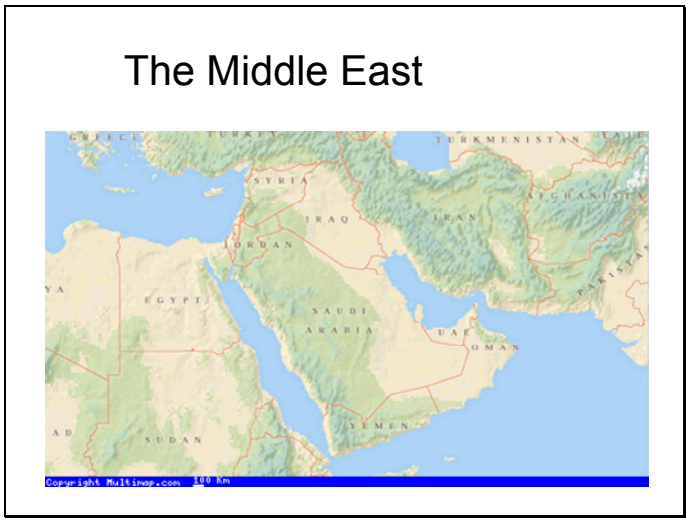

The field is located offshore in the Middle East area.

The water depth is shallow compared to European standards, typically 10 – 40 meters. The field is developed by small satellite platforms with 1 to 9 wellheads on each. Platforms are generally minimum facilities, with limited power and normally unmanned. The platforms are linked via a network of flowlines to a central processing facility.

Remote jacket

Remote Platform, Single Well

Why Well Test?

Well testing data is required for a number of reasons:

- Contractual obligations with partners and authorities.
- Well and reservoir performance monitoring and optimization
- Identification of mechanical integrity issues
- Assessment of near well-bore damage on combination with shut in data

Well Testing; Pre 1995

- Test Separators x 1.
- Could only test up to 50% of producing wells per month
- Lost production
- High OPEX
- Intermediate results for short periods, require stability in flow.

One centrally located test separator served the complete field. Not all platforms have test lines. In case a test line is not available, wells has to be shut in for the well to be tested.

A long distance between wellhead and test separator causes long stabilisation time. The test time selected is therefore a compromise between lost production costs and accuracy of well test results. Additional sources of errors are the differences in hydraulic propeties in test lines and production flow lines.

Selection of wells are done manually on wellhead platforms, hence the operation has high costs and is very weather dependent.

Technologies Trialed

- Portable Test separators
- 2 partial separation multiphase meters
- 4 inline multiphase meters

In a trial phase in 1999 – 2000 a total of 6 different multiphase meters were installed offshore in separate periods of time. Each meter was tested over a period of 1 - 3 months. During this time, the meters were tested over a selection of wells and compared with the test separator.

As a result of testing and evaluation, Roxar MPFM 1900VI was selected for field-wide implementation.

Why Roxar MPFM 1900VI

- Demonstrated performance
- Wide operating range
- Low power consumption
- Dual velocity system
- No separation or mixer
- No moving parts
- Most Competitively priced

Principles of Operation
The ROXAR 1900VI

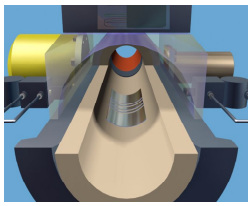

Overview

Two separate principles of measurements are used:

1. Fraction measurement (Gas/water/oil)
   - Gamma densitometer
   - Capacitance sensor
   - Inductive sensor
2. Velocity measurement (flow)
   - Venturi sensor
   - Dual Cross Correlation

1. Fraction Measurement

A) Gamma densitometer

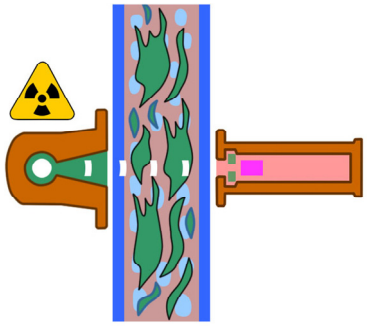

The purpose of the gamma densitometer is to measure the total density of the mixture flowing in the pipe. Because of the significant difference in the densities of the liquid and gas of an oil/gas/water mixture, the rate of the absorption gives an accurate measurement of the liquid and gas fractions of the mixture. The absorption of gamma radiation in a medium is a function of the mean density along the path of the gamma particle beam. Since the Cs beam penetrates steel, no windows or ports to the flow section is required.

The gamma detector used is a Tracerco PRI116 detector clamped on to the outside of the capacitance sensor. The radioactive source used is Cesium 137 (Cs 137). Service life for this system is 15 years. Provided instructions and regulations are followed, the gamma densitometer is totally safe, and does not constitute any source of danger.

B) Capacitance

This sensor measures fractions of oil/water/gas by measuring the permittivity' of the mixture.

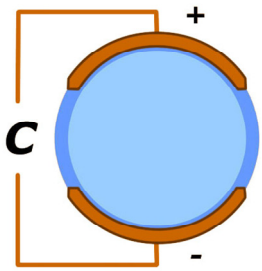

Functioning as a capacitor, the MPFM 1900VI measures the permittivity (dielectric constant) of the oil/gas/water mixture. The permittivity is different for each of the three components in an oil/gas/water mixture, and the permittivity of the mixture is therefore a measure of the fractions of the different components.

The function is achieved by locating electrodes on each side of the spool. The electrodes are isolated from the metal in the spool using a polymer plastic material (PEEK). By placing an electrode on each side on the inside of the spool, and allowing the mixture to flow through the pipe, the electrical field generated between the electrodes will be affected by the permittivity of the oil/gas/water mixture. The electrodes will act as a capacitance detector and the resulting capacitance can be measured between the electrodes. This capacitance will therefore vary when the permittivity changes, i.e. according to the amount of oil, gas and water in the mixture.

This capacitance measurement works as long as the flow is oil continuous, i.e. as long as water is dispersed in the oil and does not form a continuous path of water between the electrodes. Normally, the flow is oil continuous as long as the water cut is below approximately 60 – 70%. For higher water cuts the flow will become water continuous. For these situations the inductive sensor is used.

C) Inductive:

A set of two coils is used to induce current that flows through oil/water/gas mixture.

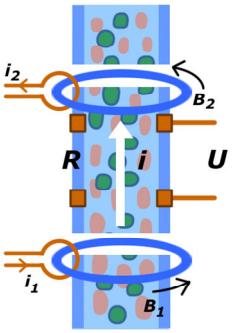

When the liquid is water-continuous, the mixture conductivity of the oil/water/gas flow is measured by an inductive sensor. Magnetic coils are used to induce a current through the liquid inside the sensor

The inductive sensor is integrated into the same sensor unit as the capacitance sensor and comprises a set of coils (B1 & B2) and also a set of electrodes. The coils are used to set up an electrical field which induces a current that flows through the oil, water and gas mixture. As long as the flow is water continuous, the water will act as a conductor and the current will flow from one side of the meter to the other side. The potential detector electrodes, also shown in the figure, will pick up the differential voltage created by the induced current. The measured signal depends on the fractions of gas and oil in the water. This information is then fed to the flow computer for calculation of oil, water and gas fractions.

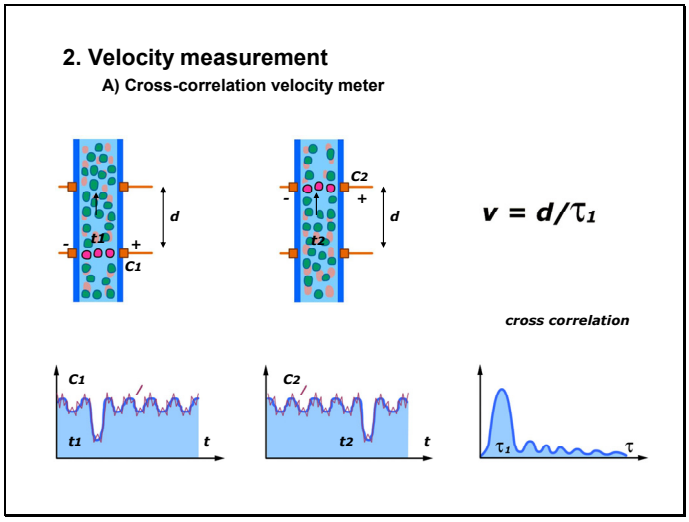

Cross correlation velocity measurement

The sensor consists of pairs of capacitance/conductance measurement electrodes, each pair of electrodes spaced a known distance apart along the direction of flow. The electrodes perform continuous measurements of the flow, utilizing the variations both in velocity and composition inherent in a multiphase flow. The sensor electronics collects data at a a high rate. The collected data forms a time serial signal, and contains information about the flow pattern inside the sensor.

The flow pattern will continuously change as the flow passes through the meter. Thus the time series signal from the two electrodes in a pair will look similar in form, and it is possible to recognize the flow pattern at the next electrode by studying the two time series.

The statistical method cross-correlation, which compares the similarities between the signals picked up by the electrode pair, are used to find the time shift. The cross correlation function

plotted versus time returns its first and highest maximum at a time representing the time shift between the signals.

Two electrode sets

The sensor contains two different shaped sets of electrodes, large and small. The large pair of electrodes will be most sensitive to variations generated by large gas bubbles, whereas the small pair of electrodes will be most sensitive to variations generated by the small gas bubbles. Hence, the velocity of the gas can be determined by cross correlating signals from the large electrodes and the liquid velocity can be determined by cross correlating signals from the small electrodes

Slip flow

In multiphase flow, almost all combinations of liquid and gas fractions results in a flow pattern where the liquid and gas phases travel at different velocities, with the gas traveling with the higher velocity. This phenomenon is called slip flow (the gas phase slips by the liquid phase). The Roxar MPFM 1900VI uses different methods for flow velocity measurement:

- Differential pressure measurement over a Venturi meter
- Cross correlation of time series signals from the capacitance and inductance sensor

The cross-correlation technique and the Venturi measurement combined constitute a very robust method of finding both the gas velocity and the liquid velocity.

B) Venturi meter:

Used at high GVFs/ Single phase

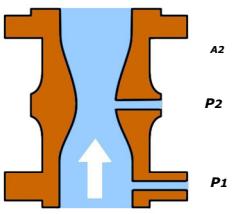

In many applications, the combination of a mass based Venturi meter and a volume based cross-correlation is beneficial. At very high GVF's (typical around 95-99%) the cross correlation technique may not work accurately due to lack of dynamics in the measurement signals from the capacitance/inductive sensor. A typical example would be annular flow where the gas mainly travels in the center of the MPFM sensor with the liquid concentrated along the walls of the sensor.

For these situations a Venturi-based flow meter will still work. Also, including a Venturi meter to the MPFM gives redundancy in velocity measurement. If one unit fails the flow computer will automatically start to use the other unit.

The standard Venturi equation is modified for use in three-phase flow. The modified equation takes into account the gas volume fraction (GVF) of the flow. Since the mixture density is measured with the composition meter, the mean liquid velocity and gas velocity can be determined from the measured differential pressure.

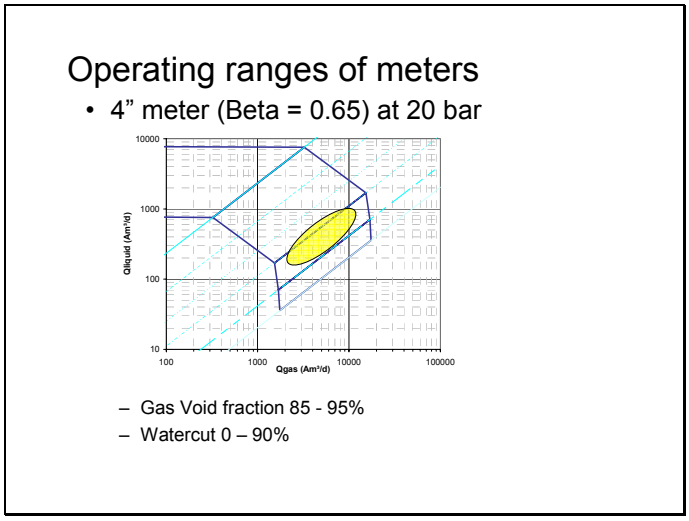

The meters where installed close to wellhead, and saw direct well stream. The wells are gas-lifted, which causes a very high GVF. The typical gas void fraction is 85 – 95%. In addition many wells were had heavy slugging, as normally occurring in gas lift wells.

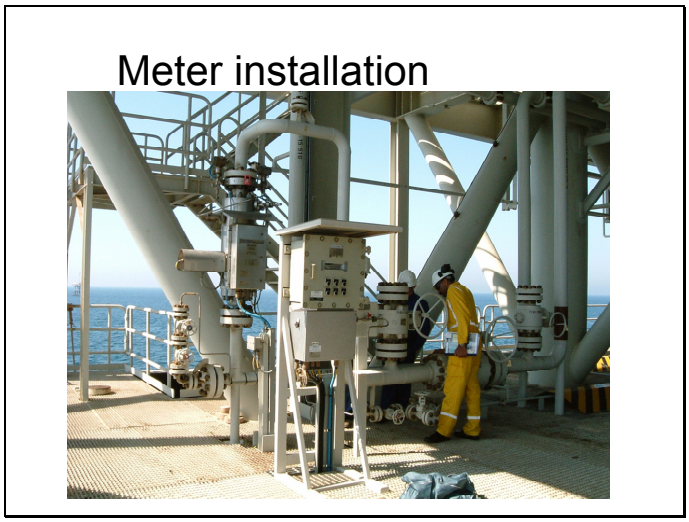

The picture shows one of the meters installed on a 9-well platform. The platform does not have safe area or control room. Therefore the flow computer is installed in a field enclosure close to the meter. The local display allows operators to directly read the flow rates, perform well tests and set up the meter in a simple way.

The installation is highly exposed to saline atmosphere and high temperatures. Special sun shades are installed on flow computer and meter electronics to protect from direct sun-exposure during the hottest periods of the day.

The meters are installed as in-lie meters rather than in a skid. The piping could then be laid more optimally, and the solution also saves valuable deck space.

Commissioning phase

- Integrated team
- Roxar services included:
  - Training courses
  - Data analysis of well tests
  - Establish filed specific procedures for maintenance, personnel training, operation, data retrieval
  - Presentation of data and integration of data into supervisery systems

Rather than a traditional installation/ commissioning exercise, an integrated team approach was selected for this project. The Roxar service engineers formed part of the operator and engineering team whoich worked cloesly together.

By this approach supplier carries out duties which normally is done by consultants or operator personnel in addition to what is normally defined as supplier scope of work.

Among the tasks carried out by supplier personnel were:
Installation supervision, setup and commissioning offshore
Well testing offshore
Supervision of well testing from onshore.
Training of personnel at various levels and at the time of need.
Data analysis
Establish filed specific procedures for operation, training, maintenance
Presentation and quality assurance of data
Integration of data into operation reporting systems.

The collaboration proved to be very fruitful. It gave an improved understanding by the operator personnel of how to optimally integrate the technology. At the same time, the supplier personnel has a much better understanding of operator priorities and needs. It is quite clear that the approach selected here reduced the time of establishing fully verified measurements and reliable integration into production reporting system.

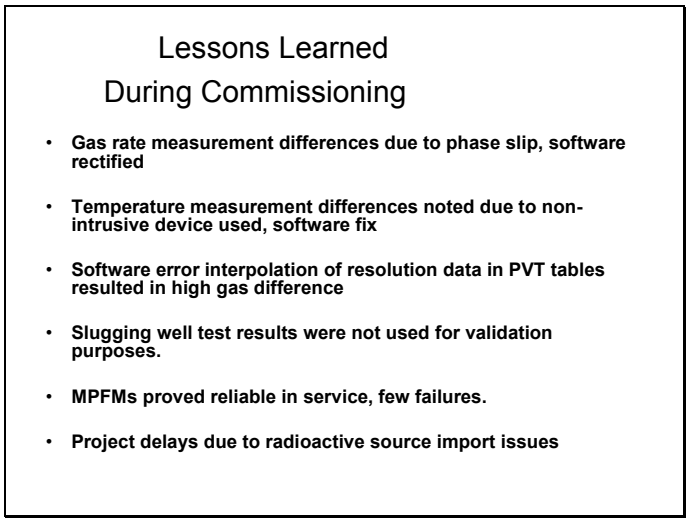

The commissioning and startup phase for the project has been performed over a period of 6 months.

The main experiences during this period are listed above.

A software adjustment of the gas flowrate calculation had to be don after first time commissioning. The exact reason for this is not clear, although it seems to be related to the high degree of slugging.

The temperature measurement showed a slow response and sometimes a lower temperature reading than correct. The reason for this was found to be in the design of the thermowell, as it was sensitive to ambient temperature. A software compensation solution solved the issue for the meters already in operation. Manufacturer has later modified the design, and then eliminated the problem for future meters.

All measurements were reported in standard conditions. Calculations from line conditions to standard conditions are based on PVT models established on black-oil composition data. The method the model initially was set up caused interpolation problems in certain conditions. By reducing the possible operating range to the expected range of pressures and temperatures, smaller steps in interpolation is required and the problems disappeared.

Slugging wells proved to be very difficult to compare with test separator. It was believed that the meter behaves better than the test lines and test separator under these conditions.

After installation of the meters, there has been very few failures, and the few which occurred were fixed quickly with a minimum of down-time.

During the project phase, a change in legislation for nucleonic source handling was introduced. Due to that supplier had to re-certify to import sources, and also get approval of working procedures, personnel training etc. It also took more time than expected to get installation licence in place. The delays are mostly contributable to introduction of new legislation, and is not expected for future installations.

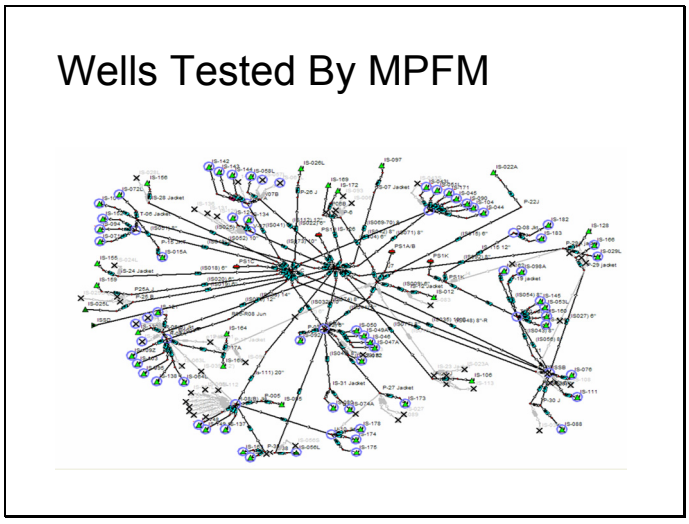

The MPFMs are installed on wellhead platforms, each with 1 – 9 wells. Most of the wells are equipped with downhole pressure and temperature sensors.

A comprehensive field wide model of the production system is established. The model simulates and correlates all available measurements on the production route, downhole, wellhead, manifold, transport lines and processing system. The welltest results are integrated and validated by this model once new data become available. Based on that, the model is corrected and optimised interactively. The tool provides an excellent way to monitor and validate all well tests and production data across the field.

It proved that comparison of well-head installed multiphase meters with test separator installed at central platform was very difficult. Long stabilisation time, operational issues with separator and slugging flow are the most likely reasons for this.

The sum of all welltest data is continuously compared with the total production as measured in the processing complex. The liquid measurements compares within typically 3% which is very satisfying, and far better than the earlier applied methods.

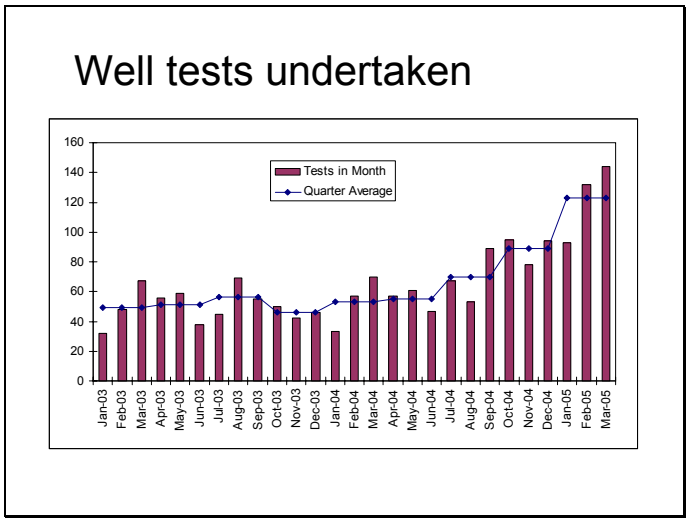

The quarterly average number of well tests taken per month has since MPFM been installed increased from average of 50 to 120.

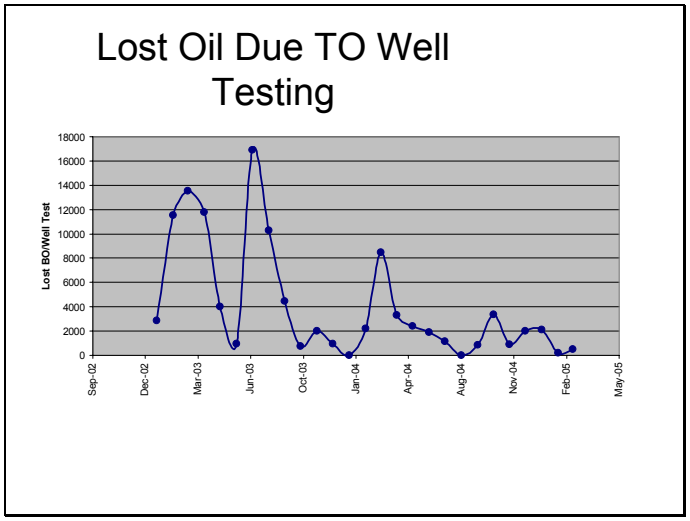

The amount of lost oil due to well testing has been greatly reduced since well testing by MPFM has been introduced. Typical figure of lost oil per month of 12 000 has been reduced to 20 – 50 barrels of oil per month.

Assuming an oil value of 40 USD/bbl the corresponding value of oil lost due to well testing has been reduced from 500 000 USD per month to a figure close to 0.

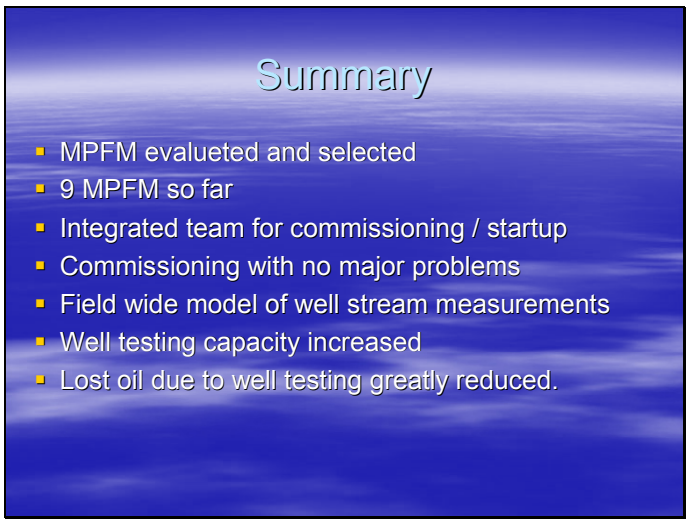
Summary
MPFM evalueted and selected
9 MPFM so far
Integrated team for commissioning / startup
Commissioning with no major problems
Field wide model of well stream measurements
Well testing capacity increased
Lost oil due to well testing greatly reduced.

North Sea Flow Measurement Workshop 2005

Allocation - The Howe Measurement Challenges.

Jim Tierney, Shell Exploration & Production, UK Limited
Paul Ove Moksnes, Dr.Ing., Framo Engineering AS

1-Abstract

The Howe Field is located in the Central North Sea Block 22/12a approximately 160km east of Aberdeen in a water depth of 85m. The reservoir lies some 12 km east of the Shell operated Nelson Platform, which is situated in adjacent Block 22/11.

The Howe project was initiated by Shell Exploration and Production to augment the operating life and production capacity of the Nelson platform, involving the development of an additional subset infrastructure and the installation of topside facilities. The owners of the Howe Field are Enterprise Oil PLC , Intrepid Energy and OMV .

The Howe well fluids are commingled with Nelson fluids. Therefore, it is required to measure the Howe well fluids to differentiate between the fields and to determine how much money each partner is allocated. The commercial agreements have stipulated that the measurements of Howe fluids are required to be measured within an accuracy of +/- 5% of reading.

In addition to accuracy constraints, it was important to minimise capex to ensure the development was economically viable. Given this, multiphase metering was considered to be a solution for allocation between the different ownerships, as opposed to traditional separator metering.

This paper will present the journey of the project activity through the selection criteria, flow loop test, installation, commissioning and the first 3 months of operation of the MPFM including verification with the Nelson test separator. Detailing with careful management and engineering support how to succeed with this type of application.

2. Background

Introduction.

The Howe development is the first of a new generation of sub sea tiebacks that benefit from government tax relief to encourage marginal field developments. Enterprise Oil discovered the field in 1987. The field is an under-saturated oil field and appraised by a further well in 2001. The reservoir is located at a depth of approximately 10,000 feet with a pressure of 455 bar and a temperature of 135 C. The tieback distance to the Nelson platform is 12 km in the easterly direction.

The Howe field has been developed by a single 14,650 feet (MD) production well, with the trajectory of the 2500 feet horizontal section being optimized by drilling a pilot-hole and through the use of geo-steering technologies.

The pipeline tie-in structure consists of an 8" pipe-in-pipe production flow line with a 3" piggy back gas lift line and multifunctional control umbilical. Oil is exported from Nelson to a Pipeline System to Grangemouth and gas exported via a Gas Line to St Fergus.

The co-venturers in Howe are Enterprise Oil. OMV (U.K.) LTD and Petro Summit Investment UK. The equities split for Howe is between Shell Intrepid and OMV . The Operator is Shell Exploration and Production.

Schematics of the process layout is shown in Figure 1.

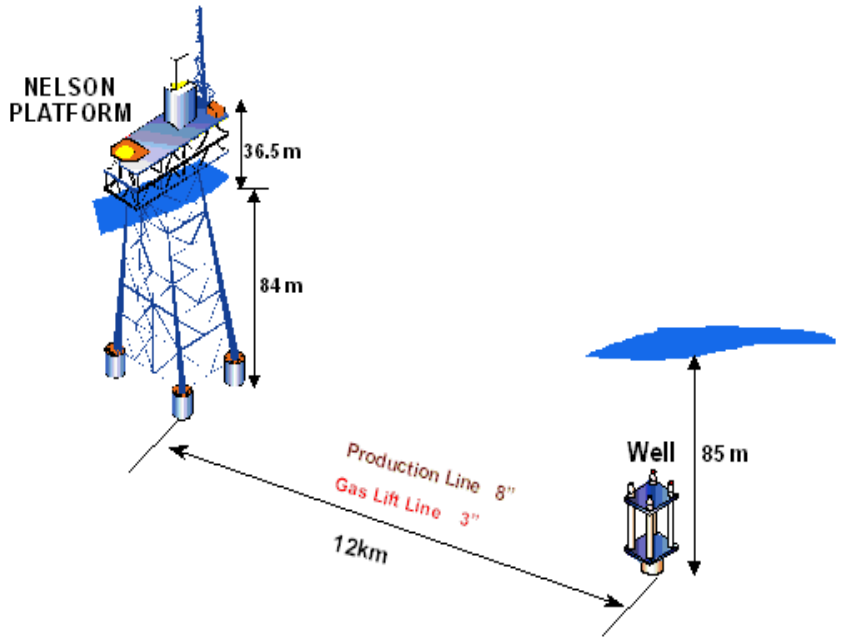

Figure 1 Process layout for Howe tieback to the Nelson Platform

Note: Howe being a marginal field has the following associated constraints:

- It will be produced without pressure support.
- It will have one production well.
- The reservoir pressure will decline rapidly.
- Nelson gas and oil are determined by difference.

3. Process Overview.

Howe Flow Line and Reception Facilities.

The Howe currently produces 11,000mstbd. The method of operating the well is to use both the subsea and topsides chokes, with the subsea choke being utilised to control the production and the topside choke being utilised to maintain the gas volume fraction (GVF) at 85%. The Multiphase Flow Meter (MPFM) is located upstream of the topsides choke valve. Downstream of the MPFM is the flowline which is connected to the 36" production header and the 10" test header. Production is normally routed to the production header and production separator V-1010.

When verification of the MPM is required the production is diverted to the test header and test separator V-1000. A schematic layout of the setup is shown in Figure 2.

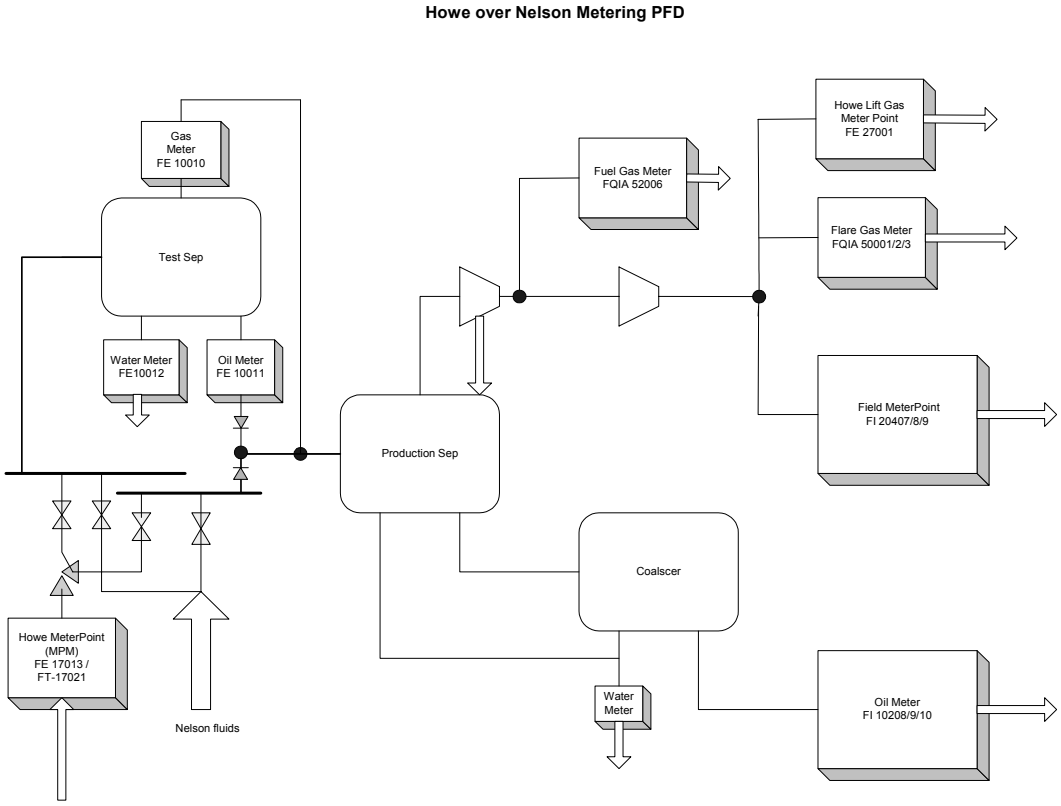

Figure 2 Schematic Howe over Nelson metering process flow.

Processing Howe Fluids.

The Howe fluids are commingled with Nelson fluids in the 36" production header and processed directly in the Production Separator V-1010. The Test separator V-1000 has a capacity of 25,000 BLPD and this separator is used for well testing and also for the verification of the MPM. The test separator is equipped with a Coriolis meter for oil measurement, a magflow meter for water and a V-Cone for the gas measurement. It

also is equipped with a venturi meter for and if gas lift is required. Figure 2 visually illustrates the above text.

4. Design Requirements and Allocation Philosophy.

Design Requirements.

The main consideration of the metering design of the Howe project was the requirement to comply with the Nelson, Forties and Segal pipeline agreements. The Nelson agreements stipulated that the measurement of the Howe fluids should be 5% for oil, 5% for gas and 10% for water utilizing a MPFM or a similar device. The test separator requirements to enable this uncertainty to be verified accurately were determined as 3% for oil, 3% for gas and 10% for water.

Howe Production Meter.

To achieve the stated uncertainties the MPFM option and other measurement devices were investigated, i.e Wet Gas Meters (WGM), this also included the option of installing a production separator. The cost and size considerations immediately eliminated the separator option and it was quickly realised that a multiphase meter was the practical and feasible solution.

In later field life the GVF is expected to exceed 90%. Thus, it will be a requirement to revisit the MPFM uncertainties for this condition. A WGM has been accounted for in this case if the initially installed MPFM cannot meet the uncertainty requirements. The GVF is expected to increase as the well pressure decreases but for the initial production years a MPFM turned out to be the choice.

The other consideration is that the MPFM will benefit from being installed upstream the topside choke. To provide comfortable operating conditions for the MPFM and thus good uncertainty figures, the Howe fluids will be produced at 80% GVF at MPFM conditions. The GVF at MPFM conditions can to a certain degree be controlled if the topside choke is positioned downstream of the MPFM.

MPFM uncertainties are influenced by the accuracy of their input parameters. Hence it is important that good quality samples are obtained. Therefore, to ensure good quality samples of the fluid for analysis a fully engineered sampling point is required preferably not too far from the MPFM.

Allocation Philosophy:

The equity divisions of the Howe reservoir are different to the Nelson reservoir. Consequently, the requirement for a method for measuring and allocating Howe Field production volumes needed to be agreed between the Howe Field and Nelson Field owners. In addition, for the gas allocation, the gas purchaser also had to be included as a party to the agreement. Furthermore, approval of the allocation procedure to ensure the correct reporting of oil quantities for tariff purposes was required from the pipeline system operator.

The main allocation principle was to establish the rules for determining the Howe Field and Nelson Field production quantities. It was agreed that Nelson Field would be calculated "by difference"

Nelson Field Gas Production = Nelson Platform Gas -Howe Field Produced Gas and
Nelson Field Oil Production = Nelson Platform Oil Export - Howe Field Produced Oil
Nelson Field Water Production = Nelson Platform Water - Howe Field Produced Water

The Howe Field fluid is firstly measured by means of a MPFM to determine the quantity of oil, gas and water at the MPFM location. Based upon process modelling oil and gas recovery factors are calculated and applied to determine what these quantities will be at the export meter point. For the avoidance of doubt Howe Field will not use water injection.

The commercial framework for the metering and allocation rules is included in two main agreements covering oil and gas separately.

Allocation Principles – Outputs

The allocation outputs are:

a) The determination of the Howe Field and Nelson Field production quantities
b) The allocation of the fuel gas and flare gas utilised on the Nelson Platform
c) The allocation of the gas export quantity between the Howe Field and Nelson Field to meet the reporting requirement of the Segal Operator i.e. gas disposal system
d) The allocation of the oil export quantity between the Howe Field and Nelson Field to meet the reporting requirement of the Pipeline Operator i.e. oil disposal system

5. Meter Selection.

Howe Production Meter.

The choices of meters were limited. It was known that in the first year of production a 3 phase flow measurement would be required. This narrowed the possible selection to multiphase meters. There were not many MPFMs available for this application providing an uncertainty of 5% for oil and gas, with a GVF of approximately 80%.

In later field life when pressure drops and GVF increases above 90%, the uncertainties of the MPFM will be revisited and compared with alternative metering devices.

Further criteria for selecting a MPFM make were track record, uncertainty specifications, operational experience and level of support. Using these selection criteria across a range of MPFMs it was decided that the Framo/Schlumberger PhaseWatcher Vx was the prefered choice.

It later became known, that the PhaseWatcher technology has been further developed so it can be utilized for high GVF applications by changing software. This has to be assessed for the Howe fluids when the pressure drops in the future. The consequence is that it might not be necessary to install a dedicated WGM for late field life.

The selected vendor has been producing MPFMs since beginning of the 1990s and has continuously developed the technology. On the UK sector several MPFMs are installed and feedback from the market is positive. In addition, an attractive characteristic of selected technology is that it is based on fluid physical properties and well known physical relations and thus does not need dynamic flow calibration. This point is important as it has a bearing on how to validate, setup and to do commissioning of the MPFM.

Another point to consider is whether or not the MPFM is flow regime dependent. The selected MPFM is not. The flow regime independence is obtained by using a blind tee immediately upstream the measurement section as a part of the MPFM design. Prior to entering the measurement section of the meter the fluids are conditioned into a predictable flow pattern by the blind tee.

The working principle of the selected MPFM is comprised of a venturi and a dual energy spectral nuclear detector. The total flow is measured by the venturi and the split between the phases is indirectly measured by a gamma ray detector. From these data sources the flow rates of each phase through the meter are calculated. A cutaway schematic of the MPFM is shown in Figure 3.

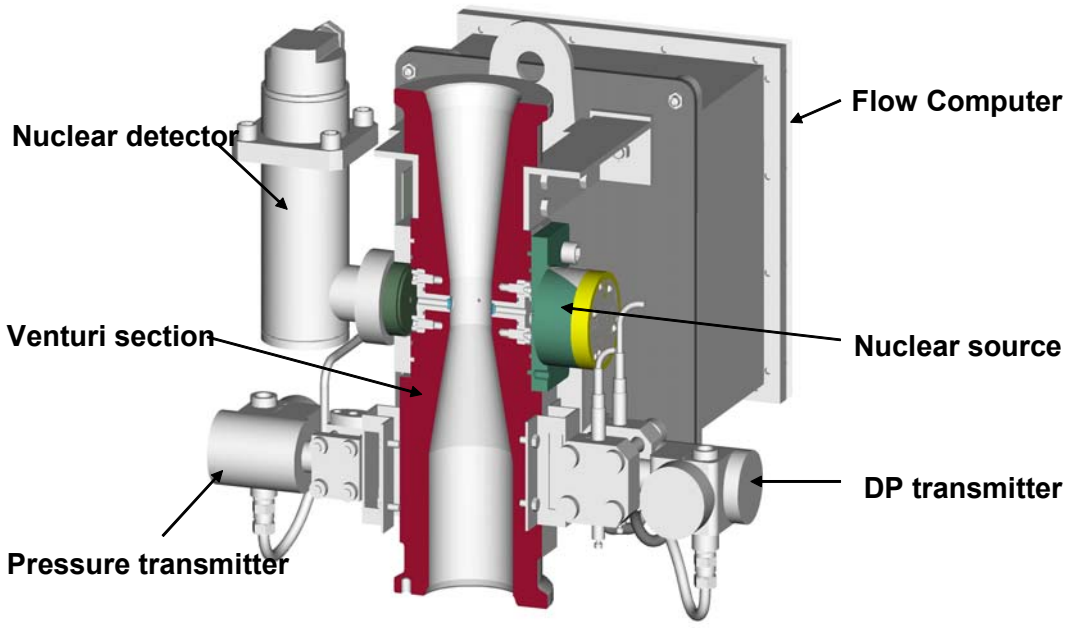

Figure 3 Cutaway schematics of the selected PhaseWatcher Vx.

As for all multiphase flow meters it is important to get a good understanding of the required input parameters. For meters utilizing the selected technology it is necessary

to provide PVT data of the fluid. It is recommended that PVT information is derived from a sample taken at line conditions and analysed at a laboratory that can produce the correct analysis for uploading into the MPFM.

Although no dynamic calibration is required a static calibration on an empty meter must be allowed for before production starts. The vendor will acquire data on an empty meter and use that as a baseline reference. Since this meter will be used for allocation it will be written into the commercial agreement, and compared against a test separator from time to time.

6. Testing Requirements.

A critical part of the Howe metering project was the functional acceptance testing of the selected meter to prove that it can achieve the stated accuracy.
Ideally the MPFM should be tested at conditions as close to the operation envelop as reasonably practicable. This can cause difficulties in selecting a testing facility that can simulate the pressure, flow, temperature and phase conditions.

It was initially planned to send the PhaseWatcher to a laboratory that was specialised in testing equipment for gas metering and could be operated under realistic conditions. The other alternative was to utilise the Framo multi phase test facility at Flatoy. This facility did have the equipment to conduct the test over the GVF and WLR range, however, it did not have the capability to simulate the pressure range that the MPFM would be exposed to at start up as the maximum pressure the flow loop could operate at was 9.0 bar.

After assurances from Framo, that the meter could perform to expectations and to the uncertainties expected, the decision was made to proceed with the Framo flow loop. The multiphase flow loop test of the PWVx was being performed in a closed loop on Exxol D80, fresh water and nitrogen. The flow loop test set-up, see Figure 4, includes a large horizontal three-phase separator from where single-phase streams of oil, water and gas are drawn, boosted and measured individually. Flow rates of the single-phase oil, water and gas streams are adjusted by means of remotely operated control valves before being commingled into a multiphase oil-water-gas stream. The multiphase stream is routed through the PWVx and back to the separator via a remotely operated control valve, which is used to adjust the operating pressure.

Single-phase flow measurements will serve as references for the PWVx. Single-phase flow rate measurements are found by measuring differential pressures over KEMETMA V-cone flow meters. In addition, pressure and temperature will be measured on the multiphase stream immediately upstream and downstream the PWVx, and in the separator for process control purposes. Also a secondary measurement is done both on the gas and the liquids in order to quality check the primary measurement. For the gas, a Venturi meter is used as secondary measurement and on the liquid a Micromotion Coriolis meter is used.

Key engineering variables such as pressure, temperature, total volumetric flow rate, gas volume fraction and water cut at PWVx inlet conditions were calculated by the flow loop control system and displayed on a computerized flow diagram. The control

system comprises built in alarms and emergency shutdown (ESD) functions in case of system failure.

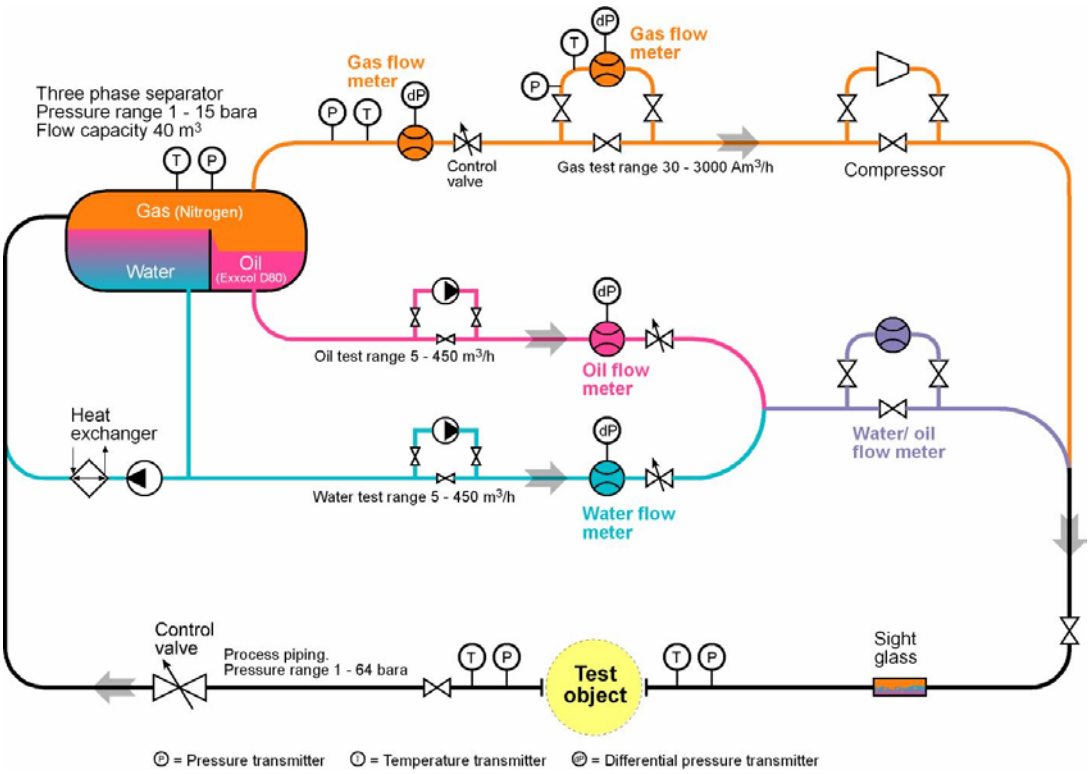

Figure 4 Framo multi phase test loop facility schematics.

The Results.

To understand the test results one has to understand how the MPFM works and how the corresponding uncertainties are specified. The uncertainties are specified in GVF ranges. That is, at lower GVFs the MPFM will perform better than at higher GVFs. This is due to the inherent nature of dual energy gamma ray venturi meters. The GVF range from 0 to 100% is usually split into 3 or 4 ranges for which the uncertainties are specified. In addition, the uncertainties are specified differently at lower pressure than at higher pressure. The pressure ranges is usually split between lower and higher pressure. Higher pressure usually means higher than 20 barg and higher GVFs usually means above 80% GVF. Our stipulations were for a 5 % uncertainty on oil and gas for the Howe conditions. Howe conditions cover both high and low GVFs but at higher pressures. Framos expectation for the flow loop conditions were 10% uncertainty for the gas flow rate measured by the PWVx + 1.5% uncertainty for the gas as measured by the flow loop, however, it was stated that the meter would perform better than this.

The test results showed that up to 60% GVF the Shell Howe requirements were met as shown in Table 1. The pressure during the test was 8 bara. The units are m3/h at MPFM conditions. Above 60% GVF the MPFM met Shell requirements were met for oil and water but not for the gas. Although the vendor specifications were met this was not satisfactorily to Shell. A graphical visualization of the gas flow comparison is shown in Figure 5. The red horizontal lines show the Shell expectations; whereas the grey horizontal lines represent the Shell expectation added to the flow loop

uncertainty. On the y-axis is plotted the difference between the flow loop reference system and the MPFM readings. The x-axis represents the tested GVF. The rest of the test results are summarized in Table 1.

	Reference			PhaseWatcher Vx Measurements						
FP Id	Qliq	Qgas	WLR	Qliq	rel.dev%	Qgas	rel.dev%	WLR	abs dev. %	GVF %
FP001	79.46	36.89	40.22	78.70	-0.95	35.87	-2.74	39.88	-0.34	31.03
FP002	79.09	37.95	70.43	79.57	0.60	36.74	-3.19	69.15	-1.28	31.38
FP003	81.35	49.55	40.12	80.92	-0.54	48.17	-2.79	40.54	0.42	36.80
FP004	79.10	48.44	70.10	79.19	0.11	47.51	-1.92	69.69	-0.40	37.13
FP005	88.97	71.84	29.92	88.08	-1.01	71.15	-0.96	30.27	0.35	44.14
FP006	88.49	70.12	60.19	87.81	-0.77	68.54	-2.25	59.84	-0.35	43.18
FP007	85.22	98.93	20.72	85.45	0.27	98.70	-0.23	21.26	0.54	52.76
FP008	84.70	99.85	60.26	83.89	-0.95	97.58	-2.28	60.96	0.70	52.73
FP009	82.86	154.40	20.59	81.82	-1.25	147.30	-4.60	21.04	0.45	63.34

Table 1 Flatøy test results at low pressure.

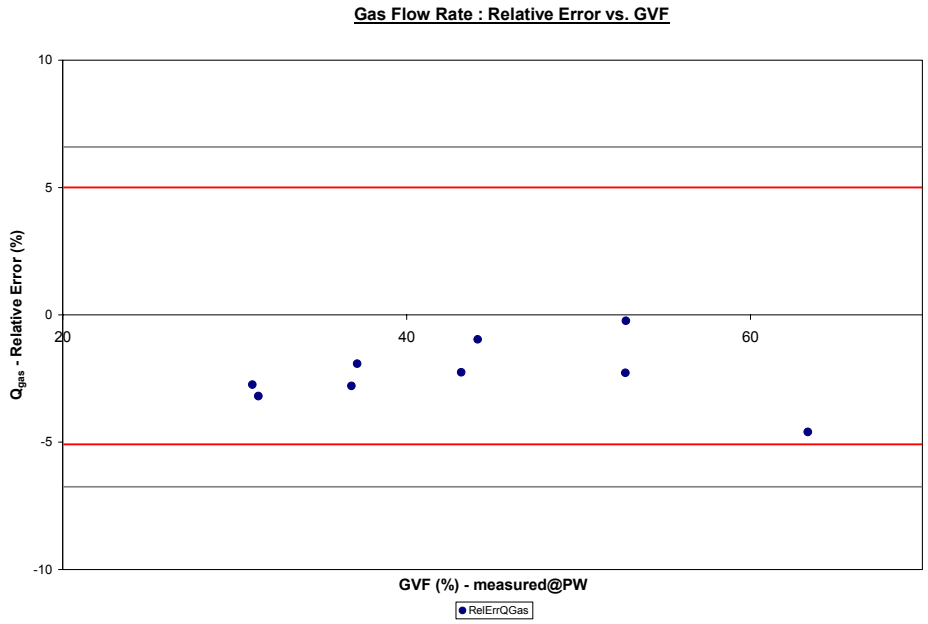

Figure 5 Flatøy test results, gas flow rate.

To verify the MPFM at a higher pressure the option was either to remove the meter to a specialised facility or design a flow loop at Flatøy to operate at the expected operating pressure of the meter. The first option was to utilise a specialised facility as the flow loop could operate at higher pressures. Obtaining a test week however proved difficult and it was then that Framo, as their flow loop had not an alternative, engineered a solution. They modified the existing facility to accommodate one of their multiphase pumps that could deliver 25 barg. The only restriction with this was that the 3 phase measurement would be reduced to 2 phase (water and N2). However, according to Table 1, the WLR uncertainty does not seem to be an issue at all and the proposal was accepted. Figure 6 shows the modified test loop schematics with the multiphase pump. With the pump the GVF test range was set to 60 to 95% GVF.

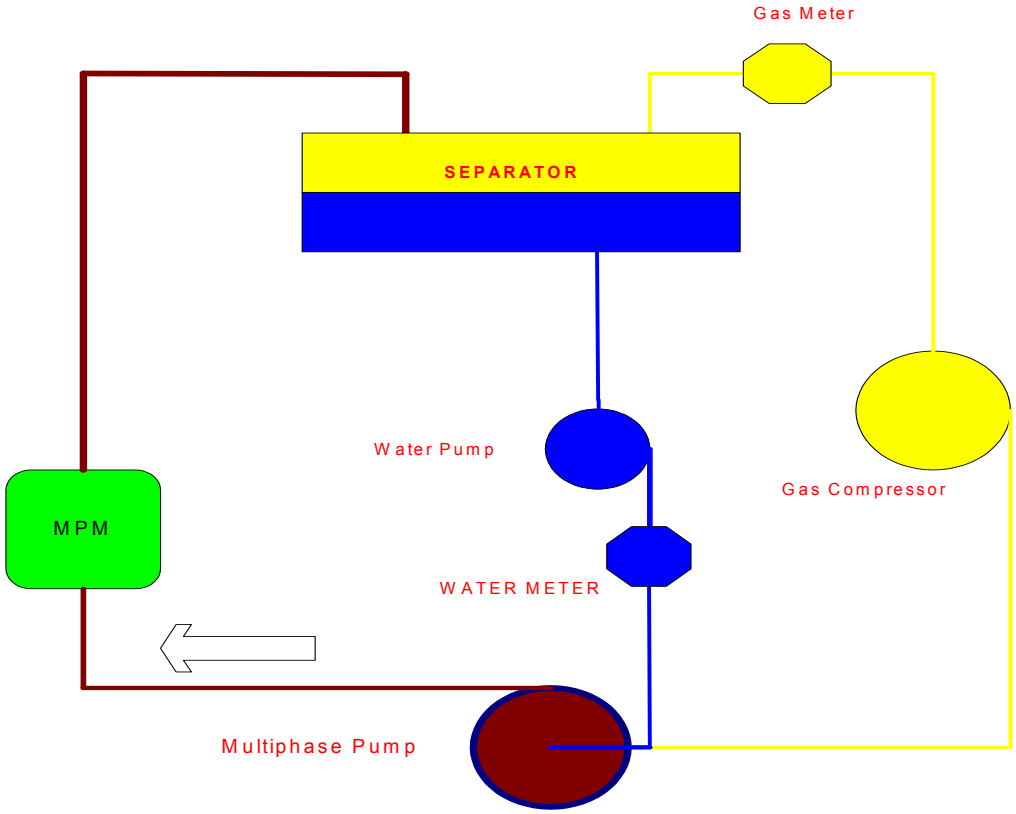

Figure 6 Framo multiphase test loop with a multiphase pump to boost the loop pressure.

The test results are shown in Table 2.

	Reference			PhaseWatcher Vx Measurements						
FP Id	Qliq	Qgas	WLR	Qliq	rel.dev%	Qgas	rel.dev%	WLR %	abs dev. %	GVF %
FP002	80.12	129.84	100.00	81.67	1.9%	123.47	-4.91	101.09	1.09	59.79
FP003	42.49	167.31	100.00	44.08	3.8%	161.52	-3.46	100.07	0.07	77.58
FP004	23.24	201.28	100.00	23.72	2.0%	196.61	-2.32	98.60	-1.40	88.92
FP005	12.78	245.19	100.00	12.94	1.3%	237.23	-3.25	102.20	2.20	94.32

Table 2 Flatøy test results at elevated pressure.

The test results showed a significant improvement due to higher pressure, as expected. All flow points are within stated limits for the Shell requirements.

Uncertainty

The uncertainty of the multiphase meter was an area that was defined prior to purchase of the meter. The results from the testing fell within the theoretical results.

The uncertainty of the facility at Flatøy was stated as:

- 1% relative of reading for the oil flow rate.
- 1% relative of reading for the water flow rate.
- 1.5% relative of reading for the gas flow rate.

Although all the test meters on the flow loop had traceable certification the flow loop itself only produced a functional test of the MPM. The flow loop is not an accredited facility, however, better documentation to substantiate the stated uncertainties would be preferable. On the other hand, the flow loops secondary instrumentation give a good indication of the measurement quality of the primary reference instruments. And above all, the MPFM passed the test within the MPFMs specifications. That is, the requirement is really MPFM spec + flow loop spec.

Therefore, it was considered proved that the uncertainty that was likely to be obtained once the meter was operational would be within the specified range for all three phases.

7. Commissioning.

The commissioning and set up of the MPFM once installed on the platform is critical to its success in measuring the fluids from Howe. Commissioning of the MPFM involves communication checks and set up of the MPFM configurations. This section will concentrate on the setup of the MPFM due to its significance for obtaining good quality measurements.

Required input data

The MPFM needs to be setup with fluid property data. The required input data for the MPFM are:

- Pressure,Volume and Temperature (PVT) data. Oil, water and gas densities at MPFM conditions. Typically tables for different temperatures and pressures around the expected operating temperature and pressure.
- Oil, water and gas compositions. Alternatively, oil and water samples and a gas compositional analysis.
- A baseline reference measurement.

For this MPFM there as basically two options for supplying PVT data. One can either choose:

- Generic black oil model which requires a limited number of input parameters
- Fluids ID model, which requires PVT data for the specific fluid at MPFM conditions as described above.

For this application, the Fluids ID model was chosen for optimum accuracy since the MPFM is used for allocation. The need for PVT data is not unique for MPFMs and should not be of particular concern for MPFMs. PVT data is equally important to other flow measurement devices at a test separator.

A reference measurement is required for the nuclear system as a base line for the number of gamma photons acquired by the system when the MPFM is empty. If possible, the vendor recommends doing this on site after installation. The baseline reference recording requires that the MPFM is empty, that is, free of hydrocarbons.

The compositional data or physical samples are used to find the mass attenuation values for the fluid. The mass attenuation value for a fluid is a measure of how much the gamma photons are attenuated when they are passing through that fluid. Oil, water and gas have different mass attenuation values and they are a characteristic of the fluid in the same way as density The mass attenuation value is determined by the atomic composition of the fluid and can be found from published tables.

The mass attenuation values can be found in three ways, from a theoretical computation based on compositional data for that fluid, by filling the measurement section of the MPFM with a representative sample or finally by measuring the fluid sample with another fully tested MPFM. Filling the MPFM with a fluid one can measure the mass attenuation value directly for that fluid. If the sample is representative for the fluid and it is practically possible, the vendor preference is to measure the mass attenuation value with the actual MPFM. There is dedicated tool for doing this so the required amount fluid sample is about 0.5 litres.

The MPFM provides data for both line and standard conditions. The black oil model does not require further input to provide this information. The Fluids ID model require fluid specific data about shrinkage factors, gas in solution etc. This is standard information needed to convert flow rate data between line and standard conditions.

Howe MPFM setup

The goal was to use the MPFM to measure the well fluids from first oil and on. At the beginning limited fluid property data were available and the vendor was asked to use this data knowing that the setup would need to be updated when samples were taken and analysed.

The plan was to bring Howe on line to clear the impurities, and then complete an ESD check on the platform. Before restarting, pressurised samples were taken to update the MPFM with results from the sample analysis. Some samples were analysed offshore and other shipped to an onshore laboratory. The offshore analysis data would be an enhancement to the setup based on the limited data available before first oil. The offshore analysis was performed using a portable laboratory and software package (PVT express). This is an analytical service provided by Schlumberger. The final setup was based on the Pressure,Volume, and Temp analysis report from the onshore lab when that was available.

Further assurance can be attained, by diverting to the test separator until either a Howe fluid sample has been analysed or a full setup of the MPFM was performed. In addition to measuring the Howe fluids, the test separator can be used in series with the MPFM for comparison during the different setup stages outlined above.

Baseline reference: Prior to start up, we believe it is essential to have a representative from the manufacturer, mobilised to the platform to ensure that the meter was installed correctly and that communications with the meter to the data trending package (PI), distributed control system (DCS) and the service computer were functioning correctly. As it was practically possible the service engineer rechecked the air calibration of the gamma source i.e. to determine how many counts per second

were received from the gamma source by the detector in air – this then provides the baseline reference.

PVT data and mass attenuations: The initial data for the mass attenuations and fluid PVT data were obtained from the on site analysis and input to the MPFM. The vendor did all the calculations and updating at this stage. The on site data were updated later when the onshore laboratory finished their analysis. The logistics in the North Sea is quite good and the laboratory provided a swift service. The experience is that, at least for North Sea applications, the time savings on doing on site analysis compared to shipping samples on-shore for analysis is not big. The last update was done by sending the onshore laboratory results to the vendor, which then did the appropriate calculations and updated the MPFM configuration file accordingly. The file was then sent offshore and downloaded to the MPFM.

8.Verification.

As soon as the meter calibration procedures were completed and the meter was once again brought on line, it was decided to compare the meter against an external source. The uncertainty requirements for the test separator were stated earlier as 3% for oil, 3% for gas and 10% for water. The operational plan was to use the test separator and MPFM in series to compare the measurements and establish confidence in using the MPFM.

A procedure had been developed to enable automatic verification. This was carried out by obtaining the data from PI for both the MPFM and the test separator instrumentation. This information was automatically transfered into a spreadsheet for direct comparison.

The start up performance against the test separator was based on the input from the on site fluid analysis. The sample analysed was taken after the clean up and ESD test.

The comparison showed that the gas results were extremely good; the deviation between the test separator and the MPFM was within 2%. The oil comparison showed a variation between 3 to 8%. It was also clear that the default input water properties could benefit from an update since traces of water were shown when in fact there should be no water produced. In interpreting these data one should consider the added uncertainties for both the MPFM and the test separator.

It later became apparent that the values read from the MPFM had shrinkage factors applied, whereas it was believed they had not. The consequence was that shrinkage factors were applied twice to the oil. This was rectified by the vendor since the MPFM can hand off both line and standard conditions data. It was decided to fetch only line condition data into the data trending package (PI) and do PVT conversion on a common basis for both the test separator and MPFM.

Since the production was very stable it was considered that the comparison was of good quality and further improvement could be obtained by updating the PVT data based on the on-shore laboratory PVT analysis.

The full laboratory analysis allowed for updating the oil, water and gas density. The results showed an improvement in performance and most results met the specifications, however, it was found that on two occasions the gas was out of specification and on one occasion the oil was out of specification. The cause was found to be that the PVT data range uploaded to the MPFM were not sufficiently large to incorporate the operating range required.

After the final update of PVT data the comparison between the MPFM and test separator clearly demonstrated that the MPM performs to 5 % on oil and 5% on gas. The performance has now been verified over half a year. Figure 7 show comparison results from January to July 2005. The x-axis show when the comparisons are made and the y-axis show the relative difference between the test separator and the MPFM. Bear in mind that these comparisons are based on raw data from the MPFM and test separator, no adjustment factors have been applied to either measurement.

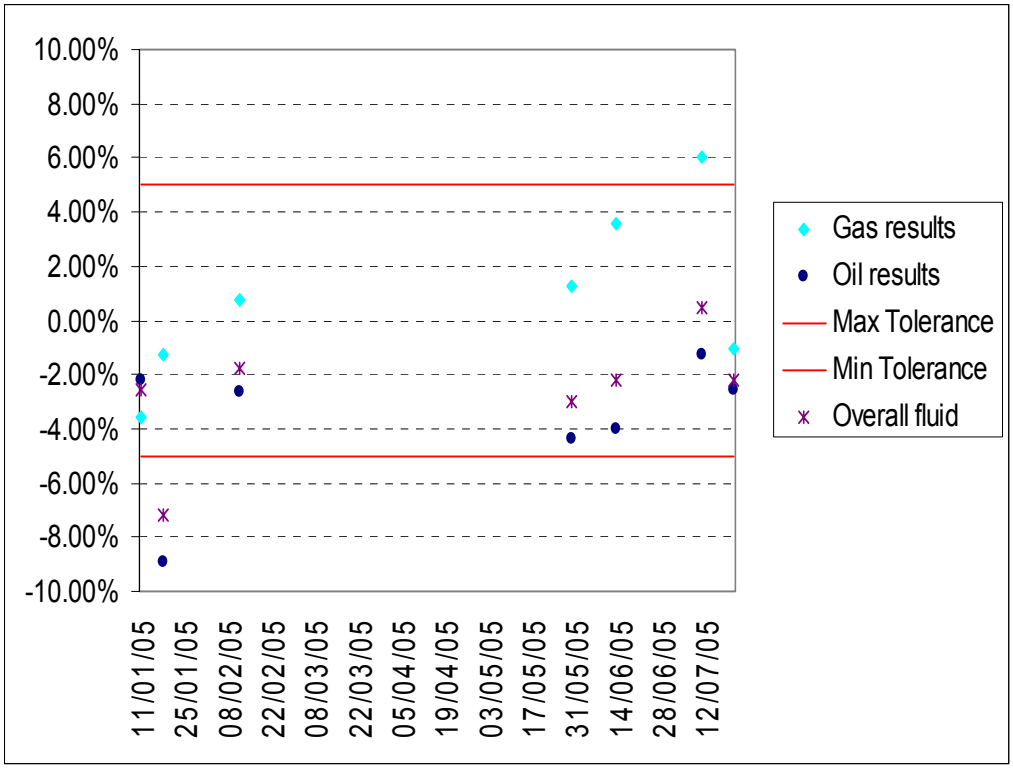

Figure 7 MPFM and test separator comparisons from January to July 2005.

9.0 Conclusion.

The overall performance of the meter, once set up with the correct PVT data has been exceptional. It should be remembered that this was a marginal field that was always under scrutiny and challenges from partners and owners alike. The data in section 8 proves without question that the performance of the meter achieves the +/-5% relative difference of reading for oil and gas that was promised to the operator for the Howe fluids.

In the first year that the MPM has operated, no failures or under performance has occurred. In the initial start up period and until the meter was correctly configured

some issues did arise. They did not impact on the overall performance and reliability and were rectified by providing temporary shrinkage and expansion factors. It should also be realised that at no time was any doubt raised on the meters ability to measure the hydrocarbons, but only to the numerical values that were being handed off. The point that should be highlighted is that it is essential that the sampling and analysis regime are strictly adhered to. This will ensure that the meter can be uploaded with the correct PVT as and when the well conditions change.

As the well conditions change it should also be realised that the MPFM PVT data should be updated. The assumption that the performance of the meter will not be affected by a change in the PVT is incorrect. The sensitivity to a PVT change will depend on operating conditions and initial fluid properties. The MPFM is robust to changes in hydrocarbon compositions, however, the sensitivity can readily be calculated by the vendor for the field in question. Then, the allowed change in PVT data before an update is necessary can be advised. A sampling regime should be initiated from the start up of the field. The change in composition can be identified by comparing with previous PVT analysis or when the meter is verified against the test separator. The technicians should be made aware of the significance of a disagreement between the MPFM and test separator and the required remedial action. Then the accuracy of the MPFM will not be affected.

The other factor that is essential for good performance is the initial dry calibration and adherence to the set up procedures. This should be carried out in location at start up and preferably repeated at every shutdown. It is essential that this is performed by an experienced engineer, using the manufacturer procedures. To cover this requirement, consideration should be given to placing a contract with the manufacturer of the MPFM. Issues around personnel protection from the nuclear source and other HSE issues are then covered.

It should be noted that the success of this project was due to the close co-operation between Framo and Shell. In the initial production phases the engineering challenges that occurred were dealt with immediately and therefore removing any doubts on the validity of the measurements. The other key points were the constant analysis and surveillance that followed the commissioning of the meter.

It should be realised that it is essential that in-house specialist for MPFM support is available, as well as support from manufacturers.

North Sea Flow Measurement Workshop
18th - 21st October 2005

Development of Recommended Practices and Guidance Documents for Upstream Oil and Gas Flow Measurement

Eivind Dahl, Christian Michelsen Research AS
Lex Scheers, Shell
Frank Ting, Chevron
Chip Letton, Letton-Hall Group

1 INTRODUCTION

Commercial multiphase and wet gas flow meters have come a long way in their accuracy, reliability, and versatility since their introduction fifteen years ago. Furthermore, considerable experience has been gained in how to select, test, verify, implement, maintain and use these devices in various applications. Particularly in applications that are located offshore, either subsea or topside, the use of multiphase or wet gas flow meters in some cases may be the only practical method of individual phase flow rate measurement.

While the maturity and acceptance of the techniques and products has steadily improved during this period, they are sufficiently different from the traditional methods of measurement that their introduction and acceptance has at times been slow. Even experienced personnel who might use them must learn not just the distinctly new technology, but also a whole new set of concepts and terminology describing the complexities of multiphase fluid flow dynamics, and the technologies used to measure the individual flow rates.

Within the major oil and gas production companies this problem has been addressed by developing courses, manuals, seminars, and other training materials. All this will bring the measurement engineers and other staff, who should have an interest in the production data, up to date with regard to how the meters work, what are their flow measurement uncertainties and limitations, what vendor companies can offer, what advantages and disadvantages are provided by each, and so on.

Nowadays, as perhaps never before, producing companies and governments worldwide are working in partnership together in the production of hydrocarbons, leading to more complex infrastructures and to questions on ownership of the various oil and gas streams. In those applications which are most likely to make use of multiphase or wet gas flow meters, it is rare that a single entity is the sole owner and completely responsible for measurement. Consequently it is not sufficient that multiphase flow measurement be well understood inside one company, but that throughout the industry this understanding is the norm rather than the exception.

The most common method for developing this kind of understanding through the industry is by the creation of documentation that discusses at length the various issues that must be confronted. Typically this has been done through the publication of white papers, technical reports, recommended practices, and standards.

There are numerous reasons why it is important that documents such as these be written and periodically updated. The ultimate reason is obviously is to reduce the capital and operational expenditure in the oil and gas projects; in support of this, the following three reasons seem particularly noteworthy:

1. **Knowledge Distribution.** The technology and practice of multiphase and wet gas flow measurement is admittedly arcane. As discussed above, not many staff involved in production measurement have any depth of understanding of multiphase flow metering, even in large production companies.
2. **Common Language and Understanding.** As the meters become commonplace in large projects in which there are many partners, it is important for all parties to "speak the same language". Not only will the documentation foster this objective, but actual participation by potential partners in its creation will do likewise.
3. **Meet the Needs of Governing Regulatory Authorities.** Since regulators often have enormous portfolios of projects for which they are responsible, any means through which their oversight responsibilities can be simplified is a welcome addition. In these complex measurement problems, such documentation can provide them some relief.

Three organizations that historically have been active in developing such documentation are the American Petroleum Institute (API), the International Organization for Standardization (ISO), and the Norwegian Society for Oil and Gas Measurement (NFOGM). Within API, ISO, and NFOGM attempts have been made to create awareness of this new measurement technology, and to provide guidance and steering on how to make its application a success.

Each organization's goals have been somewhat different from those of the others. However, in recent times the groups responsible for creating new documentation on multiphase and wet gas flow measurement have worked quite closely with one another. The purpose has been to remove, as much as possible, any ambiguity or confusion among users of the documents, and thereby to enhance the likelihood of success of all three in their respective domains.

However, in the course of working together on such similar documents, two questions continue to arise. The first is why these documents take so long to develop once the need is recognized. The second is why the industry needs three documents rather than only one. More will be said on this second topic later.

2 WHERE WE ARE IN THE WORLD OF MULTIPHASE FLOW MEASUREMENT

The adoption of multiphase and wet gas meters, though at times seeming to be almost painfully slow, has in very recent times achieved a more rapid rate of introduction. While in part due to greater familiarity among users, it is also true that new applications requiring measurement have left the user with no realistic alternative.

Here we consider the current state of multiphase and wet gas flow metering, review the various technologies used in the devices, and discuss how and where standards, recommended practices, and other similar documents can be applied in this domain.

2.1 Current State of Multiphase and Wet Gas Flow Metering.

The applications for which multiphase flow measurement was initially considered trustworthy could be broadly classed as Well Testing, Well Surveillance, or Well Management. While this is still an area where the meters find application, in recent times they have begun to see service in those applications where ownership and royalties are involved, i.e. allocation. While it is quite unlikely that meters will ever be used for the ultimate in fiscal measurement, i.e. custody transfer of hydrocarbons, they will likely become commonplace on many allocation applications.

Early meters were often installed on land – perhaps so the vendors could access them if needed. Now multiphase meters are used extensively offshore, and not simply topside but in what is termed *ultra*-deepwater. Meters have been operational in water depths ranging up to 2300 meters for

almost three years now, and others are scheduled for installation in depths approaching 3000 meters as early as 2007.

A next logical step in the evolution of multiphase flow meters, after topside and subsea, will be the development of downhole multiphase flow meters. With the multi-lateral wells being drilled today, it is desirable to measure oil, water and gas flow rates before they are commingled in the well bore. Although use can be made of existing multiphase flow measurement technology, the challenge is clearly in designing equipment for high pressure (up to 1000 bar) and high temperature (150-200 °C) applications. Of these two, the high temperature challenge is probably the more difficult to overcome as it requires electronics and sensors to work reliably at those elevated temperatures.

An early use of multiphase meters was in the replacement of mobile test separators by oilfield service companies. They recognized early on that it was far easier to transport a multiphase flow meter from one well site to another than a large separator and all its associated equipment.

In the earliest days of multiphase measurement the only means of test and verification of meters was at the facilities built by each manufacturer. Now there are well-recognized, third-party reference loops available for multiphase and wet-gas flow in the US, the UK, Norway, and China.

2.2 Diversity of Technologies Used.

In the measurement of multiphase flow, one obvious characteristic of the technology is the fact that there is no standard way of measuring flow. Unlike the case with some single-phase methodologies (e.g. orifice meters), the sensor technology and multiphase flow models used to come up with oil, gas, and water flow rates vary widely. Some of the more important sensors and technologies used are:

- Electromagnetic – Dielectric, Conductivity
- Nuclear Gamma Ray – Densitometry, Spectroscopy
- Pressure/Differential Pressure – Mass Flow, Density
- Acoustic/Ultrasound – Flow Rate, Gas-Liquid Separation
- Separation – Measurement Simplification
- Tomography – Flow Rates, Flow Regimes, Geometry

2.3 What Can be Standardized, and What Cannot.

Due to the diversity in measurement technologies used here, it is impossible to write standards for the physical designs of the meters themselves. However, the meters have common measurement objectives in spite of their differences, and there are certain key aspects of multiphase flow measurement, which clearly lend themselves to standardization. Some of these are:

- **Meter Specification**. There are numerous items that can be standardized with regard to meter specification: A few of these are:
  - Weight of complete meter package.
  - Physical dimensions of complete meter package.
  - Available pressure ratings.
  - Communications protocols and data rates available.
  - Minimum/maximum flow rates at available sizes.
  - Uncertainty of flow rates and composition.

- **Testing/Presentation of Test Results**. One of the most badly needed areas for standardization is in the area of determination of uncertainty through testing, and in the presentation of those results. Not only have there been instances in which common practice in our industry has been at odds with accepted practice in most other endeavors – for example in the use of a 90% confidence interval – but the use of confusing or misleading methods of presenting test results is commonplace. For users to make informed buying decisions, there need to be accepted methods of estimating and displaying uncertainty of measurement – i.e., standards.
- **Maintenance/Operation/Verification**. Many aspects of these activities can lend themselves to standardization. An example is the recommended schedule for verification of meters, along with a template for all the information that must be collected in routine verification activities. Although individual meters will have their own particular verification activities, there should be certain kinds of information that can be "standardized".

3 STANDARDIZATION BODIES

Although standards-making groups have been active since the time of the Industrial Revolution, and flow measurement standards were issued periodically throughout most of the 20th Century, it has only been in the last 15 years that a serious attempt has been made to document recommendations and practices for multiphase and wet gas flow metering.

Of the three groups that stepped in to fill this void, two – API and ISO – are commonly associated with such activities throughout the oilfield and elsewhere. The third represented here, the Norwegian Society for Oil and Gas Measurement, stepped up because it was needed, because the expertise existed in Norway to do the job, and because no one else seemed ready to take on the task. Thus the first "how-to" document on multiphase flow measurement was the 1995 NFOGM Handbook of Multiphase Metering.

3.1 Norwegian Society for Oil and Gas Measurement (NFOGM)

The Norwegian Society for Oil and Gas Measurement (NFOGM)[1] is an independent society for personnel engaged in measurement of oil and gas in the Norwegian oil and gas business. In the technical area the Society's activities include flow measurement, sampling and online quality measurement in processing and transportation facilities. The Society's work is to a large extent based on voluntary work by experienced personnel in oil companies, the manufacturer industry and authorities. As one of its activities, NFOGM initiate and support projects for example to produce handbooks and development of E-learning courses. The work is to a large extent based on voluntary work by experienced personnel in the oil companies, the manufacturers, and governing regulatory authorities.

In cooperation with manufacturers and end users, the first edition of the *Handbook of Multiphase Metering* was published by NFOGM in 1995 to provide a common basis for the classification of applications and multiphase flow meters, as well as guidance and recommendations for the implementation of such meters. Since then the development and use of multiphase flow meters has increased significantly, and in 2003 NFOGM and the Norwegian Society of Chartered Technical and Scientific Professionals (Tekna) therefore decided to start the work to revise this handbook.

An international workgroup was established to carry out this work, with participants from Shell GS International, TOTAL, Norsk Hydro, BP Norway, ConocoPhillips, Framo/Schlumberger, Roxar and CMR. Other than CMR, who were contracted to coordinate the work, the participants

[1] http://www.nfogm.no

contributed on a voluntary basis with sponsorship from their employer, bringing broad and varied skills and experience from oil and gas flow measurement.

The new revision of the handbook was published in March 2005 [Ref. 1], and NFOGM is now also developing an E-learning course in multiphase flow measurement based on the handbook. This new course will add to the already available E-learning course on fiscal flow metering.

3.2 International Organization for Standardization (ISO)

The International Organization for Standardization is the world's largest developer of standards, with more than 15,000 International Standards published. The name ISO is an acronym that comes from the Greek word "isos" which means equal. By using ISO as the name for the organization it would also become independent of the language, as it would have been abbreviated by IOS (International Organization for Standardization) in English and OIS in French (Organisation Internationale de Standardisation). Therefore, whatever the country, whatever the language, the short form of the organization's name is always ISO.

ISO is a non-governmental organization and is a network of national standards institutes of 150 countries, on the basis of one member per country[2]. The Central Secretariat has a coordinating role and is based in Geneva, Switzerland. Some examples of national standardization bodies that are a member are: BSI for the United Kingdom, AFNOR for France, DIN for Germany, NEN for the Netherlands, GOST for the Russian Federation and ANSI for the USA.

ISO standards are developed according to strict rules intended to make the process both transparent and fair. Most of the standard development work is done in Technical Committees (TC's) with experts from the industry, research institutes, government authorities, consumer bodies, etc. Depending on the diversity of subjects, TC's may be further split into Sub-Committees (SC's) and Working Groups (WG's). Each published International Standard has followed an extensive route through the ISO organization, which can be summarized as follows:

- Starting with a new work item proposal
- Building expert consensus, leading to a Committee Draft (CD)
- Consensus building in TC/SC expert environment, leading to a Draft International Standard (DIS)
- Enquiry on DIS, here all ISO members are entitled to comment and vote, resulting in a Final Draft International Standard (FDIS)
- Formal voting on FDIS
- Publication of International Standard (IS)

ISO TC193[3], entitled "Natural Gas", was established in 1989 to develop International Standards for natural gas and natural gas substitutes (gaseous fuels). It covers the supply chain from production to delivery to end-users across national boundaries. These standards include terminology, quality specifications, methods of measurement, sampling, analyses, calculations and testing. A total of 55 International Standards have been published so far under TC193 responsibility. TC193 was mainly "downstream" oriented, i.e. toward the gas transportation and distribution business. However with the liberalization of the gas markets and the more complex infrastructure of oil and gas production and gathering systems, the group's standardization activities have moved further into the "upstream" world. Hence, within TC193 SC3, entitled "Upstream Area", was established with the

[2] http://www.iso.org/iso/en/aboutiso/introduction/index.html
[3] http://www.iso.ch/iso/en/stdsdevelopment/tc/tclist/TechnicalCommitteeDetailPage.TechnicalCommitteeDetail?COMMID=4437

aim to look into this new area. A first WG (WG1) in this SC was established in 2002 to look into the metering and allocation methodology for gas and condensate fields (Section 4.9).

3.3 American Petroleum Institute

The American Petroleum Institute (API)[4] is a trade association representing America's oil and natural gas industry with more than 400 member companies. API draws on the experience and expertise of its members and staff to support the oil and natural gas industry, engaging in federal and state legislative and regulatory advocacy. It also provides industry forums to develop consensus policies. In addition and of particular interest here, API provides opportunity for development of standards, recommended practices, and other similar kinds of documentation. Finally, it encourages technical cooperation among peers to improve the industry's competitiveness through program sponsorship.

API has four primary standards committees, each serving the oil and gas industry in a specific area of interest. Within one of these, the API Executive Committee on Drilling and Production Operations, a special interest group called the Upstream Allocation Task Group (UATG) is found. UATG develops industry recommended practices in flow measurement and allocation, especially those needed to meet the rapidly changing technical and regulatory needs of those deepwater developments where conventional separation processes are not applicable. These recommended practices help to ensure that production from remote subsea fields with different ownership, and perhaps different royalty rates, is accurately measured and properly allocated back to the operators. Current API flow measurement standards do not fully address many measurement and allocation applications in the upstream environment. Two such recommended practices have been developed in the past four years, the most recent of which is RP 86, described below.

3.4 Recent Developments of API, ISO, and NFOGM Documentation

Each of the three groups has recently developed a document to help users who require assistance with navigating the difficulties of multiphase or wet gas measurement or allocation. Although each activity was initiated independently from the others, those working on the three were aware of the existence of the other activities. Close relationships between personnel working on each led to a high level of cooperation between the groups, more of which will be discussed in Section 3.5.

As mentioned in Section 3.1, the 2005 revision of what over time has become familiarly known as the "Norwegian Handbook" is a particularly noteworthy event. Because Norwegian oil and gas producers and manufacturers were in the forefront of developing and using multiphase and wet gas flow meters, it was perhaps natural that they would take a leadership role. During the past ten years, in the absence of other documentation, the NFOGM Handbook was often used as a *de facto* standard for this form of measurement. The new version was made available for use in the second quarter of 2005 [Ref. 1].

The ISO TC 193 WG 1 document took a somewhat different approach from the other two. While it addresses many of the issues in flow measurement, its primary emphasis is on the allocation of hydrocarbons under various situations. Because of the many different methodologies that were already available in the area of gas and condensate allocation, for the purposes of ISO it was decided that a Technical Report (TR) would be the best first approach. This WG has now delivered a draft TR called "Allocation of Gas and Condensate in the Upstream Area" [Ref. 2]. Currently this draft TR is in circulation for comments through the central ISO secretariat. A TR is often used for subjects that are still too complicated for an International Standard; through a draft TR an inventory of best practices is presented, and a level of awareness is created. A similar well-known example in

[4] **http://api-ep.api.org/publications**

gas metering is the recently developed TR on Ultrasonic Flow Meters that will now be followed by an International Standard.

The API Upstream Allocation Task Group (UATG) was tasked with developing a recommended practice that addressed the kinds of issues a user would be faced with no matter how he chose to measure a well stream. As such, the resulting document, called API RP 86 [Ref. 3], deals with the points to consider in separator-based measurement as well as various forms of multiphase flow measurement. Besides the various kinds of routine topics, special emphasis is placed on uncertainty in multiphase measurement and how it should be described, specified, and displayed.

Instructions for obtaining both electronic and print copies of each of the three documents are found in the Appendix.

3.5 Cooperation Among the Groups

It is well known that the community of those engaged in multiphase flow measurement is not large, and that many of those who are seriously engaged in this area know one another. Consequently, as each of the groups listed above began planning the development of documentation in their respective organizations, it was natural that they should discuss how they might work together.

Although there was never a formal arrangement created for cooperation among the groups, the fact is that an informal affiliation has existed during the period of the creation of the documents. Some examples of the cooperation were:

- Lex Scheers and Eivind Dahl attended numerous API UATG meetings, e.g. vendor meetings at 2003 NSFMW. This even dates back to the period of development of API RP 85.
- Lex Scheers (chair of ISO TC193) participated in NFOGM development.
- Roy Meyer of API UATG participated in ISO TR development.
- API RP 86 adopted NFOGM handbook descriptions to explain multiphase flow regimes, almost without modification.
- API and NFOGM concurrently adopted common uncertainty presentation graphics and methodology. NFOGM developed and made available to the industry an Excel tool for creating these uncertainty plots.
- API UATG was given access to NFOGM handbook development area, including drafts of new version, invited to comment on and use as necessary.
- API RP 86 adopted a number of definitions from the NFOGM Handbook. In all but one instance, common terminology was agreed between the groups.

4 TOPICS COVERED IN THE DOCUMENTS

Although the three documents have a number of similarities – and in some cases are virtually identical – they were developed independently for somewhat different purposes. In discussing content here, some of the subjects are found in two or three of the reports (e.g., Terms and Definitions), while other topics are highlighted more in one of the documents than in the other two (e.g. Allocation).

4.1 Terms and Definitions

All three reports dedicate considerable space to defining the terms that are used in both the document and in practice. Of course, the specific terms defined in each document reflect the particular emphasis of that work. For example, the ISO report has a special section called “Allocation System Terms” in which the vocabulary peculiar to allocation is presented.

As was mentioned in Section 3.5, there is a significant duplication of terms and definitions among the documents, particularly between RP 86 and the NFOGM Handbook. This was of course by design, and hopefully will prevent confusion among interested users.

The only significant exception to the harmonization of Terms and Definitions was in the use of the word *calibration*. The ISO definition [Ref. 6] of the term *calibration,* also used in the NFOGM Handbook, is fundamentally different from its definition in API RP 86, Measurement of Multiphase Flow, since API RP 86 uses definitions consistent with the API Manual of Petroleum Measurement Standards (MPMS) [Ref. 4]. According to the MPMS, the term *calibration* prescribes an adjustment to the meter should it be found out of range, whereas the ISO definition does not permit such an *adjustment*. ISO identifies *adjustment* as a separate activity, not part of a *calibration*. The ISO definition of *calibration* is similar to that defined in the API RP 86 as *verification*.

4.2 Tutorials

4.2.1 Multiphase Flow Regimes

For those who are not familiar with the nature of multiphase flow, one of its most difficult concepts to grasp is the variety of ways that the fluids travel through the pipe. Unlike the case of single-phase flow, multiphase flow through a pipe can be quite chaotic and unrepeatable.

One of the strong points of the 1995 NFOGM Handbook was its clear explanation of the various flow regimes found in both horizontal and vertical flow, complete with figures showing how the liquid and gas distribution might appear in the pipe. This section has been updated with improved verbiage and figures in the latest release of the Handbook.

Rather than re-write something, which had already been done very well, API asked for and was granted permission to use the NFOGM material on this subject in RP 86. This was accomplished with only a few minor revisions.

4.2.2 Metering Principles

Both the NFOGM Handbook and RP 86 discuss the principles involved in measuring multiphase flow rates. This includes descriptions of the sensors used for various purposes, as well as the ways the sensors are combined – at times with a partial separation system – to achieve the desired results.

4.3 Metering Philosophy and Applications

Multiphase flow measurement technology may be an attractive alternative for a number of applications since it enables measurement of unprocessed well streams very close to the well. However the technology is complex and has its limitations. Care must therefore be exercised when planning installations that include one or more MPFMs. Chapter 5 in the NFOGM Handbook and chapter 6 in API RP 86 cover the general and overall reasoning for selection, installation and operation of multiphase flow metering systems for a wide range of applications.

A number of different MPFMs are available on the market, employing a great diversity of measurement principles and solutions. Some MPFMs work better in certain applications than others, and hence a careful comparison and selection process is required to work out the optimal MPFM installation for each specific application. Amongst other things one must:

- Ensure that the selected MPFM is capable of continuously measuring the representative phases and volumes within the required uncertainties, taking into account that the well stream flow rates vary over the lifetime of the well (see 4.2.2).
- Most MPFMs on the market need some kind of a priori information about the properties of the fluids being measured, and since no standard method for multiphase fluid sampling is yet available, alternative ways to gather this fluid information must be addressed when planning an MPFM installation.

- One must ensure that an MPFM installation includes adequate auxiliary test facilities to enable calibration and adjustment of the MPFM in field during operation.

If periodic verification of the MPFM is not carried out, increased measurement uncertainty must be expected. The extent of such regular testing will depend on the criticality of the application and operation, and for some applications field verification may also be subject to approval by regulating authorities. These and other issues are covered in more detail in the API and NFOGM documents and should be addressed in an early design phase. To ensure a successful installation, an overall metering philosophy should be developed for the specific application taking into account all relevant aspects concerning the installation from selection of technology, performance specifications, design considerations to field installation, commissioning and finally field operation.

The range of applications for multiphase flow measurement is broad and expanding rapidly, and it is difficult to specify a framework in which to describe how it is practiced. Both the NFOGM Handbook (chapter 5) and the API RP 86 (chapter 6) characterize the applications by identifying all those functions in which some form of multiphase well flow rate determination is performed. The API RP 86 also characterizes the applications by the physical locations where the meters will reside, and the documents elaborate on pertinent issues concerning the various identified applications.

4.4.Acceptance, Calibration, Installation, Verification, Operability

The API RP 86 and NFOGM Handbook are each concerned primarily with multiphase and wet gas flow measurement, hence each devotes a generous amount of space to those activities that are common in this domain.

For example, in chapter 9 of API RP 86 multiphase flow meter acceptance, calibration, and verification are addressed. Depending on the requirements of the application, such as reservoir management and fiscal metering, different levels of acceptance, calibration and verification tests are recommended. A detailed recommendation regarding factory acceptance tests (FAT) is also included in the RP, along with examples and checklists.

The document deals with issues in field verification of well rate determination using the separator well test method. It encourages field verification as an integral part of the routine multiphase flow meter operation. It also points out that using a test separator as a reference device for such verification work should be approached with great care, especially for attempting accuracy determination. In-situ (field) re-calibration is another issue addressed, recognizing that while re-calibration can be performed on land-based or topsides flow meters, it is still an enormous challenge to test and possibly calibrate a subsea flow meter in-situ.

Installation, reliability and operability are discussed, suggesting guidelines and practices during both normal and abnormal operating conditions, as well as operating environment considerations. The subject of material (system) balance checking is also discussed, in which it is recommended that the system balance be done in mass terms.

4.5 Multiphase Meter Uncertainty

When faced with the task of writing a recommended practice for measurement of multiphase flow, the API UATG identified a number of technology gaps that needed to be addressed. It was agreed that the most significant of these was the uncertainty of measurement of all forms of multiphase flow. In the view of the working group, nowhere was the topic addressed in sufficient depth for the purposes required. A simple example is the lack of uniformity of presentation of multiphase measurement uncertainty by manufacturers, making comparisons difficult. In addition, producers, manufacturers, and the regulatory authority needed a common vocabulary to describe measurement

uncertainty in the estimation of oil, gas, and water flow rates for allocation calculations. In a break with today's commonly used practice, the working group recommended expressing multiphase metering uncertainty at a confidence level of 95% (two-standard-deviations), rather than at 90%. Also recommended were three levels for uncertainty determination and presentation:

- Level 1: Primary and Secondary Devices – the uncertainties of all instrument sensor readings, such as pressure, temperature, density, radiation detector counts, capacitance, and conductivity should be made available to the user.
- Level 2: Observed Conditions - the uncertainties of flow rates (both mass and volumetric) of gas, oil, and water at meter flowing conditions, plus GVF and WLR are presented at this level. It is possible to develop the flow rate uncertainties from those of the sensors combined with a multiphase flow model or equations. However, the higher uncertainty of using a flow model and equations are not ordinarily accounted for. It is common to use reference flow loop tests to determine the flow rate uncertainty at the flow loop conditions.
- Level 3: Reference Conditions – the uncertainties of flow rates of gas, oil, and water at reference conditions are presented at this level. The reference flow rates are calculated using uncertainties at Level 2 conditions in conjunction with a PVT model. Thus, the uncertainties of the PVT model, sampling, and analysis must be combined with the uncertainty at observed flow rate conditions to derive the overall uncertainty at the reference conditions. The reference flow rates are typically used for the allocation process.

Other flow rate uncertainty topics covered are uncertainty changes during field life, presentation of results (as in 4.2.2 below), calibrations, influence factors, sensitivity, and verification.

4.6 Display of Multiphase Meter Uncertainty

Currently, many different ways are used to present the outcome of a MPFM evaluation program. Often the liquid flow rate or gas flow rate as measured by the MPFM is plotted against the reference liquid or gas flow rate as measured by the test loop, however, there is no information in these plots on the actual two-phase conditions, and in particular which flow regime was present. A second and better way is to plot the deviations in liquid and gas flow rates and the deviation in watercut against the GVF. A third way of presentation often seen is the use of the composition map and contour plots. Deviations in liquid flow rate, oil flow rate, and watercut are given as function of both the watercut and the GVF. Again, the performance as a function of GVF and watercut becomes visible, but there is no information on the flow rate dependency in these plots. A fourth way recently proposed [Ref. 5] is to use both the two-phase flow map and the composition map, and to plot both the reference (test loop) measurement and the MPFM measurement together (see Figure 4.1 for an example). The direction of the lines indicates whether deviations are in the liquid flow rate (vertical lines) or in the gas flow rates (horizontal lines). The length of the line indicates the magnitude of the deviation. A logarithmic flow map has the advantage that vectors of the same relative deviation are the same length, regardless of position in the plot. This is contrary to flow maps with a linear scale, where a vector of 10% relative deviation in the low flow rates shows up much smaller than a 10% deviation at high flow rates.

A significant consideration is that deviations in MPFM's readings / results are often systematic because of inaccuracies in the flow models used or differences between configured and actual basic fluid parameters. These systematic errors appear as vectors between reference and MPFM measurement points, with consistent direction of the vector. Hence, the relative position between the reference point and measurement points indicates the presence of systematic deviations. As can be seen in the example shown in Figure 4.1, there is greater deviation is in the gas flow rates than in the liquid flow rates. The same set of test points can also be plotted in the composition map. The deviation in watercut and GVF is plotted, and the largest deviations are easily identified. The length

of the vectors between reference and MPFM measurement points again indicates an absolute deviation between the reference and MPFM measurements, this time in composition. Also clearly visible are the higher deviations at the higher GVF's, and the transition zone between oil-continuous and water-continuous emulsions.

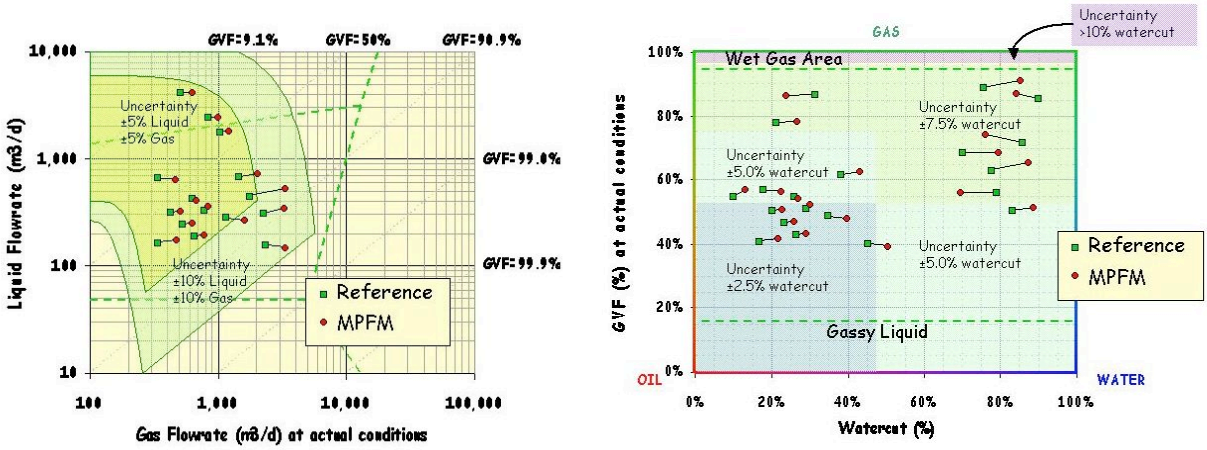

Figure 4.1. Two-phase flow map and composition map with production envelope, MPFM operating envelope, and test results

At present there is no standard method to present the overall uncertainties of multi-phase flow meters, with a variety of different methods being used in practice, making it difficult to compare the performance of different multiphase flow meters. In general MPFM uncertainties are quoted in relative uncertainties for gas and liquid flowrate, and absolute uncertainties for the watercut or WLR fraction measurements. All three will be a function of the GVF and/or WLR. With this combination, also the relative uncertainties in the oil and water flow rates are dependent on the actual watercut level, and need assessment by the user.

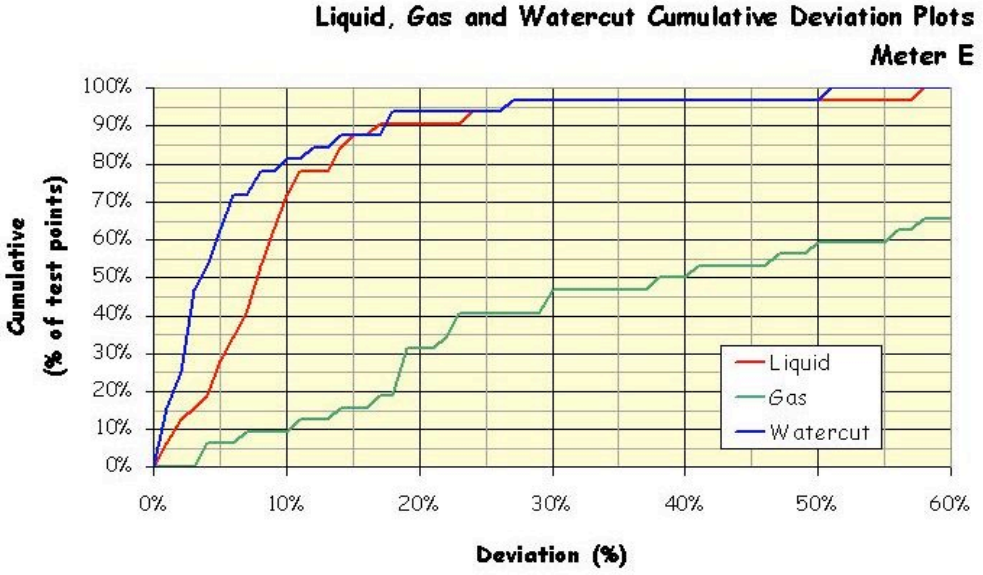

Figure 4.2. Example of cumulative deviation plots for liquid flow rates, gas flow rates and watercut.

Cumulative deviation plots are a convenient way to compare the performance of different MPFM's. In Figure 4.2 the deviation between the MPFM measurement and the reference measurement is plotted along the x-axis and the y-axis represents the percentage of test points that fulfill a certain

deviation criteria. This example shows that 70% of all the test points exhibit relative deviations in liquid flow rate that are smaller than 10%. In addition, 80% of all the test points show absolute deviations in watercut that are smaller than 10%. Finally, this MPFM performs poorly for gas, as only some 10% of the test points fulfill a 10% deviation criterion. If the operating envelope is specified with various GVF ranges, it is recommended that one construct cumulative deviation plots for each GVF range.

4.7 Site Design Considerations

In 4.1.2.1 the various flow regimes are mentioned and very practical and convenient presentations to be used in both the design and the testing phase are the two-phase flow map and the composition map. This is extensively reported in an earlier paper [Ref. 5] and is covered in both the NFOGM and API documents. In both the two-phase flow map (actual gas vs. liquid flow rates) and the composition map (watercut and Gas Volume Fraction) well trajectories, production envelopes and MPFM's operating envelopes can be plotted. This is the first step in the selection of a suitable multi-phase meter for a particular application. In Figure 4.3 an example is given with the well trajectory and the MPFM operating envelope for two uncertainty specifications.

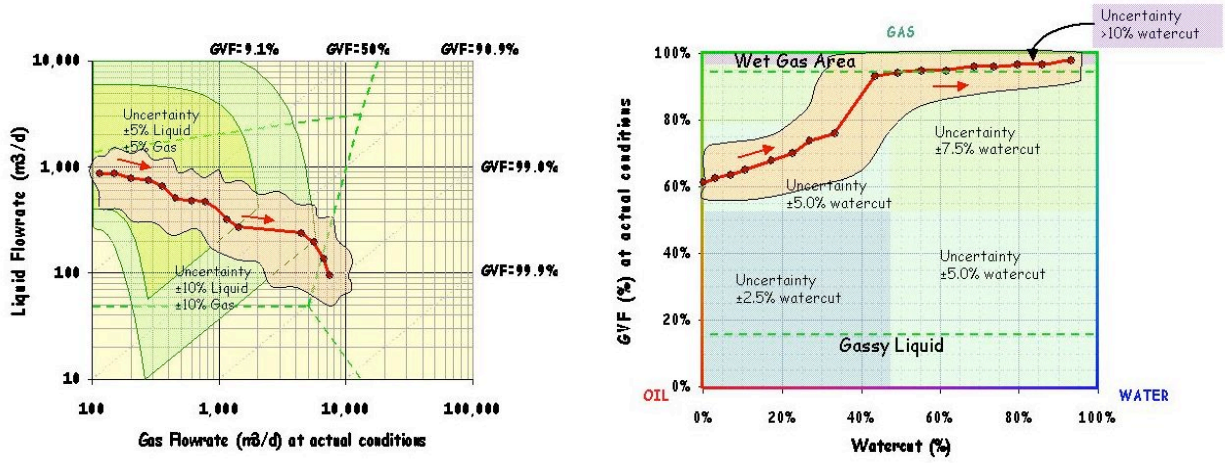

Figure 4.3. An MPFM operating envelope plotted together with the production envelope in the two-phase flow and composition maps.

4.8 Tools for Display of Multiphase Flow Meter Uncertainty

Both the NFOGM Handbook and the API RP 86 introduce new design tools and ways to display MPFM uncertainties in terms of two-phase flow maps and composition maps as described in Section 4.6. To underpin the introduction of these plots and promote their use within the industry, a Microsoft Excel software program for generating these plots has been developed and included as part of the NFOGM Handbook.

The user may enter information about the measurement uncertainty of a meter for given ranges of liquid and gas flow rates and WLR. GVF is automatically calculated from the other inputs. Well data may be specified at several time positions to indicate the evolution of a well over time, and up to five wells may be included in the same plot. By including test-data one may also illustrate graphically any difference between test data and meter specifications in all plots.

The various plots that can be generated with this software tool are:

- Two-phase flow map (Liquid flow rate vs. Gas flow rate)

- Composition map (GVF vs. WLR)
- Deviation plots
  - Gas flow rate vs. GVF
  - Liquid flow rate vs. GVF
  - WLR vs. GVF
- Cumulative plot

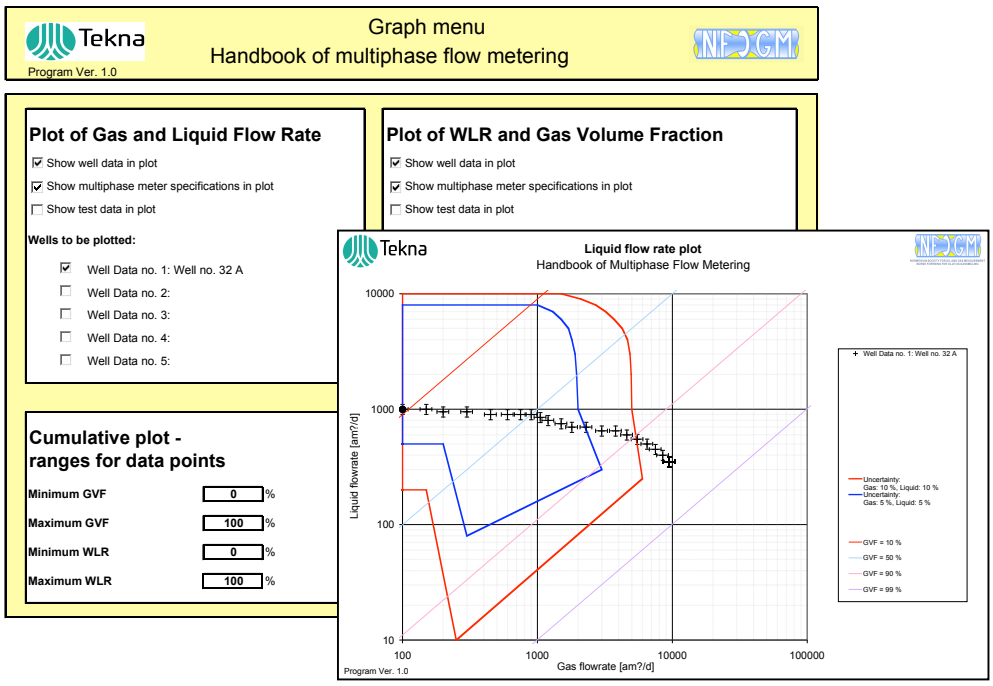

Figure 4.4. Screenshots from the Excel software tool of the graph menu and a two-phase flow map.

4.9 Allocation of Quantities

The TR *Allocation of Gas and Condensate in the Upstream Area* [Ref. 2] describes the topics/issues that are relevant if metering and allocation for gas fields are under discussion, or need to be documented for contractual reasons. It starts with a general introduction regarding the economics of gas developments through the "value of information principle", i.e., metering and allocation cost money (capex and opex) but also deliver value (data), which is used to make business decisions (again, instances where money is involved). In a subsequent chapter various allocation systems and terminology are discussed. There is also a chapter regarding the measurement technology specific to the upstream area, e.g., the use of specific single phase flow meters in non-single phase environment. The best-known example of this is in the use of wet gas differential meters, and the most widely used wet gas overreading correlation is that of de Leeuw. In addition to quantity measurements (flow rates), quality measurements (composition) are also described.

Finally, because the ISO TR is directed primarily at the allocation issue, it does so in a very comprehensive manner, dealing not just with allocation of the produced hydrocarbons, but with everything whose cost of use (or disposal) must be shared, e.g. fuel gas, flare gas, injection gas, etc.

5 CONCLUSIONS. WHAT'S NEXT? THE CHALLENGE.

As first stated in the Introduction, improvements in multiphase flow meters during the last 15 years have resulted in their increased usage in upstream oil and gas applications, especially in difficult offshore locations both topside and deep subsea. To address user needs for information and standardization in the area, documentation has recently been created under the auspices of the NFOGM, API, and ISO.

Our intent here was to familiarize potential users with the three new documents, which should be helpful in a number of respects, e.g., (a) distribution of best knowledge and operational practices on the subject, (b) provision of a common language for discussing multiphase flow, and (c) accounting for the requirements of governing regulatory authorities.

At this stage of completion of NFOGM, API, and ISO reports, a natural question arises as to what the future holds for another round of flow measurement documentation. Candidate areas include:

- In Situ Verification of Multiphase Flow Meters
- Wet Gas Flow Measurement
- Flare Gas Meters
- Virtual Metering
- Composition and Phase Behavior Issues In Measurement
- Flow Measurement Uncertainty

Addressing certain of these is already being proposed in several possible venues, among which are (1) the DeepStar Consortium, (2) a JIP for investigating total system (meter + flowline + separator) uncertainty organized by a group at Tulsa University, and (3) a program for development of drilling and production capabilities in ultradeep water to be sponsored by the US Department of Energy.

The creation of the three documents discussed in this paper demonstrates the benefits that strong international cooperation can achieve in producing standardization documents, ensuring their true global input and acceptance. On the other hand, it should also be questioned why two or more documents are required, which are the result of much duplication of effort. For example, although there are differences between API RP86 and the NFOGM Handbook, they do not differ much in content. Cost saving is often mentioned as a benefit of standardization, and here cost savings can be achieved by combined standards. In the oil and natural gas industry there are numerous examples, particularly in the area of materials, equipment and offshore structures, where API and ISO (TC67) share some 30 co-branded standards, i.e. the standards carry both the ISO and API trademarks.

The authors feel most strongly that there is no reason to repeat this in the future, and that a single document that can be adopted by all the groups be created for a given subject. If it requires that one group take the lead and that the others adopt what has been done by the leader, then this should be acceptable, if the needs of the follower groups have been adequately expressed and accounted for in the final document.

Thus, for potential new standardization activities in our area of flow measurement such as those mentioned above, we recommend the following:

- Do It Once,
- Do It Right,
- Do It Internationally

This will lead to a true international standard. In today's World where the need for speed and efficiency dominates, there is no good reason for developing these documents as we have done in the past.

6 REFERENCES

1. Norwegian Society for Oil and Gas Measurement – *Handbook of Multiphase Flow Metering*, March 2005, ISBN-82-91341-89-3.
2. International Organization for Standardization - *Allocation of Gas and Condensate in the Upstream Area,* [TR in process of publication].
3. American Petroleum Institute Recommended Practice RP 86 - *Recommended Practice for Measurement of Multiphase Flow*, August 2005.
4. American Petroleum Institute (API), *Manual of Petroleum Measurement Standards (MPMS)*.
5. Scheers, A.M., *Use of the Two-Phase Flow Map and the Composition Map in Multiphase Flow Meter Applications*. South East Asia Hydrocarbon Flow Measurement Workshop, Kuala Lumpur, March 2005.
6. International Organization for Standardization, *International Vocabulary of Basic and General Terms in Metrology*, 2003, ISBN 92-67-01075-1.

7 ACKNOWLEDGEMENTS

The authors would like to gratefully acknowledge those groups that sponsored the work reported here.

For sponsoring development of the new NFOGM Handbook, thanks are due the Norwegian Society for Oil and Gas Measurement (NFOGM) and the Norwegian Society of Chartered Technical and Scientific Professionals (Tekna)**.**

The new API Recommended Practice 86 was jointly sponsored by the American Petroleum Institute and the US Minerals Management Service (MMS), to whom our appreciation is tendered.

Finally, we would like to thank those who worked as volunteers in developing each of the three documents. We are especially grateful to their companies, which generously contributed their valuable time to these efforts. Without the hard work of these volunteer contributors, none of what has been described here would have been possible.

APPENDIX – HOW TO OBTAIN THE DOCUMENTS.

For copies of API RP 86:

Electronic copy: http://api-ep.api.org/publications

Hard copy: American Petroleum Institute
1220 L Street NW
Washington, DC, USA 20005-4070

For copies of the NFOGM Handbook:

Electronic copy: http://www.nfogm.no (free download of handbooks and E-learning courses)

Hard copy: Not available

For copies of the ISO TR on Allocation of Gas and Condensate in the Upstream Area (expected publication date Q1/2006):

Electronic copy: http://www.iso.org/iso/en/prods-services/ISOstore/store.html

Hard copy: http://www.iso.org/iso/en/prods-services/ISOstore/memberstores.html

(search by country name to order hard copies from local source)